MARMARA UNIVERSITY
INSTUTE FOR GRADUATE STUDIES
IN PURE AND APPLIED SCIENCES

MOLECULAR SUBTYPING IN COLON CANCER THROUGH CONSENSUS CLUSTERING OF MULTI-OMICS DATA

GÜLLÜ ELİF ÖZDEMİR

MASTER THESIS

Department of Bioengineering

Thesis Supervisor
Prof. Dr. Kazım Yalçın ARGA

ISTANBUL, 2025

MARMARA UNIVERSITY
INSTUTE FOR GRADUATE STUDIES
IN PURE AND APPLIED SCIENCES

MOLECULAR SUBTYPING IN COLON CANCER THROUGH CONSENSUS CLUSTERING OF MULTI-OMICS DATA

GÜLLÜ ELİF ÖZDEMİR
524221021

MASTER THESIS
Department of Bioengineering

Thesis Supervisor
Prof. Dr. Kazım Yalçın ARGA

ISTANBUL, 2025

ACKNOWLEDGEMENT

My master's degree journey has been crowned with the indescribable support and invaluable contributions of many people in my life. Above all, my first thanks go to my esteemed advisor, Prof. Dr. Kazım Yalçın Arga, who guided, supported, and encouraged me throughout the entire process. His wisdom, kindness, and endless patience have been a true source of inspiration for me. Completing this education under the guidance of such a distinguished advisor, admired not only for his academic success but also for his demeanor and character, was a great privilege for me. I extend my heartfelt thanks to Prof. Dr. Betül Yılmaz, the coordinator of the ADEP project I was involved in during my master's, for her constant kindness. Additionally, I would like to thank the members of my thesis committee for taking the time to read my thesis and provide their valuable feedback. Finally, I would like to sincerely thank PhD. Gizem Gülfidan for her patience, unwavering support, and genuine guidance whenever I had a question. Her help made this journey so much smoother for me.

It is impossible to express my gratitude to my beloved family, who have always been there for me throughout my life, never ceasing to support me. I owe my place in life and everything that makes me who I am to my one-of-a-kind family. From the moment I opened my eyes to this world, I thank my dear mother, Kadriye Özdemir, who has strived to protect me, paved my way with flowers, and has been selfless and loyal, for everything. Everything I have and will have in life, I owe to her endless love and support. To my precious sister, Specialist in Child Development Gülsüm Özdemir, who has always been my companion and like a mother to me, I extend my heartfelt thanks for never withholding her support and belief in me, and for her best wishes and assistance that have made my life and thesis process easier. I am deeply grateful to my dear father, Murat Özdemir, the greatest pillar of my life, for always being by my side through all my good and bad times, for supporting me even in my moments of deepest despair, and for always being a light in my darkness. I extend my heartfelt thanks to my dear İsmihan Küçükbaş, who is like family to me, for always cheering me up with her high energy and for always believing in me. Looking back, I am infinitely grateful to my family for always being there and for all the real, lived, and yet-to-be-lived moments we share.

I am deeply connected to the Atay family, who supported me both materially and spiritually with their endless kindness throughout my entire education and training life, and most importantly, always believed in me. This support, which allows me to realize my dreams, is very valuable to me. I will be grateful for a lifetime for the hope and support they gave me.

I would like to thank my beautiful friend Balca Baysan, whose name reflects her name, first of all, for always believing in me and most importantly for having such a big place in the healing path of my self. I am very lucky that he made me experience and feel what the most important things in life are.

I would like to thank my dear friend and colleague Betül Özbek, who fascinated me with her stance and strength in life and shaped my path with her unique perspective, for being being a friend to me in both good and bad times. I am very lucky that she is always by my side sincerely, even when she faces the great difficulties of life.

I would like to wholeheartedly thank Mr. Public Prosecutor Salih Gürcan Soylu, whom I met late but I am glad he has been in my life from the very beginning, and whose presence in my life I liken to a father figure, so to speak, for always being by my side and always making me feel safe with his support. I am as lucky as everyone else in his life with his kind heart and sincerity.

I would like to present my last thank to my beautiful colleague PhD. Hazal Soylu, who leads science with her unique thinking ability at Koç University and is one of the greatest chances of my life. I am grateful to my beautiful friend, whom I met at the very beginning of the path of finding myself, for always being able to see my heart, and for showing me that such great love, devotion and trust can be received from someone other than my family. I am very lucky that she can embrace me even when she was not there in my life and that he always believed in me.

January, 2025 **Güllü Elif ÖZDEMİR**

TABLE OF CONTENTS

ACKNOWLEDGEMENT ……..i

TABLE OF CONTENTS ……...ii

ÖZET ……...v

ABSTRACT ……...vi

SYMBOLS ……vii

ABBREVIATIONS …….viii

LIST OF FIGURES ……..xi

LIST OF TABLES ……xxix

1. INTRODUCTION ……..1

1.1. Colon Cancer ……1

1.2. Epidemiology ……....1

1.3. Treatment ……..6

1.4. Personalized Treatment ……..…..7

1.5. The Scope of COAD Omic Studies ……...…8

1.6. The Scope of This Study ……10

2. MATERIALS AND METHODS …….12

2.1. Multi-Omics Data Extraction From COAD Discovery Cohort ……12

2.2. External Validation Cohorts ……..12

2.3. Identification of Molecular Subtypes by Integrative Analysis ……..13

2.4. Pathway Enrichment Analysis ……..…..14

2.5. Characteristics of Genetic Alterations Among Subtypes ……..14

2.6. Chemotherapeutic Response Prediction ……15

2.7. Validation of External Cohorts ……..15

3. RESULTS AND DISCUSSION ……...…16

3.1. Analysis Results for Two Subtypes ……18

3.1.1. The multi-omics classification of COAD ……18

3.1.2. Differentially expressed genes and signaling pathways ...…..…….22

3.1.3. The effect of genetic alteration on subtypes ……....34

3.1.4. Precision treatment recommendations for COAD patients ……40

3.1.5. Validation of subtypes in four external cohorts ..……47

3.2. Analysis Results for Three Subtypes ……90

3.2.1. The multi-omics classification of COAD ……90

3.2.2. Differentially expressed genes and signaling pathways ……..94

3.2.3. The effect of genetic alteration on subtypes ……..108

3.2.4. Precision treatment recommendations for COAD patients ……...113

3.2.5. Validation of subtypes in four external cohorts ……120

3.3. Analysis Results for Four Subtypes ……..154

3.3.1. The multi-omics classification of COAD ……..154

3.3.2. Clinical characteristics ……...…158

3.3.3. Differentially expressed genes and signaling pathways ……....159

3.3.4. The effect of genetic alteration on subtypes ……..179

3.3.5. Precision treatment recommendations for COAD patients ……...184

3.3.6. Validation of subtypes in four external cohorts ……194

4. CONCLUSIONS ……233

REFERENCES ……...237

APPENDIX A DEGs for All Clusters ……...253

APPENDIX B Drug Sensitivity Results of All Subtypes ……388

AUTOBIOGRAPHY ……..…395

ÖZET

ÇOKLU OMİK VERİLERİNİN KONSENSUS KÜMELEMESİ ARACILIĞIYLA KOLON KANSERİNİN MOLEKÜLER ALT TİPLEMESİ

Kolon kanseri, dünya çapında kansere bağlı ölümlerin en yaygın nedenlerinden biridir ve en yaygın histolojik alt tiplerinden biri kolon adenokarsinomudur. Kolon kanseri hastaları, hastalığın çok çeşitli heterojen yapısından dolayı mevcut tedavi stratejilerinden yeterince yararlanamamaktadır. Kanserin moleküler alt tiplendirilmesi, kanserin heterojenliği hakkında derinlemesine bilgi sağlayabilir ve en uygun hedefe yönelik tedavi stratejilerinin seçimine katkıda bulunabilir.

Bu çalışmanın temel amacı, çoklu omik verilere ve bütünleştirici kümeleme algoritmalarına dayalı konsensüs kümeleri oluşturarak kolon kanserinin kapsamlı moleküler karakterizasyon analizini gerçekleştirmektir. Ayrıca hastalar sistematik olarak sınıflandırılarak spesifik moleküler özellikleri belirlenerek hassas onkoloji uygulamalarının önü açıldı.

Bu tez çalışmasında kolon adenokarsinomu, R paketi "MOVICS" kullanılarak multi-omik verilere ve 10 bütünleştirici kümeleme algoritmasına dayalı konsensüs kümeleri oluşturularak sistematik olarak sınıflandırılmış ve tanımlanan alt tipler çeşitli açılardan incelenerek kişiye özel tedavi seçenekleri değerlendirilmiştir. Sağlam bir kümeleme çıktısı elde etmek için doğrulama kohortunda eş zamanlı olarak alt tipleme analizleri de yapıldı ve her iki analizin sonuçları tutarlılık ve tekrarlanabilirlik açısından değerlendirildi.

Sonuç olarak COAD'ın yüksek hassasiyetle tespit edilen 2, 3 ve 4 alt kümesi ayrı ayrı değerlendirildi. Her üç değerlendirme sonucunda alt tiplerin mRNA, lncRNA, miRNA, metilasyon ve mutasyon açısından farklılık gösterdiği belirlendi. Özellikle APC mutasyonu her üç değerlendirmede de en sık mutasyona uğrayan gendi. Evreye bağlı farklılıklar sadece 4 alt tipleme çalışmasında görüldü. Her üç değerlendirme sonucunda 5-fluorouracil, cisplatin, paclitaxel, SN-38, rapamycin ve imatinib ilaç tedavilerine istatistiksel olarak anlamlı yanıt olduğu belirlendi. Ayrıca validasyon analizleri ile analizlerin doğruluğu teyit edilmiştir.

ABSTRACT

MOLECULAR SUBTYPING IN COLON CANCER THROUGH CONSENSUS CLUSTERING OF MULTI-OMICS DATA

Colon cancer is one of the most common causes of cancer-related deaths worldwide, and one of the most common histological subtypes is adenocarcinoma of the colon. Colon cancer patients cannot benefit sufficiently from current treatment strategies due to the great diversity and heterogeneity of the disease. Molecular subtyping of cancer can provide profound information about the heterogeneity of the cancer and contribute to the selection of the most appropriate targeted treatment strategies.

The main objective of this thesis study was to perform a comprehensive molecular characterization analysis of colon cancer by creating consensus clusters based on multi-omics data and integrative clustering. In addition, patients were systematically classified, their specific molecular characteristics were determined and the way for precision oncology applications has been paved.

In this thesis study, adenocarcinoma of the colon was systematically classified by creating consensus clusters based on multi-omics data and 10 integrative clustering algorithms using the R package "MOVICS", and personalized treatment options were evaluated by examining the defined subtypes with respect to various parameters. In order to obtain a robust clustering output, subtyping analyses were also performed simultaneously in the validation cohort and the results of both analyses were evaluated for consistency and reproducibility.

In conclusion, 2, 3 and 4 subsets of COAD, which were detected with high sensitivity, were evaluated separately. As a result of all three evaluations, it was determined that the subtypes differed in terms of mRNA, lncRNA, miRNA, methylation and mutation. In particular, APC mutation was the most frequently mutated gene in all three evaluations. Differences depending on stage were seen only in 4 subtyping studies. As a result of all three evaluations, it was determined that there was a statistically significant response to 5-fluorouracil, cisplatin, paclitaxel, SN-38, rapamycin and imatinib drug treatments. In addition, the accuracy of the analyzes was confirmed by validation analyses.

SYMBOLS

k **:** The optimum number of clusters

p **:** The significance level

ABBREVIATIONS

AAPC : Average annual percentage change

ACAP1 : ArfGAP with coiled-coil, ankyrin repeat and PH domains 1

ADCK1 : AarF domain-containing protein kinase 1

ADIPOQ : Adiponectin

APC : Adenomatous polyposis coli

BH : Benjamini-Hochberg

BRAF : B-Raf proto-oncogene

CIMP : *CpG* island methylator phenotype

CIN : Chromosomal instability

CNA : Copy number alteration

COAD : Colon adenocarcinoma

CPI : Cluster prediction index

CRC : Colorectal cancer

CRYAB : Crystallin alpha B

DEG : Differentially expressed genes

DTX3 : Deltex E3 ubiquitin ligase 3

EGFR : Epidermal growth factor receptor

EMT : Epithelial-mesenchymal transition

EPHA4 : Ephrin type-A receptor 4

ES : Enrichment score

ETV4 : ETS translocation variant 4

FABP1 : Fatty acid-binding protein 1

FC : Fold change

FDR : False discovery rate

FGA : Fraction genome altered

FGFR3 : Fibroblast growth factor receptor 3

FPKM : Fragments per kilobase of transcript per million mapped reads

GDSC : Genomics of Drug Sensitivity in Cancer

GEO : Gene Expression Omnibus

GO : Gene Ontology

GSEA : Gene set enrichment analysis
HDI : Human development index
IC50 : Half-maximal inhibitory concentration
ICI : Immune checkpoint inhibitor
IGF2 : Insulin-like growth factor 2
IGP : In-group proportion
KRAS : Kirsten rat sarcoma
KRT23 : Keratin 23
lncRNA : Long noncoding RNA
log2FC : Log 2 fold change
MAD : Median absolute deviation
MAGED1 : Melanoma-associated antigen D1
miRNA : Micro RNA
mRNA : Messenger rna
MSI : Microsatellite instability
MsigDB : Molecular Signatures Database
MUC16 : Mucin 16
NES : Normalized enrichment score
NOTUM : Notum, palmitoleoyl-protein carboxylesterase
NTP : Nearest template prediction
Padj : Adjusted p-values
PAEP : Progestagen associated endometrial protein
PAM : Partition around medoids
PCA : Principle component analysis
PIK3CA : Phosphatidylinositol-4,5-bisphosphate 3-kinase catalytic subunit alpha
PIWIL2 : Piwi like RNA-mediated gene silencing 2
POFUT1 : Protein o-fucosyltransferase 1
PRSS56 : Serine protease 56
Rapa : Rapamycin
REG1A : Regenerating family member 1 alpha
REG4 : Regenerating family member
SCNA : Somatic copy number alteration

SD : Standard deviation

SFRP2 : Secreted frizzled related protein 2

SNV : Single nucleotide variant

SOGA1 : Suppressor of glucose, autophagy associated 1

ssGSEA : Single sample gene set enrichment analysis

SYNE1 : Spectrin repeat containing nuclear envelope protein 1

TCGA : The Cancer Genome Atlas

TFAP2B : Transcription factor AP-2 beta

TIL : Tumor-infiltrating lymphocyte

TiTv : Transitions and transversions

TMB : Tumor mutation burden

TP53 : Tumor protein p53

TPM : Transcripts per kilobase million

TS : Thymidylate synthase

TTN : Titin

TYMP : Thymidine phosphorylase

VEGF : Vascular endothelial growth factor

VMC : Vanderbilt Medical Center

WHO : World Health Organization

WIF1 : Wnt inhibitory factor 1

LIST OF FIGURES

Figure 1.1. Distribution of Cases and Deaths for the Top 10 Most Common Cancers in 2020 for (A) Both Sexes, (B) Men, and (C) Women [18]…….2

Figure 1.2. (A) Average annual percentage change (AAPC) of colorectal cancer incidence and mortality in the most recent period (10 years), males [22]…….5

Figure 3.1. Identification of optimal cluster number in TCGA-COAD cohort……..17

Figure 3.2. Consensus heatmap based on results from 10 multi-omics integrative clustering algorithms with number of clusters of 2…….19

Figure 3.3. Quantification of sample similarity using Silhoutte width based on consensus ensembles result…….20

Figure 3.4. Comprehensive heatmap based on consensus across 10 algorithms with clinicopathological and potential drivers' annotation……..……...21

Figure 3.5. Heatmap of subtype-specific upregulated pathways using limma algorithm for 2 identified subtypes in TCGA-COAD cohort……..…32

Figure 3.6. Heatmap of subtype-specific downregulated pathways using limma algorithm for 2 identified subtypes in TCGA-COAD cohort……..….32

Figure 3.7. Heatmap of enrichment score of tumor-associated pathways for 2 identified subtypes in TCGA-COAD cohort. …….34

Figure 3.8. Mutational OncoPrint of 2 identified subtypes of colon adenocancinoma in TCGA-COAD cohort……..…35

Figure 3.9. Bar plot of fraction genome altered among 2 identified subtypes of colon adenocarcinoma in TCGA-COAD cohort……..….38

Figure 3.10. Comparison of TMB and TiTv among 2 identified subtypes of colon adenocarcinoma in TCGA-COAD cohort……...39

Figure 3.11. Agreement of 2 identified subtypes of colon adenocarcinoma with the most common 5 mutant genes in TCGA-COAD cohort…….40

Figure 3.12. Boxviolin for estimated IC50 of 5-Fluorouracil among 2 identified subtypes of colon adenocarcinoma in TCGA-COAD cohort……..42

Figure 3.13. Boxviolin for estimated IC50 of Cisplatin among 2 identified subtypes of colon adenocarcinoma in TCGA-COAD cohort…….43

Figure 3.14. Boxviolin for estimated IC50 of Paclitaxel among 2 identified subtypes of colon adenocarcinoma in TCGA-COAD cohort…….44

Figure 3.15. Boxviolin for estimated IC50 of SN-38 among 2 identified subtypes of colon adenocarcinoma in TCGA-COAD cohort…….45

Figure 3.16. Boxviolin for estimated IC50 of Rapamycin among 2 identified subtypes of colon adenocarcinoma in TCGA-COAD cohort…….....46

Figure 3.17. Boxviolin for estimated IC50 of Imatinib among 2 identified subtypes of colon adenocarcinoma in TCGA-COAD cohort…….47

Figure 3.18. Heatmap of NTP in GSE16125 cohort using subtype-specific upregulated biomarkers identified using edgeR from TCGA-COAD cohort…….48

Figure 3.19. Heatmap of NTP in GSE16125 cohort using subtype-specific upregulated biomarkers identified using DESeq2 from TCGA-COAD cohort……..…49

Figure 3.20. Heatmap of NTP in GSE16125 cohort using subtype-specific upregulated biomarkers identified using limma from TCGA-COAD cohort…….....49

Figure 3.21. Kaplan-Meier survival curve of 2 colon adenocarcinoma subtypes predicted by edgeR in the GSE16125 cohort……..50

Figure 3.22. Kaplan-Meier survival curve of 2 colon adenocarcinoma subtypes predicted by DESeq2 in the GSE16125 cohort……...51

Figure 3.23. Kaplan-Meier survival curve of 2 colon adenocarcinoma subtypes predicted by limma in the GSE16125 cohort……..52

Figure 3.24. Consistency heatmap between current and NTP-predicted Kappa statistics for edgeR results in TCGA-COAD cohort…….….53

Figure 3.25. Consistency heatmap between current and PAM-predicted Kappa statistics for edgeR results in TCGA-COAD cohort…..…….……54

Figure 3.26. Consistency heatmap between current and NTP-predicted Kappa statistics for DESeq2 results in TCGA-COAD cohort.…….…….……54

Figure 3.27. Consistency heatmap between current and PAM-predicted Kappa statistics for DESeq2 results in TCGA-COAD cohort…….…….….55

Figure 3.28. Consistency heatmap between current and NTP-predicted Kappa statistics for limma results in TCGA-COAD cohort……..55

Figure 3.29. Consistency heatmap between current and PAM-predicted Kappa statistics for limma results in TCGA-COAD cohort……..56

Figure 3.30. Consistency heatmap between NTP and PAM-predicted subtype for edgeR results in GSE16125……..……..…57

Figure 3.31. Consistency heatmap between NTP and PAM-predicted subype for DESeq2 results in GSE16125……..57

Figure 3.32. Consistency heatmap between NTP and PAM-predicted subtype for limma results in GSE16125……....58

Figure 3.33. Heatmap of NTP in GSE39582 cohort using subtype-specific upregulated biomarkers identified using edgeR from TCGA-COAD cohort…….59

Figure 3.34. Heatmap of NTP in GSE39582 cohort using subtype-specific upregulated biomarkers identified using DESeq2 from TCGA-COAD cohort…….....59

Figure 3.35. Heatmap of NTP in GSE39582 cohort using subtype-specific upregulated biomarkers identified using limma from TCGA-COAD cohort……..…...60

Figure 3.36. Kaplan-Meier survival curve of 2 colon adenocarcinoma subtypes predicted by edgeR in the GSE39582 cohort…….…….61

Figure 3.37. Kaplan-Meier survival curve of 2 colon adenocarcinoma subtypes predicted by DESeq2 in the GSE39582 cohort……..…….…62

Figure 3.38. Kaplan-Meier survival curve of 2 colon adenocarcinoma subtypes predicted by limma in the GSE39582 cohort…….….63

Figure 3.39. Consistency heatmap between current and NTP-predicted Kappa statistics for edgeR results in TCGA-COAD cohort……..64

Figure 3.40. Consistency heatmap between current and PAM-predicted Kappa statistics for edgeR results in TCGA-COAD cohort……..64

Figure 3.41. Consistency heatmap between current and NTP-predicted Kappa statistics for DESeq2 results in TCGA-COAD cohort…….…..65

Figure 3.42. Consistency heatmap between current and PAM-predicted Kappa statistics for DESeq2 results in TCGA-COAD cohort…….…..65

Figure 3.43. Consistency heatmap between current and NTP-predicted Kappa statistics for limma results in TCGA-COAD cohort…….….66

Figure 3.44. Consistency heatmap between current and PAM-predicted Kappa statistics for limma results in TCGA-COAD cohort……..66

Figure 3.45. Consistency heatmap between NTP and PAM-predicted subtype for edgeR results in GSE39582……..……..67

Figure 3.46. Consistency heatmap between NTP and PAM-predicted subtype for DESeq2 results in GSE39582……..68

Figure 3.47. Consistency heatmap between NTP and PAM-predicted subtype for limma results in GSE39582……....68

Figure 3.48. Heatmap of NTP in GSE17536 cohort using subtype-specific upregulated biomarkers identified using edgeR from TCGA-COAD cohort……..…...69

Figure 3.49. Heatmap of NTP in GSE17536 cohort using subtype-specific upregulated biomarkers identified using DESeq2 from TCGA-COAD cohort…….....70

Figure 3.50. Heatmap of NTP in GSE17536 cohort using subtype-specific upregulated biomarkers identified using limma from TCGA-COAD cohort……..…...70

Figure 3.51. Kaplan-Meier survival curve of 2 colon adenocarcinoma subtypes predicted by edgeR in the GSE17536 cohort…….….71

Figure 3.52. Kaplan-Meier survival curve of 2 colon adenocarcinoma subtypes predicted by DESeq2 in the GSE17536 cohort…….…..72

Figure 3.53. Kaplan-Meier survival curve of 2 colon adenocarcinoma subtypes predicted by limma in the GSE17536 cohort…….….73

Figure 3.54. Consistency heatmap between current and NTP-predicted Kappa statistics for edgeR results in TCGA-COAD cohort…….….74

Figure 3.55. Consistency heatmap between current and PAM-predicted Kappa statistics for edgeR results in TCGA-COAD cohort…….…….74

Figure 3.56. Consistency heatmap between current and NTP-predicted Kappa statistics for DESeq2 results in TCGA-COAD cohort……...75

Figure 3.57. Consistency heatmap between current and PAM-predicted Kappa statistics for DESeq2 results in TCGA-COAD cohort…….……..76

Figure 3.58. Consistency heatmap between current and NTP-predicted Kappa statistics for limma results in TCGA-COAD cohort…….….76

Figure 3.59. Consistency heatmap between current and PAM-predicted Kappa statistics for limma results in TCGA-COAD cohort…….…….77

Figure 3.60. Consistency heatmap between NTP and PAM-predicted subtype for edgeR results in GSE17536……..…..78

Figure 3.61. Consistency heatmap between NTP and PAM-predicted subtype for DESeq2 results in GSE17536……..78

Figure 3.62. Consistency heatmap between NTP and PAM-predicted subtype for limma results in GSE17536……..…..79

Figure 3.63. Heatmap of NTP in GSE17537 cohort using subtype-specific upregulated biomarkers identified using edgeR from TCGA-COAD cohort……..…...80

Figure 3.64. Heatmap of NTP in GSE17537 cohort using subtype-specific upregulated biomarkers identified using DESeq2 from TCGA-COAD cohort…….....80

Figure 3.65. Heatmap of NTP in GSE17537 cohort using subtype-specific upregulated biomarkers identified using limma from TCGA-COAD cohort…….....81

Figure 3.66. Kaplan-Meier survival curve of 2 colon adenocarcinoma subtypes predicted by edgeR in the GSE17537 cohort……..82

Figure 3.67. Kaplan-Meier survival curve of 2 colon adenocarcinoma subtypes predicted by DESeq2 in the GSE17537 cohort…….…..83

Figure 3.68. Kaplan-Meier survival curve of 2 colon adenocarcinoma subtypes predicted by limma in the GSE17537 cohort……..84

Figure 3.69. Consistency heatmap between current and NTP-predicted Kappa statistics for edgeR results in TCGA-COAD cohort….…….……85

Figure 3.70. Consistency heatmap between current and PAM-predicted Kappa statistics for edgeR results in TCGA-COAD cohort……..85

Figure 3.71. Consistency heatmap between current and NTP-predicted Kappa statistics for DESeq2 results in TCGA-COAD cohort…….…..….86

Figure 3.72. Consistency heatmap between current and PAM-predicted Kappa statistics for DESeq2 results in TCGA-COAD cohort…….…..….87

Figure 3.73. Consistency heatmap between current and NTP-predicted Kappa statistics for limma results in TCGA-COAD cohort……..87

Figure 3.74. Consistency heatmap between current and PAM-predicted Kappa statistics for limma results in TCGA-COAD cohort…….88

Figure 3.75. Consistency heatmap between NTP and PAM-predicted subtype for edgeR results in GSE17537……....89

Figure 3.76. Consistency heatmap between NTP and PAM-predicted subtype for DESeq2 results in GSE17537……..89

Figure 3.77. Consistency heatmap between NTP and PAM-predicted subtype for limma results in GSE17537……...….90

Figure 3.78. Consensus heatmap based on results from 10 multi-omics integrative clustering algorithms with cluster number of 3……..….91

Figure 3.79. Quantification of sample similarity using Silhoutte width based on consensus ensembles result…….....92

Figure 3.80. Comprehensive heatmap based on consensus across 10 algorithms with clinicopathological and potential drivers annotation…….....93

Figure 3.81. Heatmap of subtype-specific upregulated pathways using limma algorithm for 3 identified subtypes in TCGA-COAD cohort……..……..106

Figure 3.82. Heatmap of subtype-specific downregulated pathways using limma algorithm for 3 identified subtypes in TCGA-COAD cohort……..…..107

Figure 3.83. Heatmap of enrichment score of tumor-associated pathways for 3 identified subtypes in TCGA-COAD cohort…….....108

Figure 3.84. Mutational OncoPrint of 3 identified subtypes of colon adenocancinoma in TCGA-COAD cohort……....109

Figure 3.85. Bar plot of fraction genome altered among 3 identified subtypes of colon adenocarcinoma in TCGA-COAD cohort…….....111

Figure 3.86. Comparison of TMB and TiTv among 3 identified subtypes of colon adenocarcinoma in TCGA-COAD cohort…….....112

Figure 3.87. Agreement of 3 identified subtypes of colon adenocarcinoma with the most common 5 mutant genes in TCGA-COAD cohort……...113

Figure 3.88. Boxviolin for estimated IC50 of 5-Fluorouracil among 3 identified subtypes of colon adenocarcinoma in TCGA-COAD cohort……...…….115

Figure 3.89. Boxviolin for estimated IC50 of Cisplatin among 3 identified subtypes of colon adenocarcinoma in TCGA-COAD cohort……...116

Figure 3.90. Boxviolin for estimated IC50 of Paclitaxel among 3 identified subtypes of colon adenocarcinoma in TCGA-COAD cohort……...117

Figure 3.91. Boxviolin for estimated IC50 of SN-38 among 3 identified subtypes of colon adenocarcinoma in TCGA-COAD cohort……...118

Figure 3.92. Boxviolin for estimated IC50 of Rapamycin among 3 identified subtypes of colon adenocarcinoma in TCGA-COAD cohort……..….119

Figure 3.93. Boxviolin for estimated IC50 of Imatinib among 3 identified subtypes of colon adenocarcinoma in TCGA-COAD cohort. …….120

Figure 3.94. Heatmap of NTP in GSE16125 cohort using subtype-specific upregulated biomarkers identified using edgeR from TCGA-COAD cohort……..…….121

Figure 3.95. Heatmap of NTP in GSE16125 cohort using subtype-specific upregulated biomarkers identified using limma from TCGA-COAD cohort……..….122

Figure 3.96. Kaplan-Meier survival curve of 3 colon adenocarcinoma subtypes predicted by edgeR in the GSE16125 cohort…….……...123

Figure 3.97. Kaplan-Meier survival curve of 3 colon adenocarcinoma subtypes predicted by limma in the GSE16125 cohort……124

Figure 3.98. Consistency heatmap between current and NTP-predicted Kappa statistics for edgeR results in TCGA-COAD cohort…….…..….125

Figure 3.99. Consistency heatmap between current and PAM-predicted Kappa statistics for edgeR results in TCGA-COAD cohort…….……...126

Figure 3.100. Consistency heatmap between current and NTP-predicted Kappa statistics for DESeq2 results in TCGA-COAD cohort……..126

Figure 3.101. Consistency heatmap between current and PAM-predicted Kappa statistics for DESeq2 results in TCGA-COAD cohort…….....127

Figure 3.102. Consistency heatmap between current and NTP-predicted Kappa statistics for limma results in TCGA-COAD cohort…….127

Figure 3.103. Consistency heatmap between current and PAM-predicted Kappa statistics for limma results in TCGA-COAD cohort…….128

Figure 3.104. Consistency heatmap between NTP and PAM-predicted subtype for edgeR results in GSE16125……..…….129

Figure 3.105. Consistency heatmap between NTP and PAM-predicted subtype for limma results in GSE16125……...…129

Figure 3.106. Heatmap of NTP in GSE39582 cohort using subtype-specific upregulated biomarkers identified using edgeR from TCGA-COAD cohort……..….130

Figure 3.107. Heatmap of NTP in GSE39582 cohort using subtype-specific upregulated biomarkers identified using limma from TCGA-COAD cohort……...……131

Figure 3.108. Kaplan-Meier survival curve of 3 colon adenocarcinoma subtypes predicted by edgeR in the GSE39582 cohort……..…...132

Figure 3.109. Kaplan-Meier survival curve of 3 colon adenocarcinoma subtypes predicted by limma in the GSE39582 cohort……..…..133

Figure 3.110. Consistency heatmap between current and NTP-predicted Kappa statistics for edgeR results in TCGA-COAD cohort…….....134

Figure 3.111. Consistency heatmap between current and PAM-predicted Kappa statistics for edgeR results in TCGA-COAD cohort…….134

Figure 3.112. Consistency heatmap between current and NTP-predicted Kappa statistics for DESeq2 results in TCGA-COAD cohort……..135

Figure 3.113. Consistency heatmap between current and PAM-predicted Kappa statistics for DESeq2 results in TCGA-COAD cohort…….....135

Figure 3.114. Consistency heatmap between current and NTP-predicted Kappa statistics for limma results in TCGA-COAD cohort…….....136

Figure 3.115. Consistency heatmap between current and PAM-predicted Kappa statistics for limma results in TCGA-COAD cohort…….....136

Figure 3.116. Consistency heatmap between NTP and PAM-predicted subtype for edgeR results in GSE39582…….....137

Figure 3.117. Consistency heatmap between NTP and PAM-predicted subtype for limma results in GSE39582……..…138

Figure 3.118. Heatmap of NTP in GSE17536 cohort using subtype-specific upregulated biomarkers identified using edgeR from TCGA-COAD cohort……...139

Figure 3.119. Heatmap of NTP in GSE17536 cohort using subtype-specific upregulated biomarkers identified using limma from TCGA-COAD cohort……...139

Figure 3.120. Kaplan-Meier survival curve of 3 colon adenocarcinoma subtypes predicted by edgeR in the GSE17536 cohort……....140

Figure 3.121. Kaplan-Meier survival curve of 3 colon adenocarcinoma subtypes predicted by limma in the GSE17536 cohort……141

Figure 3.122. Consistency heatmap between current and NTP-predicted Kappa statistics for edgeR results in TCGA-COAD cohort…….....142

Figure 3.123. Consistency heatmap between current and PAM-predicted Kappa statistics for edgeR results in TCGA-COAD cohort…….....142

Figure 3.124. Consistency heatmap between current and NTP-predicted Kappa statistics for DESeq2 results in TCGA-COAD cohort…….....143

Figure 3.125. Consistency heatmap between current and PAM-predicted Kappa statistics for DESeq2 results in TCGA-COAD cohort…….....143

Figure 3.126. Consistency heatmap between current and NTP-predicted Kappa statistics for limma results in TCGA-COAD cohort…….....144

Figure 3.127. Consistency heatmap between current and PAM-predicted Kappa statistics for limma results in TCGA-COAD cohort…….144

Figure 3.128. Consistency heatmap between NTP and PAM-predicted subtype for edgeR results in GSE17536…….....145

Figure 3.129. Consistency heatmap between NTP and PAM-predicted subtype for limma results in GSE17536…….....146

Figure 3.130. Heatmap of NTP in GSE17537 cohort using subtype-specific upregulated biomarkers identified using edgeR from TCGA-COAD cohort……...147

Figure 3.131. Heatmap of NTP in GSE17537 cohort using subtype-specific upregulated biomarkers identified using limma from TCGA-COAD cohort……...147

Figure 3.132. Kaplan-Meier survival curve of 3 colon adenocarcinoma subtypes predicted by edgeR in the GSE17537 cohort……....148

Figure 3.133. Kaplan-Meier survival curve of 3 colon adenocarcinoma subtypes predicted by limma in the GSE17537 cohort……....149

Figure 3.134. Consistency heatmap between current and NTP-predicted Kappa statistics for edgeR results in TCGA-COAD cohort…….....150

Figure 3.135. Consistency heatmap between current and PAM-predicted Kappa statistics for edgeR results in TCGA-COAD cohort…….150

Figure 3.136. Consistency heatmap between current and NTP-predicted Kappa statistics for DESeq2 results in TCGA-COAD cohort……..151

Figure 3.137. Consistency heatmap between current and PAM-predicted Kappa statistics for DESeq2 results in TCGA-COAD cohort……..…151

Figure 3.138. Consistency heatmap between current and NTP-predicted Kappa statistics for limma results in TCGA-COAD cohort…….....152

Figure 3.139. Consistency heatmap between current and PAM-predicted Kappa statistics for limma results in TCGA-COAD cohort…….152

Figure 3.140. Consistency heatmap between NTP and PAM-predicted subtype for edgeR results in GSE17537…….....153

Figure 3.141. Consistency heatmap between NTP and PAM-predicted subtype for limma results in GSE17537…….....154

Figure 3.142. Consensus heatmap based on results from 10 multi-omics integrative clustering algorithms with cluster number of 4…….....155

Figure 3.143. Quantification of sample similarity using silhoutte score based on consensus ensembles result……..…..156

Figure 3.144. Comprehensive heatmap based on consensus across 10 algorithms with clinicopathological and potential drivers' annotation……...157

Figure 3.145. Heatmap of subtype-specific upregulated pathways using DESeq2 algorithm for 4 identified subtypes in TCGA-COAD cohort…….…...175

Figure 3.146. Heatmap of subtype-specific downregulated pathways using DESeq2 algorithm for 4 identified subtypes in TCGA-COAD cohort……176

Figure 3.147. Heatmap of subtype-specific upregulated pathways using limma algorithm for 4 identified subtypes in TCGA-COAD cohort……....177

Figure 3.149. Heatmap of enrichment score of tumor-associated pathways for 4 identified subtypes in TCGA-COAD cohort…….....178

Figure 3.150. Mutational OncoPrint of 4 identified subtypes of colon adenocancinoma in TCGA-COAD cohort……180

Figure 3.151. Barplot of fraction genome altered among 4 identified subtypes of colon adenocarcinoma in TCGA-COAD cohort…….....182

Figure 3.152. Comparison of TMB and TiTv among 4 identified subtypes of colon adenocarcinoma in TCGA-COAD cohort…….....183

Figure 3.153. Agreement of 4 identified subtypes of colon adenocarcinoma with the most common 5 mutant genes in TCGA-COAD cohort……...184

Figure 3.154. Boxviolin for estimated IC50 of 5-Fluorouracil among 4 identified subtypes of colon adenocarcinoma in TCGA-COAD cohort……186

Figure 3.155. Boxviolin for estimated IC50 of Cisplatin among 4 identified subtypes of colon adenocarcinoma in TCGA-COAD cohort…….....187

Figure 3.156. Boxviolin for estimated IC50 of Paclitaxel among 4 identified subtypes of colon adenocarcinoma in TCGA-COAD cohort……..188

Figure 3.157. Boxviolin for estimated IC50 of SN-38 among 4 identified subtypes of colon adenocarcinoma in TCGA-COAD cohort……...189

Figure 3.158. Boxviolin for estimated IC50 of Rapamycin among 4 identified subtypes of colon adenocarcinoma in TCGA-COAD cohort……190

Figure 3.159. Boxviolin for estimated IC50 of Imatinib among 4 identified subtypes of colon adenocarcinoma in TCGA-COAD cohort……...191

Figure 3.160. Boxviolin for estimated IC50 of Cetuximab among 4 identified subtypes of colon adenocarcinoma in TCGA-COAD cohort……..….192

Figure 3.161. Boxviolin for estimated IC50 of MG-132 among 4 identified subtypes of colon adenocarcinoma in TCGA-COAD cohort……...193

Figure 3.162. Heatmap of NTP in GSE16125 cohort using subtype-specific upregulated biomarkers identified using edgeR from TCGA-COAD cohort……...195

Figure 3.163. Heatmap of NTP in GSE16125 cohort using subtype-specific upregulated biomarkers identified using DESeq2 from TCGA-COAD cohort……195

Figure 3.164. Kaplan-Meier survival curve of 4 colon adenocarcinoma subtypes predicted by edgeR in the GSE16125 cohort……...196

Figure 3.165. Kaplan-Meier survival curve of 4 colon adenocarcinoma subtypes predicted by DESeq2 in the GSE16125 cohort…….....197

Figure 3.166. Consistency heatmap between current and NTP-predicted Kappa statistics for edgeR results in TCGA-COAD cohort…...…….……198

Figure 3.167. Consistency heatmap between current and PAM-predicted Kappa statistics for edgeR results in TCGA-COAD cohort…….199

Figure 3.168. Consistency heatmap between current and NTP-predicted Kappa statistics for DESeq2 results in TCGA-COAD cohort…….....199

Figure 3.169. Consistency heatmap between current and PAM-predicted Kappa statistics for DESeq2 results in TCGA-COAD cohort…….....200

Figure 3.170. Consistency heatmap between current and NTP-predicted Kappa statistics for limma results in TCGA-COAD cohort. ……...200

Figure 3.171. Consistency heatmap between current and PAM-predicted Kappa statistics for limma results in TCGA-COAD cohort. ……...201

Figure 3.172. Consistency heatmap between NTP and PAM-predicted subtype for edgeR results in GSE16125……..……202

Figure 3.173. Consistency heatmap between NTP and PAM-predicted subtype for DESeq2 results in GSE16125……202

Figure 3.174. Heatmap of NTP in GSE39582 cohort using subtype-specific upregulated biomarkers identified using edgeR from TCGA-COAD cohort……...203

Figure 3.175. Heatmap of NTP in GSE39582 cohort using subtype-specific upregulated biomarkers identified using DESeq2 from TCGA-COAD cohort……204

Figure 3.176. Heatmap of NTP in GSE39582 cohort using subtype-specific upregulated biomarkers identified using limma from TCGA-COAD cohort……...204

Figure 3.177. Kaplan-Meier survival curve of 4 colon adenocarcinoma subtypes predicted by edgeR in the GSE39582 cohort.……...205

Figure 3.178. Kaplan-Meier survival curve of 4 colon adenocarcinoma subtypes predicted by DESeq2 in the GSE39582 cohort…….....206

Figure 3.179. Kaplan-Meier survival curve of 4 colon adenocarcinoma subtypes predicted by limma in the GSE39582 cohort……...…….207

Figure 3.180. Consistency heatmap between current and NTP-predicted Kappa statistics for edgeR results in TCGA-COAD cohort……..……...208

Figure 3.181. Consistency heatmap between current and PAM-predicted Kappa statistics for edgeR results in TCGA-COAD cohort…….208

Figure 3.182. Consistency heatmap between current and NTP-predicted Kappa statistics for DESeq2 results in TCGA-COAD cohort…….….209

Figure 3.183. Consistency heatmap between current and PAM-predicted Kappa statistics for DESeq2 results in TCGA-COAD cohort…….....209

Figure 3.184. Consistency heatmap between current and NTP-predicted Kappa statistics for limma results in TCGA-COAD cohort…….210

Figure 3.185. Consistency heatmap between current and PAM-predicted Kappa statistics for limma results in TCGA-COAD cohort…….....210

Figure 3.186. Consistency heatmap between NTP and PAM-predicted subtype for edgeR results in GSE39582…….....211

Figure 3.187. Consistency heatmap between NTP and PAM-predicted subtype for DESeq2 results in GSE39582……....212

Figure 3.188. Heatmap of NTP in GSE17536 cohort using subtype-specific upregulated biomarkers identified using edgeR from TCGA-COAD cohort……...213

Figure 3.189. Heatmap of NTP in GSE17536 cohort using subtype-specific upregulated biomarkers identified using DESeq2 from TCGA-COAD cohort……....213

Figure 3.190. Heatmap of NTP in GSE17536 cohort using subtype-specific upregulated biomarkers identified using limma from TCGA-COAD cohort……...214

Figure 3.191. Kaplan-Meier survival curve of 4 colon adenocarcinoma subtypes predicted by edgeR in the GSE17536 cohort…….....215

Figure 3.192. Kaplan-Meier survival curve of 4 colon adenocarcinoma subtypes predicted by DESeq2 in the GSE17536 cohort…….…....216

Figure 3.193. Kaplan-Meier survival curve of 4 colon adenocarcinoma subtypes predicted by limma in the GSE17536 cohort……....217

Figure 3.194. Consistency heatmap between current and NTP-predicted Kappa statistics for edgeR results in TCGA-COAD cohort……...….218

Figure 3.195. Consistency heatmap between current and PAM-predicted Kappa statistics for edgeR results in TCGA-COAD cohort…….....218

Figure 3.196. Consistency heatmap between current and NTP-predicted Kappa statistics for DESeq2 results in TCGA-COAD cohort…….....219

Figure 3.197. Consistency heatmap between current and PAM-predicted Kappa statistics for DESeq2 results in TCGA-COAD cohort……..219

Figure 3.198. Consistency heatmap between current and NTP-predicted Kappa statistics for limma results in TCGA-COAD cohort…….....220

Figure 3.199. Consistency heatmap between current and PAM-predicted Kappa statistics for limma results in TCGA-COAD cohort…….....220

Figure 3.200. Consistency heatmap between NTP and PAM-predicted subtype for edgeR results in GSE17536…….....221

Figure 3.201. Consistency heatmap between NTP and PAM-predicted subtype for DESeq2 results in GSE17536……....222

Figure 3.202. Heatmap of NTP in GSE17537 cohort using subtype-specific upregulated biomarkers identified using edgeR from TCGA-COAD cohort……...223

Figure 3.203. Heatmap of NTP in GSE17537 cohort using subtype-specific upregulated biomarkers identified using DESeq2 from TCGA-COAD cohort……223

Figure 3.204. Heatmap of NTP in GSE17537 cohort using subtype-specific upregulated biomarkers identified using limma from TCGA-COAD cohort……..….224

Figure 3.205. Kaplan-Meier survival curve of 4 colon adenocarcinoma subtypes predicted by edgeR in the GSE17537 cohort..…….….225

Figure 3.206. Kaplan-Meier survival curve of 4 colon adenocarcinoma subtypes predicted by DESeq2 in the GSE17537 cohort…….....226

Figure 3.207. Kaplan-Meier survival curve of 4 colon adenocarcinoma subtypes predicted by limma in the GSE17537 cohort……227

Figure 3.208. Consistency heatmap between current and NTP-predicted Kappa statistics for edgeR results in TCGA-COAD cohort……..…...228

Figure 3.209. Consistency heatmap between current and PAM-predicted Kappa statistics for edgeR results in TCGA-COAD cohort…….....228

Figure 3.210. Consistency heatmap between current and NTP-predicted Kappa statistics for DESeq2 results in TCGA-COAD cohort……..229

Figure 3.211. Consistency heatmap between current and PAM-predicted Kappa statistics for DESeq2 results in TCGA-COAD cohort…….....229

Figure 3.212. Consistency heatmap between current and NTP-predicted Kappa statistics for limma results in TCGA-COAD cohort…….....230

Figure 3.213. Consistency heatmap between current and PAM-predicted Kappa statistics for limma results in TCGA-COAD cohort…….....230

Figure 3.214. Consistency heatmap between NTP and PAM-predicted subtype for edgeR results in GSE17537…….....231

Figure 3.215. Consistency heatmap between NTP and PAM-predicted subtype for DESeq2 results in GSE17537…….....232

LIST OF TABLES

Table 1.1. Estimated numbers of new invasive colorectal cancer cases and deaths by age, 2023, United States [20] …….....3

Table 2.1. The GEO datasets employed in the present study……13

Table 2.2. Data extracted for multi-omics data integration……14

Table 3.1. Differentially expressed upregulated transcripts identified in the CS1 subtype using edgeR…….....23

Table 3.2. Differentially expressed downregulated transcripts identified in the CS1 subtype using edgeR…….....23

Table 3.3. Differentially expressed upregulated transcripts identified in the CS2 subtype using edgeR…….....24

Table 3.4. Differentially expressed downregulated transcripts identified in the CS2 subtype using edgeR…….....24

Table 3.5. Differentially expressed upregulated transcripts identified in the CS1 subtype using DESeq2…….....25

Table 3.6. Differentially expressed downregulated transcripts identified in the CS1 subtype using DESeq2…….....26

Table 3.7. Differentially expressed upregulated transcripts identified in the CS2 subtype using DESeq2…….....26

Table 3.8. Differentially expressed downregulated transcripts identified in the CS2 subtype using DESeq2…….....27

Table 3.9. Differentially expressed upregulated transcripts identified in the CS1 subtype using limma…….....28

Table 3.10. Differentially expressed downregulated transcripts identified in the CS1 subtype using limma…….....28

Table 3.11. Differentially expressed upregulated transcripts identified in the CS2 subtype using limma…….....29

Table 3.12. Differentially expressed downregulated transcripts identified in the CS2 subtype using limma…….....30

Table 3.13. Comparison of mutational frequency among 2 identified subtype of colon adenocarcinoma in TCGA-COAD cohort…….....36

Table 3.14. Demo of comparison of fraction genome altered among 2 identified subtype of colon adenocarcinoma in TCGA-COAD cohort…….38

Table 3.15. Demo of comparison of TMB among 2 identified subtype of colon adenocarcinoma in TCGA-COAD cohort……...39

Table 3.16. IGP information in four validation cohorts of the PAM classifier trained on the TCGA-COAD cohort…….....53

Table 3.17. Differentially expressed upregulated transcripts identified in the CS1 subtype using edgeR…….....94

Table 3.18. Differentially expressed downregulated transcripts identified in the CS1 subtype using edgeR…….....95

Table 3.19. Differentially expressed upregulated transcripts identified in the CS2 subtype using edgeR…….....95

Table 3.20. Differentially expressed downregulated transcripts identified in the CS2 subtype using edgeR……96

Table 3.21. Differentially expressed upregulated transcripts identified in the CS3 subtype using edgeR……97

Table 3.22. Differentially expressed downregulated transcripts identified in the CS3 subtype using edgeR……97

Table 3.23. Differentially expressed upregulated transcripts identified in the CS1 subtype using DESeq2…….98

Table 3.24. Differentially expressed downregulated transcripts identified in the CS1 subtype using DESeq2…….99

Table 3.25. Differentially expressed upregulated transcripts identified in the CS2 subtype using DESeq2…….99

Table 3.26. Differentially expressed downregulated transcripts identified in the CS2 subtype using DESeq2..……100

Table 3.27. Differentially expressed upregulated transcripts identified in the CS3 subtype using DESeq2……...100

Table 3.28. Differentially expressed downregulated transcripts identified in the CS3 subtype using DESeq2……...101

Table 3.29. Differentially expressed upregulated transcripts identified in the CS1 subtype using limma……..102

Table 3.30. Differentially expressed downregulated transcripts identified in the CS1 subtype using limma……..103

Table 3.31. Differentially expressed upregulated transcripts identified in the CS2 subtype using limma……..103

Table 3.32. Differentially expressed downregulated transcripts identified in the CS2 subtype using limma……..104

Table 3.33. Differentially expressed upregulated transcripts identified in the CS3 subtype using limma……..105

Table 3.34. Differentially expressed downregulated transcripts identified in the CS3 subtype using limma……..105

Table 3.35. Comparison of mutational frequency among 3 identified subtype of colon adenocarcinoma in TCGA-COAD cohort…….110

Table 3.36. Demo of comparison of fraction genome altered among 3 identified subtype of colon adenocarcinoma in TCGA-COAD cohort……...111

Table 3.37. Demo of comparison of TMB among 3 identified subtype of colon adenocarcinoma in TCGA-COAD cohort…….112

Table 3.38. IGP information in four validation cohorts of the PAM classifier trained on the TCGA-COAD cohort……...125

Table 3.39. Clinicopathologic characteristics of COAD participants in the CS1, CS2, CS3 and CS4……..158

Table 3.40. Differentially expressed upregulated transcripts identified in the CS1 subtype using edgeR……..160

Table 3.41. Differentially expressed downregulated transcripts identified in the CS1 subtype using edgeR……..161

Table 3.42. Differentially expressed upregulated transcripts identified in the CS2 subtype using edgeR……..161

Table 3.43. Differentially expressed downregulated transcripts identified in the CS2 subtype using edgeR……..162

Table 3.44. Differentially expressed upregulated transcripts identified in the CS3 subtype using edgeR……..162

Table 3.45. Differentially expressed downregulated transcripts identified in the CS3 subtype using edgeR……..163

Table 3.46. Differentially expressed upregulated transcripts identified in the CS4 subtype using edgeR……..163

Table 3.47. Differentially expressed downregulated transcripts identified in the CS4 subtype using edgeR……..164

Table 3.48. Differentially expressed upregulated transcripts identified in the CS1 subtype using DESeq2……...165

Table 3.49. Differentially expressed downregulated transcripts identified in the CS1 subtype using DESeq2……...166

Table 3.50. Differentially expressed upregulated transcripts identified in the CS2 subtype using DESeq2……...166

Table 3.51. Differentially expressed downregulated transcripts identified in the CS2 subtype using DESeq2……...167

Table 3.52. Differentially expressed upregulated transcripts identified in the CS3 subtype using DESeq2……...167

Table 3.53. Differentially expressed downregulated transcripts identified in the CS3 subtype using DESeq2……...168

Table 3.54. Differentially expressed upregulated transcripts identified in the CS4 subtype using DESeq2……...169

Table 3.55. Differentially expressed downregulated transcripts identified in the CS4 subtype using DESeq2……...169

Table 3.56. Differentially expressed upregulated transcripts identified in the CS1 subtype using limma……..170

Table 3.57. Differentially expressed downregulated transcripts identified in the CS1 subtype using limma……..171

Table 3.58. Differentially expressed upregulated transcripts identified in the CS2 subtype using limma……..171

Table 3.59. Differentially expressed downregulated transcripts identified in the CS2 subtype using limma……..172

Table 3.60. Differentially expressed upregulated transcripts identified in the CS3 subtype using limma……..172

Table 3.61. Differentially expressed downregulated transcripts identified in the CS3 subtype using limma……..173

Table 3.62. Differentially expressed upregulated transcripts identified in the CS4 subtype using limma……..174

Table 3.63. Differentially expressed downregulated transcripts identified in the CS4 subtype using limma……..174

Table 3.64. Comparison of mutational frequency among 4 identified subtype of colon adenocarcinoma in TCGA-COAD cohort…….181

Table 3.65. Demo of comparison of fraction genome altered among 4 identified subtype of colon adenocarcinoma in TCGA-COAD cohort……...182

Table 3.66. Demo of comparison of TMB among 4 identified subtype of colon adenocarcinoma in TCGA-COAD cohort…….183

Table 3.67. IGP information in four validation cohorts of the PAM classifier trained on the TCGA-COAD cohort……...198

Table A.1. The list of the top 100 upregulated DEGs identified in the CS1 subtype using edgeR as a result of two clustering analyzes……...253

Table A.2. The list of the top 100 downregulated DEGs identified in the CS1 subtype using edgeR as a result of two clustering analyzes……...255

Table A.3. The list of the top 100 upregulated DEGs identified in the CS2 subtype using edgeR as a result of two clustering analyzes……...258

Table A.4. The list of the top 100 downregulated DEGs identified in the CS2 subtype using edgeR as a result of two clustering analyzes……...260

Table A.5. The list of the top 100 upregulated DEGs identified in the CS1 subtype using DESeq2 as a result of two clustering analyzes……....263

Table A.6. The list of the top 100 downregulated DEGs identified in the CS1 subtype using DESeq2 as a result of two clustering analyzes……....265

Table A.7. The list of the top 100 upregulated DEGs identified in the CS2 subtype using DESeq2 as a result of two clustering analyzes……....268

Table A.8. The list of the top 100 downregulated DEGs identified in the CS2 subtype using DESeq2 as a result of two clustering analyzes……....271

Table A.9. The list of the top 100 upregulated DEGs identified in the CS1 subtype using limma as a result of two clustering analyzes…….....273

Table A.10. The list of the top 100 downregulated DEGs identified in the CS1 subtype using limma as a result of two clustering analyzes…….....276

Table A.11. The list of the top 100 upregulated DEGs identified in the CS2 subtype using limma as a result of two clustering analyzes……...278

Table A.12. The list of the top 100 downregulated DEGs identified in the CS2 subtype using limma as a result of two clustering analyzes…….....281

Table A.13. The list of the top 100 upregulated DEGs identified in the CS1 subtype using edgeR as a result of three clustering analyzes…….....283

Table A.14. The list of the top 100 downregulated DEGs identified in the CS1 subtype using edgeR as a result of three clustering analyzes…….....286

Table A.15. The list of the top 100 upregulated DEGs identified in the CS2 subtype using edgeR as a result of three clustering analyzes…….....288

Table A.16. The list of the top 100 downregulated DEGs identified in the CS2 subtype using edgeR as a result of three clustering analyzes…….....291

Table A.17. The list of the top 100 upregulated DEGs identified in the CS3 subtype using edgeR as a result of three clustering analyzes…….....294

Table A.18. The list of the top 100 downregulated DEGs identified in the CS3 subtype using edgeR as a result of three clustering analyzes…….....296

Table A.19. The list of the top 100 upregulated DEGs identified in the CS1 subtype using DESeq2 as a result of three clustering analyzes……..299

Table A.20. The list of the top 100 downregulated DEGs identified in the CS1 subtype using DESeq2 as a result of three clustering analyzes……..301

Table A.21. The list of the top 100 upregulated DEGs identified in the CS2 subtype using DESeq2 as a result of three clustering analyzes……..304

Table A.22. The list of the top 100 downregulated DEGs identified in the CS2 subtype using DESeq2 as a result of three clustering analyzes……..306

Table A.23. The list of the top 100 upregulated DEGs identified in the CS3 subtype using DESeq2 as a result of three clustering analyzes……..309

Table A.24. The list of the top 100 downregulated DEGs identified in the CS3 subtype using DESeq2 as a result of three clustering analyzes……..312

Table A.25. The list of the top 100 upregulated DEGs identified in the CS1 subtype using limma as a result of three clustering analyzes…….314

Table A.26. The list of the top 100 downregulated DEGs identified in the CS1 subtype using limma as a result of three clustering analyzes…….....317

Table A.27. The list of the top 100 upregulated DEGs identified in the CS2 subtype using limma as a result of three clustering analyzes…….....319

Table A.28. The list of the top 100 downregulated DEGs identified in the CS2 subtype using limma as a result of three clustering analyzes……...…..322

Table A.29. The list of the top 65 upregulated DEGs identified in the CS3 subtype using limma as a result of three clustering analyzes…….324

Table A.30. The list of the top 100 downregulated DEGs identified in the CS3 subtype using limma as a result of three clustering analyzes…….326

Table A.31. The list of the top 100 upregulated DEGs identified in the CS1 subtype using edgeR as a result of four clustering analyzes……...329

Table A.32. The list of the top 100 downregulated DEGs identified in the CS1 subtype using edgeR as a result of four clustering analyzes……...331

Table A.33. The list of the top 100 upregulated DEGs identified in the CS2 subtype using edgeR as a result of four clustering analyzes……..334

Table A.34. The list of the top 100 downregulated DEGs identified in the CS2 subtype using edgeR as a result of four clustering analyzes…….……..336

Table A.35. The list of the top 100 upregulated DEGs identified in the CS3 subtype using edgeR as a result of four clustering analyzes……...339

Table A.36. The list of the top 100 downregulated DEGs identified in the CS3 subtype using edgeR as a result of four clustering analyzes……...341

Table A.37. The list of the top 100 upregulated DEGs identified in the CS4 subtype using edgeR as a result of four clustering analyzes…….…..344

Table A.38. The list of the top 100 downregulated DEGs identified in the CS4 subtype using edgeR as a result of four clustering analyzes…….…..347

Table A.39. The list of the top 100 upregulated DEGs identified in the CS1 subtype using DESeq2 as a result of four clustering analyzes……....349

Table A.40. The list of the top 100 downregulated DEGs identified in the CS1 subtype using DESeq2 as a result of four clustering analyzes……352

Table A.41. The list of the top 100 upregulated DEGs identified in the CS2 subtype using DESeq2 as a result of four clustering analyzes……354

Table A.42. The list of the top 100 downregulated DEGs identified in the CS2 subtype using DESeq2 as a result of four clustering analyzes……357

Table A.43. The list of the top 100 upregulated DEGs identified in the CS3 subtype using DESeq2 as a result of four clustering analyzes……359

Table A.44. The list of the top 100 downregulated DEGs identified in the CS3 subtype using DESeq2 as a result of four clustering analyzes……362

Table A.45. The list of the top 100 upregulated DEGs identified in the CS4 subtype using DESeq2 as a result of four clustering analyzes……365

Table A.46. The list of the top 100 downregulated DEGs identified in the CS4 subtype using DESeq2 as a result of four clustering analyzes……....367

Table A.47. The list of the top 100 upregulated DEGs identified in the CS1 subtype using limma as a result of four clustering analyzes……..370

Table A.48. The list of the top 6 downregulated DEGs identified in the CS1 subtype using limma as a result of four clustering analyzes……...372

Table A.49. The list of the top 100 upregulated DEGs identified in the CS2 subtype using limma as a result of four clustering analyzes……...372

Table A.50. The list of the top 100 downregulated DEGs identified in the CS2 subtype using limma as a result of four clustering analyzes……..375

Table A.51. The list of the top 100 upregulated DEGs identified in the CS3 subtype using limma as a result of four clustering analyzes……...378

Table A.52. The list of the top 100 downregulated DEGs identified in the CS3 subtype using limma as a result of four clustering analyzes……...380

Table A.53. The list of the top 100 upregulated DEGs identified in the CS4 subtype using limma as a result of four clustering analyzes……...383

Table A.54. The list of the top 100 downregulated DEGs identified in the CS4 subtype using limma as a result of four clustering analyzes……...385

Table B.1. Response of all clustering results to chemotherapeutic drugs in p-value...388

INTRODUCTION

1.2. Colon Cancer

Colon cancer occurs as a result of polyps becoming arises from polyps that become cancerous over time, defined as abnormal cell growth in the inner lining of the colon, the second and longest part of the large intestine [1-3]. Colon cancer is one of the most common malignant tumours of the digestive system [4]. Adenocarcinoma of the colon (COAD), which accounts for 95% of all cases of colorectal cancer [5], is one of the most commonly diagnosed cancers in both sexes worldwide, but also one of the most deadly cancers [6]. While most colon cancers occur sporadically due to acquired somatic mutations and epigenetic factors, the rest develop due to hereditary factors [2, 4, 7-11]. Sporadic cases of colon cancer are individuals who have no family history of colon cancer and no genetic mutations that would trigger the development of colon cancer [2, 4, 12]. The great heterogeneity in colon cancer, which is the main reason why cases do not benefit sufficiently from treatment, is due to genetic and epigenetic factors such as chromosomal instability (CIN), microsatellite instability (MSI) and CpG island methylator phenotype (CIMP), which occur singly or simultaneously and cause inconsistency in the genome [13-15]. The fact that these factors leading to the development of colon cancer vary from person to person results in patients responding differently to the same treatment [16]. Risk factors for colon cancer also include age, ethnicity, lifestyle and dietary habits [2, 17].

1.2. Epidemiology

Colorectal cancer (CRC), a type of cancer that affects the colon or rectum, is the third most common cancer worldwide and the second leading cause of cancer-related deaths. The study conducted by the World Health Organisation (WHO) for 36 types of cancer in 185 countries shows that men with colorectal cancer are in third place for both incidence and mortality, while women are only in third place for mortality and second place for incidence (Figure 1.1) [18]. According to GLOBOCAN 2020 estimates, the estimated 1.15 million new cases of colorectal cancer worldwide in 2020 are expected to increase by 60 %, leading to 1.92 million new cases in 2040 [18, 19].

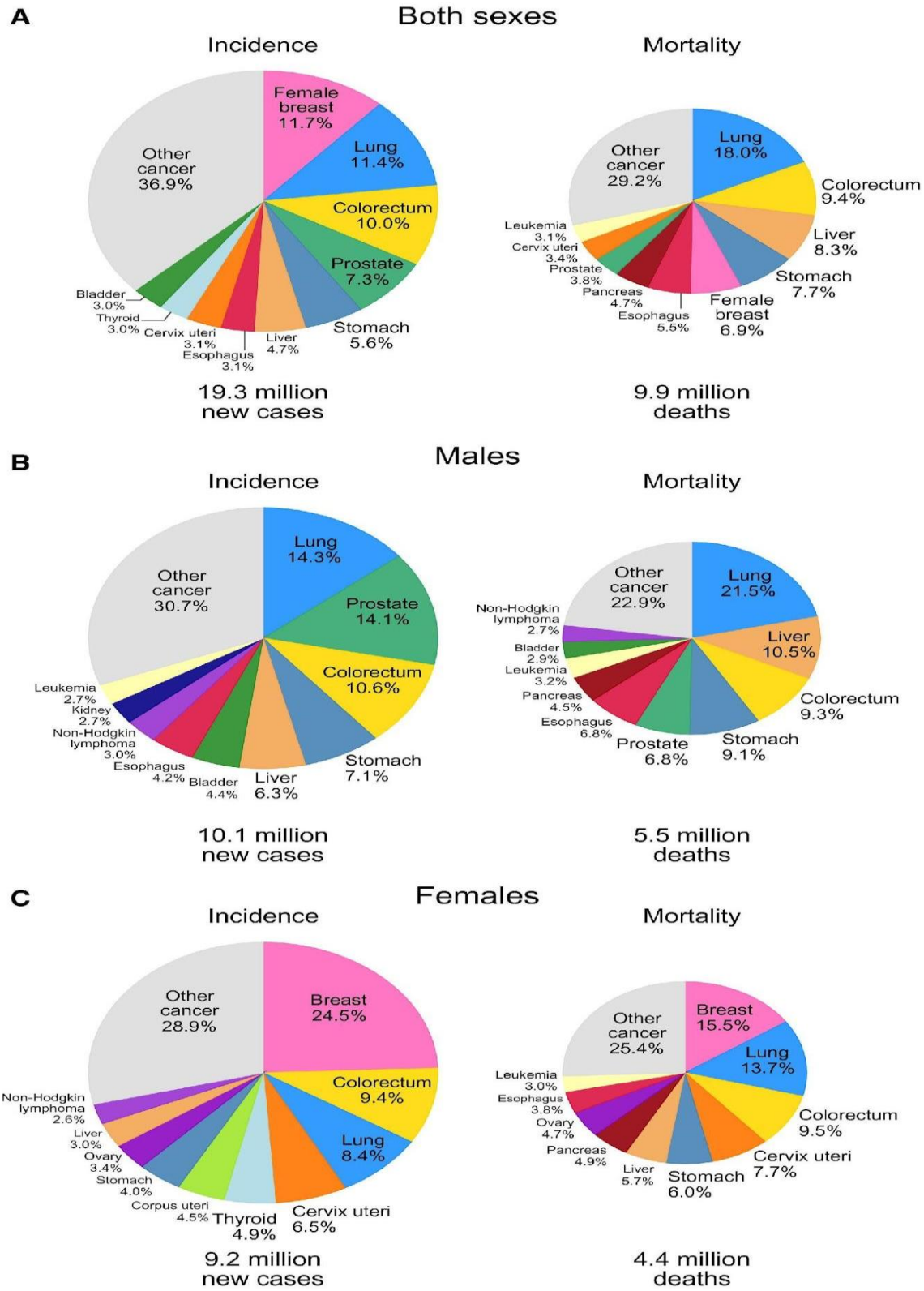


Figure 1.1. Distribution of Cases and Deaths for the Top 10 Most Common Cancers in 2020 for (A) Both Sexes, (B) Men, and (C) Women [18].

According to the American Cancer Society [20], approximately 106,970 new cases of colon cancer are expected to occur in the United States in 2023, with the majority of these cases occurring in people aged 65 years and older. On the other hand, 12,370 cases (12%) will occur in people under the age of 50 and just over a quarter will occur in people between the ages of 50 and 64. In addition, there will be an estimated 52,550 deaths from colorectal cancer in 2023, of which 3,750 (7%) will be under the age of 50. At this point, a separate classification of deaths from colon and rectal cancer would lead to an incorrect classification result, so they were analysed together.

Table 1.1. Estimated numbers of new invasive colorectal cancer cases and deaths by age, 2023, United States [20].

Age, years	Cases				Deaths			
	Colon				Colorectum			
	Male	Female	Total	Percent	Male	Female	Total	Percent
0-49	6410	5960	12,370	12%	2150	1,600	3750	7%
50-64	17,500	12,300	29,800	28%	8030	5130	13,160	25%
65+	30,510	34,290	64,800	61%	18,290	17,350	35,640	68%
Total	54,420	52,550	106,970	100%	28,470	24,080	52,550	100%

The incidence of colon cancer runs parallel to the Human Development Index (HDI) [19]. The incidence of colon cancer is significantly higher in countries with a high HDI than in countries with a low HDI. The GLOBOCAN 2020 statistics provide age-standardised incidence rates of colon cancer for men and women in different regions of the world. According to the statistics, colon cancer incidence rates for men vary between 25.3 and 2.9 with an 8-fold difference per 100,000 when comparing Southern Europe and Middle Africa, while for women they vary between 20.0 and 2.2 with an approximately 9-fold difference when comparing Australia/New Zealand and South and Central Asia [18]. In addition, shown in Figure 1.2, the mortality rate from colon cancer varies according to a country's level of development, although to a lesser extent than the difference in incidence rates between low and high HDI countries [21]. In a study by Arnold et al., the relationship between the HDI and colorectal cancer incidence and mortality was analysed in three different categories. The first category consists of countries with medium HDI, and the countries in this category have experienced an increase in CRC incidence and mortality. While the reason for the increase in incidence in these countries could be that they are in a period of economic transition, the main reason for the increase in mortality

could be that they are still exposed to high risk factors and have limited improved treatment options. In the second category, which mainly includes countries with a high HDI, such as Canada, the UK, Denmark and Singapore, incidence has increased but mortality has decreased due to improved treatment options. Finally, in countries in the third highest HDI category, such as the United States, Iceland, Japan and France, both incidence and mortality have decreased due to improved screening, control of risk factors and improved treatment options [22]. In addition, Arnold et al. also analysed the changes in CRC incidence and mortality in men and women in these regions over the last 10 years in their relevant study (Figure 1.2). The largest statistically significant increase in the number of CRC cases in men was recorded in Costa Rica and Bulgaria, which are in the first category, at 3.6 %. In addition, the largest increase in CRC cases in women was found in Brazil with 4.8%, followed by Colombia and Bulgaria with 2.7%. Moreover, the incidence of CRC in both sexes has decreased the most in America. On the other hand, it was reported that the highest mortality rate for both sexes was in the Philippines, although it was higher for women. The lowest mortality rate was found in the Czech Republic with a decrease of 4.6% in men and 4.2% in women [22].

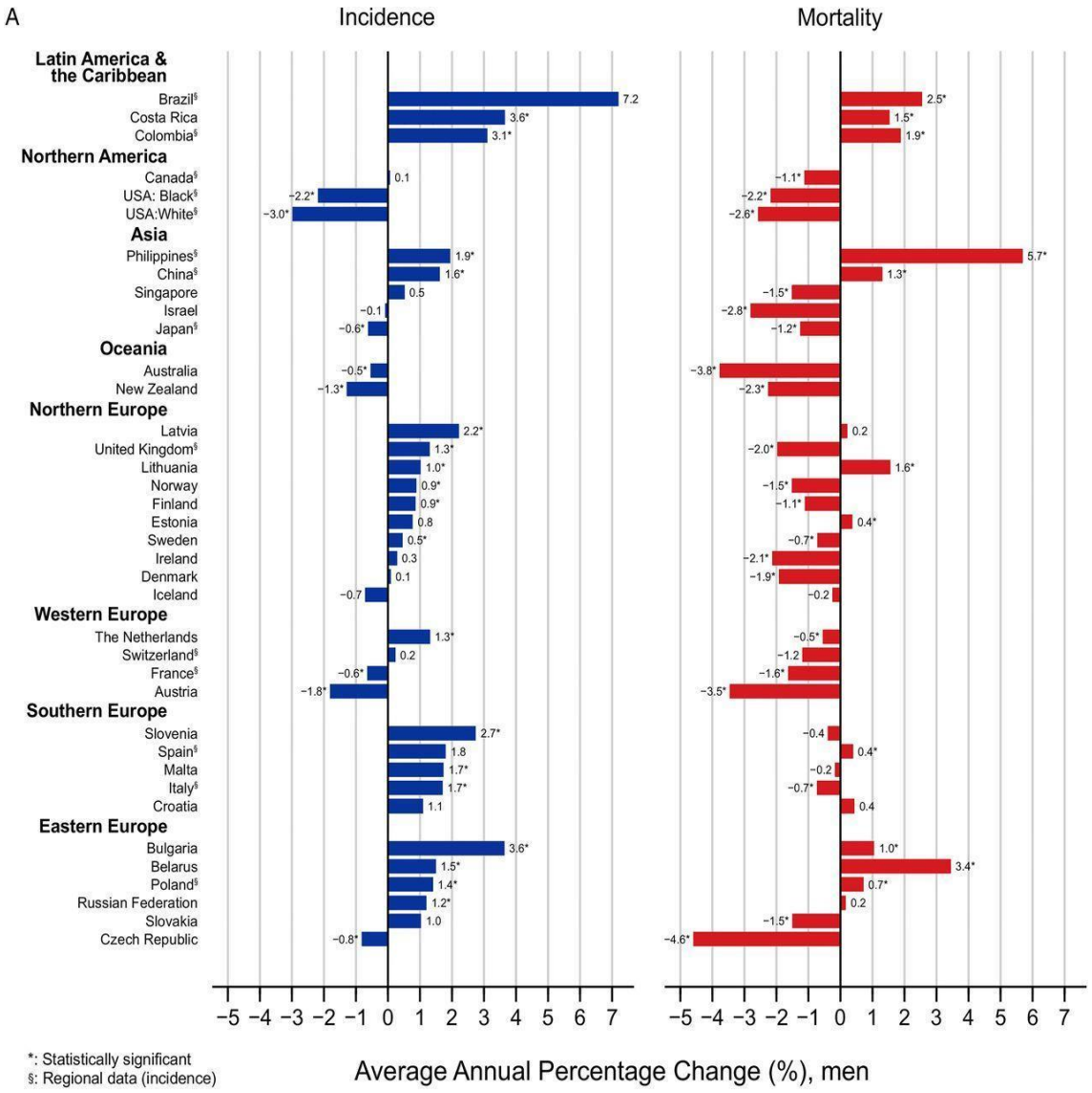


Figure 1.2. **(A)** Average annual percentage change (AAPC) of colorectal cancer incidence and mortality in the most recent period (10 years), males [22].

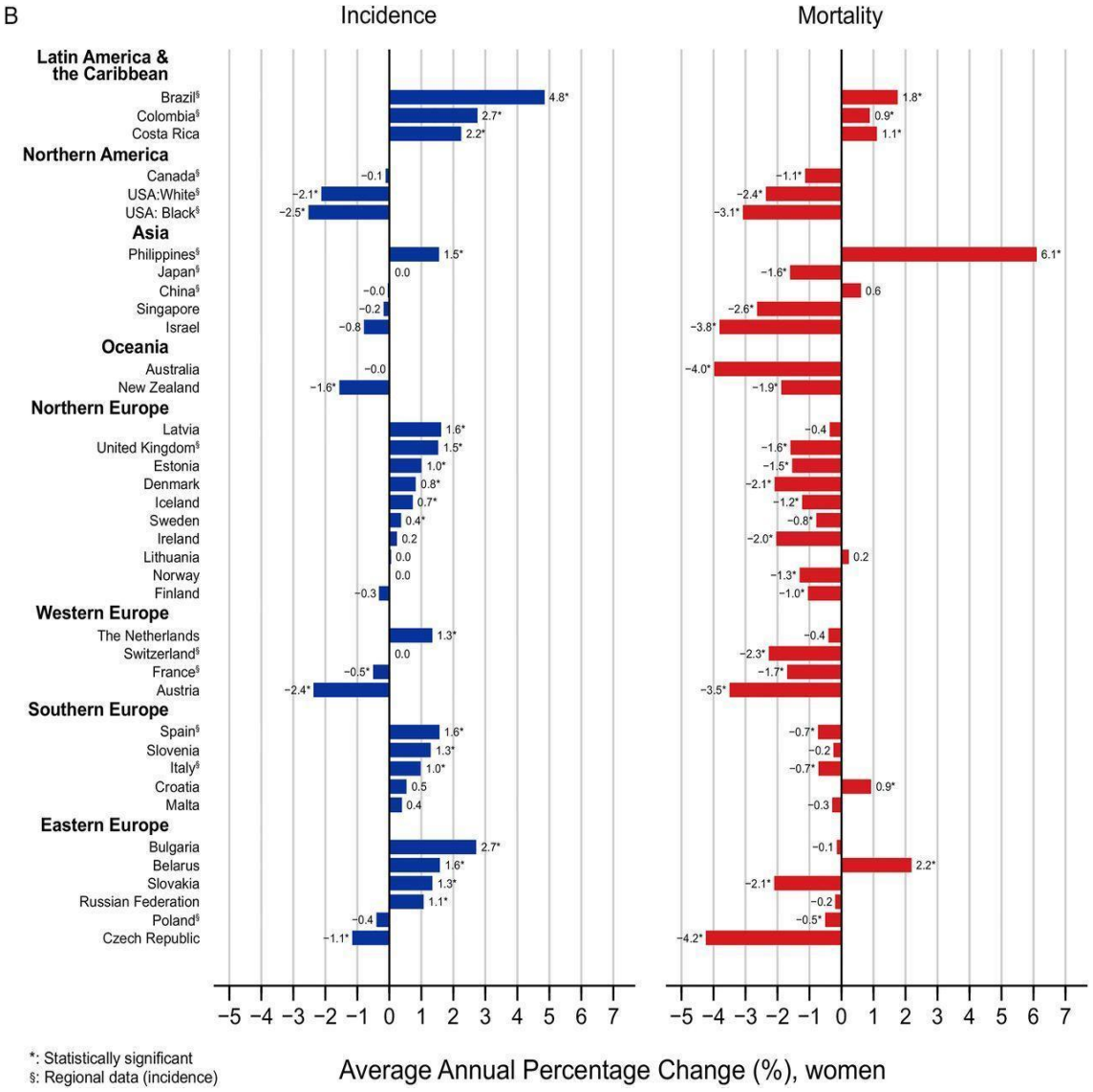


Figure 1.2 (continued). (B) AAPC of colorectal cancer incidence and mortality in the most recent period (10 years), females [22].

1.3. Treatment

Current treatment options for colon cancer include surgery and chemotherapy [23, 24]. The choice of treatment depends on various factors, such as tumour size and stage [3, 23, 24]. For early-stage colorectal cancer in particular, the tumour is removed by surgical resection, while for advanced-stage patients, chemotherapy with chemotherapeutic agents is used to shrink the tumour and prevent metastasis [23, 25, 26]. In addition, neoadjuvant chemotherapy is used to support surgery by shrinking the tumour before surgery, and adjuvant chemotherapy is used to prevent recurrence and stabilise tumour size after surgery [23, 25, 27, 28]. However, these treatment options have some limitations.

Surgical resection carries the risk of metastasis due to mechanical disruption of tumour integrity during surgery [24, 29]. The limitations of chemotherapy primarily include the short- and long-term toxicities to which patients are exposed from chemotherapeutic agents and the low tumour-specific selectivity [25, 27]. In addition, due to the high heterogeneity and complex molecular structure of COAD, an adequate response cannot be achieved with this treatment. Factors limiting the efficacy of treatment also include the high cost and invasiveness of the treatments. However, the main reason why colon cancer patients do not respond adequately to these traditional treatments is that these treatments are not sensitive enough [16]. Therefore, it is an undeniable fact that there is a great need for treatment strategies that better customise treatment options for colon cancer by taking into account patient-specific genetic and epigenetic factors.

1.4. Personalized Treatment

The effectiveness of conventional treatments is largely limited due to the highly heterogeneous nature of COAD in each patient [30]. Therefore, there is a great need for the development of personalised treatment strategies that take into account the patient's genetic and epigenetic factors and are tailored to the needs of each individual patient. Personalised treatment can be defined as the development of the best treatment strategies for each individual, taking into account the unique biological characteristics of each disease [13, 16, 30]. With its unique strategies for each patient, personalised medicine follows a more precise and faster path in the prevention and treatment of diseases than conventional methods, which can also avoid unnecessary interventions [30].

Omics technologies, which look at complex systems from a holistic perspective, produce large amounts of data [31] that allow the cell, the molecules and the organism to be analysed in a comprehensive and detailed manner [32]. At this point, the systems biology approach, which looks at biological systems such as genomics, epigenomics, transcriptomics, proteomics and metabolomics from a holistic perspective, examines the interactions of these biological systems and the effects of these interactions on the systems [33, 34]. This enables a detailed investigation at all levels, from the cell to the organism. The basic logic of the systems biology approach is to combine large amounts of data and reduce them to different omics levels such as the genomic, epigenomic and transcriptomic levels [34, 35]. Systems biology strategies enable a profound understanding of the

underlying disease mechanisms and fundamental biological processes. They provide new diagnostic, prognostic and therapeutic biomarkers and also enable the development of new treatment strategies [34, 36]. The complex nature of colon cancer is based on the interaction of several biological levels. Therefore, limiting the scope of studies conducted to understand the mechanisms of this disease and to improve the diagnosis and treatment process to a single omics level will ignore the relationships between the different molecular levels and thus provide only a limited perspective on the biological mechanism of the disease [36]. On the other hand, the systems biology approach allows the effective integration of multi-omics data obtained from different omics technologies that have complementary roles in the realisation of a particular biological function. This allows analysing the underlying mechanisms of the disease from a holistic perspective [34, 37].

1.5. Scope of COAD Omic Studies

The relationship between a patient's genotype and the phenotype of colon cancer is not based on a simple one-to-one correlation. Rather, the phenotype interacts with the genotype at many biological levels in complex ways [38]. Examination of omics studies on colon cancer reveals that the scope of these studies is generally limited to a single omics level [39-43]. However, in contrast to studies relying on single omics data analysis [44], studies integratively analysing multi-omics datasets provide a more comprehensive perspective on the nature of colorectal cancer and allow a better understanding of the disease process [36, 45]. The number of studies on multi-microbial analysis of colon cancer is quite small, and these studies usually refer to two different omic levels [46, 47] or, much less frequently, to three different omics levels [48, 49]. The shortcomings of these studies also include the fact that they used only a few integrative multi-omics algorithms to classify patients into homogeneous subtypes and did not validate their resulting subtypes in an external cohort.

The main reason why the number of comprehensive multi-omics studies on colorectal cancer is so low is the difficulty of data integration [32, 36, 45]. The concatenation-based integration method is based on the idea of obtaining a large data matrix by combining the matrices of the individual omics data before building the model. One of the biggest advantages of this method is that it facilitates the use of various machine learning algorithms that can find any relationship between the features of combined multi-omics data to analyse continuous or discrete data [45]. There are a variety of algorithms for

integrative clustering of multi-omics data written in different programming languages [50]. However, these algorithms often only examine subtypes based on differences in prediction rather than characterising them systematically. Furthermore, the lack of combined inputs and outputs of different algorithms makes it difficult to combine downstream analyses that allow in-depth characterisation of the subtypes. When investigating different R packages that combine the format of inputs and outputs (CancerSubtypes and CEPICS), it was found that they integrate few algorithms for the integration of multi-automated data, do not provide functions for the systematic analysis of subtypes and do not include somatic mutations, which play a key role in cancer heterogeneity, in the analysis [51, 52]. In addition, there are few pipelines that provide functionality to identify subtype-specific biomarkers and validate these subtypes identified in the discovery dataset in an external cohort to test the consistency and reproducibility of the subtypes [53].

On the other hand, the MOVICS R package [53], an integrated pipeline that provides a unified interface for 10 state-of-the-art multi-omic clustering algorithms (CIMLR [54], iClusterBayes [55], MoCluster [56], COCA [57], ConsensusClustering [58], IntNMF [59], LRAcluster [60], NEMO [61], PINSPlus [62], and SNF [63]), was published by Xu et al. in 2017. MOVICS encompasses the most commonly used downstream analyses in cancer subtyping research, including characterisation and comparison of identified subtypes from different angles (e.g. prognosis, somatic mutation, fractional genome alteration proportion, drug susceptibility, matching of partitions) and verification of subtypes in external cohorts using two model-free approaches for multiclass prediction.

As a result of literature searches, it appears that there is a great need to perform comprehensive integrative multi-omics analyzes for colon cancer, which will shed light on the tumorigenesis process and enable the evaluation of the most appropriate personalized treatment strategies.

1.6. The Scope of This Study

In this dissertation, a comprehensive molecular characterisation analysis of colon adenocarcinoma was performed, accompanied by integrative multi-omic analyses, providing detailed information on the heterogeneity of the cancer and a comprehensive overview of the COAD tumourigenesis process to select the most sensitive and

appropriate treatment strategies in the diagnosis and treatment process. In this dissertation study, COAD was systematically categorised into 2 to 5 separate subclasses by creating consensus clusters based on multi-omic data and 10 integrative clustering algorithms using the "R package "MOVICS" for various reasons. In addition, personalised treatment options were evaluated by examining the defined subtypes with respect to various parameters. To obtain a robust clustering result, in addition to the analyses in the discovery cohort, subtyping analyses were also performed in the validation cohort and the results of both analyses were evaluated for consistency and reproducibility. In this analysis, full transcriptome expression (messenger RNA (mRNA), long non-coding RNA (lncRNA), microRNA (miRNA)) in The Cancer Genome Atlas (TCGA) database, Illumina 450K DNA methylation, somatic mutation and copy number alteration (CNA) data, and clinicopathological data from COAD patients were used to determine specific molecular characteristics and facilitate the use of precision medicine in patients. In addition, validation datasets were obtained from the Gene Expression Omnibus (GEO) cohort containing mRNA expression data and clinical information from COAD patients. After the COAD patients in this study were classified into corresponding subtypes with high robustness, molecular biomarkers and functional signalling pathways specific to the defined subtypes were identified and each subtype was evaluated with different analyses such as mutation frequencies or sensitivities to chemotherapeutic agents.

In this study, a comprehensive molecular characterisation analysis of colon cancer was performed using the consensus clustering method based on multi-omic data and integrative clustering algorithms. By classifying the multimicrobial data of COAD patients with different integrative clustering algorithms, more correlative evidence of the biological mechanisms of the disease could be obtained, allowing a deeper understanding of complex biological processes. In this study, COAD-specific molecular subtypes were systematically and comprehensively defined, biomarkers specific to each subtype were identified, and personalised treatment options for COAD patients were evaluated based on analyses of immune response and sensitivity to chemotherapeutic agents specific to each subtype. This study ultimately performed a comprehensive molecular characterisation analysis of COAD using multi-omic data and integrative clustering algorithms for personalised treatment applications that allow for more accurate diagnosis and treatment based on each patient's unique genetic structure.

To our knowledge, this study was the first to evaluate COAD based on multi-omic data (genomic, epigenomic and transcriptomic) and 10 integrative multi-clustering algorithms and to perform a comprehensive characterisation of the identified subtypes and validation analyses of the obtained results. All results of this comprehensive molecular characterisation analysis will shed light on future studies on COAD and enable the further development of new precise treatment options for COAD patients. In addition, the striking molecular features of the individual subtypes will provide promising insights for drug repurposing studies or the development of new drugs.

2. MATERIALS AND METHODS

2.1. Multi-Omics Data Extraction From COAD Discovery Cohort

COAD cases (n=461) containing full-length transcriptome expression (mRNA, lncRNA, miRNA), somatic mutation, copy number alteration, DNA methylation and clinicopathological information of the TCGA-COAD cohort were downloaded from the TCGA database using the R package "TCGAbiolinks" [64]. miRNA expression data were renamed to filter out mature miRNAs by using the package “miRNAmeConverter” [65] in R with miRbase 21.0. Fragments per kilobase of transcript per million mapped reads (FPKM) and transcripts per kilobase million (TPM) expression data for mRNA, lncRNA and miRNA were first log2-transformed. After comparing the gene expression, methylation, mutation and copy number variation data as well as the clinical data of 461 COAD patients, the multi-omics data of 297 patients were finally included in the follow-up analysis.

2.2. External Validation Cohorts

To confirm the findings of the discovery cohort, the mRNA expression matrix and clinical information were obtained from four external Gene Expression Omnibus (GEO) cohorts, including GSE39582 [66], GSE16125 [67], GSE17536 and GSE17537 [68]. GSE39582 contains mRNA expression profiles and clinicopathological information of 562 primary colorectal adenocarcinoma tumour samples from patients of the French Ligue Nationale Contre le Cancer. GSE17536 contains gene expression data and clinical information from 177 colon cancer patients from the Moffitt Cancer Center. GSE17537 contained gene expression profiles and clinical information from 55 colorectal cancer patients from the Vanderbilt Medical Center (VMC). GSE16125 contained gene expression data from 36 microsatellite-stable sporadic colon cancer patients characterised by adenomatous polyposis coli (APC), tumour protein p53 (TP53) and Kirsten-Ratten sarcoma (KRAS) mutations. Affymetrix Human Genome U133 Plus 2.0 Array was used for GSE39582, GSE17536 and GSE17537, while Affymetrix Human Exon 1.0 ST Array [transcript (gene) version] was used for GSE16125.

Table 2.1. The GEO datasets employed in the present study.

Dataset ID	Number of samples	Platform
GSE39582	562	Affymetrix Human Genome U133 Plus 2.0 Array
GSE17536	177	Affymetrix Human Genome U133 Plus 2.0 Array
GSE17537	55	Affymetrix Human Genome U133 Plus 2.0 Array
GSE16125	36	Affymetrix Human Exon 1.0 ST Array [transcript (gene) version]

2.3. Identification of Molecular Subtypes by Integrative Analysis

The R package "MOVICS" [53] was used to identify subtypes of COAD patients based on mRNA expression, lncRNA expression, miRNA expression, DNA methylation and somatic mutation data. The data size was reduced using five filtering methods to filter out features that fulfil some stringent requirements. The filtering methods offered by MOVICS are "mad" for median absolute deviation, "sd" for standard deviation, "pca" for principal components analysis, "cox" for univariate cox proportional hazards regression and "freq" for binary omics data. At this stage, it is also possible to remove "NA" values directly or assign them to k nearest neighbours using the Euclidean metric. The transcriptome data from the TCGA-COAD dataset was pre-processed to identify the top 2000 mRNAs, 2000 lncRNAs and 800 miRNAs with high variation based on "mad". The top 1343 DNA CpG methylation sites were then selected by filtering out DNA methylation CpG sites with a P-value < 0.05 and analysed by univariate Cox regression. Finally, genes with a mutation frequency above 10%, selected by the "freq" method, were determined as mutated genes. Cluster Prediction Index (CPI) [59] and gap statistic analysis [69] based on multi-omics data were evaluated to find the appropriate number of subtypes. Ten clustering algorithms were then used to categorise the patients into different subtypes. Finally, the combined classification was determined by consensus ensembles and the subtypes were identified with high robustness. The similarity of samples between subtypes was quantified using the silhouette score.

Table 2.2. Data extracted for multi-omics data integration.

Data Type	Raw Data Size	Data Size After Pre-processing	Filtering Method
mRNA	19962	19463	2000 - mad
lncRNA	16901	16193	2000 - mad
miRNA	1881	847	800 - mad
Methylation	485577	24944	1343 - cox
Mutation	17753	17034	- freq

2.4. Pathway Enrichment Analysis

Using normalised expression data (TPM), subtype-specific upregulated and downregulated genes were calculated by setting both the nominal and the adjusted P-value <0.05 as the significance threshold and using the "edgeR" [70, 71], "DESeq2" [72], and "limma" [73] packages in R. Additionally, the filtering parameters are set to: |log 2 fold change (log2 FC)| > 1. Gene Ontology (GO) terms of each patient were annotated in R using Single Sample Gene Set Enrichment Analysis (ssGSEA) [74] using the “GSVA” package [75]. The nominal and adjusted P-value set as the significance threshold for the enrichment score (ES) for a single gene set is < 0.05. Gene sets of GO biological processes, oncogenic signatures and immunological signatures [76] were downloaded from the Molecular Signatures Database [77]. The specific signalling pathways of one subtype differed significantly from those of other subtypes. The mean enrichment score for each subtype was used for visualisation with a heat map. The enrichment score of each sample in each subtype was then calculated by gene set variation analysis based on a gene list of cancer hallmarks [78] from the Molecular Signatures Database (MsigDB).

2.5. Characteristics of Genetic Alterations Among Subtypes

The somatic copy number alteration (SCNA) data were downloaded from TCGA. The fraction of genome alterations (FGA) [79, 80], which expresses the percentage of the genome affected by copy number gains or losses, was calculated.

Subsequently, the “Maftools” package [81] was used to calculate the differences in mutation frequencies between the individual samples, mutations with significant differences ($p < 0.05$) were identified and an overall map of the mutational landscape was

generated using oncoprint. In addition, the number of non-synonymous mutations per million bases was also calculated to assess the tumour mutation burden (TMB).

2.6. Chemotherapeutic Response Prediction

The response to chemotherapy was estimated for each sample based on the Genomics of Drug Sensitivity in Cancer (GDSC) database [82]. Accordingly, the widely used 249 chemotherapeutic agents offered by the MOVICS package were included in the analysis. Responses to these drugs were compared by estimating the half-maximal inhibitory concentration (IC50) values of the samples by ridge regression. A lower IC50 indicates a higher sensitivity to the drug.

2.7. Validation of External Cohorts

For the prediction of subtypes in validation cohorts, we used Nearest Template Prediction (NTP) [83], which can be used flexibly for cross-platform, cross-species and cross-class predictions without optimising the analysis parameters. In addition to NTP, another model-independent approach is used to predict subspecies. A partition around medoids (PAM) classifier is first trained in the discovery cohort to predict the subtype for patients in the external validation cohort. Each sample in the validation cohort is assigned a subtype label with the highest Pearson correlation with the central sample [84]. Next, an in-group proportion (IGP) statistic is performed to assess the similarity and reproducibility of the identified subtypes between the discovery and validation cohorts [85]. Finally, the kappa statistic is used to find out how consistent the different prediction results are.

3. RESULTS AND DISCUSSION

Current treatment strategies based on the "one-drug-fits-all" model for colon cancer do not provide sufficient benefit because each patient has a different genetic signature [86]. In-depth characterisation of the molecular nature of the disease for each patient plays a key role in deciding the treatment process. Therefore, identifying and thoroughly characterising the molecular subtype of tumours in each patient is clinically important [87]. At this point, subtyping analysis performed at the system level, rather than molecular subtyping based on a single mutation-centered perspective, will provide a more detailed and reliable result [87]. Estimating the appropriate number of clusters is the most important step in subtyping, i.e. cluster analysis [88]. The most important parameters to consider when choosing the optimal number of clusters are that it should be small enough to reduce noise but large enough to retain important information [53].

In this thesis study, a comprehensive molecular characterisation analysis of adenocarcinomas of the colon (COAD) was performed, accompanied by integrative multi-omics analyses. In this study, 297 samples were included in the further analysis after comparison of the multi-omics data. COAD was systematically categorised into subclasses by creating consensus clusters based on multi-omics data and 10 integrative clustering algorithms using the “R package "MOVICS". At this point, CPI and gap statistics, which are the best methods, were used to determine the optimal number of k clusters. The CPI, which is calculated as the average of the adjusted rand indices, and the gap statistic, which compares the change in distribution within clusters with the change expected under an appropriate reference null distribution, estimates the optimal number of clusters with the best precision while preserving important information. The larger the value of the CPI and gap statistics, the better the cluster effect. As a result of this analysis, the k2 cluster number at which the sum of the two statistics reaches the maximum is considered arbitrarily optimal (Figure 3.1). Therefore, performing future analyses based on the optimal k2 result may yield promising results.

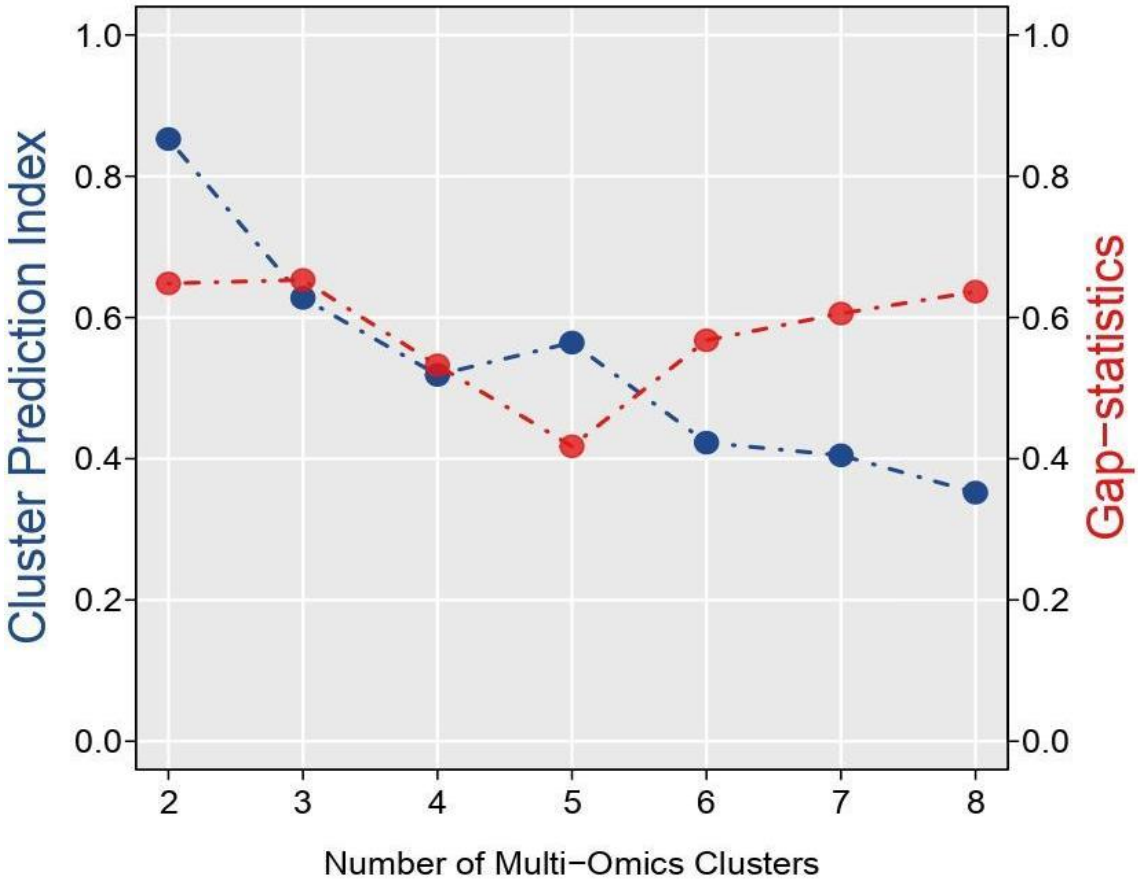


Figure 3.1. Identification of optimal cluster number in TCGA-COAD cohort.

However, the choice of this k2 value is not absolutely necessary to determine the number of clusters. When determining the optimal number of clusters, information already available on the molecular subtypes of the cancer type in question can also be used, as well as information on new molecular subtypes that are considered potentially promising. However, when determining the number of clusters based on different references, it is important to choose the k value at which the values of the CPI and gap statistics do not drop too much.

In addition to using the k2 value, which was determined to be the optimal number of clusters in this study, clusters 3, 4 and 5, which are thought to contain promising results, were also included and characterised separately in the analysis. Each defined subtype was analysed with respect to different parameters and personalised treatment options were evaluated. To obtain a robust clustering result, in addition to the analyses in the discovery cohort, subtyping analyses were also performed in the validation cohort and the results of

both analyses were assessed for consistency and reproducibility. In the following, the characterisation results of each cluster analysis are examined under separate headings.

3.1. Analysis Results for Two Subtypes

3.1.1. The multi-omics classification of COAD

Cluster analysis, an approach based on grouping similar data, increases intra-cluster similarity by grouping patients with similar characteristics into the same subtype while reducing inter-cluster similarity [89]. This allows a more accurate and precise diagnosis and treatment regimen to be determined for each subtype. Based on the results of CPI and gap statistics to estimate the optimal number of clusters, the number of clusters was determined as k2. The clustering results were then determined by running each of the 10 clustering algorithms in turn. To improve the robustness of the clustering, the clustering results of the different algorithms were combined based on consensus ensembles [90]. Consensus ensembles are based on obtaining a single clustering by combining multiple clustering results obtained from different algorithms for a given dataset [89]. In this way, a more accurate and robust result is obtained by overcoming the shortcomings of approaches based on a single algorithm that cannot capture some important structures in the data. In this approach, an M(t)n×n matrix is first calculated for each algorithm, where t is the number of algorithms and n is the number of samples. While M(t)ij=1 indicates that two different samples (sample i and j) are clustered in the same subtype, M(t)ij=0 reflects the opposite situation. Then, considering the strengths and similarities of the specified algorithms, a consensus matrix is created that summarises the similarity between pairs of data points in all clustering results. This consensus matrix represents a robust pairwise similarity for samples as it takes into account the strengths and similarities of the different integrative multi-omic clustering algorithms [91]. In short, the consensus matrix indicates how often samples of the same subtype can be clustered together by different multi-omics clustering methods [53]. A final stable clustering result is then obtained by applying the hierarchical clustering algorithm to the consensus matrix. Finally, a consensus heatmap is created, which should show a smooth diagonal rectangle (Figure 3.2). Ultimately, the patients were categorised into two subtypes: CS1 and CS2.

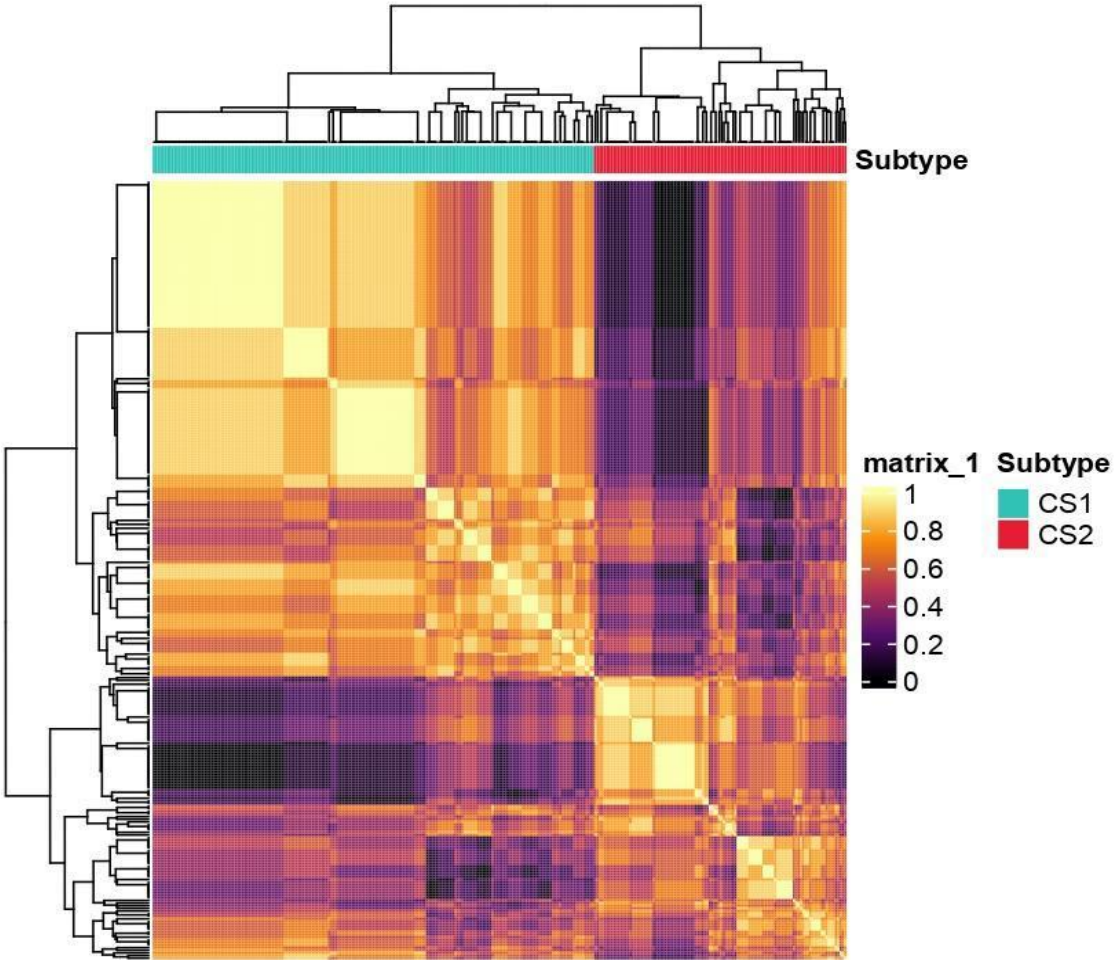


Figure 3.2. Consensus heatmap based on results from 10 multi-omics integrative clustering algorithms with number of clusters of 2.

In addition, the similarity of the samples was measured by the silhouette width to verify the clustering result (Figure 3.3) [92]. The silhouette width is a measure of how similar an object is to its own cluster (cohesion) compared to other clusters (separation). The value of the silhouette width ranges from -1, which means that the clusters are mismatched, to 1, which means that the clusters are quite clearly separated from each other. If the silhouette width is 0, this may mean that different clusters overlap [93]. The results showed that these subtypes were well differentiated and distinguishable from each other with silhouette widthes of 0.39 and 0.58, respectively.

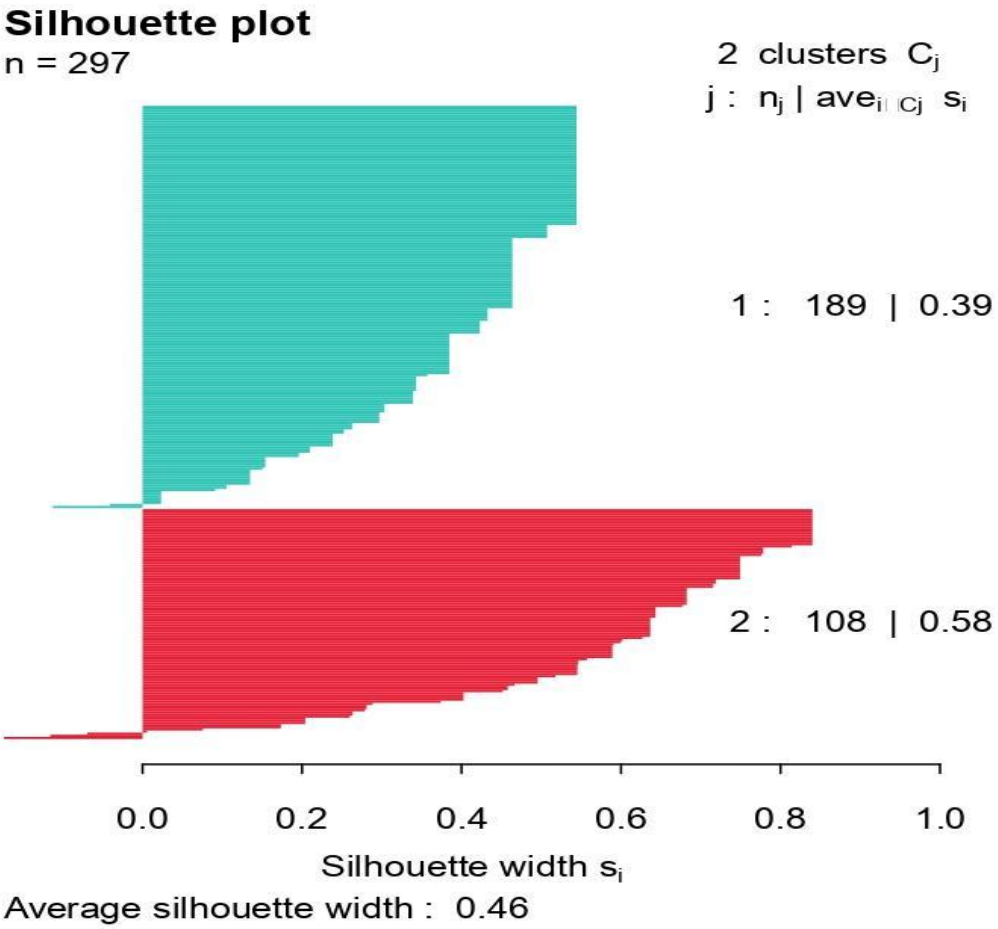


Figure 3.3. Quantification of sample similarity using Silhoutte width based on consensus ensembles result.

A genome-wide heatmap was then created based on the mRNA, lncRNA, miRNA, methylation and mutation data (Figure 3.4). This heatmap provides information on how the samples/genes are clustered for each omic, but also provides information on possible sample biases and other artefacts. In addition, the top 10 features for each omics data were selected using the iClusterBayes algorithm, which enables feature selection. The selected features may have a specific biological meaning that determines the heterogeneity of cancers. This heatmap includes clinicopathological features such as age, stage, race and gender as well as information on APC mutations. As a result, it can be said that each subtype is clearly differentiated on the basis of the mRNA heatmap. In addition, a relatively pronounced hypermethylated region was observed in the CS2 subtype, and the CS2 subtype is more strongly mutated than CS1.

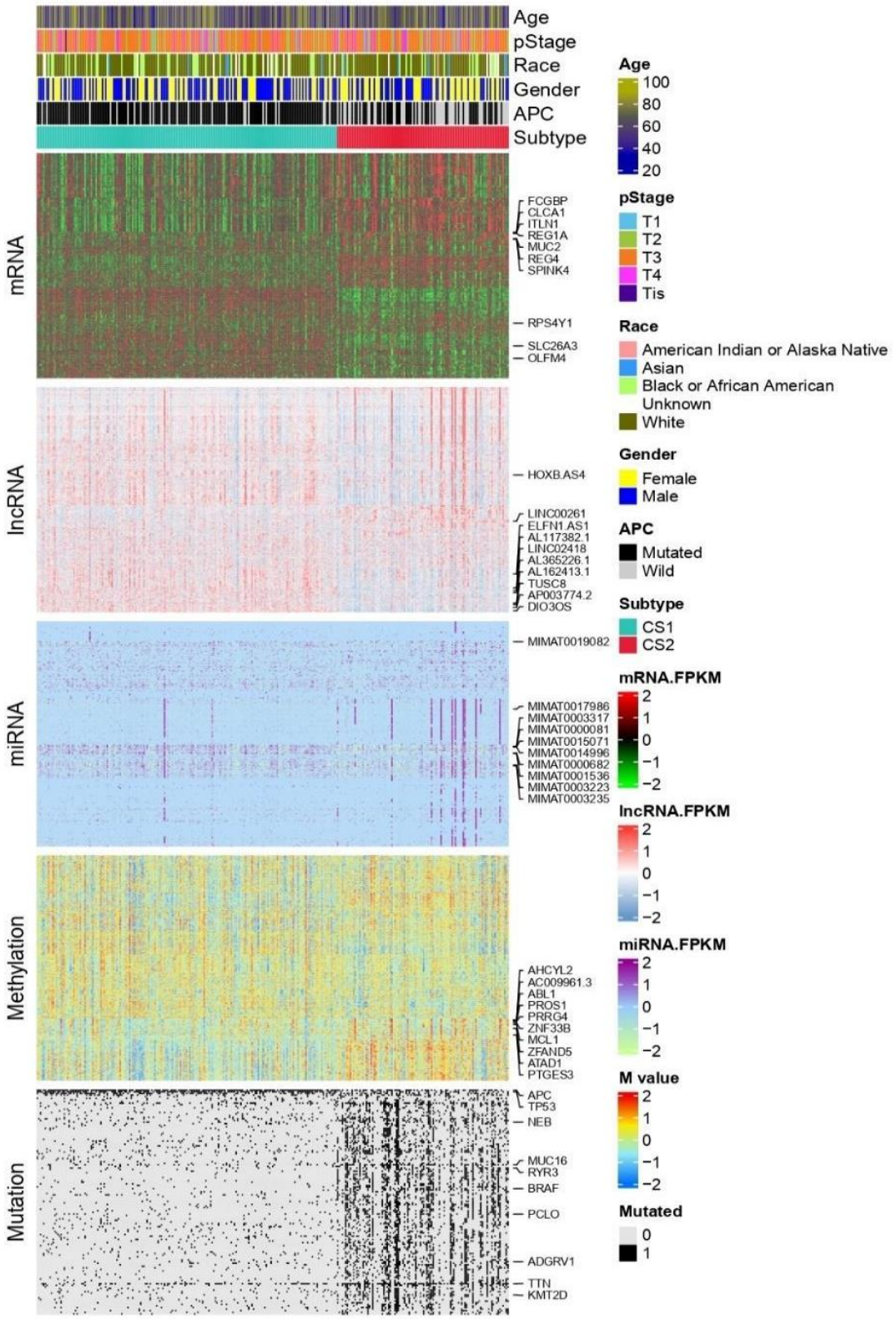


Figure 3.4. Comprehensive heatmap based on consensus across 10 algorithms with clinicopathological and potential drivers' annotation.

3.1.2. Differentially expressed genes and signaling pathways

DEGs, defined as differentially expressed genes obtained as a result of differential gene expression analysis to study differences in the abundance of gene transcripts within a transcriptome, are used to obtain mechanistic information about diseases and also serve as clinical biomarkers for early diagnosis [94, 95]. The identification of diagnostic and prognostic biomarkers not only provides insight into the occurrence and development of the disease, but also paves the way for early diagnosis and effective treatment [95, 96]. To further investigate the characteristics of subtypes, DEGs between subtypes were identified using the "edgeR", "DESeq2" and "limma" packages, which are among the most effective tools for differential expression analysis. Although the three protocols of limma, DESeq2 and edgeR are generally similar, there are some differences between the analysis methods [97]. In limma, a linear model is used for the statistics [73], while in edgeR [70, 71] and DESeq2 [72] a negative binomial distribution is used. Furthermore, edgeR and DESeq2 are preferred for RNA-Seq count data, while limma is used for microarray and normalised expression data. According to the results of edgeR, DESeq2 and limma, upregulated biomarkers were selected with the parameters threshold, adjusted P-value < 0.05 and Fold Change (FC) > 2, while downregulated biomarkers were determined with the filters adjusted P-value < 0.05 and fold change < 0.5.

UsingWith edgeR, 1168 and 11999 upregulated biomarkers were identified for CS1 and CS2, respectively. Tables 3.1-3.4 show the top 20 up- most upregulated and down-regulateddownregulated transcripts identified in with edgeR for the CS1 and CS2 subtype using edgeRsubtypes and sorted by FC. All other DEGs detected in the differential expression analysis with edgeR are listed in Appendix A.1. Overexpression of protein O-fucosyltransferase 1 (POFUT1), one of the significantly upregulated DEGs in CS1, can promote the metastatic process of colon cancer by activating the NOTCH signalling pathway [98]. On the other hand, downregulation of this gene in CS2 inhibits tumour growth by inhibiting cell proliferation and triggering apoptosis [99].

Table 3.1. Differentially expressed upregulated transcripts identified in the CS1 subtype using edgeR.

CS1 – Differentially Expressed Up-Regulated Transcripts

	fc	log2fc	pvalue	padj
WIF1	$5.04x10^{1}$	$5.65x10^{0}$	4.68x10-30	$9.46x10^{-28}$
BX322234.2	$4.61x10^{1}$	$5.53x10^{0}$	$1.63x10^{-7}$	$9.53x10^{-7}$
RNA5.8SP5	$3.90x10^{1}$	$5.28x10^{0}$	$2.00x10^{-3}$	$5.35x10^{-3}$
AC152010.1	$3.73x10^{1}$	$5.22x10^{0}$	$5.40x10^{-3}$	$1.27x10^{-2}$
ORM1	$3.02x10^{1}$	$4.92x10^{0}$	$2.02x10^{-18}$	$6.97x10^{-17}$
RNA5SP267	$2.79x10^{1}$	$4.80x10^{0}$	$1.83x10^{-2}$	$3.66x10^{-2}$
RNA5SP211	$2.77x10^{1}$	$4.79x10^{0}$	$2.21x10^{-2}$	$4.29x10^{-2}$
RN7SL618P	$2.65x10^{1}$	$4.73x10^{0}$	$1.44x10^{-2}$	$2.97x10^{-2}$
PTF1A	$2.29x10^{1}$	$4.52x10^{0}$	$6.23x10^{-16}$	$1.47x10^{-14}$
RNA5SP389	$2.15x10^{1}$	$4.42x10^{0}$	$2.16x10^{-2}$	$4.21x10^{-2}$
SFTPC	$2.10x10^{1}$	$4.39x10^{0}$	$2.04x10^{-6}$	$9.73x10^{-6}$
KRT31	$1.83x10^{1}$	$4.20x10^{0}$	$2.95x10^{-12}$	$3.84x10^{-11}$
SOHLH1	$1.62x10^{1}$	$4.02x10^{0}$	$2.38x10^{-10}$	$2.26x10^{-9}$
RN7SL149P	$1.58x10^{1}$	$3.98x10^{0}$	$2.07x10^{-2}$	$4.06x10^{-2}$
AC127459.2	$1.44x10^{1}$	$3.85x10^{0}$	$8.57x10^{-6}$	$3.65x10^{-5}$
AC114291.1	$1.40x10^{1}$	$3.80x10^{0}$	$9.34x10^{-37}$	$5.14x10^{-34}$
AC026336.3	$1.37x10^{1}$	$3.77x10^{0}$	$1.45x10^{-22}$	$9.41x10^{-21}$
LINC01896	$1.36x10^{1}$	$3.77x10^{0}$	$1.29x10^{-3}$	$3.50x10^{-3}$
PRR9	$1.29x10^{1}$	$3.69x10^{0}$	$3.38x10^{-9}$	$2.66x10^{-8}$
RN7SL762P	$1.29x10^{1}$	$3.68x10^{0}$	$1.29x10^{-8}$	$9.18x10^{-8}$

Table 3.2. Differentially expressed downregulated transcripts identified in the CS1 subtype using edgeR.

CS1 – Differentially Expressed Down-Regulated Transcripts				
	fc	**log2fc**	**pvalue**	**padj**
RNY4	$6.02x10^{-3}$	$-7.37x10^{0}$	$4.67x10^{-9}$	$3.59x10^{-8}$
PAEP	$7.39x10^{-3}$	$-7.08x10^{0}$	$2.59x10^{-63}$	$1.48x10^{-58}$
FBXO40	$9.29x10^{-3}$	$-6.75x10^{0}$	$5.33x10^{-31}$	$1.21x10^{-28}$
MTND5P32	$1.08x10^{-2}$	$-6.53x10^{0}$	$5.77x10^{-16}$	$1.37x10^{-14}$
RNU1.28P	$1.11x10^{-2}$	$-6.49x10^{0}$	$1.22x10^{-6}$	$6.08x10^{-6}$
RNVU1.2	$1.14x10^{-2}$	$-6.46x10^{0}$	$1.74x10^{-14}$	$3.24x10^{-13}$
CLDN18	$1.19x10^{-2}$	$-6.40x10^{0}$	$2.72x10^{-58}$	$7.78x10^{-54}$
AC066616.2	$1.20x10^{-2}$	$-6.38x10^{0}$	$6.04x10^{-16}$	$1.43x10^{-14}$
RNU1.52P	$1.20x10^{-2}$	$-6.38x10^{0}$	$4.68x10^{-9}$	$3.60x10^{-8}$
TFAP2B	$1.28x10^{-2}$	$-6.29x10^{0}$	$4.78x10^{-16}$	$1.15x10^{-14}$
RNU1.19P	$1.29x10^{-2}$	$-6.27x10^{0}$	$1.10x10^{-10}$	$1.10x10^{-9}$
RNU1.83P	$1.31x10^{-2}$	$-6.26x10^{0}$	$4.91x10^{-12}$	$6.19x10^{-11}$
RNU1.20P	$1.32x10^{-2}$	$-6.24x10^{0}$	$1.14x10^{-8}$	$8.21x10^{-8}$
AC090220.1	$1.36x10^{-2}$	$-6.20x10^{0}$	$3.50x10^{-17}$	$1.00x10^{-15}$
RNVU1.18	$1.42x10^{-2}$	$-6.14x10^{0}$	$2.01x10^{-7}$	$1.16x10^{-6}$
RNU1.139P	$1.45x10^{-2}$	$-6.10x10^{0}$	$5.53x10^{-8}$	$3.53x10^{-7}$

Table 3.2 (continued). Differentially expressed downregulated transcripts identified in the CS1 subtype using edgeR.

MTCYBP23	$1.46x10^{-2}$	$-6.09x10^{0}$	$4.97x10^{-15}$	$1.02x10^{-13}$
RNU1.46P	$1.54x10^{-2}$	$-6.02x10^{0}$	$9.51x10^{-9}$	$6.92x10^{-8}$

RNU2.59P	$1.56x10^{-2}$	$-6.01x10^{0}$	$8.94x10^{-9}$	$6.54x10^{-8}$
Y_RNA.209	$1.56x10^{-2}$	$-6.00x10^{0}$	$7.92x10^{-8}$	$4.92x10^{-7}$

Table 3.3. Differentially expressed upregulated transcripts identified in the CS2 subtype using edgeR.

CS2 – Differentially Expressed Up-Regulated Transcripts				
	fc	**log2fc**	**pvalue**	**padj**
RNY4	$1.66x10^{2}$	$7.38x10^{0}$	$4.67x10^{-9}$	$3.59x10^{-8}$
PAEP	$1.35x10^{2}$	$7.08x10^{0}$	$2.59x10^{-63}$	$1.48x10^{-58}$
FBXO40	$1.08x10^{2}$	$6.75x10^{0}$	$5.33x10^{-31}$	$1.21x10^{-28}$
MTND5P32	$9.22x10^{1}$	$6.53x10^{0}$	$5.77x10^{-16}$	$1.37x10^{-14}$
RNU1.28P	$8.99x10^{1}$	$6.49x10^{0}$	$1.22x10^{-6}$	$6.08x10^{-6}$
RNVU1.2	$8.80x10^{1}$	$6.46x10^{0}$	$1.74x10^{-14}$	$3.24x10^{-13}$
CLDN18	$8.42x10^{1}$	$6.40x10^{0}$	$2.72x10^{-58}$	$7.78x10^{-54}$
AC066616.2	$8.36x10^{1}$	$6.38x10^{0}$	$6.04x10^{-16}$	$1.43x10^{-14}$
RNU1.52P	$8.30x10^{1}$	$6.38x10^{0}$	$4.68x10^{-9}$	$3.60x10^{-8}$
TFAP2B	$7.80x10^{1}$	$6.29x10^{0}$	$4.78x10^{-16}$	$1.15x10^{-14}$
RNU1.19P	$7.74x10^{1}$	$6.27x10^{0}$	$1.10x10^{-10}$	$1.10x10^{-9}$
RNU1.83P	$7.64x10^{1}$	$6.26x10^{0}$	$4.91x10^{-12}$	$6.19x10^{-11}$
RNU1.20P	$7.58x10^{1}$	$6.24x10^{0}$	$1.14x10^{-8}$	$8.21x10^{-8}$
AC090220.1	$7.37x10^{1}$	$6.20x10^{0}$	$3.50x10^{-17}$	$1.00x10^{-15}$
RNVU1.18	$7.04x10^{1}$	$6.14x10^{0}$	$2.01x10^{-7}$	$1.16x10^{-6}$
RNU1.139P	$6.88x10^{1}$	$6.10x10^{0}$	$5.53x10^{-8}$	$3.53x10^{-7}$
MTCYBP23	$6.83x10^{1}$	$6.09x10^{0}$	$4.97x10^{-15}$	$1.02x10^{-13}$
RNU1.46P	$6.51x10^{1}$	$6.02x10^{0}$	$9.51x10^{-9}$	$6.92x10^{-8}$
RNU2.59P	$6.43x10^{1}$	$6.01x10^{0}$	$8.94x10^{-9}$	$6.54x10^{-8}$
Y_RNA.209	$6.40x10^{1}$	$6.00x10^{0}$	$7.92x10^{-8}$	$4.92x10^{-7}$

Table 3.4. Differentially expressed downregulated transcripts identified in the CS2 subtype using edgeR.

CS2 – Differentially Expressed Down-Regulated Transcripts				
	fc	**log2fc**	**pvalue**	**padj**
WIF1	$1.99x10^{-2}$	$-5.65x10^{0}$	$4.68x10^{-30}$	$9.46x10^{-28}$
BX322234.2	$2.17x10^{-2}$	$-5.53x10^{0}$	$1.63x10^{-7}$	$9.53x10^{-7}$
RNA5.8SP5	$2.57x10^{-2}$	$-5.28x10^{0}$	$2.07x10^{-3}$	$5.35x10^{-3}$
AC152010.1	$2.68x10^{-2}$	$-5.22x10^{0}$	$5.46x10^{-3}$	$1.27x10^{-2}$
ORM1	$3.31x10^{-2}$	$-4.92x10^{0}$	$2.02x10^{-18}$	$6.97x10^{-17}$
RNA5SP267	$3.58x10^{-2}$	$-4.80x10^{0}$	$1.83x10^{-2}$	$3.66x10^{-2}$
RNA5SP211	$3.62x10^{-2}$	$-4.79x10^{0}$	$2.21x10^{-2}$	$4.29x10^{-2}$
RN7SL618P	$3.78x10^{-2}$	$-4.73x10^{0}$	$1.44x10^{-2}$	$2.97x10^{-2}$
PTF1A	$4.36x10^{-2}$	$-4.52x10^{0}$	$6.23x10^{-16}$	$1.47x10^{-14}$

Table 3.4 (continued). Differentially expressed downregulated transcripts identified in the CS2 subtype using edgeR.

RNA5SP389	$4.66x10^{-2}$	$-4.42x10^{0}$	$2.16x10^{-2}$	$4.21x10^{-2}$
SFTPC	$4.76x10^{-2}$	$-4.39x10^{0}$	$2.04x10^{-6}$	$9.73x10^{-6}$
KRT31	$5.45x10^{-2}$	$-4.20x10^{0}$	$2.95x10^{-12}$	$3.84x10^{-11}$

SOHLH1	$6.17x10^{-2}$	$-4.02x10^{0}$	$2.38x10^{-10}$	$2.26x10^{-9}$
RN7SL149P	$6.33x10^{-2}$	$-3.98x10^{0}$	$2.07x10^{-2}$	$4.06x10^{-2}$
AC127459.2	$6.92x10^{-2}$	$-3.85x10^{0}$	$8.57x10^{-6}$	$3.65x10^{-5}$
AC114291.1	$7.16x10^{-2}$	$-3.80x10^{0}$	$9.34x10^{-37}$	$5.14x10^{-34}$
AC026336.3	$7.32x10^{-2}$	$-3.77x10^{0}$	$1.45x10^{-22}$	$9.41x10^{-21}$
LINC01896	$7.33x10^{-2}$	$-3.77x10^{0}$	$1.29x10^{-3}$	$3.50x10^{-3}$
PRR9	$7.76x10^{-2}$	$-3.69x10^{0}$	$3.38x10^{-9}$	$2.66x10^{-8}$
RN7SL762P	$7.78x10^{-2}$	$-3.68x10^{0}$	$1.29x10^{-8}$	$9.18x10^{-8}$

As a result of the differential expression analysis performed with DESeq2, 954 and 10872 upregulated biomarkers were identified for the CS1 and CS2 subtypes, respectively. Tables 3.5-3.8 show the 20 most up- and downregulated transcripts identified with DESeq2 for the CS1 and CS2 subtypes and sorted by FC. All other DEGs identified with DESeq2 during differential expression analysis are listed in Appendix A.2. In CS1, Wnt inhibitory factor 1 (WIF1) was expressed more than 24-fold higher. WIF1 inhibits the Wnt signalling pathway, a metabolic-related pathway that is inactive in normal cells but whose abnormal activation triggers cell proliferation and metastasis. On the other hand, silencing of WIF1, a tumour suppressor, in CS2 can trigger tumour development [100].

Table 3.5. Differentially expressed upregulated transcripts identified in the CS1 subtype using DESeq2.

CS1 – Differentially Expressed Up-Regulated Transcripts				
	fc	**log2fc**	**pvalue**	**padj**
WIF1	$4.83x10^{1}$	$5.59x10^{0}$	$1.03x10^{-50}$	$3.02x10^{-47}$
PTF1A	$2.59x10^{1}$	$4.69x10^{0}$	$3.33x10^{-22}$	$1.34x10^{-20}$
PRSS56	$2.33x10^{1}$	$4.54x10^{0}$	$6.35x10^{-26}$	$4.62x10^{-24}$
IGF2	$2.10x10^{1}$	$4.39x10^{0}$	$4.96x10^{-34}$	$1.22x10^{-31}$
AL356433.1	$1.97x10^{1}$	$4.30x10^{0}$	$1.57x10^{-23}$	$8.02x10^{-22}$
LY6G6D	$1.77x10^{1}$	$4.14x10^{0}$	$3.59x10^{-40}$	$2.01x10^{-37}$
KRT35	$1.52x10^{1}$	$3.93x10^{0}$	$2.63x10^{-16}$	$4.21x10^{-15}$
AC114291.1	$1.35x10^{1}$	$3.76x10^{0}$	$3.55x10^{-49}$	$7.01x10^{-46}$
AC026336.3	$1.32x10^{1}$	$3.72x10^{0}$	$3.64x10^{-31}$	$5.85x10^{-29}$
AC026774.1	$1.31x10^{1}$	$3.71x10^{0}$	$3.68x10^{-21}$	$1.26x10^{-19}$
LY6G6F.LY6G6D	$1.30x10^{1}$	$3.70x10^{0}$	$1.08x10^{-30}$	$1.63x10^{-28}$
MAGEB17	$1.18x10^{1}$	$3.56x10^{0}$	$5.29x10^{-26}$	$3.92x10^{-24}$
GOLGA6L2	$1.16x10^{1}$	$3.53x10^{0}$	$1.48x10^{-22}$	$6.27x10^{-21}$

Table 3.5 (continued). Differentially expressed upregulated transcripts identified in the CS1 subtype using DESeq2.

KRT43P	$1.11x10^{1}$	$3.47x10^{0}$	$1.42x10^{-14}$	$1.73x10^{-13}$
NOTUM	$1.05x10^{1}$	$3.39x10^{0}$	$1.36x10^{-32}$	$2.82x10^{-30}$
LCN15	$1.04x10^{1}$	$3.38x10^{0}$	$8.61x10^{-21}$	$2.75x10^{-19}$
KRT32	$9.98x10^{0}$	$3.32x10^{0}$	$1.51x10^{-14}$	$1.84x10^{-13}$

KRT37	$9.89x10^{0}$	$3.31x10^{0}$	$2.73x10^{-18}$	$5.89x10^{-17}$
CDH9	$9.89x10^{0}$	$3.31x10^{0}$	$8.97x10^{-6}$	$2.93x10^{-5}$
BX510359.5	$9.66x10^{0}$	$3.27x10^{0}$	$6.11x10^{-13}$	$5.87x10^{-12}$

Table 3.6. Differentially expressed downregulated transcripts identified in the CS1 subtype using DESeq2.

CS1 – Differentially Expressed Down-Regulated Transcripts				
	fc	**log2fc**	**pvalue**	**padj**
RN7SKP227	$3.33x10^{-4}$	$-1.16x10^{1}$	$2.66x10^{-7}$	$1.11x10^{-6}$
CLDN18	$5.37x10^{-3}$	$-7.54x10^{0}$	$1.18x10^{-118}$	$5.16x10^{-114}$
RN7SKP203	$7.80x10^{-3}$	$-7.00x10^{0}$	$3.10x10^{-15}$	$4.22x10^{-14}$
AL139274.1	$8.64x10^{-3}$	$-6.85x10^{0}$	$7.13x10^{-17}$	$1.24x10^{-15}$
RNU1.88P	$8.91x10^{-3}$	$-6.81x10^{0}$	$2.41x10^{-15}$	$3.33x10^{-14}$
MIR3609	$1.33x10^{-2}$	$-6.23x10^{0}$	$2.44x10^{-27}$	$2.28x10^{-25}$
ANXA10	$1.37x10^{-2}$	$-6.19x10^{0}$	$5.87x10^{-88}$	$1.29x10^{-83}$
RN7SKP9	$1.40x10^{-2}$	$-6.16x10^{0}$	$1.56x10^{-29}$	$2.03x10^{-27}$
AL390318.1	$1.43x10^{-2}$	$-6.13x10^{0}$	$2.90x10^{-5}$	$8.75x10^{-5}$
RN7SKP186	$1.48x10^{-2}$	$-6.07x10^{0}$	$5.57x10^{-3}$	$1.10x10^{-2}$
RNU1.11P	$1.49x10^{-2}$	$-6.07x10^{0}$	$4.00x10^{-9}$	$2.19x10^{-8}$
RN7SKP255	$1.60x10^{-2}$	$-5.96x10^{0}$	$2.48x10^{-11}$	$1.89x10^{-10}$
AL139120.1	$1.66x10^{-2}$	$-5.91x10^{0}$	$4.41x10^{-9}$	$2.40x10^{-8}$
RAD51AP1P1	$1.67x10^{-2}$	$-5.90x10^{0}$	$1.00x10^{-8}$	$5.19x10^{-8}$
LPP.AS1	$1.67x10^{-2}$	$-5.90x10^{0}$	$6.89x10^{-8}$	$3.14x10^{-7}$
IFNK	$1.75x10^{-2}$	$-5.83x10^{0}$	$1.27x10^{-14}$	$1.57x10^{-13}$
AC010997.6	$1.82x10^{-2}$	$-5.78x10^{0}$	$2.99x10^{-9}$	$1.67x10^{-8}$
EIF4E2P1	$1.86x10^{-2}$	$-5.75x10^{0}$	$8.47x10^{-8}$	$3.81x10^{-7}$
AL606517.2	$1.87x10^{-2}$	$-5.74x10^{0}$	$1.72x10^{-6}$	$6.30x10^{-6}$
AC008533.1	$1.92x10^{-2}$	$-5.70x10^{0}$	$8.17x10^{-24}$	$4.33x10^{-22}$

Table 3.7. Differentially expressed upregulated transcripts identified in the CS2 subtype using DESeq2.

CS2 – Differentially Expressed Up-Regulated Transcripts				
	fc	**log2fc**	**pvalue**	**padj**
RN7SKP227	$3.00x10^{3}$	$1.16x10^{1}$	$2.66x10^{-7}$	$1.11x10^{-6}$
CLDN18	$1.86x10^{2}$	$7.54x10^{0}$	$1.18x10^{-118}$	$5.16x10^{-114}$
RN7SKP203	$1.28x10^{2}$	$7.00x10^{0}$	$3.10x10^{-15}$	$4.22x10^{-14}$
AL139274.1	$1.16x10^{2}$	$6.85x10^{0}$	$7.13x10^{-17}$	$1.24x10^{-15}$
RNU1.88P	$1.12x10^{2}$	$6.81x10^{0}$	$2.41x10^{-15}$	$3.34x10^{-14}$
MIR3609	$7.52x10^{1}$	$6.23x10^{0}$	$2.44x10^{-27}$	$2.28x10^{-25}$

Table 3.7 (continued). Differentially expressed upregulated transcripts identified in the CS2 subtype using DESeq2.

ANXA10	$7.31x10^{1}$	$6.19x10^{0}$	$5.87x10^{-88}$	$1.29x10^{-83}$
RN7SKP9	$7.16x10^{1}$	$6.16x10^{0}$	$1.56x10^{-29}$	$2.03x10^{-27}$
AL390318.1	$7.00x10^{1}$	$6.13x10^{0}$	$2.90x10^{-5}$	$8.75x10^{-5}$
RN7SKP186	$6.74x10^{1}$	$6.07x10^{0}$	$5.57x10^{-3}$	$1.10x10^{-2}$
RNU1.11P	$6.73x10^{1}$	$6.07x10^{0}$	$4.00x10^{-9}$	$2.19x10^{-8}$

RN7SKP255	$6.24x10^{1}$	$5.96x10^{0}$	$2.48x10^{-11}$	$1.89x10^{-10}$
AL139120.1	$6.02x10^{1}$	$5.91x10^{0}$	$4.41x10^{-9}$	$2.40x10^{-8}$
RAD51AP1P1	$5.97x10^{1}$	$5.90x10^{0}$	$1.00x10^{-8}$	$5.19x10^{-8}$
LPP.AS1	$5.97x10^{1}$	$5.90x10^{0}$	$6.89x10^{-8}$	$3.14x10^{-7}$
IFNK	$5.71x10^{1}$	$5.83x10^{0}$	$1.27x10^{-14}$	$1.57x10^{-13}$
AC010997.6	$5.48x10^{1}$	$5.78x10^{0}$	$2.99x10^{-9}$	$1.67x10^{-8}$
EIF4E2P1	$5.37x10^{1}$	$5.75x10^{0}$	$8.47x10^{-8}$	$3.81x10^{-7}$
AL606517.2	$5.33x10^{1}$	$5.74x10^{0}$	$1.72x10^{-6}$	$6.30x10^{-6}$
AC008533.1	$5.21x10^{1}$	$5.70x10^{0}$	$8.17x10^{-24}$	$4.33x10^{-22}$

Table 3.8. Differentially expressed downregulated transcripts identified in the CS2 subtype using DESeq2.

CS2 – Differentially Expressed Down-Regulated Transcripts				
	fc	**log2fc**	**pvalue**	**padj**
WIF1	$2.07x10^{-2}$	$-5.59x10^{0}$	$1.03x10^{-50}$	$3.02x10^{-47}$
PTF1A	$3.86x10^{-2}$	$-4.69x10^{0}$	$3.33x10^{-22}$	$1.34x10^{-20}$
PRSS56	$4.29x10^{-2}$	$-4.54x10^{0}$	$6.35x10^{-26}$	$4.63x10^{-24}$
IGF2	$4.77x10^{-2}$	$-4.39x10^{0}$	$4.95x10^{-34}$	$1.22x10^{-31}$
AL356433.1	$5.09x10^{-2}$	$-4.30x10^{0}$	$1.57x10^{-23}$	$8.04x10^{-22}$
LY6G6D	$5.65x10^{-2}$	$-4.14x10^{0}$	$3.59x10^{-40}$	$2.01x10^{-37}$
KRT35	$6.56x10^{-2}$	$-3.93x10^{0}$	$2.63x10^{-16}$	$4.22x10^{-15}$
AC114291.1	$7.39x10^{-2}$	$-3.76x10^{0}$	$3.55x10^{-49}$	$7.01x10^{-46}$
AC026336.3	$7.57x10^{-2}$	$-3.72x10^{0}$	$3.64x10^{-31}$	$5.85x10^{-29}$
AC026774.1	$7.65x10^{-2}$	$-3.71x10^{0}$	$3.68x10^{-21}$	$1.26x10^{-19}$
LY6G6F.LY6G6D	$7.71x10^{-2}$	$-3.70x10^{0}$	$1.08x10^{-30}$	$1.63x10^{-28}$
MAGEB17	$8.45x10^{-2}$	$-3.56x10^{0}$	$5.29x10^{-26}$	$3.93x10^{-24}$
GOLGA6L2	$8.65x10^{-2}$	$-3.53x10^{0}$	$1.48x10^{-22}$	$6.27x10^{-21}$
KRT43P	$9.01x10^{-2}$	$-3.47x10^{0}$	$1.42x10^{-14}$	$1.73x10^{-13}$
NOTUM	$9.53x10^{-2}$	$-3.39x10^{0}$	$1.36x10^{-32}$	$2.82x10^{-30}$
LCN15	$9.63x10^{-2}$	$-3.38x10^{0}$	$8.61x10^{-21}$	$2.76x10^{-19}$
KRT32	$1.00x10^{-1}$	$-3.32x10^{0}$	$1.51x10^{-14}$	$1.84x10^{-13}$
KRT37	$1.01x10^{-1}$	$-3.31x10^{0}$	$2.73x10^{-18}$	$5.89x10^{-17}$
CDH9	$1.01x10^{-1}$	$-3.31x10^{0}$	$8.97x10^{-6}$	$2.93x10^{-5}$
BX510359.5	$1.03x10^{-1}$	$-3.27x10^{0}$	$6.11x10^{-13}$	$5.87x10^{-12}$

Finally, 279 upregulated biomarkers for CS1 and 228 for CS2 were identified as a result of the analysis performed with the Limma algorithm. Tables 3.9-3.12 show the 20 most up- and down-regulated transcripts identified by Limma for the CS1 and CS2 subtypes and sorted by FC. All other DEGs identified by differential expression analysis with Limma are listed in Appendix A.3. Regenerating family member 4 (REG4), a member of the calcium-dependent lectin gene superfamily that is abnormally expressed in colon cancer, is associated with important cancer hallmarks such as cell proliferation and apoptosis [101]. In addition, REG4-positive cancer cells are associated with poor

prognosis due to their high resistance to 5-FU-based therapy [102], one of the most commonly used chemotherapeutic agents in the treatment of colon cancer, and this gene was upregulated more than 5-fold in CS2.

Table 3.9. Differentially expressed upregulated transcripts identified in the CS1 subtype using limma.

CS1 – Differentially Expressed Up-Regulated Transcripts				
	fc	**log2fc**	**pvalue**	**padj**
TNNC2	$9.77x10^{0}$	$3.29x10^{0}$	$1.27x10^{-47}$	$7.28x10^{-43}$
AP003774.2	$7.71x10^{0}$	$2.95x10^{0}$	$4.49x10^{-40}$	$1.28x10^{-35}$
CEL	$7.68x10^{0}$	$2.94x10^{0}$	$7.42x10^{-24}$	$4.04x10^{-21}$
C10orf99	$7.48x10^{0}$	$2.90x10^{0}$	$2.02x10^{-23}$	$1.01x10^{-20}$
KRT23	$6.47x10^{0}$	$2.69x10^{0}$	$9.17x10^{-22}$	$3.26x10^{-19}$
QPRT	$6.01x10^{0}$	$2.59x10^{0}$	$1.71x10^{-36}$	$1.22x10^{-32}$
NOTUM	$5.38x10^{0}$	$2.43x10^{0}$	$1.57x10^{-15}$	$1.49x10^{-13}$
GNG4	$5.37x10^{0}$	$2.43x10^{0}$	$2.78x10^{-22}$	$1.13x10^{-19}$
CDHR1	$5.22x10^{0}$	$2.38x10^{0}$	$1.19x10^{-24}$	$7.64x10^{-22}$
ASCL2	$5.13x10^{0}$	$2.36x10^{0}$	$2.14x10^{-31}$	$5.33x10^{-28}$
DPEP1	$5.06x10^{0}$	$2.34x10^{0}$	$1.80x10^{-17}$	$2.56x10^{-15}$
SLC26A3	$5.00x10^{0}$	$2.32x10^{0}$	$1.72x10^{-11}$	$6.46x10^{-10}$
SLC39A5	$4.78x10^{0}$	$2.26x10^{0}$	$1.55x10^{-30}$	$3.07x10^{-27}$
TDGF1	$4.58x10^{0}$	$2.19x10^{0}$	$1.64x10^{-32}$	$5.51x10^{-29}$
Y_RNA.244	$4.46x10^{0}$	$2.16x10^{0}$	$6.98x10^{-25}$	$4.65x10^{-22}$
FABP1	$4.38x10^{0}$	$2.13x10^{0}$	$9.65x10^{-11}$	$3.10x10^{-9}$
VAV3	$4.30x10^{0}$	$2.10x10^{0}$	$4.32x10^{-32}$	$1.18x10^{-28}$
CYP2B6	$4.25x10^{0}$	$2.09x10^{0}$	$1.67x10^{-25}$	$1.31x10^{-22}$
CXCL14	$4.20x10^{0}$	$2.07x10^{0}$	$1.20x10^{-16}$	$1.43x10^{-14}$
CYP2W1	$4.20x10^{0}$	$2.07x10^{0}$	$2.95x10^{-13}$	$1.68x10^{-11}$

Table 3.10. Differentially expressed downregulated transcripts identified in the CS1 subtype using limma.

CS1 – Differentially Expressed Down-Regulated Transcripts				
	fc	**log2fc**	**pvalue**	**padj**
REG4	$9.27x10^{-2}$	$-3.43x10^{0}$	$1.42x10^{-16}$	$1.65x10^{-14}$
CTSE	$1.44x10^{-1}$	$-2.80x10^{0}$	$2.55x10^{-19}$	$5.28x10^{-17}$

Table 3.10 (continued). Differentially expressed downregulated transcripts identified in the CS1 subtype using limma.

PLA2G2A	$1.87x10^{-1}$	$-2.42x10^{0}$	$3.16x10^{-13}$	$1.77x10^{-11}$
CLDN18	$1.92x10^{-1}$	$-2.38x10^{0}$	$4.82x10^{-20}$	$1.17x10^{-17}$
DUSP4	$2.02x10^{-1}$	$-2.31x10^{0}$	$1.99x10^{-35}$	$1.26x10^{-31}$
GJB5	$2.57x10^{-1}$	$-1.96x10^{0}$	$4.14x10^{-18}$	$6.50x10^{-16}$
MUC2	$2.59x10^{-1}$	$-1.95x10^{0}$	$6.37x10^{-8}$	$1.09x10^{-6}$
MUC5AC	$2.64x10^{-1}$	$-1.92x10^{0}$	$9.37x10^{-17}$	$1.14x10^{-14}$
LYZ	$2.68x10^{-1}$	$-1.90x10^{0}$	$8.39x10^{-14}$	$5.45x10^{-12}$
TCN1	$2.73x10^{-1}$	$-1.87x10^{0}$	$3.81x10^{-10}$	$1.08x10^{-8}$

CXCL13	$2.74x10^{-1}$	$-1.87x10^{0}$	$1.38x10^{-19}$	$3.08x10^{-17}$
RAMP1	$2.76x10^{-1}$	$-1.86x10^{0}$	$1.32x10^{-14}$	$1.02x10^{-12}$
REG1A	$2.81x10^{-1}$	$-1.83x10^{0}$	$7.78x10^{-5}$	$4.91x10^{-4}$
VNN1	$2.83x10^{-1}$	$-1.82x10^{0}$	$1.31x10^{-21}$	$4.50x10^{-19}$
TFF2	$2.84x10^{-1}$	$-1.82x10^{0}$	$1.49x10^{-10}$	$4.55x10^{-9}$
TNNT1	$2.88x10^{-1}$	$-1.80x10^{0}$	$1.04x10^{-19}$	$2.35x10^{-17}$
RAB27B	$2.99x10^{-1}$	$-1.74x10^{0}$	$1.42x10^{-37}$	$1.16x10^{-33}$
CCL18	$3.02x10^{-1}$	$-1.73x10^{0}$	$4.96x10^{-11}$	$1.69x10^{-9}$
CXCL9	$3.14x10^{-1}$	$-1.67x10^{0}$	$1.69x10^{-13}$	$1.02x10^{-11}$
TRNP1	$3.19x10^{-1}$	$-1.65x10^{0}$	$4.52x10^{-21}$	$1.33x10^{-18}$

Table 3.11. Differentially expressed upregulated transcripts identified in the CS2 subtype using limma.

CS2 – Differentially Expressed Up-Regulated Transcripts				
	fc	**log2fc**	**pvalue**	**padj**
REG4	$1.08x10^{1}$	$3.43x10^{0}$	$1.42x10^{-16}$	$1.65x10^{-14}$
CTSE	$6.95x10^{0}$	$2.80x10^{0}$	$2.55x10^{-19}$	$5.28x10^{-17}$
PLA2G2A	$5.36x10^{0}$	$2.42x10^{0}$	$3.16x10^{-13}$	$1.77x10^{-11}$
CLDN18	$5.22x10^{0}$	$2.38x10^{0}$	$4.82x10^{-20}$	$1.17x10^{-17}$
DUSP4	$4.95x10^{0}$	$2.31x10^{0}$	$1.99x10^{-35}$	$1.26x10^{-31}$
GJB5	$3.90x10^{0}$	$1.96x10^{0}$	$4.14x10^{-18}$	$6.50x10^{-16}$
MUC2	$3.86x10^{0}$	$1.95x10^{0}$	$6.37x10^{-8}$	$1.09x10^{-6}$
MUC5AC	$3.78x10^{0}$	$1.92x10^{0}$	$9.37x10^{-17}$	$1.14x10^{-14}$
LYZ	$3.74x10^{0}$	$1.90x10^{0}$	$8.39x10^{-14}$	$5.45x10^{-12}$
TCN1	$3.66x10^{0}$	$1.87x10^{0}$	$3.81x10^{-10}$	$1.08x10^{-8}$
CXCL13	$3.66x10^{0}$	$1.87x10^{0}$	$1.38x10^{-19}$	$3.08x10^{-17}$
RAMP1	$3.62x10^{0}$	$1.86x10^{0}$	$1.32x10^{-14}$	$1.02x10^{-12}$
REG1A	$3.56x10^{0}$	$1.83x10^{0}$	$7.78x10^{-5}$	$4.91x10^{-4}$
VNN1	$3.54x10^{0}$	$1.82x10^{0}$	$1.31x10^{-21}$	$4.50x10^{-19}$
TFF2	$3.52x10^{0}$	$1.82x10^{0}$	$1.49x10^{-10}$	$4.55x10^{-9}$
TNNT1	$3.48x10^{0}$	$1.80x10^{0}$	$1.04x10^{-19}$	$2.35x10^{-17}$
RAB27B	$3.34x10^{0}$	$1.74x10^{0}$	$1.42x10^{-37}$	$1.16x10^{-33}$
CCL18	$3.31x10^{0}$	$1.73x10^{0}$	$4.96x10^{-11}$	$1.69x10^{-9}$
CXCL9	$3.19x10^{0}$	$1.67x10^{0}$	$1.69x10^{-13}$	$1.02x10^{-11}$
TRNP1	$3.13x10^{0}$	$1.65x10^{0}$	$4.52x10^{-21}$	$1.33x10^{-18}$

Table 3.12. Differentially expressed downregulated transcripts identified in the CS2 subtype using limma.

CS2 – Differentially Expressed Up-Regulated Transcripts				
	fc	**log2fc**	**pvalue**	**padj**
TNNC2	$1.02x10^{-1}$	$-3.29x10^{0}$	$1.27x10^{-47}$	$7.28x10^{-43}$
AP003774.2	$1.30x10^{-1}$	$-2.95x10^{0}$	$4.49x10^{-40}$	$1.28x10^{-35}$
CEL	$1.30x10^{-1}$	$-2.94x10^{0}$	$7.42x10^{-24}$	$4.04x10^{-21}$
C10orf99	$1.34x10^{-1}$	$-2.90x10^{0}$	$2.02x10^{-23}$	$1.01x10^{-20}$
KRT23	$1.55x10^{-1}$	$-2.69x10^{0}$	$9.17x10^{-22}$	$3.26x10^{-19}$
QPRT	$1.67x10^{-1}$	$-2.59x10^{0}$	$1.71x10^{-36}$	$1.22x10^{-32}$
NOTUM	$1.86x10^{-1}$	$-2.43x10^{0}$	$1.57x10^{-15}$	$1.49x10^{-13}$

GNG4	$1.86x10^{-1}$	$-2.43x10^{0}$	$2.78x10^{-22}$	$1.13x10^{-19}$
CDHR1	$1.92x10^{-1}$	$-2.38x10^{0}$	$1.19x10^{-24}$	$7.64x10^{-22}$
ASCL2	$1.95x10^{-1}$	$-2.36x10^{0}$	$2.14x10^{-31}$	$5.33x10^{-28}$
DPEP1	$1.98x10^{-1}$	$-2.34x10^{0}$	$1.80x10^{-17}$	$2.56x10^{-15}$
SLC26A3	$2.00x10^{-1}$	$-2.32x10^{0}$	$1.72x10^{-11}$	$6.46x10^{-10}$
SLC39A5	$2.09x10^{-1}$	$-2.26x10^{0}$	$1.55x10^{-30}$	$3.07x10^{-27}$
TDGF1	$2.19x10^{-1}$	$-2.19x10^{0}$	$1.64x10^{-32}$	$5.51x10^{-29}$
Y_RNA.244	$2.24x10^{-1}$	$-2.16x10^{0}$	$6.98x10^{-25}$	$4.65x10^{-22}$
FABP1	$2.28x10^{-1}$	$-2.13x10^{0}$	$9.65x10^{-11}$	$3.10x10^{-9}$
VAV3	$2.33x10^{-1}$	$-2.10x10^{0}$	$4.32x10^{-32}$	$1.18x10^{-28}$
CYP2B6	$2.35x10^{-1}$	$-2.09x10^{0}$	$1.67x10^{-25}$	$1.31x10^{-22}$
CXCL14	$2.38x10^{-1}$	$-2.07x10^{0}$	$1.20x10^{-16}$	$1.43x10^{-14}$
CYP2W1	$2.38x10^{-1}$	$-2.07x10^{0}$	$2.95x10^{-13}$	$1.68x10^{-11}$

Gene Set Enrichment Analysis (GSEA) is the association of a disease phenotype with a group of significantly expressed genes or proteins [103, 104]. The disease phenotype is thus characterised by the identification of functional pathways specific for the gene/protein list in question. In GSEA, the list of differentially expressed genes/proteins (e.g. the S-list) is first classified using a metric suitable for expression changes. The list of sequenced genes is then compared to a set of genes known to be associated with a specific biological process or oncogenic pathway (e.g. L-list). This comparison calculates an enrichment score that reflects the extent to which the relevant S-list is over-represented at the extremes of the L-list. The most basic logic in calculating this score is based on increasing the overall statistic if there is an overlap with the genes in the S-list as you move from top to bottom in a biological gene list (L-list), and decreasing it otherwise. The size of this score depends on the correlation of the gene with the phenotype. The statistical significance of the ES is then estimated. Due to the use of gene sets of different sizes in the analysis, ES differences occur between the gene sets. To correct for these differences, the NES value is determined by normalising the enrichment score. A positive value of the normalised enrichment score (NES) means that the corresponding gene in the S-list is upregulated in the L-list, while a negative value indicates that the gene in the S-list is downregulated in the L-list [104]. Finally, the false discovery rate (FDR) [105, 106] is calculated for each NES value to estimate the probability that a given NES represents a false positive [104].

A GSEA was conducted on the TCGA-COAD cohort as part of this work. A dataset containing all gene sets derived from GO biological processes from the Molecular

Signature Database was used to better understand the biology of COAD and to identify subtype-specific functional pathways. When analysing the enrichment of gene sets, the edgeR, DESeq2 and limma algorithms were used to identify subtype-specific upregulated or downregulated pathways. However, only significant results that exceeded the significance threshold (nominal P-value < 0.05 and adjusted P-value < 0.05) and did not overlap with a pathway defined for other subtypes were obtained with limma. Once the subtype-specific pathways were determined, single-sample GSEA (ssGSEA) [74] was used to calculate the single-sample enrichment score. This method calculates separate enrichment scores for each match between a sample and a gene set. Each ssGSEA score represents the extent to which genes are upregulated or downregulated in a particular gene set within a sample. In addition, the median was used as a normalisation method when calculating the subtype-specific enrichment score. As a result, a cross-sectional heat map was drawn to visualise the 10 most upregulated or downregulated subtype-specific pathways. The result of the analysis was that CS2 was upregulated in almost four times as many biological pathways as CS1 (Figure 3.5). On the other hand, CS1 is enriched in 467 downregulated pathways, in contrast to CS2, which is downregulated in 80 pathways (Figure 3.6). CS1 is downregulated in several biological pathways, such as immune cell migration, immune response and chemokine response, while CS2 is upregulated in these pathways. The immune response to tumour tissue by tumour-infiltrating lymphocytes (TILs) influences cell proliferation and metastasis in patients with colon adenocarcinoma [107]. An increased intratumoural density of TILs is a good prognostic marker. Therefore, it can be said that upregulation of this pathway in CS2 may result in low local tumour spread and low possibility of metastasis in patients of this group with lymphocyte-rich tumours [107, 108]. It is also considered that abnormally expressed chemokines play an important role in tumour development [109, 110].

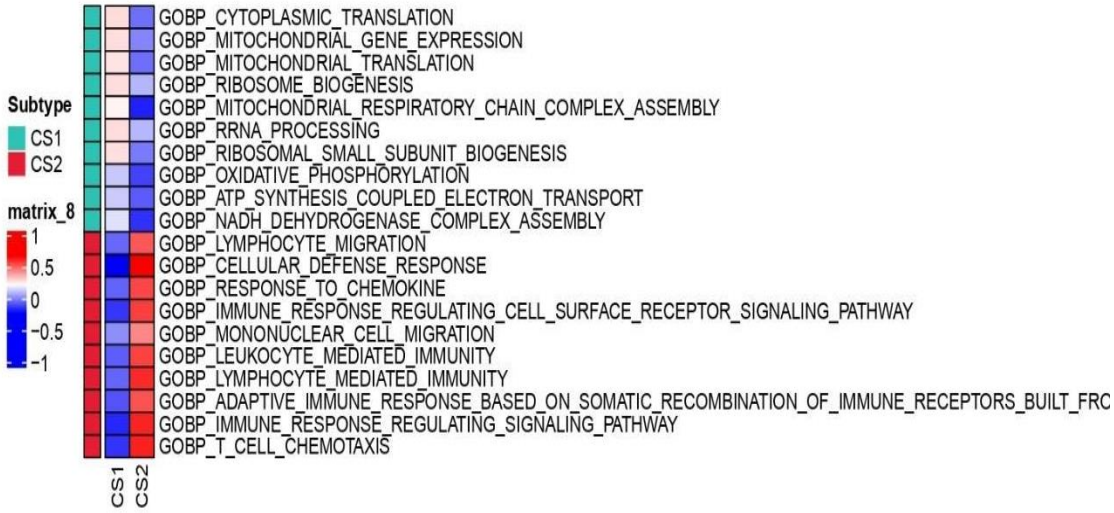


Figure 3.5. Heatmap of subtype-specific upregulated pathways using limma algorithm for 2 identified subtypes in TCGA-COAD cohort.

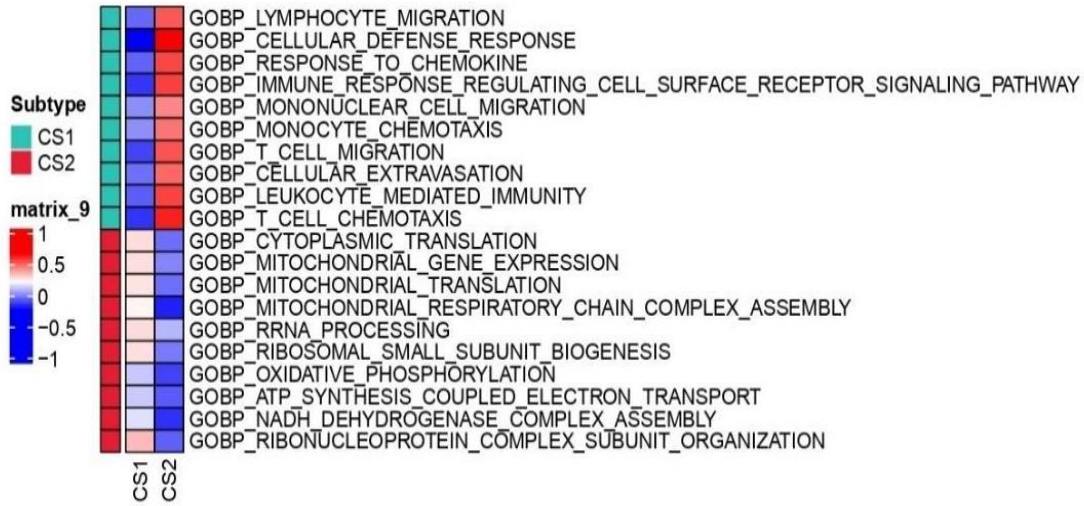


Figure 3.6. Heatmap of subtype-specific downregulated pathways using limma algorithm for 2 identified subtypes in TCGA-COAD cohort.

Tumour-associated genes largely regulate carcinogenesis [111]. Hanahan and Weinberg [112, 113] have identified ten cancer hallmarks that occur in almost all types of cancer. These hallmarks ((i) activation of invasion and metastasis, (ii) facilitation of replicative immortality, (iii) evasion of growth suppressors, (iv) evasion of destruction by the immune system, (v) genome instability and mutation, (vi) initiation of angiogenesis, (vii) deregulation of cellular energetics, (viii) resistance to cell death, (ix) maintenance of proliferative signalling and (x) tumour-promoting inflammation) play a crucial role in the initiation, development and progression of cancer. Therefore, to better understand the process of tumourigenesis in each subtype, the activation status of 50 tumour-related

signalling pathways, including these 10 hallmarks, was compared (Figure 3.7). The results showed that interferon-alpha response, interferon-gamma response, allograft rejection, IL-2-STAT5 signalling, IL-6/JAKK/STAT3 signalling and inflammatory response are highly active in CS2 cells. These results suggest that the CS2 subtype is associated with the immune response and inflammation. The process by which epithelial cells transform into mesenchymal cells, which increases the mobility of cancer cells, is called epithelial-mesenchymal transition (EMT), and this EMT plays an important role in cancer metastasis [114, 115]. The epithelial-mesenchymal signalling pathway is activated in CS2, which may be associated with a poor prognosis.

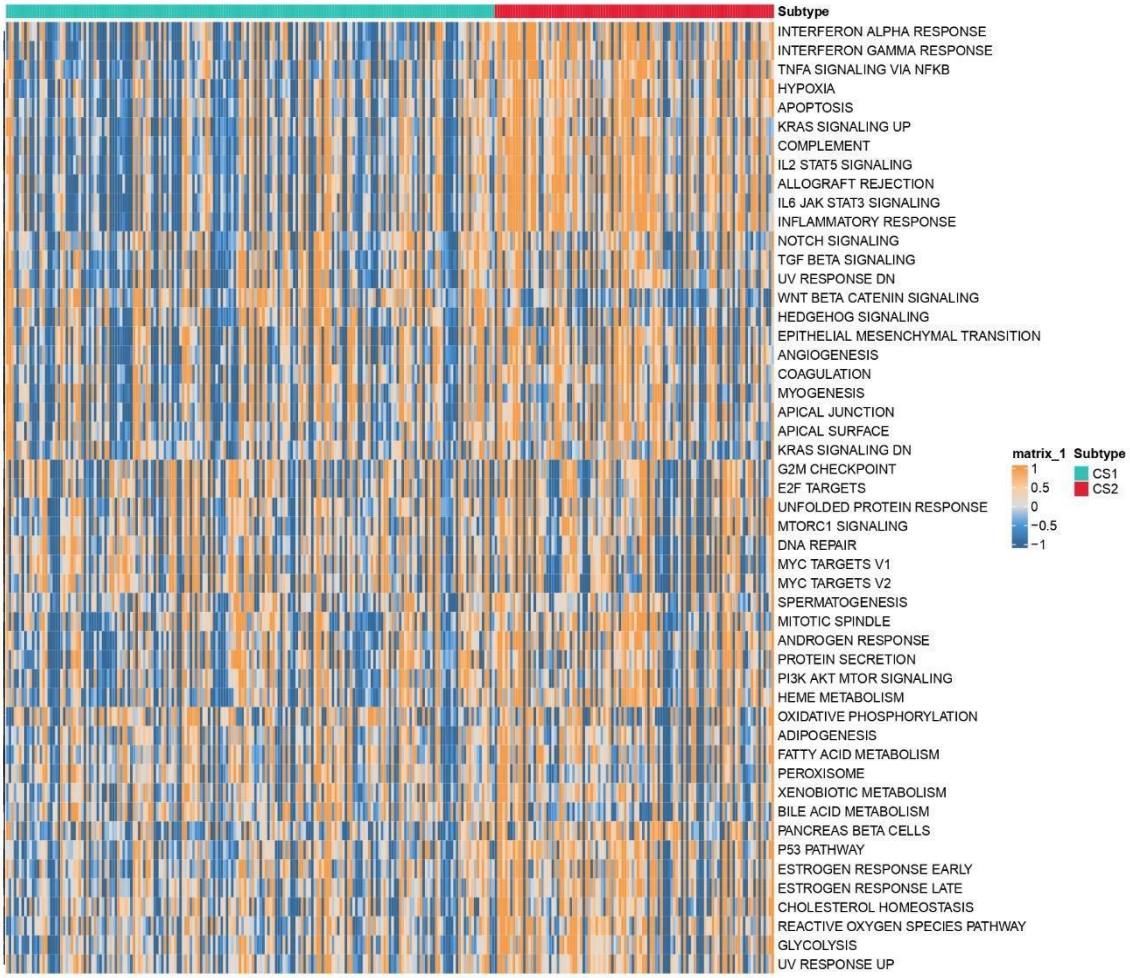


Figure 3.7. Heatmap of enrichment score of tumor-associated pathways for 2 identified subtypes in TCGA-COAD cohort.

3.1.3. The effect of genetic alteration on subtypes

Gene mutations are of crucial importance for the development, progression and metastasis of colon cancer. Mutational gene signatures serve as preventive biomarkers in colon cancer patients and are also very important markers for predicting treatment and prognosis [116, 117]. Therefore, the mutational differences between all subtypes were analysed and promising markers were evaluated. In this analysis, Fisher's exact method was chosen as an independent test for each mutation and Benjamini-Hochberg (BH) as an adjusted p-value method for multiple comparisons. In addition, $p < 0.05$ was chosen as the significance threshold and a Freq.cuttof value of 0.15 was chosen as the mutation cut-off for the data. As shown in Figure 3.8, the analysis of somatic mutations revealed that 297 patients with colon adenocarcinoma had a mutation, and most of them were missense.

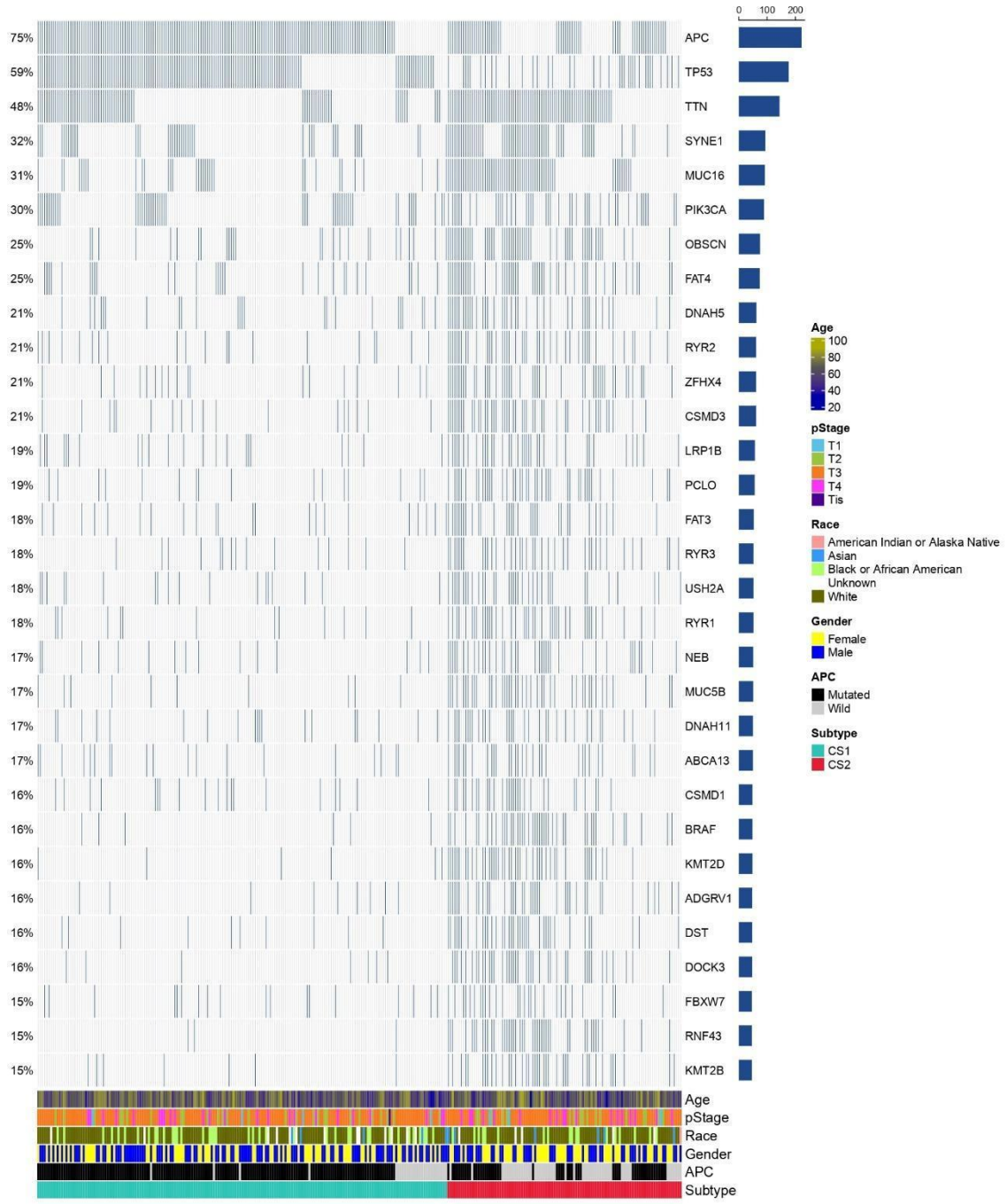


Figure 3.8. Mutational OncoPrint of 2 identified subtypes of colon adenocancinoma in TCGA-COAD cohort.

The overall mutation rate of the thirty mutated genes was at least 15%. Compared to the CS1 subtype, the CS2 subtype had a higher number of mutated genes. APC, TP53, titin (TTN), spectrin repeat containing nuclear envelope protein 1 (SYNE1) and mucin 16 (MUC16) were the five most frequently mutated genes in the colon adenocarcinoma

samples (Table 3.13). APC had the highest mutation frequency, with mutations occurring in 75% of the samples.

Table 3.13. Comparison of mutational frequency among 2 identified subtype of colon adenocarcinoma in TCGA-COAD cohort.

Gene (Mutated)	TMB	CS1	CS2	pvalue	padj
APC	222 (75%)	165 (87.3%)	57 (52.8%)	1.14e-10	3.76e-10
TP53	176 (59%)	140 (74.1%)	36 (33.3%)	7.26e-12	3.42e-11
TTN	144 (48%)	68 (36.0%)	76 (70.4%)	1.10e-08	2.14e-08
SYNE1	94 (32%)	41 (21.7%)	53 (49.1%)	2.28e-06	3.42e-06
MUC16	92 (31%)	33 (17.5%)	59 (54.6%)	5.85e-11	2.15e-10

APC is the most frequently mutated gene in colon cancer and plays a key role in oncogenesis and the progression of colon cancer. It acts as a gatekeeper gene of COAD by inducing apoptosis and is also involved in cell migration, adhesion, transcriptional activation and other processes [118-122]. Considering that inactivation or deletion of the APC tumour suppressor gene occurs in the early stages of COAD development, as indicated by the studies [123], APC mutations could be useful for early diagnosis and personalised treatment of COAD.

In non-hypermutated colorectal cancers, the mutation rate of TP53, which is associated with a poor prognosis, is around 55-60%, making it the second most common mutation observed in colorectal cancer [124-126]. TP53 mutations lead to a poorer prognosis in colon cancer patients treated with chemotherapy than in patients treated with surgery [127, 128].

The titin (TTN) mutation, which has been identified as a risk factor for colon cancer, has the potential to transform the tumour microenvironment into an immunosuppressive type [129]. In addition, abnormal activation of Spectrin Repeat Containing Nuclear Envelope Protein 1 (SYNE1) in colon cancer cell lines has been found in studies to play an oncogenic role in colon cancer by promoting cell proliferation and migration [130].

KRAS, the most frequently mutated gene among the three human ras isoforms, is found in almost a quarter of all cancers, but is also mutated in about 30–40% of colorectal cancers [131]. As a result of the studies, COAD patients with KRAS mutation have been reported to be treatment resistant and have poorer survival [131-133]. Activation of

phosphatidylinositol-4,5-bisphosphate 3-kinase catalytic subunit alpha (PIK3CA), which is mutated in 10-20% of colorectal cancer patients and is involved in the PI3K/Akt signalling pathway, triggers tumour formation [134, 135]. In addition, patients with stage II and III colon cancer who have a PIK3CA mutation have a poorer survival rate than patients without this mutation [136].

APC, TP53 and KRAS mutations, which are considered crucial for the development of colorectal cancer, are more common in the CS1 subtype. These mutations are of great importance for diagnosis, treatment and prognosis, as they control the transition from healthy colon epithelium to cancerous tissue [122, 137]. As a result of the studies, it was found that patients with B-Raf proto-oncogene (BRAF) and PIK3CA mutations respond negatively to treatment with epidermal growth factor receptor (EGFR) inhibitors [138, 139]. Therefore, detection of mutations in the combination of BRAF and PIK3CA can be used to predict patient response to EGFR pathway inhibitors. BRAF was more common in the CS2 group, and the PIK3CA mutation occurred mainly in the CS1 group.

In addition to genetic mutations, colon cancer is also strongly influenced by copy number alterations [117]. Copy number changes lead to genome instability, which promotes the accumulation of mutations in the tumour and triggers the rapid evolution of cancer genomes. Genomic lesions associated with immune checkpoint activation also play a role in patient response to immunotherapy [53]. Therefore, total mutation burden (TMB) and fraction genome altered (FGA) were calculated to measure these genomic alterations that may impact immunotherapy, which has become the critical point of cancer treatment. The FGA values, expressed as the percentage of genomes affected by copy number gains or losses of the two subtypes, i.e. copy number alterations, were analysed first. Compared to the CS2 subtype, the CS1 group had more CNAs in both the lost and gained genomes (Figure 3.9). On the other hand, in the CS2 group, the percentage of genomes gained was higher than that of genomes lost (Table 3.14).

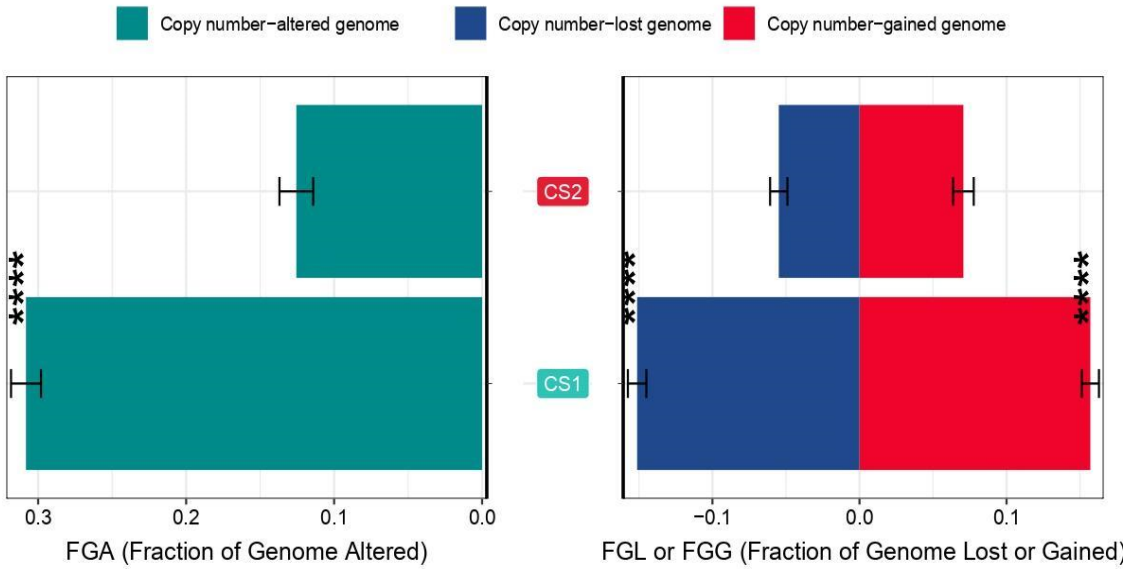


Figure 3.9. Bar plot of fraction genome altered among 2 identified subtypes of colon adenocarcinoma in TCGA-COAD cohort.

Table 3.14. Demo of comparison of fraction genome altered among 2 identified subtype of colon adenocarcinoma in TCGA-COAD cohort.

samID	FGA	FGG	FGL	Subtype
TCGA-3L-AA1B-01A	0.14303125	0.07289238	0.07013886	CS1
TCGA-4N-A93T-01A	0.33418894	0.10710504	0.2270839	CS1
TCGA-4T-AA8H-01A	0.26618216	0.21583491	0.05034725	CS1
TCGA-5M-AAT4-01A	0.44477464	0.19556139	0.24921325	CS1
TCGA-5M-AAT6-01A	0.06718986	0.03419735	0.03299251	CS2

Tumour mutation burden (TMB), defined as the total number of somatic coding errors, base substitutions and indel mutations per million bases of DNA, can be used to assess the response of colon cancer patients to immune checkpoint inhibitor (ICI) therapy [140, 141]. When calculating the TMB, only non-synonymous variables were considered, including frame shift del, frame shift ins, splice site, translation start site, nonsense mutation, nonstop mutation, in frame del, in frame ins and missense mutation. The number of non-synonymous mutations per million bases was calculated to assess the TMB. We observed a significantly higher mean TMB value for CS2 ($P < 0.001$, Figure 3.10) (Table 3.15). Tumours with high TMB levels harbour a high number of neoantigens, making them more likely to be recognised by the immune system and respond to immunotherapy [142]. In addition, single nucleotide variants (SNVs) were visualised after they were classified into transitions and transversions (TiTv).

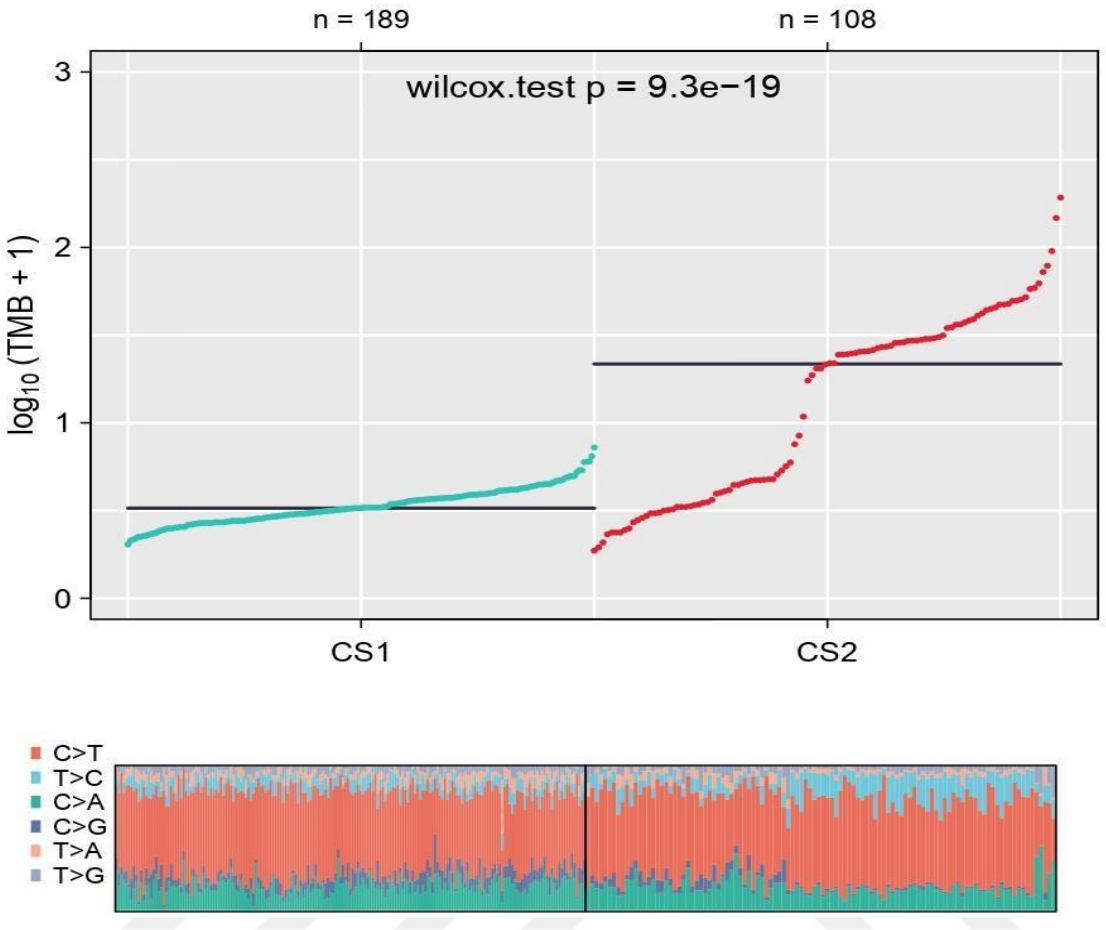


Figure 3.10. Comparison of TMB and TiTv among 2 identified subtypes of colon adenocarcinoma in TCGA-COAD cohort.

Table 3.15. Demo of comparison of TMB among 2 identified subtype of colon adenocarcinoma in TCGA-COAD cohort.

	samID	variants	TMB	log10TMB	Subtype
295	TCGA-A6-2685-01A	39	1.026316	0.3067071	CS1
293	TCGA-A6-A567-01A	43	1.131579	0.3287014	CS1
292	TCGA-CM-5863-01A	44	1.157895	0.3340303	CS1
291	TCGA-CK-6748-01A	45	1.184211	0.3392945	CS1
289	TCGA-CM-5344-01A	47	1.236842	0.3496353	CS1

Moreover, an alluvial diagram was created to visualize how often the present subtypes contained the 5 most common mutant genes in COAD (Figure 3.11).

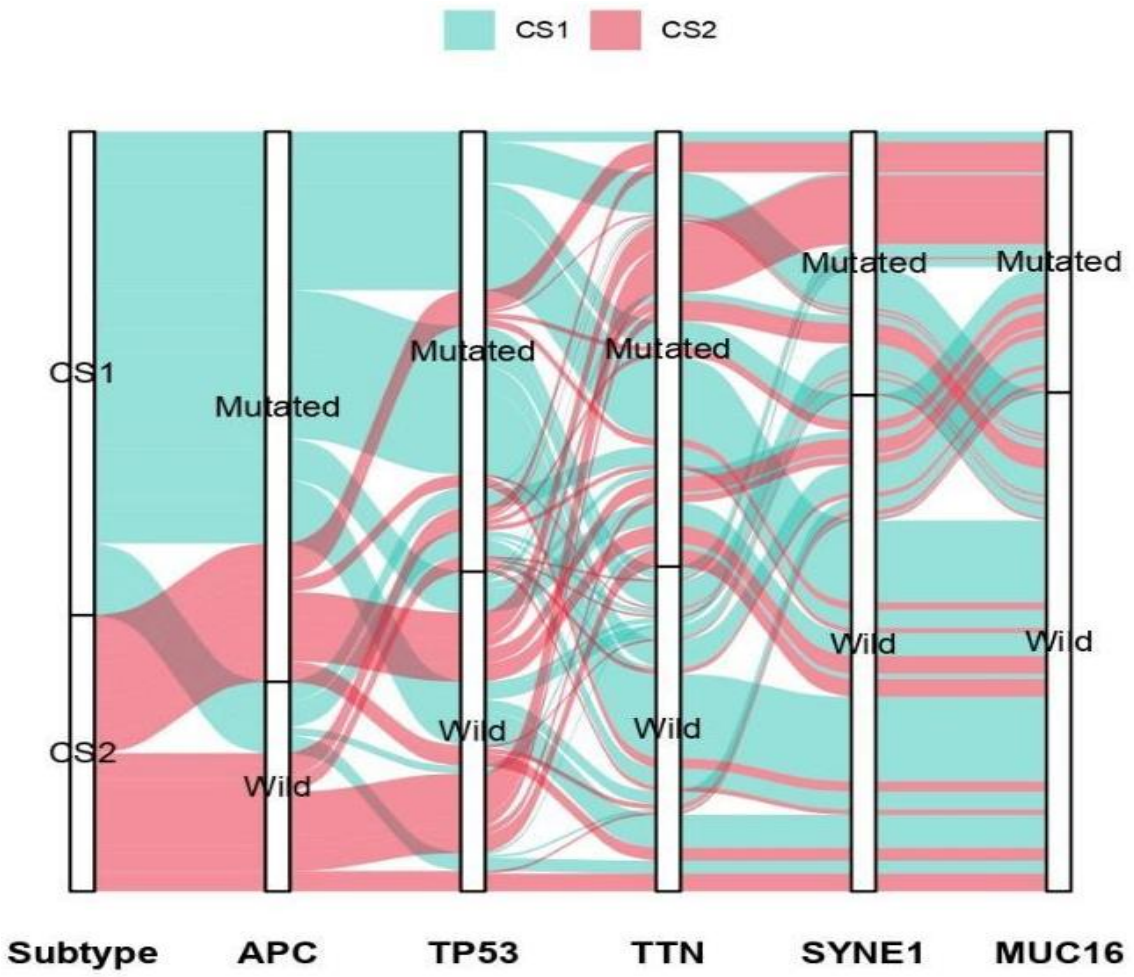


Figure 3.11. Agreement of 2 identified subtypes of colon adenocarcinoma with the most common 5 mutant genes in TCGA-COAD cohort.

3.1.4. Precision treatment recommendations for COAD patients

Chemotherapy is one of the two basic treatment methods for colorectal cancer. Standard protocols are used in the selection of chemotherapeutic agents, taking into account various factors such as the stage of the tumour, the patient's state of health and the overall response rate to the drug [143]. However, incorrect drug selection without taking into account the individual differences of each patient and the biological characteristics of the tumour leads to cellular stress, increases drug resistance and ultimately prevents the success of the treatment. In addition, choosing the wrong drug can lead to potentially fatal side effects. Therefore, it is very important to assess the response of a particular tumour to a particular drug before starting treatment for each patient [144]. Therefore, to enable individualised treatment selection, the potential response to commonly administered

chemotherapeutic agents in COAD patients was assessed by estimating IC50 values based on gene expression profiling and data from the GDSC database. As part of this drug sensitivity analysis, in addition to analysing the chemotherapeutic agents commonly used in the treatment of COAD, sensitivity analyses of 249 packaged drugs that could be potentially promising for the treatment of COAD were performed. In this way, the sensitivities of subtypes, which are differentiated according to their molecular characteristics, were determined.

Here, the response of each subtype to some of the most commonly used and promising drugs in the treatment of colon cancer is analysed in detail. A list of the drugs to which the subtypes responded statistically significantly among 249 drugs is presented in Appendix B.1. When analysing drug sensitivity, the IC50 criterion was used to determine the efficacy of a drug. The IC50 value indicates how much drug is needed to inhibit half of a certain biological process. This gives an idea of the effect of antagonistic drugs that bind to the receptor in question and prevent its biological activation. A high IC50 value indicates drug resistance, while a low value indicates a better effect of the drug.

Chemotherapy is a treatment method that can be used for patients with advanced colon cancer. 5-Fluorouracil is one of the most commonly used chemotherapeutic agents as it improves survival rates. However, its mechanism of action in patients with advanced colon cancer decreases to 10% [145]. CS2 subtype patients have lower IC50 values for 5-fluorouracil than CS1 patients, which means that CS2 patients benefit more from treatment with 5-FU (Figure 3.12).

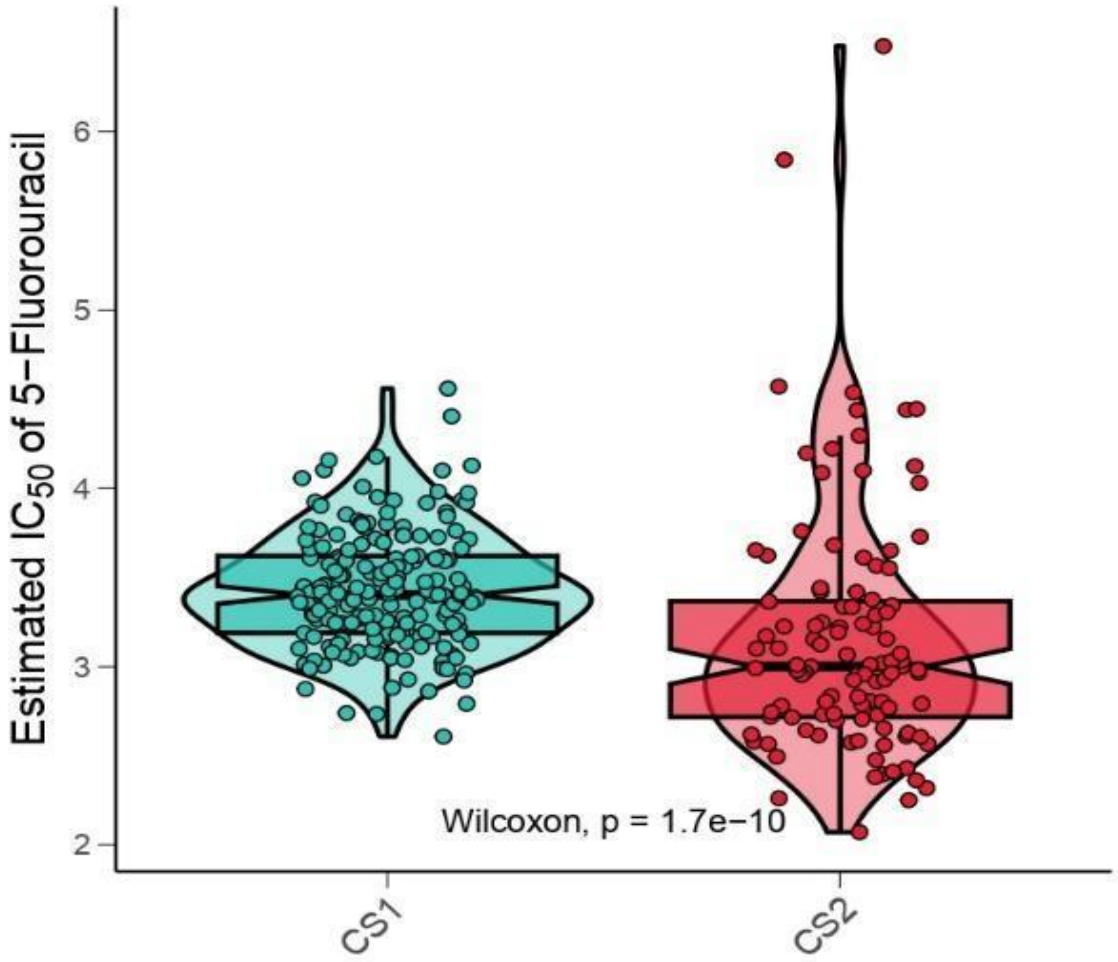


Figure 3.12. Boxviolin for estimated IC50 of 5-Fluorouracil among 2 identified subtypes of colon adenocarcinoma in TCGA-COAD cohort.

While the CS1 subtype shows a high resistance to cisplatin, one of the most effective chemotherapeutic agents for colon cancer [146], with high IC50 values, CS2 patients show a better response (Figure 3.13).

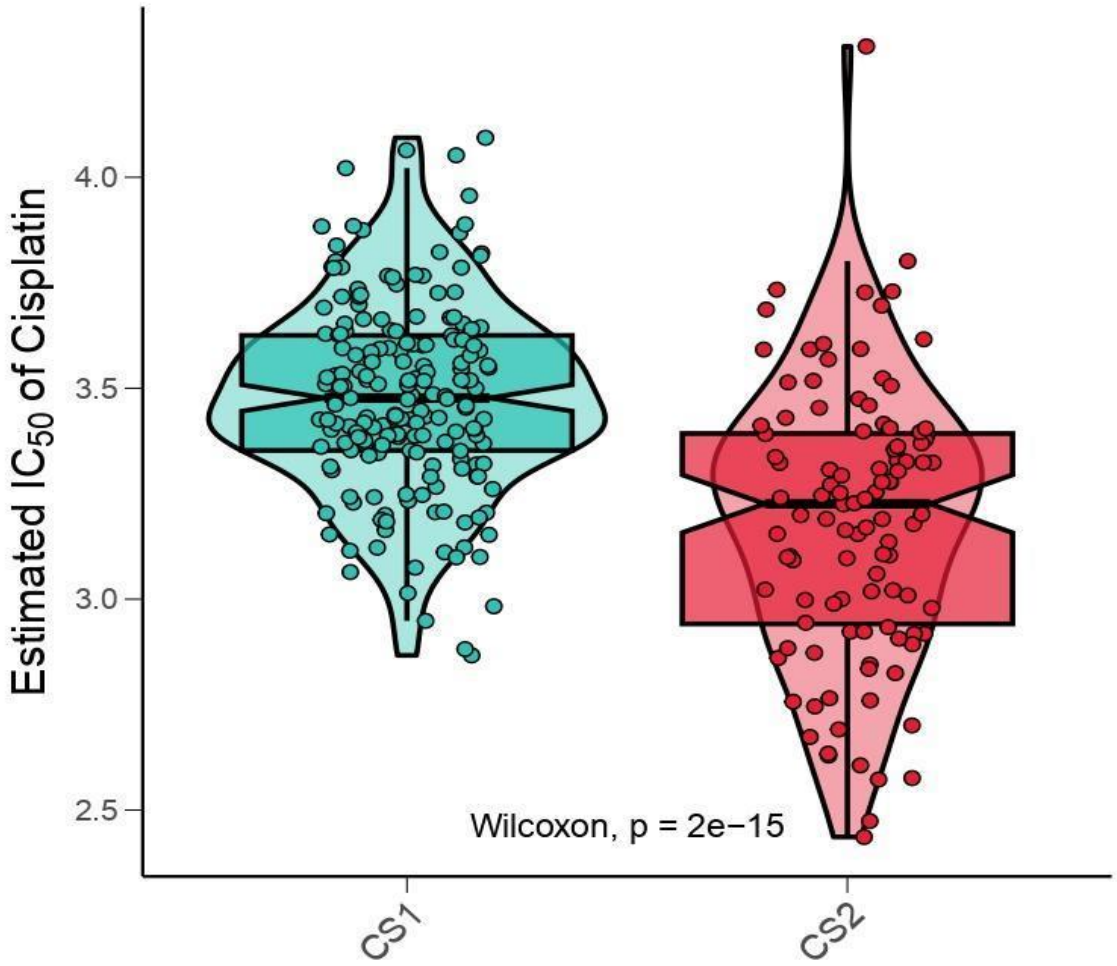


Figure 3.13. Boxviolin for estimated IC50 of Cisplatin among 2 identified subtypes of colon adenocarcinoma in TCGA-COAD cohort.

CS2 patients respond better to paclitaxel, which has anti-cancer properties by playing a role in proliferation and apoptosis and is used in the treatment of advanced colon cancer (Figure 3.14) [147, 148].

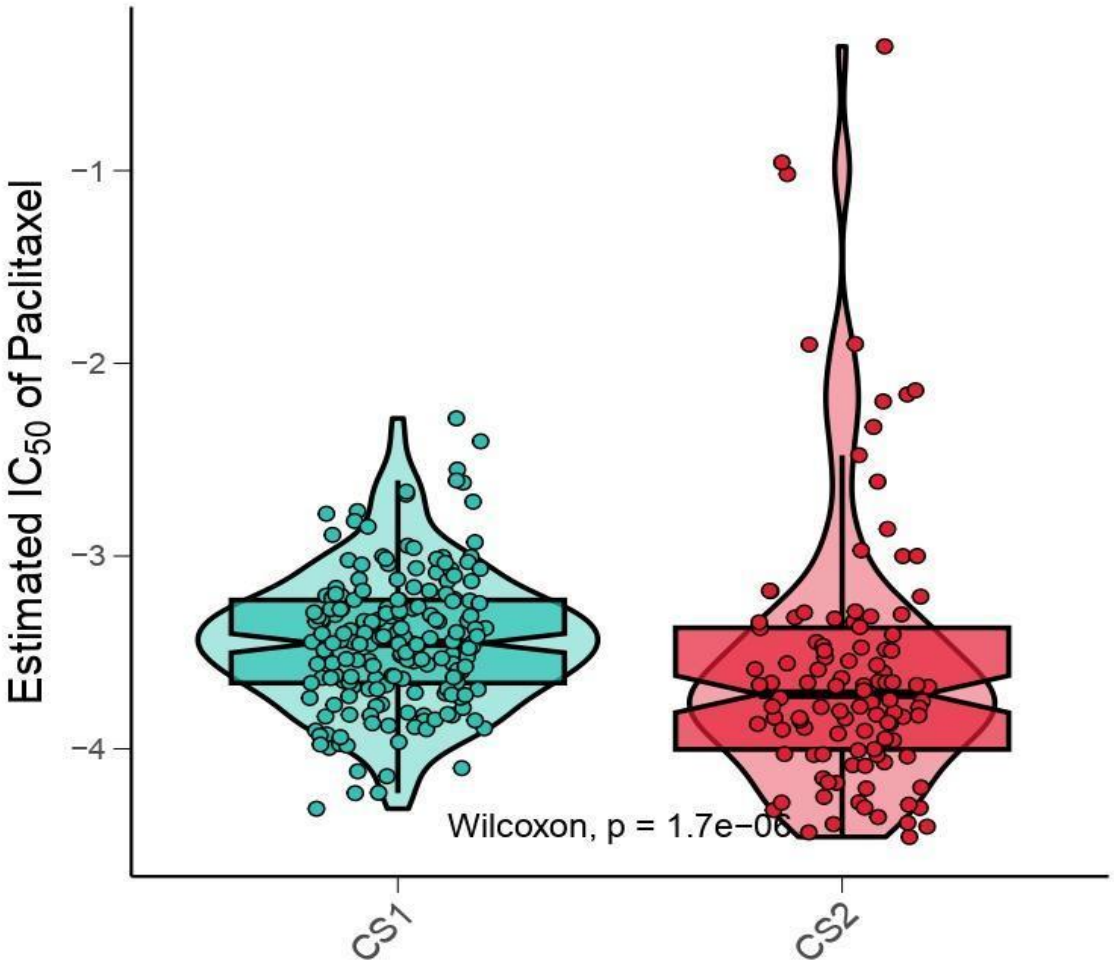


Figure 3.14. Boxviolin for estimated IC50 of Paclitaxel among 2 identified subtypes of colon adenocarcinoma in TCGA-COAD cohort.

Some cancer cells can become resistant to treatment under hypoxic conditions [149]. SN-38, which acts as an active metabolite of irinotecan, a common chemotherapeutic agent for colorectal cancer, overcomes chemoresistance in a hypoxic environment, resulting in an antitumour effect in colon cancer [150]. As a result of the analysis, it was found that CS2 patients responded better to SN-38 than CS1 patients (Figure 3.15).

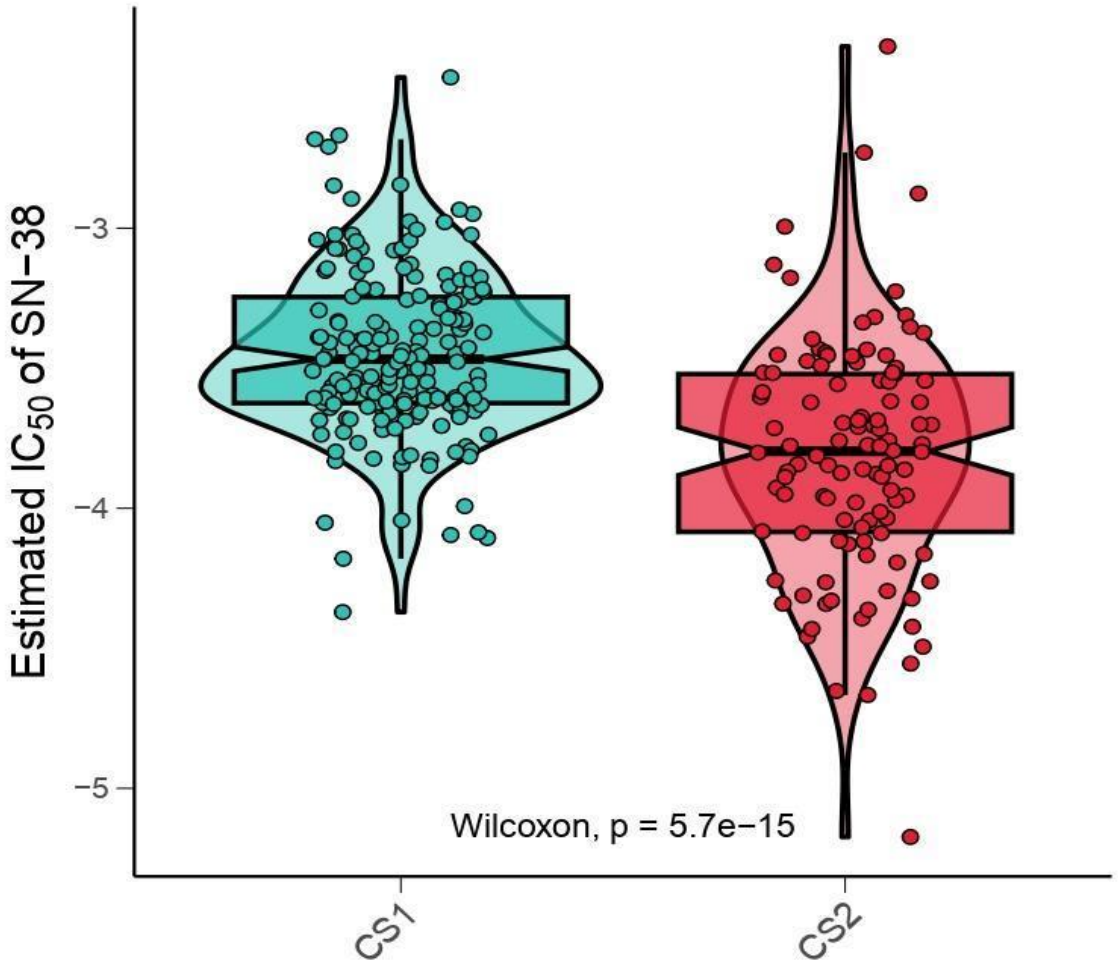


Figure 3.15. Boxviolin for estimated IC50 of SN-38 among 2 identified subtypes of colon adenocarcinoma in TCGA-COAD cohort.

Rapamycin (Rapa), which is used as an immunosuppressant, also exhibits antitumour properties by inhibiting cell proliferation and inducing apoptosis [151]. Some studies have reported that the combination of Rapa and 5-FU reveals the antitumour property of Rapa and thus suppresses the progression of colon cancer [152, 153]. The CS1 subtype responded significantly better to treatment with Rapa, which could be promising for the treatment of colon cancer (Figure 3.16).

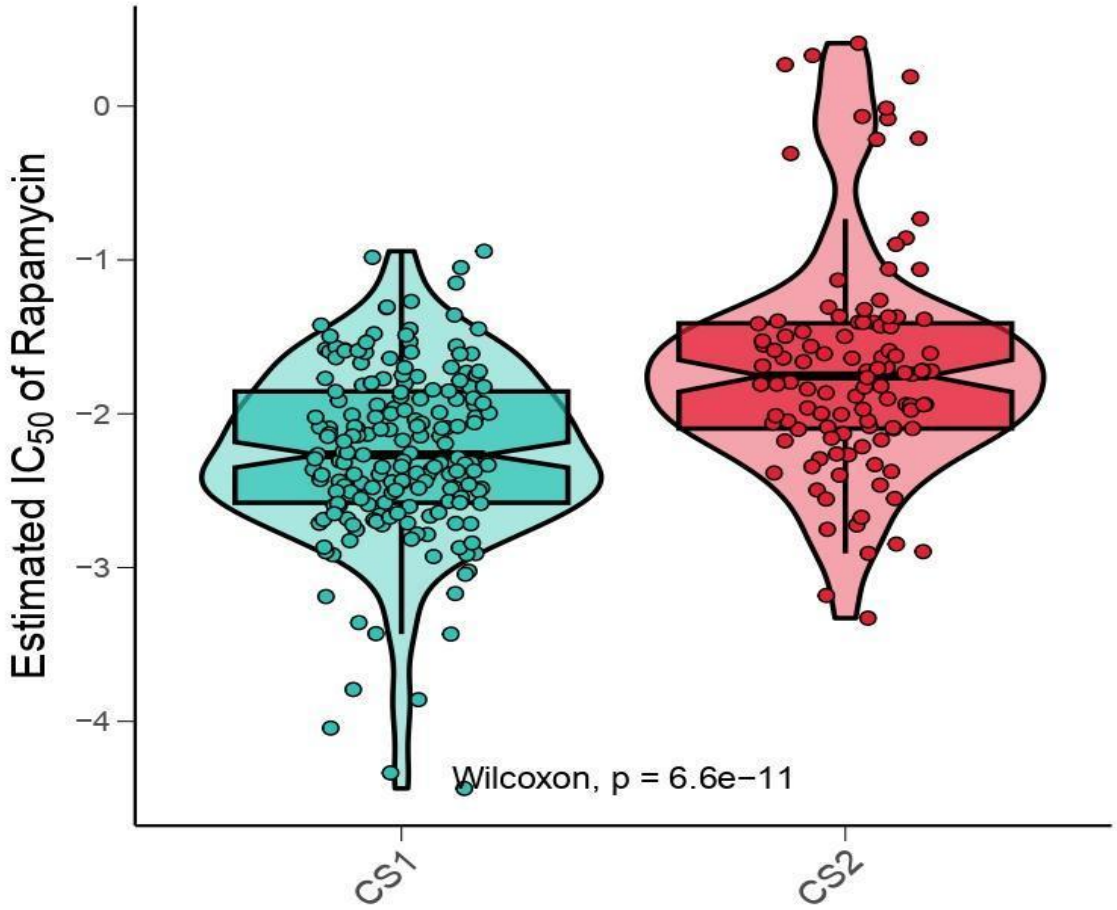


Figure 3.16. Boxviolin for estimated IC50 of Rapamycin among 2 identified subtypes of colon adenocarcinoma in TCGA-COAD cohort.

While differentiated cancer cells are destroyed during treatment with cytotoxic drugs, resistant stem-like cancer cells, which can cause relapse, are not destroyed and show high expression under normoxic conditions. Activation of receptor tyrosine kinases reduces the sensitivity of COAD to cytotoxic drugs, making them resistant to treatment. In 2019, Kotlarz and colleagues [154] investigated the effect of imatinib, which inhibits receptor tyrosine kinases, on resistance to cytotoxic drugs after conventional cytotoxic therapy. They reported that the number of cells resistant to 5-FU after cytotoxic treatment decreased under both normoxic and hypoxic conditions after treatment with imatinib. Therefore, imatinib, which can be used to inhibit tumour growth after chemotherapy and to reduce the expression of stem-like cancer cells that can trigger relapse, showed a much better effect in the CS2 type (Figure 3.17).

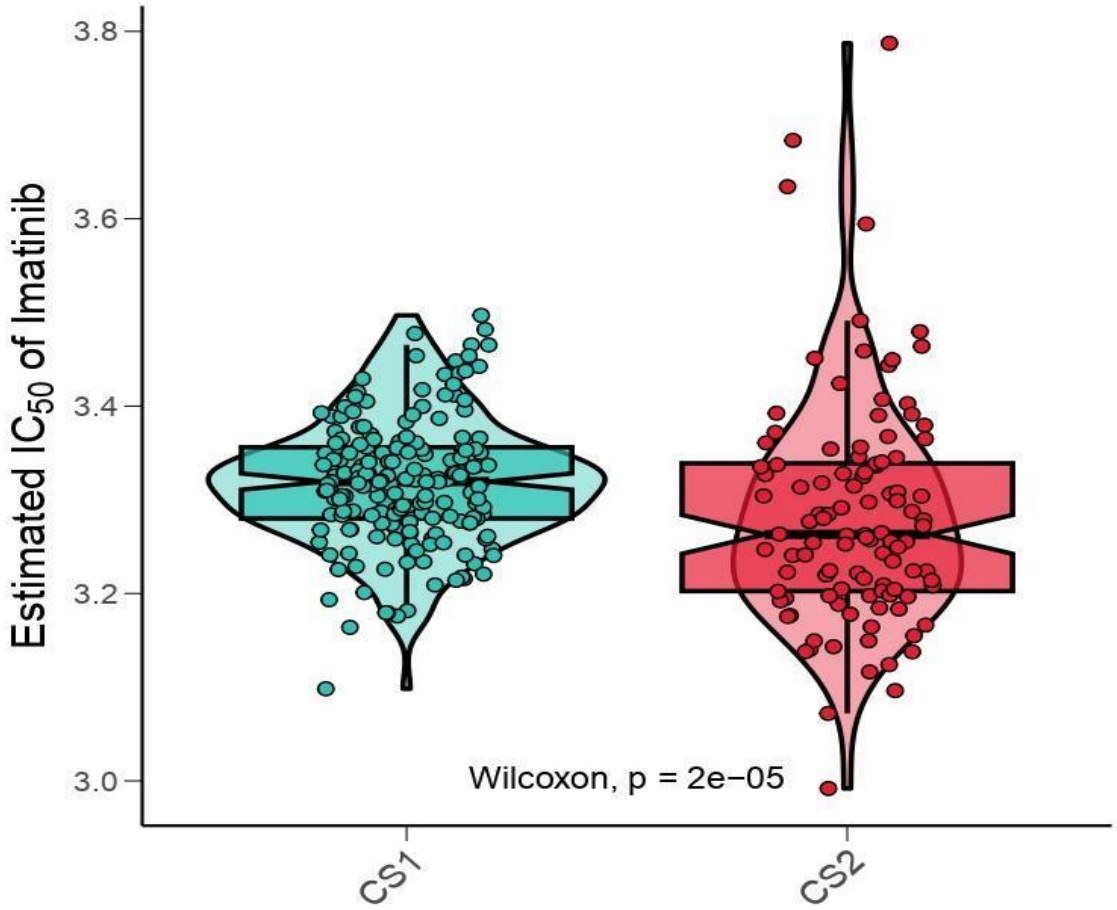


Figure 3.17. Boxviolin for estimated IC50 of Imatinib among 2 identified subtypes of colon adenocarcinoma in TCGA-COAD cohort.

3.1.5. Validation of subtypes in four external cohorts

Four external cohorts GSE39582, GSE16125, GSE17536 and GSE17537 were used to validate the reliability of the subtypes. Subtype-specific upregulated biomarkers previously identified with edgeR, DESeq2 and limma were used to confirm the current subtypes of patients in external cohorts. Estimates were made in each cohort using the NTP method based on specific upregulation of biomarkers in the subtypes, one of two model-independent approaches used for subtype prediction in the validation cohort. Another subtype prediction method is to train a PAM classifier in the discovery cohort to predict the subtype for the patients in the external validation cohort, and each sample in the validation cohort is assigned a subtype label with the highest Pearson correlation with the central sample. Finally, the IGP statistic was performed to assess the similarity and

reproducibility of the subtypes identified between the discovery and validation cohorts. Subtype prediction was then performed using NTP and PAM for the discovery dataset. Subsequently, the agreement between the subtypes present in the discovery dataset and the subtypes predicted by NTP and PAM was measured using the kappa statistic. In addition, the accuracy and agreement between the subtype predicted by NTP and PAM were analysed in the validation cohort.

First, NTP was performed for the prediction of subspecies with edgeR, DESeq2 and limma in GSE16125 (Figure 3.18-3.20). As a result of the NTP analysis performed based on the biomarkers predicted using edgeR, only the CS2 subtype matched 1 sample in the GSE16125 dataset, which consists of 32 samples, while no sample matches were detected between the subtypes using the biomarkers obtained as a result of DESeq2. On the other hand, in the NTP analysis based on the Limma results, CS1 and CS2 were matched with 12 and 11 samples, respectively, showing that a better subtyping analysis was obtained with Limma compared to the other two algorithms.

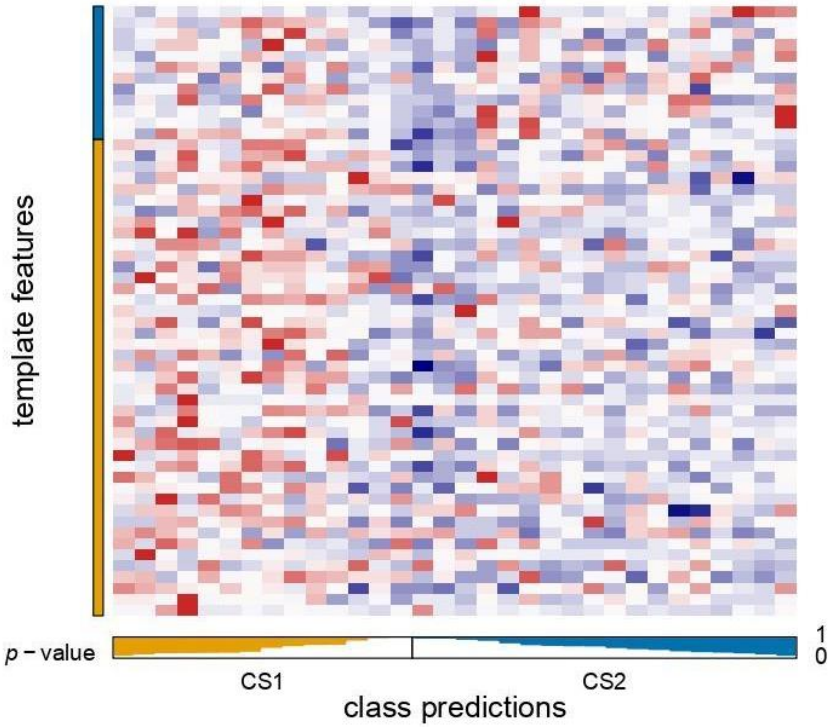


Figure 3.18. Heatmap of NTP in GSE16125 cohort using subtype-specific upregulated biomarkers identified using edgeR from TCGA-COAD cohort.

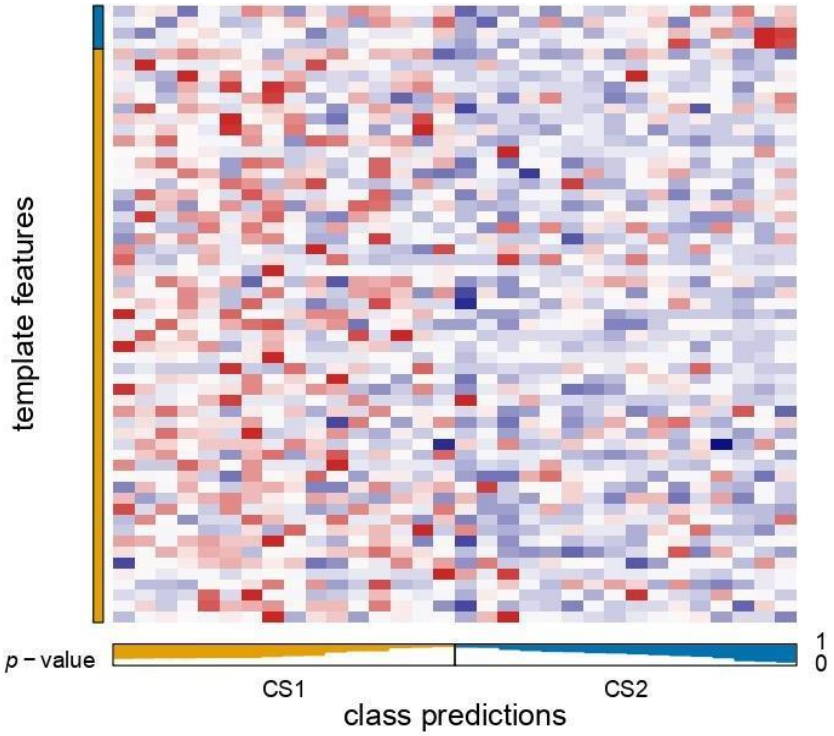


Figure 3.19. Heatmap of NTP in GSE16125 cohort using subtype-specific upregulated biomarkers identified using DESeq2 from TCGA-COAD cohort.

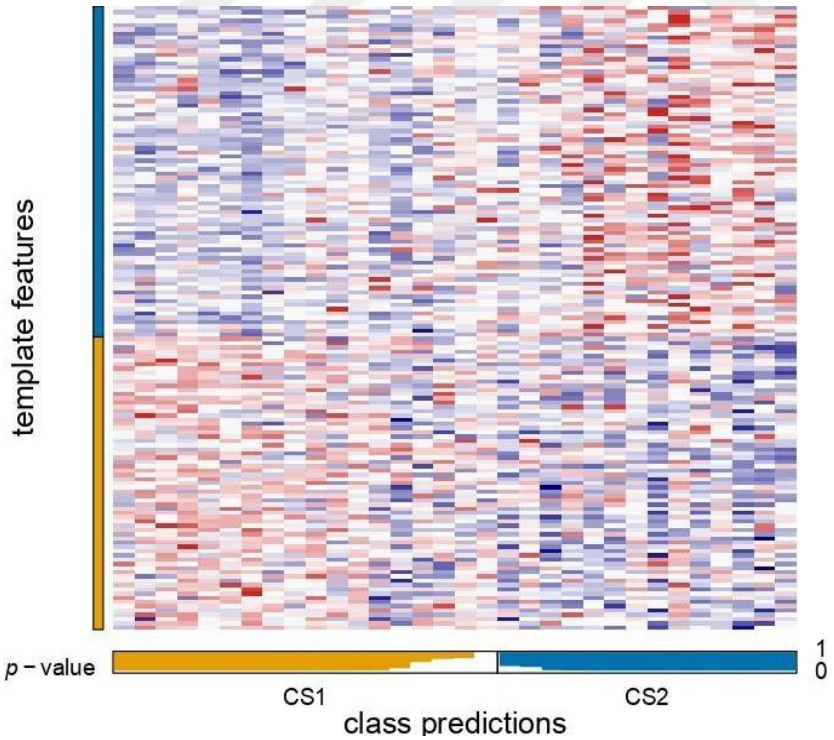


Figure 3.20. Heatmap of NTP in GSE16125 cohort using subtype-specific upregulated biomarkers identified using limma from TCGA-COAD cohort.

In addition, a survival analysis of the subtypes predicted by NTP was performed in the validation cohort based on the edgeR, DESeq2 and limma methods. According to the

results of the edgeR and DESeq2 algorithms, a statistically significant difference in the survival rates of patients in the GSE16125 cohort was observed (Figure 3.21-3.22). The survival analysis performed in this cohort showed that the clinical prognosis of CS2 was worse than that of CS1 in both edgeR and DESeq2 results, but the result of the survival analysis performed with the markers obtained by the Limma algorithm was not statistically significant (Figure 3.23).

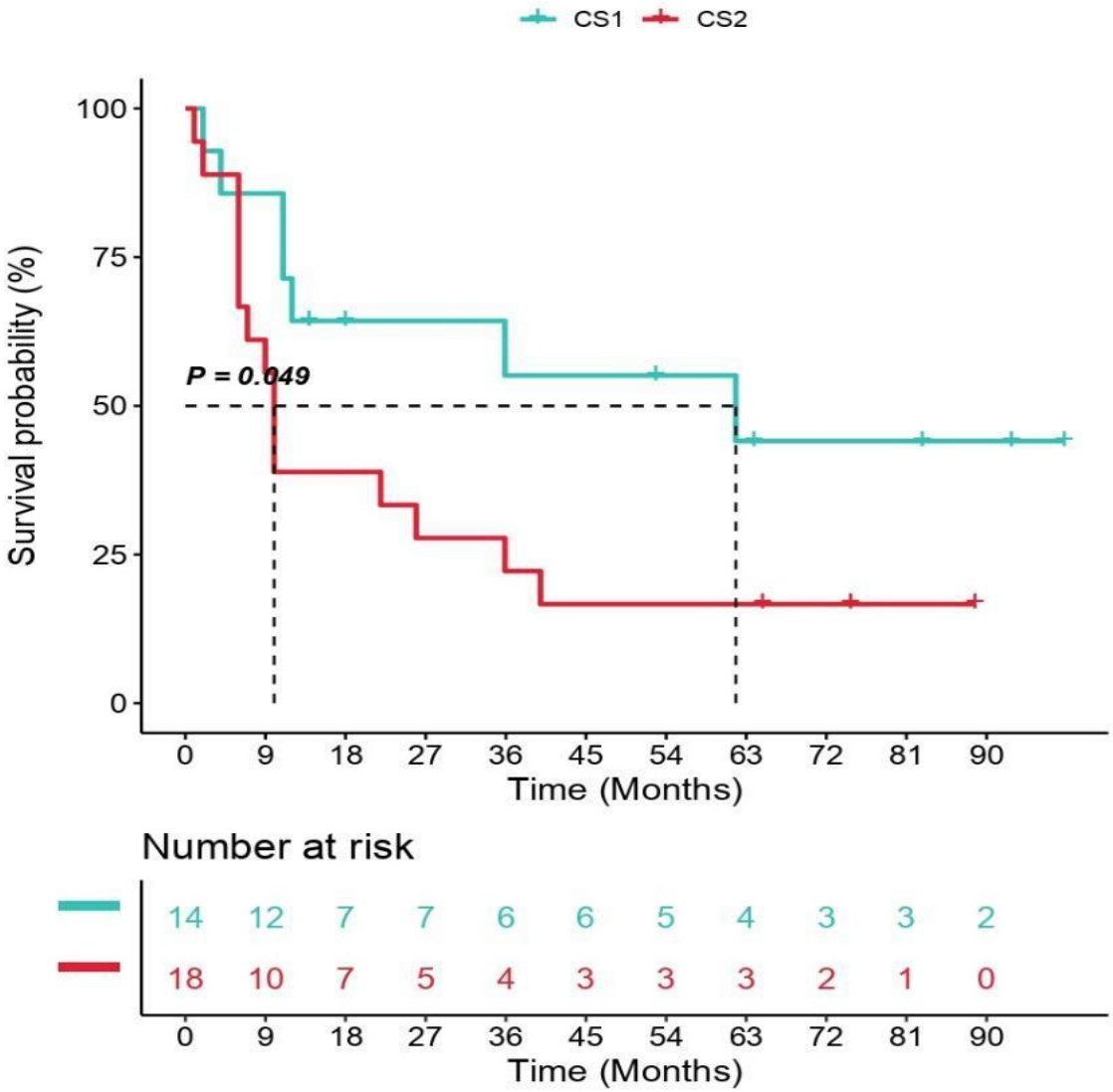


Figure 3.21. Kaplan-Meier survival curve of 2 colon adenocarcinoma subtypes predicted by edgeR in the GSE16125 cohort.

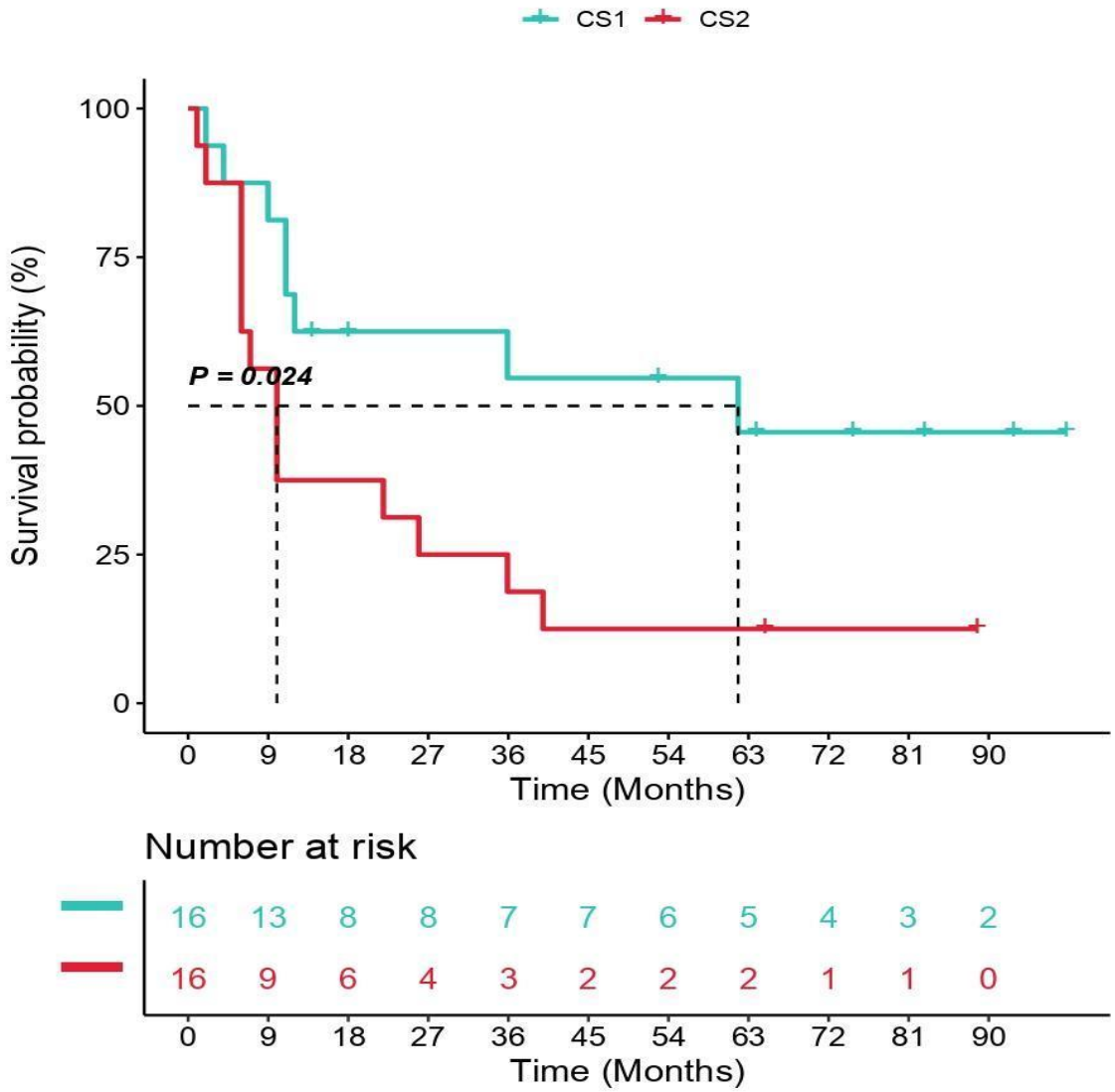


Figure 3.22. Kaplan-Meier survival curve of 2 colon adenocarcinoma subtypes predicted by DESeq2 in the GSE16125 cohort.

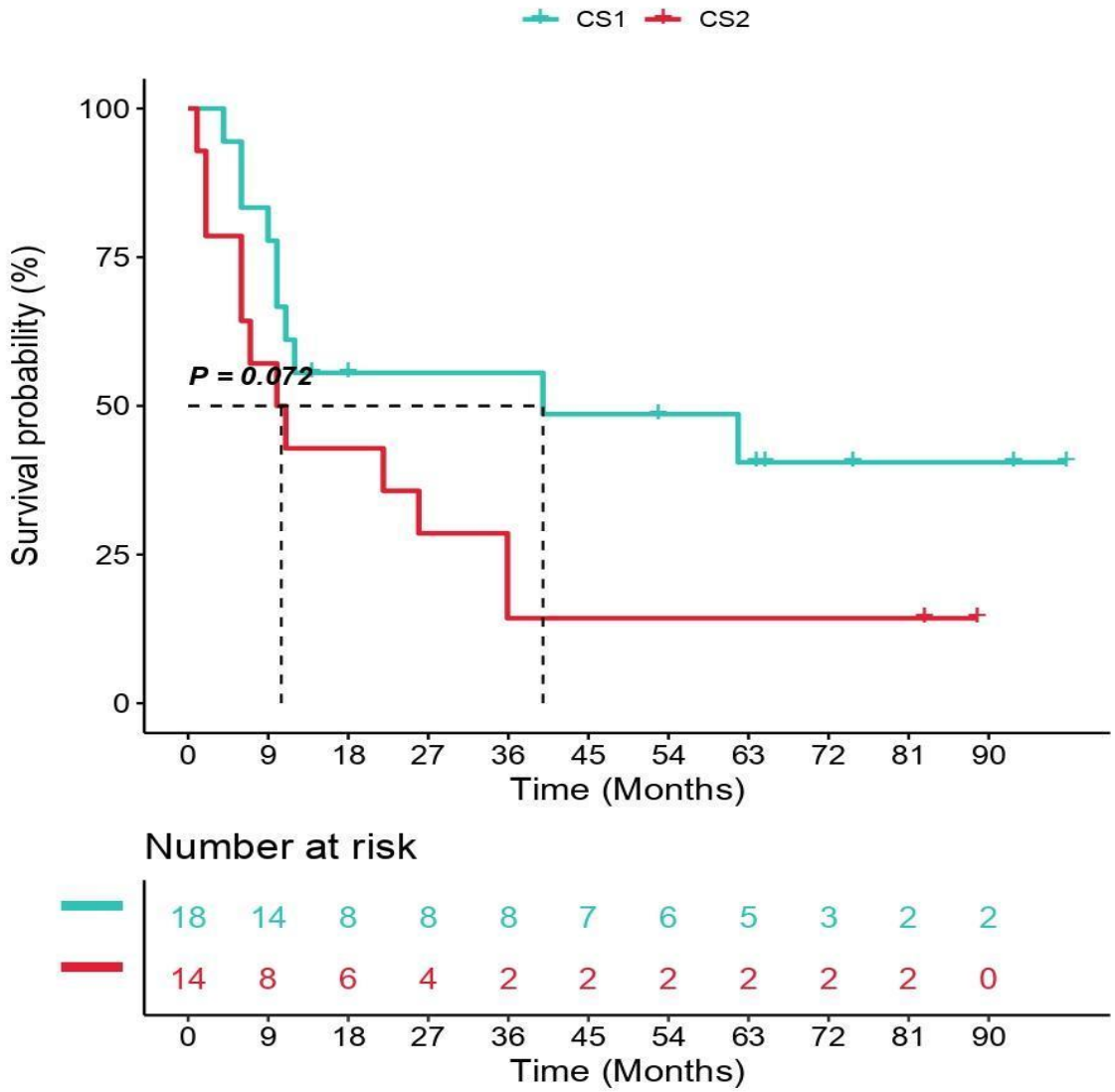


Figure 3.23. Kaplan-Meier survival curve of 2 colon adenocarcinoma subtypes predicted by limma in the GSE16125 cohort.

Another method for subtype prediction is to train a PAM classifier in the discovery group to predict the subtype for patients in the external validation group. The similarity and reproducibility of subtypes identified by PAM was assessed using the IGP statistic. As can be seen in Table 3.16, the IGP statistic of the GSE16125 cohort was close to 1. It was concluded that the subtypes identified between the discovery and validation groups were similar and reproducible.

Table 3.16. IGP information in four validation cohorts of the PAM classifier trained on the TCGA-COAD cohort.

Dataset Name	CS1	CS2
GSE16125	0.8750	0.8125
GSE39582	0.7870968	0.7896825
GSE17536	0.7755102	0.8101266
GSE17537	0.7692308	0.8275862

The results of the kappa statistic can be between -1 and +1, where 0 stands for a match that would be expected by chance, while 1 stands for a perfect match between the raters [155]. According to the results of edgeR (Figure 3.24-3.25), the agreement between the subtypes present in the TCGA dataset and the subtypes predicted by NTP was much more significant than those predicted by PAM, while according to the results of DESeq2 (Figure 3.26-3.27) and limma (Figure 3.28-3.29), the subtypes predicted by PAM were much more significant.

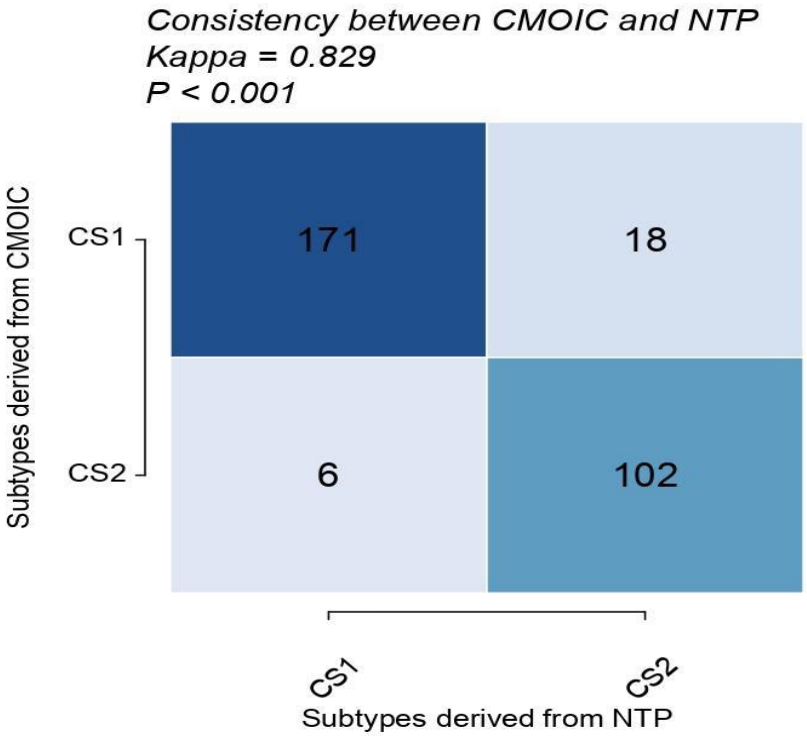


Figure 3.24. Consistency heatmap between current and NTP-predicted Kappa statistics for edgeR results in TCGA-COAD cohort.

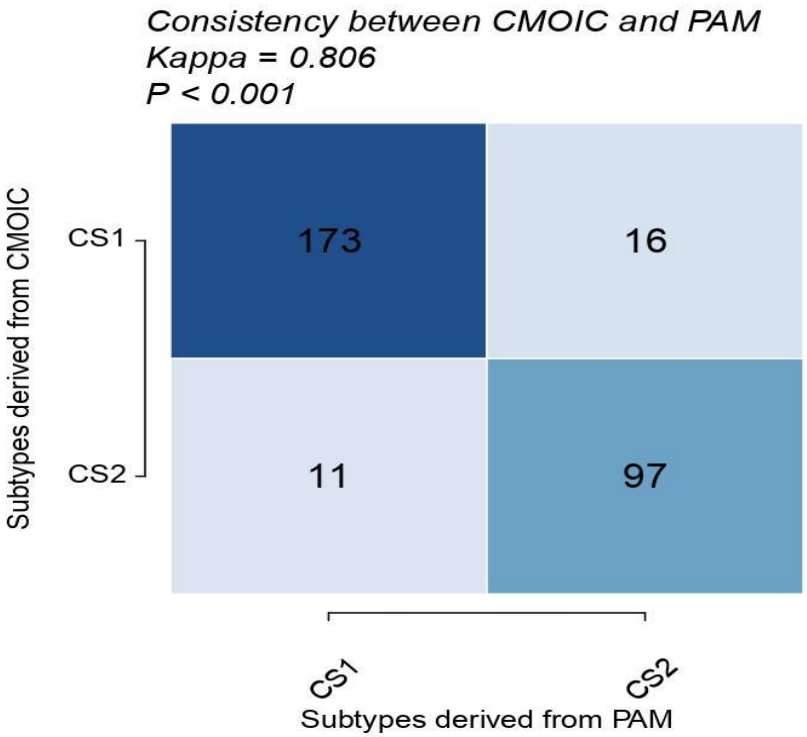


Figure 3.25. Consistency heatmap between current and PAM-predicted Kappa statistics for edgeR results in TCGA-COAD cohort.

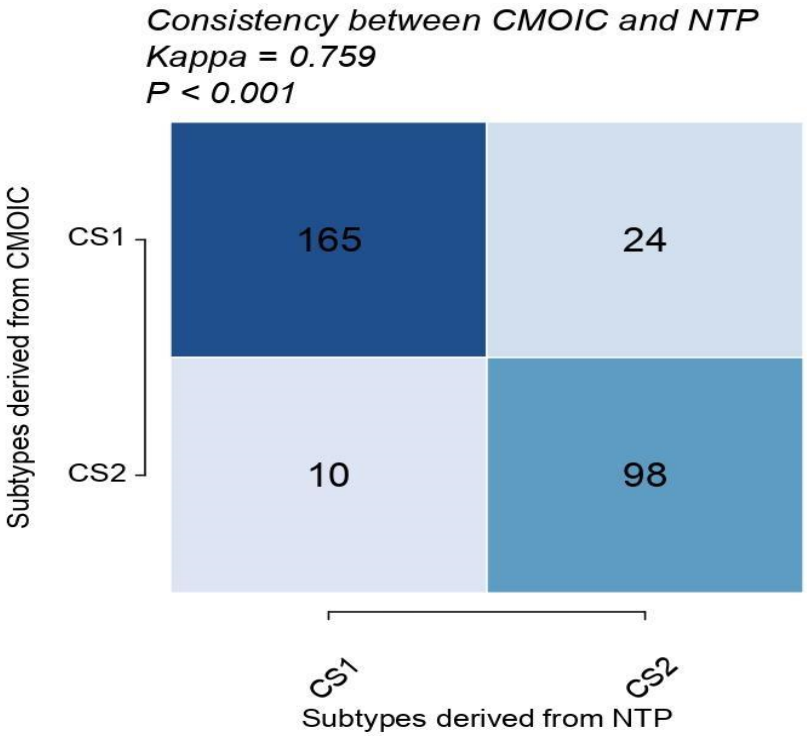


Figure 3.26. Consistency heatmap between current and NTP-predicted Kappa statistics for DESeq2 results in TCGA-COAD cohort.

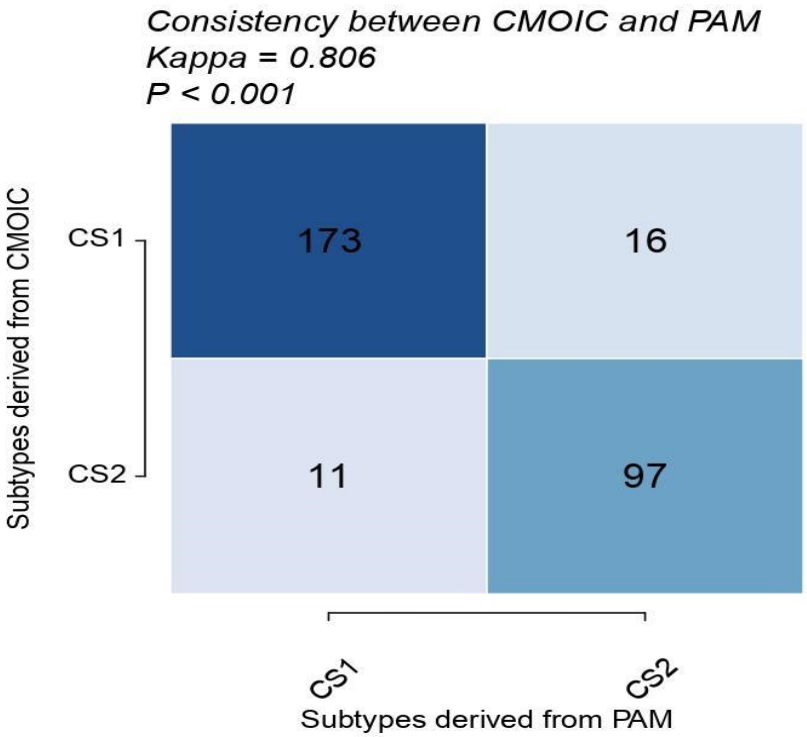


Figure 3.27. Consistency heatmap between current and PAM-predicted Kappa statistics for DESeq2 results in TCGA-COAD cohort.

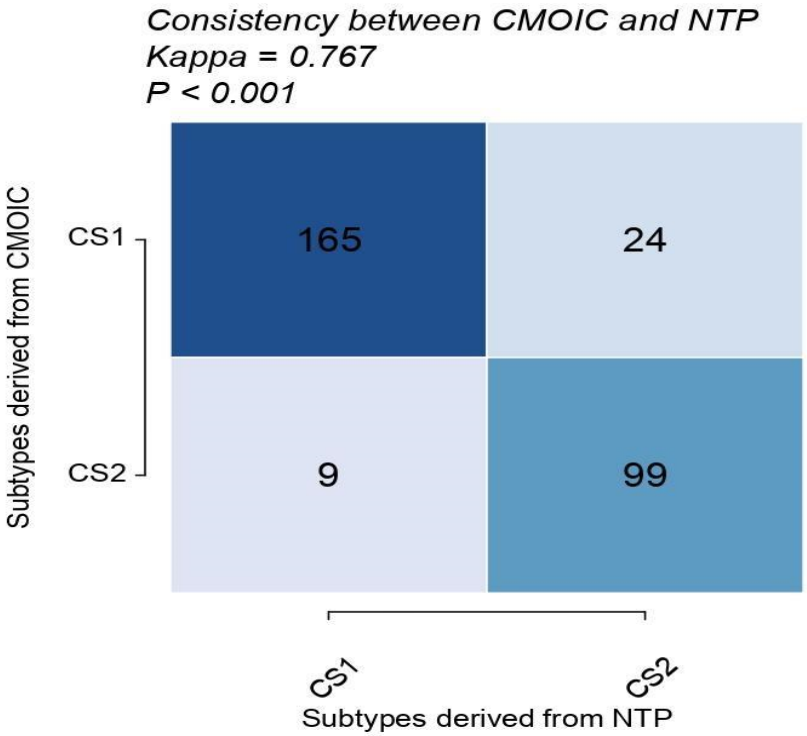


Figure 3.28. Consistency heatmap between current and NTP-predicted Kappa statistics for limma results in TCGA-COAD cohort.

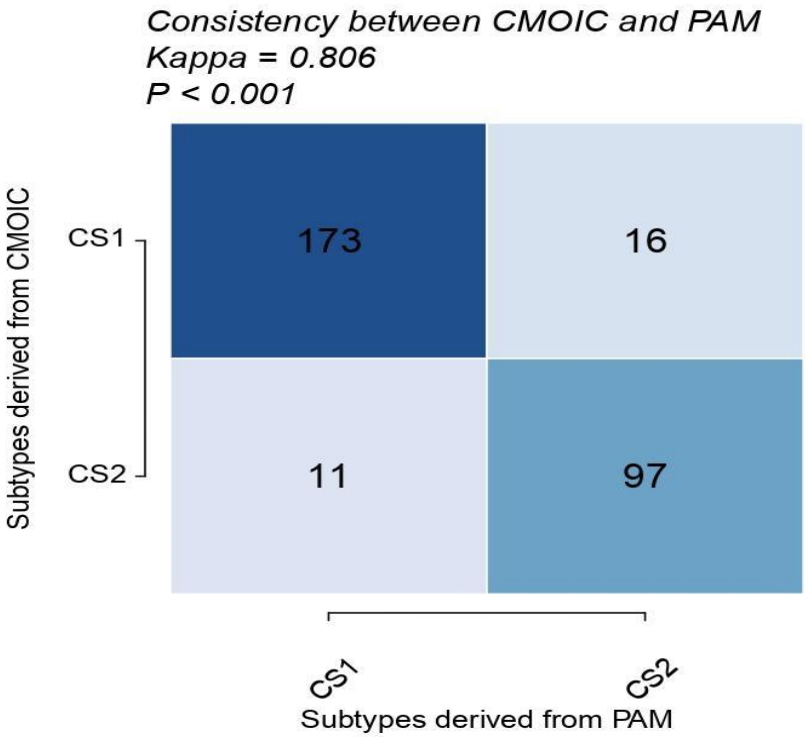


Figure 3.29. Consistency heatmap between current and PAM-predicted Kappa statistics for limma results in TCGA-COAD cohort.

The results of edgeR and DESeq2 also show that the agreement between the subtypes detected by NTP and PAM in the GEO dataset is 0.375 (Figure 3.30-3.31). In other words, the agreement between the subtypes detected by NTP and PAM in the validation dataset is defined as fair. According to the results of Limma, the agreement between them is 0.750, which is quite high (Figure 3.32).

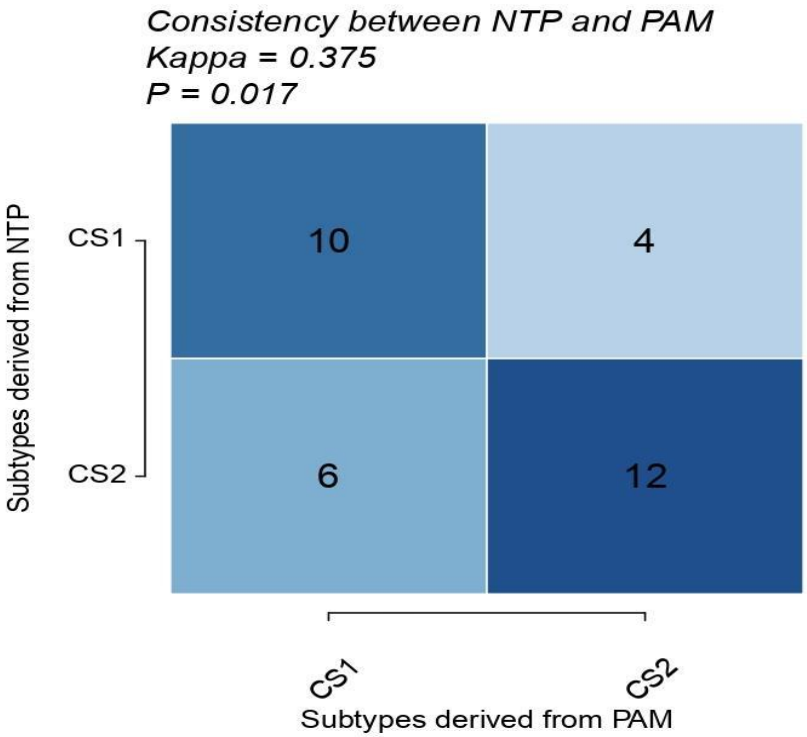


Figure 3.30. Consistency heatmap between NTP and PAM-predicted subtype for edgeR results in GSE16125.

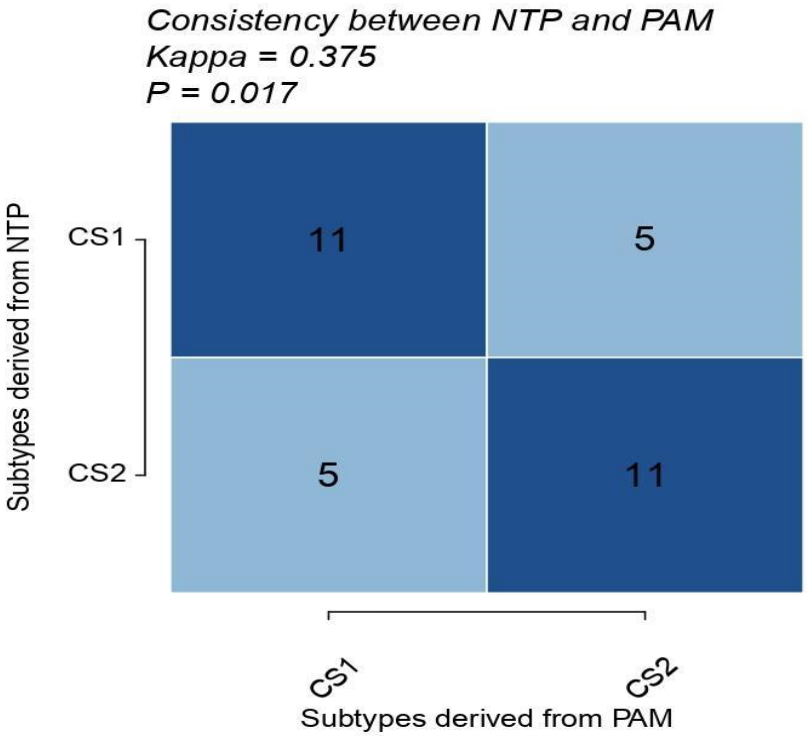


Figure 3.31. Consistency heatmap between NTP and PAM-predicted subype for DESeq2 results in GSE16125.

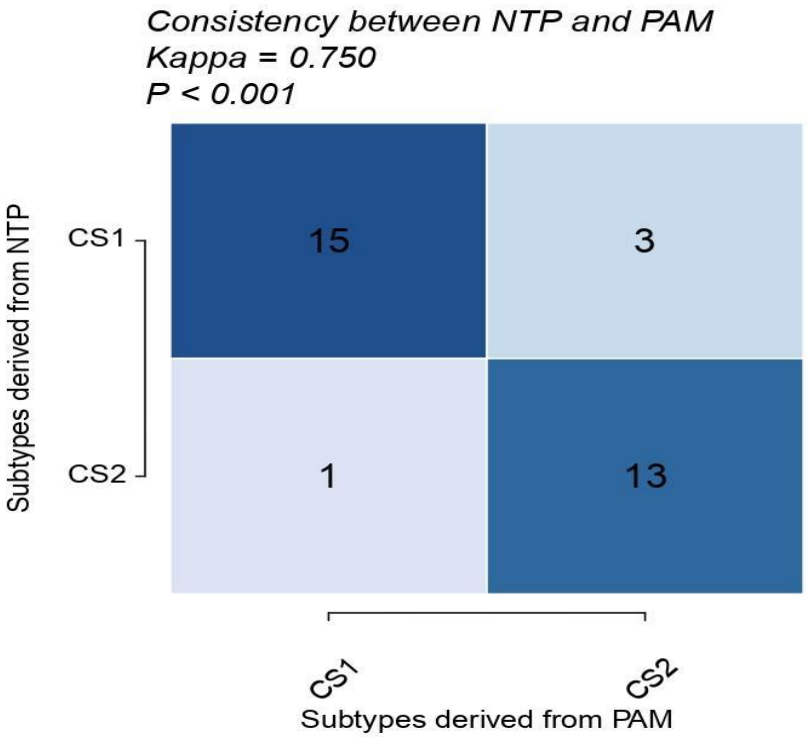


Figure 3.32. Consistency heatmap between NTP and PAM-predicted subtype for limma results in GSE16125.

To predict subtypes in the GSE39582 cohort, which consists of 562 samples, NTP was performed based on upregulated markers detected with edgeR, DESeq2 and limma in the discovery dataset (Figures 3.33-3.35). However, as a result of the NTP analysis based on the edgeR and DESeq2 results, none of the 562 samples could be assigned to the corresponding subtypes. On the other hand, as a result of the NTP performed with limma, 261 patients were categorised in CS1 and 185 patients in CS2.

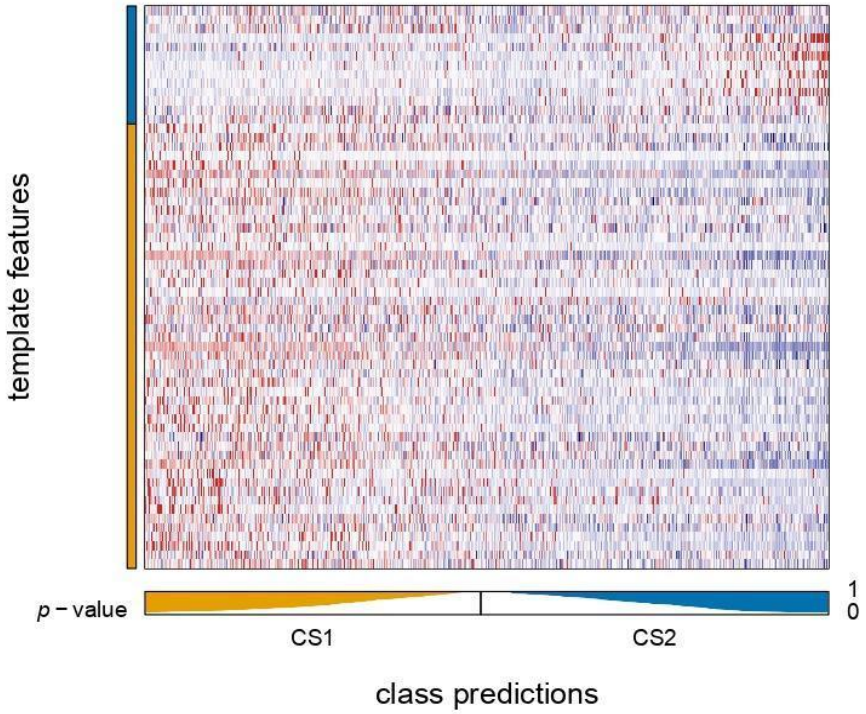


Figure 3.33. Heatmap of NTP in GSE39582 cohort using subtype-specific upregulated biomarkers identified using edgeR from TCGA-COAD cohort.

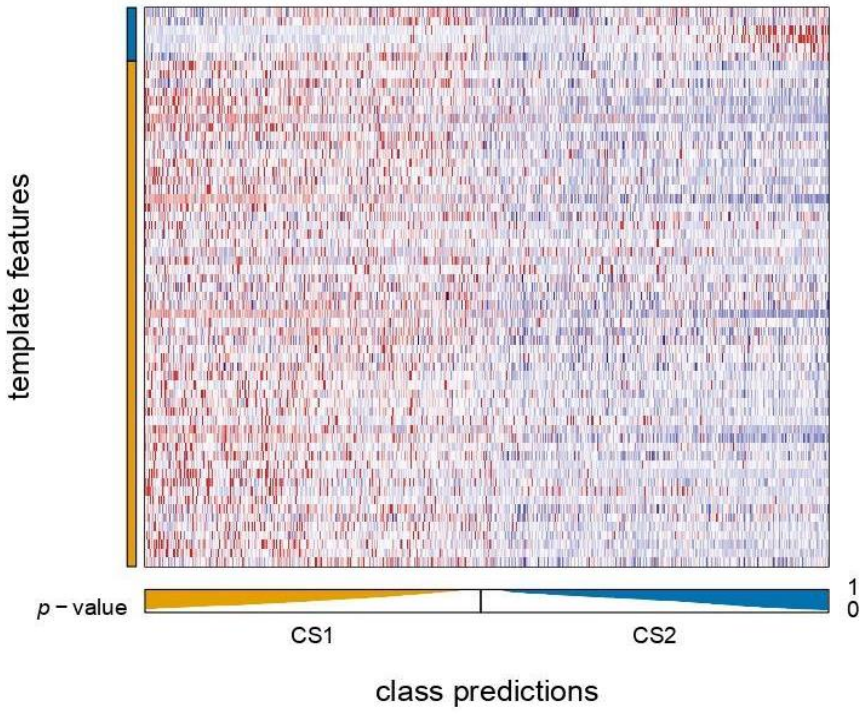


Figure 3.34. Heatmap of NTP in GSE39582 cohort using subtype-specific upregulated biomarkers identified using DESeq2 from TCGA-COAD cohort.

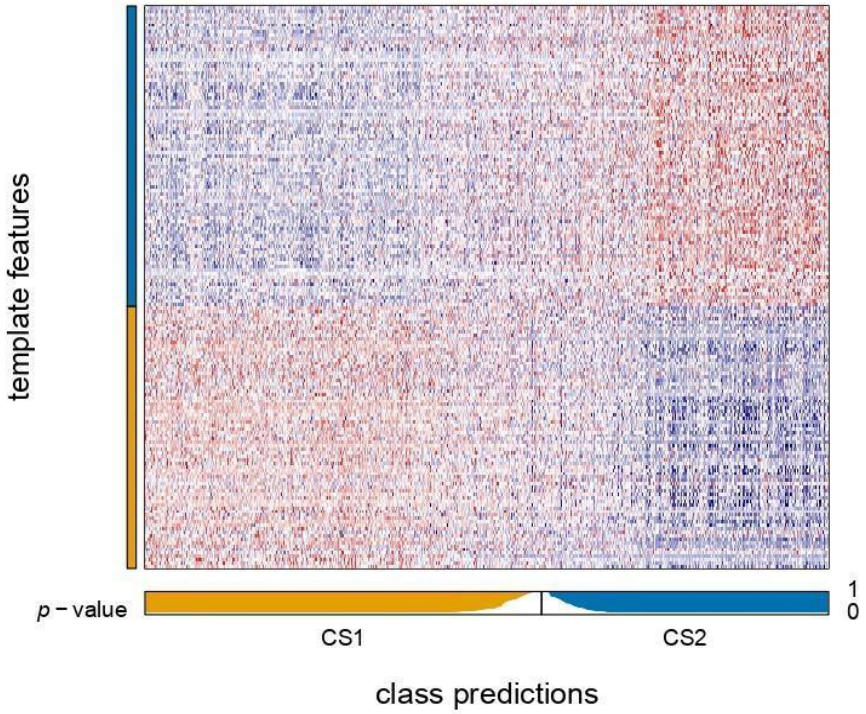


Figure 3.35. Heatmap of NTP in GSE39582 cohort using subtype-specific upregulated biomarkers identified using limma from TCGA-COAD cohort.

No significant survival differences were found in the GSE39582 cohort based on the results of the three algorithms (Figure 3.36-3.38).

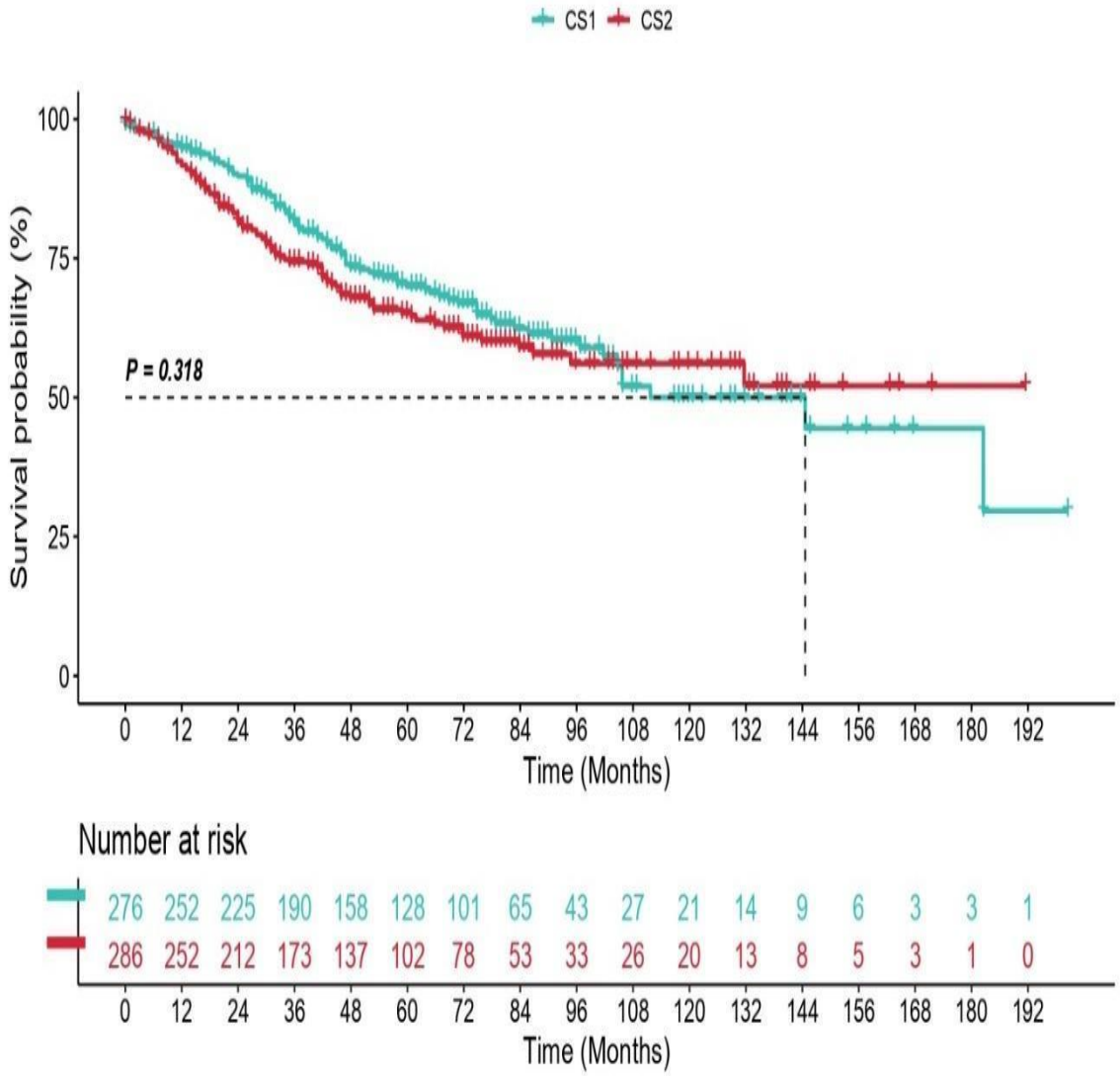


Figure 3.36. Kaplan-Meier survival curve of 2 colon adenocarcinoma subtypes predicted by edgeR in the GSE39582 cohort.

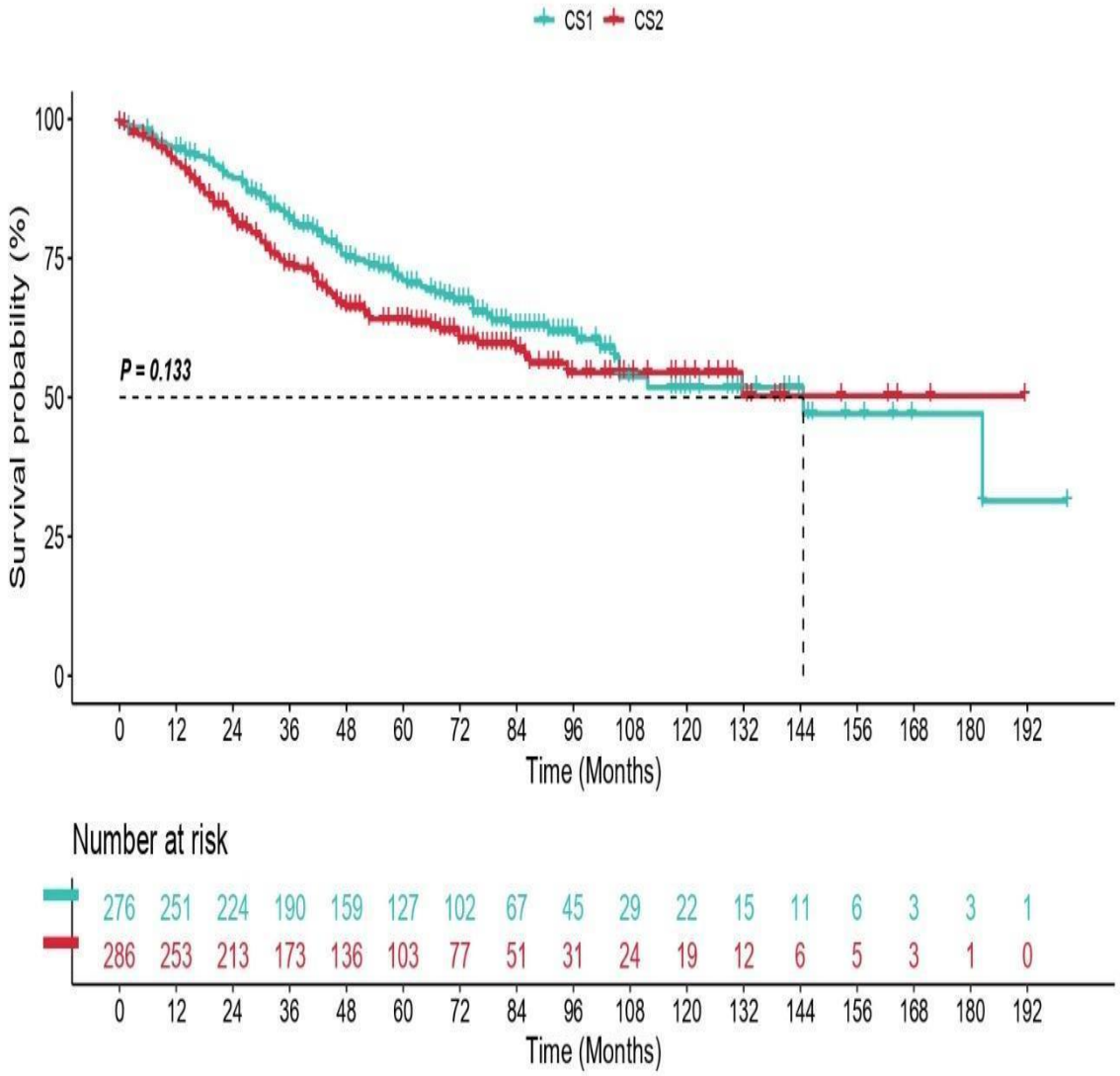


Figure 3.37. Kaplan-Meier survival curve of 2 colon adenocarcinoma subtypes predicted by DESeq2 in the GSE39582 cohort.

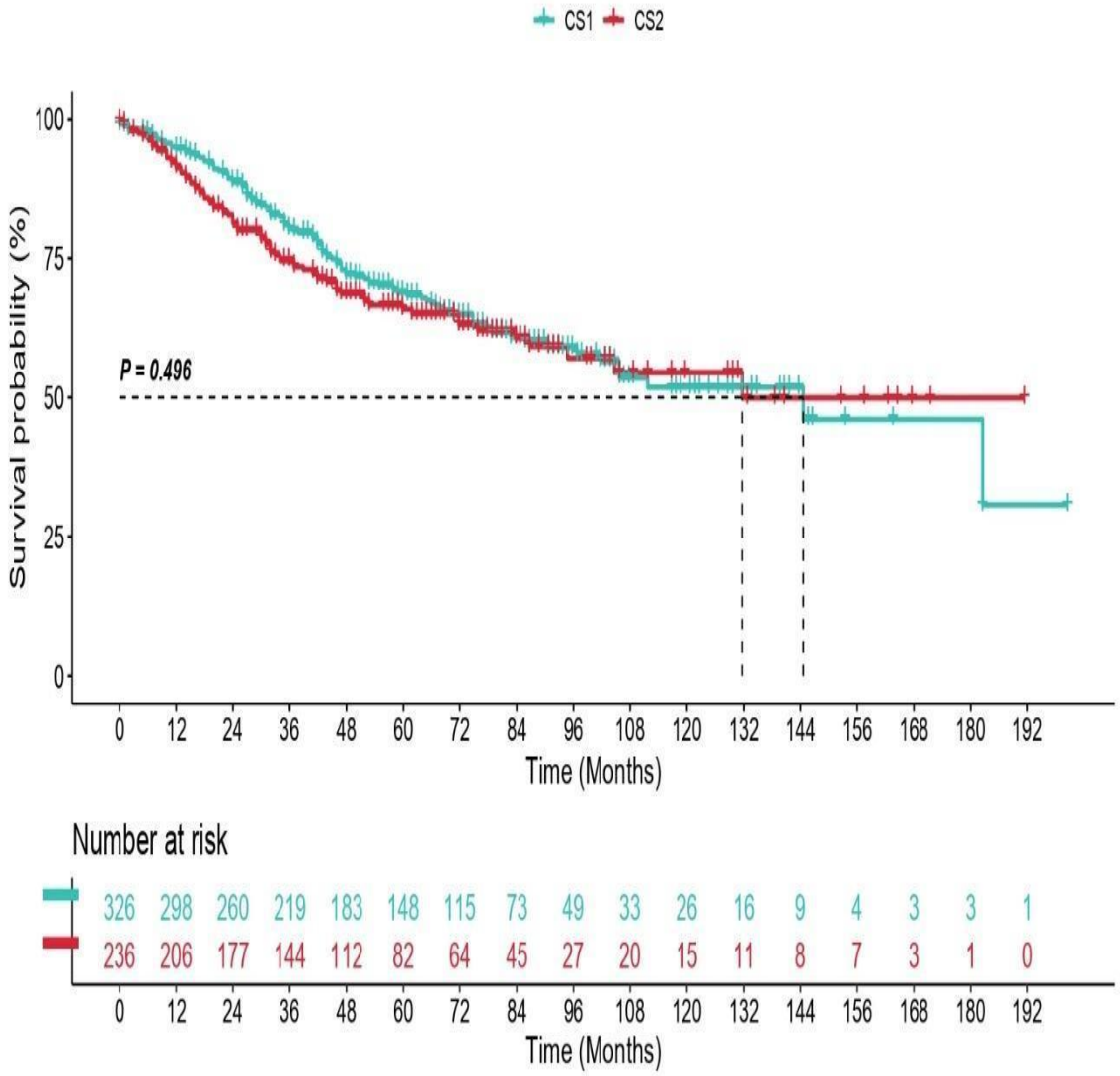


Figure 3.38. Kaplan-Meier survival curve of 2 colon adenocarcinoma subtypes predicted by limma in the GSE39582 cohort.

Based on the IGP statistics obtained as a result of the PAM analysis of the GSE39582 cohort, the subtypes identified between the discovery and validation groups were found to be similar and reproducible (Table 3.16).

According to the results of edgeR (Figure 3.39-3.40), the consistency between the subtypes present in the TCGA dataset and the subtypes predicted by NTP was much more significant than those predicted by PAM, while according to the results of DESeq2 (Figure 3.41-3.42) and limma (Figure 3.43-3.44), the subtypes predicted by PAM were much more significant.

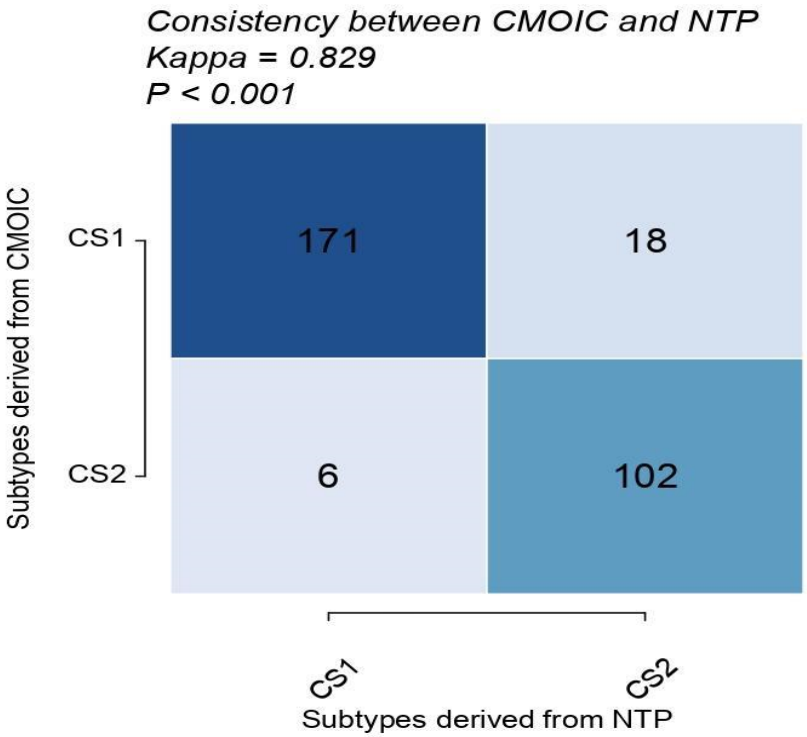


Figure 3.39. Consistency heatmap between current and NTP-predicted Kappa statistics for edgeR results in TCGA-COAD cohort.

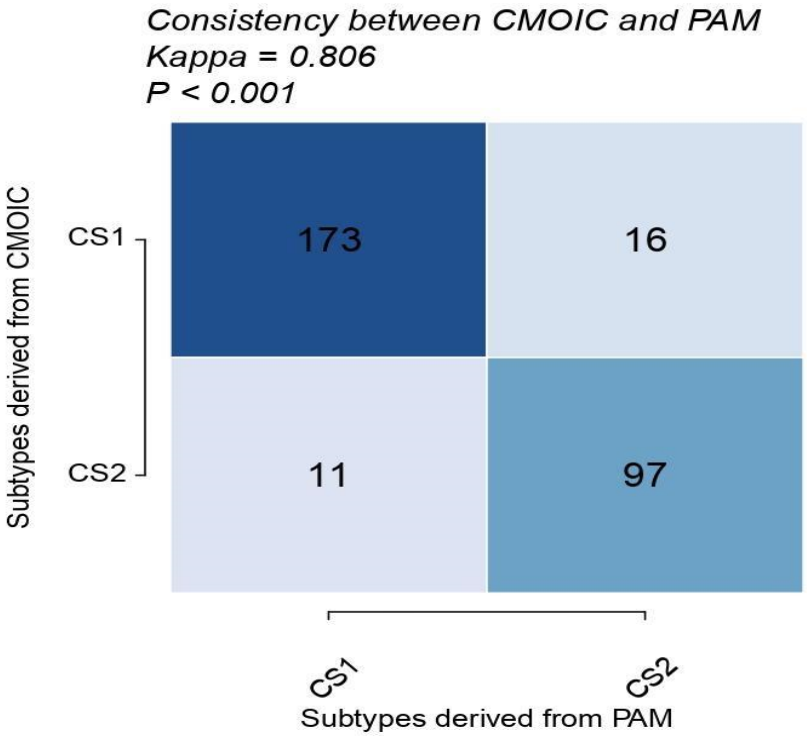


Figure 3.40. Consistency heatmap between current and PAM-predicted Kappa statistics for edgeR results in TCGA-COAD cohort.

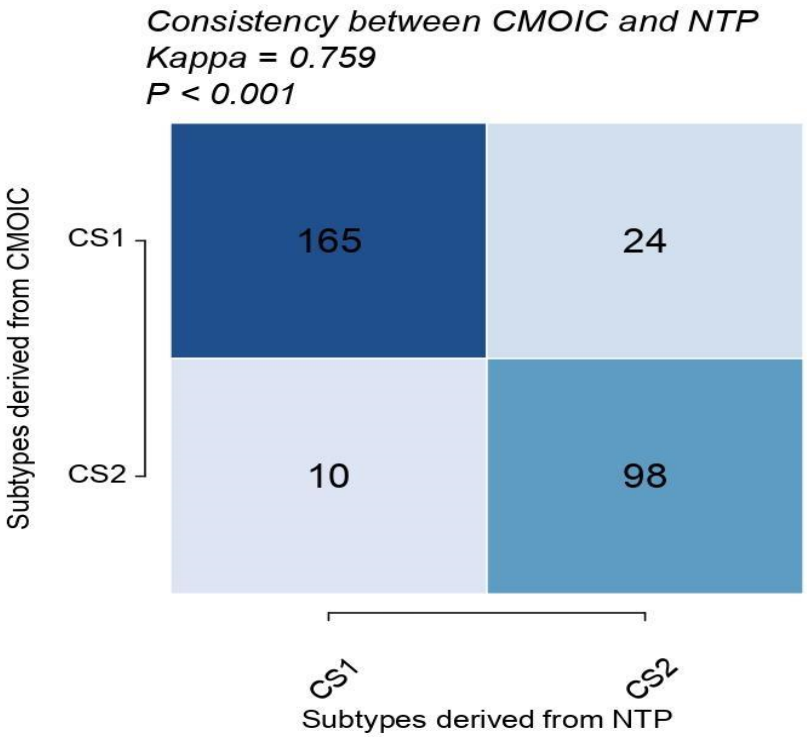


Figure 3.41. Consistency heatmap between current and NTP-predicted Kappa statistics for DESeq2 results in TCGA-COAD cohort.

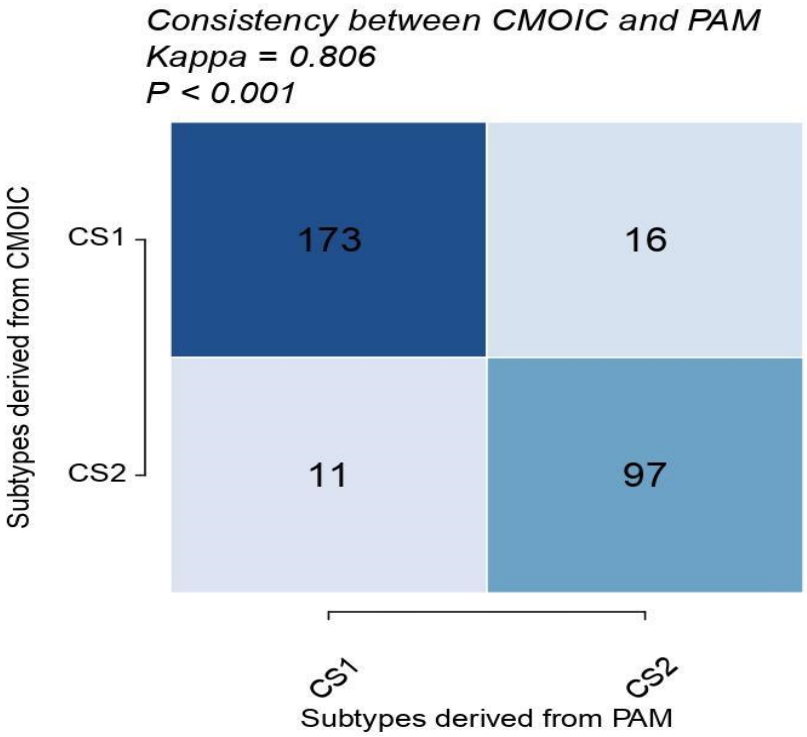


Figure 3.42. Consistency heatmap between current and PAM-predicted Kappa statistics for DESeq2 results in TCGA-COAD cohort.

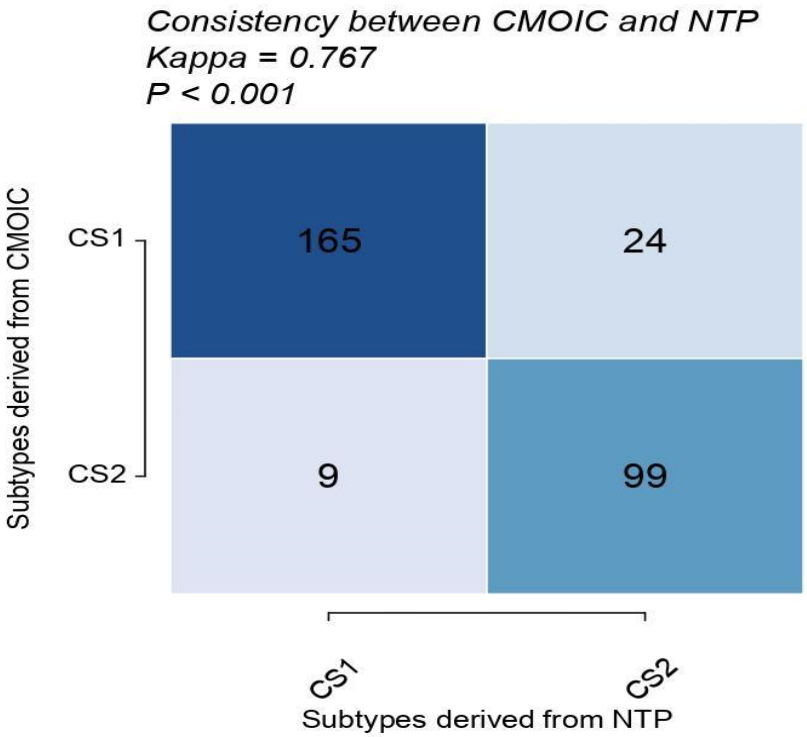


Figure 3.43. Consistency heatmap between current and NTP-predicted Kappa statistics for limma results in TCGA-COAD cohort.

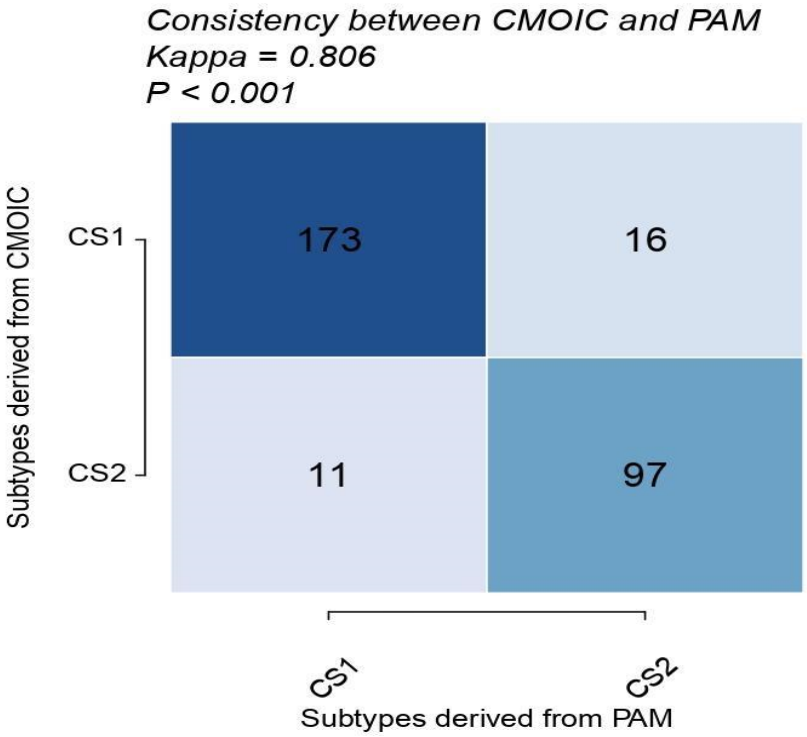


Figure 3.44. Consistency heatmap between current and PAM-predicted Kappa statistics for limma results in TCGA-COAD cohort.

In addition, the consistency results of the subtypes recognised by NTP and PAM in the validation dataset were best obtained with Limma and worst with edgeR (0.711, 0.538 and 0.474 for Limma, DESeq2 and edgeR, respectively) (Figure 3.45-3.47).

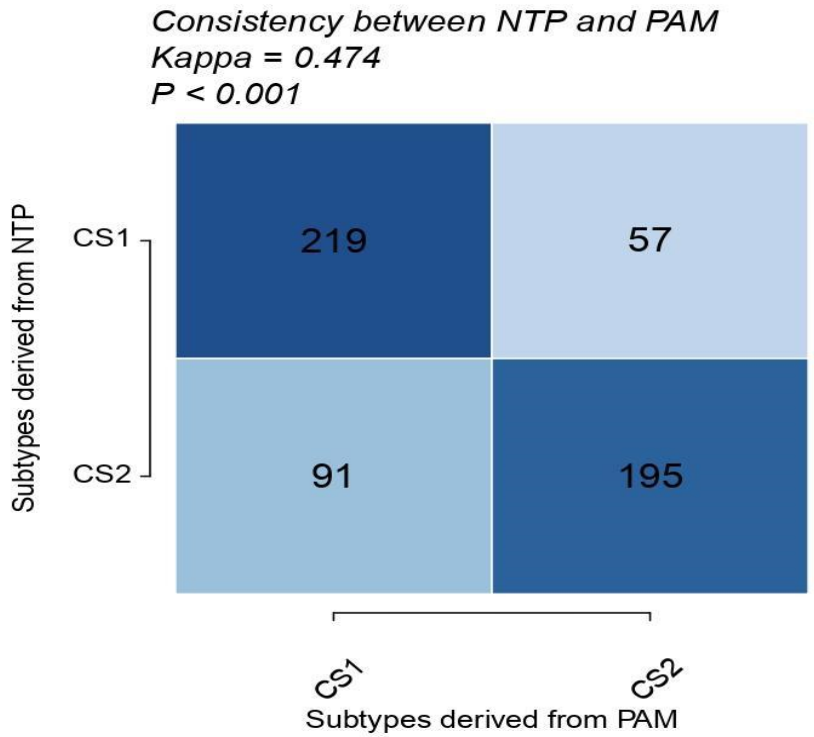


Figure 3.45. Consistency heatmap between NTP and PAM-predicted subtype for edgeR results in GSE39582.

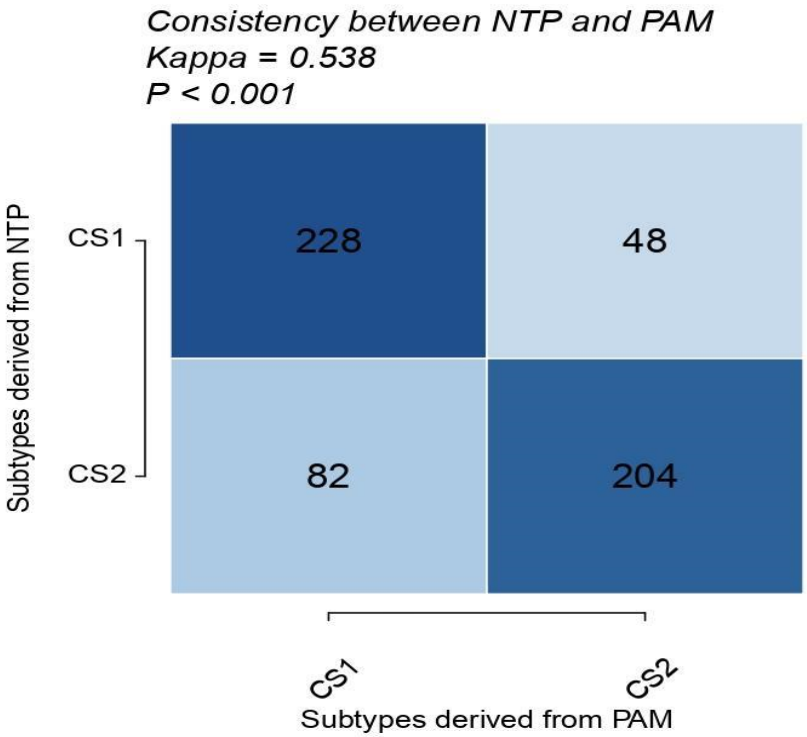


Figure 3.46. Consistency heatmap between NTP and PAM-predicted subtype for DESeq2 results in GSE39582.

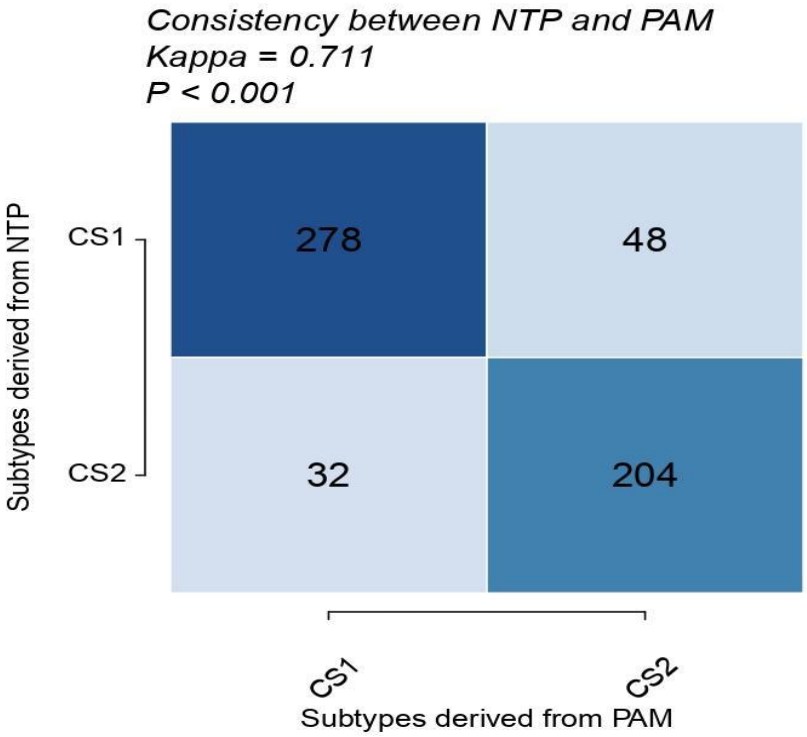


Figure 3.47. Consistency heatmap between NTP and PAM-predicted subtype for limma results in GSE39582.

To predict subtypes in the GSE1756 cohort, which consists of 177 samples, NTP was performed based on upregulated markers detected with edgeR, DESeq2 and limma in the discovery dataset (Figure 3.48-3.50). However, the NTP analysis based on the edgeR and DESeq2 results showed that none of the 177 samples could be assigned to the corresponding subtypes. On the other hand, as a result of the NTP performed with limma, 82 patients were categorised in CS1 and 61 patients in CS2.

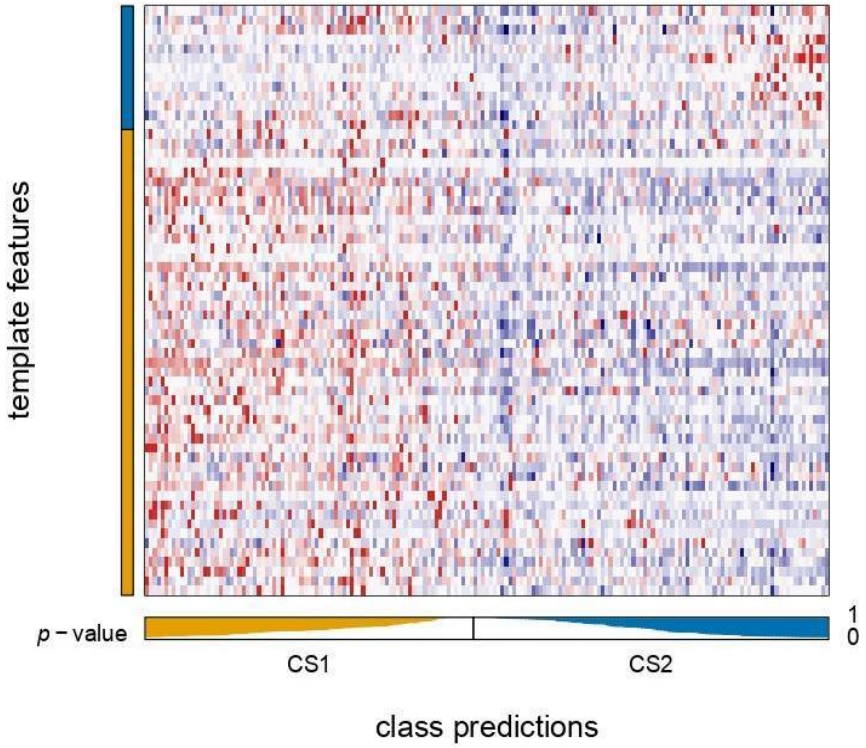


Figure 3.48. Heatmap of NTP in GSE17536 cohort using subtype-specific upregulated biomarkers identified using edgeR from TCGA-COAD cohort.

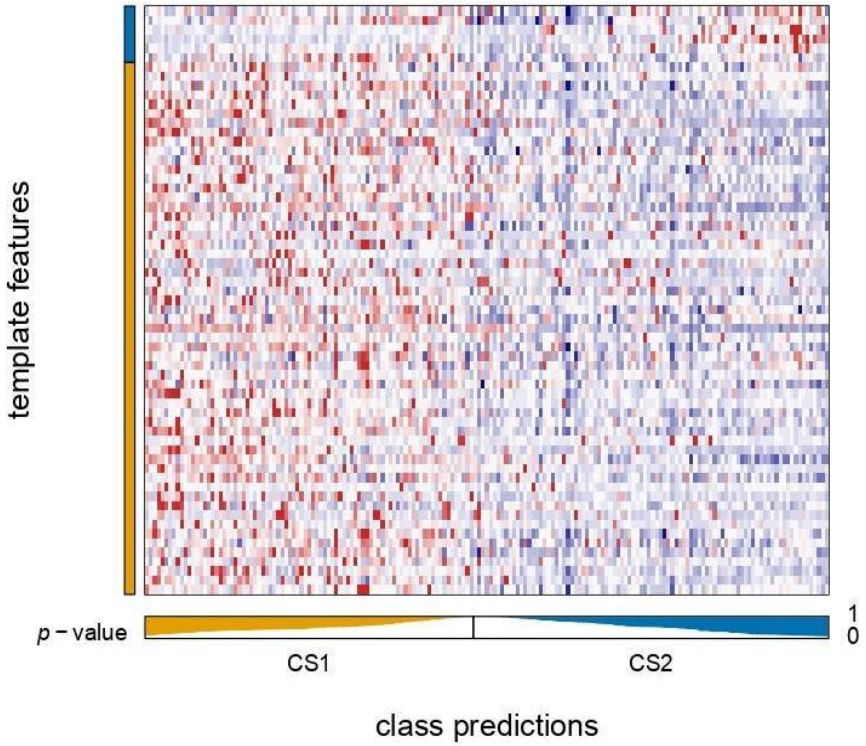


Figure 3.49. Heatmap of NTP in GSE17536 cohort using subtype-specific upregulated biomarkers identified using DESeq2 from TCGA-COAD cohort.

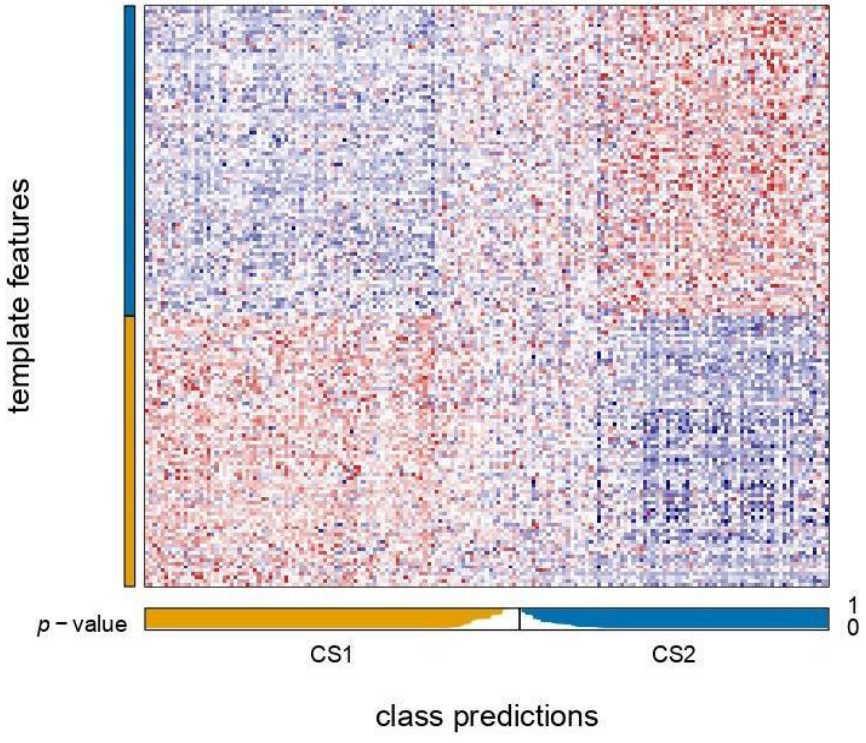


Figure 3.50. Heatmap of NTP in GSE17536 cohort using subtype-specific upregulated biomarkers identified using limma from TCGA-COAD cohort.

No significant differences in survival were found in the GSE17536 cohort based on the results of the three algorithms (Figure 3.51-3.53).

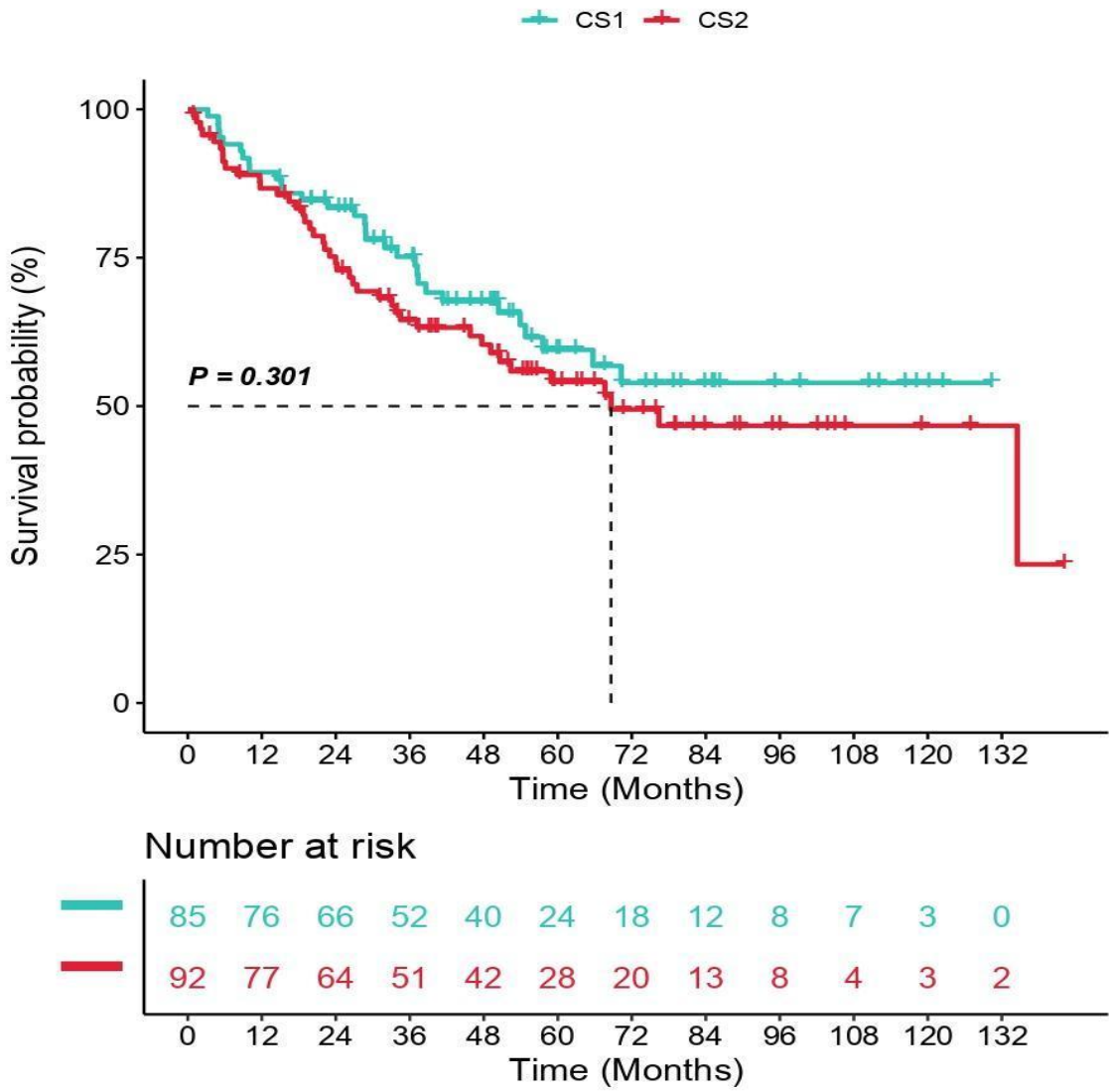


Figure 3.51. Kaplan-Meier survival curve of 2 colon adenocarcinoma subtypes predicted by edgeR in the GSE17536 cohort.

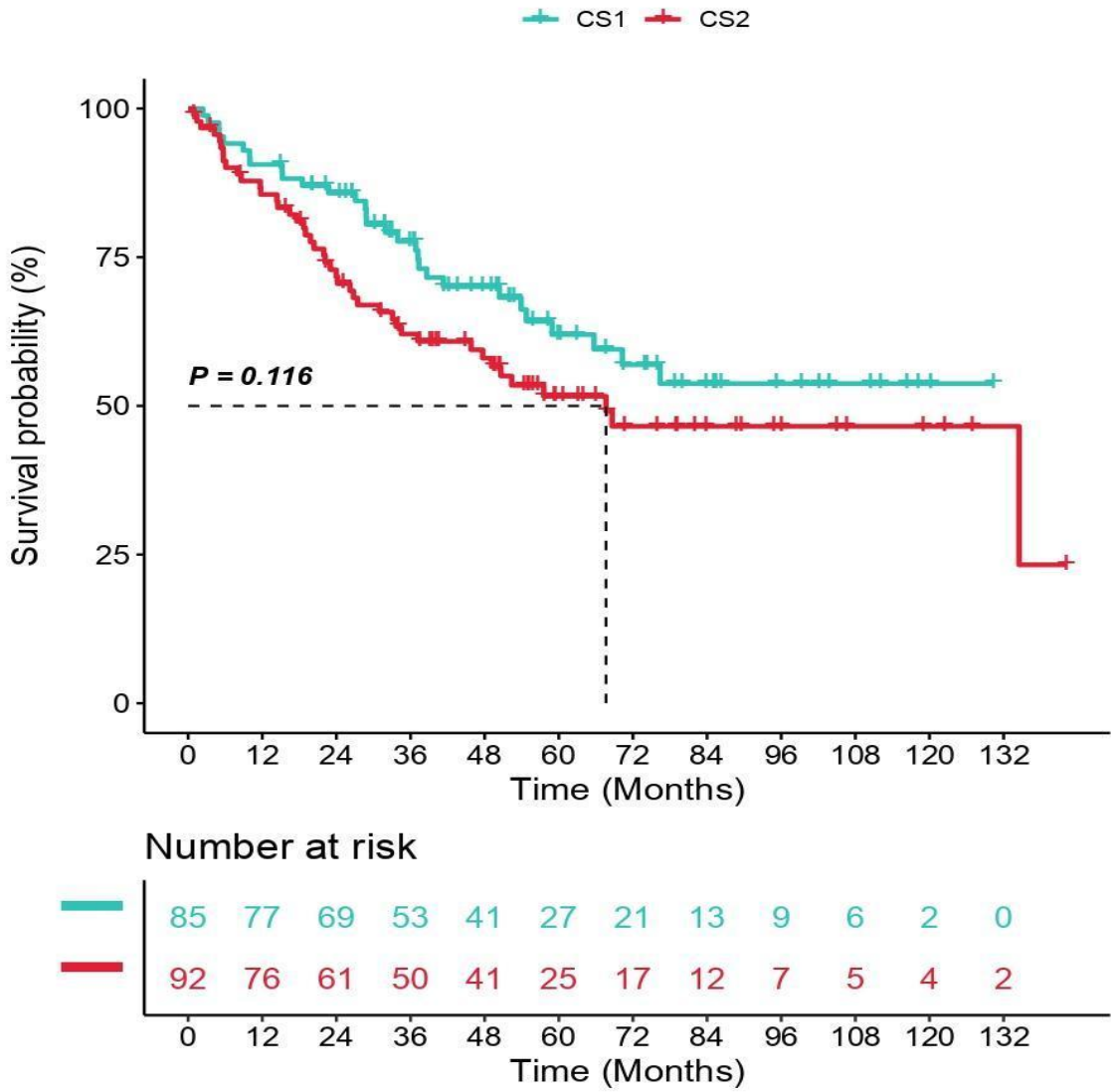


Figure 3.52. Kaplan-Meier survival curve of 2 colon adenocarcinoma subtypes predicted by DESeq2 in the GSE17536 cohort.

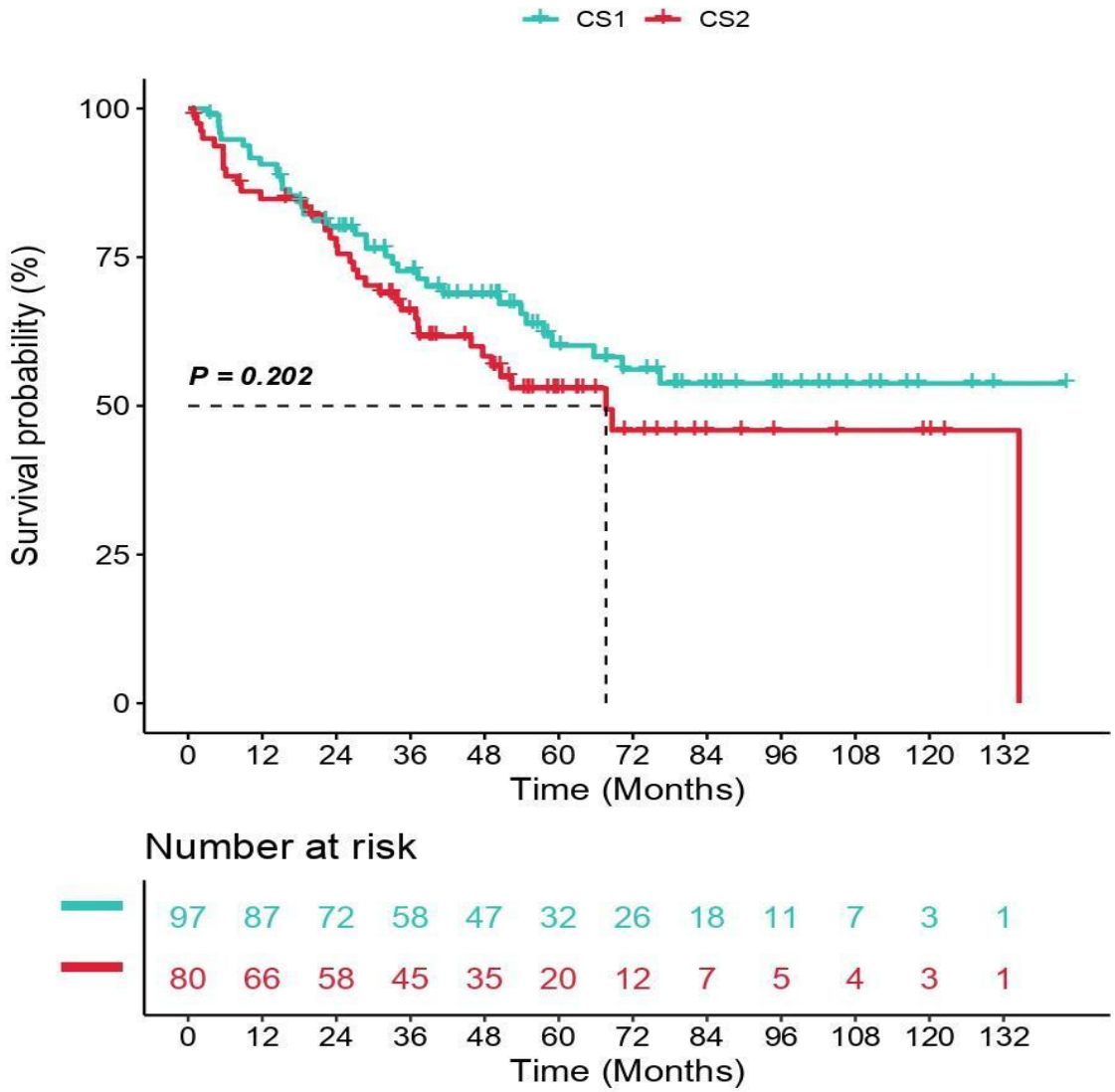


Figure 3.53. Kaplan-Meier survival curve of 2 colon adenocarcinoma subtypes predicted by limma in the GSE17536 cohort.

Based on the IGP statistics obtained as a result of the PAM analysis of the GSE17536 cohort, it was concluded that the subtypes obtained between the discovery and validation groups were similar and reproducible (Table 3.16).

According to the edgeR results (Figure 3.54-3.55), the consistency between the subspecies present in the TCGA dataset and the subspecies predicted by NTP was much clearer.

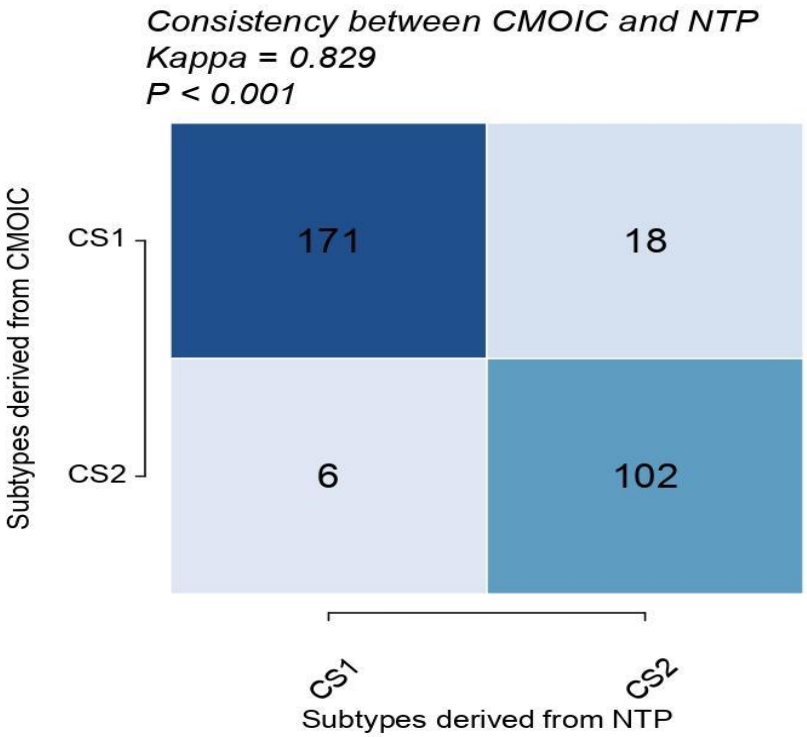


Figure 3.54. Consistency heatmap between current and NTP-predicted Kappa statistics for edgeR results in TCGA-COAD cohort.

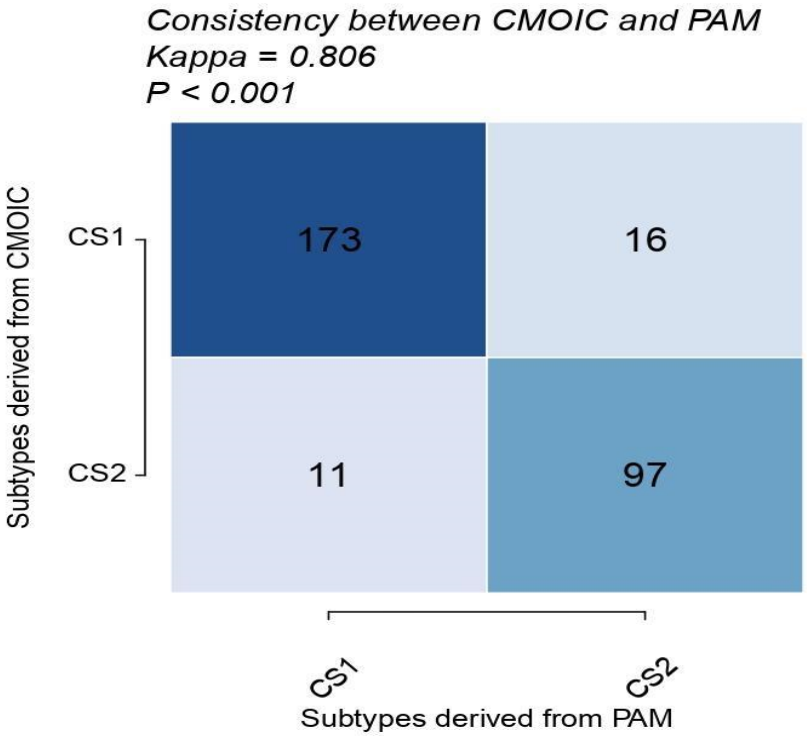


Figure 3.55. Consistency heatmap between current and PAM-predicted Kappa statistics for edgeR results in TCGA-COAD cohort.

Compared to DESeq2 (Figure 3.56-3.57) and limma results (Figure 3.58-3.59), the results obtained with PAM were much more significant.

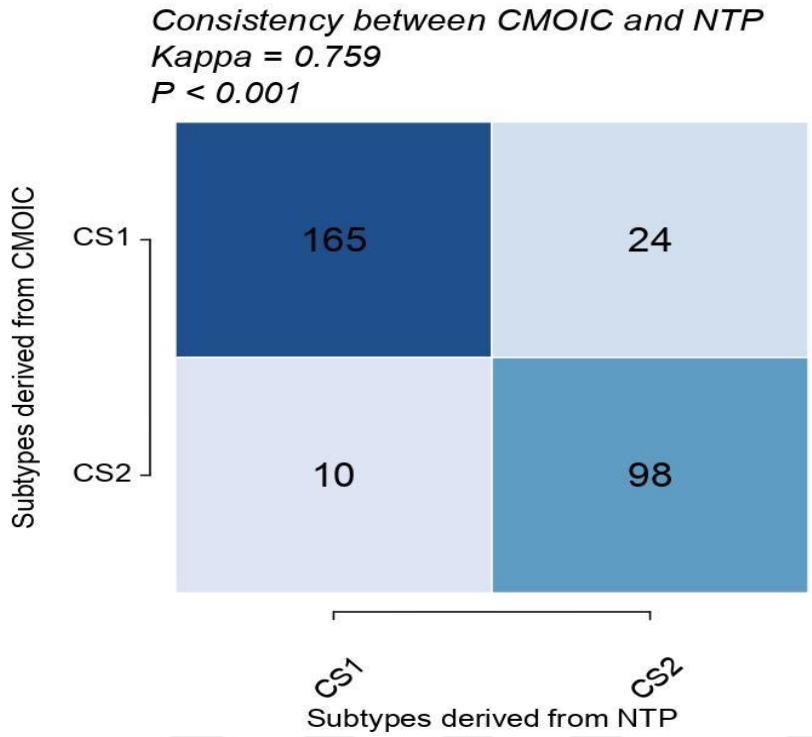


Figure 3.56. Consistency heatmap between current and NTP-predicted Kappa statistics for DESeq2 results in TCGA-COAD cohort.

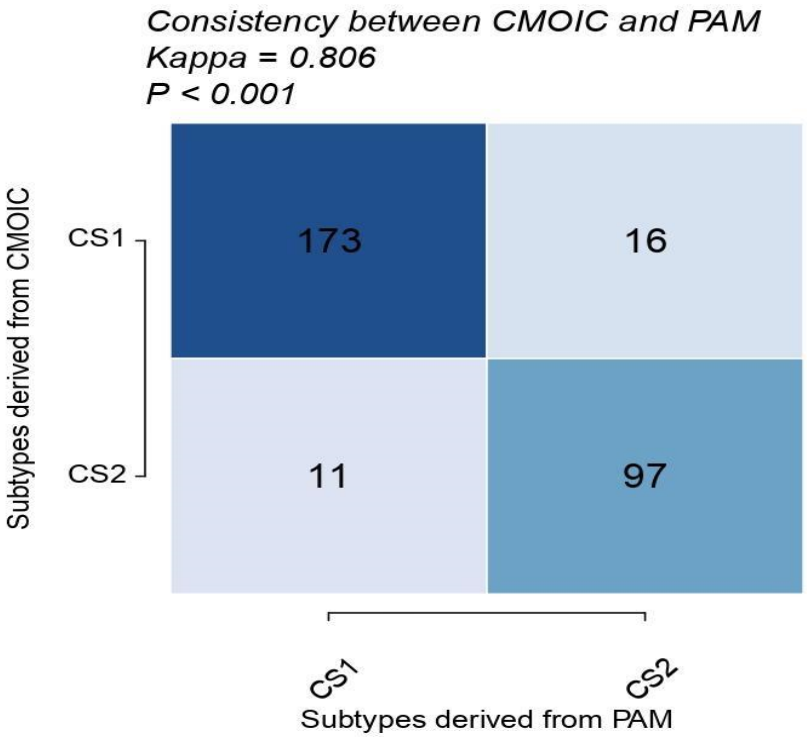


Figure 3.57. Consistency heatmap between current and PAM-predicted Kappa statistics for DESeq2 results in TCGA-COAD cohort.

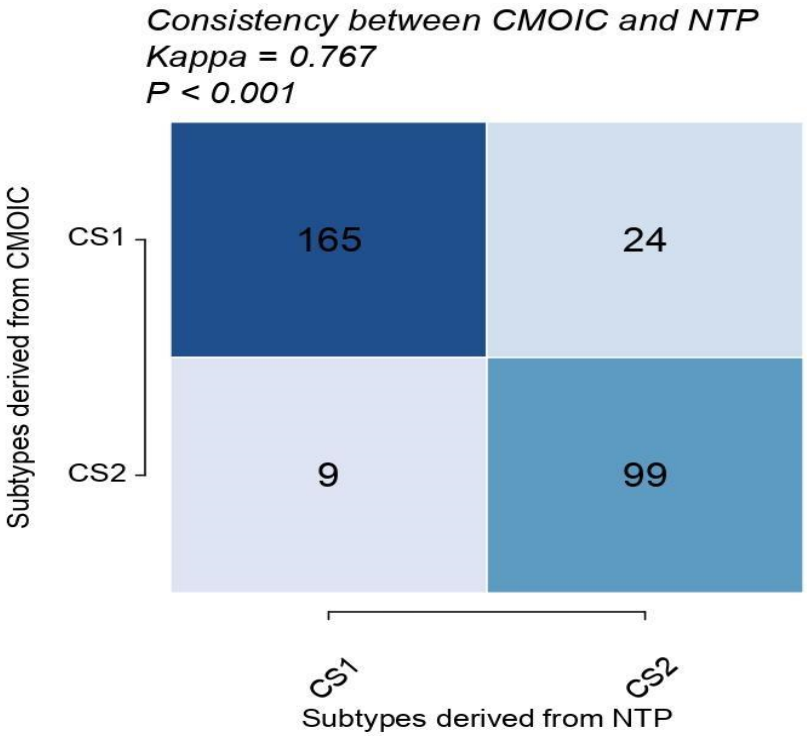


Figure 3.58. Consistency heatmap between current and NTP-predicted Kappa statistics for limma results in TCGA-COAD cohort.

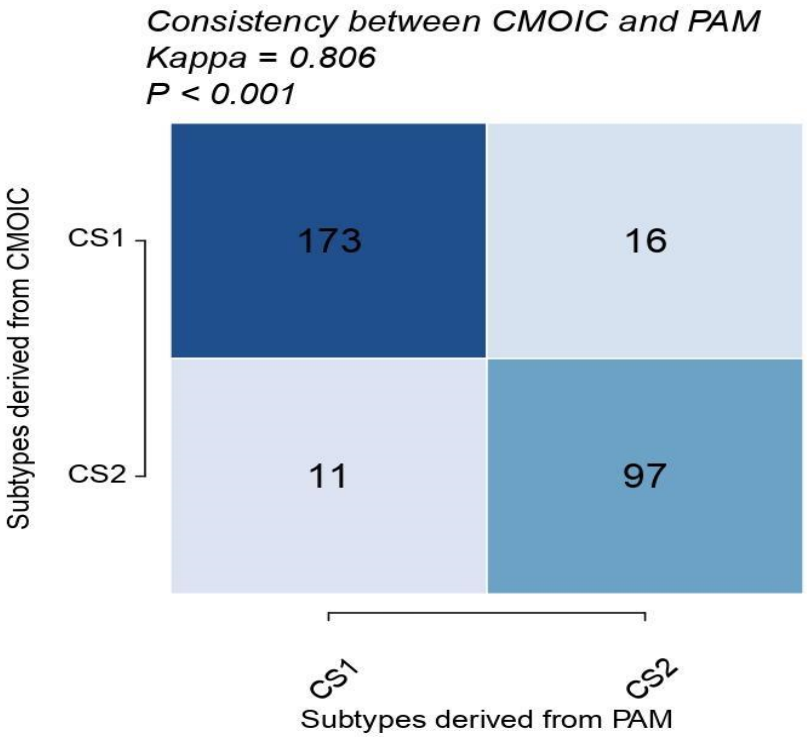


Figure 3.59. Consistency heatmap between current and PAM-predicted Kappa statistics for limma results in TCGA-COAD cohort.

In addition, the consistency results of the subtypes recognised by NTP and PAM in the validation dataset were obtained with the best limma and the worst edgeR in the GSE17536 cohort (0.760, 0.539 and 0.516 for limma, DESeq2 and edgeR, respectively) (Figure 3.60-3.62).

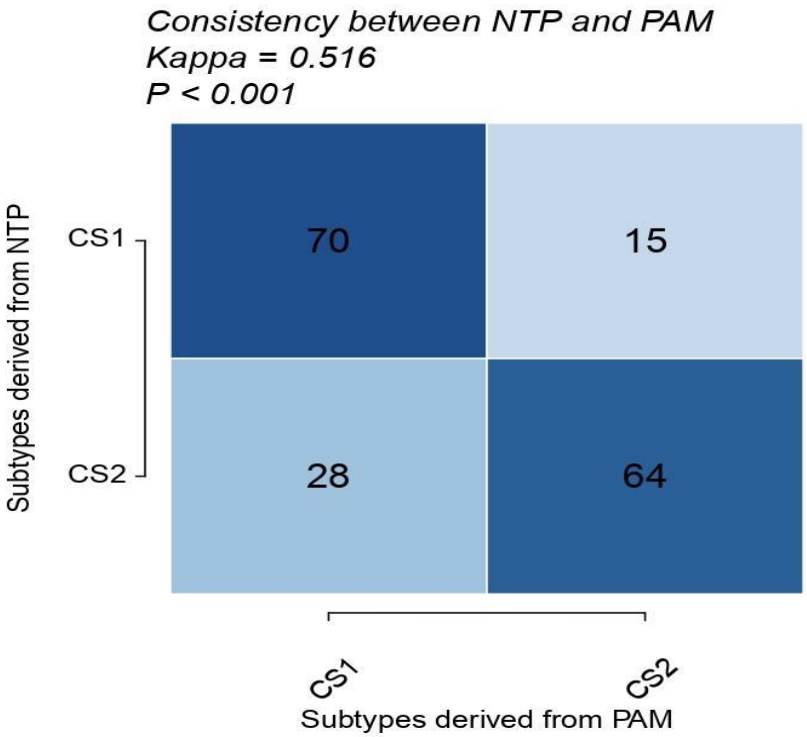


Figure 3.60. Consistency heatmap between NTP and PAM-predicted subtype for edgeR results in GSE17536.

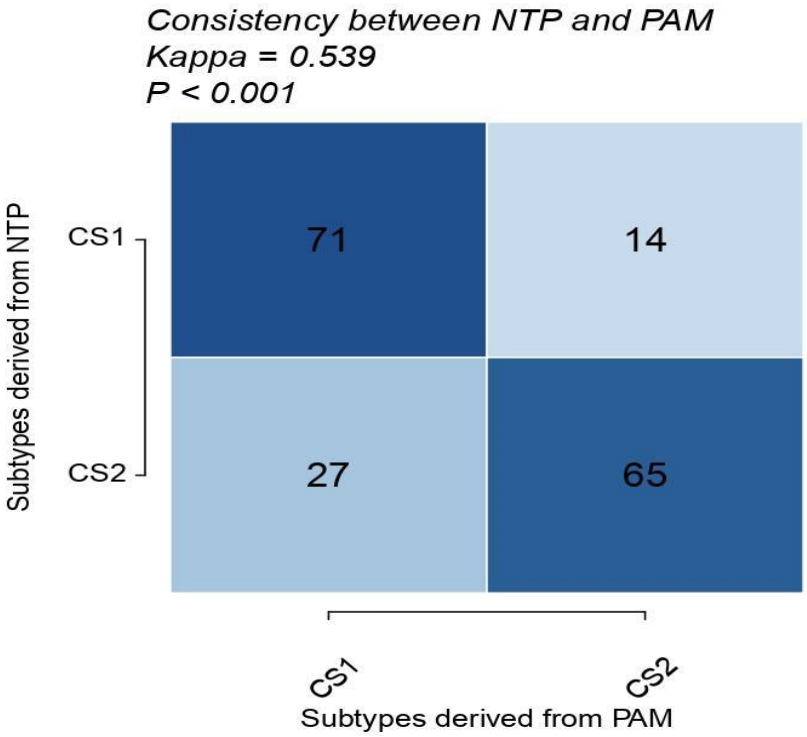


Figure 3.61. Consistency heatmap between NTP and PAM-predicted subtype for DESeq2 results in GSE17536.

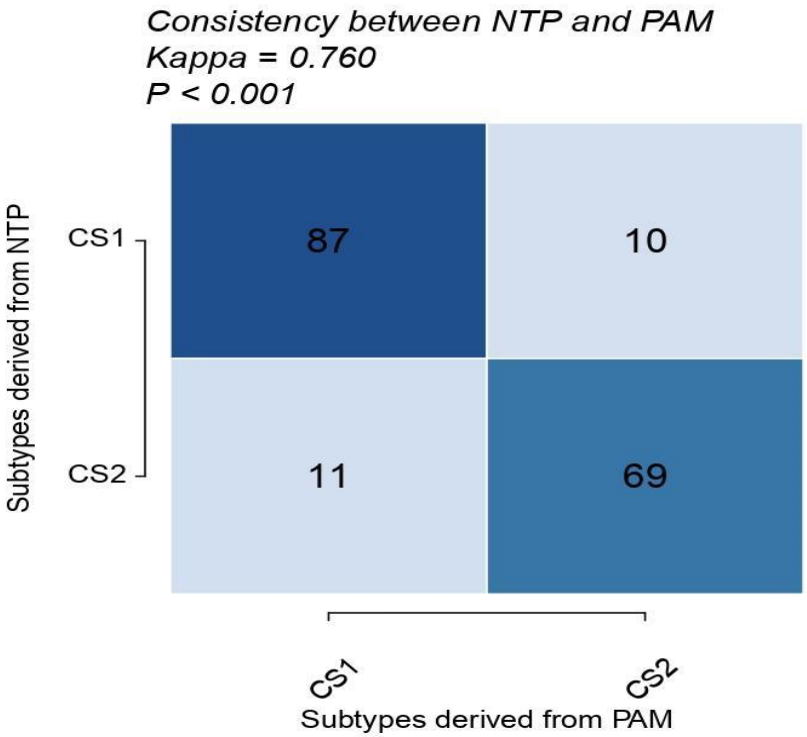


Figure 3.62. Consistency heatmap between NTP and PAM-predicted subtype for limma results in GSE17536.

To predict subtypes in the GSE17537 cohort, which consists of 55 samples, NTP was performed based on upregulated markers detected with edgeR, DESeq2 and limma in the discovery dataset (Figure 3.63-3.65). However, the NTP analysis based on the results of edgeR and DESeq2 revealed that none of the 177 samples could be assigned to the corresponding subtypes. On the other hand, as a result of the NTP performed with Limma, 21 patients were categorised in CS1 and 20 patients in CS2.

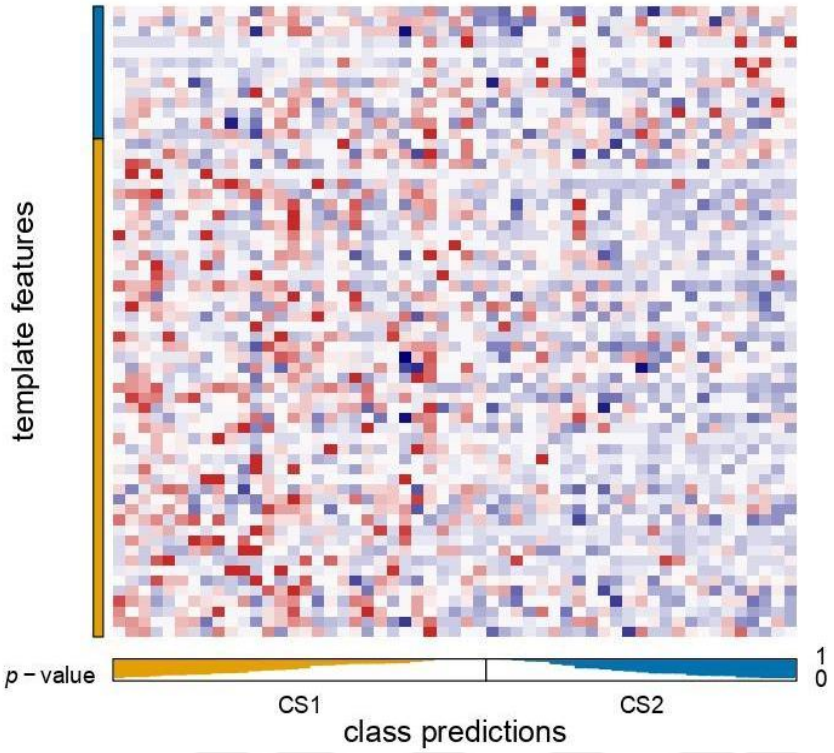


Figure 3.63. Heatmap of NTP in GSE17537 cohort using subtype-specific upregulated biomarkers identified using edgeR from TCGA-COAD cohort.

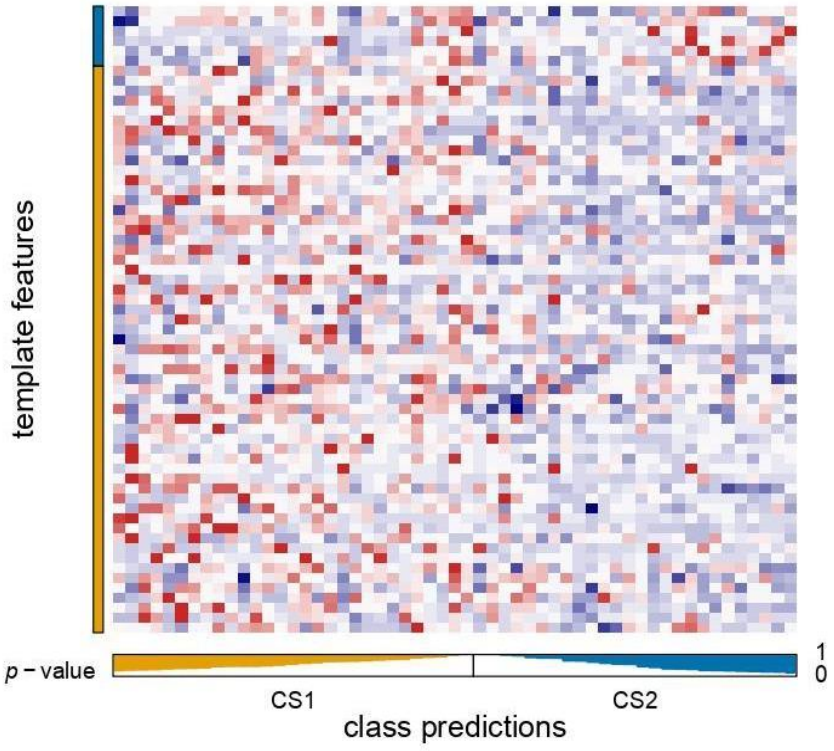


Figure 3.64. Heatmap of NTP in GSE17537 cohort using subtype-specific upregulated biomarkers identified using DESeq2 from TCGA-COAD cohort.

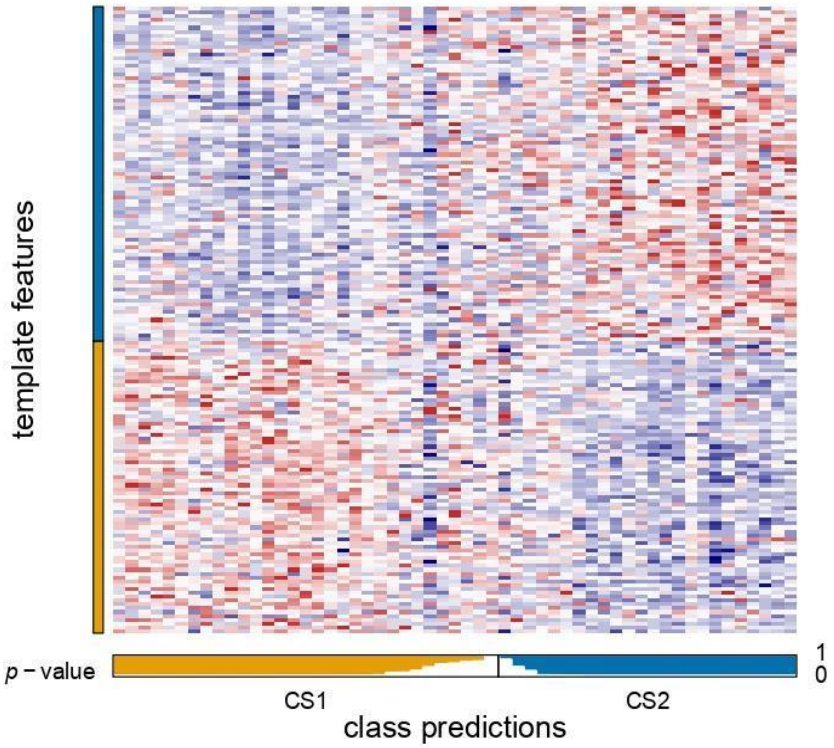


Figure 3.65. Heatmap of NTP in GSE17537 cohort using subtype-specific upregulated biomarkers identified using limma from TCGA-COAD cohort.

No significant difference was detected as a result of the survival analysis performed in the GSE17537 cohort (Figure 3.66-3.68).

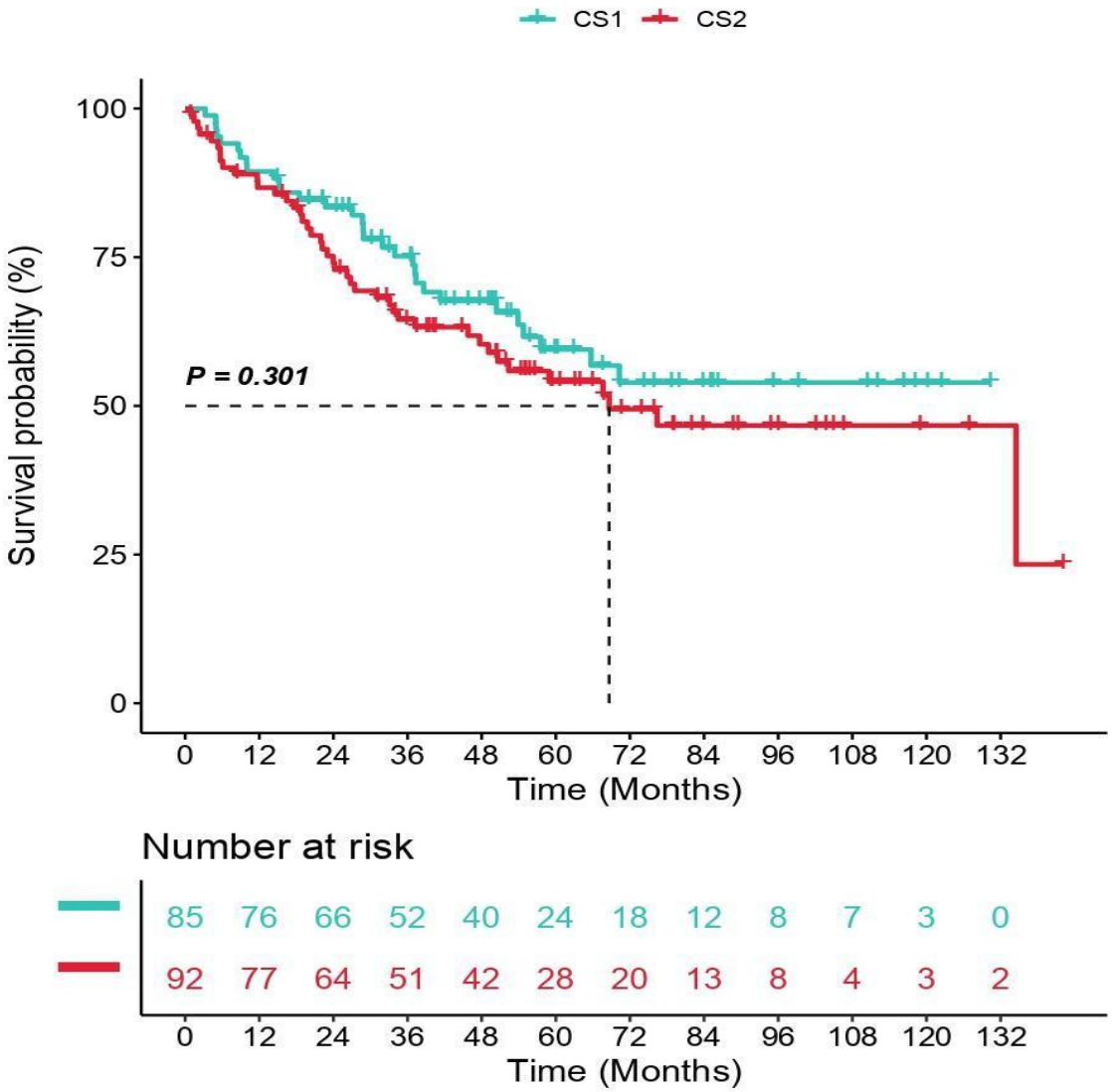


Figure 3.66. Kaplan-Meier survival curve of 2 colon adenocarcinoma subtypes predicted by edgeR in the GSE17537 cohort.

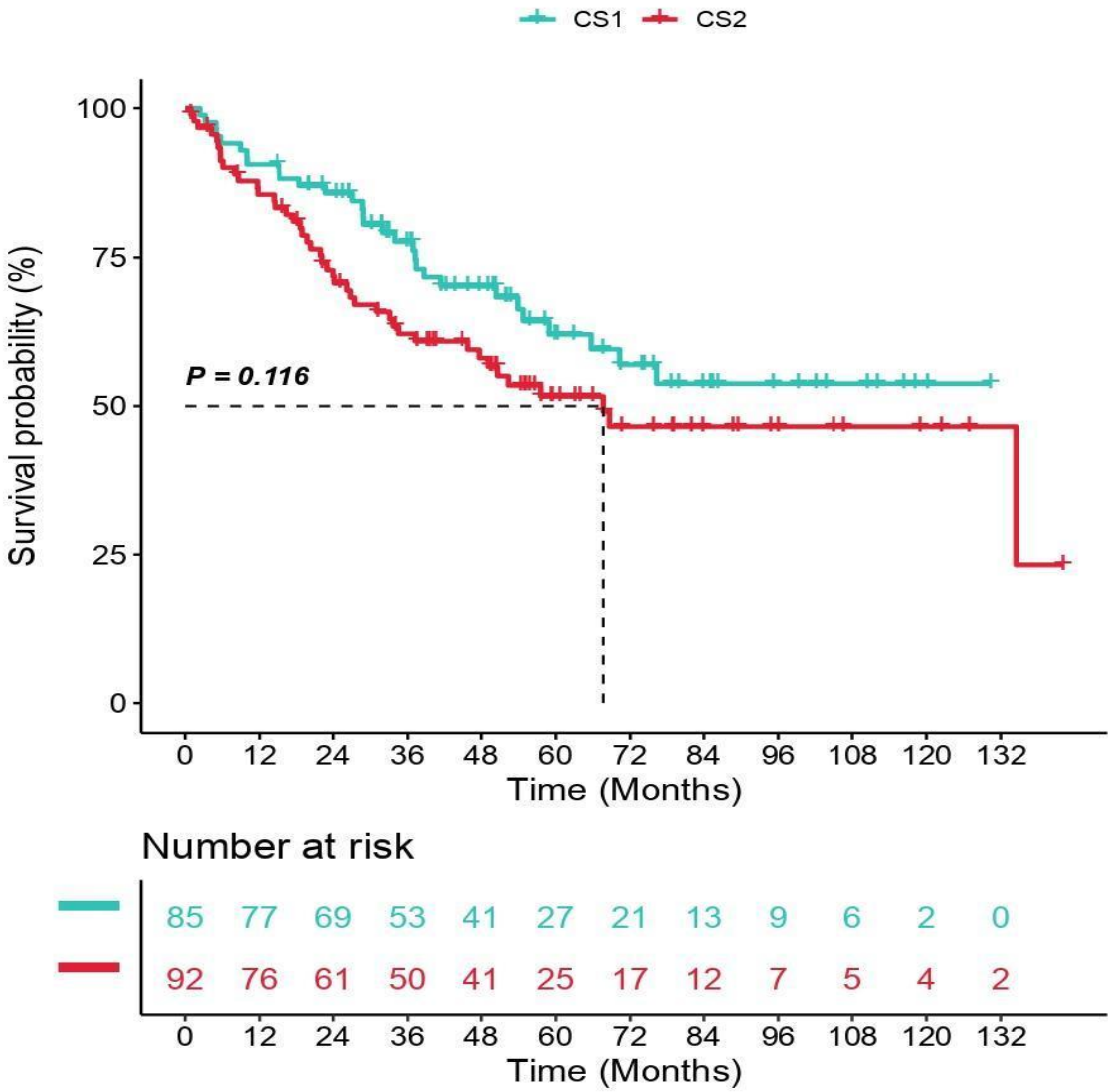


Figure 3.67. Kaplan-Meier survival curve of 2 colon adenocarcinoma subtypes predicted by DESeq2 in the GSE17537 cohort.

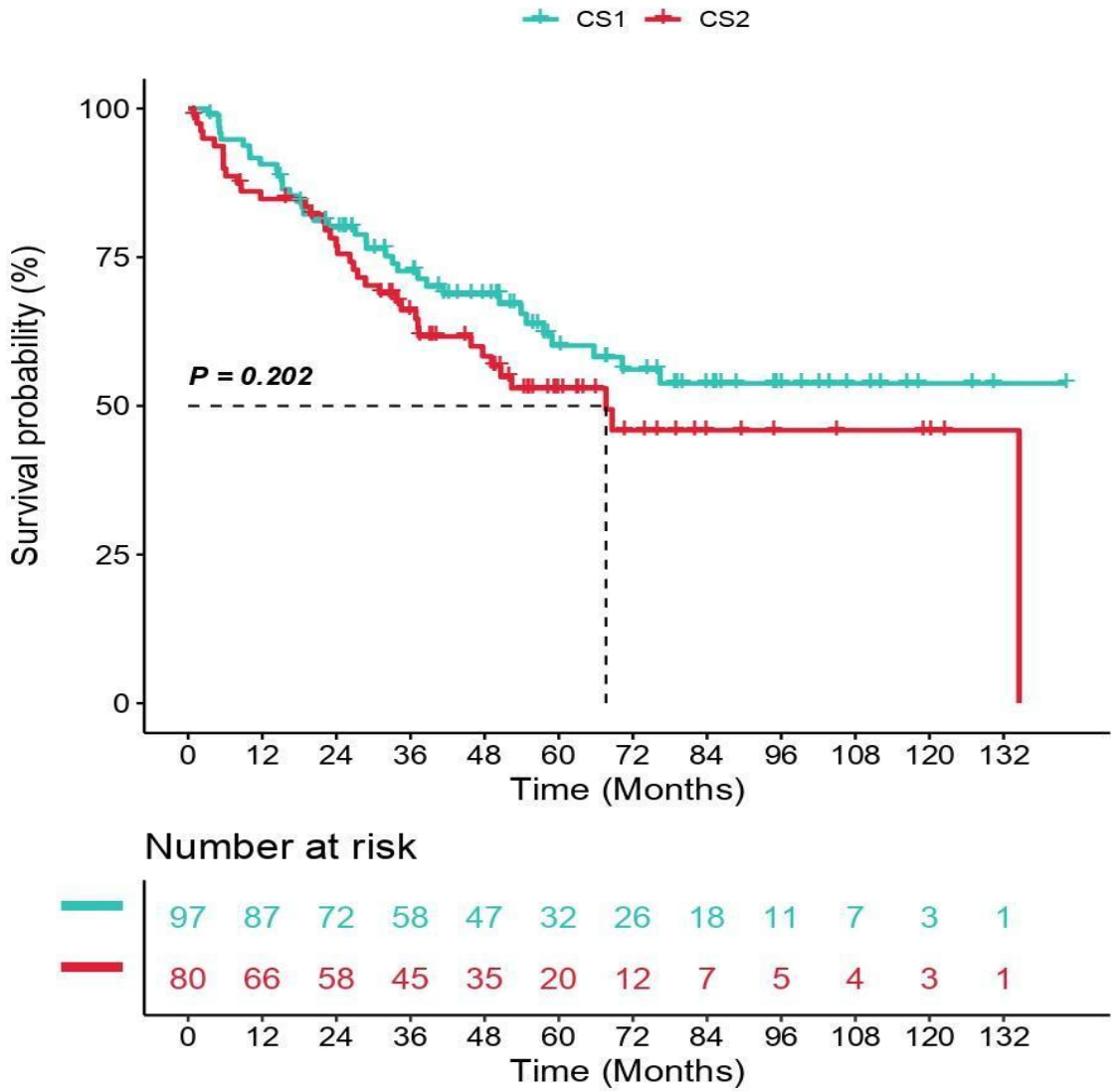


Figure 3.68. Kaplan-Meier survival curve of 2 colon adenocarcinoma subtypes predicted by limma in the GSE17537 cohort.

Based on the IGP statistics obtained as a result of the PAM analysis of the GSE17537 cohort, the subtypes identified between the discovery and validation groups were found to be similar and reproducible (Table 3.16).

According to the EdgeR results (Figure 3.69-3.70), the consistency between the subtypes present in the TCGA dataset and the subtypes predicted by NTP was much clearer.

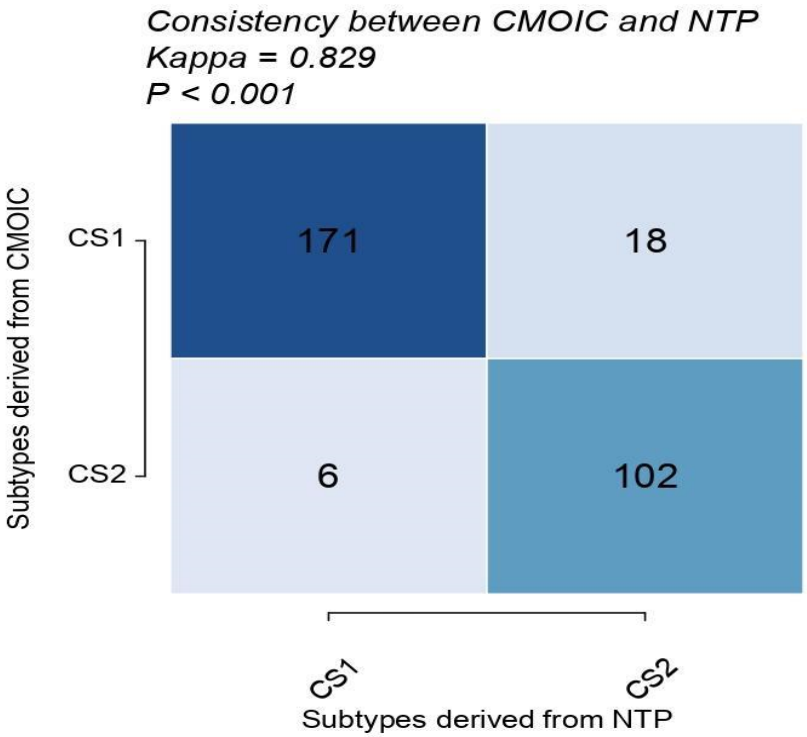


Figure 3.69. Consistency heatmap between current and NTP-predicted Kappa statistics for edgeR results in TCGA-COAD cohort.

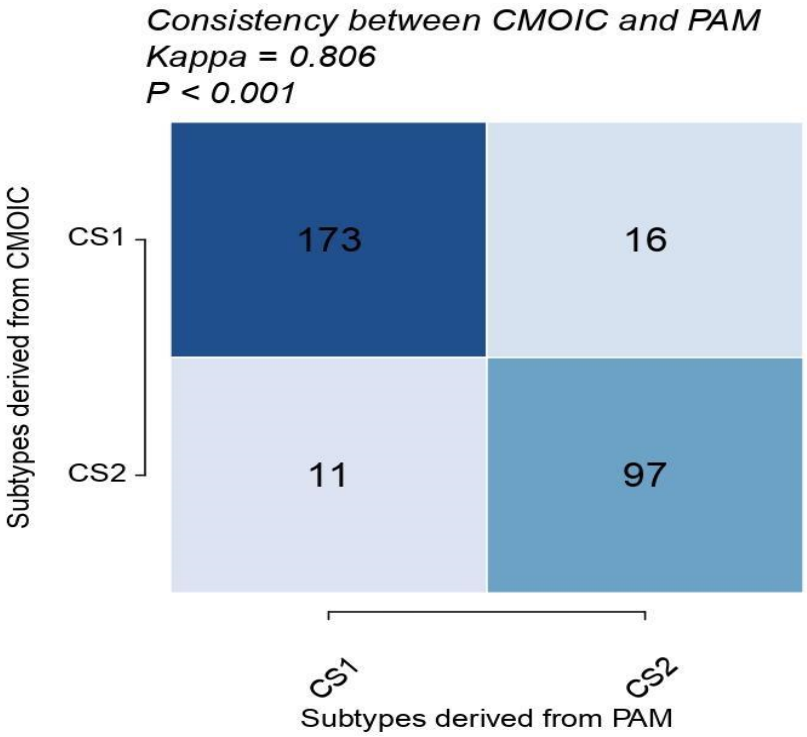


Figure 3.70. Consistency heatmap between current and PAM-predicted Kappa statistics for edgeR results in TCGA-COAD cohort.

Compared to DESeq2 (Figure 3.71-3.72) and limma results (Figure 3.73-3.74), the results obtained with PAM were much more significant.

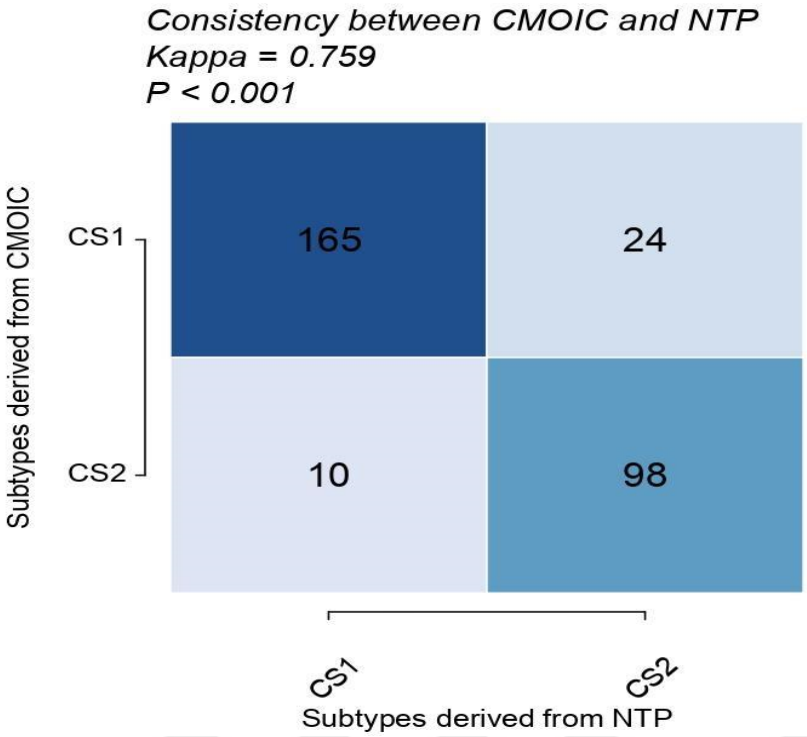


Figure 3.71. Consistency heatmap between current and NTP-predicted Kappa statistics for DESeq2 results in TCGA-COAD cohort.

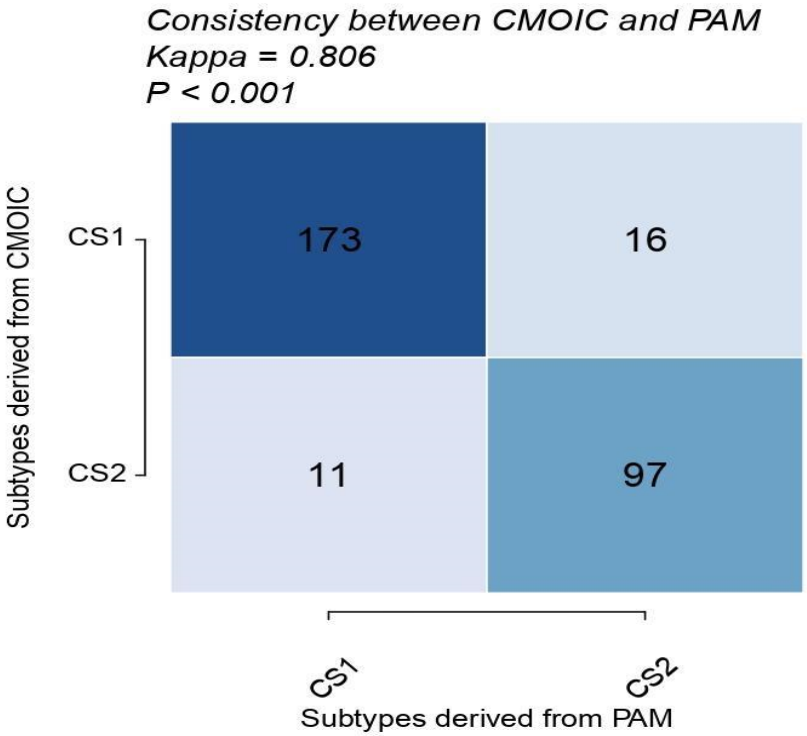


Figure 3.72. Consistency heatmap between current and PAM-predicted Kappa statistics for DESeq2 results in TCGA-COAD cohort.

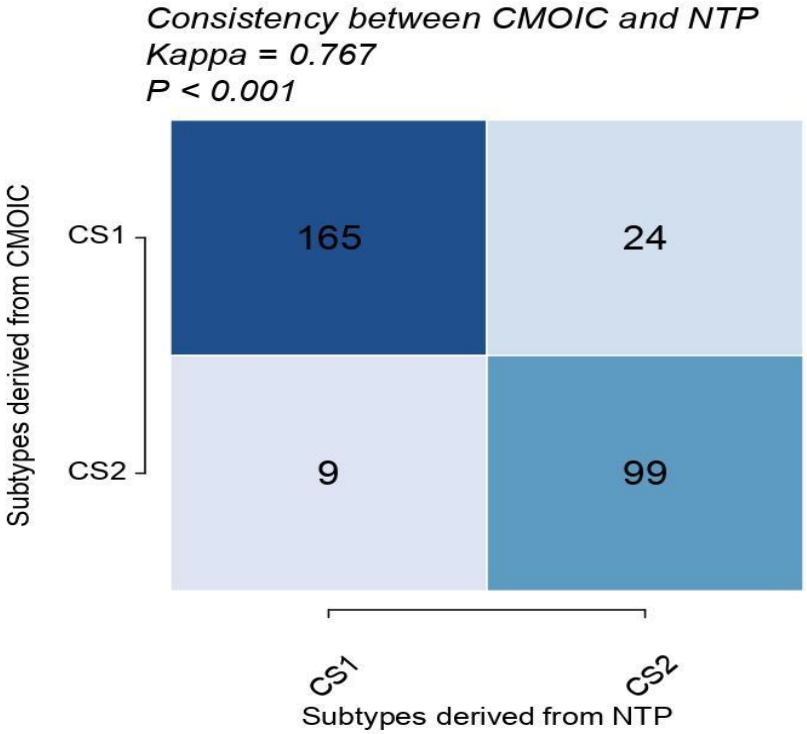


Figure 3.73. Consistency heatmap between current and NTP-predicted Kappa statistics for limma results in TCGA-COAD cohort.

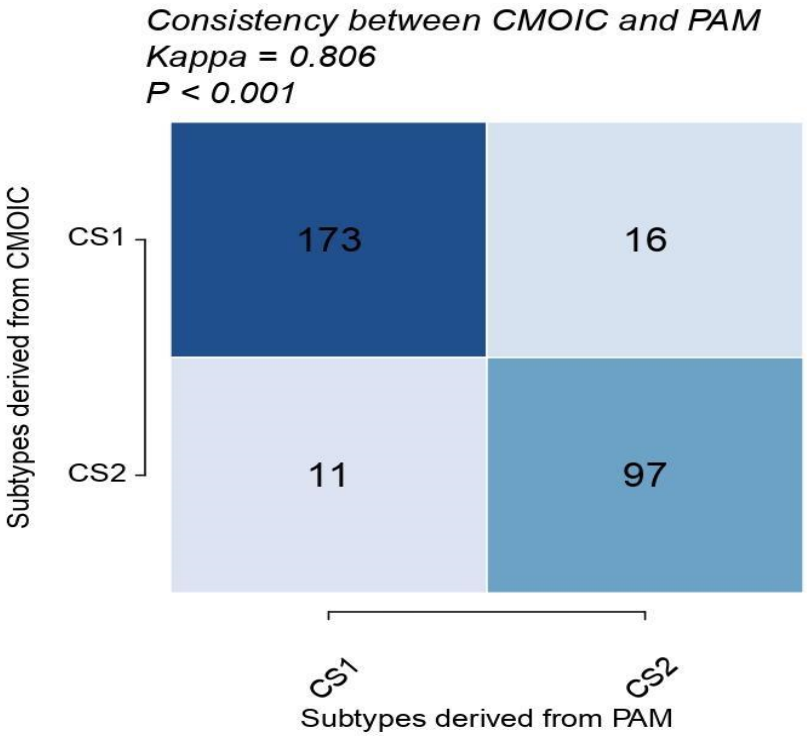


Figure 3.74. Consistency heatmap between current and PAM-predicted Kappa statistics for limma results in TCGA-COAD cohort.

In addition, the consistency results of the subtypes recognised by NTP and PAM in the validation dataset were best obtained with Limma and worst with DESeq2 (0.747, 0.529 and 0.566 for Limma, DESeq2 and EdgeR, respectively) (Figure 3.75-3.77).

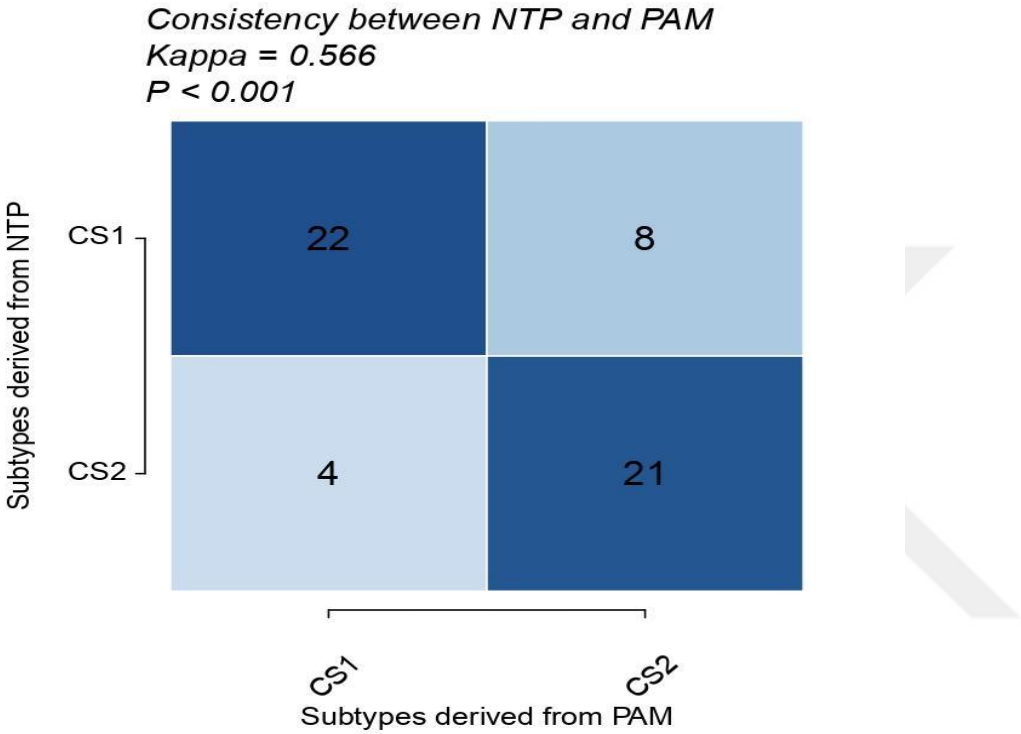


Figure 3.75. Consistency heatmap between NTP and PAM-predicted subtype for edgeR results in GSE17537.

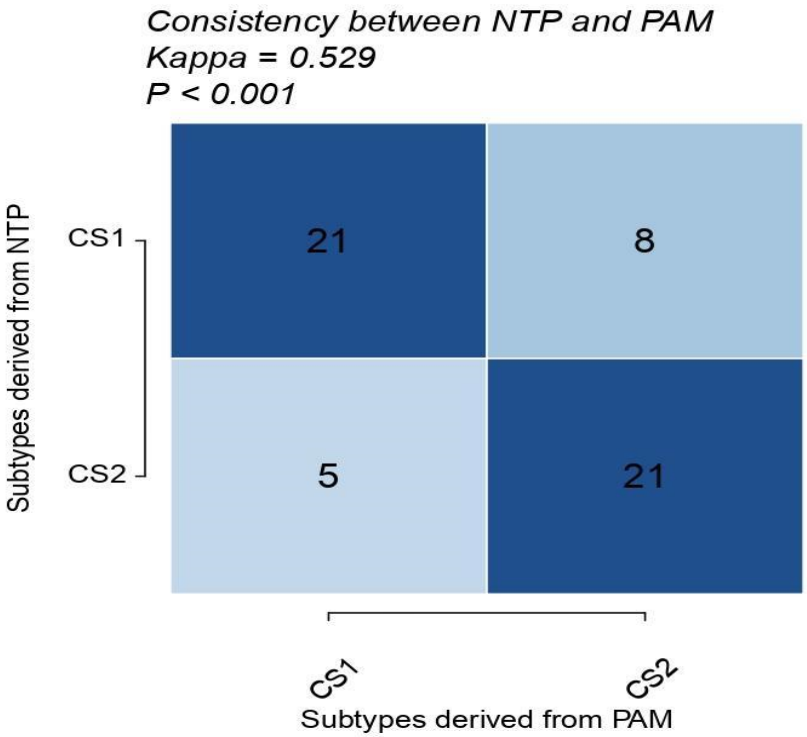


Figure 3.76. Consistency heatmap between NTP and PAM-predicted subtype for DESeq2 results in GSE17537.

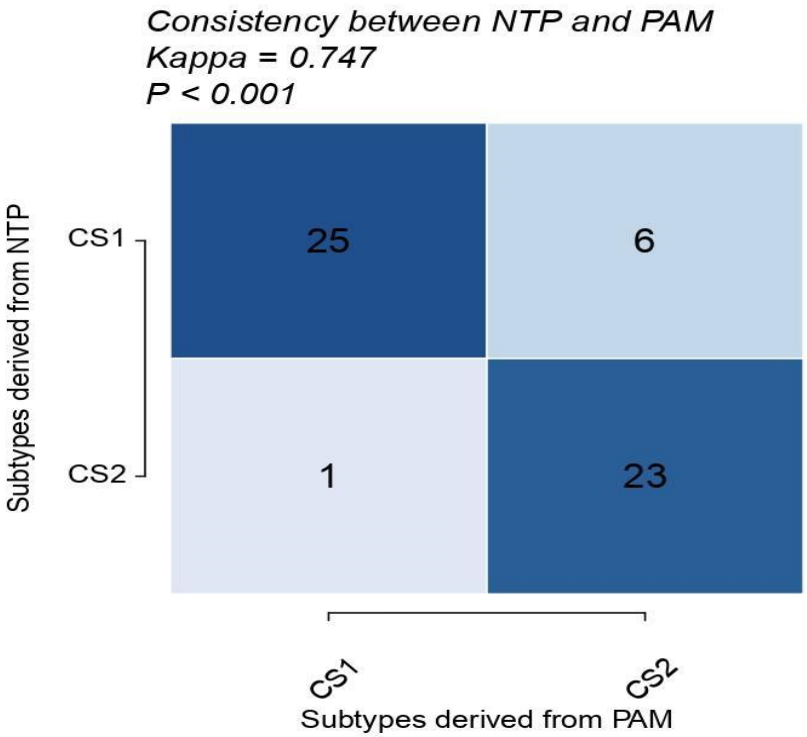


Figure 3.77. Consistency heatmap between NTP and PAM-predicted subtype for limma results in GSE17537.

As a result, the results of the survival analysis were only significant in the GSE16125 cohort with the edgeR and DESeq2 algorithms. For all cohorts, the consistency between the subspecies present and those predicted by NTP in the discovery dataset according to the edgeR algorithm was much more significant than that predicted by PAM, while the consistency results obtained with the DESeq2 and limma algorithms were best with PAM. When examining the consistency between the subtypes recognised by NTP and PAM in the validation dataset in all cohorts, it was also found that the Kappa statistic result was best obtained with the limma algorithm.

3.2. Analysis Results for Three Subtypes

3.2.1. The multi-omics classification of COAD

Based on the results of the CPI and gap statistics, the optimal number of clusters was determined as k2 (Figure 3.1). However, it is not necessary to choose this k2 value when determining the number of clusters. It has already been mentioned that when deciding on the optimal number of clusters, previous molecular classifications of the cancer type in question and new cluster numbers that could potentially be promising after appropriate analyses should also be taken into account. It was also mentioned that the number of clusters at which the values for CPI and gap statistics do not decrease too much can be considered optimal. Therefore, k3, where the CPI and gap statistics are the highest right after k2, is promising and was determined as the optimal number of clusters. The results of the 10 clustering algorithms were then combined based on the idea of consensus ensembles to improve the robustness of clustering (Figure 3.78). Ultimately, patients were categorised into three subtypes: CS1, CS2 and CS3.

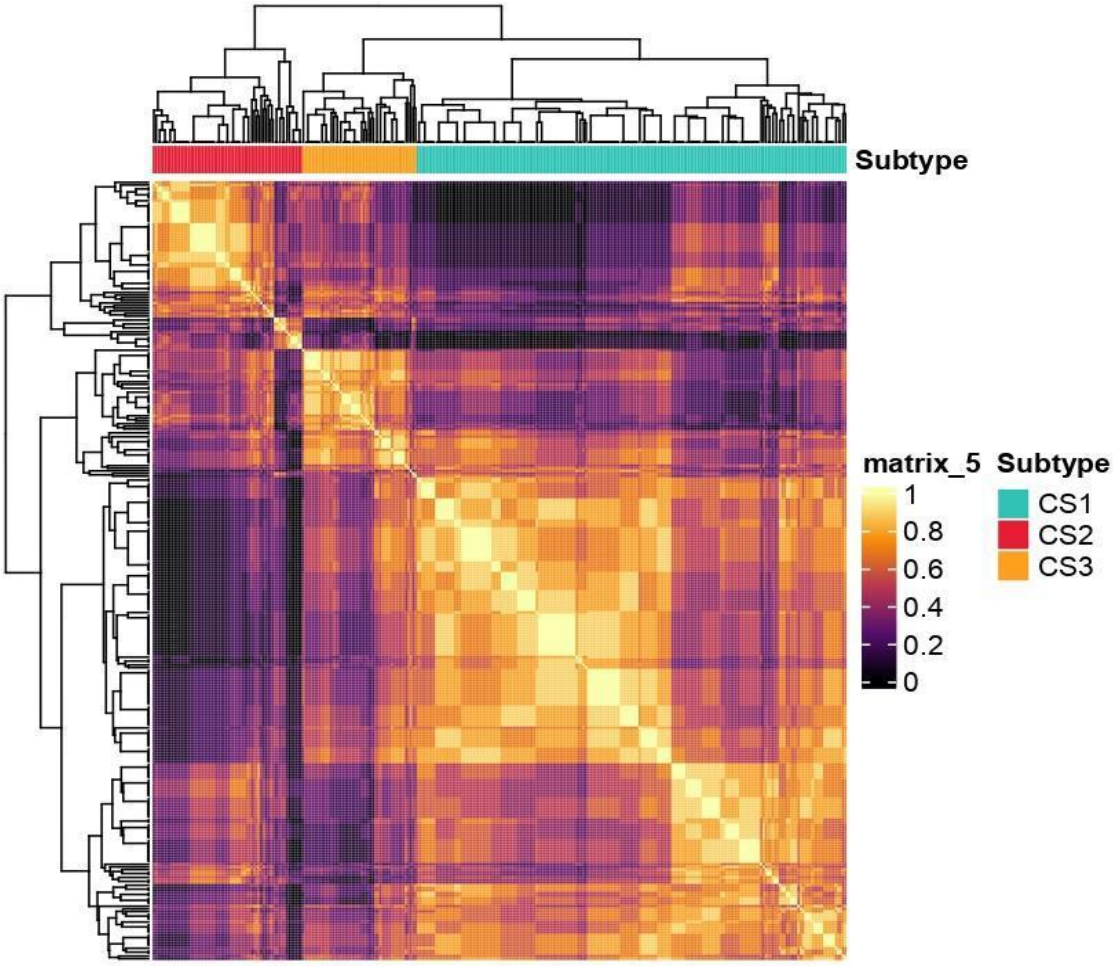


Figure 3.78. Consensus heatmap based on results from 10 multi-omics integrative clustering algorithms with cluster number of 3.

In addition, the similarity of the samples was measured using the silhouette width to verify the clustering result (Figure 3.79). The results showed that these subtypes were distinguishable from each other with silhouette scores of 0.18, 0.53 and 0.27 respectively, but there was still a possibility that some clusters could overlap, with an overall silhouette width of 0.27.

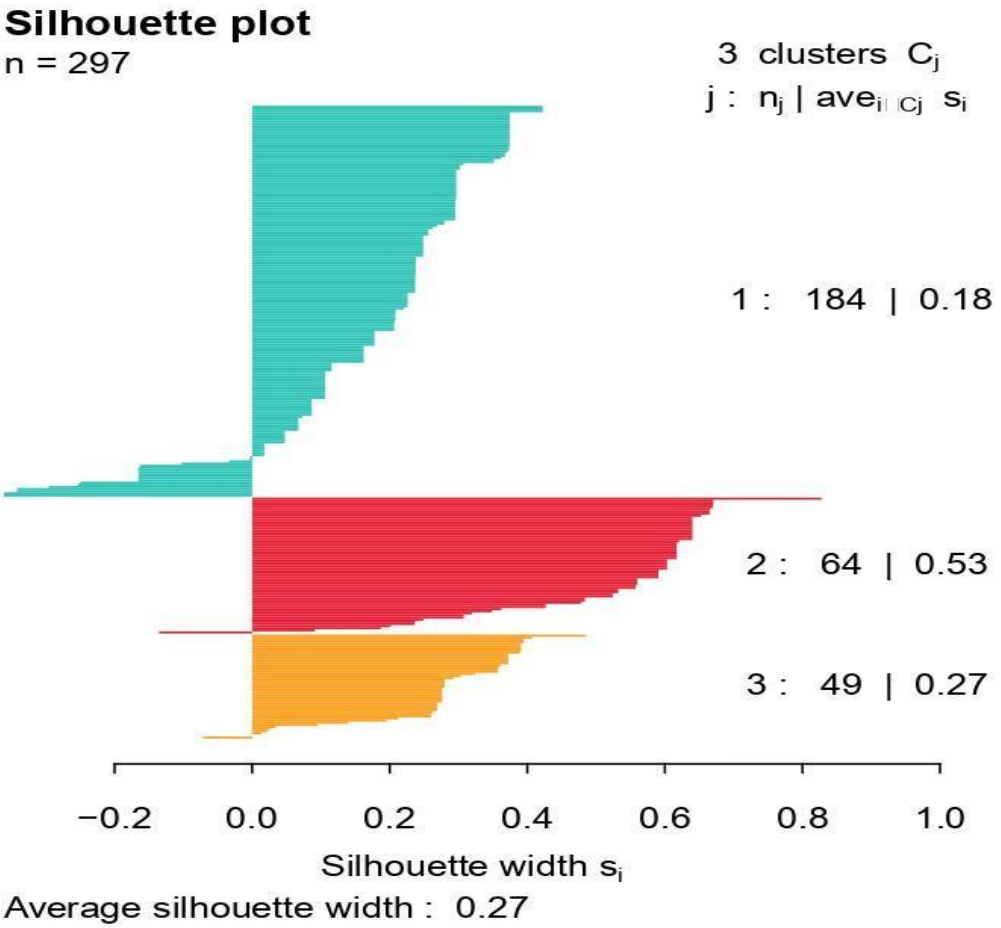


Figure 3.79. Quantification of sample similarity using Silhoutte width based on consensus ensembles result.

A genome-wide heatmap was then created based on mRNA, lncRNA, miRNA, methylation and mutation data and the top 10 features for each omics data were selected using the iClusterBayes algorithm, which allows feature selection (Figure 3.80). This heatmap includes clinicopathological features such as age, stage, race and gender, as well as information on APC mutations. As a result, a relatively pronounced hypermethylated region was observed in subtype CS2. In addition, subtypes CS2 and CS3 are more highly mutated than CS1.

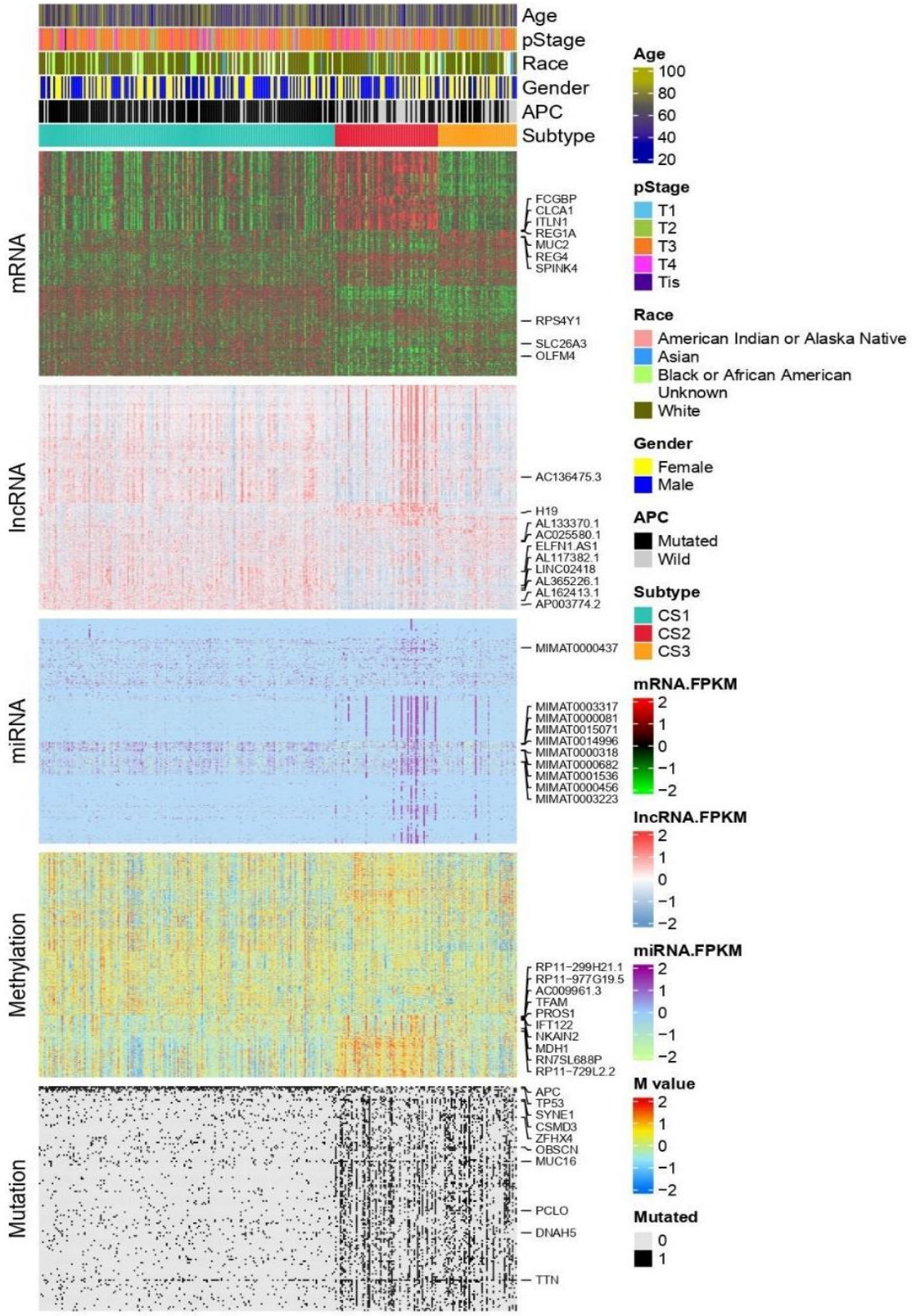


Figure 3.80. Comprehensive heatmap based on consensus across 10 algorithms with clinicopathological and potential drivers annotation.

3.2.2. Differentially expressed genes and signaling pathways

To further investigate the characteristics of the subtypes, DEGs between the subtypes were identified using the packages "edgeR", "DESeq2" and "limma", which are among the most effective tools for differential expression analysis. Based on the results of edgeR, DESeq2 and limma, upregulated biomarkers with the threshold adjusted P-value < 0.05 and Fold Change > 2 parameters were selected, while downregulated biomarkers with adjusted P-value < 0.05 and fold change < 0.5 filters were determined. Using the edgeR method, 1070, 17280 and 956 upregulated and 10327, 814 and 1564 downregulated biomarkers were detected in the CS1, CS2 and CS3 subtypes, respectively. Tables 3.17-3.22 show the 20 most upregulated and downregulated transcripts identified in the CS1, CS2 and CS3 subtypes with edgeR and sorted by FC. All other DEGs identified with edgeR during differential expression analysis are listed in Appendix A.4. WIF1, which inhibits activation of the Wnt/β-catenin signalling pathway that occurs primarily in the majority of colon cancers, was expressed more than 23-fold in CS1 [156]. Thus, WIF1 acts as a tumour suppressor in CS1 and progestagen- associated endometrial protein (PAEP), an immunosuppressive glycoprotein, was expressed more than 100-fold in CS2 [157]. The ETS translocation variant 4 (ETV4), whose low expression inhibits tumour growth, was downregulated in CS2 [158]. The deletion of Deltex E3 ubiquitin ligase 3 (DTX3), which is downregulated in CS3, triggers colony formation and proliferation [159].

Table 3.17. Differentially expressed upregulated transcripts identified in the CS1 subtype using edgeR.

CS1 – Differentially Expressed Up-Regulated Transcripts				
	fc	**log2fc**	**pvalue**	**padj**
BX322234.2	$4.93x10^{1}$	$5.62x10^{0}$	$5.19x10^{-8}$	$2.92x10^{-7}$
WIF1	$4.68x10^{1}$	$5.55x10^{0}$	$1.41x10^{-30}$	$1.59x10^{-28}$
RNA5.8SP5	$4.02x10^{1}$	$5.33x10^{0}$	$1.54x10^{-3}$	$3.91x10^{-3}$
AC152010.1	$3.87x10^{1}$	$5.27x10^{0}$	$4.21x10^{-3}$	$9.65x10^{-3}$
RNA5SP267	$2.94x10^{1}$	$4.88x10^{0}$	$1.48x10^{-2}$	$2.93x10^{-2}$
RNA5SP211	$2.69x10^{1}$	$4.75x10^{0}$	$2.08x10^{-2}$	$3.96x10^{-2}$
RNA5SP389	$2.25x10^{1}$	$4.49x10^{0}$	$1.75x10^{-2}$	$3.41x10^{-2}$
SFTPC	$2.23x10^{1}$	$4.48x10^{0}$	$7.99x10^{-7}$	$3.71x10^{-6}$
SOHLH1	$1.70x10^{1}$	$4.08x10^{0}$	$4.89x10^{-11}$	$4.37x10^{-10}$
KRT31	$1.66x10^{1}$	$4.05x10^{0}$	$4.92x10^{-12}$	$5.12x10^{-11}$

Table 3.17 (continued). Differentially expressed upregulated transcripts identified in the CS1 subtype using edgeR.

AC127459.2	$1.50x10^{1}$	$3.91x10^{0}$	$3.77x10^{-6}$	$1.57x10^{-5}$
LINC01896	$1.42x10^{1}$	$3.83x10^{0}$	$7.61x10^{-4}$	$2.07x10^{-3}$
PRR9	$1.17x10^{1}$	$3.55x10^{0}$	$5.55x10^{-9}$	$3.64x10^{-8}$
AC114291.1	$1.14x10^{1}$	$3.51x10^{0}$	$1.17x10^{-32}$	$1.68x10^{-30}$
AC009446.1	$1.14x10^{1}$	$3.51x10^{0}$	$1.47x10^{-3}$	$3.75x10^{-3}$
PTF1A	$1.14x10^{1}$	$3.51x10^{0}$	$1.46x10^{-10}$	$1.22x10^{-9}$
XAGE2	$1.14x10^{1}$	$3.51x10^{0}$	$7.55x10^{-7}$	$3.52x10^{-6}$
GALP	$1.10x10^{1}$	$3.46x10^{0}$	$1.06x10^{-3}$	$2.80x10^{-3}$
PNLIP	$1.09x10^{1}$	$3.45x10^{0}$	$1.39x10^{-2}$	$2.79x10^{-2}$
SLC5A8	$1.07x10^{1}$	$3.42x10^{0}$	$7.22x10^{-8}$	$3.97x10^{-7}$

Table 3.18. Differentially expressed downregulated transcripts identified in the CS1 subtype using edgeR.

CS1 – Differentially Expressed Down-Regulated Transcripts				
	fc	**log2fc**	**pvalue**	**padj**
RN7SKP227	$3.14x10^{-3}$	$-8.32x10^{0}$	$2.56x10^{-13}$	$3.21x10^{-12}$
RNU1.28P	$3.51x10^{-3}$	$-8.15x10^{0}$	$3.30x10^{-14}$	$4.72x10^{-13}$
RN7SKP203	$4.66x10^{-3}$	$-7.75x10^{0}$	$1.58x10^{-16}$	$3.14x10^{-15}$
RNU1.88P	$4.98x10^{-3}$	$-7.65x10^{0}$	$3.66x10^{-17}$	$7.97x10^{-16}$
MIR3609	$5.02x10^{-3}$	$-7.64x10^{0}$	$4.36x10^{-31}$	$5.17x10^{-29}$
RNY4	$5.31x10^{-3}$	$-7.56x10^{0}$	$5.67x10^{-10}$	$4.34x10^{-9}$
H2BC3	$5.37x10^{-3}$	$-7.54x10^{0}$	$4.44x10^{-28}$	$3.67x10^{-26}$
RNY1	$5.45x10^{-3}$	$-7.52x10^{0}$	$7.83x10^{-18}$	$1.87x10^{-16}$
SCARNA5	$5.70x10^{-3}$	$-7.45x10^{0}$	$1.60x10^{-67}$	$6.54x10^{-64}$
RNU5B.1	$5.80x10^{-3}$	$-7.43x10^{0}$	$2.00x10^{-13}$	$2.55x10^{-12}$
RNVU1.18	$6.25x10^{-3}$	$-7.32x10^{0}$	$7.34x10^{-14}$	$1.00x10^{-12}$
RN7SKP255	$6.49x10^{-3}$	$-7.27x10^{0}$	$6.83x10^{-14}$	$9.36x10^{-13}$
RNU2.59P	$6.54x10^{-3}$	$-7.26x10^{0}$	$5.36x10^{-15}$	$8.61x10^{-14}$
RN7SL149P	$6.82x10^{-3}$	$-7.20x10^{0}$	$6.89x10^{-13}$	$8.12x10^{-12}$
RNU1.11P	$7.00x10^{-3}$	$-7.16x10^{0}$	$1.71x10^{-11}$	$1.64x10^{-10}$
RN7SKP9	$7.06x10^{-3}$	$-7.15x10^{0}$	$4.02x10^{-31}$	$4.82x10^{-29}$
RNU5A.1	$7.39x10^{-3}$	$-7.08x10^{0}$	$8.84x10^{-21}$	$3.16x10^{-19}$
AL139274.1	$7.69x10^{-3}$	$-7.02x10^{0}$	$3.58x10^{-20}$	$1.17x10^{-18}$
RN7SKP186	$8.25x10^{-3}$	$-6.92x10^{0}$	$5.33x10^{-14}$	$7.41x10^{-13}$
AL356057.1	$8.82x10^{-3}$	$-6.83x10^{0}$	$1.59x10^{-18}$	$4.18x10^{-17}$

Table 3.19. Differentially expressed upregulated transcripts identified in the CS2 subtype using edgeR.

CS2 – Differentially Expressed Up-Regulated Transcripts				
	fc	**log2fc**	**pvalue**	**padj**
RNY4	$2.84x10^{2}$	$8.15x10^{0}$	$1.62x10^{-16}$	$1.81x10^{-15}$
PAEP	$2.04x10^{2}$	$7.67x10^{0}$	$1.48x10^{-94}$	$2.12x10^{-90}$
FBXO40	$1.99x10^{2}$	$7.63x10^{0}$	$5.97x10^{-60}$	$4.27x10^{-57}$

Table 3.19 (continued). Differentially expressed upregulated transcripts identified in the CS2 subtype using edgeR.

RNU1.28P	$1.74x10^{2}$	$7.44x10^{0}$	$9.62x10^{-11}$	$5.70x10^{-10}$
RNVU1.2	$1.67x10^{2}$	$7.39x10^{0}$	$2.05x10^{-24}$	$5.11x10^{-23}$
MTND5P32	$1.48x10^{2}$	$7.20x10^{0}$	$2.85x10^{-27}$	$9.33x10^{-26}$
AC066616.2	$1.41x10^{2}$	$7.14x10^{0}$	$2.47x10^{-29}$	$9.92x10^{-28}$
RNU1.19P	$1.37x10^{2}$	$7.10x10^{0}$	$7.00x10^{-20}$	$1.09x10^{-18}$
RNVU1.18	$1.34x10^{2}$	$7.07x10^{0}$	$1.08x10^{-12}$	$7.97x10^{-12}$
RNU1.20P	$1.33x10^{2}$	$7.05x10^{0}$	$5.85x10^{-16}$	$6.18x10^{-15}$
TFAP2B	$1.30x10^{2}$	$7.02x10^{0}$	$3.53x10^{-27}$	$1.14x10^{-25}$
RNU1.83P	$1.28x10^{2}$	$7.00x10^{0}$	$3.76x10^{-21}$	$6.67x10^{-20}$
AC090220.1	$1.27x10^{2}$	$6.99x10^{0}$	$1.57x10^{-30}$	$7.04x10^{-29}$
RNU2.59P	$1.26x10^{2}$	$6.98x10^{0}$	$4.90x10^{-15}$	$4.70x10^{-14}$
RNU1.52P	$1.23x10^{2}$	$6.94x10^{0}$	$2.97x10^{-12}$	$2.09x10^{-11}$
RNU1.139P	$1.18x10^{2}$	$6.89x10^{0}$	$3.67x10^{-14}$	$3.20x10^{-13}$
SERPINB13	$1.17x10^{2}$	$6.88x10^{0}$	$1.01x10^{-22}$	$2.10x10^{-21}$
MTCYBP23	$1.12x10^{2}$	$6.81x10^{0}$	$5.16x10^{-26}$	$1.49x10^{-24}$
RNU1.46P	$1.12x10^{2}$	$6.81x10^{0}$	$3.02x10^{-16}$	$3.28x10^{-15}$
Y_RNA.241	$1.09x10^{2}$	$6.77x10^{0}$	$6.93x10^{-20}$	$1.08x10^{-18}$

Table 3.20. Differentially expressed downregulated transcripts identified in the CS2 subtype using edgeR.

CS2 – Differentially Expressed Down-Regulated Transcripts				
	fc	**log2fc**	**pvalue**	**padj**
RNA5.8SP5	$3.34x10^{-2}$	$-4.90x10^{0}$	$2.48x10^{-2}$	$4.18x10^{-2}$
CLEC2A	$4.82x10^{-2}$	$-4.37x10^{0}$	$4.83x10^{-4}$	$1.16x10^{-3}$
RPL35P2	$4.93x10^{-2}$	$-4.34x10^{0}$	$3.39x10^{-6}$	$1.14x10^{-5}$
ALB	$5.73x10^{-2}$	$-4.13x10^{0}$	$5.41x10^{-10}$	$2.93x10^{-9}$
ORM1	$5.83x10^{-2}$	$-4.10x10^{0}$	$9.71x10^{-9}$	$4.56x10^{-8}$
FP236383.7	$7.76x10^{-2}$	$-3.69x10^{0}$	$1.31x10^{-2}$	$2.36x10^{-2}$
AC079804.2	$7.89x10^{-2}$	$-3.66x10^{0}$	$6.28x10^{-7}$	$2.34x10^{-6}$
BHLHA9	$7.92x10^{-2}$	$-3.66x10^{0}$	$3.54x10^{-11}$	$2.20x10^{-10}$
AC018695.1	$8.04x10^{-2}$	$-3.64x10^{0}$	$8.43x10^{-9}$	$3.99x10^{-8}$
APOA2	$8.25x10^{-2}$	$-3.60x10^{0}$	$6.14x10^{-10}$	$3.30x10^{-9}$
DEFA6	$9.44x10^{-2}$	$-3.41x10^{0}$	$5.25x10^{-9}$	$2.54x10^{-8}$
AL049830.1	$1.03x10^{-1}$	$-3.28x10^{0}$	$5.95x10^{-9}$	$2.86x10^{-8}$
SRIP3	$1.07x10^{-1}$	$-3.23x10^{0}$	$1.01x10^{-4}$	$2.72x10^{-4}$
AC074085.2	$1.11x10^{-1}$	$-3.17x10^{0}$	$1.12x10^{-11}$	$7.39x10^{-11}$
ATP12A	$1.13x10^{-1}$	$-3.15x10^{0}$	$4.81x10^{-8}$	$2.07x10^{-7}$
GALP	$1.20x10^{-1}$	$-3.05x10^{0}$	$2.92x10^{-2}$	$4.84x10^{-2}$
AC087612.1	$1.25x10^{-1}$	$-3.00x10^{0}$	$1.20x10^{-4}$	$3.20x10^{-4}$
AC244102.3	$1.26x10^{-1}$	$-2.98x10^{0}$	$2.19x10^{-2}$	$3.74x10^{-2}$
SNHG25	$1.28x10^{-1}$	$-2.97x10^{0}$	$2.08x10^{-12}$	$1.49x10^{-11}$
RPS5P8	$1.28x10^{-1}$	$-2.97x10^{0}$	$3.84x10^{-8}$	$1.67x10^{-7}$

Table 3.21. Differentially expressed upregulated transcripts identified in the CS3 subtype using edgeR.

CS3 – Differentially Expressed Up-Regulated Transcripts				
	fc	**log2fc**	**pvalue**	**padj**
RN7SL618P	$1.22x10^{2}$	$6.93x10^{0}$	$5.37x10^{-8}$	$1.92x10^{-6}$
RN7SL149P	$1.15x10^{2}$	$6.85x10^{0}$	$2.25x10^{-10}$	$2.10x10^{-8}$
RN7SL783P	$4.79x10^{1}$	$5.58x10^{0}$	$7.17x10^{-7}$	$1.71x10^{-5}$
RN7SL822P	$4.51x10^{1}$	$5.49x10^{0}$	$1.62x10^{-6}$	$3.40x10^{-5}$
RN7SL122P	$4.48x10^{1}$	$5.49x10^{0}$	$8.84x10^{-10}$	$6.22x10^{-8}$
RN7SL7P	$4.08x10^{1}$	$5.35x10^{0}$	$1.09x10^{-8}$	$5.07x10^{-7}$
RN7SL762P	$4.05x10^{1}$	$5.34x10^{0}$	$1.13x10^{-33}$	$2.16x10^{-29}$
RN7SL837P	$3.99x10^{1}$	$5.32x10^{0}$	$1.22x10^{-7}$	$3.82x10^{-6}$
RN7SL217P	$3.88x10^{1}$	$5.28x10^{0}$	$2.82x10^{-12}$	$5.37x10^{-10}$
RN7SL507P	$3.61x10^{1}$	$5.17x10^{0}$	$1.96x10^{-10}$	$1.88x10^{-8}$
RN7SL546P	$3.14x10^{1}$	$4.97x10^{0}$	$7.22x10^{-31}$	$6.88x10^{-27}$
RN7SL253P	$3.00x10^{1}$	$4.91x10^{0}$	$8.55x10^{-19}$	$1.36x10^{-15}$
GP2	$2.99x10^{1}$	$4.90x10^{0}$	$6.31x10^{-33}$	$9.04x10^{-29}$
RN7SL792P	$2.66x10^{1}$	$4.73x10^{0}$	$6.97x10^{-12}$	$1.18x10^{-9}$
RN7SL126P	$2.57x10^{1}$	$4.68x10^{0}$	$1.71x10^{-6}$	$3.55x10^{-5}$
RN7SL575P	$2.39x10^{1}$	$4.58x10^{0}$	$2.38x10^{-6}$	$4.65x10^{-5}$
RN7SL714P	$2.31x10^{1}$	$4.53x10^{0}$	$6.68x10^{-5}$	$7.52x10^{-4}$
RN7SL14P	$2.28x10^{1}$	$4.51x10^{0}$	$2.39x10^{-6}$	$4.67x10^{-5}$
RN7SL498P	$2.01x10^{1}$	$4.33x10^{0}$	$8.10x10^{-8}$	$2.69x10^{-6}$
LINC01790	$1.92x10^{1}$	$4.26x10^{0}$	$6.34x10^{-4}$	$4.67x10^{-3}$

Table 3.22. Differentially expressed downregulated transcripts identified in the CS3 subtype using edgeR.

CS3 – Differentially Expressed Down-Regulated Transcripts				
	fc	**log2fc**	**pvalue**	**padj**
PNMA5	$5.86x10^{-3}$	$-7.41x10^{0}$	$1.46x10^{-10}$	$1.48x10^{-8}$
PAGE1	$1.49x10^{-2}$	$-6.07x10^{0}$	$2.61x10^{-4}$	$2.29x10^{-3}$
MAGEA3	$2.12x10^{-2}$	$-5.56x10^{0}$	$8.80x10^{-5}$	$9.44x10^{-4}$
MAGEA4	$2.19x10^{-2}$	$-5.51x10^{0}$	$1.45x10^{-4}$	$1.43x10^{-3}$
COL2A1	$2.38x10^{-2}$	$-5.39x10^{0}$	$6.01x10^{-16}$	$4.19x10^{-13}$
MAGEA12	$2.80x10^{-2}$	$-5.16x10^{0}$	$1.36x10^{-4}$	$1.36x10^{-3}$
CSAG1	$2.97x10^{-2}$	$-5.07x10^{0}$	$4.67x10^{-6}$	$8.10x10^{-5}$
CDH9	$3.57x10^{-2}$	$-4.81x10^{0}$	$1.25x10^{-4}$	$1.27x10^{-3}$
CIDEA	$3.91x10^{-2}$	$-4.68x10^{0}$	$6.18x10^{-5}$	$7.05x10^{-4}$
MAGEA10	$4.16x10^{-2}$	$-4.59x10^{0}$	$9.06x10^{-5}$	$9.67x10^{-4}$
LINC02864	$4.33x10^{-2}$	$-4.53x10^{0}$	$1.94x10^{-6}$	$3.93x10^{-5}$
MAGEA4.AS1	$4.34x10^{-2}$	$-4.53x10^{0}$	$1.00x10^{-4}$	$1.05x10^{-3}$
TMEM132D.AS1	$4.77x10^{-2}$	$-4.39x10^{0}$	$5.89x10^{-4}$	$4.41x10^{-3}$
LINC01419	$4.79x10^{-2}$	$-4.38x10^{0}$	$1.18x10^{-5}$	$1.78x10^{-4}$
MAGEA6	$5.10x10^{-2}$	$-4.29x10^{0}$	$1.50x10^{-3}$	$9.35x10^{-3}$
SALL3	$5.30x10^{-2}$	$-4.24x10^{0}$	$1.26x10^{-3}$	$8.15x10^{-3}$

Table 3.22 (continued). Differentially expressed downregulated transcripts identified in the CS3 subtype using edgeR.

SFTPA1	$5.52x10^{-2}$	$-4.18x10^{0}$	$2.17x10^{-5}$	$2.97x10^{-4}$

GABRA3	$5.55x10^{-2}$	$-4.17x10^{0}$	$1.39x10^{-9}$	$8.97x10^{-8}$
AC009446.1	$5.59x10^{-2}$	$-4.16x10^{0}$	$1.66x10^{-3}$	$1.01x10^{-2}$
AC244102.4	$5.65x10^{-2}$	$-4.14x10^{0}$	$6.70x10^{-3}$	$3.02x10^{-2}$

As a result of the differential expression analysis with DESeq2, 831, 14968 and 563 upregulated and 7479, 693 and 1340 downregulated biomarkers were identified for the subtypes CS1, CS2 and CS3, respectively. Tables 3.23-3.28 show the 20 most upregulated and downregulated transcripts identified in the CS1, CS2 and CS3 subtypes with DESeq2 and sorted by FC. All other DEGs identified with DESeq2 during differential expression analysis are listed in Appendix A.5.

Insulin-like growth factor 2 (IGF2), whose overexpression has been associated with colon cancer metastasis, was upregulated more than 10-fold in CS1 [160]. Thymidine phosphorylase (TYMP), which prevents T cell exhaustion by triggering immunological cell death, is downregulated in CS1 [161]. Piwi like RNA-mediated gene silencing 2 (PIWIL2), the overexpression of which contributes to the development and metastasis of colon cancer, is downregulated in the CS2 subtype [162].

Table 3.23. Differentially expressed upregulated transcripts identified in the CS1 subtype using DESeq2.

CS1 – Differentially Expressed Up-Regulated Transcripts				
	fc	**log2fc**	**pvalue**	**padj**
WIF1	$4.37x10^{1}$	$5.45x10^{0}$	$2.86x10^{-49}$	$3.92x10^{-46}$
PTF1A	$2.66x10^{1}$	$4.74x10^{0}$	$3.00x10^{-23}$	$1.12x10^{-21}$
PRSS56	$2.25x10^{1}$	$4.49x10^{0}$	$5.39x10^{-26}$	$3.01x10^{-24}$
IGF2	$2.18x10^{1}$	$4.45x10^{0}$	$7.08x10^{-36}$	$1.78x10^{-33}$
LY6G6D	$1.59x10^{1}$	$3.99x10^{0}$	$3.99x10^{-38}$	$1.36x10^{-35}$
AC026774.1	$1.20x10^{1}$	$3.58x10^{0}$	$2.42x10^{-20}$	$5.74x10^{-19}$
KRT35	$1.13x10^{1}$	$3.50x10^{0}$	$2.73x10^{-13}$	$2.47x10^{-12}$
AL356433.1	$1.12x10^{1}$	$3.48x10^{0}$	$2.45x10^{-16}$	$3.33x10^{-15}$
LY6G6F.LY6G6D	$1.10x10^{1}$	$3.46x10^{0}$	$2.77x10^{-27}$	$1.92x10^{-25}$
NOTUM	$1.09x10^{1}$	$3.44x10^{0}$	$1.60x10^{-34}$	$3.21x10^{-32}$
AC114291.1	$1.07x10^{1}$	$3.41x10^{0}$	$2.09x10^{-40}$	$9.46x10^{-38}$
GOLGA6L2	$1.05x10^{1}$	$3.39x10^{0}$	$1.10x10^{-21}$	$3.22x10^{-20}$
LCN15	$9.89x10^{0}$	$3.31x10^{0}$	$8.16x10^{-20}$	$1.78x10^{-18}$
CDH9	$9.56x10^{0}$	$3.26x10^{0}$	$9.52x10^{-6}$	$3.00x10^{-5}$
MAGEA4.AS1	$9.44x10^{0}$	$3.24x10^{0}$	$3.37x10^{-5}$	$9.73x10^{-5}$

Table 3.23 (continued). Differentially expressed upregulated transcripts identified in the CS1 subtype using DESeq2.

BHLHA9	$9.24x10^{0}$	$3.21x10^{0}$	$1.46x10^{-20}$	$3.60x10^{-19}$
AC026336.3	$9.16x10^{0}$	$3.20x10^{0}$	$6.82x10^{-23}$	$2.43x10^{-21}$

HSPB3	$8.92x10^{0}$	$3.16x10^{0}$	$3.25x10^{-21}$	$8.87x10^{-20}$
CPN1	$8.47x10^{0}$	$3.08x10^{0}$	$1.69x10^{-21}$	$4.83x10^{-20}$
SULT2A1	$8.31x10^{0}$	$3.05x10^{0}$	$8.20x10^{-20}$	$1.79x10^{-18}$

Table 3.24. Differentially expressed downregulated transcripts identified in the CS1 subtype using DESeq2.

CS1 – Differentially Expressed Down-Regulated Transcripts				
	fc	**log2fc**	**pvalue**	**padj**
RN7SKP227	$3.14x10^{-4}$	$-1.16x10^{1}$	$3.98x10^{-9}$	$2.04x10^{-8}$
CLDN18	$5.71x10^{-3}$	$-7.45x10^{0}$	$1.09x10^{-114}$	$4.77x10^{-110}$
AL139274.1	$6.89x10^{-3}$	$-7.18x10^{0}$	$3.03x10^{-19}$	$6.16x10^{-18}$
AL390318.1	$1.10x10^{-2}$	$-6.51x10^{0}$	$2.25x10^{-6}$	$7.81x10^{-6}$
AL139120.1	$1.23x10^{-2}$	$-6.34x10^{0}$	$3.42x10^{-11}$	$2.32x10^{-10}$
ANXA10	$1.38x10^{-2}$	$-6.18x10^{0}$	$2.50x10^{-87}$	$5.50x10^{-83}$
RN7SKP186	$1.47x10^{-2}$	$-6.09x10^{0}$	$1.56x10^{-3}$	$3.37x10^{-3}$
AC096741.1	$1.47x10^{-2}$	$-6.09x10^{0}$	$3.92x10^{-14}$	$3.97x10^{-13}$
LPP.AS1	$1.52x10^{-2}$	$-6.04x10^{0}$	$1.01x10^{-8}$	$4.85x10^{-8}$
RAD51AP1P1	$1.60x10^{-2}$	$-5.97x10^{0}$	$2.25x10^{-9}$	$1.19x10^{-8}$
AC010997.6	$1.61x10^{-2}$	$-5.96x10^{0}$	$3.07x10^{-10}$	$1.82x10^{-9}$
EIF4E2P1	$1.77x10^{-2}$	$-5.82x10^{0}$	$2.06x10^{-8}$	$9.53x10^{-8}$
EDDM3CP	$1.83x10^{-2}$	$-5.77x10^{0}$	$5.67x10^{-5}$	$1.58x10^{-4}$
AL606517.2	$1.85x10^{-2}$	$-5.76x10^{0}$	$6.84x10^{-7}$	$2.56x10^{-6}$
RNY3	$1.85x10^{-2}$	$-5.76x10^{0}$	$5.36x10^{-5}$	$1.50x10^{-4}$
AL136320.1	$1.86x10^{-2}$	$-5.75x10^{0}$	$6.15x10^{-16}$	$7.95x10^{-15}$
AC018398.2	$1.87x10^{-2}$	$-5.74x10^{0}$	$8.54x10^{-15}$	$9.48x10^{-14}$
METTL21AP1	$1.88x10^{-2}$	$-5.74x10^{0}$	$5.68x10^{-11}$	$3.75x10^{-10}$
AL589655.1	$1.92x10^{-2}$	$-5.70x10^{0}$	$1.67x10^{-6}$	$5.90x10^{-6}$
PIGFP2	$1.93x10^{-2}$	$-5.69x10^{0}$	$1.57x10^{-6}$	$5.59x10^{-6}$

Table 3.25. Differentially expressed upregulated transcripts identified in the CS2 subtype using DESeq2.

CS2 – Differentially Expressed Up-Regulated Transcripts				
	fc	**log2fc**	**pvalue**	**padj**
RNU1.88P	$8.61x10^{2}$	$9.75x10^{0}$	$6.85x10^{-29}$	$2.01x10^{-27}$
RN7SKP203	$6.76x10^{2}$	$9.40x10^{0}$	$6.26x10^{-27}$	$1.50x10^{-25}$
RNU2.59P	$5.33x10^{2}$	$9.06x10^{0}$	$3.20x10^{-17}$	$2.98x10^{-16}$
RNU2.23P	$5.12x10^{2}$	$9.00x10^{0}$	$2.22x10^{-12}$	$1.28x10^{-11}$
MTND5P26	$4.88x10^{2}$	$8.93x10^{0}$	$1.03x10^{-14}$	$7.51x10^{-14}$
RNY3	$4.50x10^{2}$	$8.81x10^{0}$	$4.92x10^{-10}$	$2.23x10^{-9}$
MTCYBP32	$4.28x10^{2}$	$8.74x10^{0}$	$2.14x10^{-14}$	$1.51x10^{-13}$
AC022537.1	$4.16x10^{2}$	$8.70x10^{0}$	$4.55x10^{-11}$	$2.30x10^{-10}$

Table 3.25 (continued). Differentially expressed upregulated transcripts identified in the CS2 subtype using DESeq2.

RN7SKP255	$3.82x10^{2}$	$8.58x10^{0}$	$3.27x10^{-22}$	$4.93x10^{-21}$
RNVU1.2A	$3.69x10^{2}$	$8.53x10^{0}$	$4.01x10^{-13}$	$2.49x10^{-12}$
AC010997.6	$3.27x10^{2}$	$8.35x10^{0}$	$4.50x10^{-17}$	$4.12x10^{-16}$

ZNF75BP	$3.14x10^{2}$	$8.29x10^{0}$	$3.73x10^{-14}$	$2.57x10^{-13}$
RN7SKP186	$3.08x10^{2}$	$8.27x10^{0}$	$2.70x10^{-5}$	$7.16x10^{-5}$
RNVU1.2	$3.06x10^{2}$	$8.26x10^{0}$	$1.01x10^{-22}$	$1.60x10^{-21}$
AC100800.1	$2.92x10^{2}$	$8.19x10^{0}$	$8.70x10^{-19}$	$9.42x10^{-18}$
AC090220.1	$2.71x10^{2}$	$8.08x10^{0}$	$5.06x10^{-24}$	$9.08x10^{-23}$
SCARNA5	$2.70x10^{2}$	$8.08x10^{0}$	$8.01x10^{-109}$	$1.94x10^{-104}$
RNU5A.1	$2.66x10^{2}$	$8.05x10^{0}$	$2.44x10^{-32}$	$1.00x10^{-30}$
AL391863.2	$2.57x10^{2}$	$8.00x10^{0}$	$1.87x10^{-31}$	$7.07x10^{-30}$
AL360178.2	$2.54x10^{2}$	$7.99x10^{0}$	$2.97x10^{-14}$	$2.06x10^{-13}$

Table 3.26. Differentially expressed downregulated transcripts identified in the CS2 subtype using DESeq2.

CS2 – Differentially Expressed Down-Regulated Transcripts				
	fc	**log2fc**	**pvalue**	**padj**
AC079804.2	$5.63x10^{-2}$	$-4.15x10^{0}$	$1.16x10^{-11}$	$6.21x10^{-11}$
RPL35P2	$7.11x10^{-2}$	$-3.81x10^{0}$	$7.37x10^{-9}$	$2.95x10^{-8}$
FP236383.5	$7.41x10^{-2}$	$-3.75x10^{0}$	$1.68x10^{-2}$	$2.95x10^{-2}$
SRIP3	$1.06x10^{-1}$	$-3.24x10^{0}$	$1.69x10^{-5}$	$4.60x10^{-5}$
RPL35AP21	$1.23x10^{-1}$	$-3.02x10^{0}$	$1.85x10^{-8}$	$7.11x10^{-8}$
MAGEB2	$1.27x10^{-1}$	$-2.98x10^{0}$	$8.49x10^{-4}$	$1.84x10^{-3}$
MIF	$1.36x10^{-1}$	$-2.87x10^{0}$	$6.74x10^{-7}$	$2.17x10^{-6}$
BOLA2P1	$1.53x10^{-1}$	$-2.71x10^{0}$	$1.01x10^{-4}$	$2.49x10^{-4}$
CNN2P4	$1.55x10^{-1}$	$-2.69x10^{0}$	$6.52x10^{-5}$	$1.65x10^{-4}$
RETNLB	$1.61x10^{-1}$	$-2.64x10^{0}$	$9.12x10^{-17}$	$8.08x10^{-16}$
DEFA6	$1.70x10^{-1}$	$-2.56x10^{0}$	$1.35x10^{-9}$	$5.84x10^{-9}$
DEFA5	$1.70x10^{-1}$	$-2.56x10^{0}$	$4.94x10^{-9}$	$2.02x10^{-8}$
EIF3IP1	$1.74x10^{-1}$	$-2.52x10^{0}$	$2.16x10^{-6}$	$6.57x10^{-6}$
AL138785.1	$1.75x10^{-1}$	$-2.52x10^{0}$	$6.82x10^{-15}$	$5.06x10^{-14}$
RPL35AP34	$1.76x10^{-1}$	$-2.51x10^{0}$	$7.98x10^{-5}$	$1.99x10^{-4}$
GGT4P	$1.77x10^{-1}$	$-2.50x10^{0}$	$1.79x10^{-16}$	$1.53x10^{-15}$
OR7E121P	$1.81x10^{-1}$	$-2.47x10^{0}$	$2.25x10^{-6}$	$6.83x10^{-6}$
EIF3KP3	$1.81x10^{-1}$	$-2.46x10^{0}$	$8.16x10^{-3}$	$1.52x10^{-2}$
MT.TY	$1.88x10^{-1}$	$-2.41x10^{0}$	$1.19x10^{-12}$	$7.04x10^{-12}$
AC008026.2	$1.89x10^{-1}$	$-2.40x10^{0}$	$6.66x10^{-8}$	$2.40x10^{-7}$

Table 3.27. Differentially expressed upregulated transcripts identified in the CS3 subtype using DESeq2.

CS3 – Differentially Expressed Up-Regulated Transcripts				
	fc	**log2fc**	**pvalue**	**padj**
GP2	$3.02x10^{1}$	$4.92x10^{0}$	$1.27x10^{-22}$	$5.18x10^{-19}$

Table 3.27 (continued). Differentially expressed upregulated transcripts identified in the CS3 subtype using DESeq2.

TTC29	$2.22x10^{1}$	$4.47x10^{0}$	$6.03x10^{-12}$	$5.80x10^{-10}$
RN7SL507P	$1.14x10^{1}$	$3.51x10^{0}$	$6.87x10^{-6}$	$9.41x10^{-5}$
TM4SF4	$1.01x10^{1}$	$3.34x10^{0}$	$8.68x10^{-17}$	$5.18x10^{-14}$
FGL1	$9.61x10^{0}$	$3.27x10^{0}$	$8.73x10^{-9}$	$2.98x10^{-7}$

CYP1A1	$9.53x10^{0}$	$3.25x10^{0}$	$1.93x10^{-9}$	$8.19x10^{-8}$
LINC02620	$8.93x10^{0}$	$3.16x10^{0}$	$1.13x10^{-3}$	$6.62x10^{-3}$
IGFALS	$8.77x10^{0}$	$3.13x10^{0}$	$5.67x10^{-17}$	$3.42x10^{-14}$
RBP3	$8.57x10^{0}$	$3.10x10^{0}$	$1.68x10^{-14}$	$4.03x10^{-12}$
CTSE	$8.34x10^{0}$	$3.06x10^{0}$	$1.88x10^{-15}$	$6.45x10^{-13}$
AC009078.1	$8.23x10^{0}$	$3.04x10^{0}$	$1.48x10^{-4}$	$1.24x10^{-3}$
AC253536.4	$8.23x10^{0}$	$3.04x10^{0}$	$6.96x10^{-10}$	$3.39x10^{-8}$
EIF3KP3	$8.23x10^{0}$	$3.04x10^{0}$	$1.63x10^{-3}$	$8.96x10^{-3}$
AC092435.1	$8.11x10^{0}$	$3.02x10^{0}$	$3.13x10^{-3}$	$1.52x10^{-2}$
MUC5AC	$7.78x10^{0}$	$2.96x10^{0}$	$1.19x10^{-11}$	$1.04x10^{-9}$
AC021534.1	$7.52x10^{0}$	$2.91x10^{0}$	$7.37x10^{-7}$	$1.39x10^{-5}$
IRX4.AS1	$7.38x10^{0}$	$2.88x10^{0}$	$6.49x10^{-3}$	$2.76x10^{-2}$
TFF1	$6.76x10^{0}$	$2.76x10^{0}$	$2.96x10^{-19}$	$3.94x10^{-16}$
AC009517.1	$6.74x10^{0}$	$2.75x10^{0}$	$9.48x10^{-6}$	$1.23x10^{-4}$
ALPG	$6.63x10^{0}$	$2.73x10^{0}$	$7.59x10^{-14}$	$1.47x10^{-11}$

Table 3.28. Differentially expressed downregulated transcripts identified in the CS3 subtype using DESeq2.

CS3 – Differentially Expressed Down-Regulated Transcripts				
	fc	**log2fc**	**pvalue**	**padj**
AC244102.4	$2.96x10^{-2}$	$-5.08x10^{0}$	$6.16x10^{-5}$	$5.99x10^{-4}$
TMEM132D.AS1	$4.01x10^{-2}$	$-4.64x10^{0}$	$3.29x10^{-7}$	$6.95x10^{-6}$
MAGEA3	$4.54x10^{-2}$	$-4.46x10^{0}$	$3.21x10^{-6}$	$4.93x10^{-5}$
AC244102.3	$4.64x10^{-2}$	$-4.43x10^{0}$	$2.92x10^{-5}$	$3.19x10^{-4}$
LINC00491	$4.96x10^{-2}$	$-4.33x10^{0}$	$7.64x10^{-6}$	$1.03x10^{-4}$
MAGEA4	$5.19x10^{-2}$	$-4.27x10^{0}$	$1.74x10^{-5}$	$2.06x10^{-4}$
CSAG1	$5.48x10^{-2}$	$-4.19x10^{0}$	$1.27x10^{-8}$	$4.17x10^{-7}$
MTND1P23	$5.51x10^{-2}$	$-4.18x10^{0}$	$2.84x10^{-20}$	$6.02x10^{-17}$
LINC00355	$5.51x10^{-2}$	$-4.18x10^{0}$	$3.19x10^{-8}$	$9.30x10^{-7}$
VSTM2B	$5.67x10^{-2}$	$-4.14x10^{0}$	$4.81x10^{-10}$	$2.44x10^{-8}$
AC090809.1	$5.92x10^{-2}$	$-4.08x10^{0}$	$9.35x10^{-9}$	$3.17x10^{-7}$
HTR2C	$6.22x10^{-2}$	$-4.01x10^{0}$	$6.33x10^{-5}$	$6.13x10^{-4}$
GABRA3	$6.25x10^{-2}$	$-4.00x10^{0}$	$1.06x10^{-14}$	$2.70x10^{-12}$
HAND1	$6.48x10^{-2}$	$-3.95x10^{0}$	$9.88x10^{-15}$	$2.56x10^{-12}$
MAGEA12	$6.51x10^{-2}$	$-3.94x10^{0}$	$1.17x10^{-5}$	$1.47x10^{-4}$
CIDEA	$6.78x10^{-2}$	$-3.88x10^{0}$	$4.61x10^{-6}$	$6.70x10^{-5}$
AL591501.1	$6.94x10^{-2}$	$-3.85x10^{0}$	$1.54x10^{-11}$	$1.29x10^{-9}$
AL589787.2	$7.51x10^{-2}$	$-3.73x10^{0}$	$2.53x10^{-6}$	$4.00x10^{-5}$
AC090578.1	$7.54x10^{-2}$	$-3.73x10^{0}$	$2.21x10^{-15}$	$7.30x10^{-13}$

Table 3.28 (continued). Differentially expressed downregulated transcripts identified in the CS3 subtype using DESeq2.

AL589743.3	$7.80x10^{-2}$	$-3.68x10^{0}$	$1.00x10^{-11}$	$8.97x10^{-10}$

As a result of the differential expression analysis with Limma, 275, 1039 and 65 upregulated and 185, 193 and 122 downregulated markers were identified for the

subtypes CS1, CS2 and CS3, respectively. Tables 3.29-3.34 show the 20 most upregulated and downregulated transcripts identified in the CS1, CS2 and CS3 subtypes using Limma and sorted by FC. All other DEGs identified by differential expression analysis with Limma are listed in Appendix A.6.

Keratin 23 (KRT23), which promotes cancer stem cell characteristics and triggers colon cancer development, was upregulated in CS1 [163]. Secreted frizzled related protein 2 (SFRP2), whose overexpression suppresses the development of colon cancer, was upregulated in CS2 [164]. The expression of Regenerating family member 1 alpha (REG1A), which has prognostic significance in colon cancer, is upregulated in CS3 [165]. Ephrin type A receptor 4 (EPHA4), overexpression of which reduces E-cadherin expression leading to poor prognosis, was downregulated in CS1 [166]. Blockade of fibroblast growth factor receptor 3 (FGFR3) inhibits the growth of colon cancer cells, and this gene is downregulated in the CS2 subtype [167, 168]. Crystallin alpha B (CRYAB), which contributes to cancer progression by inducing EMT, also plays an important role in the tumour microenvironment and is downregulated in CS3 [169].

Table 3.29. Differentially expressed upregulated transcripts identified in the CS1 subtype using limma.

CS1 – Differentially Expressed Up-Regulated Transcripts				
	fc	**log2fc**	**pvalue**	**padj**
TNNC2	$9.38x10^{0}$	$3.23x10^{0}$	$1.74x10^{-46}$	$9.96x10^{-42}$
CEL	$7.63x10^{0}$	$2.93x10^{0}$	$3.71x10^{-24}$	$2.28x10^{-21}$
AP003774.2	$7.58x10^{0}$	$2.92x10^{0}$	$3.60x10^{-40}$	$1.03x10^{-35}$
C10orf99	$7.10x10^{0}$	$2.83x10^{0}$	$1.51x10^{-22}$	$6.71x10^{-20}$
KRT23	$6.04x10^{0}$	$2.59x10^{0}$	$1.81x10^{-20}$	$5.12x10^{-18}$
QPRT	$6.00x10^{0}$	$2.58x10^{0}$	$2.68x10^{-37}$	$3.07x10^{-33}$
GNG4	$5.78x10^{0}$	$2.53x10^{0}$	$5.42x10^{-25}$	$4.25x10^{-22}$
NOTUM	$5.46x10^{0}$	$2.45x10^{0}$	$4.05x10^{-16}$	$4.73x10^{-14}$
DPEP1	$5.06x10^{0}$	$2.34x10^{0}$	$8.59x10^{-18}$	$1.45x10^{-15}$
ASCL2	$5.05x10^{0}$	$2.34x10^{0}$	$2.16x10^{-31}$	$5.62x10^{-28}$

Table 3.29 (continued). Differentially expressed upregulated transcripts identified in the CS1 subtype using limma.

CDHR1	$5.00x10^{0}$	$2.32x10^{0}$	$1.03x10^{-23}$	$5.91x10^{-21}$
SLC26A3	$4.98x10^{0}$	$2.32x10^{0}$	$1.22x10^{-11}$	$5.22x10^{-10}$
SLC39A5	$4.78x10^{0}$	$2.26x10^{0}$	$2.87x10^{-31}$	$6.84x10^{-28}$
TDGF1	$4.57x10^{0}$	$2.19x10^{0}$	$3.07x10^{-33}$	$1.25x10^{-29}$
Y_RNA.244	$4.36x10^{0}$	$2.13x10^{0}$	$1.29x10^{-24}$	$9.50x10^{-22}$
CXCL14	$4.28x10^{0}$	$2.10x10^{0}$	$2.11x10^{-17}$	$3.25x10^{-15}$

CYP2B6	$4.27x10^{0}$	$2.09x10^{0}$	$3.09x10^{-26}$	$2.99x10^{-23}$
CYP2W1	$4.25x10^{0}$	$2.09x10^{0}$	$9.50x10^{-14}$	$6.55x10^{-12}$
FABP1	$4.24x10^{0}$	$2.08x10^{0}$	$1.82x10^{-10}$	$6.05x10^{-9}$
VAV3	$4.15x10^{0}$	$2.05x10^{0}$	$6.09x10^{-31}$	$1.34x10^{-27}$

Table 3.30. Differentially expressed downregulated transcripts identified in the CS1 subtype using limma.

CS1 – Differentially Expressed Down-Regulated Transcripts				
	fc	**log2fc**	**pvalue**	**padj**
REG4	$1.03x10^{-1}$	$-3.28x10^{0}$	$2.14x10^{-15}$	$2.12x10^{-13}$
CTSE	$1.50x10^{-1}$	$-2.74x10^{0}$	$7.97x10^{-19}$	$1.66x10^{-16}$
CLDN18	$2.07x10^{-1}$	$-2.27x10^{0}$	$1.83x10^{-18}$	$3.42x10^{-16}$
PLA2G2A	$2.14x10^{-1}$	$-2.22x10^{0}$	$1.95x10^{-11}$	$7.98x10^{-10}$
DUSP4	$2.16x10^{-1}$	$-2.21x10^{0}$	$1.11x10^{-32}$	$4.25x10^{-29}$
GJB5	$2.62x10^{-1}$	$-1.93x10^{0}$	$7.88x10^{-18}$	$1.34x10^{-15}$
MUC5AC	$2.71x10^{-1}$	$-1.88x10^{0}$	$2.22x10^{-16}$	$2.74x10^{-14}$
TCN1	$2.76x10^{-1}$	$-1.86x10^{0}$	$3.81x10^{-10}$	$1.17x10^{-8}$
LYZ	$2.77x10^{-1}$	$-1.85x10^{0}$	$2.26x10^{-13}$	$1.43x10^{-11}$
MUC2	$2.80x10^{-1}$	$-1.84x10^{0}$	$2.89x10^{-7}$	$4.28x10^{-6}$
CXCL13	$2.84x10^{-1}$	$-1.82x10^{0}$	$8.93x10^{-19}$	$1.83x10^{-16}$
REG1A	$2.91x10^{-1}$	$-1.78x10^{0}$	$1.03x10^{-4}$	$5.55x10^{-4}$
TNNT1	$2.96x10^{-1}$	$-1.76x10^{0}$	$3.52x10^{-19}$	$7.81x10^{-17}$
RAMP1	$3.01x10^{-1}$	$-1.73x10^{0}$	$5.48x10^{-13}$	$3.16x10^{-11}$
TFF2	$3.02x10^{-1}$	$-1.73x10^{0}$	$8.71x10^{-10}$	$2.44x10^{-8}$
RAB27B	$3.14x10^{-1}$	$-1.67x10^{0}$	$9.77x10^{-35}$	$6.99x10^{-31}$
VNN1	$3.14x10^{-1}$	$-1.67x10^{0}$	$2.82x10^{-18}$	$5.14x10^{-16}$
CCL18	$3.25x10^{-1}$	$-1.62x10^{0}$	$5.26x10^{-10}$	$1.56x10^{-8}$
TRNP1	$3.29x10^{-1}$	$-1.60x10^{0}$	$3.23x10^{-20}$	$8.67x10^{-18}$
CXCL9	$3.37x10^{-1}$	$-1.57x10^{0}$	$4.03x10^{-12}$	$1.92x10^{-10}$

Table 3.31. Differentially expressed upregulated transcripts identified in the CS2 subtype using limma.

CS2 – Differentially Expressed Up-Regulated Transcripts				
	fc	**log2fc**	**pvalue**	**padj**
SFRP2	$7.52x10^{0}$	$2.91x10^{0}$	$3.30x10^{-15}$	$1.11x10^{-13}$
CCL18	$6.55x10^{0}$	$2.71x10^{0}$	$7.54x10^{-20}$	$5.77x10^{-18}$
CXCL13	$5.83x10^{0}$	$2.54x10^{0}$	$2.62x10^{-27}$	$8.14x10^{-25}$

Table 3.31 (continued). Differentially expressed upregulated transcripts identified in the CS2 subtype using limma.

CXCL9	$5.38x10^{0}$	$2.43x10^{0}$	$5.27x10^{-21}$	$4.95x10^{-19}$
IGHG1	$4.85x10^{0}$	$2.28x10^{0}$	$1.04x10^{-9}$	$1.03x10^{-8}$
COL10A1	$4.79x10^{0}$	$2.26x10^{0}$	$1.62x10^{-14}$	$4.88x10^{-13}$
CD163	$4.78x10^{0}$	$2.26x10^{0}$	$1.26x10^{-27}$	$4.05x10^{-25}$
FCGR3A	$4.77x10^{0}$	$2.25x10^{0}$	$2.01x10^{-24}$	$3.53x10^{-22}$
MRC1	$4.58x10^{0}$	$2.19x10^{0}$	$6.87x10^{-29}$	$2.93x10^{-26}$
GREM1	$4.45x10^{0}$	$2.16x10^{0}$	$2.37x10^{-19}$	$1.68x10^{-17}$

GPNMB	$4.41x10^{0}$	$2.14x10^{0}$	$6.28x10^{-21}$	$5.83x10^{-19}$
IGLV3.1	$4.34x10^{0}$	$2.12x10^{0}$	$3.50x10^{-8}$	$2.28x10^{-7}$
IGHV1.24	$4.30x10^{0}$	$2.10x10^{0}$	$4.05x10^{-9}$	$3.36x10^{-8}$
SPP1	$4.28x10^{0}$	$2.10x10^{0}$	$3.56x10^{-10}$	$4.11x10^{-9}$
POSTN	$4.26x10^{0}$	$2.09x10^{0}$	$3.86x10^{-17}$	$1.84x10^{-15}$
GAS1	$4.25x10^{0}$	$2.09x10^{0}$	$1.14x10^{-23}$	$1.69x10^{-21}$
GBP5	$4.24x10^{0}$	$2.08x10^{0}$	$1.76x10^{-34}$	$2.96x10^{-31}$
PTPRC	$4.20x10^{0}$	$2.07x10^{0}$	$1.52x10^{-32}$	$1.53x10^{-29}$
CYBB	$4.18x10^{0}$	$2.06x10^{0}$	$4.97x10^{-28}$	$1.78x10^{-25}$
ADAM12	$4.17x10^{0}$	$2.06x10^{0}$	$6.61x10^{-26}$	$1.59x10^{-23}$

Table 3.32. Differentially expressed downregulated transcripts identified in the CS2 subtype using limma.

CS2 – Differentially Expressed Down-Regulated Transcripts				
	fc	**log2fc**	**pvalue**	**padj**
FABP1	$1.34x10^{-1}$	$-2.90x10^{0}$	$2.21x10^{-14}$	$6.49x10^{-13}$
IHH	$2.03x10^{-1}$	$-2.30x10^{0}$	$1.37x10^{-32}$	$1.42x10^{-29}$
MEP1A	$2.11x10^{-1}$	$-2.24x10^{0}$	$1.93x10^{-16}$	$8.19x10^{-15}$
HMGCS2	$2.19x10^{-1}$	$-2.19x10^{0}$	$6.49x10^{-10}$	$6.92x10^{-9}$
PPP1R14D	$2.26x10^{-1}$	$-2.15x10^{0}$	$8.24x10^{-29}$	$3.47x10^{-26}$
FABP6	$2.62x10^{-1}$	$-1.93x10^{0}$	$2.72x10^{-16}$	$1.12x10^{-14}$
LYPD8	$2.65x10^{-1}$	$-1.92x10^{0}$	$3.22x10^{-9}$	$2.75x10^{-8}$
CDX2	$2.66x10^{-1}$	$-1.91x10^{0}$	$1.87x10^{-28}$	$7.23x10^{-26}$
DEFA6	$2.68x10^{-1}$	$-1.90x10^{0}$	$1.80x10^{-5}$	$6.55x10^{-5}$
PHGR1	$2.70x10^{-1}$	$-1.89x10^{0}$	$4.92x10^{-20}$	$3.89x10^{-18}$
DDC	$2.70x10^{-1}$	$-1.89x10^{0}$	$4.53x10^{-20}$	$3.59x10^{-18}$
NOX1	$2.76x10^{-1}$	$-1.86x10^{0}$	$3.11x10^{-15}$	$1.05x10^{-13}$
KRT20	$2.78x10^{-1}$	$-1.85x10^{0}$	$3.17x10^{-10}$	$3.73x10^{-9}$
CLDN3	$2.83x10^{-1}$	$-1.82x10^{0}$	$3.23x10^{-25}$	$6.88x10^{-23}$
AL354743.2	$2.97x10^{-1}$	$-1.75x10^{0}$	$3.79x10^{-20}$	$3.06x10^{-18}$
CHP2	$3.02x10^{-1}$	$-1.73x10^{0}$	$6.39x10^{-9}$	$5.03x10^{-8}$
SELENBP1	$3.03x10^{-1}$	$-1.72x10^{0}$	$5.99x10^{-17}$	$2.75x10^{-15}$
SPINK1	$3.07x10^{-1}$	$-1.71x10^{0}$	$3.33x10^{-10}$	$3.89x10^{-9}$
ISX	$3.10x10^{-1}$	$-1.69x10^{0}$	$1.95x10^{-13}$	$4.80x10^{-12}$
CKB	$3.12x10^{-1}$	$-1.68x10^{0}$	$2.38x10^{-9}$	$2.11x10^{-8}$

Table 3.33. Differentially expressed upregulated transcripts identified in the CS3 subtype using limma.

CS3 – Differentially Expressed Up-Regulated Transcripts				
	fc	**log2fc**	**pvalue**	**padj**
REG1A	$6.59x10^{0}$	$2.72x10^{0}$	$5.35x10^{-6}$	$1.55x10^{-4}$
TFF1	$6.45x10^{0}$	$2.69x10^{0}$	$6.41x10^{-13}$	$8.73x10^{-10}$
SPINK4	$5.69x10^{0}$	$2.51x10^{0}$	$1.36x10^{-6}$	$5.24x10^{-5}$
TFF2	$4.91x10^{0}$	$2.30x10^{0}$	$4.28x10^{-10}$	$1.03x10^{-7}$
MUC2	$4.87x10^{0}$	$2.28x10^{0}$	$1.16x10^{-6}$	$4.62x10^{-5}$
REG3A	$4.51x10^{0}$	$2.17x10^{0}$	$1.04x10^{-5}$	$2.62x10^{-4}$
FCGBP	$4.34x10^{0}$	$2.12x10^{0}$	$5.05x10^{-7}$	$2.43x10^{-5}$

SPDEF	$4.25x10^{0}$	$2.09x10^{0}$	$3.57x10^{-11}$	$1.53x10^{-8}$
CA9	$3.82x10^{0}$	$1.93x10^{0}$	$1.81x10^{-7}$	$1.11x10^{-5}$
PIGR	$3.78x10^{0}$	$1.92x10^{0}$	$8.91x10^{-5}$	$1.46x10^{-3}$
TM4SF4	$3.77x10^{0}$	$1.91x10^{0}$	$1.62x10^{-10}$	$4.95x10^{-8}$
AGR3	$3.69x10^{0}$	$1.88x10^{0}$	$1.48x10^{-9}$	$2.73x10^{-7}$
AGR2	$3.54x10^{0}$	$1.82x10^{0}$	$1.01x10^{-17}$	$2.88x10^{-13}$
REG1B	$3.46x10^{0}$	$1.79x10^{0}$	$7.71x10^{-5}$	$1.29x10^{-3}$
FFAR4	$3.29x10^{0}$	$1.72x10^{0}$	$2.60x10^{-11}$	$1.21x10^{-8}$
KLK11	$3.14x10^{0}$	$1.65x10^{0}$	$1.74x10^{-9}$	$3.07x10^{-7}$
KLK12	$2.95x10^{0}$	$1.56x10^{0}$	$7.24x10^{-10}$	$1.58x10^{-7}$
PRSS2	$2.92x10^{0}$	$1.55x10^{0}$	$5.35x10^{-4}$	$6.13x10^{-3}$
GP2	$2.90x10^{0}$	$1.53x10^{0}$	$2.56x10^{-11}$	$1.21x10^{-8}$
CREB3L1	$2.88x10^{0}$	$1.53x10^{0}$	$1.30x10^{-9}$	$2.47x10^{-7}$

Table 3.34. Differentially expressed downregulated transcripts identified in the CS3 subtype using limma.

CS3 – Differentially Expressed Down-Regulated Transcripts				
	fc	**log2fc**	**pvalue**	**padj**
SFRP4	$2.22x10^{-1}$	$-2.17x10^{0}$	$3.00x10^{-10}$	$7.82x10^{-8}$
COMP	$2.37x10^{-1}$	$-2.08x10^{0}$	$1.62x10^{-9}$	$2.93x10^{-7}$
CES1	$2.77x10^{-1}$	$-1.85x10^{0}$	$1.97x10^{-9}$	$3.38x10^{-7}$
PRELP	$3.40x10^{-1}$	$-1.56x10^{0}$	$5.15x10^{-9}$	$6.98x10^{-7}$
DES	$3.43x10^{-1}$	$-1.55x10^{0}$	$3.72x10^{-4}$	$4.61x10^{-3}$
MPP1	$3.47x10^{-1}$	$-1.53x10^{0}$	$1.11x10^{-16}$	$1.06x10^{-12}$
CCL21	$3.51x10^{-1}$	$-1.51x10^{0}$	$7.93x10^{-6}$	$2.13x10^{-4}$
MYH11	$3.56x10^{-1}$	$-1.49x10^{0}$	$2.78x10^{-6}$	$9.33x10^{-5}$
ASPN	$3.58x10^{-1}$	$-1.48x10^{0}$	$1.03x10^{-7}$	$7.26x10^{-6}$
FBLN1	$3.65x10^{-1}$	$-1.45x10^{0}$	$3.18x10^{-9}$	$4.78x10^{-7}$
ELN	$3.66x10^{-1}$	$-1.45x10^{0}$	$6.59x10^{-11}$	$2.55x10^{-8}$
EFEMP1	$3.66x10^{-1}$	$-1.45x10^{0}$	$1.22x10^{-9}$	$2.35x10^{-7}$
SRPX2	$3.71x10^{-1}$	$-1.43x10^{0}$	$8.47x10^{-11}$	$3.00x10^{-8}$
NPTX2	$3.74x10^{-1}$	$-1.42x10^{0}$	$9.50x10^{-6}$	$2.44x10^{-4}$
CHRDL1	$3.74x10^{-1}$	$-1.42x10^{0}$	$1.04x10^{-7}$	$7.29x10^{-6}$
PTGIS	$3.74x10^{-1}$	$-1.42x10^{0}$	$9.80x10^{-10}$	$2.01x10^{-7}$

Table 3.34 (continued). Differentially expressed downregulated transcripts identified in the CS3 subtype using limma.

RBP1	$3.75x10^{-1}$	$-1.42x10^{0}$	$4.03x10^{-8}$	$3.49x10^{-6}$
MFAP4	$3.78x10^{-1}$	$-1.40x10^{0}$	$3.13x10^{-8}$	$2.90x10^{-6}$
ZCCHC24	$3.84x10^{-1}$	$-1.38x10^{0}$	$8.75x10^{-15}$	$2.51x10^{-11}$
HSPB6	$3.86x10^{-1}$	$-1.37x10^{0}$	$1.54x10^{-9}$	$2.81x10^{-7}$

To better understand the biology of COAD, a GSEA was then performed based on the results obtained with the edgeR, DESeq2 and limma algorithms. However, pathways that exceeded the significance threshold (nominal P-value < 0.05 and corrected P-value < 0.05) and did not overlap with pathways identified for other subtypes were only captured

by limma. The result of the analysis was that CS2 was upregulated in 751 signalling pathways, while CS3 was upregulated in about one sixtieth of CS2 (Figure 3.81). Activation of the B-cell receptor signalling pathway, which has a positive effect on immunotherapy, was upregulated in the CS2 subtype (Figure 3.82). On the other hand, the downregulation of T-cell activation in CS1 could negatively influence the response of this subtype to immunotherapy.



Figure 3.81. Heatmap of subtype-specific upregulated pathways using limma algorithm for 3 identified subtypes in TCGA-COAD cohort.

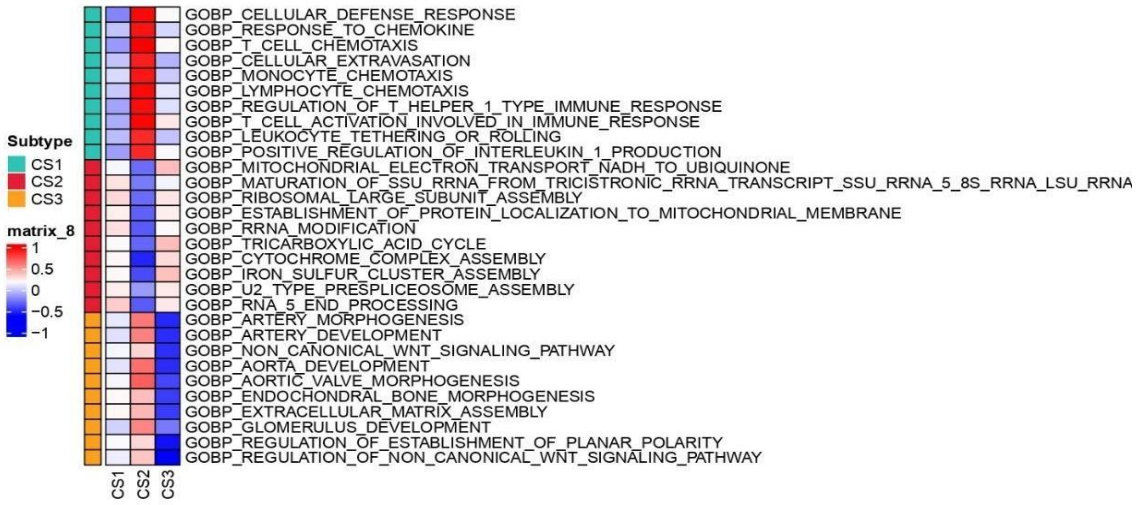


Figure 3.82. Heatmap of subtype-specific downregulated pathways using limma algorithm for 3 identified subtypes in TCGA-COAD cohort.

To gain a deeper understanding of the tumourigenesis process for each subtype, the activation status of 50 tumour-associated signalling pathways was compared (Figure

3.83). The results show that the CS2 subtype is particularly enriched in important cancer hallmarks, such as apoptosis and angiogenesis. EMT, which plays an important role in cancer metastasis, was particularly downregulated in the CS3 subtype.

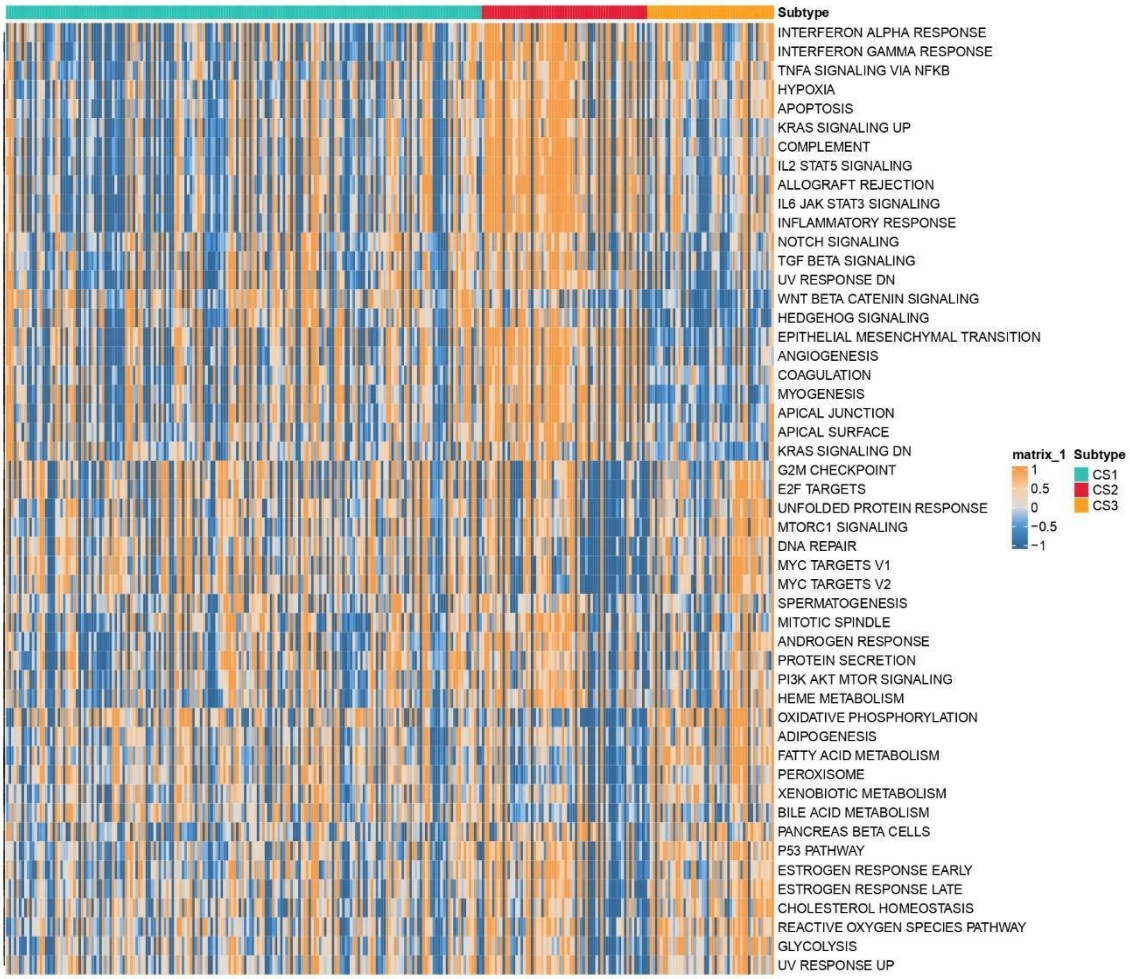


Figure 3.83. Heatmap of enrichment score of tumor-associated pathways for 3 identified subtypes in TCGA-COAD cohort.

3.2.3. The effect of genetic alteration on subtypes

Since mutated gene signatures play an important role in the development, progression and metastasis of colon cancer, the mutational differences between the subtypes were investigated. Figure 3.84 shows the genes that exceed the significance threshold ($p < 0.05$) and whose overall mutation rate is not less than 15%. This analysis of somatic mutations revealed that 297 patients with colon adenocarcinoma had mutations, most of which were missense mutations.

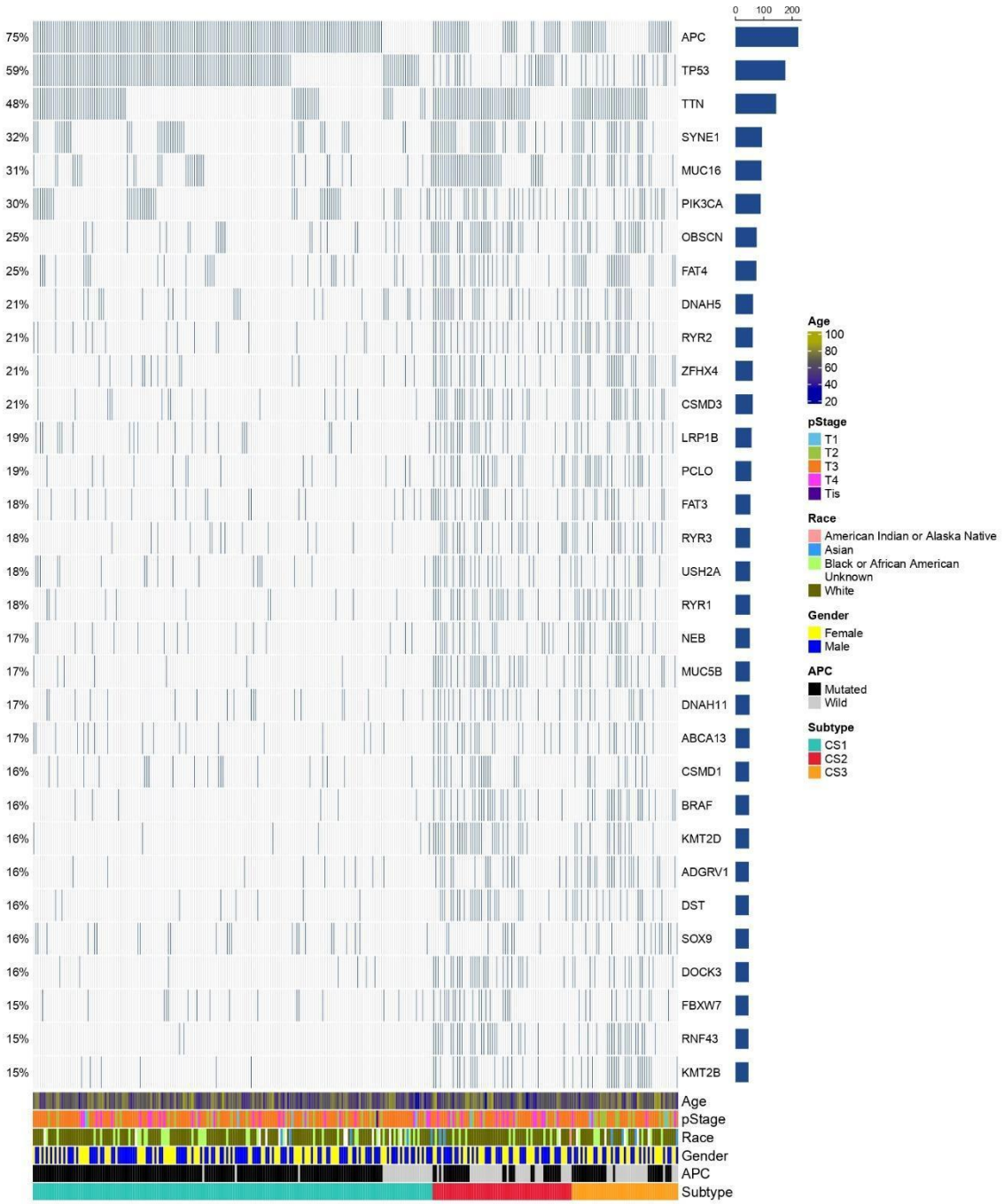


Figure 3.84. Mutational OncoPrint of 3 identified subtypes of colon adenocancinoma in TCGA-COAD cohort.

The overall mutation rate of thirty mutated genes was at least 15%. APC, TP53, TTN, SYNE1 and MUC16 were the five most frequently mutated genes in colon adenocarcinoma samples (Table 3.35). APC had the highest mutation frequency, with mutations occurring in 75% of the samples.

Table 3.35. Comparison of mutational frequency among 3 identified subtype of colon adenocarcinoma in TCGA-COAD cohort.

Gene (Mutated)	TMB	CS1	CS2	CS3	pvalue	padj
APC	222 (75%)	161 (87.5%)	34 (53.1%)	27 (55.1%)	7.31e-10	2.13e-09
TP53	176 (59%)	136 (73.9%)	25 (39.1%)	15 (30.6%)	2.38e-10	7.85e-10
TTN	144 (48%)	64 (34.8%)	45 (70.3%)	35 (71.4%)	9.19e-09	1.78e-08
SYNE1	94 (32%)	41 (22.3%)	32 (50.0%)	21 (42.9%)	4.09e-05	5.62e-05
MUC16	92 (31%)	33 (17.9%)	38 (59.4%)	21 (42.9%)	1.01e-09	2.56e-09

APC and TP53 mutations, which are considered crucial for the development of colon cancer, are more common in the CS1 subtype. APC is the most frequently mutated gene in colon cancer and TP53 is the second most frequently mutated gene. These gene mutations are of great importance for diagnosis, treatment and prognosis, as they control the transition from healthy colon epithelium to cancerous tissue. The TTN mutation, which has the potential to transform the tumour microenvironment into an immunosuppressive type, was found in 71% of the CS3 subtype. In addition, SYNE1 and PIK3CA mutations, which trigger tumour formation, were found in half of the CS2 subtype.

Furthermore, colon cancer is highly influenced by copy number alterations and genetic mutations. Genomic lesions associated with the activation of immune checkpoints play an important role in patient response to immunotherapy. Therefore, the total mutational burden (TMB) and the altered genomic fraction (FGA) were calculated to quantify these genomic alterations that may influence immunotherapy. The FGA values, expressed as the percentage of genomes affected by copy number gains or losses (i.e. copy number alterations) of the three subtypes, were first analysed. Compared to the other subtypes, the CS1 group had more CNAs in both the lost and gained genomes. (Figure 3.85). On the other hand, in the CS3 group, the percentage of genomes gained was higher than the percentage of genomes lost (Table 3.36).

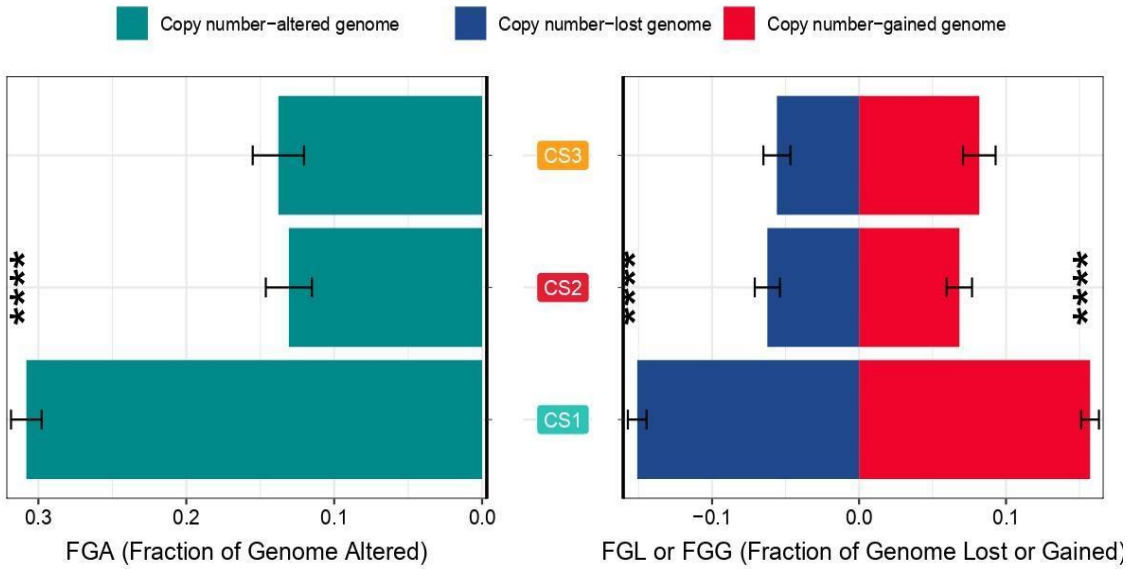


Figure 3.85. Bar plot of fraction genome altered among 3 identified subtypes of colon adenocarcinoma in TCGA-COAD cohort.

Table 3.36. Demo of comparison of fraction genome altered among 3 identified subtype of colon adenocarcinoma in TCGA-COAD cohort.

samID	FGA	FGG	FGL	Subtype
TCGA-3L-AA1B-01A	0.14303125	0.07289238	0.07013886	CS1
TCGA-4N-A93T-01A	0.33418894	0.10710504	0.2270839	CS1
TCGA-5M-AAT6-01A	0.06718986	0.03419735	0.03299251	CS2
TCGA-A6-5656-01A	0.29470538	0.1665571963	0.12814818	CS3
TCGA-A6-5659-01A	0.31950372	0.1475715395	0.17193219	CS3

Tumour mutation burden (TMB), defined as the total number of somatic coding errors, base substitutions and indel mutations per million bases of DNA, can be used to assess the response of colon cancer patients to ICI therapy. To assess TMB, the number of non-synonymous mutations per million bases was calculated. We observed a significantly higher mean TMB value for CS2 and CS3. ($P < 0.001$, Figure 3.86) (Table 3.37). Tumours with high TMB values are more likely to respond to immunotherapy. Therefore, subtypes CS2 and CS3 may respond better to immunotherapy than CS1. In addition, single nucleotide variants (SNVs) were visualised after they were classified into transitions and transformations (TiTv).

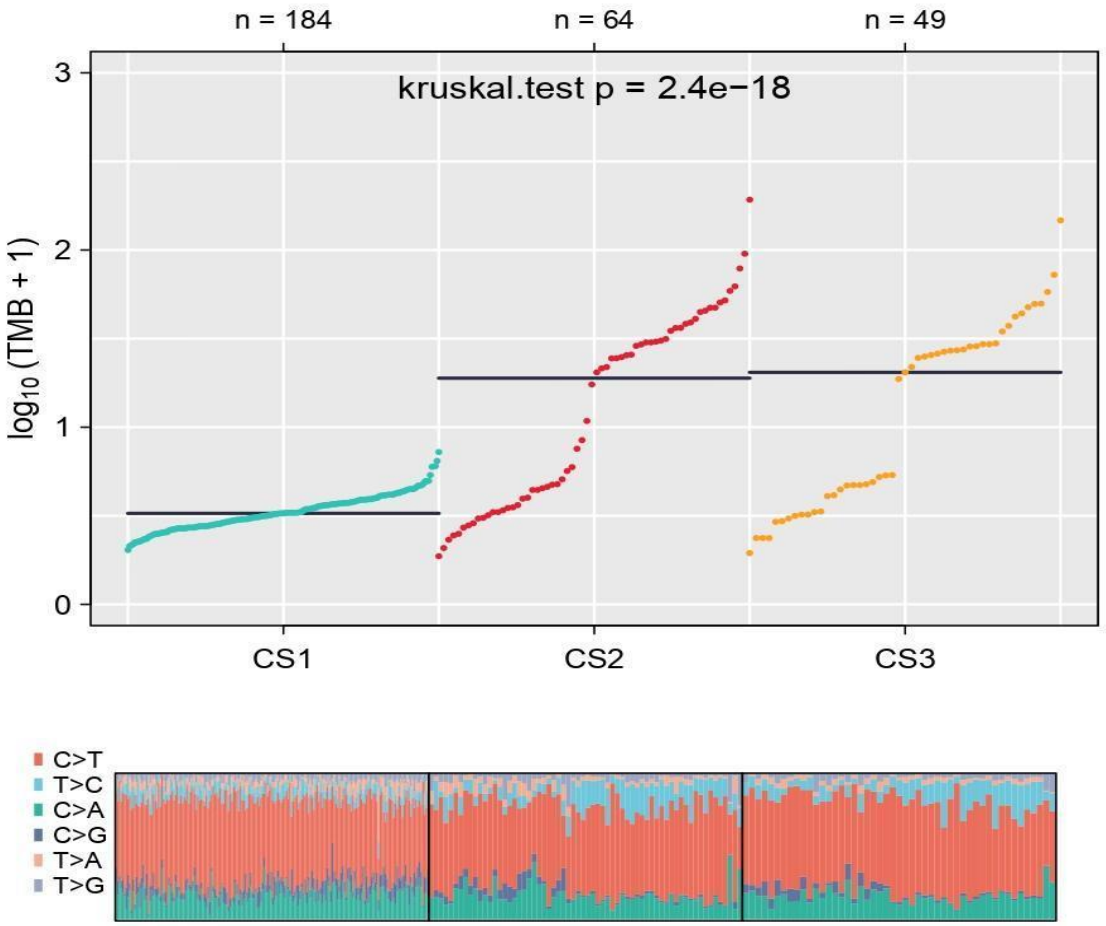


Figure 3.86. Comparison of TMB and TiTv among 3 identified subtypes of colon adenocarcinoma in TCGA-COAD cohort.

Table 3.37. Demo of comparison of TMB among 3 identified subtype of colon adenocarcinoma in TCGA-COAD cohort.

	samID	variants	TMB	log10TMB	Subtype
295	TCGA-A6-2685-01A	39	1.026316	0.3067071	CS1
293	TCGA-A6-A567-01A	43	1.131579	0.3287014	CS1
297	TCGA-AZ-4323-01A	33	0.8684211	0.2714748	CS2
294	TCGA-A6-5664-01A	41	1.0789474	0.3178435	CS2
296	TCGA-CA-5255-01A	36	0.9473684	0.2894481	CS3

Moreover, an alluvial diagram was created to illustrate how often the present subtypes contained the 5 most frequently mutated genes in COAD (Figure 3.87).

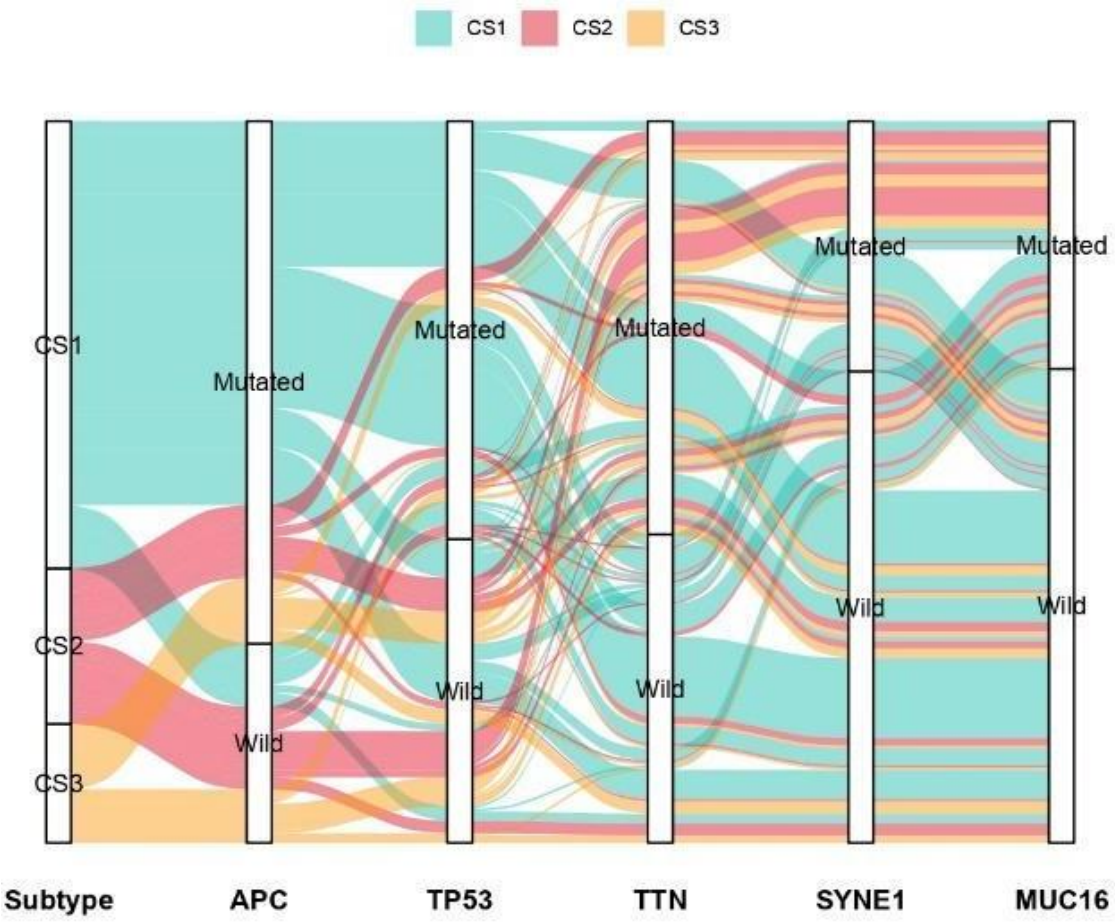


Figure 3.87. Agreement of 3 identified subtypes of colon adenocarcinoma with the most common 5 mutant genes in TCGA-COAD cohort.

3.2.4. Precision treatment recommendations for COAD patients

Chemotherapy is one of the two most important treatment methods for colorectal cancer. Various factors are taken into account when choosing chemotherapeutic agents, e.g. the stage of the tumour, the patient's state of health and the general response rate to the drug. However, choosing a drug without considering the individual differences of each patient and the biological characteristics of the tumour can lead to cellular stress and increase resistance to the drug, and even a wrong drug choice can lead to potentially fatal side effects. Therefore, it is of great importance to assess the drug response for each patient before starting treatment. Therefore, to enable individualised treatment selection, the potential response to commonly administered chemotherapeutic agents in COAD patients was assessed by estimating IC50 values based on gene expression profiling and data from

the GDSC database. As part of this drug sensitivity analysis, in addition to analysing the chemotherapeutic agents commonly used in the treatment of COAD, sensitivity analyses of 249 drugs offered by the package that might be promising for the treatment of COAD were performed. In this way, the sensitivities of subtypes, which are differentiated according to their molecular characteristics, were determined.

Here, the response of each subtype to some of the most commonly used and promising drugs in the treatment of colon cancer is analysed in detail. Appendix B.1 shows a list of drugs for which the subtypes showed a statistically significant response among 249 drugs. When analysing drug sensitivity, the IC50 values used to determine the efficacy of a drug were calculated. While a high IC50 value indicates drug resistance, a low value indicates a better effect of the drug.

Although 5-fluorouracil is one of the most commonly used chemotherapeutic agents because it increases the survival rate, its effect in patients with advanced colon cancer is low. Patients with the CS3 subtype respond better to chemotherapy with 5-fluorouracil than other subtypes (Figure 3.88).

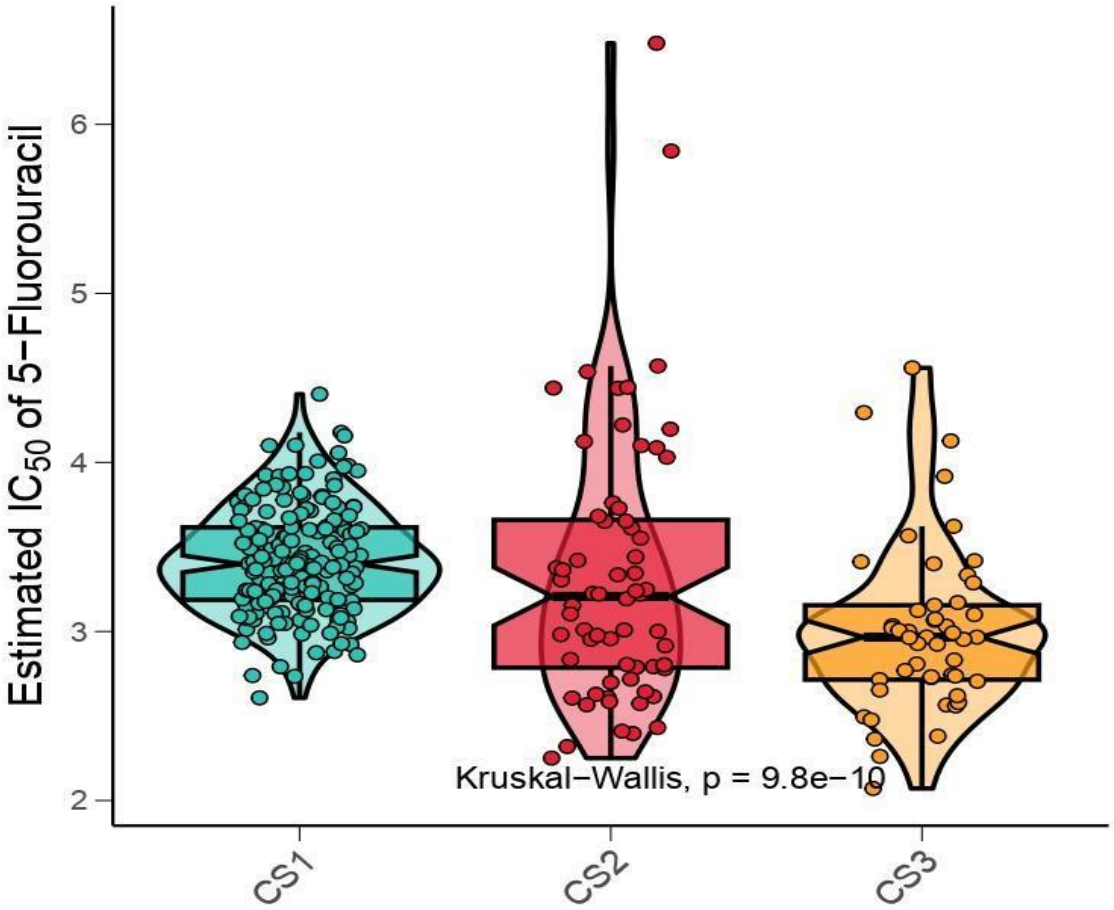


Figure 3.88. Boxviolin for estimated IC50 of 5-Fluorouracil among 3 identified subtypes of colon adenocarcinoma in TCGA-COAD cohort.

Subtypes CS1 and CS3 are highly resistant to cisplatin, one of the most effective chemotherapeutic agents for colon cancer, while CS2 patients with lower IC50 values respond better to this treatment (Figure 3.89).

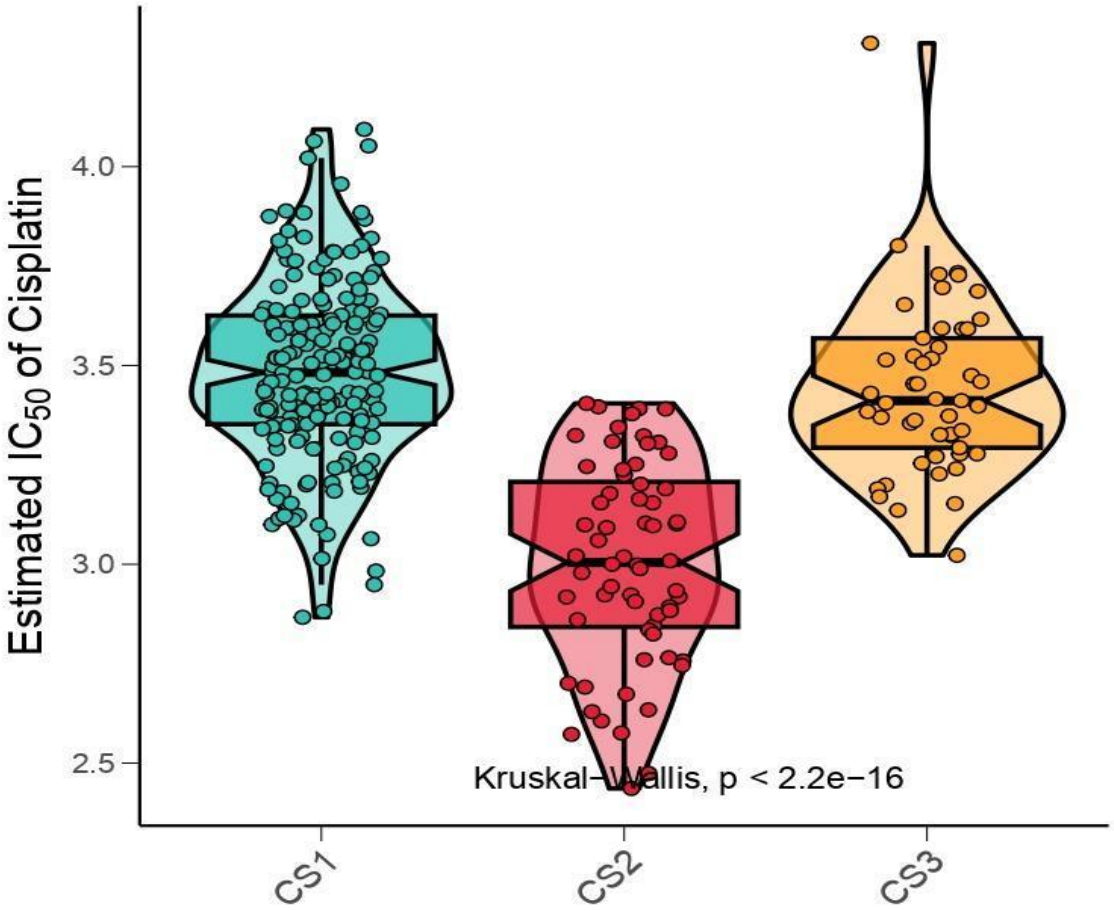


Figure 3.89. Boxviolin for estimated IC50 of Cisplatin among 3 identified subtypes of colon adenocarcinoma in TCGA-COAD cohort.

CS2 patients respond better to paclitaxel, which has anti-cancer properties by playing a role in proliferation and apoptosis and is used in the treatment of advanced colon cancer (Figure 3.90).

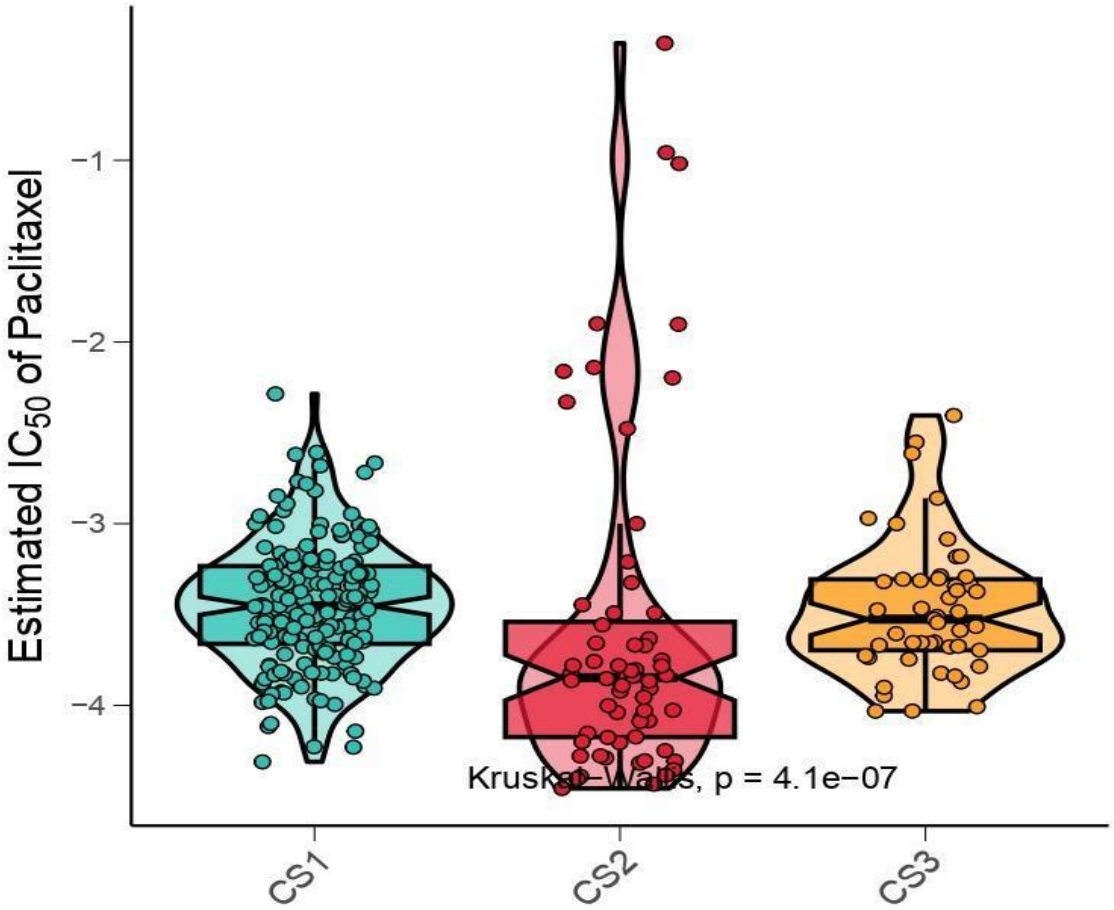


Figure 3.90. Boxviolin for estimated IC50 of Paclitaxel among 3 identified subtypes of colon adenocarcinoma in TCGA-COAD cohort.

SN-38, which acts as an active metabolite of irinotecan, a common chemotherapeutic agent for colon cancer, overcomes chemoresistance in a hypoxic environment, resulting in an anti-tumour effect in colon cancer. As a result of the analysis, it was found that CS2 patients responded better to SN-38 than patients of the other subtypes (Figure 3.91).

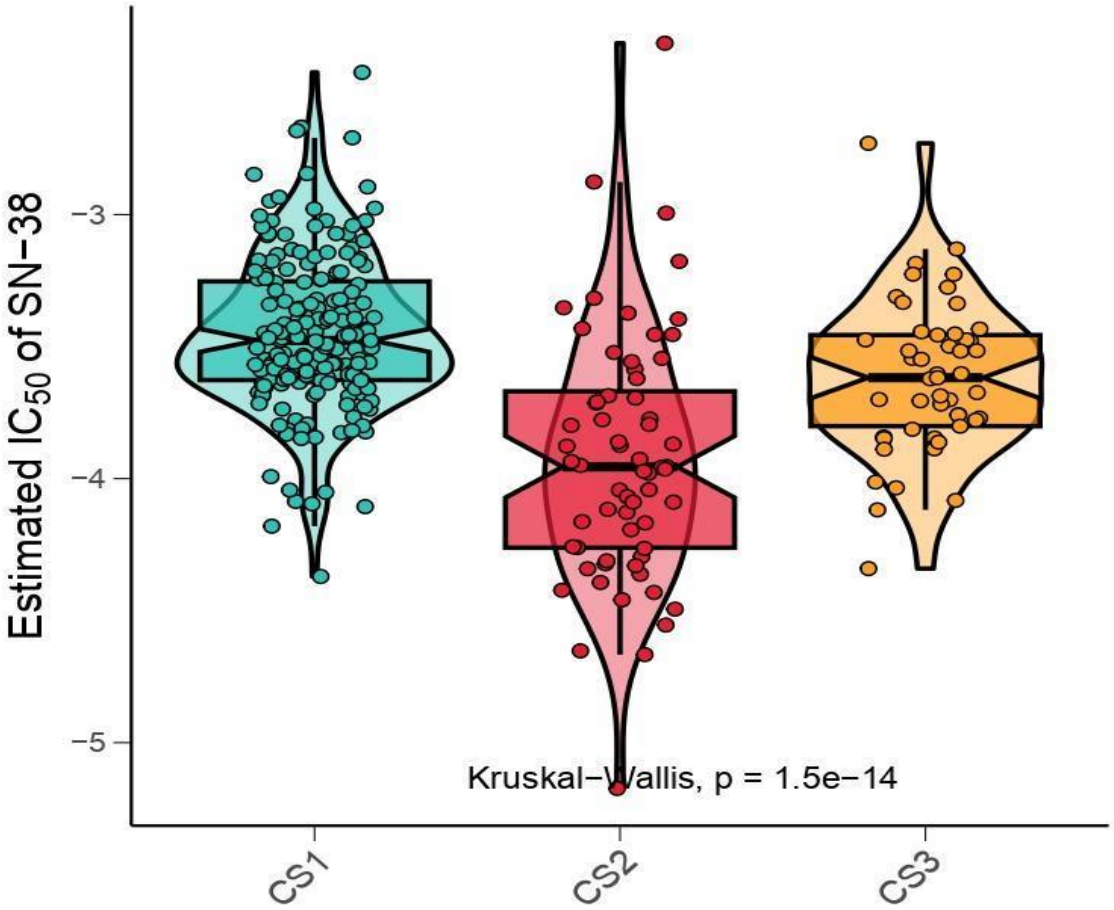


Figure 3.91. Boxviolin for estimated IC50 of SN-38 among 3 identified subtypes of colon adenocarcinoma in TCGA-COAD cohort.

Rapamycin (Rapa), used as an immunosuppressant, shows anti-tumor properties. The CS1 subtype showed a much better response to Rapa treatment, which is potentially promising for the treatment of colon cancer (Figure 3.92).

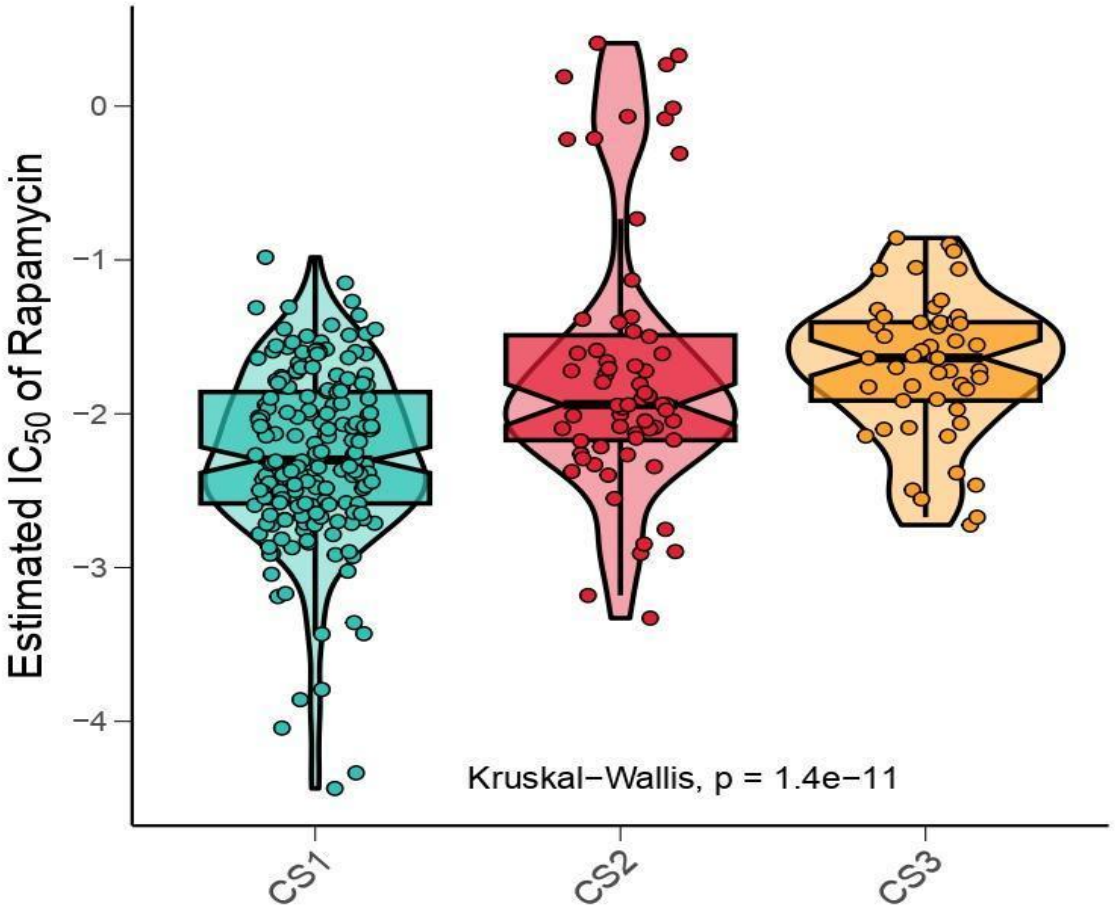


Figure 3.92. Boxviolin for estimated IC50 of Rapamycin among 3 identified subtypes of colon adenocarcinoma in TCGA-COAD cohort.

Rapamycin (Rapa), which is used as an immunosuppressant, shows antitumour properties. The CS1 subtype responded significantly better to treatment with Rapa, which could be promising for the treatment of colon cancer (Figure 3.92).

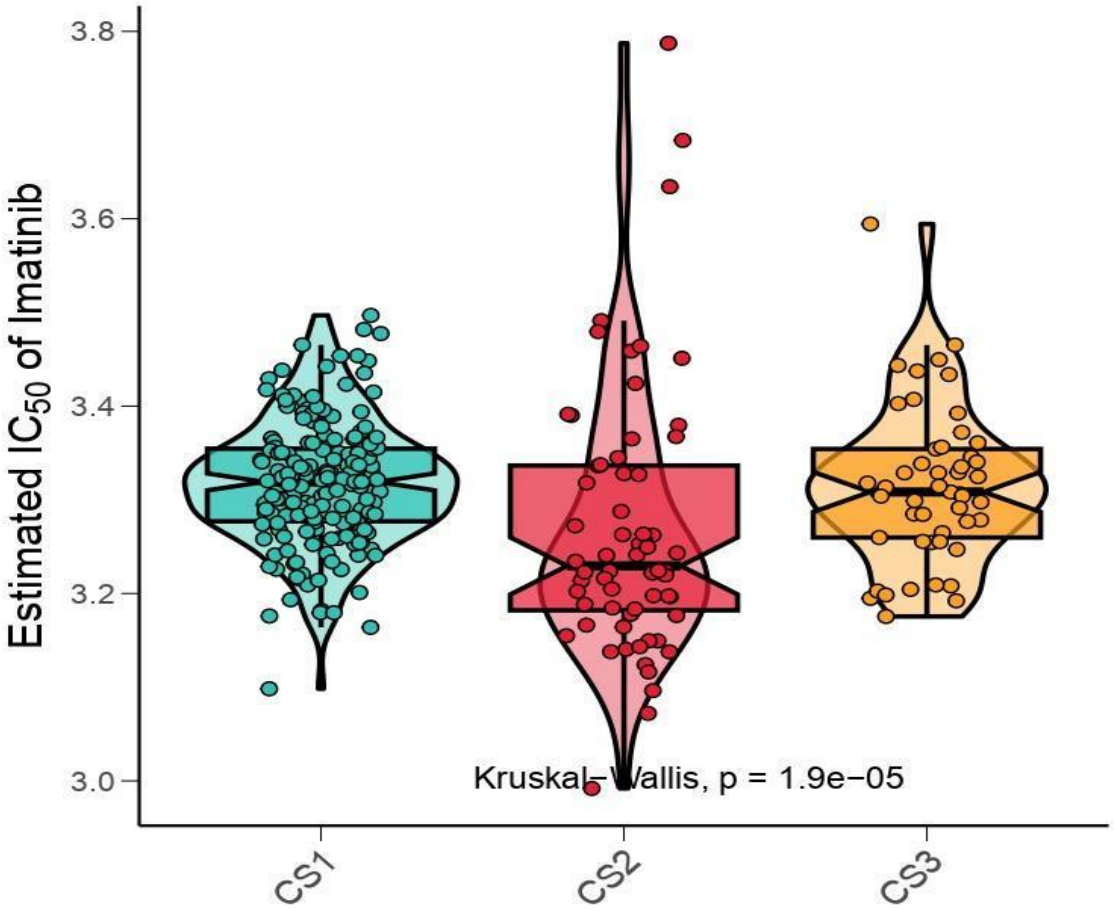


Figure 3.93. Boxviolin for estimated IC50 of Imatinib among 3 identified subtypes of colon adenocarcinoma in TCGA-COAD cohort.

3.2.5. Validation of subtypes in four external cohorts

Four external cohorts GSE39582, GSE16125, GSE17536 and GSE17537 were used to validate the reliability of the subtypes. Subtype-specific upregulated biomarkers previously identified with edgeR, DESeq2 and limma were used to confirm the current subtypes of patients in external cohorts. NTP and PAM methods were used for subtype prediction in the validation cohort. Subtype survival results obtained between NTP and the discovery and validation groups were compared. In addition, the IGP statistic was calculated to assess the similarity and reproducibility of the subtypes obtained between the discovery and validation groups with PAM. Subtype prediction was then performed using NTP and PAM for the discovery dataset. Subsequently, the agreement between the subtypes present in the discovery dataset and the subtypes predicted by NTP and PAM

was measured using the kappa statistic. The accuracy and consistency between the subtype predicted by NTP and PAM was also analysed in the validation cohort.

NTP was initially implemented for the prediction of subtypes with edgeR, DESeq2 and limma on GSE16125 (Figures 3.94-3.95). However, during the NTP analysis, no matches could be detected based on the DESeq2 results. Furthermore, in the NTP analysis based on the use of biomarkers predicted with EdgeR, no sample in the GSE16125 dataset, which consists of 32 samples, could be assigned to a subspecies. In contrast, NTP analysis based on Limma results assigned CS1, CS2 and CS3 to 9, 9 and 5 samples, respectively, demonstrating that Limma achieved a better subtyping analysis than the other two algorithms.

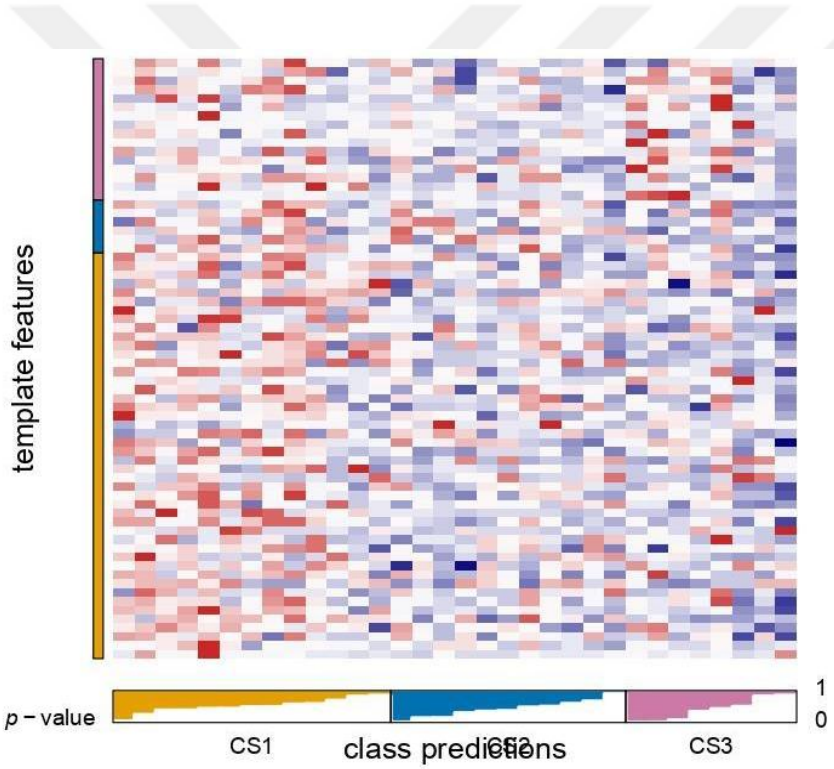


Figure 3.94. Heatmap of NTP in GSE16125 cohort using subtype-specific upregulated biomarkers identified using edgeR from TCGA-COAD cohort.

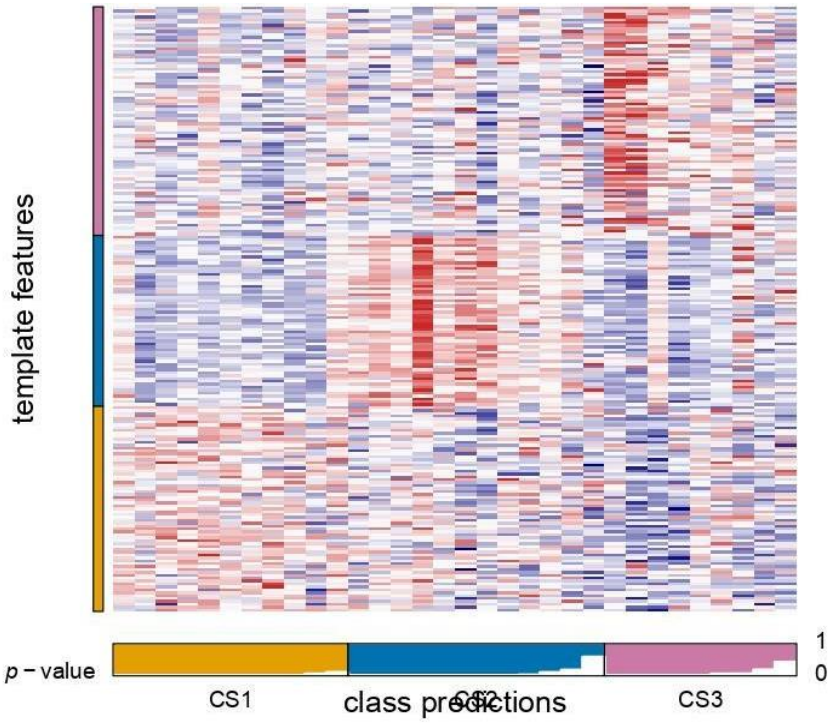


Figure 3.95. Heatmap of NTP in GSE16125 cohort using subtype-specific upregulated biomarkers identified using limma from TCGA-COAD cohort.

In addition, a survival analysis of the subtypes predicted by NTP was performed in the validation cohort based on the EdgeR and Limma methods. As a result of the survival analysis performed based on the edgeR results, a statistically significant difference in the survival rates of patients in the GSE16125 cohort was observed (Figure 3.96). Figure 3.96 shows that the clinical prognosis of CS3 is worse than other subtypes. However, no statistically significant result was found in the survival analysis based on the Limma algorithm (Figure 3.97).

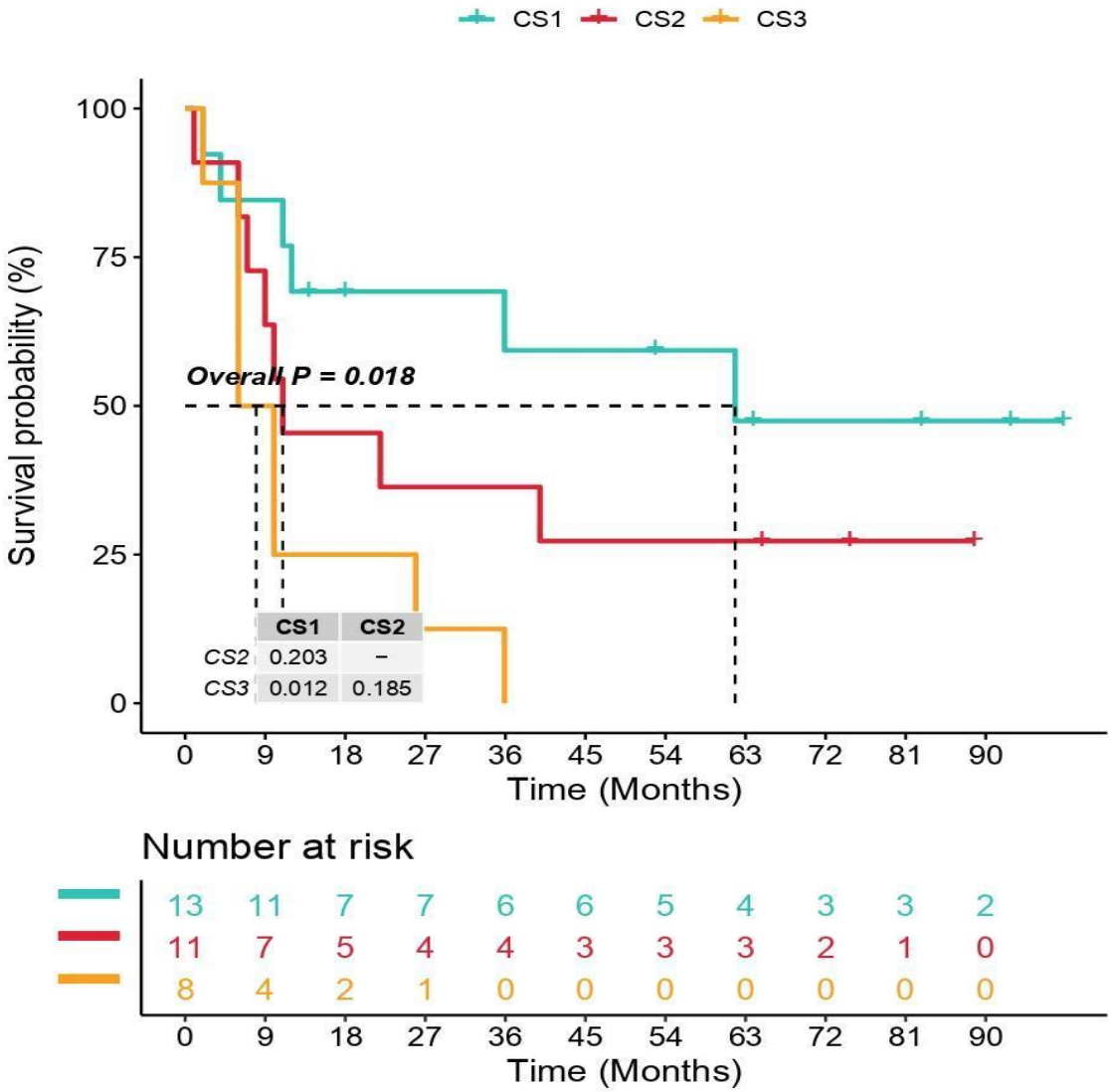


Figure 3.96. Kaplan-Meier survival curve of 3 colon adenocarcinoma subtypes predicted by edgeR in the GSE16125 cohort.

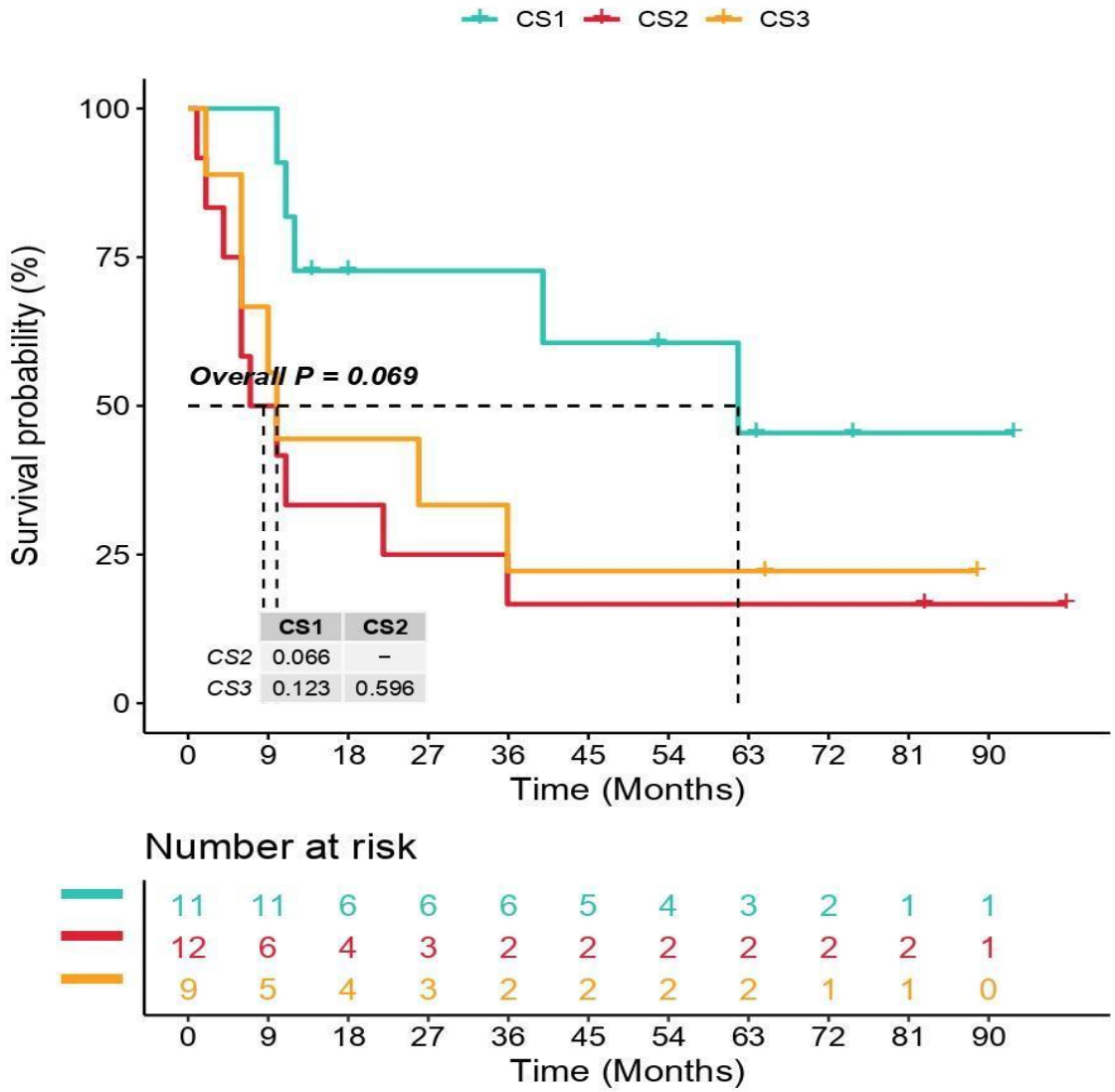


Figure 3.97. Kaplan-Meier survival curve of 3 colon adenocarcinoma subtypes predicted by limma in the GSE16125 cohort.

Another method for subtype prediction is to train a PAM classifier in the discovery group to predict the subtype for patients in the external validation group. The similarity and reproducibility of subtypes identified by PAM was assessed using the IGP statistic. As can be seen in Table 3.38, the IGP statistic of the GSE16125 cohort was close to 1. It was concluded that the subtypes identified between the discovery and validation groups were similar and reproducible.

Table 3.38. IGP information in four validation cohorts of the PAM classifier trained on the TCGA-COAD cohort.

	CS1	CS2	CS3
GSE16125	0.6923077	0.8333333	0.4285714
GSE39582	0.7773109	0.7470588	0.7597403
GSE17536	0.7594937	0.7037037	0.6590909
GSE17537	0.8181818	0.8750000	0.7647059

The results of the kappa statistic can range from -1 to +1, where 1 means perfect agreement between the raters. According to the results of EdgeR (Figure 3.98-3.99), DESeq2 (Figure 3.100-3.101) and limma (Figure 3.102-3.103), the consistency between the subtypes found in the TCGA dataset and the subtypes predicted by PAM was much greater than that predicted by NTP.

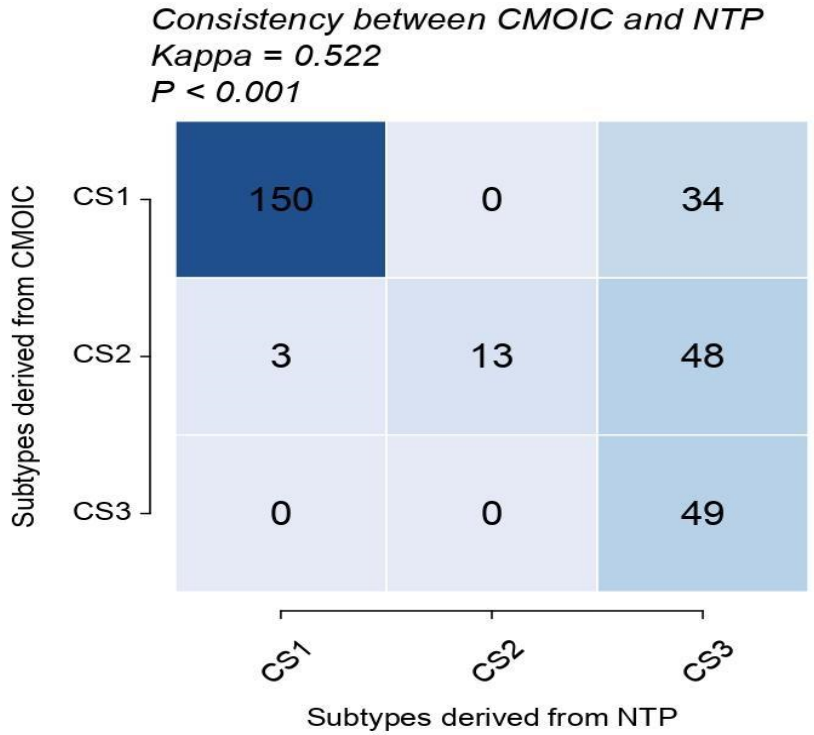


Figure 3.98. Consistency heatmap between current and NTP-predicted Kappa statistics for edgeR results in TCGA-COAD cohort.

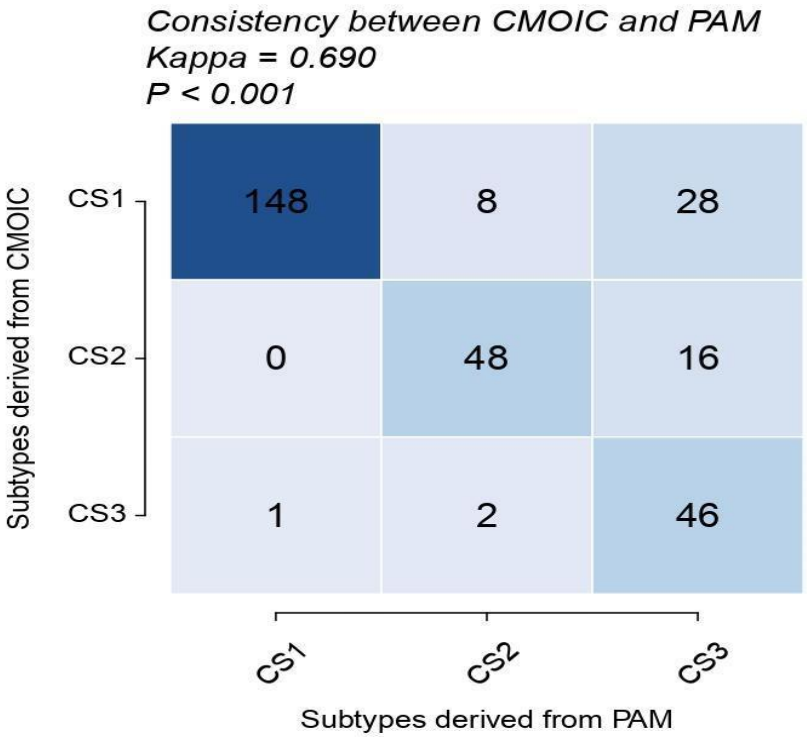


Figure 3.99. Consistency heatmap between current and PAM-predicted Kappa statistics for edgeR results in TCGA-COAD cohort.

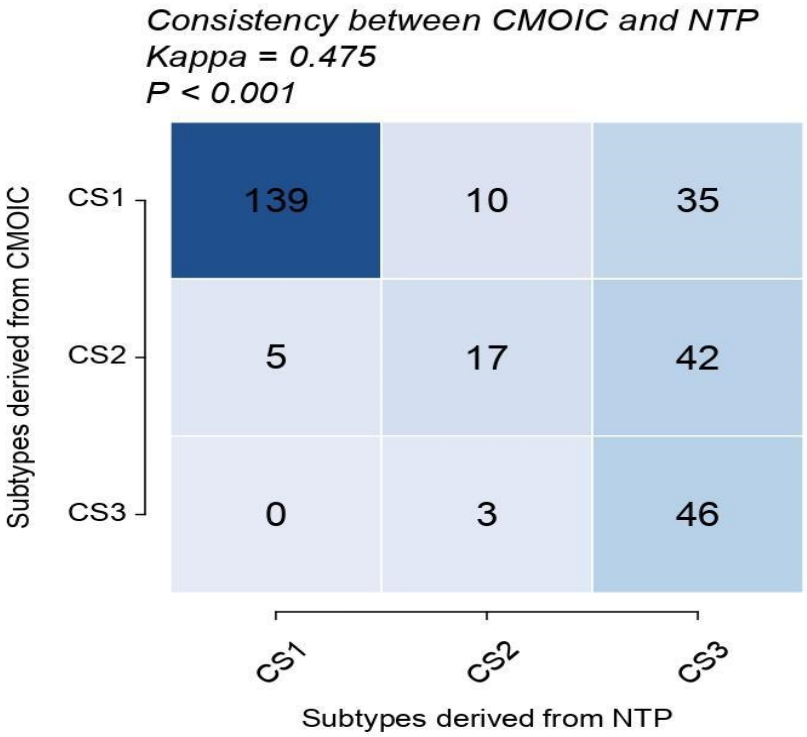


Figure 3.100. Consistency heatmap between current and NTP-predicted Kappa statistics for DESeq2 results in TCGA-COAD cohort.

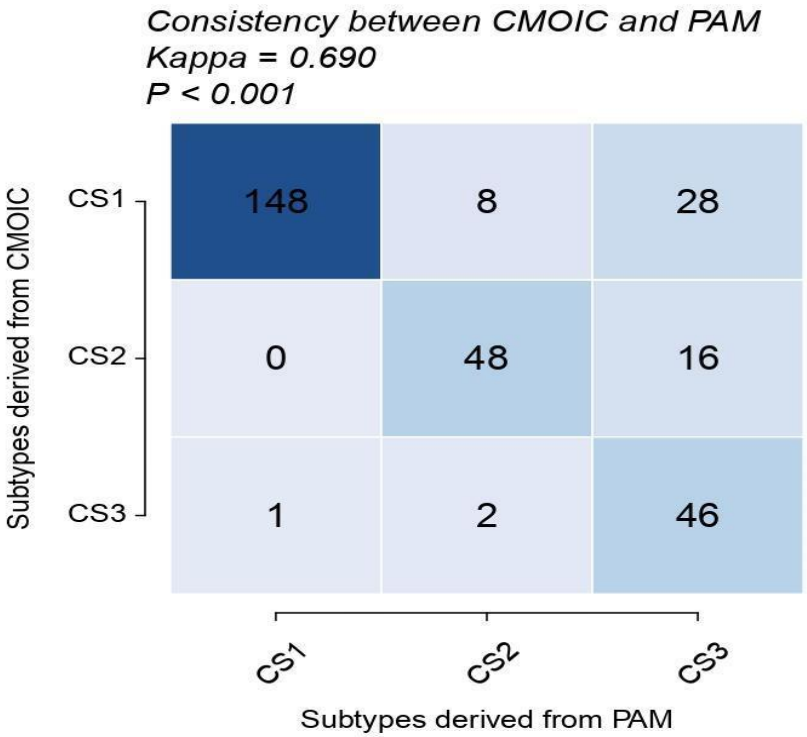


Figure 3.101. Consistency heatmap between current and PAM-predicted Kappa statistics for DESeq2 results in TCGA-COAD cohort.

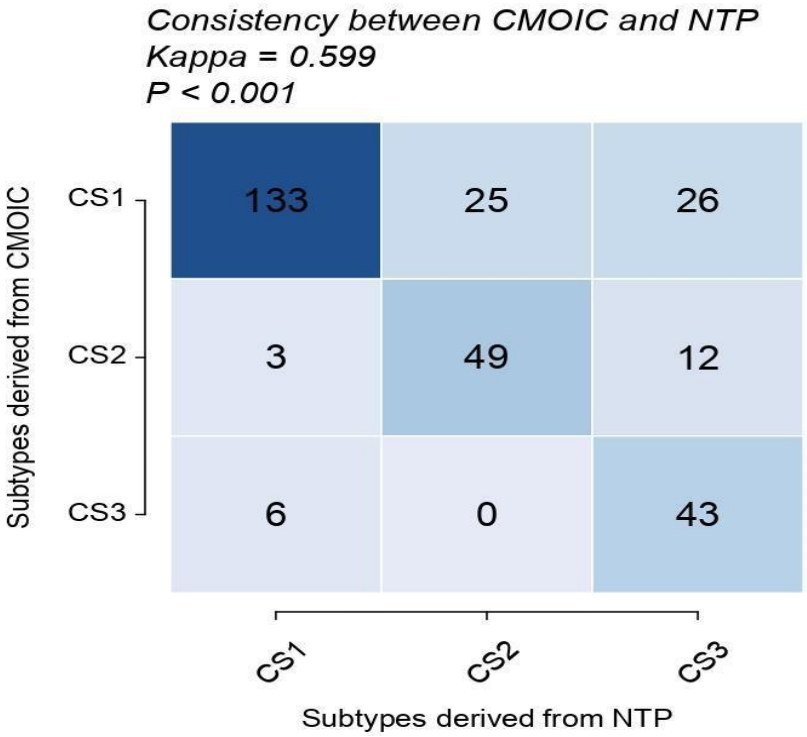


Figure 3.102. Consistency heatmap between current and NTP-predicted Kappa statistics for limma results in TCGA-COAD cohort.

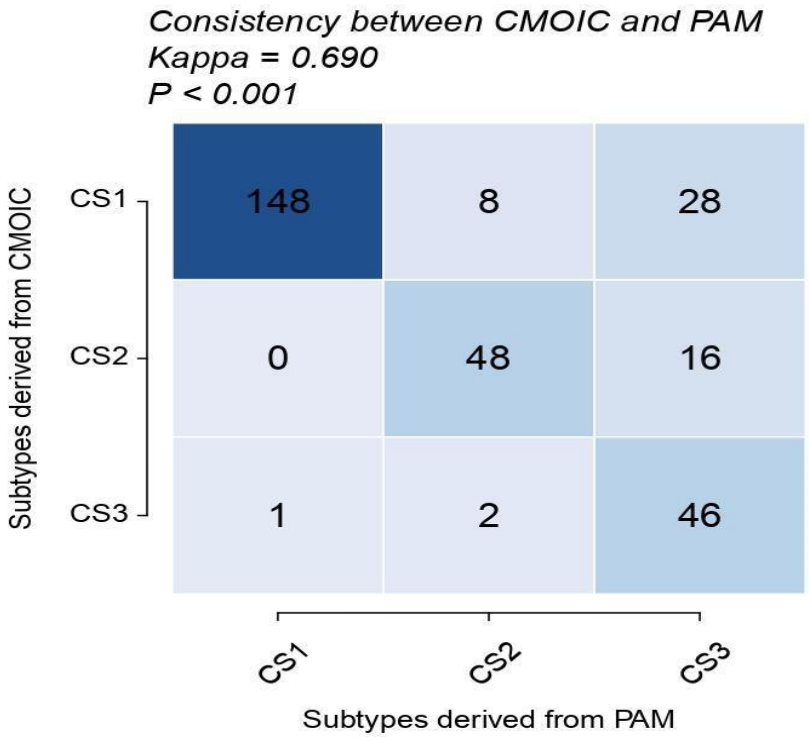


Figure 3.103. Consistency heatmap between current and PAM-predicted Kappa statistics for limma results in TCGA-COAD cohort.

Furthermore, if we examine the consistency between the subtypes recognised by NTP and PAM in the GEO dataset according to the results of edgeR and limma, we find that the result of the kappa statistic is 0.232 and 0.573, respectively (Figures 3.104-3.105). In other words, the consistency between the subtypes identified by NTP and PAM in the validation dataset is categorised as fair by edgeR and moderate by limma.

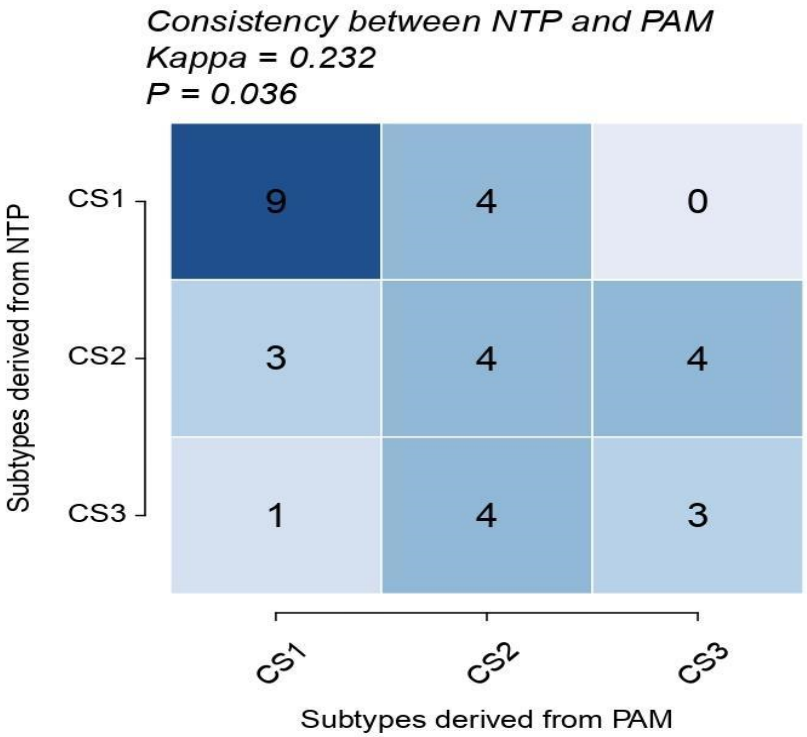


Figure 3.104. Consistency heatmap between NTP and PAM-predicted subtype for edgeR results in GSE16125.

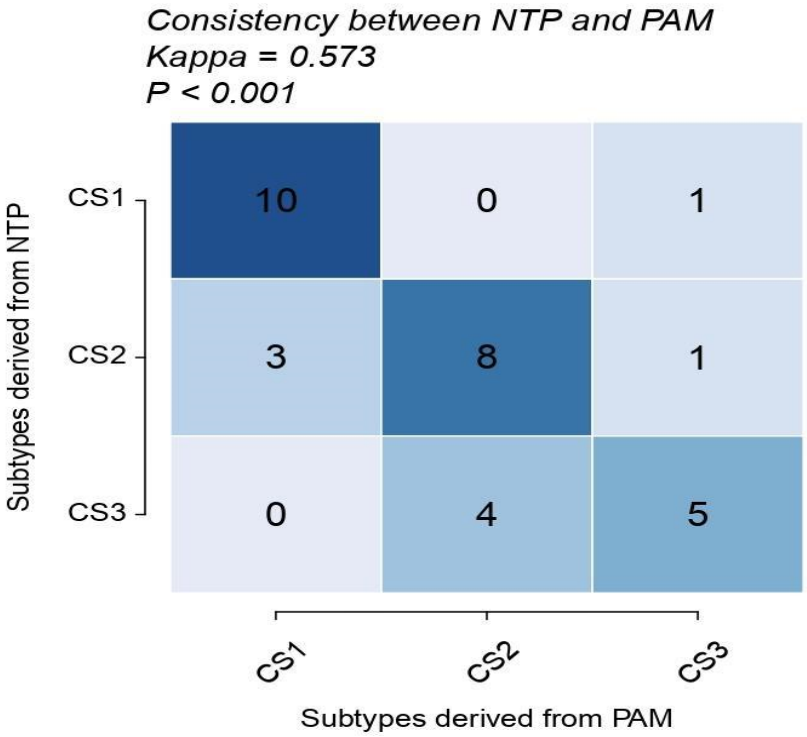


Figure 3.105. Consistency heatmap between NTP and PAM-predicted subtype for limma results in GSE16125.

To predict subtypes in the GSE39582 cohort, which consists of 562 samples, NTP was performed based on upregulated markers detected with edgeR, DESeq2 and limma in the discovery dataset. However, no matches based on DESeq2 results were detected during the NTP analysis. In addition, NTP analysis based on the use of biomarkers predicted using EdgeR failed to match any sample in the GSE39582 dataset to a subspecies (Figure 3.106). In contrast, NTP analysis using Limma revealed that CS1, CS2 and CS3 subtypes matched 213, 150 and 156 samples, respectively (Figure 3.107).

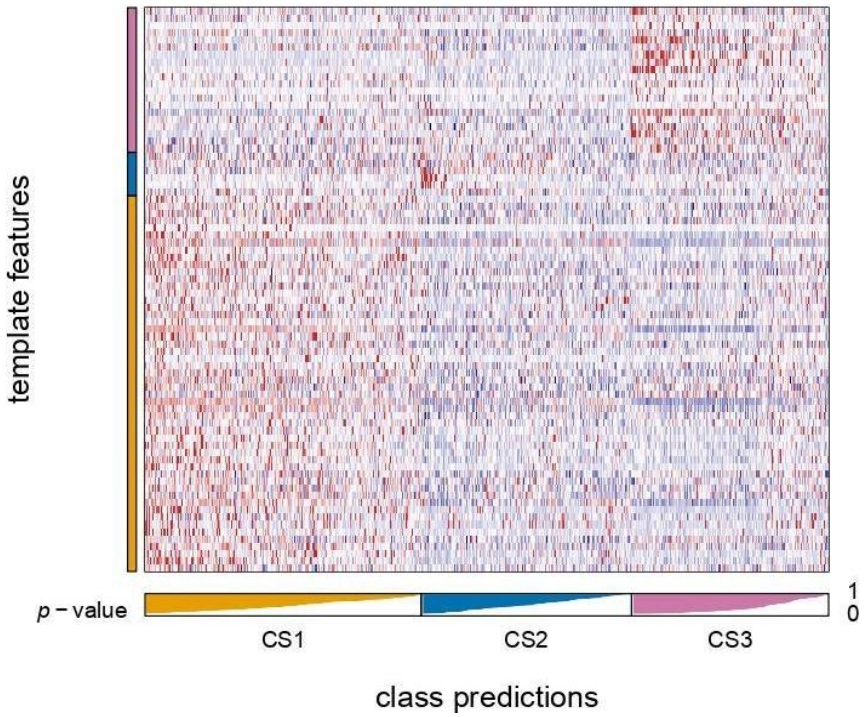


Figure 3.106. Heatmap of NTP in GSE39582 cohort using subtype-specific upregulated biomarkers identified using edgeR from TCGA-COAD cohort.

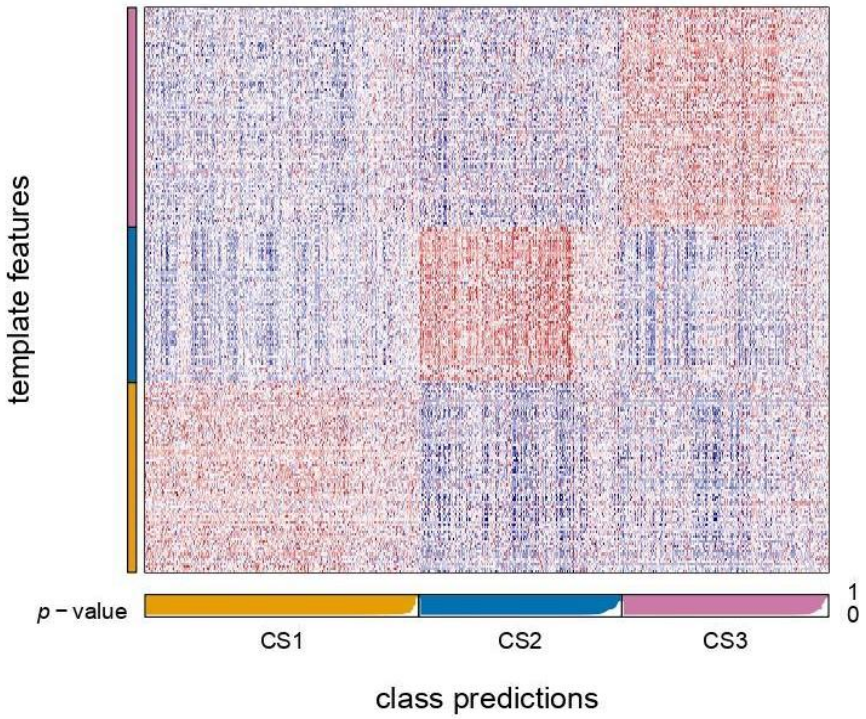


Figure 3.107. Heatmap of NTP in GSE39582 cohort using subtype-specific upregulated biomarkers identified using limma from TCGA-COAD cohort.

As a result of the survival analysis in the GSE39582 cohort, statistically significant results were only obtained with the Limma algorithm (Figures 3.108-3.109). According to the IGP statistics obtained as a result of the PAM analysis of the GSE39582 cohort, the subtypes identified between the discovery and validation groups were found to be similar and reproducible (Table 3.38).

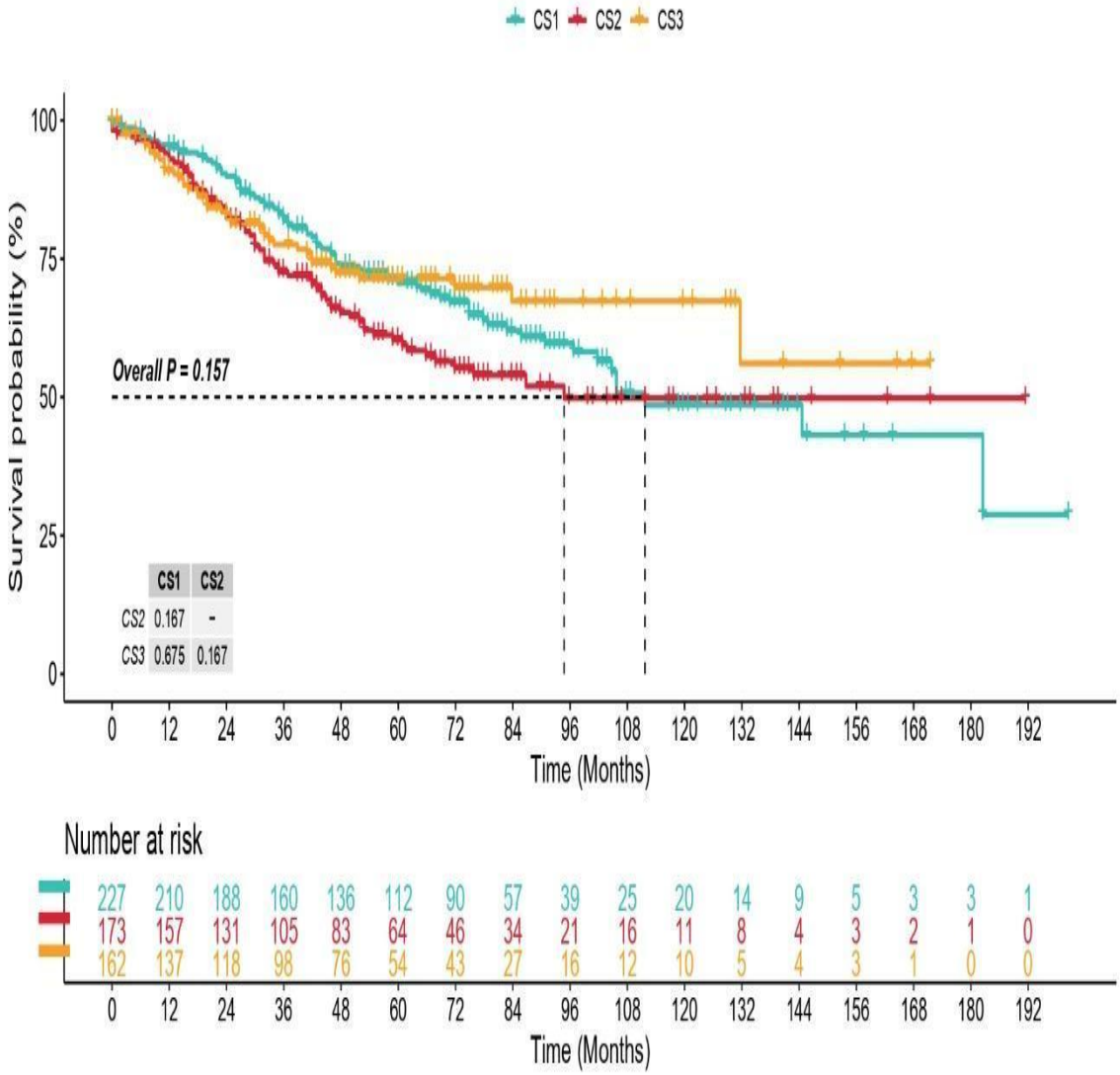


Figure 3.108. Kaplan-Meier survival curve of 3 colon adenocarcinoma subtypes predicted by edgeR in the GSE39582 cohort.

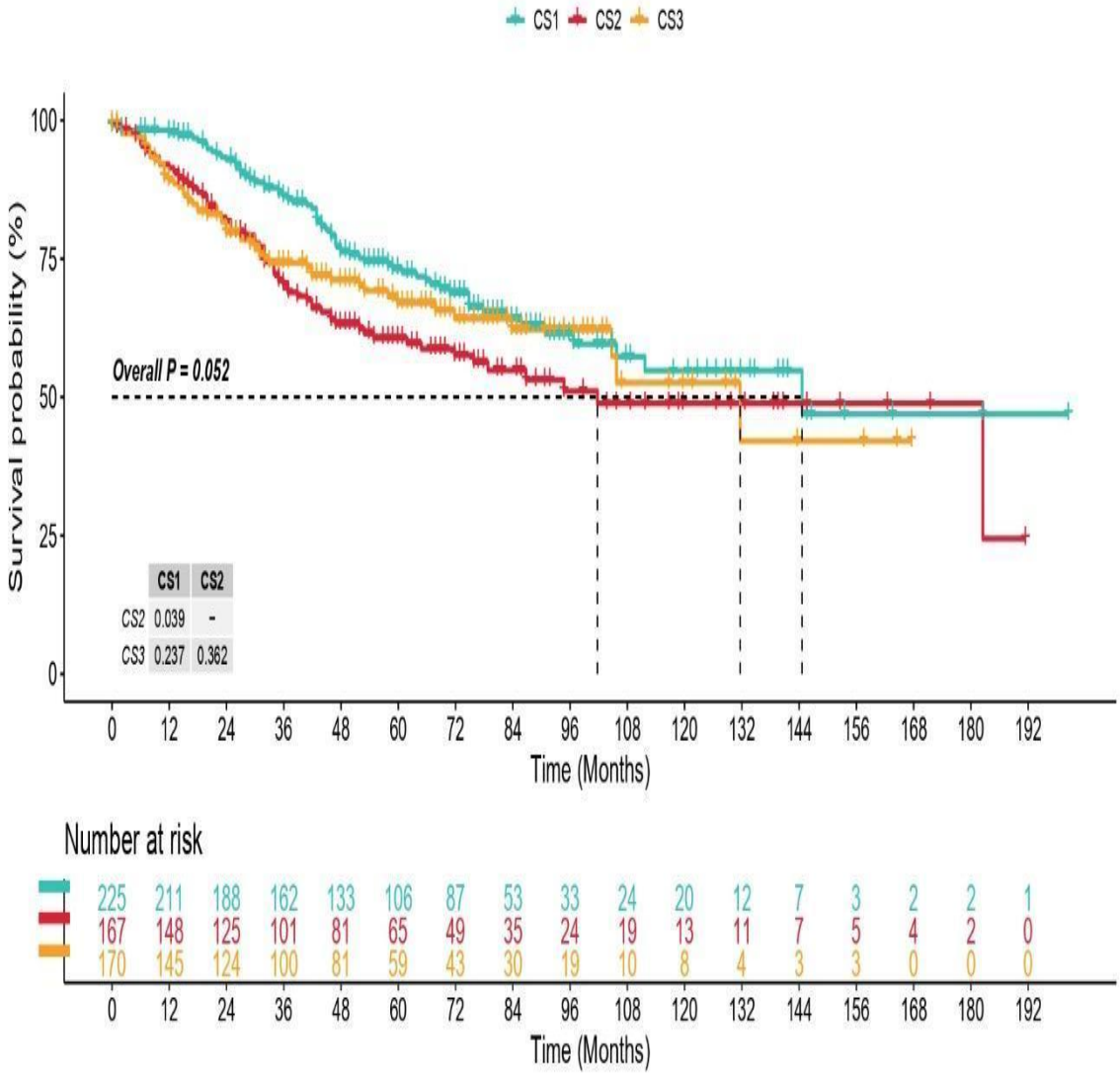


Figure 3.109. Kaplan-Meier survival curve of 3 colon adenocarcinoma subtypes predicted by limma in the GSE39582 cohort.

The results of the three algorithms (Figures 3.110-3.115) show that the consistency between the subtypes found in the TCGA dataset and the subtypes predicted by PAM is much clearer than that predicted by NTP.

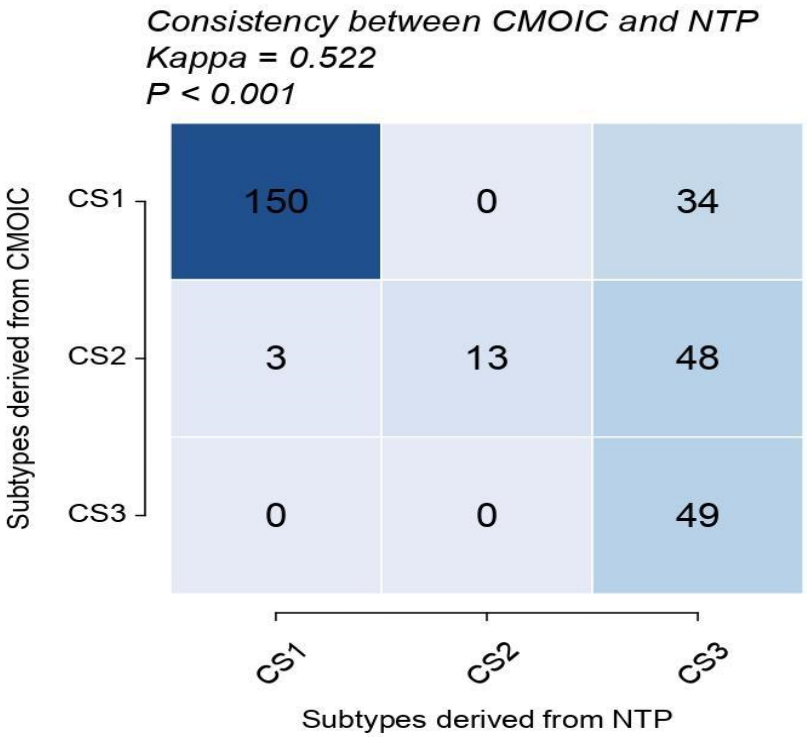


Figure 3.110. Consistency heatmap between current and NTP-predicted Kappa statistics for edgeR results in TCGA-COAD cohort.

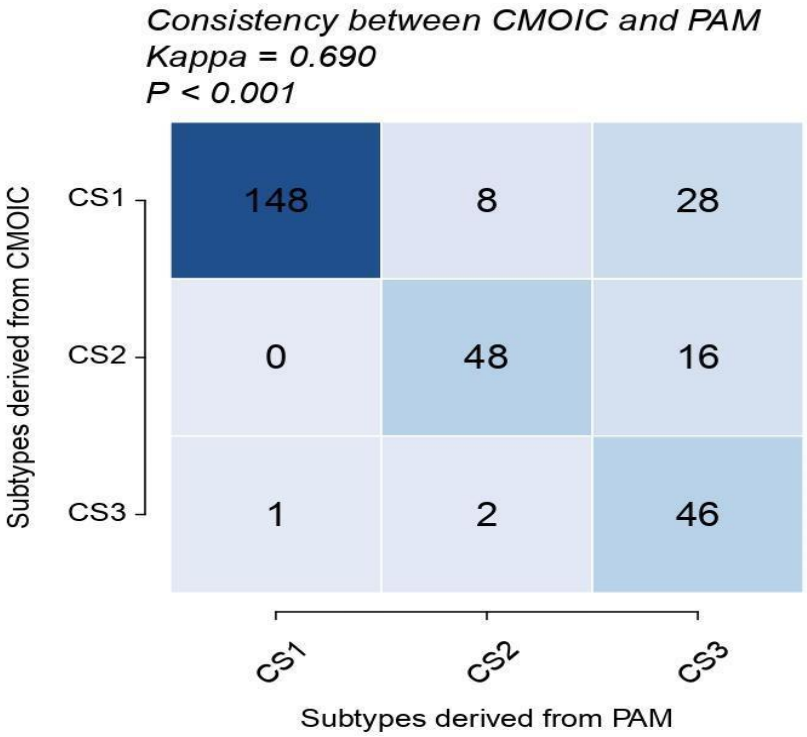


Figure 3.111. Consistency heatmap between current and PAM-predicted Kappa statistics for edgeR results in TCGA-COAD cohort.

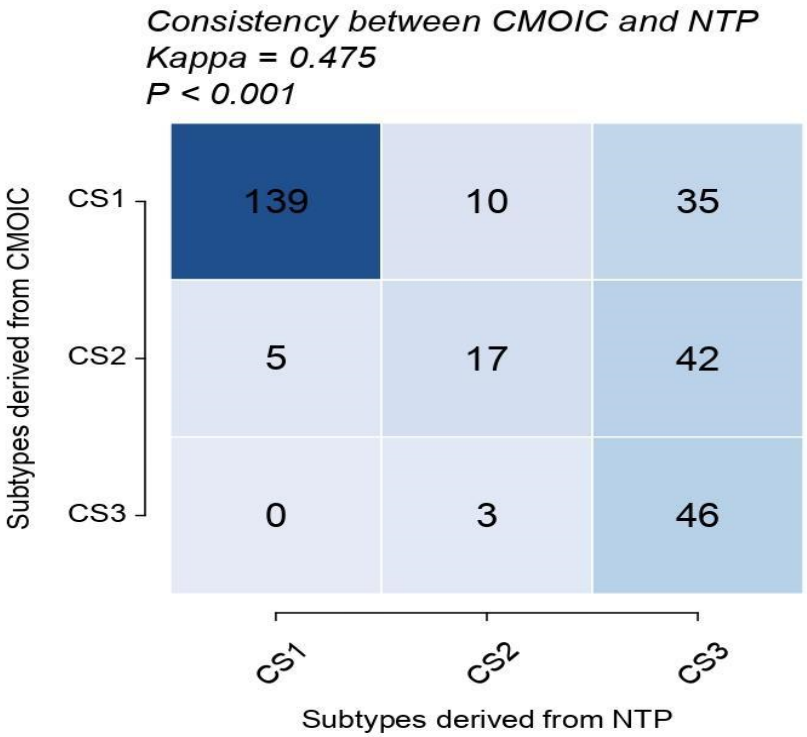


Figure 3.112. Consistency heatmap between current and NTP-predicted Kappa statistics for DESeq2 results in TCGA-COAD cohort.

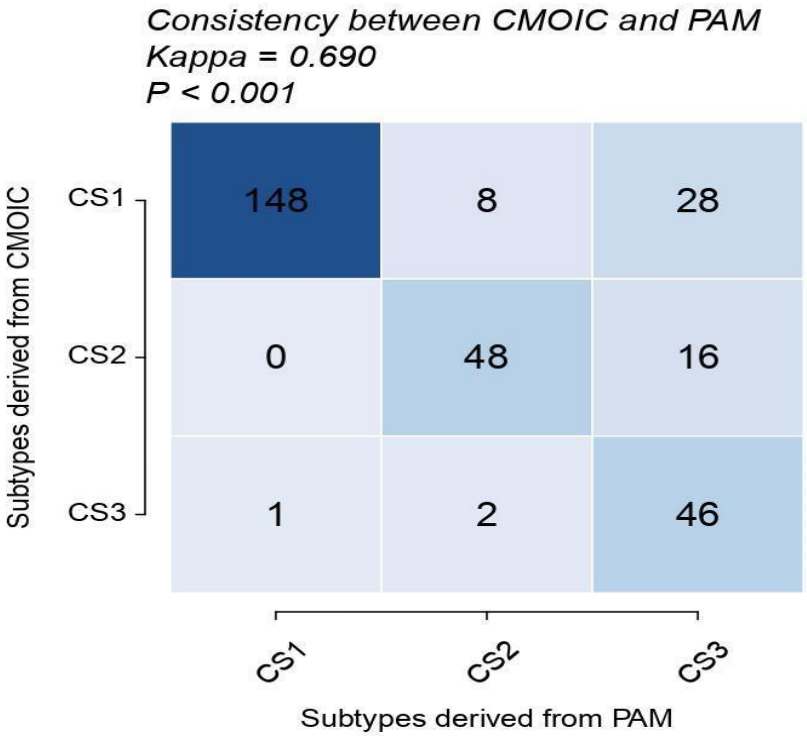


Figure 3.113. Consistency heatmap between current and PAM-predicted Kappa statistics for DESeq2 results in TCGA-COAD cohort.

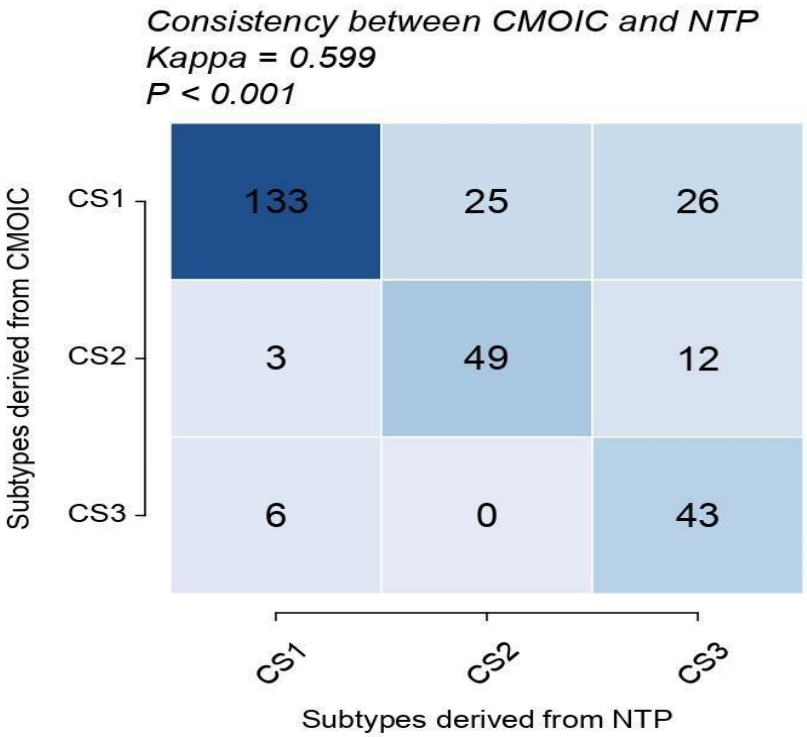


Figure 3.114. Consistency heatmap between current and NTP-predicted Kappa statistics for limma results in TCGA-COAD cohort.

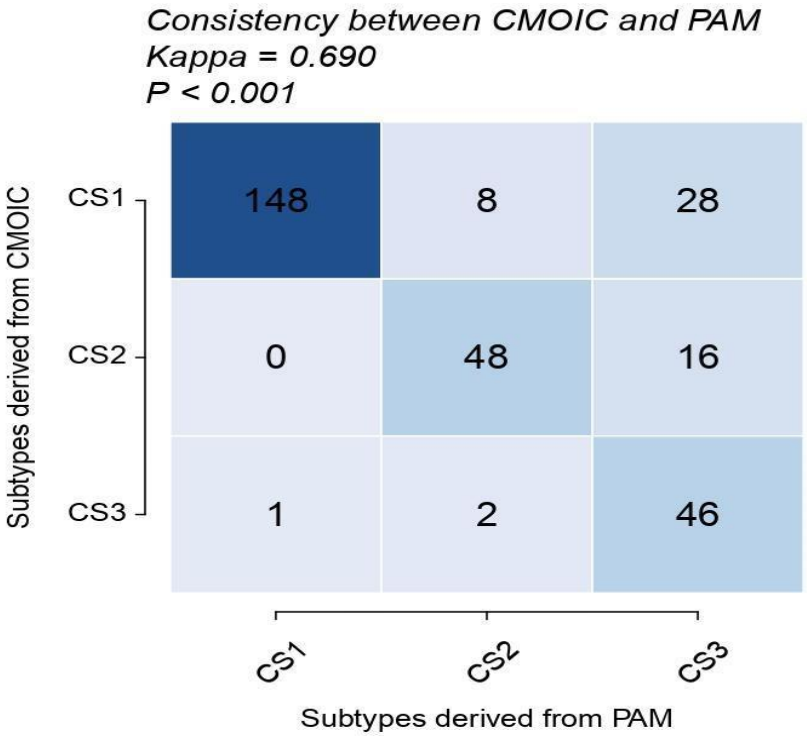


Figure 3.115. Consistency heatmap between current and PAM-predicted Kappa statistics for limma results in TCGA-COAD cohort.

In addition, the consistency results of the subtypes detected by NTP and PAM in the validation data set were best obtained with Limma (0.363 and 0.667 for edgeR and limma, respectively) (Figures 3.116-3.117).

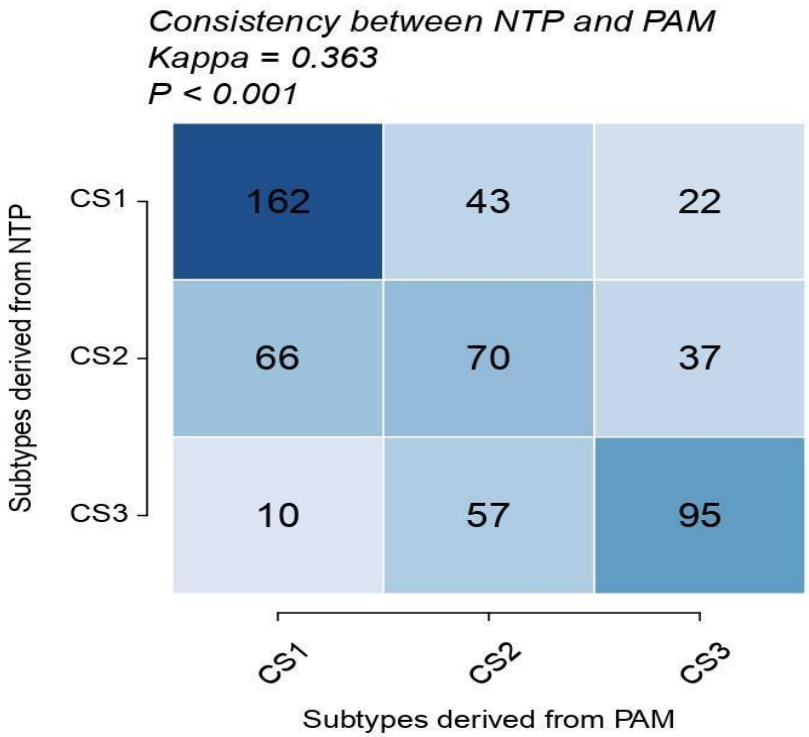


Figure 3.116. Consistency heatmap between NTP and PAM-predicted subtype for edgeR results in GSE39582.

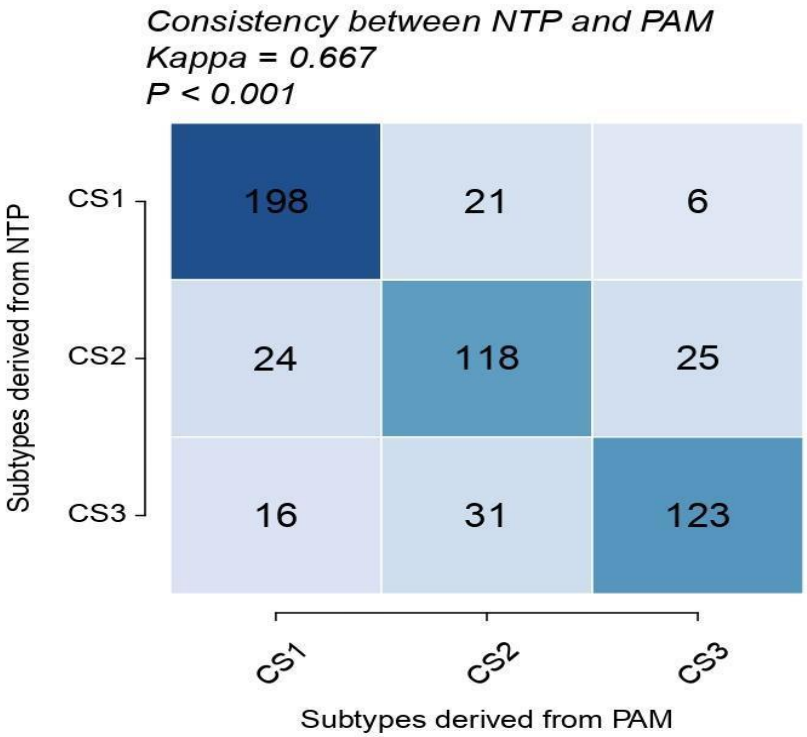


Figure 3.117. Consistency heatmap between NTP and PAM-predicted subtype for limma results in GSE39582.

To predict subtypes in the GSE1756 cohort, which consists of 177 samples, NTP was performed based on upregulated markers detected with edgeR, DESeq2 and limma in the discovery dataset. However, no matches based on DESeq2 results were detected during the NTP analysis. In addition, NTP analysis based on the use of biomarkers predicted by EdgeR failed to match any sample in the GSE39582 dataset to a subspecies (Figure 3.118). On the other hand, NTP analysis using Limma revealed that CS1, CS2 and CS3 subtypes matched 68, 47 and 42 samples, respectively (Figure 3.119).

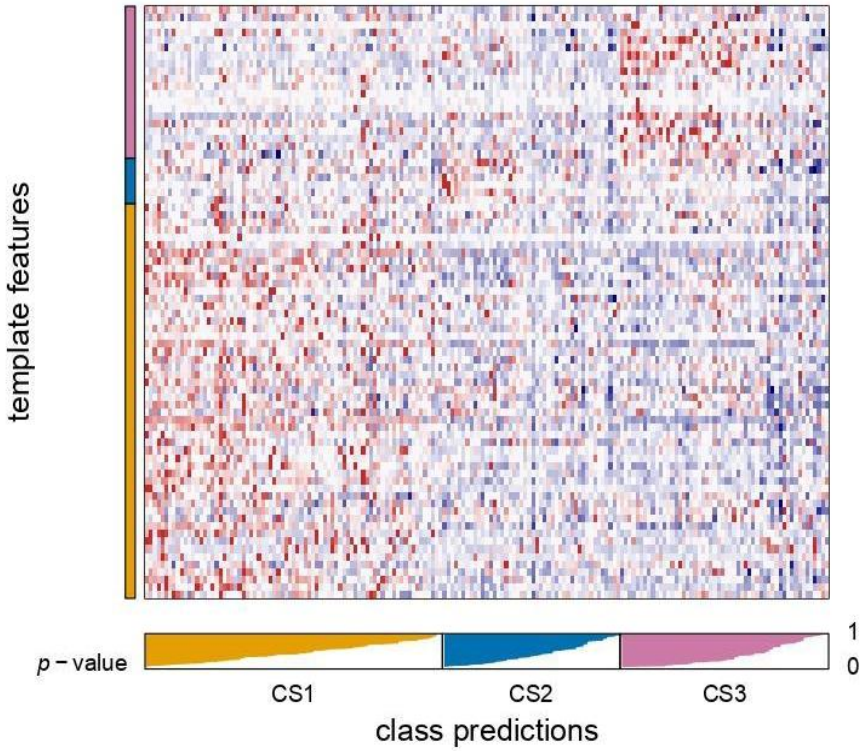


Figure 3.118. Heatmap of NTP in GSE17536 cohort using subtype-specific upregulated biomarkers identified using edgeR from TCGA-COAD cohort.

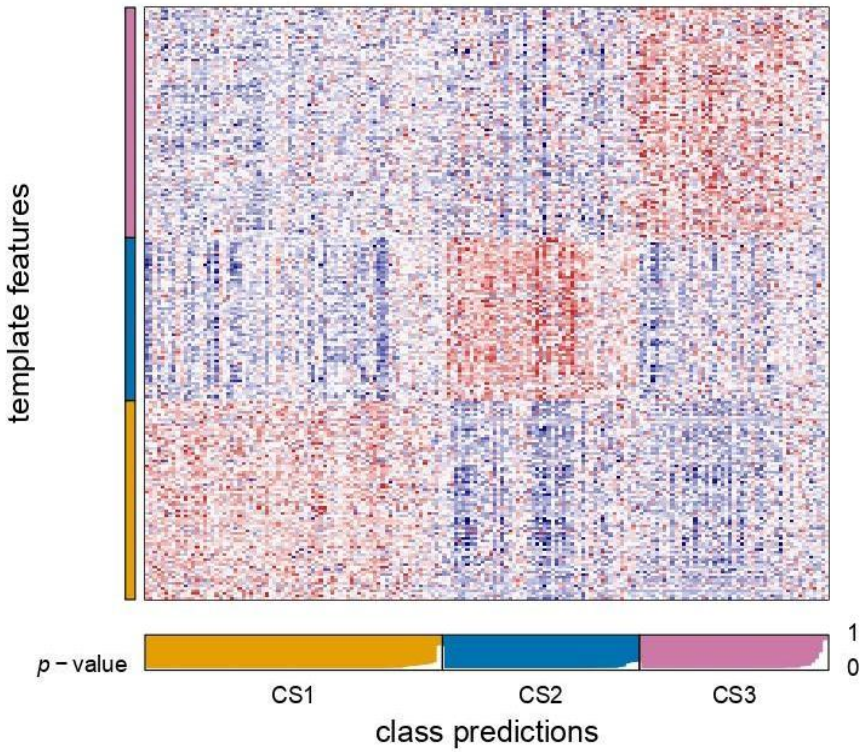


Figure 3.119. Heatmap of NTP in GSE17536 cohort using subtype-specific upregulated biomarkers identified using limma from TCGA-COAD cohort.

As a result of the survival analysis performed with edgeR and limma in the GSE17536 cohort, no statistically significant difference was found (Figures 3.120-3.121). According to the IGP statistics obtained as a result of the PAM analysis of the GSE17536 cohort, the subtypes identified between the discovery and validation groups were found to be similar and reproducible (Table 3.38).

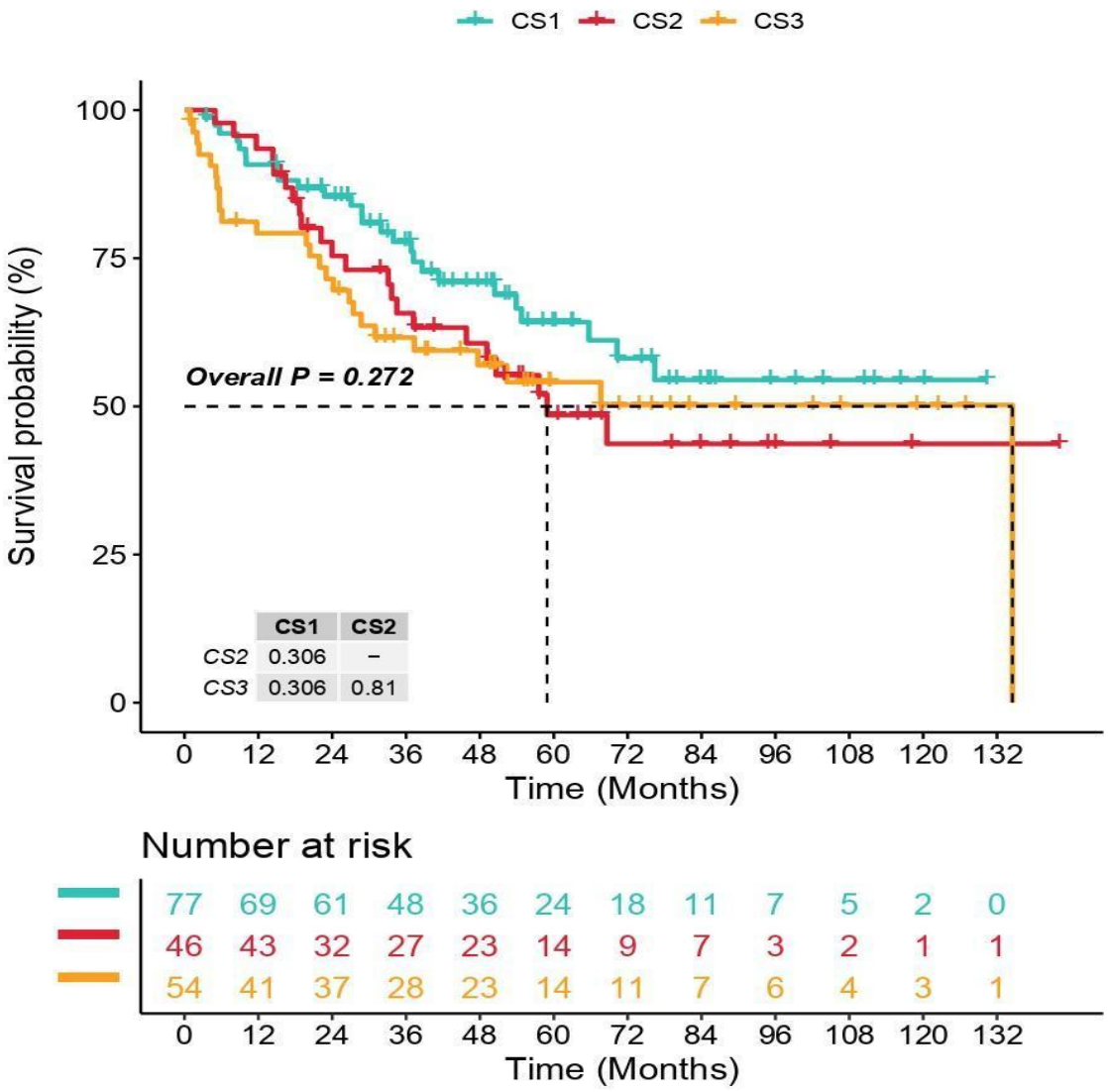


Figure 3.120. Kaplan-Meier survival curve of 3 colon adenocarcinoma subtypes predicted by edgeR in the GSE17536 cohort.

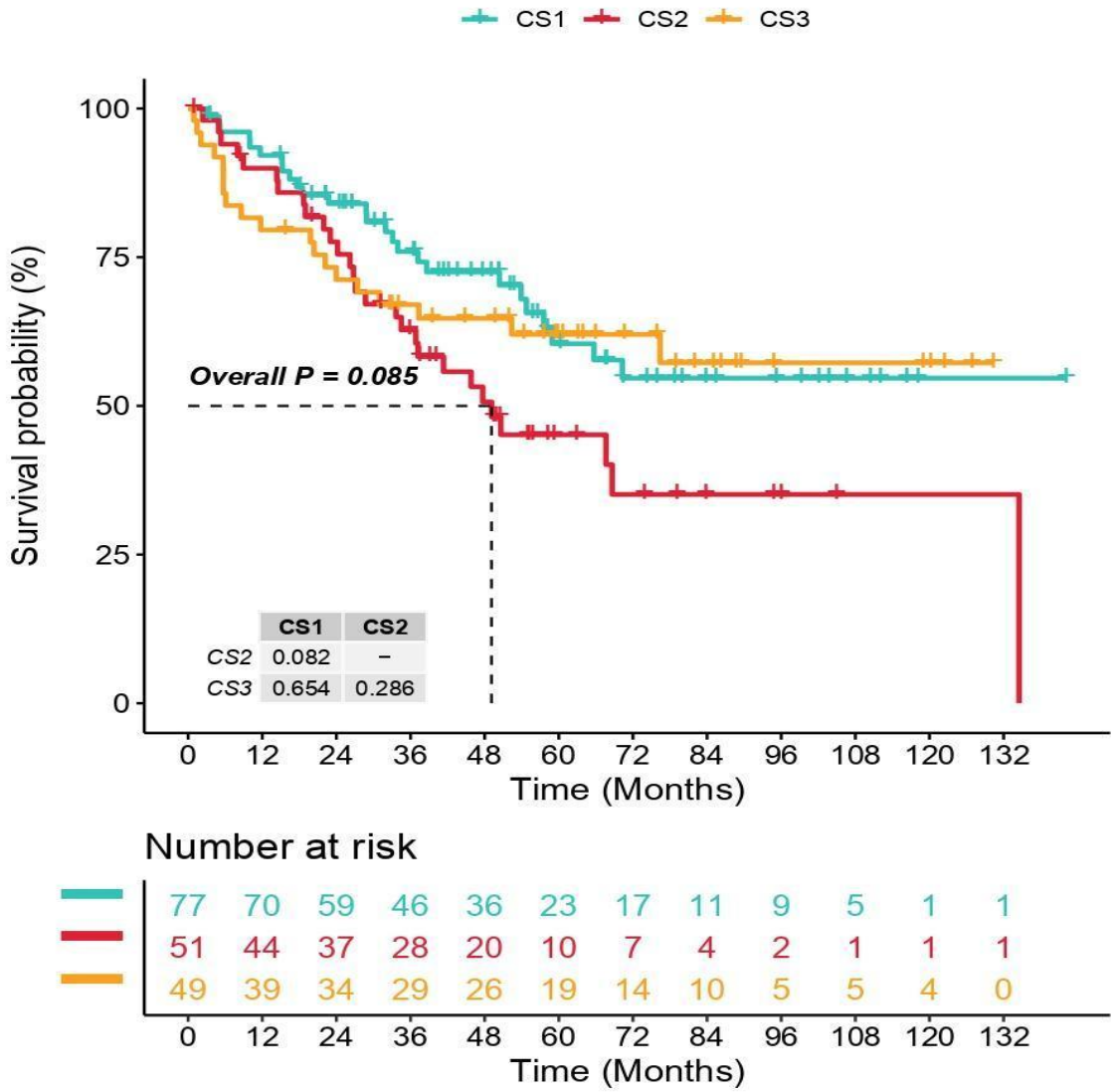


Figure 3.121. Kaplan-Meier survival curve of 3 colon adenocarcinoma subtypes predicted by limma in the GSE17536 cohort.

According to the results of the three algorithms (Figures 3.122-3.127), the consistency between the subtypes found in the TCGA dataset and those predicted by PAM is much more significant than that predicted by NTP.

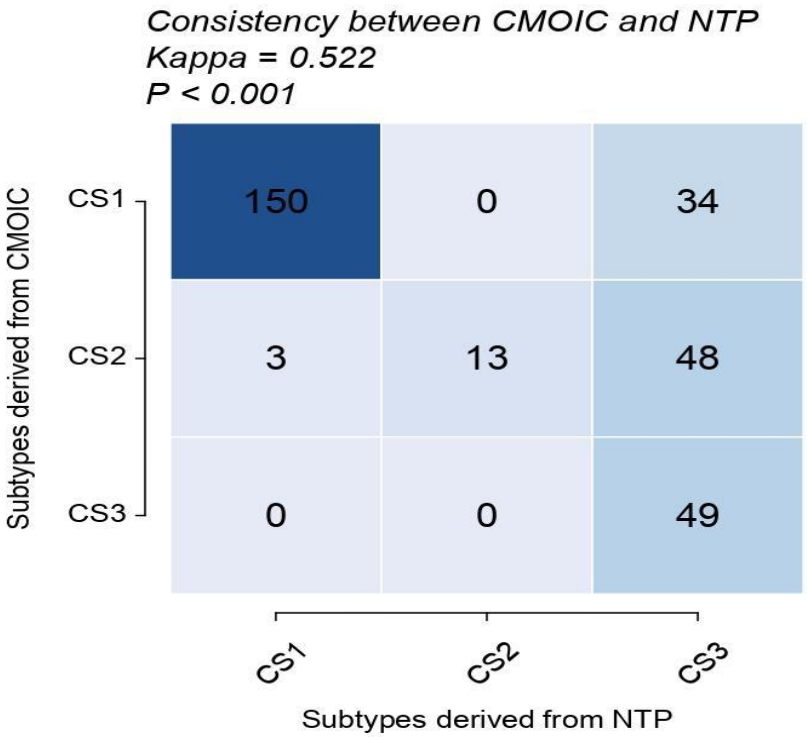


Figure 3.122. Consistency heatmap between current and NTP-predicted Kappa statistics for edgeR results in TCGA-COAD cohort.

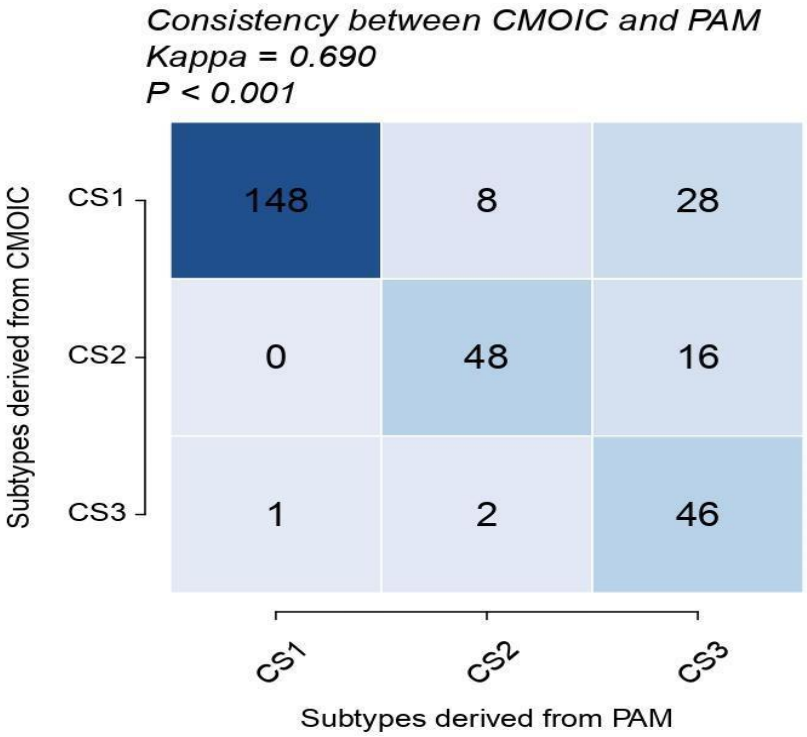


Figure 3.123. Consistency heatmap between current and PAM-predicted Kappa statistics for edgeR results in TCGA-COAD cohort.

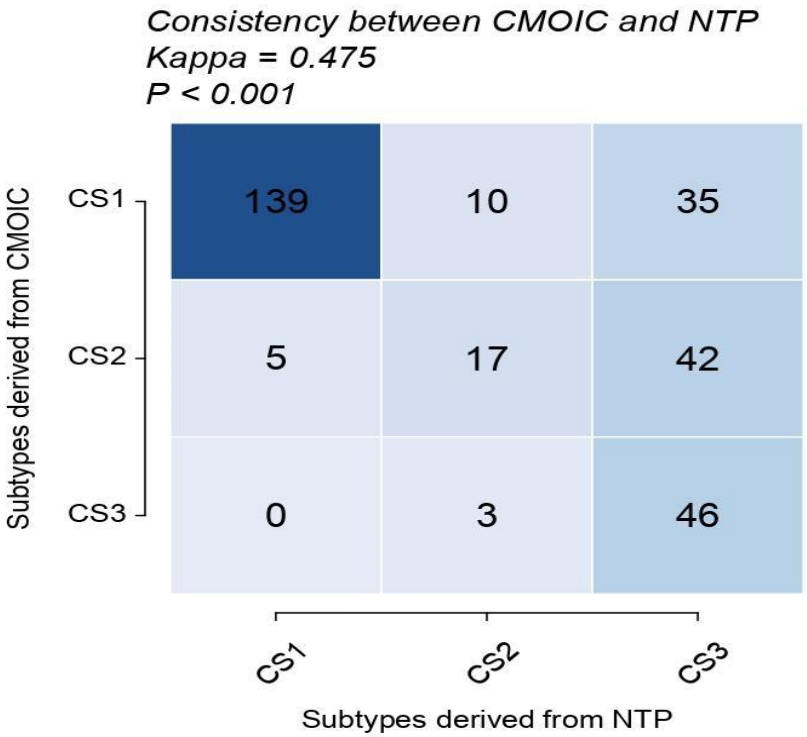


Figure 3.124. Consistency heatmap between current and NTP-predicted Kappa statistics for DESeq2 results in TCGA-COAD cohort.

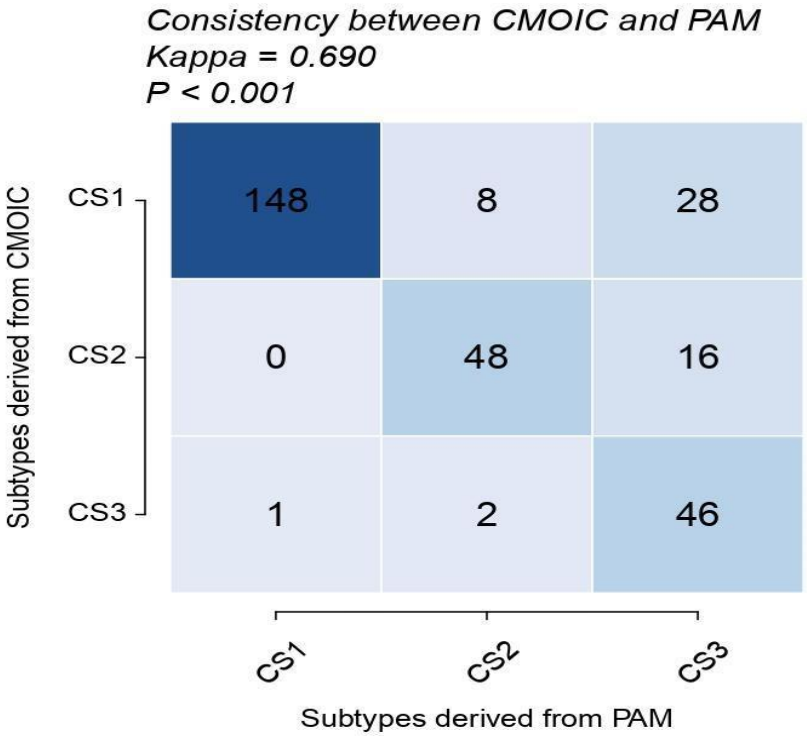


Figure 3.125. Consistency heatmap between current and PAM-predicted Kappa statistics for DESeq2 results in TCGA-COAD cohort.

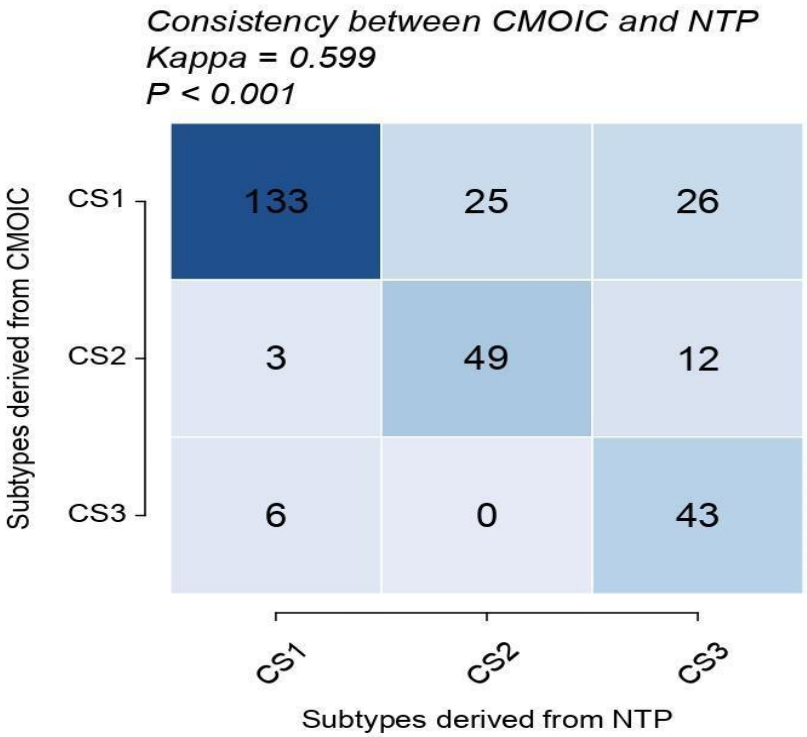


Figure 3.126. Consistency heatmap between current and NTP-predicted Kappa statistics for limma results in TCGA-COAD cohort.

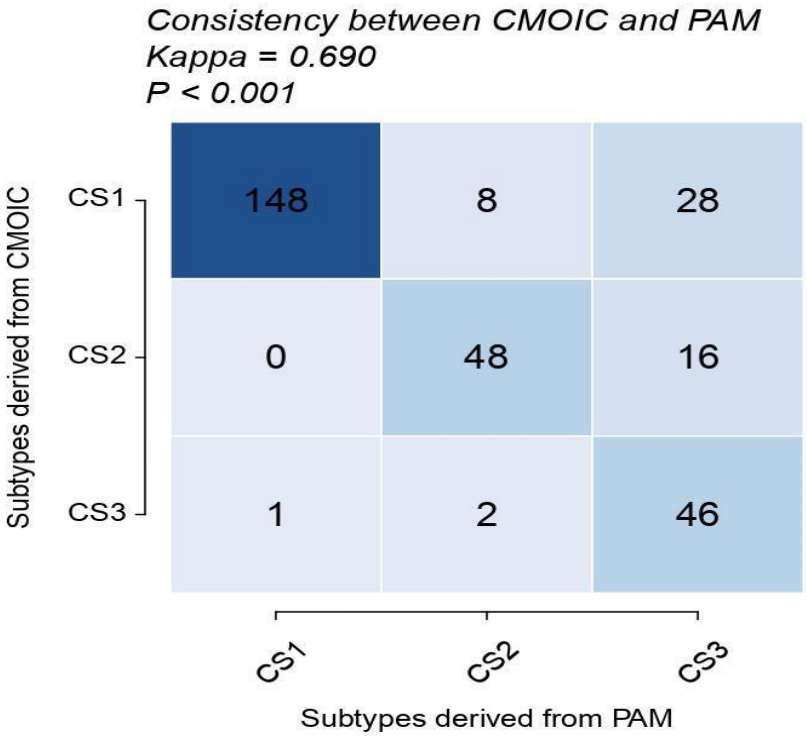


Figure 3.127. Consistency heatmap between current and PAM-predicted Kappa statistics for limma results in TCGA-COAD cohort.

In addition, the consistency results of the subtypes detected by NTP and PAM in the validation data set were best obtained with Limma (0.384 and 0.617 for edgeR and limma, respectively) (Figures 3.128-3.129).

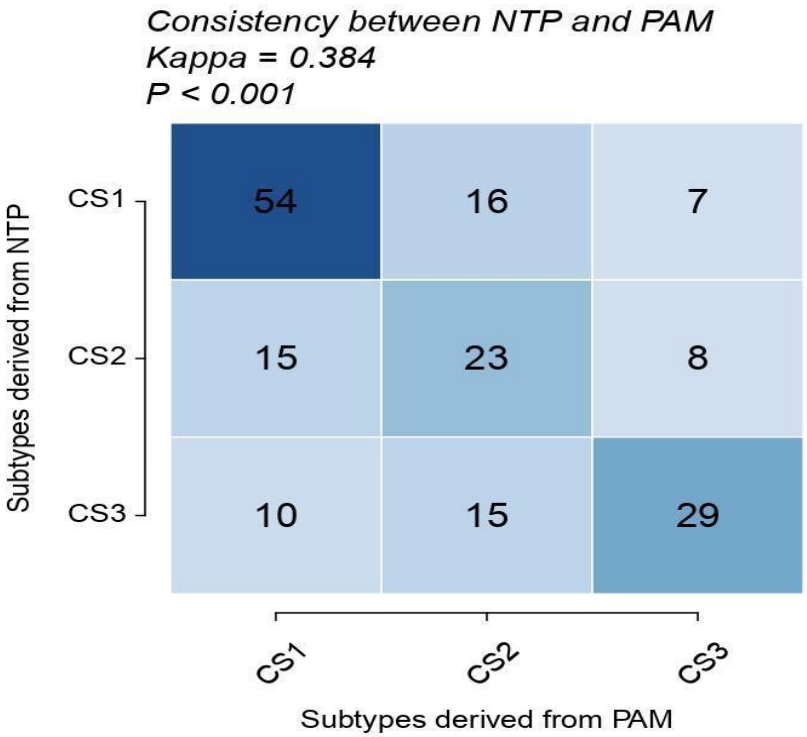


Figure 3.128. Consistency heatmap between NTP and PAM-predicted subtype for edgeR results in GSE17536.

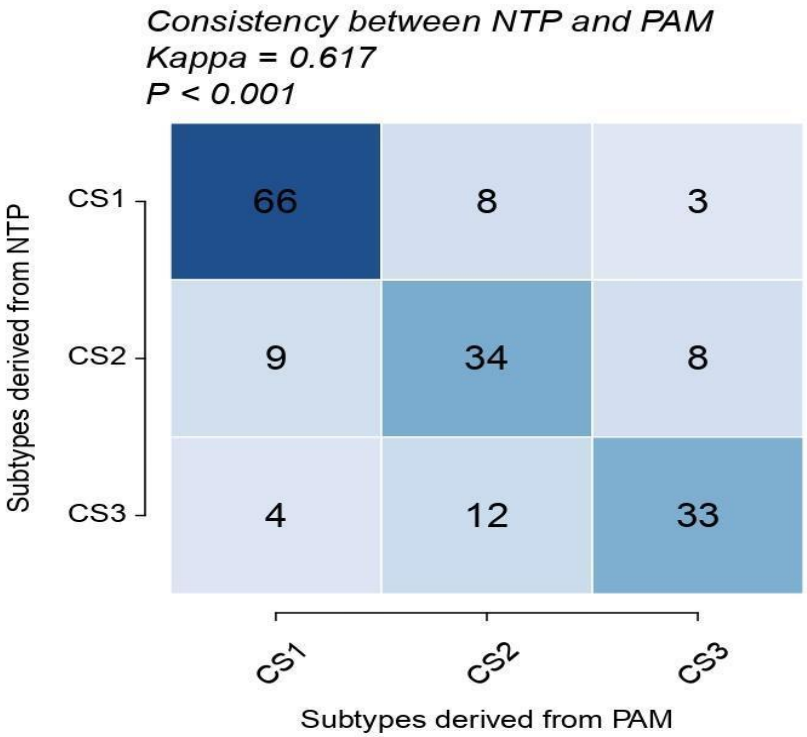


Figure 3.129. Consistency heatmap between NTP and PAM-predicted subtype for limma results in GSE17536.

To predict subtypes in the GSE17537 cohort, which consists of 55 samples, NTP was performed based on upregulated markers detected with edgeR, DESeq2 and limma in the discovery dataset. However, no matches based on DESeq2 results could be detected during NTP analysis. In addition, NTP analysis based on the use of biomarkers predicted by EdgeR failed to match any sample in the GSE17537 dataset to a subspecies (Figure 3.130). On the other hand, the NTP analysis using Limma revealed that the CS1, CS2 and CS3 subtypes could be assigned to 19, 16 and 15 samples, respectively (Figure 3.131).

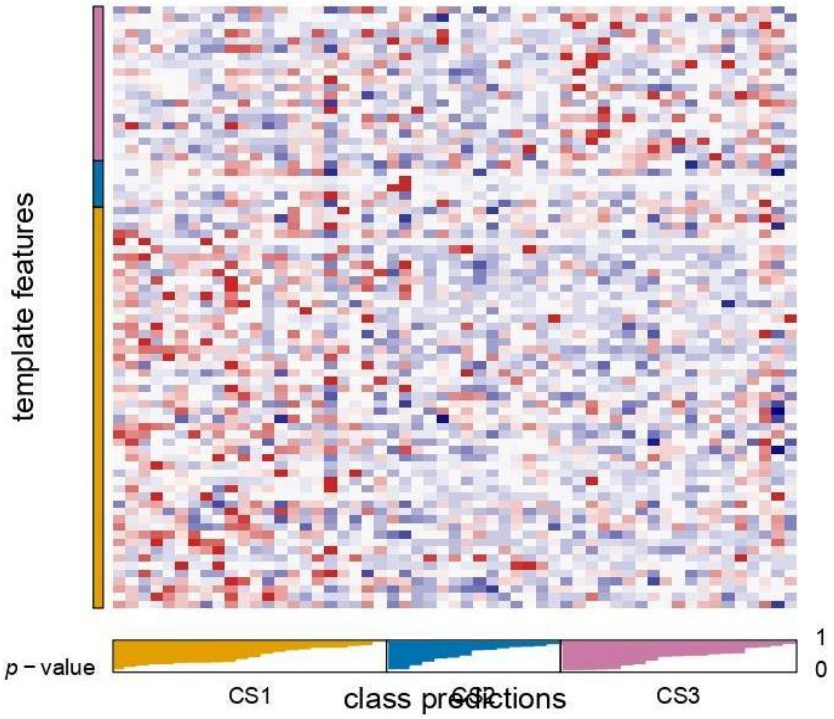


Figure 3.130. Heatmap of NTP in GSE17537 cohort using subtype-specific upregulated biomarkers identified using edgeR from TCGA-COAD cohort.

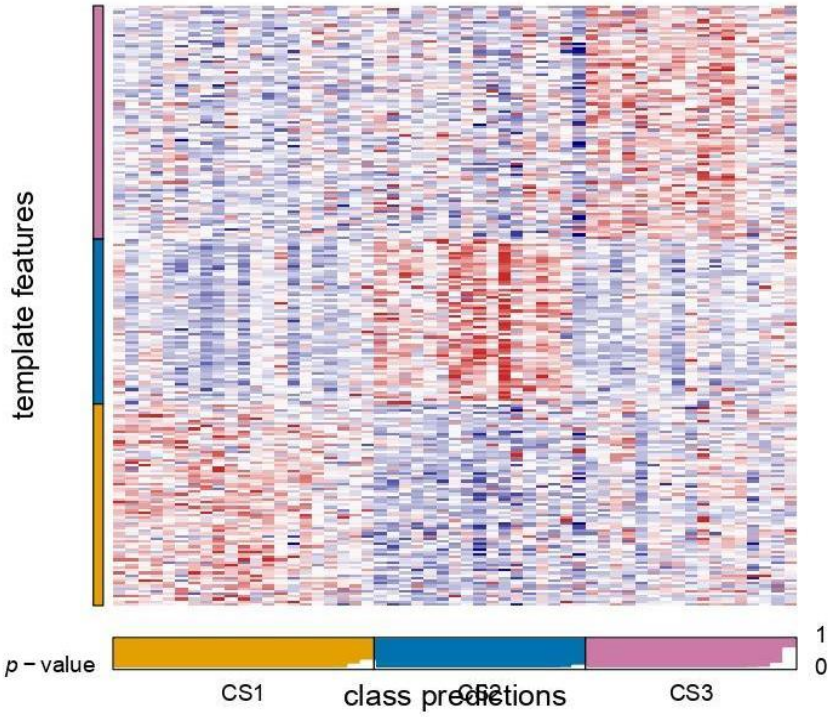


Figure 3.131. Heatmap of NTP in GSE17537 cohort using subtype-specific upregulated biomarkers identified using limma from TCGA-COAD cohort.

In the GSE17537 cohort, a survival analysis of the subtypes obtained by NTP was performed based on the results of edgeR and limma. While no statistically significant result was obtained with edgeR, a statistically significant result with a p-value of 0.045 was obtained with limma (Figures 3.132-3.133). As a result, CS2 was characterised by the worst survival. According to the IGP statistics obtained as a result of the PAM analysis of the GSE17537 cohort, the subtypes obtained between the discovery and validation groups proved to be similar and reproducible (Table 3.38).

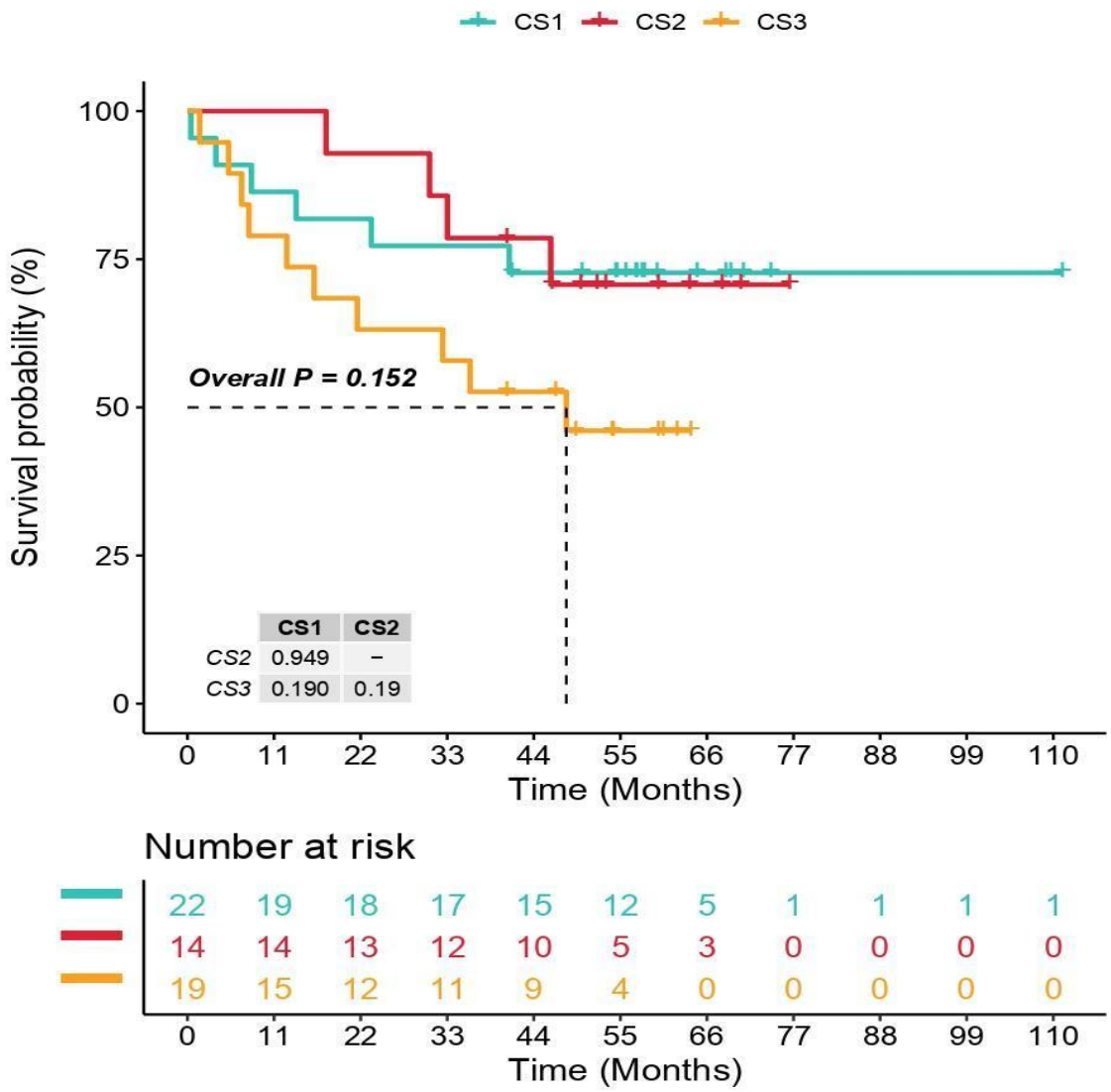


Figure 3.132. Kaplan-Meier survival curve of 3 colon adenocarcinoma subtypes predicted by edgeR in the GSE17537 cohort.

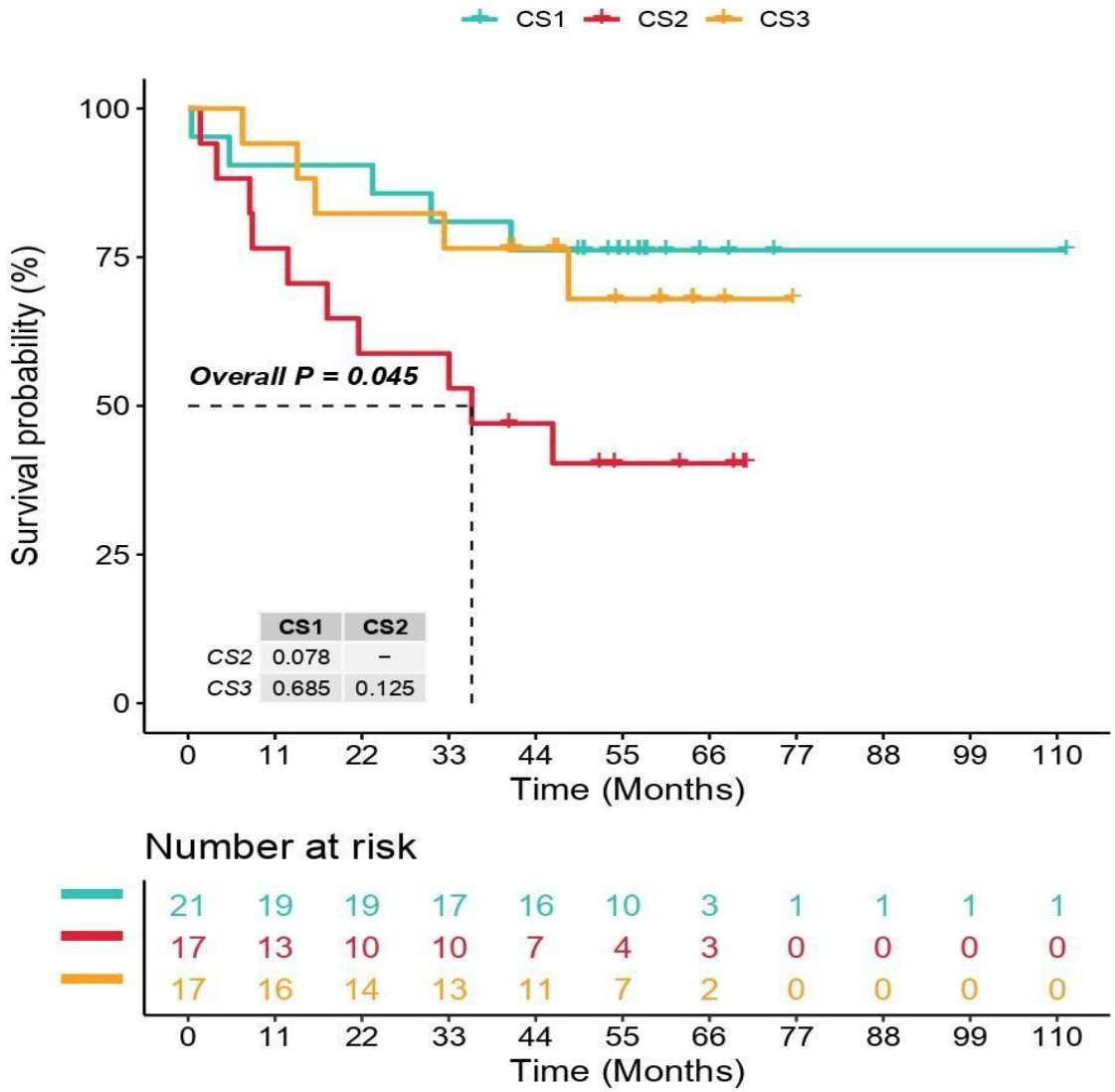


Figure 3.133. Kaplan-Meier survival curve of 3 colon adenocarcinoma subtypes predicted by limma in the GSE17537 cohort.

According to the results of the three algorithms (Figures 3.134-3.139), the consistency between the subtypes found in the TCGA dataset and those predicted by PAM is much more significant than that predicted by NTP.

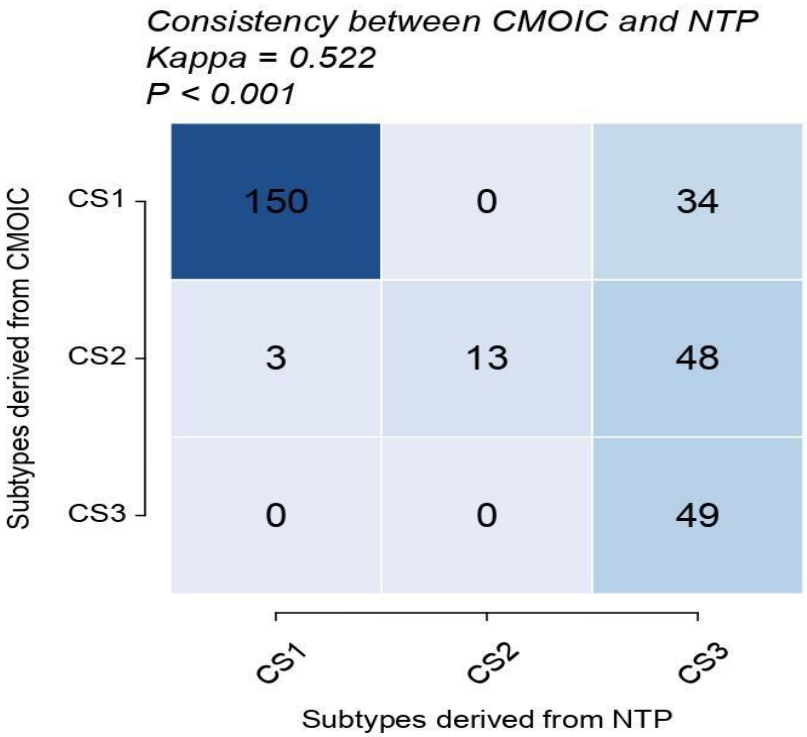


Figure 3.134. Consistency heatmap between current and NTP-predicted Kappa statistics for edgeR results in TCGA-COAD cohort.

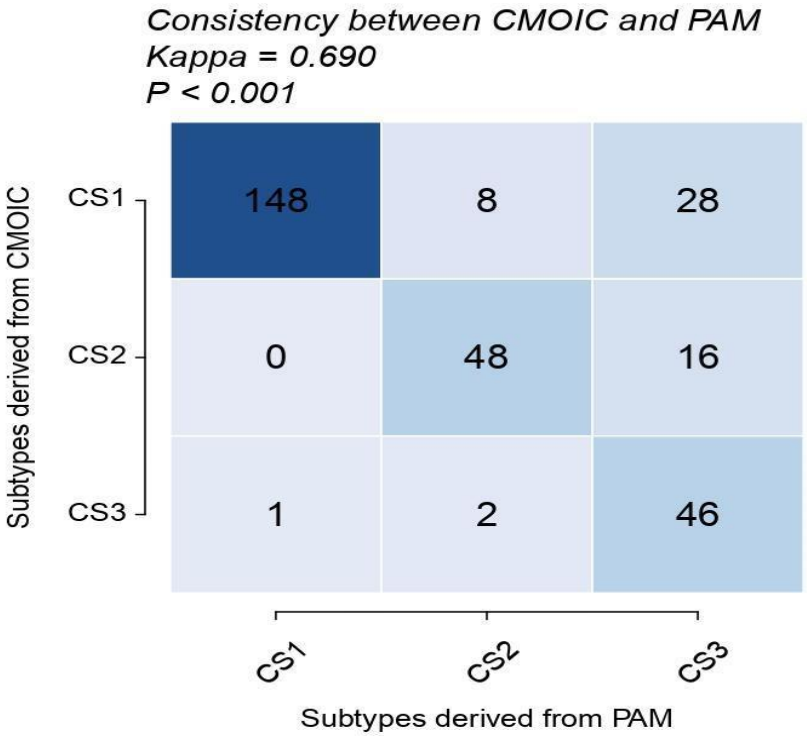


Figure 3.135. Consistency heatmap between current and PAM-predicted Kappa statistics for edgeR results in TCGA-COAD cohort.

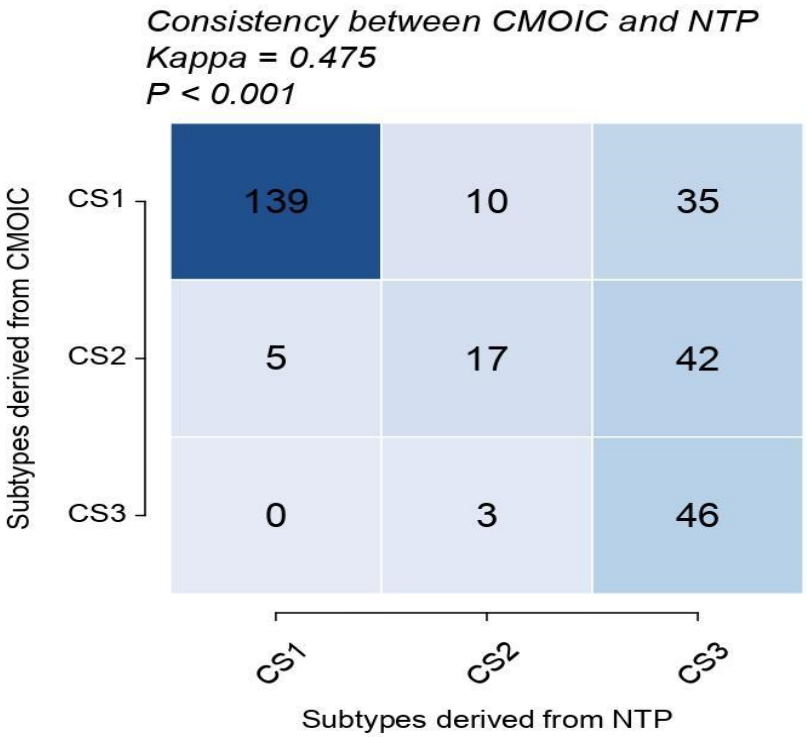


Figure 3.136. Consistency heatmap between current and NTP-predicted Kappa statistics for DESeq2 results in TCGA-COAD cohort.

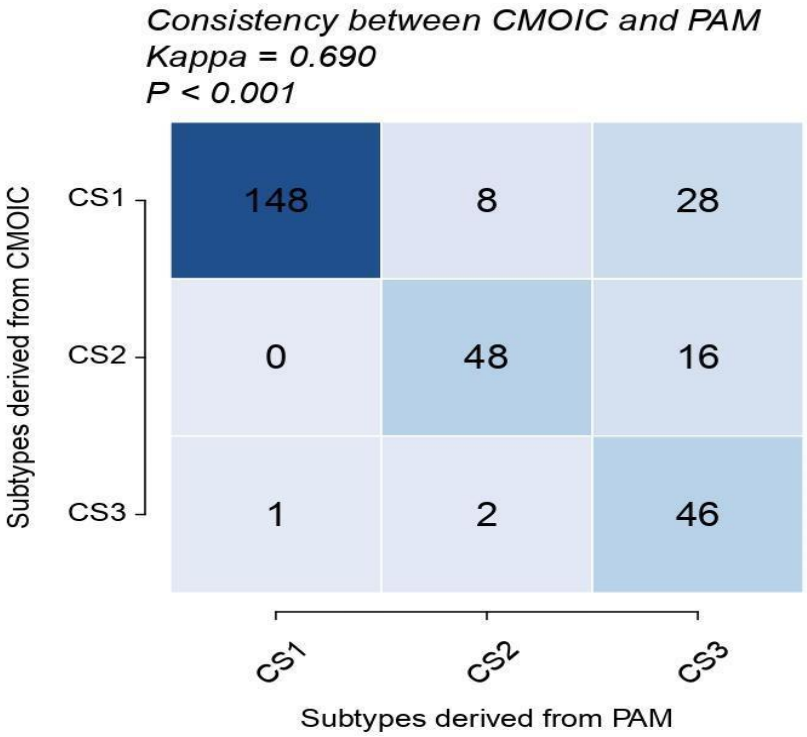


Figure 3.137. Consistency heatmap between current and PAM-predicted Kappa statistics for DESeq2 results in TCGA-COAD cohort.

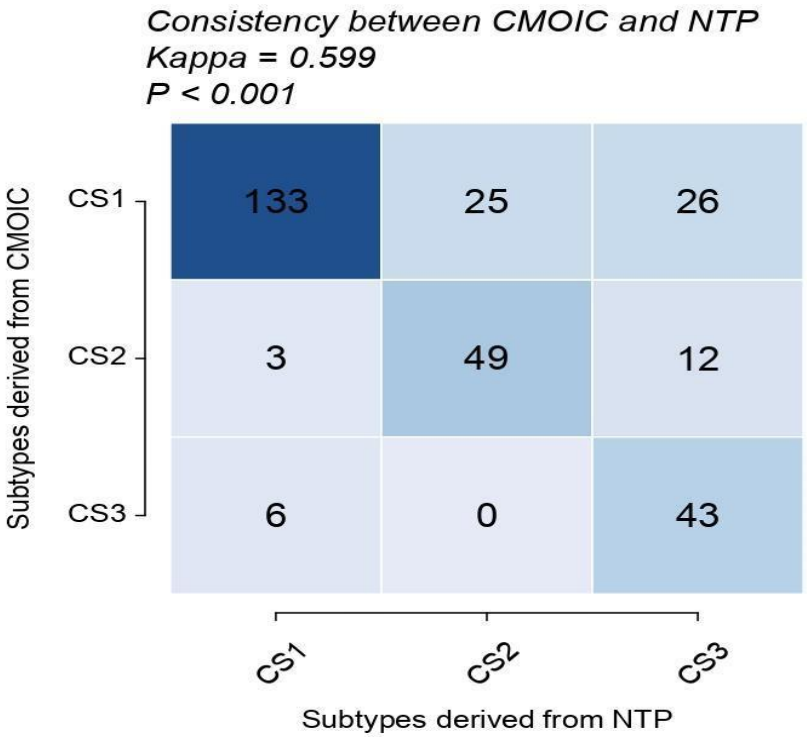


Figure 3.138. Consistency heatmap between current and NTP-predicted Kappa statistics for limma results in TCGA-COAD cohort.

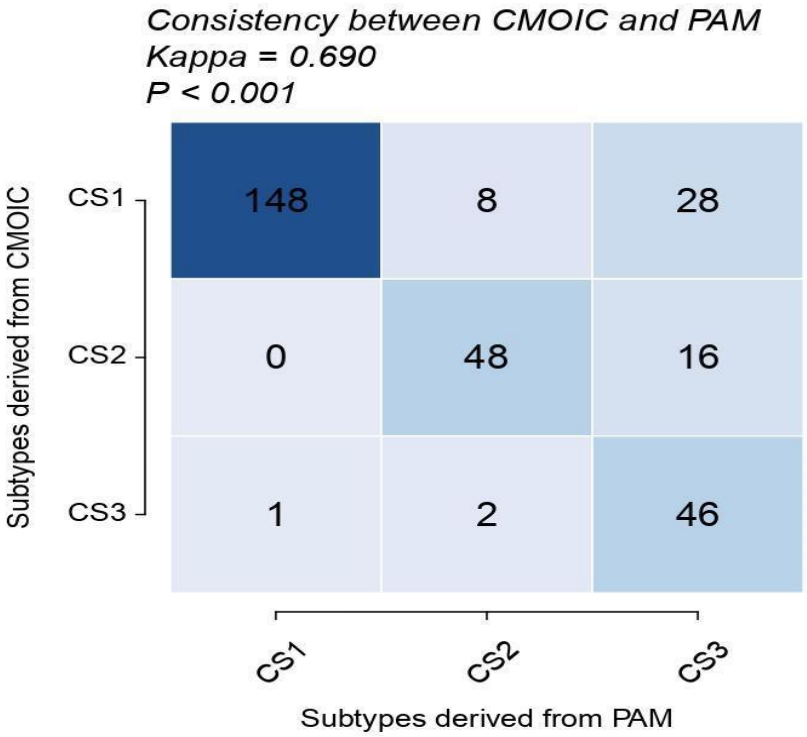


Figure 3.139. Consistency heatmap between current and PAM-predicted Kappa statistics for limma results in TCGA-COAD cohort.

In addition, the consistency results of the subtypes detected by NTP and PAM in the validation dataset were best obtained with limma (0.228 and 0.615 for edgeR and limma, respectively) (Figures 3.140-3.141).

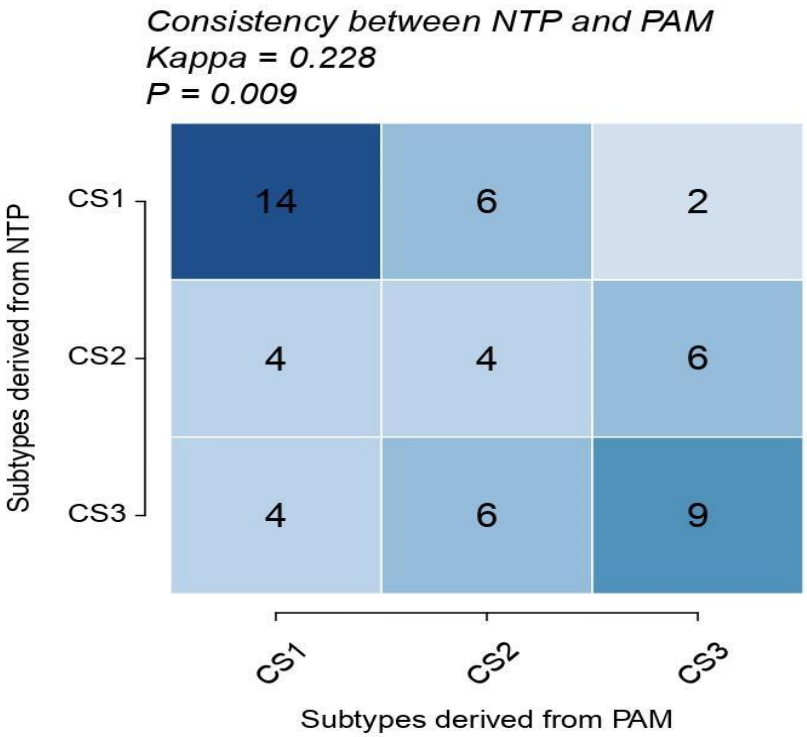


Figure 3.140. Consistency heatmap between NTP and PAM-predicted subtype for edgeR results in GSE17537.

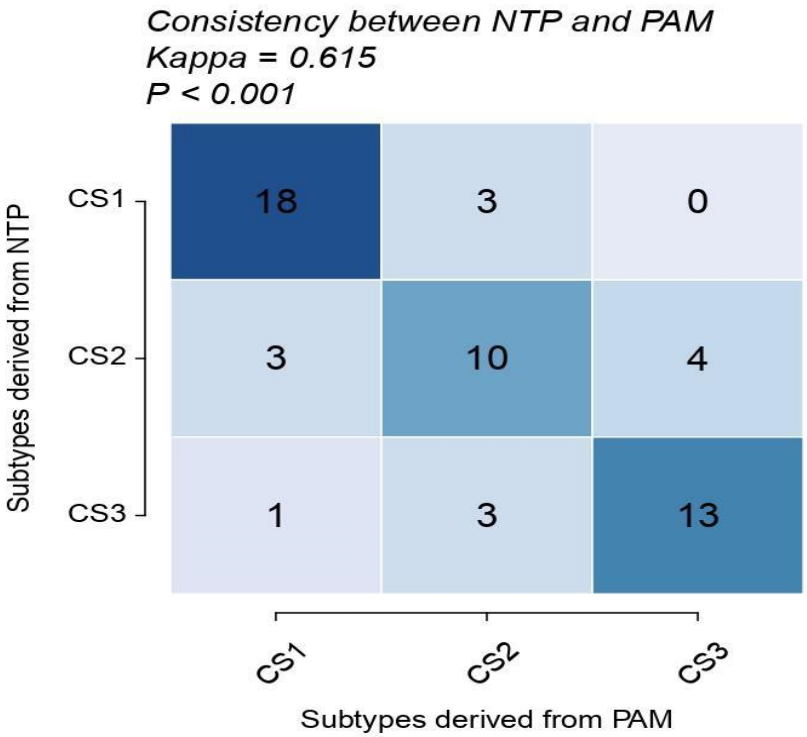


Figure 3.141. Consistency heatmap between NTP and PAM-predicted subtype for limma results in GSE17537.

3.3. Analysis Results for Four Subtypes

3.3.1. The multi-omics classification of COAD

Based on the results of the CPI and gap statistics, the optimal number of clusters was determined as k2 (Figure 3.1). However, the Consensus Molecular Subtypes (CMS) Consortium for colorectal cancer has defined 4 CMS groups, and upon closer inspection of the descriptive figure, it can be seen that both the CPI and gap statistics did not decrease greatly; therefore, four clusters were accepted as the optimal number of clusters. Subsequently, the clustering results were obtained by running each of the 10 clustering algorithms in turn. To improve the robustness of the clustering, the clustering results of the different algorithms were combined based on the idea of consensus ensemble (Figure 3.142). Ultimately, the patients were categorised into four subtypes: CS1, CS2, CS3 and CS4.

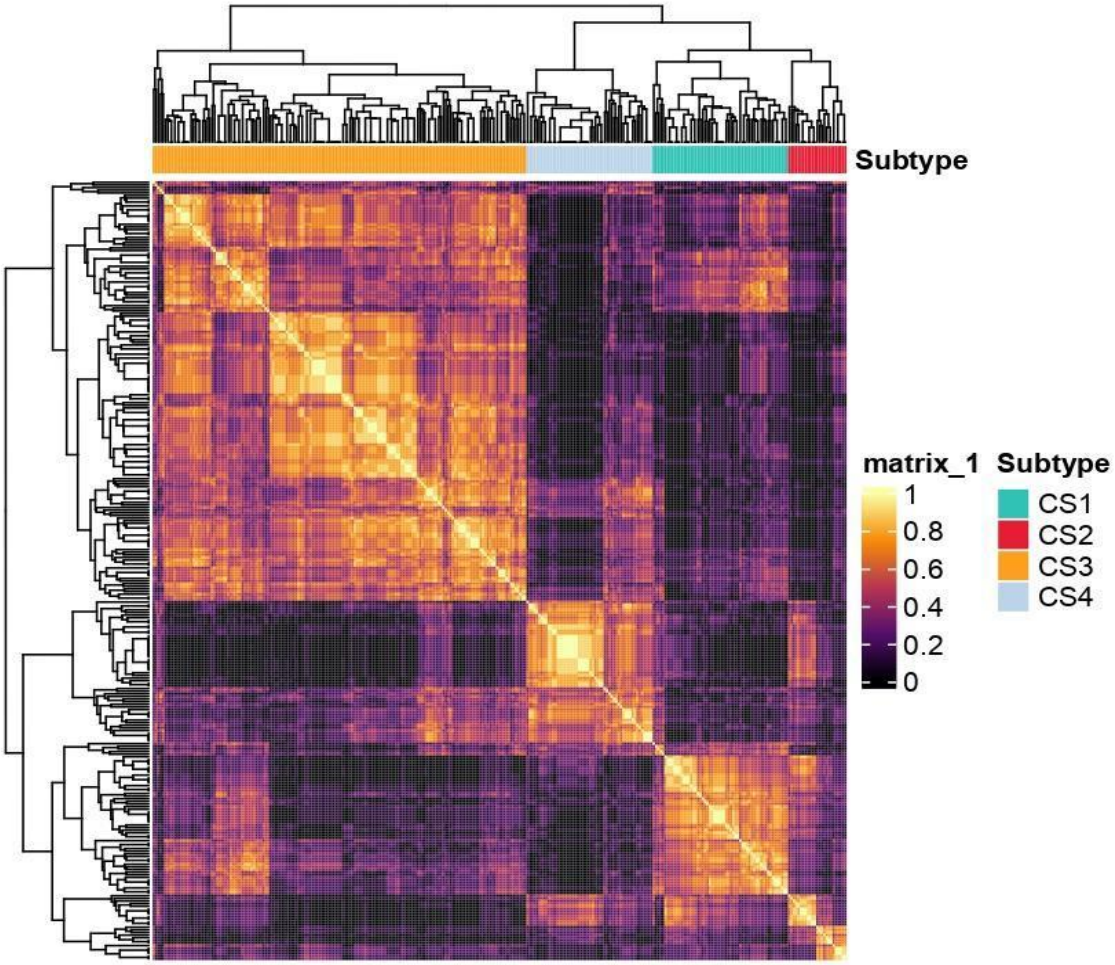


Figure 3.142. Consensus heatmap based on results from 10 multi-omics integrative clustering algorithms with cluster number of 4.

In addition, the similarity of the samples was measured using the silhouette score to verify the clustering result (Figure 3.143). The results showed that these subtypes were well differentiated and distinguishable from each other with silhouette scores of 0.34, 0.53, 0.35 and 0.53, respectively.

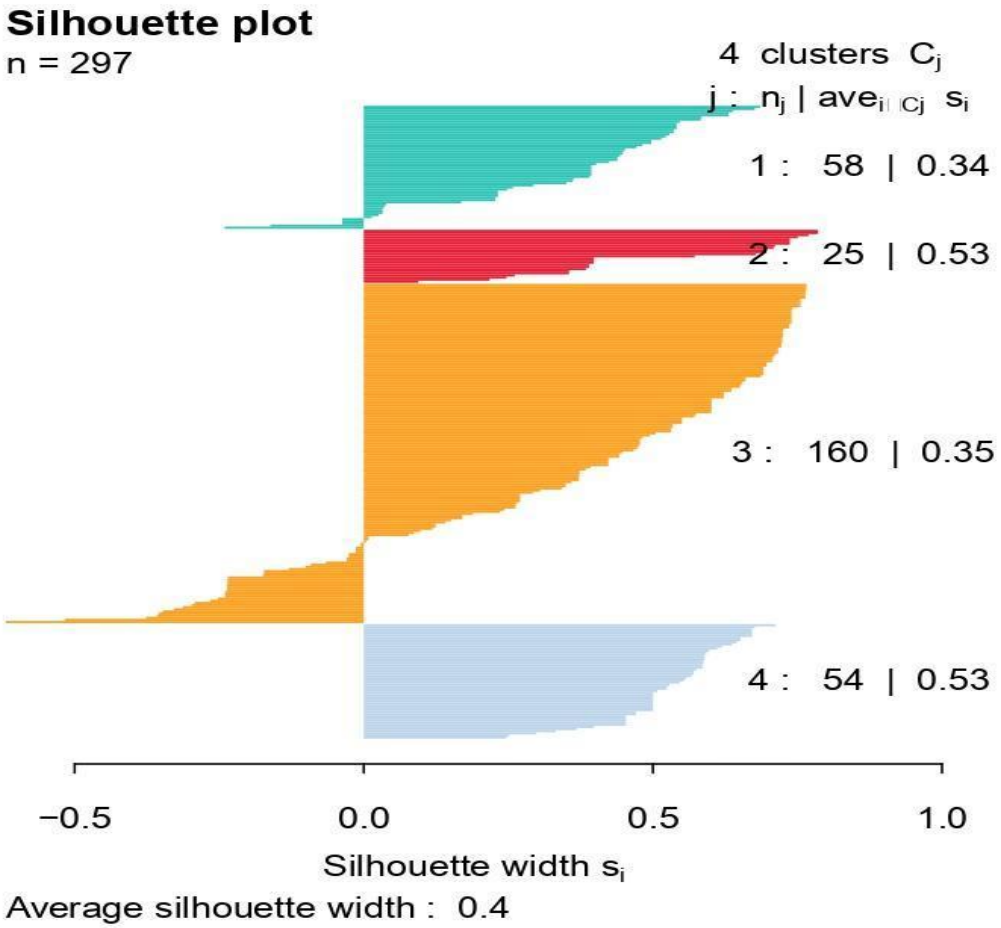


Figure 3.143. Quantification of sample similarity using silhoutte score based on consensus ensembles result.

A genome-wide heatmap was then created based on the mRNA, lncRNA, miRNA, methylation and mutation data, which provides information on how the samples/genes are clustered for each omics level (Figure 3.144). In addition, the top 10 features selected by the iClusterBayes algorithm for each omic data are shown on the right. The selected features may have a specific biological meaning that determines the heterogeneity of cancers. This heatmap includes clinicopathological characteristics such as age, stage, race and gender as well as information on APC mutations. As a result, it can be said that each subtype is clearly differentiated on the basis of the mRNA heatmap. In addition, a relatively pronounced hypermethylated region was observed in subtype CS1. In addition, the CS2 and CS4 subtypes mutated much more strongly than the other two subtypes.

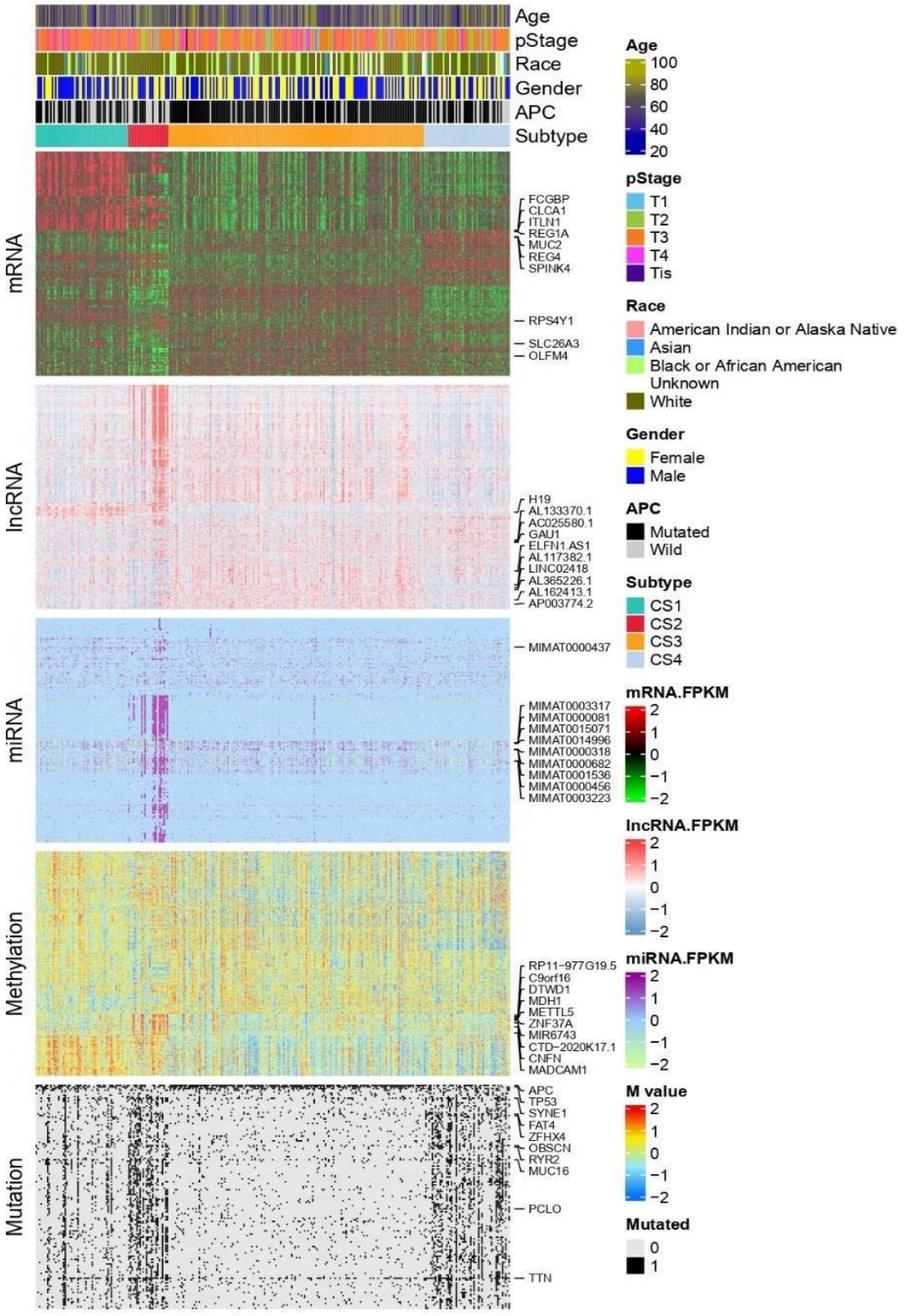


Figure 3.144. Comprehensive heatmap based on consensus across 10 algorithms with clinicopathological and potential drivers' annotation.

3.3.2. Clinical characteristics

The incidence of colon cancer varies according to age [170, 171], ethnicity [172, 173], gender [174-176] or tumour stage [177, 178]. Therefore, the evaluation of clinicopathological characteristics contributes to the development of personalised treatment strategies by providing an accurate understanding of the baseline data of each patient subtype. Moreover, the tumour suppressor gene APC [179], known as the gatekeeper gene of colon cancer [120] and found in 80% of colon tumors [180], plays a very important role in colon cancer screening and early detection studies. For this reason, the clinicopathological characteristics of the four subtypes of COAD, including age, race, pathological stage, gender and APC, were compared (Table 3.39). As a result of this comparison, a statistically significant difference in APC mutations was found between the four subtypes. The APC mutations were significantly higher in CS3 than in the other subtypes ($P < 0.001$). In addition, a significant difference in pathological staging was found between the subtypes. Among the subtypes, patients with pathological stage T3 are the most common, and in particular, three quarters of CS1 patients are in T3 stage. In addition, a survival analysis was performed to compare the clinical prognoses of the COAD subtypes. However, no significant difference was found between the COAD subtypes in terms of clinical prognosis outcomes.

Table 3.39. Clinicopathologic characteristics of COAD participants in the CS1, CS2, CS3 and CS4.

	CS1	**CS2**	**CS3**	**CS4**	**p**	**test**
n	58	25	160	54		
Age (median [IQR])	64.00 [52.75, 75.00]	68.00 [67.00, 74.00]	67.00 [55.00, 75.00]	68.00 [58.50, 75.75]	0.134	nonnorm
APC (%)					<0.001	exact
Mutated	34 (58.6)	11 (44.0)	139 (86.9)	31 (57.4)		
Wild	24 (41.4)	14 (56.0)	21 (13.1)	23 (42.6)		
pStage (%)					0.052	exact
Tis	0 (0.0)	0 (0.0)	1 (0.6)	0 (0.0)		
T1	0 (0.0)	1 (4.0)	4 (2.5)	2 (3.7)		
T2	2 (3.4)	6 (24.0)	23 (14.4)	13 (24.1)		

Table 3.39 (continued). Clinicopathologic characteristics of COAD participants in the CS1, CS2, CS3 and CS4.

T3	44 (75.9)	15 (60.0)	109 (68.1)	35 (64.8)		
T4	12 (20.7)	3 (12.0)	23 (14.4)	4 (7.4)		
Gender (%)					0.421	exact
Female	22 (37.9)	13 (52.0)	77 (48.1)	28 (51.9)		
Male	36 (62.1)	12 (48.0)	83 (51.9)	26 (48.1)		
Race (%)					0.059	exact
American Indian or Alaska Native	1 (1.7)	0 (0.0)	0 (0.0)	0 (0.0)		
Asian	3 (5.2)	0 (0.0)	4 (2.5)	4 (7.4)		
Black or African American	11 (19.0)	1 (4.0)	36 (22.5)	9 (16.7)		
Unknown	1 (1.7)	0 (0.0)	12 (7.5)	5 (9.3)		
White	42 (72.4)	24 (96.0)	108 (67.5)	36 (66.7)		
fustat (%)					0.297	exact
0	41 (70.7)	19 (76.0)	120 (75.0)	46 (85.2)		
1	17 (29.3)	6 (24.0)	40 (25.0)	8 (14.8)		
futime (median [IQR])					0.357	nonnorm
	606.00 [356.75, 1077.00]	824.00 [612.00, 1111.00]	667.50 [383.00, 1270.25]	661.50 [388.00, 1071.75]		

3.3.3. Differentially expressed genes and signaling pathways

To further investigate the characteristics of the subtypes, DEGs between the subtypes were identified using the packages “edgeR”, “DESeq2” and “limma”, which are among the most effective tools for differential expression analysis. Based on the results of edgeR, DESeq2 and limma, upregulated biomarkers with the threshold adjusted P-value < 0.05 and Fold Change > 2 parameters were selected, while downregulated biomarkers with adjusted P-value < 0.05 and fold change < 0.5 filters were determined. Using the edgeR algorithm, 3113, 20137, 878 and 1039 upregulated and 1049, 850, 4360 and 1838 downregulated biomarkers were identified for the subtypes CS1, CS2, CS3 and CS4,

respectively. Tables 3.40-3.47 show the top 20 upregulated and downregulated transcripts identified in the CS1, CS2, CS3 and CS4 subtypes with edgeR and sorted by FC. All other DEGs identified with edgeR during differential expression analysis are listed in Appendix A.7. Activation of the transcription factor AP-2 beta (TFAP2B) contributes to tumour cell development by triggering the expression of vascular endothelial growth factor (VEGF) proteins that induce angiogenesis and was upregulated approximately 48-fold in CS1 [181]. AarF domain-containing protein kinase 1 (ADCK1), which triggers tumour cell growth by activating the β-catenin/TCF pathway, was downregulated in CS2 [182]. The absence of ArfGAP with coiled-coil, ankyrin repeat and PH domains 1 (ACAP1) expressed in lymphocytes is associated with poor immunotherapeutic response [183], and ACAP1 is downregulated in CS3.

Table 3.40. Differentially expressed upregulated transcripts identified in the CS1 subtype using edgeR.

CS1 – Differentially Expressed Up-Regulated Transcripts				
	fc	**log2fc**	**pvalue**	**padj**
KRT14	$1.13x10^{2}$	$6.82x10^{0}$	$3.53x10^{-51}$	$8.15x10^{-48}$
TFAP2B	$9.77x10^{1}$	$6.61x10^{0}$	$5.16x10^{-21}$	$2.39x10^{-19}$
SERPINB13	$5.52x10^{1}$	$5.79x10^{0}$	$9.98x10^{-13}$	$2.40x10^{-11}$
CRCT1	$5.18x10^{1}$	$5.69x10^{0}$	$9.57x10^{-17}$	$3.13x10^{-15}$
SPRR2C	$4.16x10^{1}$	$5.38x10^{0}$	$1.02x10^{-10}$	$2.04x10^{-9}$
UNCX	$4.09x10^{1}$	$5.36x10^{0}$	$1.46x10^{-13}$	$3.74x10^{-12}$
SPRR2E	$4.02x10^{1}$	$5.33x10^{0}$	$5.75x10^{-17}$	$1.92x10^{-15}$
KRTAP4.6	$3.58x10^{1}$	$5.16x10^{0}$	$8.50x10^{-8}$	$1.17x10^{-6}$
KRT78	$3.31x10^{1}$	$5.05x10^{0}$	$4.58x10^{-32}$	$5.71x10^{-30}$
SPRR2B	$2.91x10^{1}$	$4.86x10^{0}$	$4.13x10^{-6}$	$3.97x10^{-5}$
NEUROD4	$2.56x10^{1}$	$4.68x10^{0}$	$7.06x10^{-7}$	$8.17x10^{-6}$
SBK2	$2.53x10^{1}$	$4.66x10^{0}$	$8.30x10^{-24}$	$4.79x10^{-22}$
TFAP2D	$2.50x10^{1}$	$4.65x10^{0}$	$1.06x10^{-5}$	$9.11x10^{-5}$
LEP	$2.41x10^{1}$	$4.59x10^{0}$	$2.78x10^{-41}$	$1.10x10^{-38}$
LHX3	$2.38x10^{1}$	$4.57x10^{0}$	$4.42x10^{-30}$	$4.55x10^{-28}$
HRH3	$2.29x10^{1}$	$4.52x10^{0}$	$2.35x10^{-24}$	$1.45x10^{-22}$
TRARG1	$2.29x10^{1}$	$4.51x10^{0}$	$6.97x10^{-24}$	$4.09x10^{-22}$
LINC00661	$2.28x10^{1}$	$4.51x10^{0}$	$5.48x10^{-11}$	$1.13x10^{-9}$
CNGA3	$2.26x10^{1}$	$4.50x10^{0}$	$7.44x10^{-70}$	$2.13x10^{-65}$
ANXA8	$2.15x10^{1}$	$4.43x10^{0}$	$1.54x10^{-34}$	$2.49x10^{-32}$

Table 3.41. Differentially expressed downregulated transcripts identified in the CS1 subtype using edgeR.

CS1 – Differentially Expressed Down-Regulated Transcripts

	fc	log2fc	pvalue	padj
PNLIP	$2.12x10^{-2}$	$-5.56x10^{0}$	$4.49x10^{-3}$	$1.59x10^{-2}$
ZNF479	$4.86x10^{-2}$	$-4.36x10^{0}$	$8.85x10^{-3}$	$2.78x10^{-2}$
GALP	$5.27x10^{-2}$	$-4.25x10^{0}$	$2.17x10^{-4}$	$1.25x10^{-3}$
CLEC2A	$5.32x10^{-2}$	$-4.23x10^{0}$	$1.27x10^{-3}$	$5.57x10^{-3}$
FAM238B	$7.27x10^{-2}$	$-3.78x10^{0}$	$4.91x10^{-5}$	$3.50x10^{-4}$
AL390961.1	$7.58x10^{-2}$	$-3.72x10^{0}$	$8.27x10^{-4}$	$3.89x10^{-3}$
RN7SL314P	$7.71x10^{-2}$	$-3.70x10^{0}$	$2.03x10^{-3}$	$8.23x10^{-3}$
RN7SL837P	$8.03x10^{-2}$	$-3.64x10^{0}$	$1.66x10^{-2}$	$4.63x10^{-2}$
RN7SL791P	$8.38x10^{-2}$	$-3.58x10^{0}$	$1.21x10^{-3}$	$5.36x10^{-3}$
OR10G4	$8.82x10^{-2}$	$-3.50x10^{0}$	$1.23x10^{-4}$	$7.68x10^{-4}$
RN7SL321P	$9.49x10^{-2}$	$-3.40x10^{0}$	$2.51x10^{-3}$	$9.79x10^{-3}$
RN7SL414P	$9.93x10^{-2}$	$-3.33x10^{0}$	$7.35x10^{-4}$	$3.52x10^{-3}$
AP002963.1	$9.99x10^{-2}$	$-3.32x10^{0}$	$1.44x10^{-2}$	$4.11x10^{-2}$
AC073530.2	$1.01x10^{-1}$	$-3.30x10^{0}$	$1.21x10^{-3}$	$5.35x10^{-3}$
SNORA35B	$1.03x10^{-1}$	$-3.28x10^{0}$	$2.87x10^{-3}$	$1.10x10^{-2}$
AC073176.2	$1.05x10^{-1}$	$-3.25x10^{0}$	$1.74x10^{-2}$	$4.80x10^{-2}$
OR8D4	$1.09x10^{-1}$	$-3.20x10^{0}$	$1.69x10^{-5}$	$1.38x10^{-4}$
RN7SL210P	$1.10x10^{-1}$	$-3.19x10^{0}$	$5.13x10^{-4}$	$2.60x10^{-3}$
RN7SL764P	$1.11x10^{-1}$	$-3.17x10^{0}$	$8.18x10^{-5}$	$5.42x10^{-4}$
RN7SKP217	$1.14x10^{-1}$	$-3.13x10^{0}$	$1.12x10^{-2}$	$3.36x10^{-2}$

Table 3.42. Differentially expressed upregulated transcripts identified in the CS2 subtype using edgeR.

CS2 – Differentially Expressed Up-Regulated Transcripts				
	fc	**log2fc**	**pvalue**	**padj**
RNU1.28P	$9.68x10^{2}$	$9.92x10^{0}$	$1.29x10^{-50}$	$2.92x10^{-49}$
RNY4	$7.74x10^{2}$	$9.60x10^{0}$	$3.10x10^{-40}$	$4.99x10^{-39}$
AL139274.1	$5.82x10^{2}$	$9.18x10^{0}$	$1.21x10^{-107}$	$1.79x10^{-105}$
RNVU1.2	$5.60x10^{2}$	$9.13x10^{0}$	$1.06x10^{-58}$	$3.16x10^{-57}$
FBXO40	$4.55x10^{2}$	$8.83x10^{0}$	$5.89x10^{-129}$	$1.66x10^{-126}$
PAEP	$4.43x10^{2}$	$8.79x10^{0}$	$4.85x10^{-138}$	$1.79x10^{-135}$
AC090220.1	$4.25x10^{2}$	$8.73x10^{0}$	$5.29x10^{-106}$	$7.55x10^{-104}$
RNU1.88P	$4.19x10^{2}$	$8.71x10^{0}$	$7.51x10^{-31}$	$8.76x10^{-30}$
RNU1.19P	$4.10x10^{2}$	$8.68x10^{0}$	$2.99x10^{-57}$	$8.48x10^{-56}$
RNVU1.18	$4.07x10^{2}$	$8.67x10^{0}$	$2.42x10^{-27}$	$2.52x10^{-26}$
RNU1.83P	$4.05x10^{2}$	$8.66x10^{0}$	$2.28x10^{-66}$	$8.95x10^{-65}$
RNU2.59P	$4.05x10^{2}$	$8.66x10^{0}$	$9.39x10^{-34}$	$1.21x10^{-32}$
Y_RNA.241	$3.93x10^{2}$	$8.62x10^{0}$	$2.16x10^{-67}$	$8.71x10^{-66}$
RNU5A.1	$3.93x10^{2}$	$8.62x10^{0}$	$4.46x10^{-37}$	$6.46x10^{-36}$
MTND5P32	$3.88x10^{2}$	$8.60x10^{0}$	$1.85x10^{-62}$	$6.41x10^{-61}$
MTCYBP32	$3.83x10^{2}$	$8.58x10^{0}$	$6.03x10^{-71}$	$2.75x10^{-69}$

Table 3.42 (continued). Differentially expressed upregulated transcripts identified in the CS2 subtype using edgeR.

AC092139.1	$3.60x10^{2}$	$8.49x10^{0}$	$6.37x10^{-91}$	$5.49x10^{-89}$
AL356057.1	$3.45x10^{2}$	$8.43x10^{0}$	$6.28x10^{-53}$	$1.53x10^{-51}$

RN7SKP227	$3.40x10^{2}$	$8.41x10^{0}$	$6.18x10^{-10}$	$2.88x10^{-9}$
AL035693.1	$3.38x10^{2}$	$8.40x10^{0}$	$1.44x10^{-94}$	$1.42x10^{-92}$

Table 3.43. Differentially expressed downregulated transcripts identified in the CS2 subtype using edgeR.

CS2 – Differentially Expressed Down-Regulated Transcripts				
	fc	**log2fc**	**pvalue**	**padj**
PPBP	$4.96x10^{-3}$	$-7.65x10^{0}$	$3.83x10^{-9}$	$1.66x10^{-8}$
AC247036.1	$1.89x10^{-2}$	$-5.73x10^{0}$	$8.69x10^{-3}$	$1.60x10^{-2}$
SPRR2F	$3.15x10^{-2}$	$-4.99x10^{0}$	$1.39x10^{-2}$	$2.46x10^{-2}$
SP9	$3.22x10^{-2}$	$-4.96x10^{0}$	$5.56x10^{-4}$	$1.27x10^{-3}$
LCN15	$4.04x10^{-2}$	$-4.63x10^{0}$	$5.49x10^{-6}$	$1.69x10^{-5}$
IGHA2	$4.12x10^{-2}$	$-4.60x10^{0}$	$1.28x10^{-10}$	$6.28x10^{-10}$
SERPINA11	$4.87x10^{-2}$	$-4.36x10^{0}$	$2.06x10^{-5}$	$5.89x10^{-5}$
MS4A12	$5.23x10^{-2}$	$-4.26x10^{0}$	$5.61x10^{-7}$	$1.95x10^{-6}$
VGLL1	$5.39x10^{-2}$	$-4.21x10^{0}$	$2.09x10^{-5}$	$5.97x10^{-5}$
FABP1	$5.87x10^{-2}$	$-4.09x10^{0}$	$8.51x10^{-13}$	$4.89x10^{-12}$
HPN	$5.92x10^{-2}$	$-4.08x10^{0}$	$1.73x10^{-8}$	$7.09x10^{-8}$
GUCA2A	$6.14x10^{-2}$	$-4.03x10^{0}$	$3.70x10^{-11}$	$1.90x10^{-10}$
PYY	$6.39x10^{-2}$	$-3.97x10^{0}$	$2.85x10^{-8}$	$1.14x10^{-7}$
GUCA2B	$6.77x10^{-2}$	$-3.89x10^{0}$	$1.07x10^{-6}$	$3.63x10^{-6}$
CALCA	$7.52x10^{-2}$	$-3.73x10^{0}$	$5.97x10^{-7}$	$2.07x10^{-6}$
SCNN1B	$7.78x10^{-2}$	$-3.68x10^{0}$	$6.17x10^{-11}$	$3.12x10^{-10}$
AC021146.12	$8.24x10^{-2}$	$-3.60x10^{0}$	$2.57x10^{-2}$	$4.29x10^{-2}$
DEFB1	$8.29x10^{-2}$	$-3.59x10^{0}$	$2.79x10^{-13}$	$1.66x10^{-12}$
REN	$8.37x10^{-2}$	$-3.58x10^{0}$	$9.83x10^{-9}$	$4.12x10^{-8}$
VSIG2	$8.57x10^{-2}$	$-3.55x10^{0}$	$1.94x10^{-9}$	$8.68x10^{-9}$

Table 3.44. Differentially expressed upregulated transcripts identified in the CS3 subtype using edgeR.

CS3 – Differentially Expressed Up-Regulated Transcripts				
	fc	**log2fc**	**pvalue**	**padj**
BX322234.2	$6.48x10^{1}$	$6.02x10^{0}$	$1.40x10^{-10}$	$1.44x10^{-9}$
AC152010.1	$4.63x10^{1}$	$5.53x10^{0}$	$3.15x10^{-4}$	$1.01x10^{-3}$
RN7SL618P	$3.42x10^{1}$	$5.10x10^{0}$	$3.84x10^{-3}$	$9.56x10^{-3}$
SFTPC	$2.92x10^{1}$	$4.87x10^{0}$	$5.86x10^{-9}$	$4.56x10^{-8}$
RNA5SP267	$2.46x10^{1}$	$4.62x10^{0}$	$1.37x10^{-2}$	$2.94x10^{-2}$
RNA5SP211	$2.26x10^{1}$	$4.50x10^{0}$	$1.83x10^{-2}$	$3.77x10^{-2}$
SOHLH1	$2.01x10^{1}$	$4.33x10^{0}$	$1.97x10^{-14}$	$3.86x10^{-13}$
RNA5SP389	$1.86x10^{1}$	$4.22x10^{0}$	$1.86x10^{-2}$	$3.82x10^{-2}$
AC127459.2	$1.84x10^{1}$	$4.20x10^{0}$	$3.72x10^{-8}$	$2.50x10^{-7}$

Table 3.44 (continued). Differentially expressed upregulated transcripts identified in the CS3 subtype using edgeR.

RN7SL149P	$1.73x10^{1}$	$4.11x10^{0}$	$7.91x10^{-3}$	$1.82x10^{-2}$
GALP	$1.46x10^{1}$	$3.87x10^{0}$	$3.90x10^{-5}$	$1.50x10^{-4}$
PNLIP	$1.46x10^{1}$	$3.87x10^{0}$	$2.91x10^{-3}$	$7.46x10^{-3}$

RN7SL762P	$1.38x10^{1}$	$3.79x10^{0}$	$5.92x10^{-11}$	$6.48x10^{-10}$
AC009446.1	$1.34x10^{1}$	$3.75x10^{0}$	$1.92x10^{-4}$	$6.40x10^{-4}$
SLC5A8	$1.30x10^{1}$	$3.70x10^{0}$	$3.05x10^{-10}$	$2.97x10^{-9}$
KRT31	$1.23x10^{1}$	$3.62x10^{0}$	$1.52x10^{-11}$	$1.84x10^{-10}$
PRSS56	$1.15x10^{1}$	$3.52x10^{0}$	$9.14x10^{-10}$	$8.18x10^{-9}$
GTF2IP11	$1.14x10^{1}$	$3.51x10^{0}$	$1.61x10^{-2}$	$3.39x10^{-2}$
MAGEB1	$1.12x10^{1}$	$3.49x10^{0}$	$3.34x10^{-3}$	$8.44x10^{-3}$
BPIFA1	$1.12x10^{1}$	$3.48x10^{0}$	$2.03x10^{-4}$	$6.72x10^{-4}$

Table 3.45. Differentially expressed downregulated transcripts identified in the CS3 subtype using edgeR.

CS3 – Differentially Expressed Down-Regulated Transcripts				
	fc	**log2fc**	**pvalue**	**padj**
CLDN18	$1.63x10^{-2}$	$-5.94x10^{0}$	$2.28x10^{-42}$	$1.09x10^{-38}$
INSL4	$1.71x10^{-2}$	$-5.87x10^{0}$	$1.09x10^{-18}$	$4.36x10^{-17}$
MSMB	$2.81x10^{-2}$	$-5.15x10^{0}$	$3.37x10^{-26}$	$5.35x10^{-24}$
DLGAP1.AS5	$2.85x10^{-2}$	$-5.13x10^{0}$	$5.57x10^{-26}$	$8.48x10^{-24}$
AL136442.1	$3.30x10^{-2}$	$-4.92x10^{0}$	$8.49x10^{-11}$	$9.07x10^{-10}$
TAAR1	$3.65x10^{-2}$	$-4.78x10^{0}$	$3.85x10^{-20}$	$1.93x10^{-18}$
RNU1.29P	$4.21x10^{-2}$	$-4.57x10^{0}$	$2.97x10^{-6}$	$1.42x10^{-5}$
LCE3D	$5.04x10^{-2}$	$-4.31x10^{0}$	$4.92x10^{-6}$	$2.25x10^{-5}$
SPRR2C	$5.18x10^{-2}$	$-4.27x10^{0}$	$1.21x10^{-5}$	$5.13x10^{-5}$
MUC5AC	$5.55x10^{-2}$	$-4.17x10^{0}$	$5.15x10^{-36}$	$4.61x10^{-33}$
LINC01790	$5.71x10^{-2}$	$-4.13x10^{0}$	$6.90x10^{-5}$	$2.52x10^{-4}$
AC013437.1	$5.89x10^{-2}$	$-4.09x10^{0}$	$1.74x10^{-10}$	$1.75x10^{-9}$
PSAPL1	$5.96x10^{-2}$	$-4.07x10^{0}$	$2.09x10^{-18}$	$8.02x10^{-17}$
RNU1.104P	$6.13x10^{-2}$	$-4.03x10^{0}$	$2.50x10^{-6}$	$1.21x10^{-5}$
TFAP2D	$6.36x10^{-2}$	$-3.97x10^{0}$	$9.18x10^{-6}$	$3.99x10^{-5}$
MAGEA1	$6.41x10^{-2}$	$-3.96x10^{0}$	$1.47x10^{-4}$	$5.03x10^{-4}$
MIR548K	$6.44x10^{-2}$	$-3.96x10^{0}$	$1.25x10^{-8}$	$9.13x10^{-8}$
Y_RNA.291	$6.55x10^{-2}$	$-3.93x10^{0}$	$6.90x10^{-5}$	$2.52x10^{-4}$
NEUROD4	$6.56x10^{-2}$	$-3.93x10^{0}$	$5.87x10^{-5}$	$2.18x10^{-4}$
AC093001.1	$6.78x10^{-2}$	$-3.88x10^{0}$	$1.35x10^{-18}$	$5.33x10^{-17}$

Table 3.46. Differentially expressed upregulated transcripts identified in the CS4 subtype using edgeR.

CS4 – Differentially Expressed Up-Regulated Transcripts				
	fc	**log2fc**	**pvalue**	**padj**
GP2	$3.82x10^{1}$	$5.26x10^{0}$	$1.98x10^{-40}$	$5.67x10^{-36}$
MLN	$2.29x10^{1}$	$4.52x10^{0}$	$4.47x10^{-19}$	$1.77x10^{-16}$

Table 3.46 (continued). Differentially expressed upregulated transcripts identified in the CS4 subtype using edgeR.

TTC29	$2.16x10^{1}$	$4.43x10^{0}$	$3.68x10^{-17}$	$8.50x10^{-15}$
COX8C	$1.61x10^{1}$	$4.01x10^{0}$	$8.47x10^{-23}$	$6.83x10^{-20}$
AL136442.1	$1.60x10^{1}$	$4.00x10^{0}$	$8.72x10^{-5}$	$5.94x10^{-4}$
LIPF	$1.59x10^{1}$	$3.99x10^{0}$	$8.58x10^{-13}$	$6.49x10^{-11}$

CIB4	$1.56x10^{1}$	$3.96x10^{0}$	$1.06x10^{-33}$	$1.35x10^{-29}$
ANXA10	$1.56x10^{1}$	$3.96x10^{0}$	$1.18x10^{-21}$	$8.21x10^{-19}$
CYP1A1	$1.46x10^{1}$	$3.87x10^{0}$	$4.98x10^{-16}$	$8.56x10^{-14}$
SEMG2	$1.45x10^{1}$	$3.86x10^{0}$	$7.87x10^{-15}$	$9.90x10^{-13}$
RPS17P1	$1.39x10^{1}$	$3.80x10^{0}$	$1.39x10^{-17}$	$3.61x10^{-15}$
IRGM	$1.38x10^{1}$	$3.78x10^{0}$	$1.18x10^{-33}$	$1.35x10^{-29}$
PRSS2	$1.36x10^{1}$	$3.77x10^{0}$	$4.14x10^{-19}$	$1.65x10^{-16}$
AC126323.1	$1.34x10^{1}$	$3.74x10^{0}$	$8.39x10^{-11}$	$3.62x10^{-9}$
UGT2B4	$1.30x10^{1}$	$3.70x10^{0}$	$2.08x10^{-14}$	$2.35x10^{-12}$
BCAR4	$1.30x10^{1}$	$3.70x10^{0}$	$9.10x10^{-27}$	$2.17x10^{-23}$
FGL1	$1.26x10^{1}$	$3.66x10^{0}$	$1.48x10^{-15}$	$2.21x10^{-13}$
DEFA11P	$1.24x10^{1}$	$3.63x10^{0}$	$3.80x10^{-4}$	$2.05x10^{-3}$
CTSE	$1.17x10^{1}$	$3.55x10^{0}$	$2.19x10^{-32}$	$1.79x10^{-28}$
TM4SF4	$1.13x10^{1}$	$3.49x10^{0}$	$1.50x10^{-27}$	$4.52x10^{-24}$

Table 3.47. Differentially expressed downregulated transcripts identified in the CS4 subtype using edgeR.

CS4 – Differentially Expressed Down-Regulated Transcripts				
	fc	**log2fc**	**pvalue**	**padj**
TMEM132D.AS1	$1.40x10^{-2}$	$-6.16x10^{0}$	$2.45x10^{-6}$	$2.77x10^{-5}$
PTF1A	$2.42x10^{-2}$	$-5.37x10^{0}$	$2.23x10^{-10}$	$8.47x10^{-9}$
CDH9	$2.51x10^{-2}$	$-5.32x10^{0}$	$3.12x10^{-6}$	$3.41x10^{-5}$
AC152010.1	$2.59x10^{-2}$	$-5.27x10^{0}$	$1.25x10^{-2}$	$3.63x10^{-2}$
RN7SL618P	$2.76x10^{-2}$	$-5.18x10^{0}$	$1.30x10^{-2}$	$3.74x10^{-2}$
RNA5.8SP5	$2.98x10^{-2}$	$-5.07x10^{0}$	$1.36x10^{-2}$	$3.88x10^{-2}$
MAGEA10	$3.76x10^{-2}$	$-4.73x10^{0}$	$2.24x10^{-5}$	$1.86x10^{-4}$
CT45A1	$3.84x10^{-2}$	$-4.70x10^{0}$	$1.43x10^{-2}$	$4.05x10^{-2}$
RN7SL783P	$3.96x10^{-2}$	$-4.66x10^{0}$	$6.17x10^{-3}$	$2.05x10^{-2}$
CHRND	$4.05x10^{-2}$	$-4.63x10^{0}$	$5.65x10^{-9}$	$1.43x10^{-7}$
MAGEA4.AS1	$4.14x10^{-2}$	$-4.59x10^{0}$	$2.92x10^{-5}$	$2.33x10^{-4}$
LINC02128	$4.37x10^{-2}$	$-4.52x10^{0}$	$4.18x10^{-14}$	$4.38x10^{-12}$
OR1N2	$4.52x10^{-2}$	$-4.47x10^{0}$	$8.04x10^{-5}$	$5.54x10^{-4}$
RNA5SP225	$4.84x10^{-2}$	$-4.37x10^{0}$	$1.36x10^{-2}$	$3.88x10^{-2}$
EYA1	$5.36x10^{-2}$	$-4.22x10^{0}$	$3.71x10^{-19}$	$1.50x10^{-16}$
MAGEA9B	$5.40x10^{-2}$	$-4.21x10^{0}$	$1.75x10^{-3}$	$7.28x10^{-3}$
LINC01419	$5.67x10^{-2}$	$-4.14x10^{0}$	$1.15x10^{-5}$	$1.05x10^{-4}$
AL589787.2	$5.70x10^{-2}$	$-4.13x10^{0}$	$1.31x10^{-4}$	$8.38x10^{-4}$
AL110505.1	$5.75x10^{-2}$	$-4.12x10^{0}$	$2.25x10^{-6}$	$2.58x10^{-5}$
AC110772.2	$6.01x10^{-2}$	$-4.06x10^{0}$	$1.07x10^{-11}$	$5.87x10^{-10}$

As a result of the differential expression analysis with DESeq2, 2162, 16007, 660 and 752 upregulated and 909, 435, 3490 and 1314 downregulated biomarkers were identified for each subtype. Tables 3.48-3.55 show the 20 most upregulated and downregulated transcripts identified in the CS1, CS2, CS3 and CS4 subtypes with DESeq2, sorted by FC. All other DEGs identified with DESeq2 during differential expression analysis are

listed in Appendix A.8. Low levels of the gene adiponectin (ADIPOQ), an adipokine produced only by adipose tissue, trigger the development of colorectal cancer [184]. The ADIPOQ gene was upregulated in CS1. Melanoma-associated antigen D1 (MAGED1), whose low expression is associated with poor survival [185], was downregulated in CS2. Serine protease 56 (PRSS56) is upregulated approximately 11-fold in CS3, and its activation is associated with tumour cell proliferation and migration in colorectal cancer [186]. Although increased expression of the oncogene Suppressor of Glucose, Autophagy Associated 1 (SOGA1) is associated with metastasis, this gene is downregulated in CS4 [187].

Table 3.48. Differentially expressed upregulated transcripts identified in the CS1 subtype using DESeq2.

CS1 – Differentially Expressed Up-Regulated Transcripts				
	fc	**log2fc**	**pvalue**	**padj**
TRARG1	$2.40x10^{1}$	$4.59x10^{0}$	$3.11x10^{-18}$	$1.33x10^{-16}$
ADIPOQ	$2.10x10^{1}$	$4.39x10^{0}$	$2.21x10^{-9}$	$3.01x10^{-8}$
FABP4	$1.76x10^{1}$	$4.14x10^{0}$	$3.22x10^{-31}$	$7.23x10^{-29}$
LINCADL	$1.58x10^{1}$	$3.98x10^{0}$	$1.12x10^{-4}$	$4.34x10^{-4}$
LEP	$1.58x10^{1}$	$3.98x10^{0}$	$6.27x10^{-27}$	$7.32x10^{-25}$
CIDEA	$1.51x10^{1}$	$3.92x10^{0}$	$2.03x10^{-7}$	$1.75x10^{-6}$
MYOC	$1.44x10^{1}$	$3.84x10^{0}$	$8.70x10^{-19}$	$3.98x10^{-17}$
PLIN4	$1.35x10^{1}$	$3.76x10^{0}$	$2.63x10^{-31}$	$6.08x10^{-29}$
PRG4	$1.27x10^{1}$	$3.66x10^{0}$	$2.43x10^{-57}$	$1.01x10^{-52}$
PLIN1	$1.19x10^{1}$	$3.58x10^{0}$	$6.68x10^{-32}$	$1.69x10^{-29}$
TCF23	$1.12x10^{1}$	$3.48x10^{0}$	$9.38x10^{-28}$	$1.23x10^{-25}$
TCEAL2	$1.08x10^{1}$	$3.44x10^{0}$	$1.52x10^{-23}$	$1.17x10^{-21}$
NGB	$1.08x10^{1}$	$3.44x10^{0}$	$2.07x10^{-17}$	$8.02x10^{-16}$
TCEAL5	$1.08x10^{1}$	$3.43x10^{0}$	$2.31x10^{-28}$	$3.34x10^{-26}$
THSD7B	$1.06x10^{1}$	$3.40x10^{0}$	$1.01x10^{-26}$	$1.14x10^{-24}$
SPOCK3	$1.05x10^{1}$	$3.39x10^{0}$	$7.57x10^{-17}$	$2.75x10^{-15}$
NPTX1	$9.76x10^{0}$	$3.29x10^{0}$	$1.14x10^{-34}$	$5.47x10^{-32}$
SLC7A14	$9.60x10^{0}$	$3.26x10^{0}$	$2.14x10^{-18}$	$9.32x10^{-17}$
PROK1	$9.46x10^{0}$	$3.24x10^{0}$	$1.05x10^{-11}$	$2.09x10^{-10}$

Table 3.48 (continued). Differentially expressed upregulated transcripts identified in the CS1 subtype using DESeq2.

FCER2	$9.31x10^{0}$	$3.22x10^{0}$	$3.68x10^{-23}$	$2.69x10^{-21}$

Table 3.49. Differentially expressed downregulated transcripts identified in the CS1 subtype using DESeq2.

CS1 – Differentially Expressed Down-Regulated Transcripts				
	fc	**log2fc**	**pvalue**	**padj**
MT.TY	$5.09x10^{-2}$	$-4.30x10^{0}$	$8.67x10^{-32}$	$2.17x10^{-29}$

PRDX2P1	$9.22x10^{-2}$	$-3.44x10^{0}$	$9.35x10^{-11}$	$1.63x10^{-9}$
IFITM3P9	$1.07x10^{-1}$	$-3.22x10^{0}$	$9.14x10^{-7}$	$6.54x10^{-6}$
CNN2P4	$1.10x10^{-1}$	$-3.19x10^{0}$	$6.78x10^{-6}$	$3.76x10^{-5}$
LIN28B	$1.11x10^{-1}$	$-3.17x10^{0}$	$1.78x10^{-3}$	$4.90x10^{-3}$
RPL35AP34	$1.29x10^{-1}$	$-2.96x10^{0}$	$7.20x10^{-6}$	$3.96x10^{-5}$
AC009362.1	$1.35x10^{-1}$	$-2.89x10^{0}$	$9.23x10^{-15}$	$2.67x10^{-13}$
AL353662.1	$1.41x10^{-1}$	$-2.82x10^{0}$	$1.42x10^{-19}$	$6.99x10^{-18}$
OR10G4	$1.43x10^{-1}$	$-2.81x10^{0}$	$5.23x10^{-4}$	$1.68x10^{-3}$
AC004884.1	$1.51x10^{-1}$	$-2.73x10^{0}$	$5.41x10^{-11}$	$9.77x10^{-10}$
EIF3IP1	$1.56x10^{-1}$	$-2.68x10^{0}$	$1.40x10^{-6}$	$9.53x10^{-6}$
KRTCAP2P1	$1.58x10^{-1}$	$-2.66x10^{0}$	$2.43x10^{-8}$	$2.64x10^{-7}$
AC098591.3	$1.68x10^{-1}$	$-2.57x10^{0}$	$2.86x10^{-13}$	$7.05x10^{-12}$
RPS5P8	$1.71x10^{-1}$	$-2.55x10^{0}$	$6.37x10^{-9}$	$7.84x10^{-8}$
BOLA2P1	$1.71x10^{-1}$	$-2.55x10^{0}$	$4.60x10^{-4}$	$1.50x10^{-3}$
COX7A2P2	$1.73x10^{-1}$	$-2.53x10^{0}$	$5.79x10^{-8}$	$5.80x10^{-7}$
SELENOWP1	$1.75x10^{-1}$	$-2.52x10^{0}$	$1.99x10^{-5}$	$9.58x10^{-5}$
MTCO2P22	$1.75x10^{-1}$	$-2.52x10^{0}$	$2.23x10^{-16}$	$7.68x10^{-15}$
EIF3KP3	$1.78x10^{-1}$	$-2.49x10^{0}$	$1.01x10^{-2}$	$2.19x10^{-2}$
MIF	$1.78x10^{-1}$	$-2.49x10^{0}$	$3.30x10^{-5}$	$1.50x10^{-4}$

Table 3.50. Differentially expressed upregulated transcripts identified in the CS2 subtype using DESeq2.

CS2 – Differentially Expressed Up-Regulated Transcripts				
	fc	**log2fc**	**pvalue**	**padj**
Y_RNA.713	$1.16x10^{4}$	$1.35x10^{1}$	$2.40x10^{-5}$	$6.29x10^{-5}$
RNU1.46P	$7.33x10^{3}$	$1.28x10^{1}$	$1.80x10^{-5}$	$4.77x10^{-5}$
RNU1.28P	$4.97x10^{3}$	$1.23x10^{1}$	$5.11x10^{-13}$	$2.79x10^{-12}$
Y_RNA.209	$4.46x10^{3}$	$1.21x10^{1}$	$1.76x10^{-4}$	$4.11x10^{-4}$
RNVU1.18	$4.07x10^{3}$	$1.20x10^{1}$	$4.18x10^{-14}$	$2.47x10^{-13}$
RNY4	$2.86x10^{3}$	$1.15x10^{1}$	$1.05x10^{-9}$	$4.31x10^{-9}$
MTND3P12	$2.47x10^{3}$	$1.13x10^{1}$	$1.72x10^{-5}$	$4.59x10^{-5}$
RNU1.19P	$1.68x10^{3}$	$1.07x10^{1}$	$6.02x10^{-13}$	$3.26x10^{-12}$
MTCYBP32	$1.64x10^{3}$	$1.07x10^{1}$	$3.12x10^{-16}$	$2.14x10^{-15}$
RNU1.83P	$1.60x10^{3}$	$1.06x10^{1}$	$8.30x10^{-16}$	$5.51x10^{-15}$
Y_RNA.241	$1.22x10^{3}$	$1.02x10^{1}$	$6.82x10^{-20}$	$5.81x10^{-19}$
RNVU1.2	$1.15x10^{3}$	$1.02x10^{1}$	$3.17x10^{-27}$	$4.02x10^{-26}$

Table 3.50 (continued). Differentially expressed upregulated transcripts identified in the CS2 subtype using DESeq2.

MTND5P32	$1.10x10^{3}$	$1.01x10^{1}$	$1.23x10^{-21}$	$1.16x10^{-20}$
AC066616.2	$1.09x10^{3}$	$1.01x10^{1}$	$6.08x10^{-19}$	$4.91x10^{-18}$
RNU1.42P	$1.03x10^{3}$	$1.00x10^{1}$	$7.40x10^{-7}$	$2.29x10^{-6}$
MTCYBP23	$1.02x10^{3}$	$1.00x10^{1}$	$1.23x10^{-16}$	$8.64x10^{-16}$
AL139274.1	$1.00x10^{3}$	$9.97x10^{0}$	$7.92x10^{-33}$	$1.35x10^{-31}$
FBXO40	$9.69x10^{2}$	$9.92x10^{0}$	$1.51x10^{-62}$	$1.36x10^{-60}$
RNU2.59P	$9.28x10^{2}$	$9.86x10^{0}$	$1.16x10^{-12}$	$6.16x10^{-12}$
H2BC3	$9.21x10^{2}$	$9.85x10^{0}$	$3.03x10^{-54}$	$1.69x10^{-52}$

Table 3.51. Differentially expressed downregulated transcripts identified in the CS2 subtype using DESeq2.

CS2 – Differentially Expressed Down-Regulated Transcripts				
	fc	**log2fc**	**pvalue**	**padj**
NKX2.1	$2.36x10^{-2}$	$-5.41x10^{0}$	$4.52x10^{-8}$	$1.59x10^{-7}$
ZG16	$3.09x10^{-2}$	$-5.02x10^{0}$	$1.43x10^{-17}$	$1.06x10^{-16}$
SOX2	$3.36x10^{-2}$	$-4.90x10^{0}$	$6.18x10^{-14}$	$3.60x10^{-13}$
VGLL1	$3.64x10^{-2}$	$-4.78x10^{0}$	$1.62x10^{-10}$	$7.13x10^{-10}$
LCN15	$3.77x10^{-2}$	$-4.73x10^{0}$	$2.81x10^{-14}$	$1.68x10^{-13}$
IGHA2	$5.14x10^{-2}$	$-4.28x10^{0}$	$2.15x10^{-19}$	$1.79x10^{-18}$
AQP8	$5.86x10^{-2}$	$-4.09x10^{0}$	$7.61x10^{-13}$	$4.09x10^{-12}$
PRDM13	$6.04x10^{-2}$	$-4.05x10^{0}$	$4.39x10^{-10}$	$1.86x10^{-9}$
GUCA2A	$6.58x10^{-2}$	$-3.93x10^{0}$	$1.43x10^{-19}$	$1.20x10^{-18}$
FABP1	$7.09x10^{-2}$	$-3.82x10^{0}$	$3.42x10^{-21}$	$3.13x10^{-20}$
UCN3	$7.34x10^{-2}$	$-3.77x10^{0}$	$2.02x10^{-14}$	$1.22x10^{-13}$
SERPINA11	$7.51x10^{-2}$	$-3.74x10^{0}$	$1.32x10^{-6}$	$3.96x10^{-6}$
GUCA2B	$7.82x10^{-2}$	$-3.68x10^{0}$	$2.86x10^{-10}$	$1.23x10^{-9}$
SP9	$8.94x10^{-2}$	$-3.48x10^{0}$	$3.84x10^{-4}$	$8.56x10^{-4}$
DEFB1	$9.12x10^{-2}$	$-3.46x10^{0}$	$1.51x10^{-20}$	$1.33x10^{-19}$
VSIG2	$9.64x10^{-2}$	$-3.37x10^{0}$	$1.11x10^{-14}$	$6.83x10^{-14}$
CA4	$9.80x10^{-2}$	$-3.35x10^{0}$	$2.68x10^{-9}$	$1.06x10^{-8}$
RPL10P9	$1.01x10^{-1}$	$-3.31x10^{0}$	$3.37x10^{-15}$	$2.15x10^{-14}$
SLC6A19	$1.01x10^{-1}$	$-3.30x10^{0}$	$1.89x10^{-8}$	$6.92x10^{-8}$
DAPL1	$1.06x10^{-1}$	$-3.24x10^{0}$	$2.67x10^{-13}$	$1.49x10^{-12}$

Table 3.52. Differentially expressed upregulated transcripts identified in the CS3 subtype using DESeq2.

CS3 – Differentially Expressed Up-Regulated Transcripts				
	fc	**log2fc**	**pvalue**	**padj**
PRSS56	$2.38x10^{1}$	$4.57x10^{0}$	$4.21x10^{-30}$	$8.34x10^{-28}$
IGF2	$1.32x10^{1}$	$3.73x10^{0}$	$6.50x10^{-27}$	$7.20x10^{-25}$
WIF1	$1.18x10^{1}$	$3.56x10^{0}$	$2.92x10^{-21}$	$1.17x10^{-19}$
LINC02864	$9.57x10^{0}$	$3.26x10^{0}$	$1.95x10^{-12}$	$1.80x10^{-11}$
MAGEA4.AS1	$9.05x10^{0}$	$3.18x10^{0}$	$2.13x10^{-5}$	$6.57x10^{-5}$

Table 3.52 (continued). Differentially expressed upregulated transcripts identified in the CS3 subtype using DESeq2.

NOTUM	$8.00x10^{0}$	$3.00x10^{0}$	$1.67x10^{-27}$	$2.04x10^{-25}$
PTF1A	$7.97x10^{0}$	$3.00x10^{0}$	$2.57x10^{-10}$	$1.72x10^{-9}$
BX510359.5	$6.76x10^{0}$	$2.76x10^{0}$	$1.30x10^{-10}$	$9.05x10^{-10}$
LY6G6D	$6.55x10^{0}$	$2.71x10^{0}$	$1.31x10^{-17}$	$2.81x10^{-16}$
AL356433.1	$6.24x10^{0}$	$2.64x10^{0}$	$2.30x10^{-10}$	$1.55x10^{-9}$
AC114291.1	$6.13x10^{0}$	$2.62x10^{0}$	$5.21x10^{-24}$	$3.39x10^{-22}$
HSPB3	$6.09x10^{0}$	$2.61x10^{0}$	$1.88x10^{-15}$	$2.79x10^{-14}$
AC108865.2	$5.90x10^{0}$	$2.56x10^{0}$	$5.57x10^{-10}$	$3.53x10^{-9}$
TMEM252	$5.88x10^{0}$	$2.55x10^{0}$	$5.93x10^{-22}$	$2.66x10^{-20}$
MAGEA4	$5.60x10^{0}$	$2.49x10^{0}$	$5.01x10^{-4}$	$1.21x10^{-3}$

LY6G6F.LY6G6D	$5.59x10^{0}$	$2.48x10^{0}$	$1.65x10^{-14}$	$2.11x10^{-13}$
CPN1	$5.50x10^{0}$	$2.46x10^{0}$	$1.70x10^{-14}$	$2.18x10^{-13}$
KRT40	$5.49x10^{0}$	$2.46x10^{0}$	$4.55x10^{-14}$	$5.41x10^{-13}$
MAGEA11	$5.45x10^{0}$	$2.45x10^{0}$	$5.87x10^{-6}$	$1.98x10^{-5}$
CTNNA2	$5.43x10^{0}$	$2.44x10^{0}$	$2.22x10^{-16}$	$3.85x10^{-15}$

Table 3.53. Differentially expressed downregulated transcripts identified in the CS3 subtype using DESeq2.

CS3 – Differentially Expressed Down-Regulated Transcripts				
	fc	**log2fc**	**pvalue**	**padj**
RN7SKP227	$1.38x10^{-2}$	$-6.18x10^{0}$	$5.64x10^{-3}$	$1.11x10^{-2}$
AL390318.1	$1.55x10^{-2}$	$-6.01x10^{0}$	$5.76x10^{-5}$	$1.65x10^{-4}$
RN7SKP186	$2.22x10^{-2}$	$-5.49x10^{0}$	$1.17x10^{-2}$	$2.16x10^{-2}$
DLGAP1.AS5	$2.52x10^{-2}$	$-5.31x10^{0}$	$8.04x10^{-39}$	$6.37x10^{-36}$
RNU2.61P	$3.03x10^{-2}$	$-5.04x10^{0}$	$4.65x10^{-3}$	$9.35x10^{-3}$
EDDM3CP	$3.23x10^{-2}$	$-4.95x10^{0}$	$1.12x10^{-3}$	$2.56x10^{-3}$
AC008833.1	$3.25x10^{-2}$	$-4.94x10^{0}$	$4.26x10^{-5}$	$1.25x10^{-4}$
AL589655.1	$3.30x10^{-2}$	$-4.92x10^{0}$	$7.44x10^{-5}$	$2.08x10^{-4}$
RN7SKP48	$3.36x10^{-2}$	$-4.90x10^{0}$	$2.27x10^{-3}$	$4.86x10^{-3}$
ATG10.AS1	$3.70x10^{-2}$	$-4.76x10^{0}$	$7.34x10^{-4}$	$1.72x10^{-3}$
RNU6.522P	$3.93x10^{-2}$	$-4.67x10^{0}$	$1.36x10^{-3}$	$3.03x10^{-3}$
TRPV6	$4.43x10^{-2}$	$-4.50x10^{0}$	$1.45x10^{-59}$	$2.07x10^{-55}$
MIR3140	$4.53x10^{-2}$	$-4.46x10^{0}$	$6.69x10^{-4}$	$1.58x10^{-3}$
RN7SKP189	$4.66x10^{-2}$	$-4.42x10^{0}$	$4.81x10^{-3}$	$9.65x10^{-3}$
RN7SKP133	$4.80x10^{-2}$	$-4.38x10^{0}$	$1.11x10^{-2}$	$2.05x10^{-2}$
Y_RNA.93	$4.83x10^{-2}$	$-4.37x10^{0}$	$2.53x10^{-3}$	$5.37x10^{-3}$
AL158832.1	$4.88x10^{-2}$	$-4.36x10^{0}$	$9.65x10^{-5}$	$2.65x10^{-4}$
AL358333.2	$5.10x10^{-2}$	$-4.29x10^{0}$	$1.16x10^{-4}$	$3.13x10^{-4}$
RN7SKP56	$5.11x10^{-2}$	$-4.29x10^{0}$	$1.20x10^{-4}$	$3.23x10^{-4}$
AL117341.1	$5.17x10^{-2}$	$-4.27x10^{0}$	$3.00x10^{-4}$	$7.57x10^{-4}$

Table 3.54. Differentially expressed upregulated transcripts identified in the CS4 subtype using DESeq2.

CS4 – Differentially Expressed Up-Regulated Transcripts				
	fc	**log2fc**	**pvalue**	**padj**
GP2	$3.78x10^{1}$	$5.24x10^{0}$	$6.05x10^{-29}$	$7.04x10^{-26}$
TTC29	$2.95x10^{1}$	$4.88x10^{0}$	$1.38x10^{-15}$	$8.61x10^{-14}$
TFF2	$1.67x10^{1}$	$4.06x10^{0}$	$1.21x10^{-29}$	$1.55x10^{-26}$
ANXA10	$1.56x10^{1}$	$3.96x10^{0}$	$1.13x10^{-15}$	$7.23x10^{-14}$
SEMG2	$1.42x10^{1}$	$3.82x10^{0}$	$3.52x10^{-10}$	$6.46x10^{-9}$
FGL1	$1.34x10^{1}$	$3.74x10^{0}$	$1.13x10^{-11}$	$3.00x10^{-10}$
GUSBP7	$1.21x10^{1}$	$3.59x10^{0}$	$3.63x10^{-7}$	$3.02x10^{-6}$
TM4SF4	$1.17x10^{1}$	$3.55x10^{0}$	$6.14x10^{-21}$	$1.25x10^{-18}$
CTSE	$1.15x10^{1}$	$3.53x10^{0}$	$3.32x10^{-23}$	$1.14x10^{-20}$
IGFALS	$1.10x10^{1}$	$3.46x10^{0}$	$2.47x10^{-23}$	$8.79x10^{-21}$

MUC5AC	$1.03x10^{1}$	$3.36x10^{0}$	$2.16x10^{-16}$	$1.60x10^{-14}$
RBP3	$1.00x10^{1}$	$3.32x10^{0}$	$1.15x10^{-18}$	$1.48x10^{-16}$
LINC02620	$9.39x10^{0}$	$3.23x10^{0}$	$4.64x10^{-4}$	$1.50x10^{-3}$
REG4	$8.69x10^{0}$	$3.12x10^{0}$	$3.72x10^{-16}$	$2.64x10^{-14}$
REG1A	$8.35x10^{0}$	$3.06x10^{0}$	$1.93x10^{-11}$	$4.82x10^{-10}$
MUC6	$8.26x10^{0}$	$3.05x10^{0}$	$3.42x10^{-10}$	$6.31x10^{-9}$
NKX2.2	$8.17x10^{0}$	$3.03x10^{0}$	$6.94x10^{-12}$	$1.94x10^{-10}$
PRSS2	$7.89x10^{0}$	$2.98x10^{0}$	$1.83x10^{-10}$	$3.59x10^{-9}$
AC021534.1	$7.81x10^{0}$	$2.97x10^{0}$	$1.18x10^{-7}$	$1.12x10^{-6}$
SPRR1A	$7.81x10^{0}$	$2.97x10^{0}$	$8.44x10^{-8}$	$8.31x10^{-7}$

Table 3.55. Differentially expressed downregulated transcripts identified in the CS4 subtype using DESeq2.

CS4 – Differentially Expressed Down-Regulated Transcripts				
	fc	**log2fc**	**pvalue**	**padj**
SHISA9	$1.48x10^{-2}$	$-6.08x10^{0}$	$1.87x10^{-40}$	$1.79x10^{-36}$
LINC02128	$3.57x10^{-2}$	$-4.81x10^{0}$	$9.23x10^{-22}$	$2.31x10^{-19}$
U91319.1	$3.68x10^{-2}$	$-4.76x10^{0}$	$5.26x10^{-14}$	$2.32x10^{-12}$
TMEM132D.AS1	$3.75x10^{-2}$	$-4.74x10^{0}$	$3.17x10^{-8}$	$3.54x10^{-7}$
LINC00491	$5.32x10^{-2}$	$-4.23x10^{0}$	$5.49x10^{-6}$	$3.25x10^{-5}$
AC110772.2	$6.16x10^{-2}$	$-4.02x10^{0}$	$1.04x10^{-18}$	$1.35x10^{-16}$
EYA1	$6.27x10^{-2}$	$-4.00x10^{0}$	$4.34x10^{-31}$	$6.93x10^{-28}$
PWWP3B	$6.42x10^{-2}$	$-3.96x10^{0}$	$1.09x10^{-25}$	$6.31x10^{-23}$
KRT35	$6.58x10^{-2}$	$-3.92x10^{0}$	$1.51x10^{-9}$	$2.37x10^{-8}$
TUBAP13	$6.64x10^{-2}$	$-3.91x10^{0}$	$1.44x10^{-19}$	$2.26x10^{-17}$
AL589787.2	$6.70x10^{-2}$	$-3.90x10^{0}$	$2.61x10^{-7}$	$2.27x10^{-6}$
MAGEA4.AS1	$6.81x10^{-2}$	$-3.88x10^{0}$	$1.43x10^{-4}$	$5.46x10^{-4}$
AC016044.1	$6.84x10^{-2}$	$-3.87x10^{0}$	$3.11x10^{-7}$	$2.63x10^{-6}$
GABRA3	$6.87x10^{-2}$	$-3.86x10^{0}$	$1.54x10^{-15}$	$9.48x10^{-14}$
AC090809.1	$7.06x10^{-2}$	$-3.82x10^{0}$	$1.58x10^{-8}$	$1.89x10^{-7}$
AL035252.2	$7.09x10^{-2}$	$-3.82x10^{0}$	$1.77x10^{-14}$	$8.59x10^{-13}$

Table 3.55 (continued). Differentially expressed downregulated transcripts identified in the CS4 subtype using DESeq2.

CDH9	$7.24x10^{-2}$	$-3.79x10^{0}$	$8.82x10^{-5}$	$3.60x10^{-4}$
AC012501.2	$7.46x10^{-2}$	$-3.74x10^{0}$	$5.31x10^{-13}$	$1.87x10^{-11}$
ZNF663P	$7.52x10^{-2}$	$-3.73x10^{0}$	$4.09x10^{-11}$	$9.40x10^{-10}$
AC090578.1	$7.57x10^{-2}$	$-3.72x10^{0}$	$7.57x10^{-17}$	$6.31x10^{-15}$

Finally, using the Limma algorithm, 985, 4509, 167 and 153 upregulated and 6, 1183, 276 and 105 downregulated biomarkers were identified for the subtypes CS1, CS2, CS3 and CS4, respectively. Tables 3.56-3.63 show the 20 most upregulated and downregulated transcripts identified in the CS1, CS2, CS3 and CS4 subtypes using Limma and sorted by FC. All other DEGs identified in the differential expression analysis using Limma are listed in Appendix A.9. Overexpression of secreted frizzled-related

protein 2 (SFRP2), which is upregulated more than 6-fold in CS1, exhibits anti-tumour properties by inhibiting the activation of Wnt signalling, leading to suppression of cell proliferation and promotion of apoptosis in colon cancer [164, 188]. In addition, previous studies have reported that the expression of fatty acid-binding protein 1 (FABP1) is reduced in microsatellite unstable colorectal carcinomas characterised by a strong immune response [189-192]. Therefore, the significant decrease in FABP1 expression in CS2 provides important evidence that this subtype may be an immune subtype. Notum, the palmitoleoyl-protein carboxylesterase (NOTUM), which is significantly upregulated in CS3, promotes tumour proliferation and progression by influencing the p38 and c-JUN N-terminal kinase (JNK) signalling pathways [193]. In addition, regenerating islet-derived 4 (REG4), which supports colon cancer progression through Akt/GSK-3β/β-catenin/TCF-4 [194] and affects many important cancer hallmarks such as cell proliferation, apoptosis and metastasis, is associated with poor prognosis but is also resistant to 5-FU-based chemotherapy [102], which is commonly used in the treatment of colon cancer. The expression of REG4 was downregulated in CS3 and increased almost 16-fold in CS4.

Table 3.56. Differentially expressed upregulated transcripts identified in the CS1 subtype using limma.

CS1 – Differentially Expressed Up-Regulated Transcripts				
	fc	**log2fc**	**pvalue**	**padj**
SFRP2	$1.36x10^{1}$	$3.77x10^{0}$	$2.51x10^{-24}$	$2.22x10^{-22}$

Table 3.56 (continued). Differentially expressed upregulated transcripts identified in the CS1 subtype using limma.

COMP	$8.15x10^{0}$	$3.03x10^{0}$	$5.55x10^{-23}$	$4.11x10^{-21}$
CCL21	$7.91x10^{0}$	$2.98x10^{0}$	$6.45x10^{-24}$	$5.37x10^{-22}$
SFRP4	$7.61x10^{0}$	$2.93x10^{0}$	$4.04x10^{-21}$	$2.42x10^{-19}$
DES	$7.40x10^{0}$	$2.89x10^{0}$	$1.95x10^{-13}$	$5.41x10^{-12}$
IGHG1	$6.99x10^{0}$	$2.80x10^{0}$	$1.98x10^{-13}$	$5.47x10^{-12}$
PRELP	$6.87x10^{0}$	$2.78x10^{0}$	$2.74x10^{-34}$	$2.66x10^{-31}$
C3	$6.81x10^{0}$	$2.77x10^{0}$	$1.60x10^{-27}$	$2.42x10^{-25}$
FNDC1	$6.79x10^{0}$	$2.76x10^{0}$	$5.77x10^{-31}$	$1.83x10^{-28}$
CCL19	$6.75x10^{0}$	$2.76x10^{0}$	$7.77x10^{-28}$	$1.27x10^{-25}$
IGLV3.25	$6.73x10^{0}$	$2.75x10^{0}$	$8.03x10^{-13}$	$2.11x10^{-11}$
IGHV4.39	$6.68x10^{0}$	$2.74x10^{0}$	$2.98x10^{-12}$	$7.39x10^{-11}$
IGHG4	$6.68x10^{0}$	$2.74x10^{0}$	$3.84x10^{-13}$	$1.04x10^{-11}$
IGHV5.51	$6.64x10^{0}$	$2.73x10^{0}$	$4.61x10^{-12}$	$1.12x10^{-10}$
IGLV1.40	$6.39x10^{0}$	$2.68x10^{0}$	$6.66x10^{-12}$	$1.59x10^{-10}$
IGHV4.34	$6.32x10^{0}$	$2.66x10^{0}$	$1.92x10^{-14}$	$5.89x10^{-13}$

THBS2	$6.30x10^{0}$	$2.65x10^{0}$	$1.33x10^{-22}$	$9.34x10^{-21}$
IGHV3.15	$6.28x10^{0}$	$2.65x10^{0}$	$7.30x10^{-12}$	$1.73x10^{-10}$
IGLV6.57	$6.24x10^{0}$	$2.64x10^{0}$	$2.01x10^{-12}$	$5.09x10^{-11}$
IGLV3.21	$6.21x10^{0}$	$2.63x10^{0}$	$9.36x10^{-12}$	$2.19x10^{-10}$

Table 3.57. Differentially expressed downregulated transcripts identified in the CS1 subtype using limma.

CS1 – Differentially Expressed Down-Regulated Transcripts				
	fc	**log2fc**	**pvalue**	**padj**
MT.TY	$4.12x10^{-1}$	$-1.28x10^{0}$	$2.59x10^{-4}$	$2.44x10^{-3}$
STYXL2	$4.27x10^{-1}$	$-1.23x10^{0}$	$3.60x10^{-3}$	$2.48x10^{-2}$
SNHG25	$4.43x10^{-1}$	$-1.17x10^{0}$	$3.47x10^{-6}$	$4.45x10^{-5}$
MT.TC	$4.62x10^{-1}$	$-1.11x10^{0}$	$7.32x10^{-4}$	$6.22x10^{-3}$
MT.TL1	$4.93x10^{-1}$	$-1.02x10^{0}$	$1.02x10^{-4}$	$1.05x10^{-3}$
RNU4.1	$4.96x10^{-1}$	$-1.01x10^{0}$	$5.44x10^{-3}$	$3.50x10^{-2}$

Table 3.58. Differentially expressed upregulated transcripts identified in the CS2 subtype using limma.

CS2 – Differentially Expressed Up-Regulated Transcripts				
	fc	**log2fc**	**pvalue**	**padj**
RNU4.2	$4.52x10^{1}$	$5.50x10^{0}$	$4.21x10^{-24}$	$5.73x10^{-23}$
RNU4.1	$3.33x10^{1}$	$5.06x10^{0}$	$2.79x10^{-26}$	$4.61x10^{-25}$
RNY1	$3.33x10^{1}$	$5.06x10^{0}$	$6.95x10^{-27}$	$1.22x10^{-25}$
MIR3609	$2.94x10^{1}$	$4.88x10^{0}$	$2.98x10^{-35}$	$1.67x10^{-33}$
RNU5B.1	$2.94x10^{1}$	$4.88x10^{0}$	$8.62x10^{-29}$	$1.84x10^{-27}$
SNORA73B	$2.87x10^{1}$	$4.85x10^{0}$	$2.70x10^{-32}$	$8.87x10^{-31}$
SCARNA7	$2.79x10^{1}$	$4.80x10^{0}$	$2.10x10^{-35}$	$1.22x10^{-33}$
RNU5A.1	$2.66x10^{1}$	$4.73x10^{0}$	$4.50x10^{-26}$	$7.31x10^{-25}$

Table 3.58 (continued). Differentially expressed upregulated transcripts identified in the CS2 subtype using limma.

SCARNA5	$2.55x10^{1}$	$4.67x10^{0}$	$3.36x10^{-31}$	$9.59x10^{-30}$
RN7SL3	$2.07x10^{1}$	$4.37x10^{0}$	$2.65x10^{-30}$	$6.73x10^{-29}$
SNORA23	$1.89x10^{1}$	$4.24x10^{0}$	$3.47x10^{-32}$	$1.13x10^{-30}$
SNORA74A	$1.83x10^{1}$	$4.19x10^{0}$	$3.81x10^{-34}$	$1.70x10^{-32}$
SNORA12	$1.68x10^{1}$	$4.07x10^{0}$	$4.19x10^{-32}$	$1.35x10^{-30}$
H4C3	$1.64x10^{1}$	$4.04x10^{0}$	$2.47x10^{-35}$	$1.41x10^{-33}$
SNORD13	$1.63x10^{1}$	$4.03x10^{0}$	$3.98x10^{-21}$	$4.29x10^{-20}$
SNORA53	$1.61x10^{1}$	$4.01x10^{0}$	$2.12x10^{-33}$	$8.27x10^{-32}$
SNORA49	$1.51x10^{1}$	$3.91x10^{0}$	$7.15x10^{-32}$	$2.23x10^{-30}$
SCARNA21	$1.50x10^{1}$	$3.91x10^{0}$	$8.37x10^{-33}$	$2.98x10^{-31}$
RNU1.88P	$1.49x10^{1}$	$3.90x10^{0}$	$1.80x10^{-36}$	$1.36x10^{-34}$
SNORA79B	$1.46x10^{1}$	$3.87x10^{0}$	$1.34x10^{-28}$	$2.79x10^{-27}$

Table 3.59. Differentially expressed downregulated transcripts identified in the CS2 subtype using limma.

CS2 – Differentially Expressed Down-Regulated Transcripts

	fc	log2fc	pvalue	padj
FABP1	$1.02x10^{-1}$	$-3.29x10^{0}$	$1.05x10^{-8}$	$3.95x10^{-8}$
DEFA6	$1.22x10^{-1}$	$-3.03x10^{0}$	$3.52x10^{-6}$	$9.90x10^{-6}$
HMGCS2	$1.33x10^{-1}$	$-2.91x10^{0}$	$3.42x10^{-8}$	$1.21x10^{-7}$
CLCA1	$1.41x10^{-1}$	$-2.83x10^{0}$	$9.37x10^{-5}$	$2.20x10^{-4}$
CLDN3	$1.43x10^{-1}$	$-2.81x10^{0}$	$1.19x10^{-27}$	$2.24x10^{-26}$
AC090498.1	$1.45x10^{-1}$	$-2.79x10^{0}$	$1.94x10^{-17}$	$1.55x10^{-16}$
RPL41P1	$1.45x10^{-1}$	$-2.79x10^{0}$	$1.77x10^{-5}$	$4.55x10^{-5}$
IGHA2	$1.49x10^{-1}$	$-2.75x10^{0}$	$2.38x10^{-5}$	$6.05x10^{-5}$
OLFM4	$1.58x10^{-1}$	$-2.66x10^{0}$	$4.82x10^{-4}$	$1.03x10^{-3}$
GUCA2A	$1.59x10^{-1}$	$-2.65x10^{0}$	$1.07x10^{-8}$	$4.01x10^{-8}$
MEP1A	$1.66x10^{-1}$	$-2.59x10^{0}$	$3.33x10^{-10}$	$1.45x10^{-9}$
CKB	$1.66x10^{-1}$	$-2.59x10^{0}$	$5.00x10^{-10}$	$2.14x10^{-9}$
DEFA5	$1.72x10^{-1}$	$-2.54x10^{0}$	$3.16x10^{-4}$	$6.91x10^{-4}$
SCAND1	$1.73x10^{-1}$	$-2.53x10^{0}$	$1.90x10^{-28}$	$3.88x10^{-27}$
DEFB1	$1.82x10^{-1}$	$-2.46x10^{0}$	$5.35x10^{-12}$	$2.74x10^{-11}$
WFDC2	$1.86x10^{-1}$	$-2.43x10^{0}$	$1.75x10^{-8}$	$6.40x10^{-8}$
PPDPF	$1.90x10^{-1}$	$-2.40x10^{0}$	$2.27x10^{-31}$	$6.66x10^{-30}$
IGFBP2	$1.92x10^{-1}$	$-2.38x10^{0}$	$2.54x10^{-9}$	$1.02x10^{-8}$
C4orf48	$1.94x10^{-1}$	$-2.37x10^{0}$	$2.08x10^{-20}$	$2.12x10^{-19}$
TFF3	$1.96x10^{-1}$	$-2.35x10^{0}$	$1.04x10^{-11}$	$5.20x10^{-11}$

Table 3.60. Differentially expressed upregulated transcripts identified in the CS3 subtype using limma.

CS3 – Differentially Expressed Up-Regulated Transcripts				
	fc	**log2fc**	**pvalue**	**padj**
TNNC2	$6.22x10^{0}$	$2.64x10^{0}$	$1.07x10^{-29}$	$1.23x10^{-25}$

Table 3.60 (continued). Differentially expressed upregulated transcripts identified in the CS3 subtype using limma.

AP003774.2	$6.20x10^{0}$	$2.63x10^{0}$	$5.27x10^{-33}$	$1.51x10^{-28}$
CEL	$5.84x10^{0}$	$2.55x10^{0}$	$7.04x10^{-19}$	$1.93x10^{-16}$
C10orf99	$5.83x10^{0}$	$2.54x10^{0}$	$5.32x10^{-19}$	$1.51x10^{-16}$
NOTUM	$5.10x10^{0}$	$2.35x10^{0}$	$1.18x10^{-15}$	$1.26x10^{-13}$
QPRT	$4.80x10^{0}$	$2.26x10^{0}$	$9.49x10^{-29}$	$7.76x10^{-25}$
ASCL2	$4.54x10^{0}$	$2.18x10^{0}$	$2.02x10^{-28}$	$1.28x10^{-24}$
GNG4	$4.44x10^{0}$	$2.15x10^{0}$	$1.45x10^{-18}$	$3.51x10^{-16}$
KRT23	$4.32x10^{0}$	$2.11x10^{0}$	$3.67x10^{-14}$	$2.70x10^{-12}$
CDHR1	$4.11x10^{0}$	$2.04x10^{0}$	$5.32x10^{-19}$	$1.51x10^{-16}$
DPEP1	$3.99x10^{0}$	$2.00x10^{0}$	$1.17x10^{-13}$	$7.66x10^{-12}$
TDGF1	$3.64x10^{0}$	$1.86x10^{0}$	$3.99x10^{-24}$	$5.44x10^{-21}$
CYP2B6	$3.61x10^{0}$	$1.85x10^{0}$	$3.78x10^{-21}$	$2.10x10^{-18}$
SLC39A5	$3.59x10^{0}$	$1.84x10^{0}$	$6.10x10^{-21}$	$3.23x10^{-18}$
CYP2W1	$3.54x10^{0}$	$1.83x10^{0}$	$3.61x10^{-11}$	$1.33x10^{-9}$
SLC26A3	$3.45x10^{0}$	$1.79x10^{0}$	$1.26x10^{-7}$	$1.97x10^{-6}$
ENPP3	$3.44x10^{0}$	$1.78x10^{0}$	$1.42x10^{-16}$	$2.02x10^{-14}$
RUBCNL	$3.40x10^{0}$	$1.77x10^{0}$	$1.55x10^{-25}$	$3.45x10^{-22}$

CELP	$3.40x10^{0}$	$1.76x10^{0}$	$3.37x10^{-27}$	$1.55x10^{-23}$
FABP1	$3.24x10^{0}$	$1.70x10^{0}$	$1.32x10^{-7}$	$2.06x10^{-6}$

Table 3.61. Differentially expressed downregulated transcripts identified in the CS3 subtype using limma.

CS3 – Differentially Expressed Down-Regulated Transcripts				
	fc	**log2fc**	**pvalue**	**padj**
REG4	$1.42x10^{-1}$	$-2.82x10^{0}$	$4.59x10^{-12}$	$2.07x10^{-10}$
CTSE	$1.71x10^{-1}$	$-2.55x10^{0}$	$3.82x10^{-17}$	$6.26x10^{-15}$
PLA2G2A	$2.03x10^{-1}$	$-2.30x10^{0}$	$8.31x10^{-13}$	$4.44x10^{-11}$
CCL18	$2.31x10^{-1}$	$-2.11x10^{0}$	$1.29x10^{-17}$	$2.44x10^{-15}$
DUSP4	$2.51x10^{-1}$	$-1.99x10^{0}$	$3.79x10^{-27}$	$1.55x10^{-23}$
RAMP1	$2.61x10^{-1}$	$-1.94x10^{0}$	$4.48x10^{-17}$	$7.18x10^{-15}$
LYZ	$2.63x10^{-1}$	$-1.93x10^{0}$	$3.23x10^{-15}$	$3.10x10^{-13}$
CLDN18	$2.64x10^{-1}$	$-1.92x10^{0}$	$6.62x10^{-14}$	$4.57x10^{-12}$
CXCL13	$2.69x10^{-1}$	$-1.89x10^{0}$	$1.02x10^{-21}$	$6.74x10^{-19}$
SPP1	$2.70x10^{-1}$	$-1.89x10^{0}$	$5.30x10^{-12}$	$2.37x10^{-10}$
TCN1	$2.86x10^{-1}$	$-1.81x10^{0}$	$3.69x10^{-10}$	$1.06x10^{-8}$
REG1A	$2.88x10^{-1}$	$-1.80x10^{0}$	$5.74x10^{-5}$	$4.41x10^{-4}$
CXCL9	$2.97x10^{-1}$	$-1.75x10^{0}$	$6.30x10^{-16}$	$7.32x10^{-14}$
TFF2	$3.02x10^{-1}$	$-1.73x10^{0}$	$2.80x10^{-10}$	$8.29x10^{-9}$
VNN1	$3.17x10^{-1}$	$-1.66x10^{0}$	$5.14x10^{-19}$	$1.47x10^{-16}$
GJB5	$3.21x10^{-1}$	$-1.64x10^{0}$	$1.53x10^{-13}$	$9.72x10^{-12}$
SPON1	$3.21x10^{-1}$	$-1.64x10^{0}$	$5.02x10^{-20}$	$1.99x10^{-17}$
MUC5AC	$3.21x10^{-1}$	$-1.64x10^{0}$	$4.28x10^{-13}$	$2.43x10^{-11}$
CXCL10	$3.21x10^{-1}$	$-1.64x10^{0}$	$3.08x10^{-15}$	$2.98x10^{-13}$

Table 3.61 (continued). Differentially expressed downregulated transcripts identified in the CS3 subtype using limma.

FCGR3A	$3.25x10^{-1}$	$-1.62x10^{0}$	$3.03x10^{-18}$	$6.78x10^{-16}$

Table 3.62. Differentially expressed upregulated transcripts identified in the CS4 subtype using limma.

CS4 – Differentially Expressed Up-Regulated Transcripts				
	fc	**log2fc**	**pvalue**	**padj**
REG4	$3.33x10^{1}$	$5.06x10^{0}$	$1.14x10^{-23}$	$1.31x10^{-19}$
CTSE	$1.86x10^{1}$	$4.22x10^{0}$	$1.52x10^{-29}$	$8.70x10^{-25}$
SPINK4	$9.99x10^{0}$	$3.32x10^{0}$	$1.29x10^{-11}$	$1.93x10^{-9}$
REG1A	$8.86x10^{0}$	$3.15x10^{0}$	$3.48x10^{-8}$	$1.56x10^{-6}$
TFF1	$7.73x10^{0}$	$2.95x10^{0}$	$8.67x10^{-17}$	$6.88x10^{-14}$
MUC2	$7.56x10^{0}$	$2.92x10^{0}$	$5.23x10^{-11}$	$6.38x10^{-9}$
TFF2	$7.11x10^{0}$	$2.83x10^{0}$	$2.84x10^{-16}$	$1.91x10^{-13}$
TCN1	$6.69x10^{0}$	$2.74x10^{0}$	$9.17x10^{-14}$	$2.78x10^{-11}$
SPDEF	$6.01x10^{0}$	$2.59x10^{0}$	$1.79x10^{-18}$	$2.85x10^{-15}$
MUC5AC	$5.87x10^{0}$	$2.55x10^{0}$	$3.78x10^{-19}$	$7.47x10^{-16}$
FCGBP	$5.74x10^{0}$	$2.52x10^{0}$	$3.04x10^{-10}$	$2.87x10^{-8}$
REG3A	$5.11x10^{0}$	$2.35x10^{0}$	$6.43x10^{-7}$	$1.78x10^{-5}$

AGR3	$4.81x10^{0}$	$2.27x10^{0}$	$1.33x10^{-14}$	$5.28x10^{-12}$
GJB5	$4.54x10^{0}$	$2.18x10^{0}$	$2.42x10^{-14}$	$8.86x10^{-12}$
AGR2	$4.41x10^{0}$	$2.14x10^{0}$	$2.47x10^{-27}$	$7.06x10^{-23}$
CREB3L1	$4.34x10^{0}$	$2.12x10^{0}$	$9.67x10^{-20}$	$2.64x10^{-16}$
REG1B	$4.23x10^{0}$	$2.08x10^{0}$	$1.56x10^{-6}$	$3.71x10^{-5}$
CA9	$4.22x10^{0}$	$2.08x10^{0}$	$4.54x10^{-9}$	$2.80x10^{-7}$
MUC5B	$4.16x10^{0}$	$2.06x10^{0}$	$1.65x10^{-8}$	$8.29x10^{-7}$
SDR16C5	$4.16x10^{0}$	$2.06x10^{0}$	$9.52x10^{-15}$	$3.95x10^{-12}$

Table 3.63. Differentially expressed downregulated transcripts identified in the CS4 subtype using limma.

CS4 – Differentially Expressed Down-Regulated Transcripts				
	fc	**log2fc**	**pvalue**	**padj**
EREG	$1.69x10^{-1}$	$-2.57x10^{0}$	$4.48x10^{-16}$	$2.79x10^{-13}$
Y_RNA.244	$2.27x10^{-1}$	$-2.14x10^{0}$	$2.26x10^{-15}$	$1.16x10^{-12}$
PTPRO	$2.82x10^{-1}$	$-1.83x10^{0}$	$5.67x10^{-14}$	$1.80x10^{-11}$
SRPX2	$3.14x10^{-1}$	$-1.67x10^{0}$	$1.06x10^{-15}$	$5.84x10^{-13}$
AOAH	$3.15x10^{-1}$	$-1.67x10^{0}$	$2.73x10^{-17}$	$2.61x10^{-14}$
MPP1	$3.15x10^{-1}$	$-1.67x10^{0}$	$1.01x10^{-21}$	$5.25x10^{-18}$
NPTX2	$3.32x10^{-1}$	$-1.59x10^{0}$	$2.18x10^{-7}$	$7.21x10^{-6}$
ST6GAL1	$3.41x10^{-1}$	$-1.55x10^{0}$	$1.37x10^{-17}$	$1.51x10^{-14}$
R3HDML	$3.46x10^{-1}$	$-1.53x10^{0}$	$1.62x10^{-17}$	$1.71x10^{-14}$
CKMT2	$3.47x10^{-1}$	$-1.53x10^{0}$	$1.27x10^{-6}$	$3.13x10^{-5}$
REEP1	$3.53x10^{-1}$	$-1.50x10^{0}$	$2.90x10^{-15}$	$1.43x10^{-12}$
APOLD1	$3.67x10^{-1}$	$-1.45x10^{0}$	$4.61x10^{-12}$	$7.96x10^{-10}$

Table 3.63 (continued). Differentially expressed downregulated transcripts identified in the CS4 subtype using limma.

AC108134.3	$3.68x10^{-1}$	$-1.44x10^{0}$	$2.45x10^{-15}$	$1.24x10^{-12}$
ZCCHC24	$3.73x10^{-1}$	$-1.42x10^{0}$	$5.71x10^{-17}$	$4.81x10^{-14}$
SLC6A6	$3.75x10^{-1}$	$-1.41x10^{0}$	$3.20x10^{-21}$	$1.41x10^{-17}$
AC078993.1	$3.79x10^{-1}$	$-1.40x10^{0}$	$2.61x10^{-9}$	$1.72x10^{-7}$
SHROOM4	$3.81x10^{-1}$	$-1.39x10^{0}$	$3.05x10^{-21}$	$1.41x10^{-17}$
FARP1	$3.83x10^{-1}$	$-1.38x10^{0}$	$3.16x10^{-25}$	$6.03x10^{-21}$
HSPB6	$3.84x10^{-1}$	$-1.38x10^{0}$	$2.49x10^{-10}$	$2.41x10^{-8}$
SLC26A2	$3.91x10^{-1}$	$-1.35x10^{0}$	$2.21x10^{-7}$	$7.30x10^{-6}$

To identify subtype-specific functional pathways, a GSEA was then performed based on the results obtained with the edgeR, DESeq2 and limma algorithms. However, only DESeq2 and limma detected pathways that exceeded the significance threshold (nominal P-value < 0.05 and corrected P-value < 0.05) and did not overlap with pathways identified for other subtypes. According to the DESeq2 result, the CS1 subtype was upregulated in a total of 2539 pathways, including collagen fibril organisation, B cell receptor signalling,

cell adhesion, leukocyte activation and degranulation, while it was downregulated in only 8 pathways (Figures 3.145-3.146).

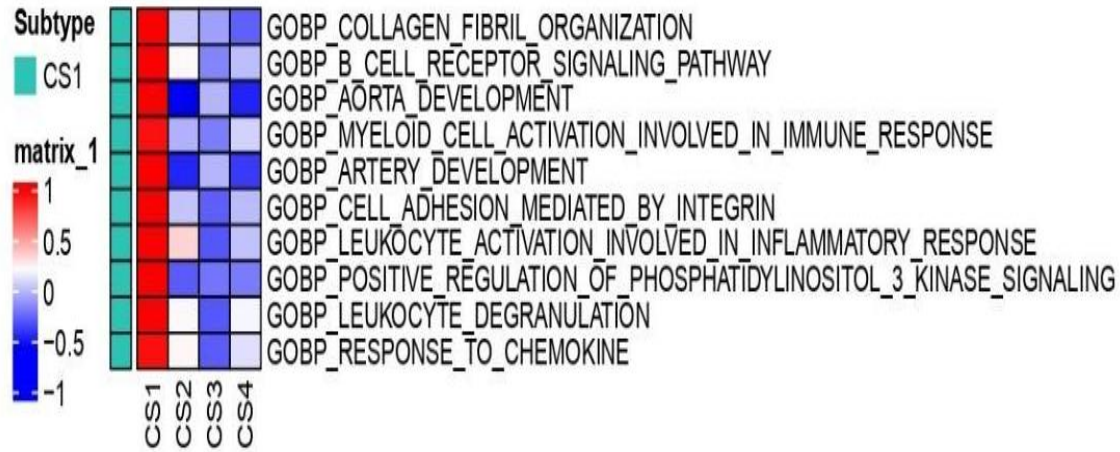


Figure 3.145. Heatmap of subtype-specific upregulated pathways using DESeq2 algorithm for 4 identified subtypes in TCGA-COAD cohort.

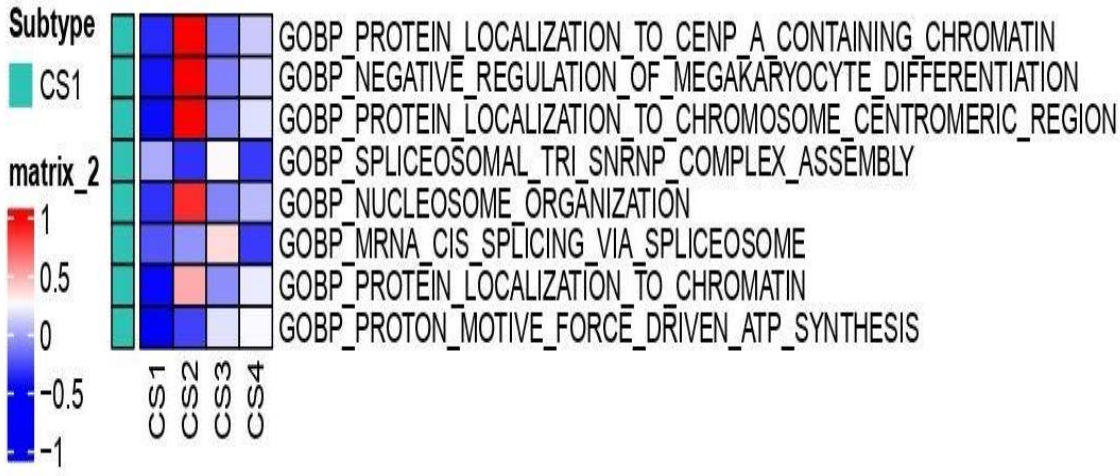


Figure 3.146. Heatmap of subtype-specific downregulated pathways using DESeq2 algorithm for 4 identified subtypes in TCGA-COAD cohort.

On the other hand, examination of the limma results revealed that the other subtypes, with the exception of CS2, were enriched in at least one pathway (Figures 3.147-3.148). Collagen fibril organisation, which is associated with poor prognosis by promoting epithelial-mesenchymal transition [195-197], is upregulated in CS1. As the chemotaxis signalling pathway promotes tumour cell dissemination and metastasis [198],

upregulation of this pathway in CS1 patients leads to tumour progression. CS3 is downregulated in various biological pathways, such as migration of immune cells, immune response and response to chemokines. Abnormally expressed chemokines are known to play an important role in tumour development and metastasis [198-200]. The non-canonical WNT signalling pathway, which contributes to tumourigenesis by regulating cell polarity and migration, is downregulated in CS4.



Figure 3.147. Heatmap of subtype-specific upregulated pathways using limma algorithm for 4 identified subtypes in TCGA-COAD cohort.

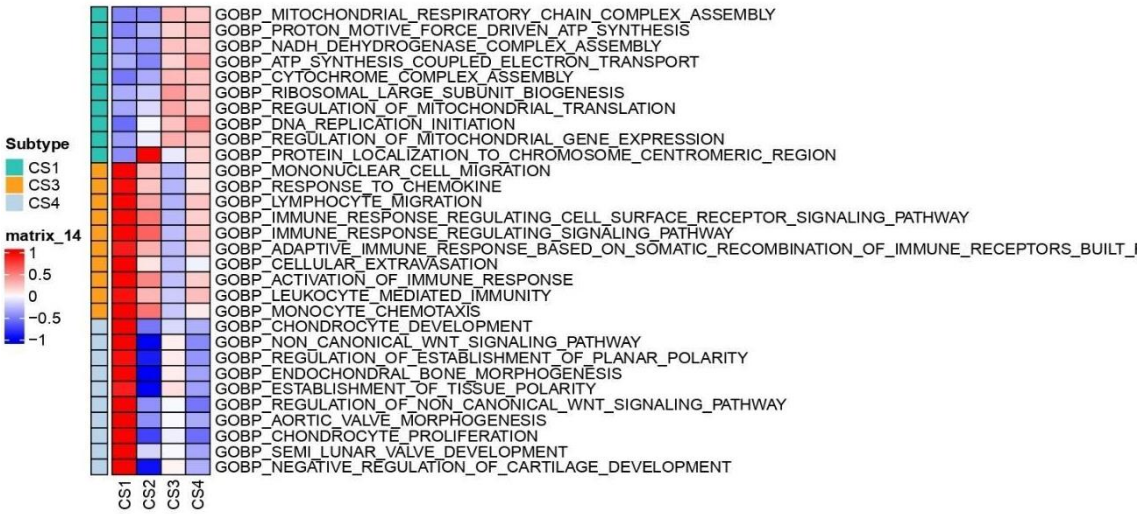


Figure 3.148. Heatmap of subtype-specific downregulated pathways using limma algorithm for 4 identified subtypes in TCGA-COAD cohort.

Next, the activation status of 50 tumour-associated signalling pathways was compared between the four subtypes (Figure 3.149). The results showed that interferon-alpha

response, interferon-gamma response, allograft rejection, IL-2-STAT5 signalling, IL-6/JAKK/STAT3 signalling, inflammatory response and other pathways were highly active in CS1 cells. These results suggest that the CS1 subtype is associated with the immune response and inflammation. At the same time, the CS1 subtype is upregulated in the Notch, Wnt/β-catenin and Hedhehog (Hh) signalling pathways, which trigger tumour progression, while the CS2 subtype is downregulated in these pathways. The G2M checkpoint, E2F targets, unfolded protein response, mTORC1 signalling, DNA repair and two MYC target pathways were activated in CS4 cells. The mTORC1 signalling pathway is involved in tumour development and progression at an early stage [201, 202]. Furthermore, silencing MYC in colorectal cancer cells can suppress cell growth [203]. Therefore, activation of these signalling pathways was positively associated with the poor prognosis of CS4, whereas they were significantly downregulated in CS1. Epithelial-mesenchymal transition (EMT) is an important process in the metastasis of cancer cells. In this process, epithelial cells take on the characteristics of mesenchymal cells, which increase the mobility and migratory capacity of cancer cells. The epithelial-mesenchymal pathway is activated in CS1, which may be associated with a poor prognosis.



Figure 3.149. Heatmap of enrichment score of tumor-associated pathways for 4 identified subtypes in TCGA-COAD cohort.

3.3.4. The effect of genetic alteration on subtypes

Since gene mutations and copy number changes are crucial in the development, progression and metastasis of colon cancer, the genetic changes were compared between the subtypes. Gene mutation signatures serve as preventive biomarkers in colon cancer patients and are also very important markers for predicting treatment and prognosis [116, 117]. Therefore, the mutational differences between all subtypes were analysed and promising markers were evaluated. Figure 3.150 shows the genes that exceed the significance threshold ($p < 0.05$) and whose overall mutation rate is not less than 15%. This analysis of somatic mutations showed that 297 patients with colon adenocarcinoma had mutations, most of which were missense mutations.

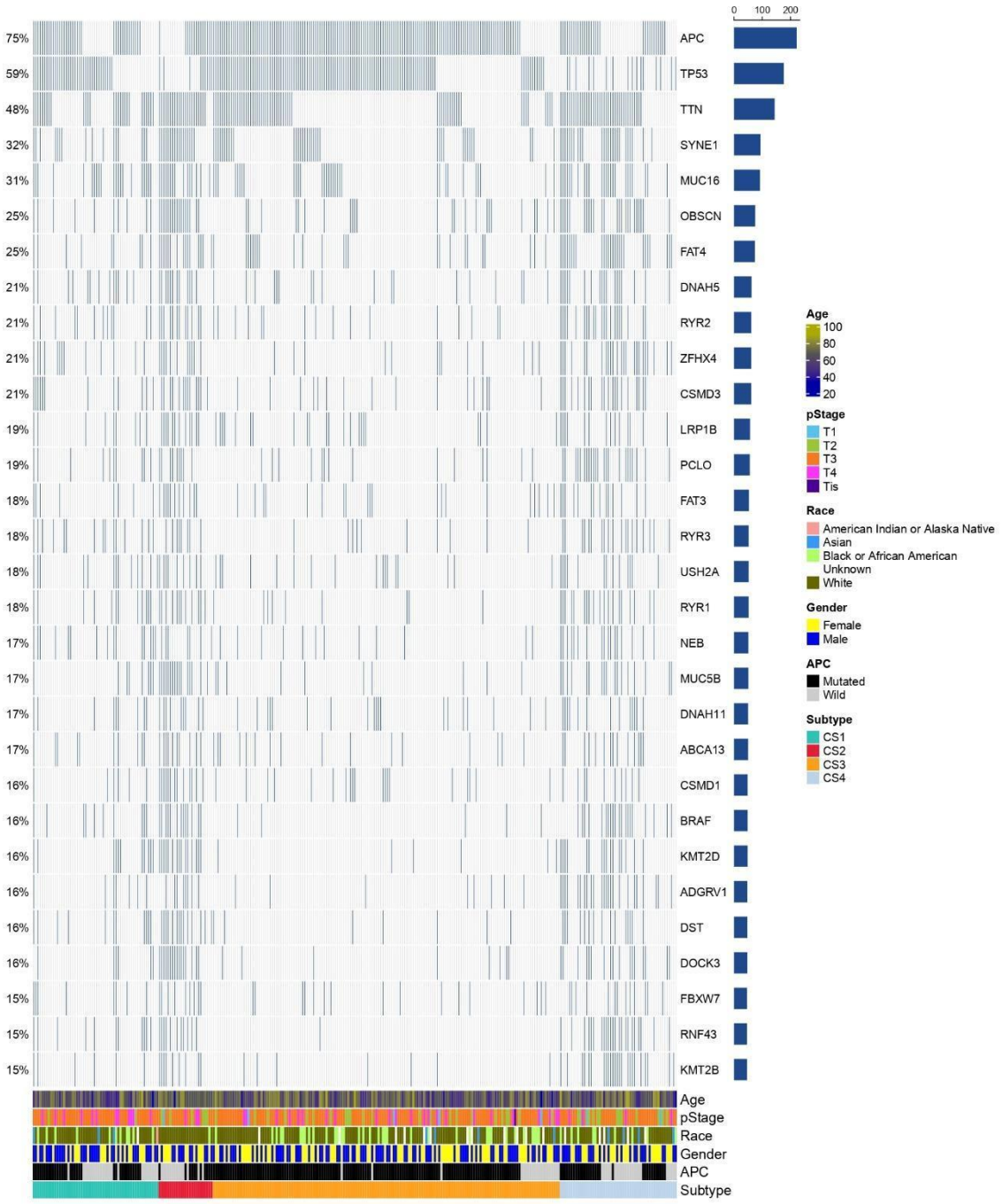


Figure 3.150. Mutational OncoPrint of 4 identified subtypes of colon adenocancinoma in TCGA-COAD cohort.

The overall mutation rate of thirty mutated genes was at least 15%. APC, TP53, TTN, SYNE1 and MUC16 were the five most frequently mutated genes in colon adenocarcinoma samples (Table 3.10). APC had the highest mutation frequency, with mutations occurring in 75% of the samples. APC and TP53 mutations, which are considered crucial for the development of colon cancer, are mutated in more than four-

fifths and three-fifths of the CS3 subtype, respectively. Considering that inactivation or deletion of the APC tumour suppressor gene occurs in the early stages of COAD development [123], it is concluded that APC mutations, which are more common in the CS3 subtype than in other subtypes, may be useful for early diagnosis and personalised treatment. In addition, TP53, the second most common mutation in colon cancer, is associated with a poorer prognosis, especially in patients treated with chemotherapy [128, 204, 205]. The titin (TTN) mutation, which has been identified as a risk factor for colon cancer and has the potential to convert the tumour microenvironment to an immunosuppressive type [129], was mutated in 88% and 70% of CS2 and CS4 subtypes, respectively. In addition, abnormal activation of Spectrin Repeat Containing Nuclear Envelope Protein 1 (SYNE1) in colon cancer cell lines plays an oncogenic role in colon cancer by promoting cell proliferation and migration [130], and is mutated in 68% of the CS2 subtype.

Table 3.64. Comparison of mutational frequency among 4 identified subtype of colon adenocarcinoma in TCGA-COAD cohort.

Gene (Mutated)	TMB	CS1	CS2	CS3	CS4	pvalue	padj
APC	222 (75%)	36 (62.1%)	14 (56.0%)	142 (88.8%)	30 (55.6%)	1.95e-08	4.95e-08
TP53	176 (59%)	37 (63.8%)	9 (36.0%)	114 (71.2%)	16 (29.6%)	9.89e-08	2.18e-07
TTN	144 (48%)	27 (46.6%)	22 (88.0%)	57 (35.6%)	38 (70.4%)	2.37e-08	5.59e-08
SYNE1	94 (32%)	16 (27.6%)	17 (68.0%)	36 (22.5%)	25 (46.3%)	8.36e-06	1.38e-05
MUC16	92 (31%)	21 (36.2%)	15 (60.0%)	32 (20.0%)	24 (44.4%)	2.26e-05	3.24e-05

In addition, colon cancer is strongly influenced by copy number alterations, which play an important role in the response to immunotherapy, and by genetic mutations. Therefore, TMB and FGA were calculated to quantify these genomic alterations that may influence immunotherapy. The FGA values, expressed as the percentage of genomes affected by copy number gains or losses (i.e. copy number alterations) of the four subtypes, were first analysed. Compared to the other subtypes, the CS3 group had more CNAs in both the lost and gained genomes (Figure 3.151). On the other hand, the CS2 group has the least copy number increased genome, while the CS4 group has the least copy number decreased genome. Table 3.11 shows the FGA, FGG and FGL values of some samples.

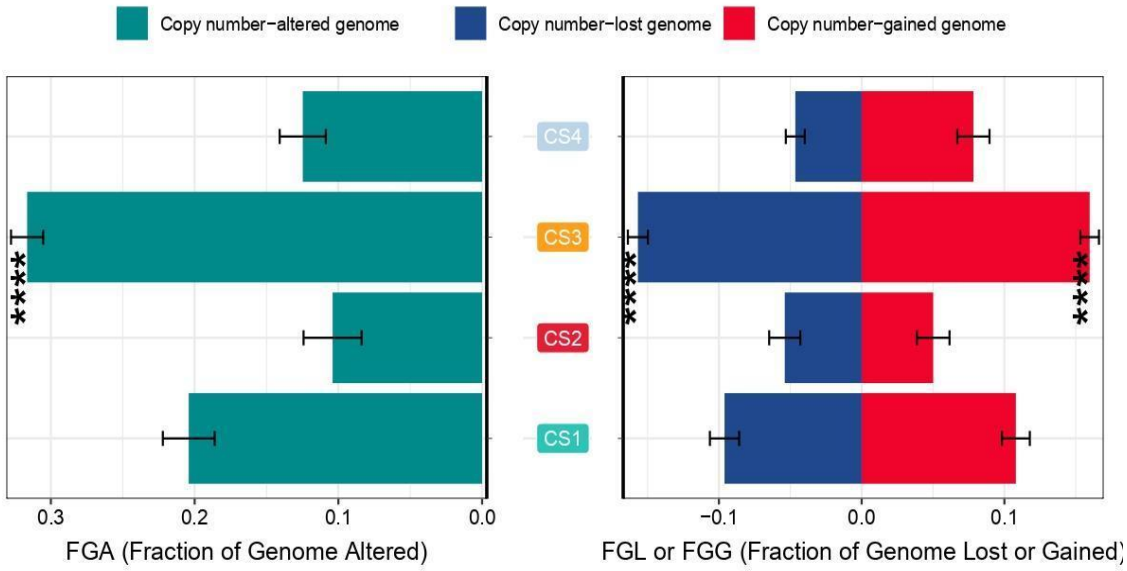


Figure 3.151. Barplot of fraction genome altered among 4 identified subtypes of colon adenocarcinoma in TCGA-COAD cohort.

Table 3.65. Demo of comparison of fraction genome altered among 4 identified subtype of colon adenocarcinoma in TCGA-COAD cohort.

samID	FGA	FGG	FGL	Subtype
TCGA-5M-AAT6-01A	0.06718986	0.0341973528	0.03299251	CS1
TCGA-A6-2672-01B	0.06181553	0.0119797499	0.04983578	CS2
TCGA-3L-AA1B-01A	0.14303125	0.072892383	0.07013886	CS3
TCGA-A6-5661-01A	0.05367073	0.0259775981	0.02769313	CS4
TCGA-A6-5665-01A	0.03291044	0.0010687047	0.03184174	CS4

TMB, defined as the total number of somatic coding errors, base substitutions and indel mutations per million bases of DNA, can be used to assess the response of colorectal cancer patients to ICI therapy. To assess TMB, the number of non-synonymous mutations per million bases was calculated. Significantly higher mean TMB values were observed for CS2 and CS4 ($P < 0.001$, Figure 3.152) (Table 3.12). Tumours with high TMB levels harbour a high number of neoantigens, making them more likely to be recognised by the immune system and respond to immunotherapy [142]. In addition, single nucleotide variants (SNVs) were visualised after they were classified into transitions and transformations (TiTv).

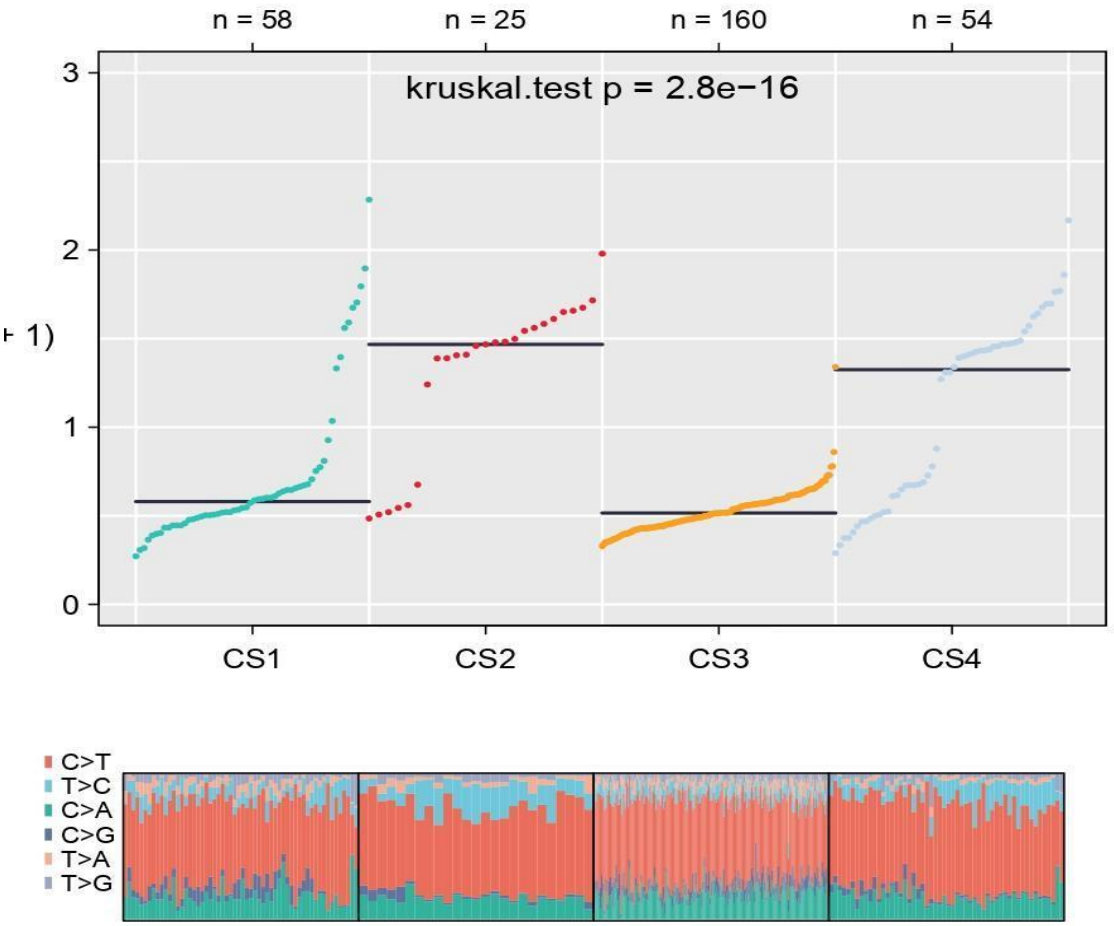


Figure 3.152. Comparison of TMB and TiTv among 4 identified subtypes of colon adenocarcinoma in TCGA-COAD cohort.

Table 3.66. Demo of comparison of TMB among 4 identified subtype of colon adenocarcinoma in TCGA-COAD cohort.

	samID	variants	TMB	log10TMB	Subtype
295	TCGA-A6-2685-01A	39	1.0263158	0.3067071	CS1
210	TCGA-A6-2684-01C	78	2.052632	0.4846744	CS2
293	TCGA-A6-A567-01A	43	1.131579	0.3287014	CS3
296	TCGA-CA-5255-01A	36	0.9473684	0.2894481	CS4
292	TCGA-CM-5863-01A	44	1.1578947	0.3340303	CS4

Moreover, an alluvial diagram was created to visualize how often the present subtypes contained the 5 most common mutant genes in COAD (Figure 3.153).

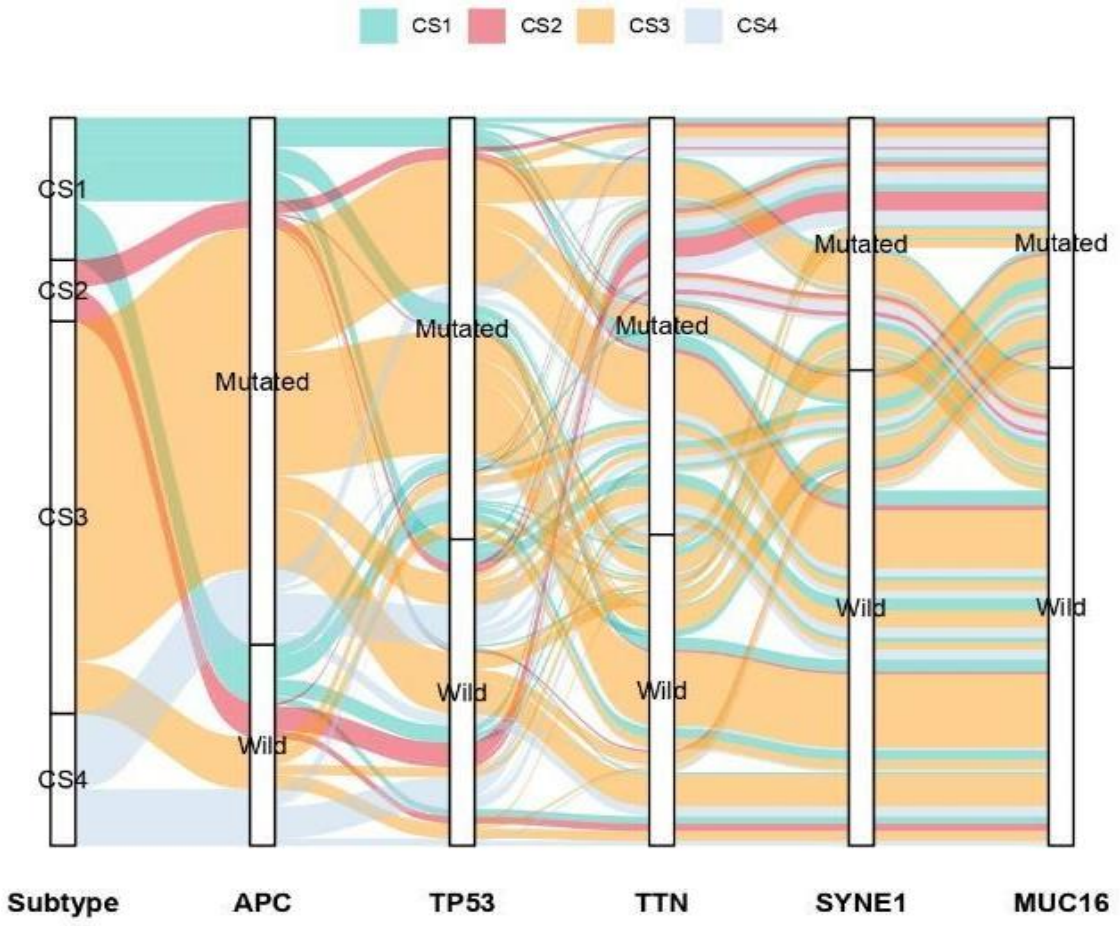


Figure 3.153. Agreement of 4 identified subtypes of colon adenocarcinoma with the most common 5 mutant genes in TCGA-COAD cohort.

3.3.5. Precision treatment recommendations for COAD patients

Determining sensitivity to the drug by taking into account the individual differences of each patient before starting treatment improves the treatment process. Therefore, to enable individualised treatment selection, the potential response to commonly administered chemotherapeutic agents in COAD patients was assessed by estimating IC50 values based on gene expression profiles and data from the GDSC database. As part of this drug sensitivity analysis, in addition to analysing the chemotherapeutic agents commonly used in the treatment of COAD, sensitivity analyses of 249 drugs offered by the package that may be promising for the treatment of COAD were performed. In this way, the sensitivities of subtypes, which are differentiated according to their molecular characteristics, were determined.

Here, the response of each subtype to some of the most frequently used and most promising drugs during colon cancer treatment is evaluated in detail. Appendix B.1 shows a list of drugs for which subtypes showed a statistically significant response among 249 drugs. During drug sensitivity analysis, IC50 values were calculated, which are used to determine the effectiveness of a drug. While a high IC50 value indicates drug resistance, a low value indicates a better effect of the drug.

5-fluorouracil is one of the most commonly used chemotherapeutics, especially in the treatment of advanced-stage colon cancer [206]. CS4 patients showed a better response to treatment with 5-FU, which acts as an inhibitor of thymidylate synthase (TS) and whose main role is to inhibit DNA synthesis (Figure 3.154) [207].

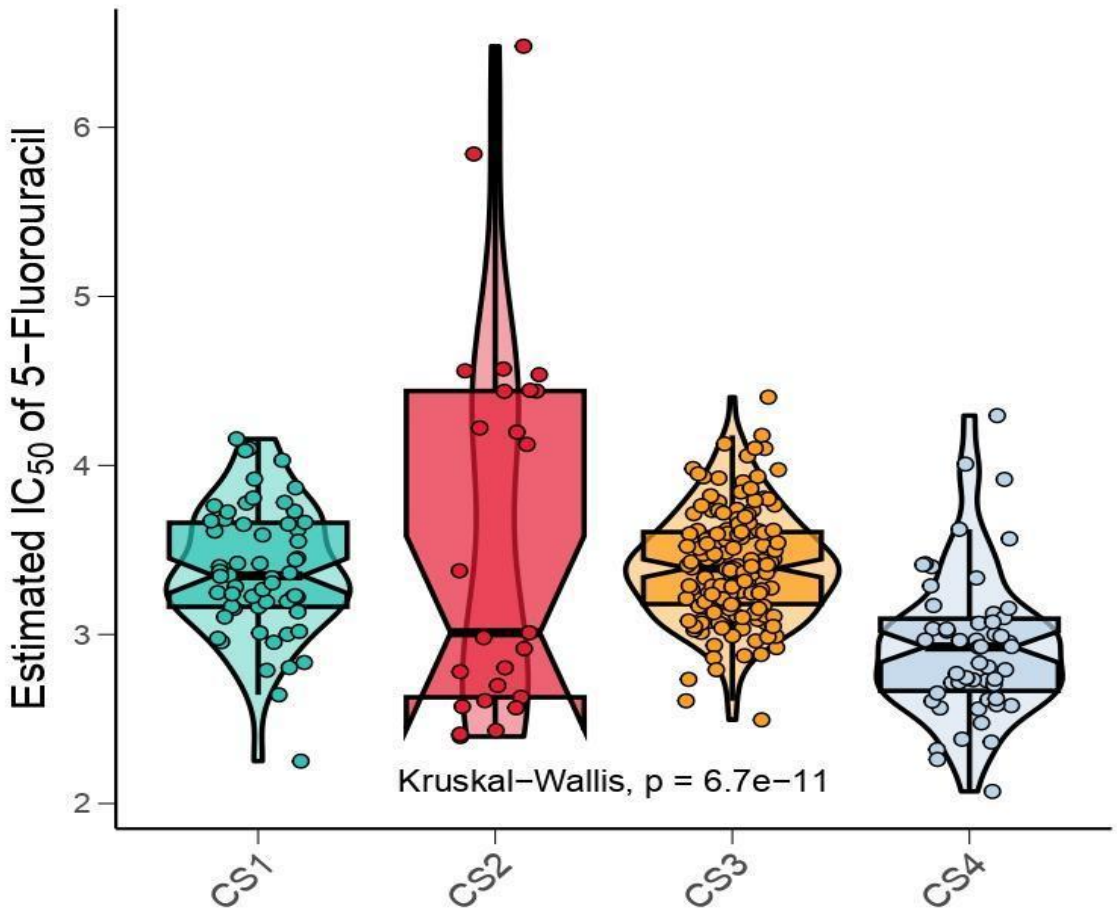


Figure 3.154. Boxviolin for estimated IC50 of 5-Fluorouracil among 4 identified subtypes of colon adenocarcinoma in TCGA-COAD cohort.

In addition, the response to cisplatin, one of the most potent chemotherapeutic agents used in the treatment of colorectal cancer, was higher, especially in patients with subtypes CS1 and CS2 (Figure 3.155). However, the high toxicity caused by the use of the drug leads to the development of drug resistance [208, 209]. As a result of the studies, however, it was found that the combination treatment of aspirin and cisplatin, which is used to enhance the effect of cisplatin, leads to effective results in tumour regression [208]. The downregulation of the anti-apoptotic protein Bcl-2, whose expression is suppressed by the use of this combination, in the CS2 subtype provides important evidence that this subtype may respond favourably to aspirin-cisplatin combination treatment.

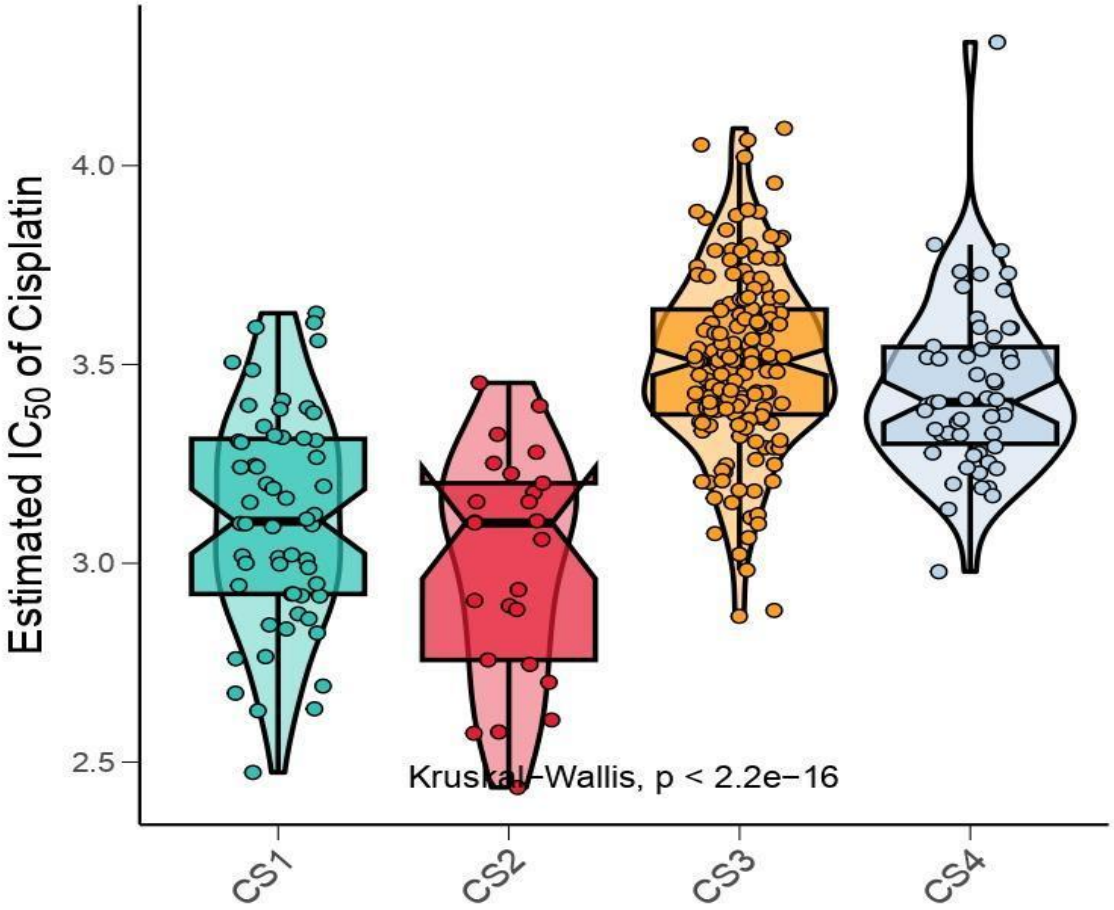


Figure 3.155. Boxviolin for estimated IC50 of Cisplatin among 4 identified subtypes of colon adenocarcinoma in TCGA-COAD cohort.

CS1 patients show a better response to Paclitaxel, which exhibits anticancer properties by playing a role in proliferation and apoptosis and is used in advanced colon cancer treatments (Figure 3.156).

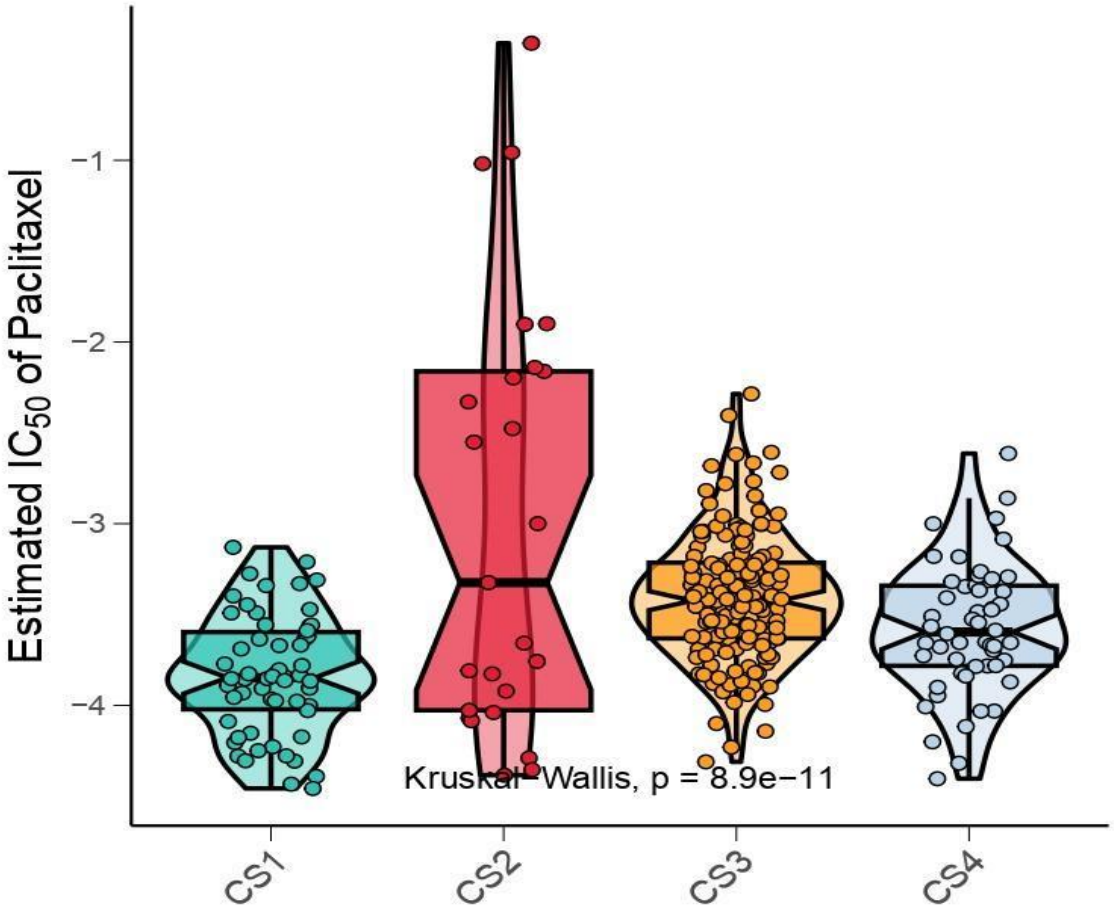


Figure 3.156. Boxviolin for estimated IC50 of Paclitaxel among 4 identified subtypes of colon adenocarcinoma in TCGA-COAD cohort.

SN-38, which acts as the active metabolite of irinotecan, a common chemotherapeutic drug of colon cancer, overcomes chemoresistance in a hypoxic environment, leading to anti-tumor effects on colon cancer. As a result of the analysis, it was determined that CS1 and CS2 patients had a better response to SN-38 than patients in the other subtypes (Figure 3.157).

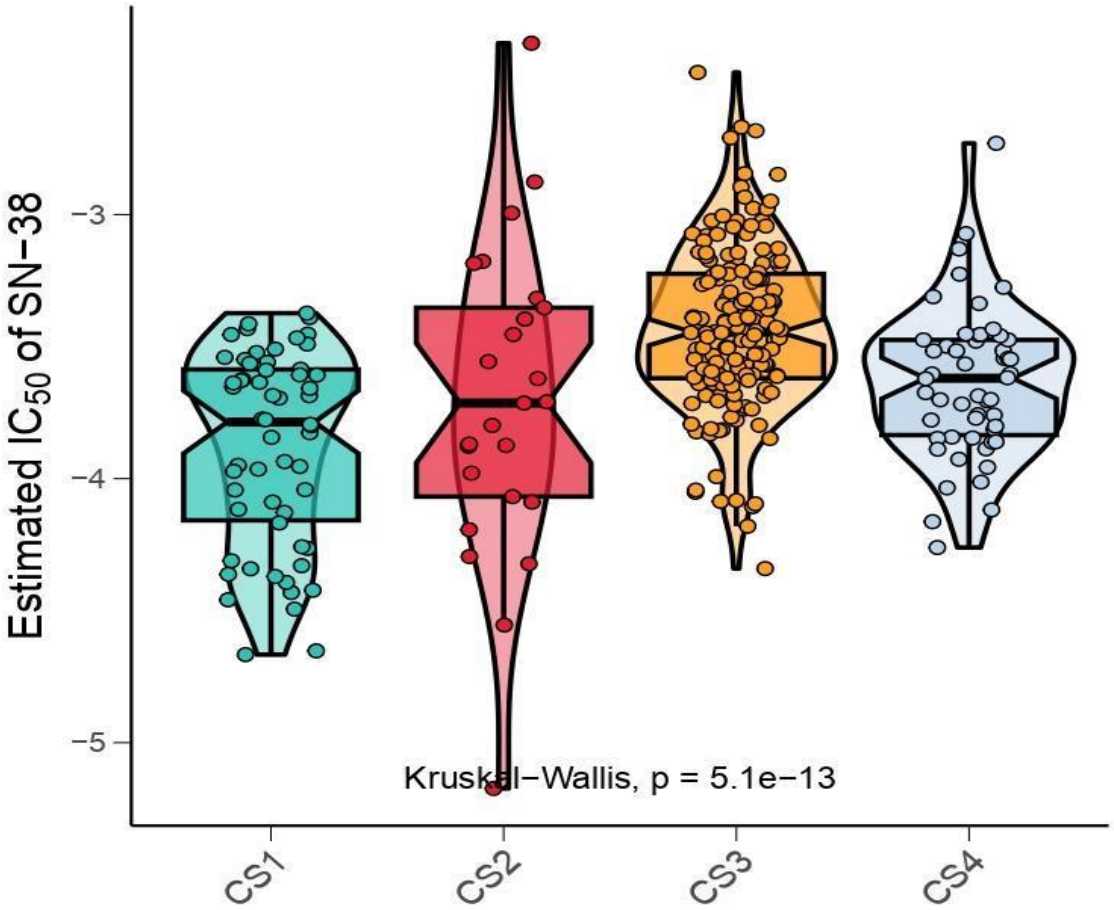


Figure 3.157. Boxviolin for estimated IC50 of SN-38 among 4 identified subtypes of colon adenocarcinoma in TCGA-COAD cohort.

Rapamycin (Rapa), used as an immunosuppressant, shows anti-tumor properties. The CS1 and CS3 subtypes showed a much better response to Rapa treatment, which is potentially promising for the treatment of colon cancer (Figure 3.158).

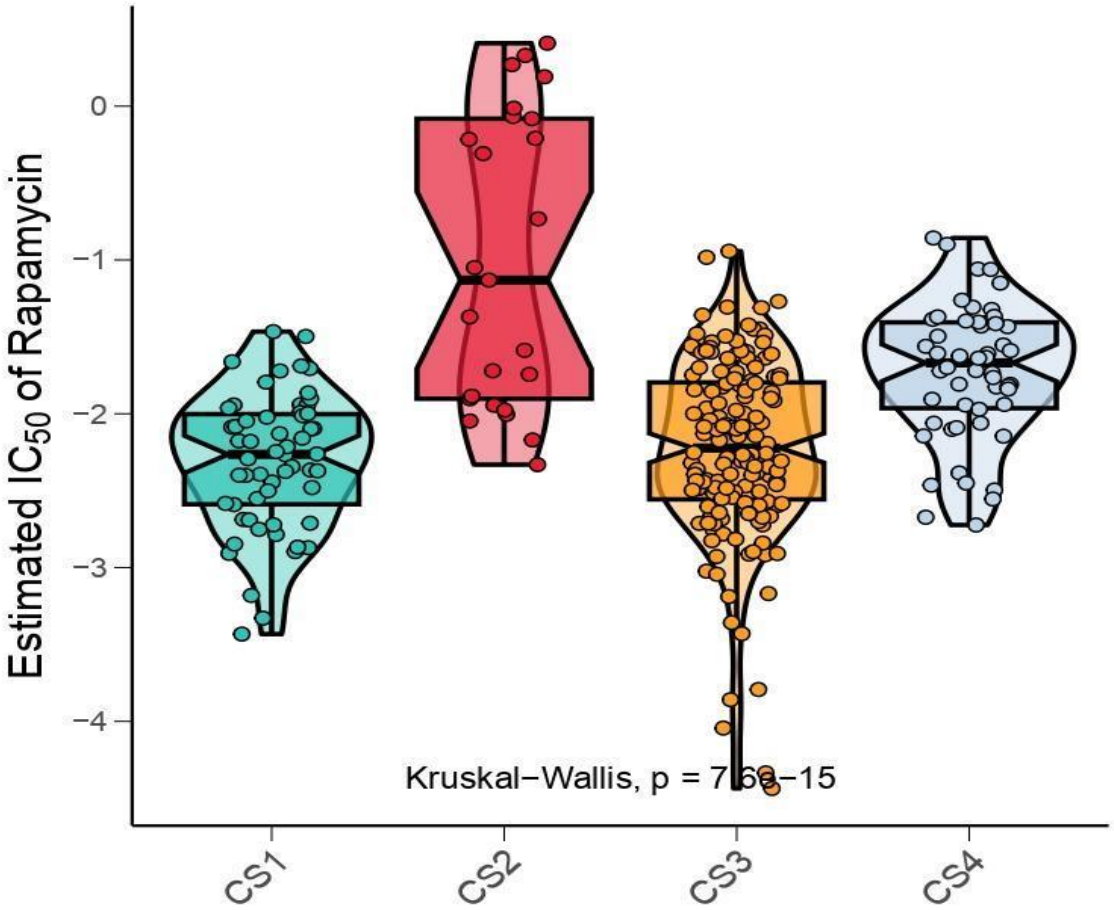


Figure 3.158. Boxviolin for estimated IC50 of Rapamycin among 4 identified subtypes of colon adenocarcinoma in TCGA-COAD cohort.

Imatinib, which can be used to inhibit tumor growth after chemotherapy and reduce the expression of stem-like cancer cells that can initiate relapse, showed a much better effect in the CS1 type (Figure 3.159).

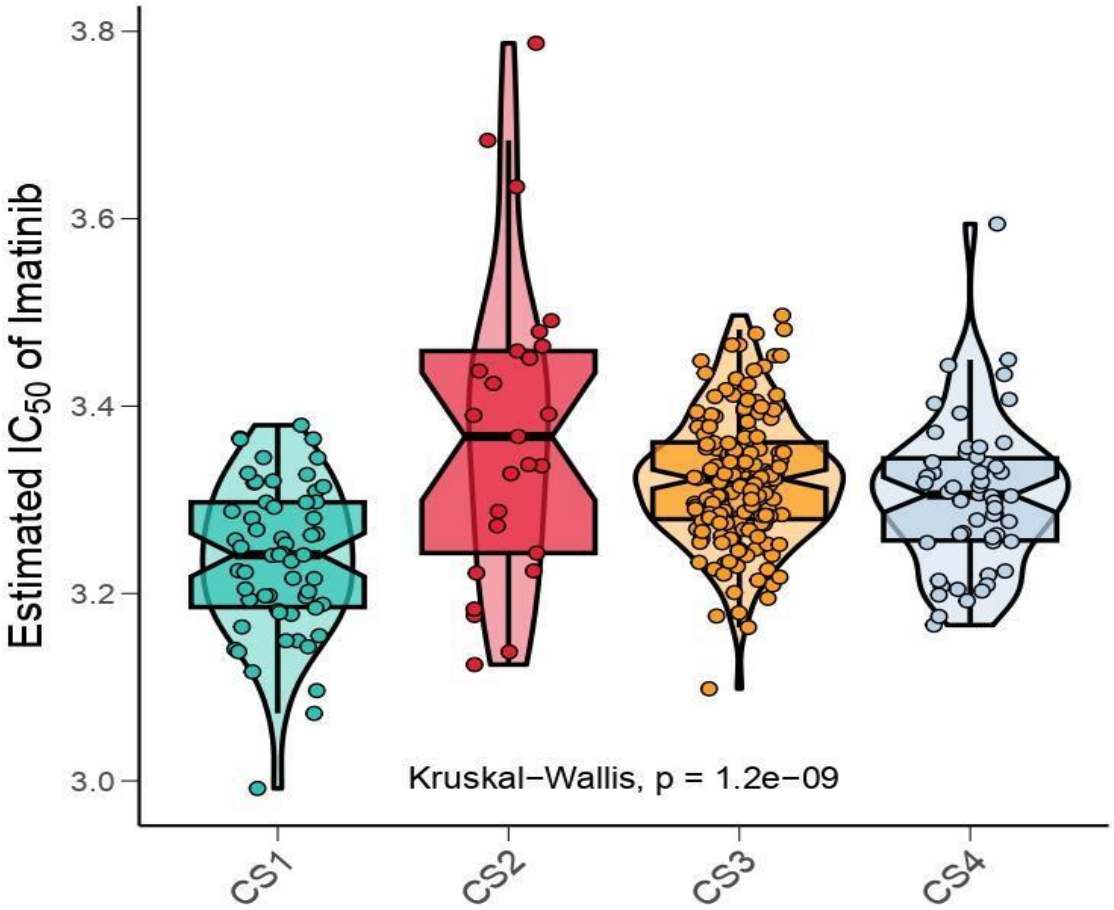


Figure 3.159. Boxviolin for estimated IC50 of Imatinib among 4 identified subtypes of colon adenocarcinoma in TCGA-COAD cohort.

However, the response to these chemotherapeutic agents is still quite low due to the high toxicity, the innate or acquired resistance mechanisms and the low tumour-specific selectivity. In order to improve the effect of chemotherapy in colorectal cancer, targeted treatment approaches that act directly on the cancer cell and significantly increase the effect of the treatment are therefore gaining in importance day by day. Monoclonal antibodies, cyclin-dependent kinases, proteasomes and poly-ADP-ribose polymerases are among the most important molecular targets of targeted therapy [25].

Cetuximab is the first FDA-approved monoclonal antibody against EGFR [25]. Cetuximab suppresses tumour cells in patients with metastatic RAS wild-type colorectal cancer by targeting EGFR [210]. Cetuximab has been reported to achieve significant results in improving overall survival (OS) and progression-free survival (PFS), both as monotherapy and in combination with various chemotherapeutic agents [25, 211, 212].

The downregulation of EREG, which stimulates cell growth by binding to EGFRs, in the CS4 subtype could be an indicator of why this subtype responds more sensitively to treatment with cetuximab (Figure 3.160) [213].

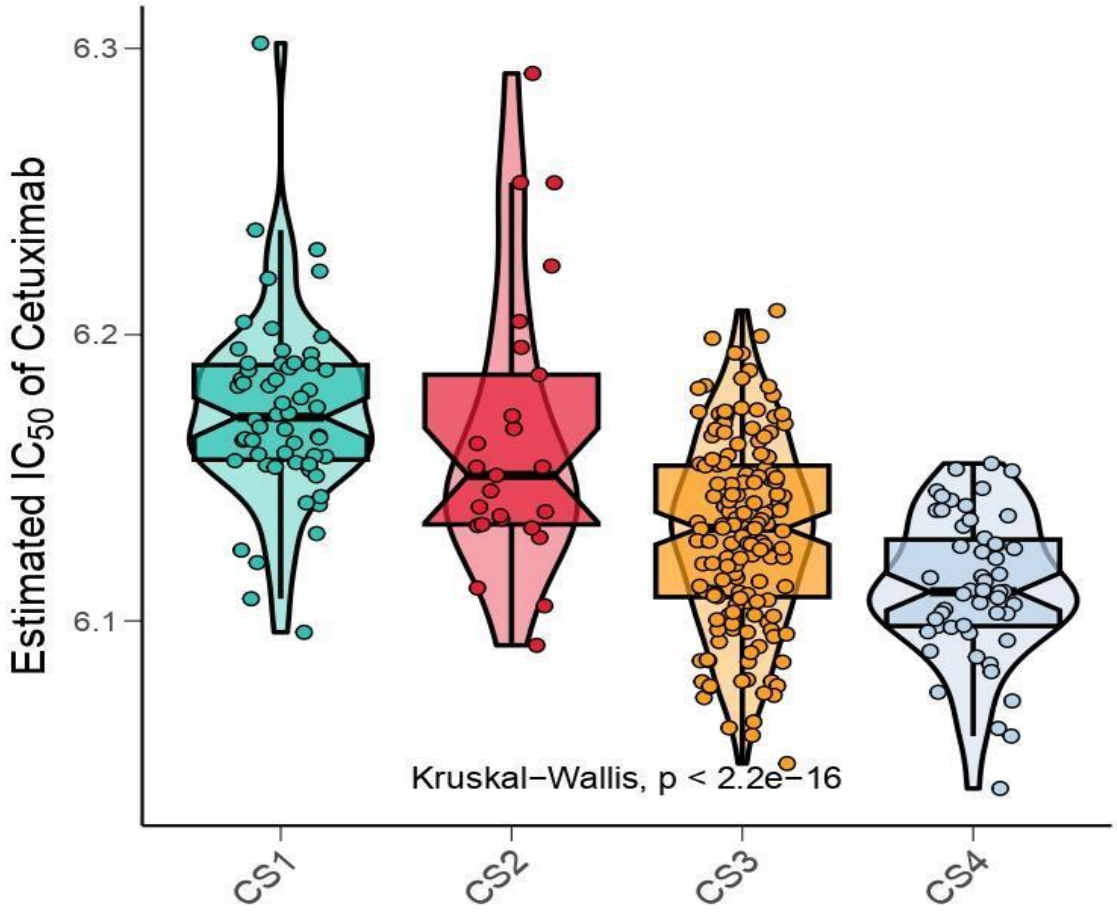


Figure 3.160. Boxviolin for estimated IC50 of Cetuximab among 4 identified subtypes of colon adenocarcinoma in TCGA-COAD cohort.

The ubiquitin-proteasome pathway (UPP), which plays a crucial role in the degradation of misfolded proteins, regulates the activity of various proteins such as p53, NFκB and β-catenin, which play an important role in tumour growth [214]. Therefore, as a result of various studies targeting the degradation of UPP, proteasome inhibitors have been found to induce apoptosis in cancer and can therefore be used as an effective treatment strategy [215]. The peptide aldehyde proteasome inhibitor MG132 (carbobenzoxyl-L-leucyl-L-leucyl-L-leucinal) induces cell cycle arrest but also triggers apoptosis [216]. After treatment with MG-132, the expression of the tumour suppressor p53 and the pro-apoptotic PUMA is induced in the cells, which in turn causes the activation of Bax, which

triggers apoptosis. In addition, cycloheximide, a translational inhibitor that reduces Bax activation and apoptosis by suppressing PUMA and p53, plays an important role in this treatment [215]. Therefore, regulation of p53-, PUMA- and Bax-mediated mitochondrial activation of the CS2 subtype, which may be more responsive to treatment with the proteasome inhibitor MG-132, will further improve the response to the respective treatment (Figure 3.161).

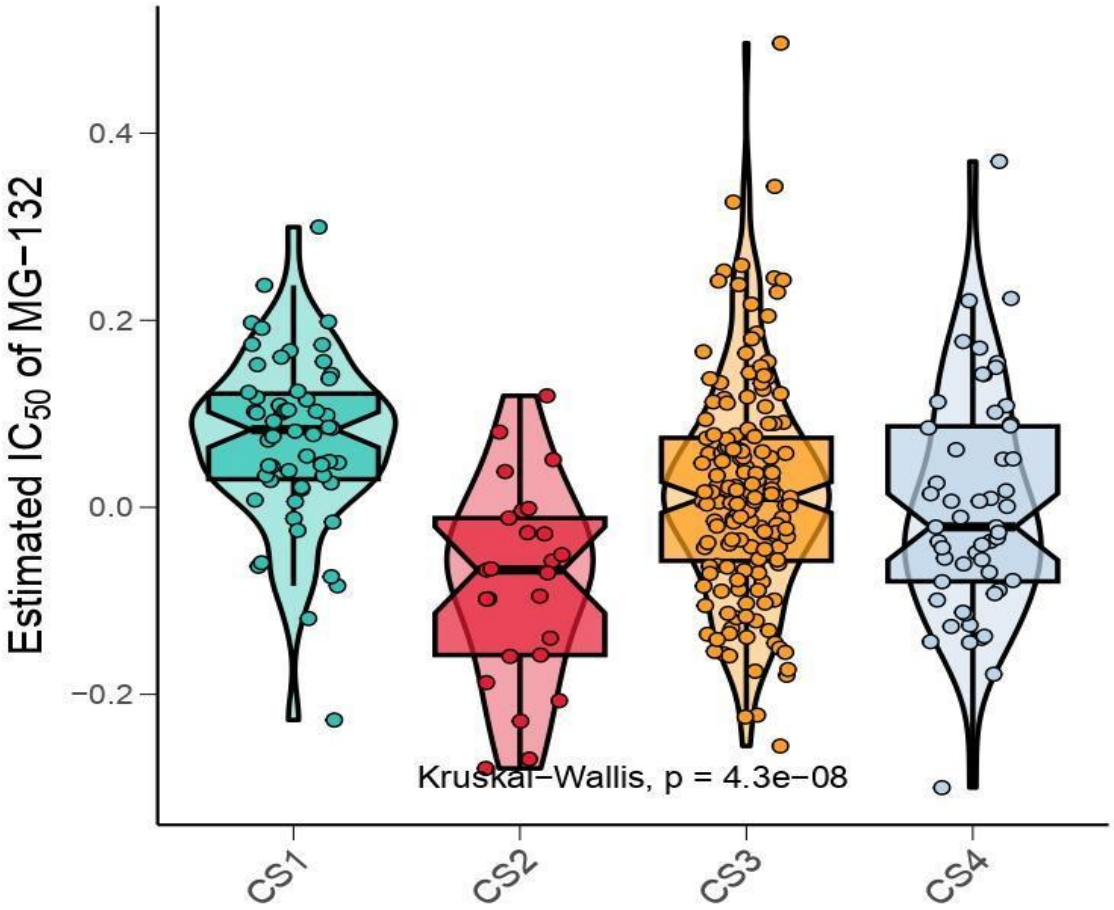


Figure 3.161. Boxviolin for estimated IC50 of MG-132 among 4 identified subtypes of colon adenocarcinoma in TCGA-COAD cohort.

3.3.6. Validation of subtypes in four external cohorts

Four external cohorts GSE39582, GSE16125, GSE17536 and GSE17537 were used to validate the reliability of the subtypes. Subtype-specific upregulated biomarkers previously identified with edgeR, DESeq2 and limma were used to confirm the current subtypes of patients in external cohorts. NTP and PAM methods were used for subtype

prediction in the validation cohort. Subtype survival results obtained between NTP and the discovery and validation groups were compared. In addition, the IGP statistic was calculated to assess the similarity and reproducibility of the subtypes obtained between the discovery and validation groups with PAM. Subtype prediction was then performed using NTP and PAM for the discovery dataset. The agreement between the subtypes present in the discovery dataset and the subtypes predicted by NTP and PAM was then measured using the kappa statistic. The accuracy and consistency between the subtype predicted by NTP and PAM was also analysed in the validation cohort.

NTP was initially implemented for the prediction of subtypes with edgeR, DESeq2 and limma on GSE16125 (Figures 3.162-3.163). However, no matches based on the limma results could be detected during the NTP analysis. Furthermore, in the NTP analysis based on the use of biomarkers predicted with EdgeR, no sample in the GSE16125 dataset, which consists of 32 samples, could be assigned to a subspecies. In contrast, in the NTP analysis based on DESeq2 results, CS1, CS2, CS3 and CS4 could be assigned to 8, 1, 3 and 2 samples, respectively, showing that DESeq2 achieved a better subtyping analysis than the other two algorithms.

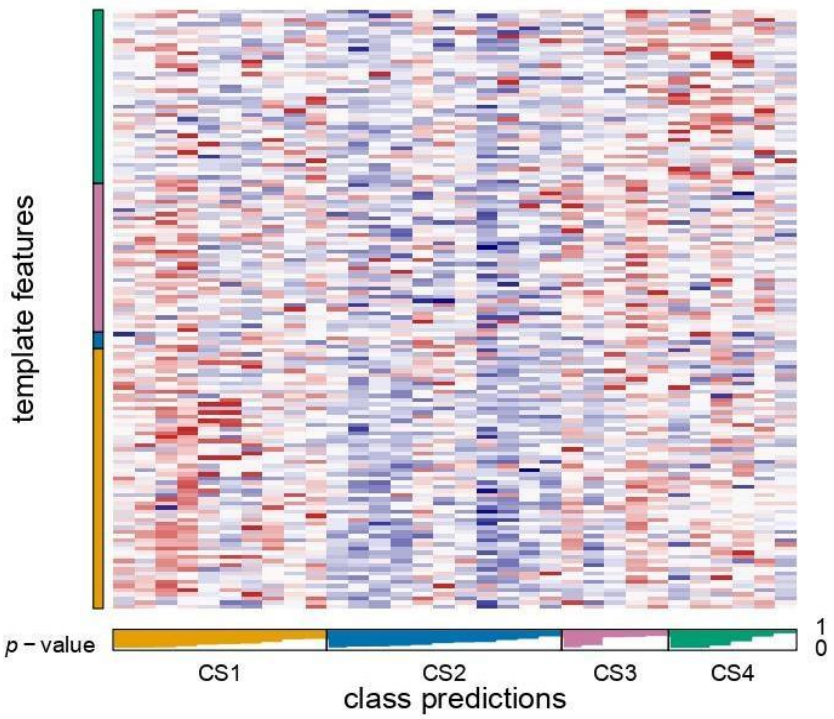


Figure 3.162. Heatmap of NTP in GSE16125 cohort using subtype-specific upregulated biomarkers identified using edgeR from TCGA-COAD cohort.

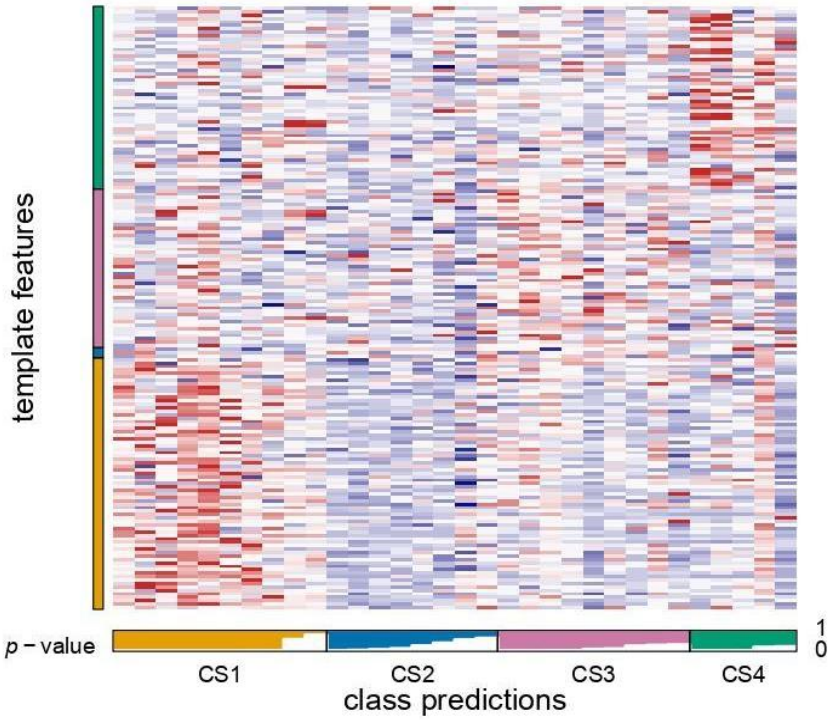


Figure 3.163. Heatmap of NTP in GSE16125 cohort using subtype-specific upregulated biomarkers identified using DESeq2 from TCGA-COAD cohort.

In addition, a survival analysis of the subtypes predicted by NTP was performed in the validation cohort based on the edgeR and DESeq2 methods. As a result of the survival analysis performed based on the edgeR results, no statistically significant difference in the survival rates of patients in the GSE16125 cohort was observed (Figure 3.164). However, when survival was analysed based on the DESeq2 algorithm, a statistically significant result was found (Figure 3.165). Figure 3.165 shows that the clinical prognosis of CS1 is worse than that of other subtypes.

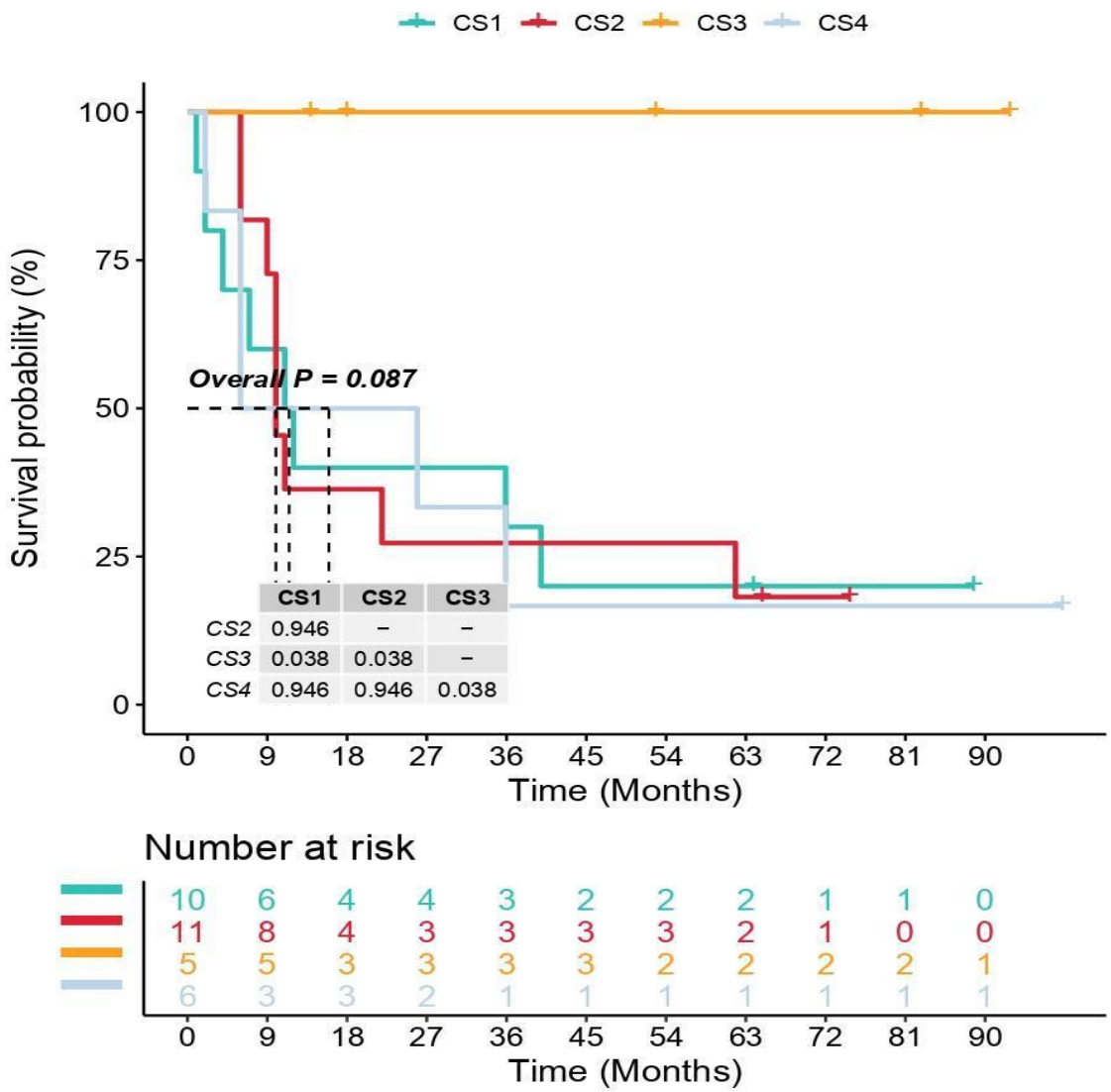


Figure 3.164. Kaplan-Meier survival curve of 4 colon adenocarcinoma subtypes predicted by edgeR in the GSE16125 cohort.

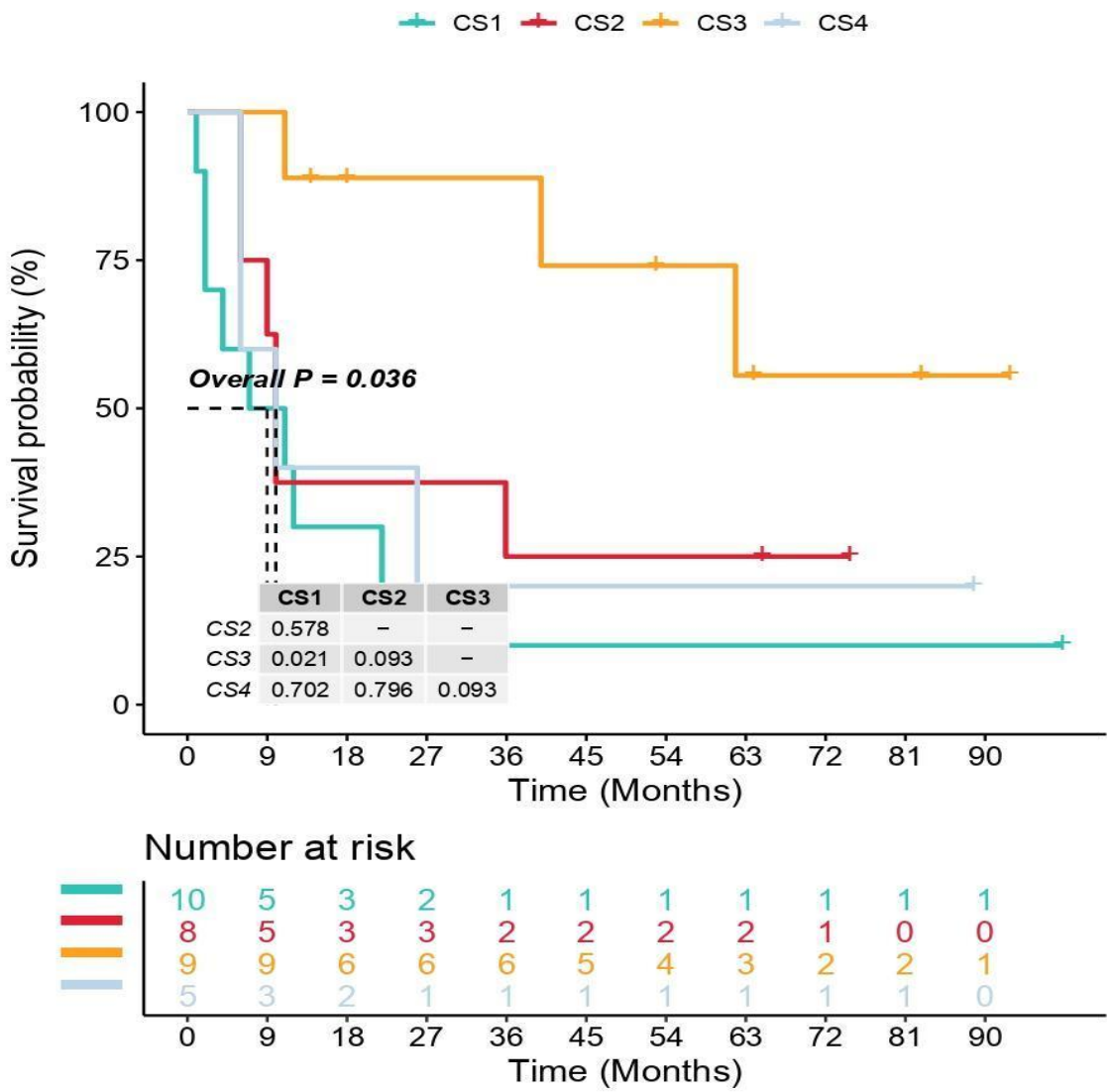


Figure 3.165. Kaplan-Meier survival curve of 4 colon adenocarcinoma subtypes predicted by DESeq2 in the GSE16125 cohort.

Another method for subtype prediction is to train a PAM classifier in the discovery group to predict the subtype for patients in the external validation group. The similarity and reproducibility of subtypes identified by PAM was assessed using the IGP statistic. As can be seen in Table 3.9, the IGP statistic of the GSE16125 cohort was close to 1, indicating that the subtypes identified between the discovery and validation groups were similar and reproducible.

Table 3.67. IGP information in four validation cohorts of the PAM classifier trained on the TCGA-COAD cohort.

	CS1	CS2	CS3	CS4
GSE16125	0.7272727	0.6250000	0.8000000	0.0000000
GSE39582	0.8359375	0.3253012	0.7393365	0.7214286
GSE17536	0.4772727	0.4347826	0.6060606	0.6818182
GSE17537	0.4545455	0.8571429	0.8000000	0.7058824

The results of the kappa statistic can range from -1 to +1, where 1 means perfect agreement between the raters. According to the results of EdgeR (Figure 3.166-3.167), DESeq2 (Figure 3.168-3.169) and limma (Figure 3.170-3.171), the agreement between the subtypes found in the TCGA dataset and the subtypes predicted by PAM was much greater than that predicted by NTP.

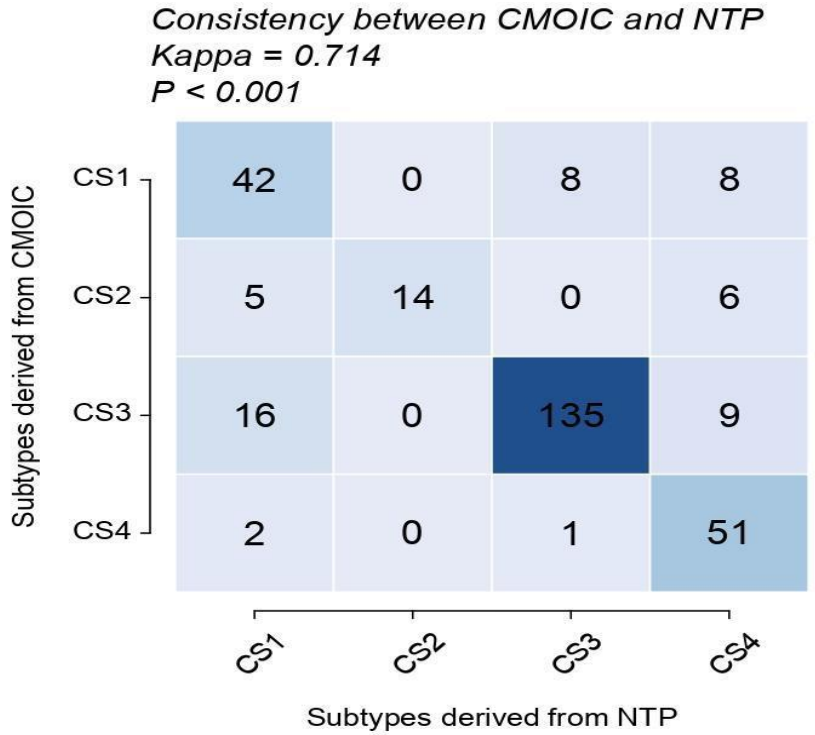


Figure 3.166. Consistency heatmap between current and NTP-predicted Kappa statistics for edgeR results in TCGA-COAD cohort.

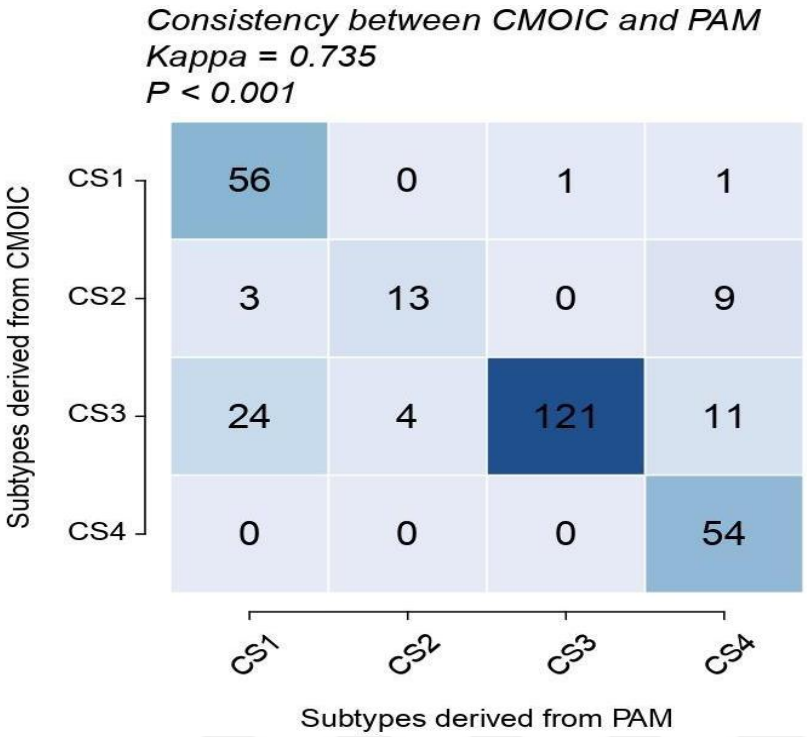


Figure 3.167. Consistency heatmap between current and PAM-predicted Kappa statistics for edgeR results in TCGA-COAD cohort.

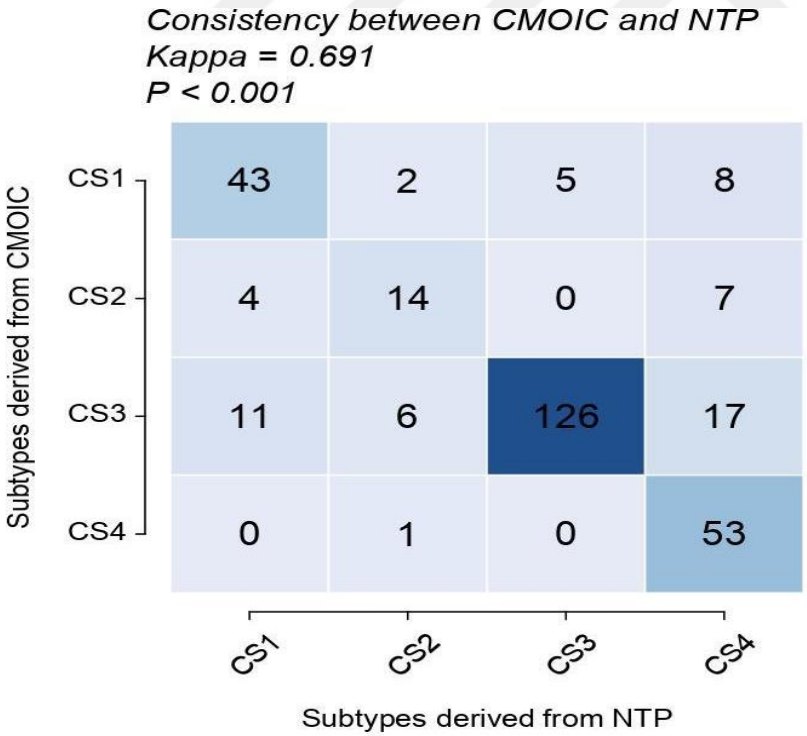


Figure 3.168. Consistency heatmap between current and NTP-predicted Kappa statistics for DESeq2 results in TCGA-COAD cohort.

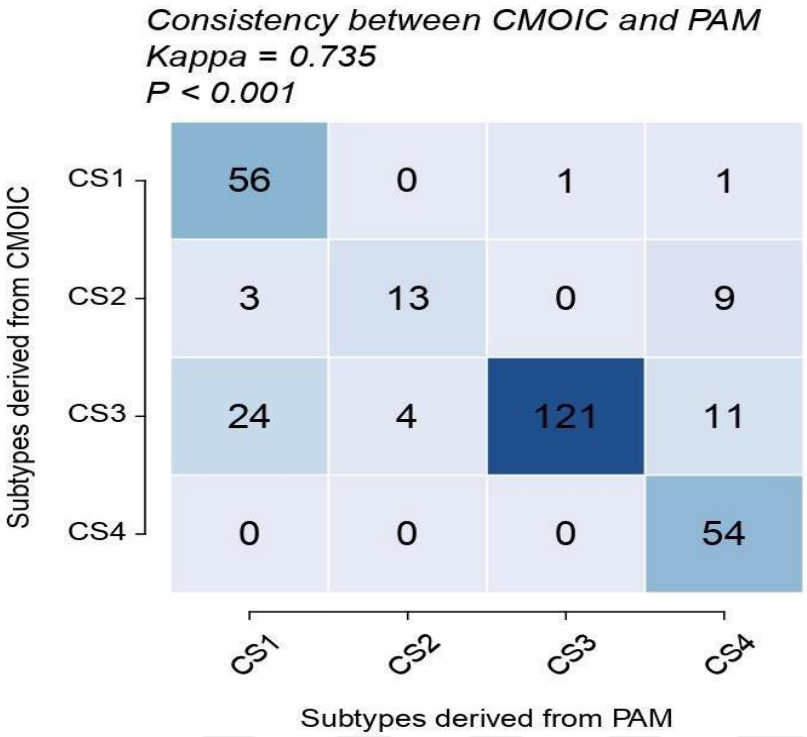


Figure 3.169. Consistency heatmap between current and PAM-predicted Kappa statistics for DESeq2 results in TCGA-COAD cohort.

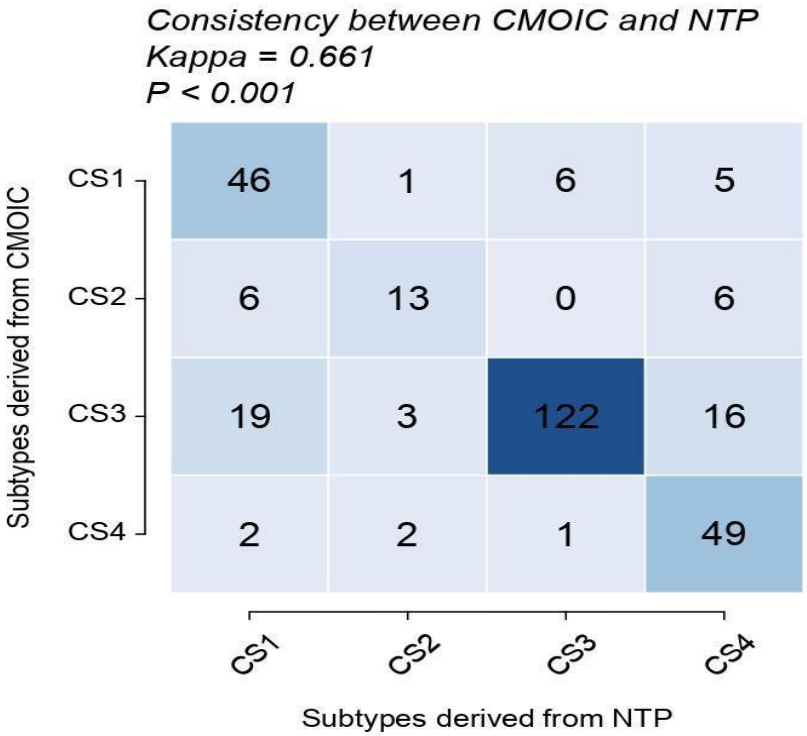


Figure 3.170. Consistency heatmap between current and NTP-predicted Kappa statistics for limma results in TCGA-COAD cohort.

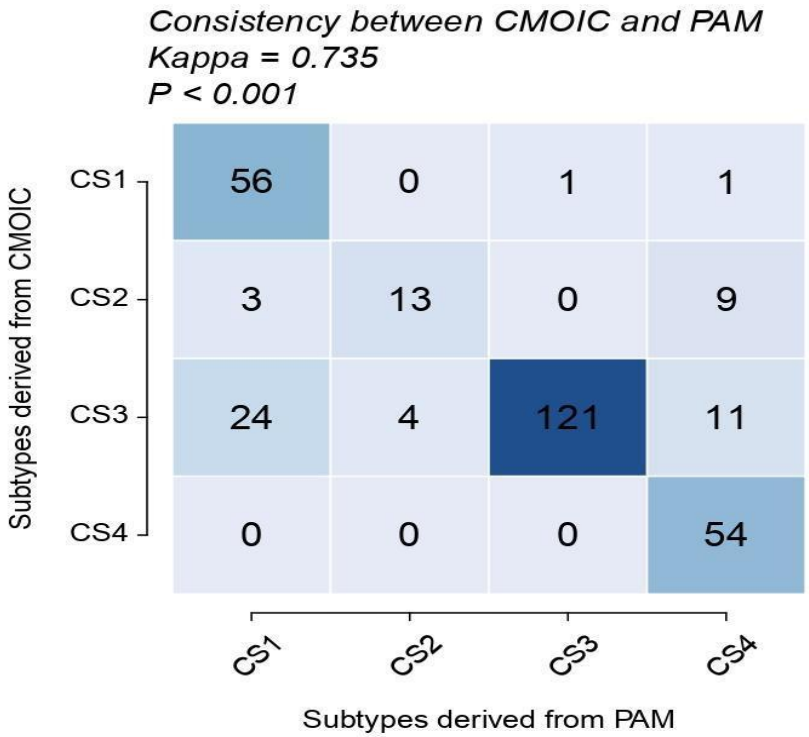


Figure 3.171. Consistency heatmap between current and PAM-predicted Kappa statistics for limma results in TCGA-COAD cohort.

Furthermore, if we examine the agreement between the subtypes recognised by NTP and PAM in the GEO dataset according to the results of edgeR and DESeq2, we find that the result of the kappa statistic is 0.451 and 0.528, respectively (Figures 3.172-3.173). In other words, the agreement between the subtypes identified by NTP and PAM in the validation dataset is categorised as moderate by edgeR and DESeq2.

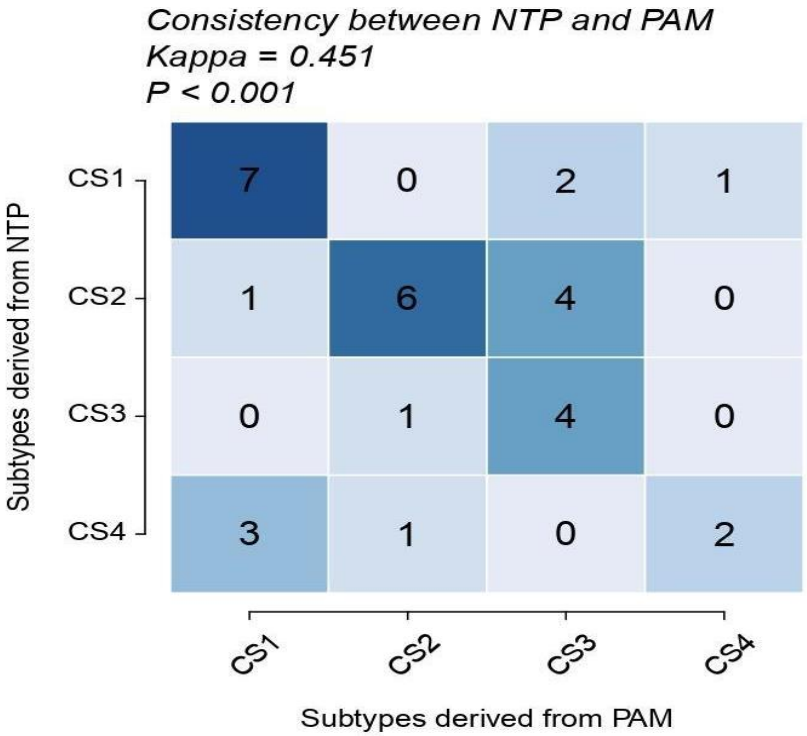


Figure 3.172. Consistency heatmap between NTP and PAM-predicted subtype for edgeR results in GSE16125.

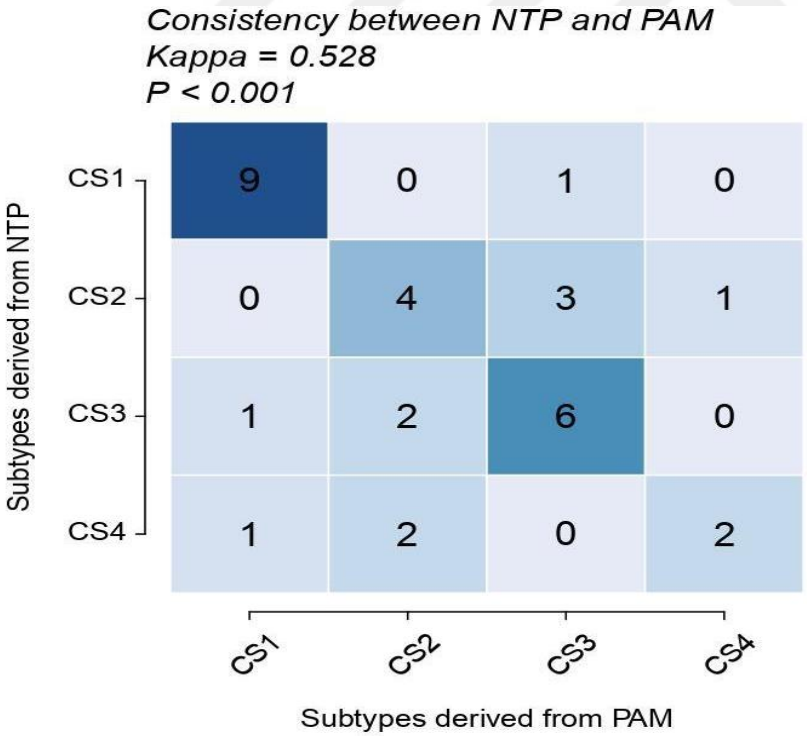


Figure 3.173. Consistency heatmap between NTP and PAM-predicted subtype for DESeq2 results in GSE16125.

To predict subtypes in the GSE39582 cohort, which consists of 562 samples, NTP was performed based on upregulated markers detected with edgeR, DESeq2 and limma in the discovery dataset. However, no matches based on the edgeR results were detected during the NTP analysis (Figure 3.174). In contrast, the NTP analysis performed with DESeq2 between the CS1, CS2, CS3 and CS4 subtypes compared 60, 8, 75 and 95 samples, respectively (Figure 3.175). In addition, NTP analysis using Limma revealed that 141, 0, 208 and 154 samples were matched in the CS1, CS2, CS3 and CS4 subtypes, respectively (Figure 3.176).

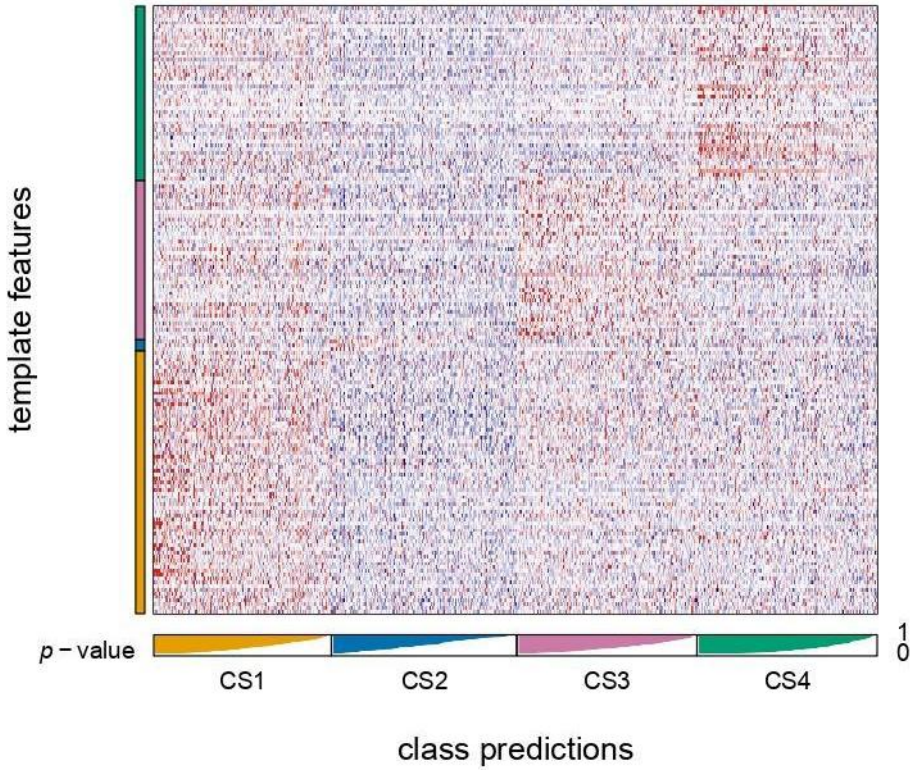


Figure 3.174. Heatmap of NTP in GSE39582 cohort using subtype-specific upregulated biomarkers identified using edgeR from TCGA-COAD cohort.

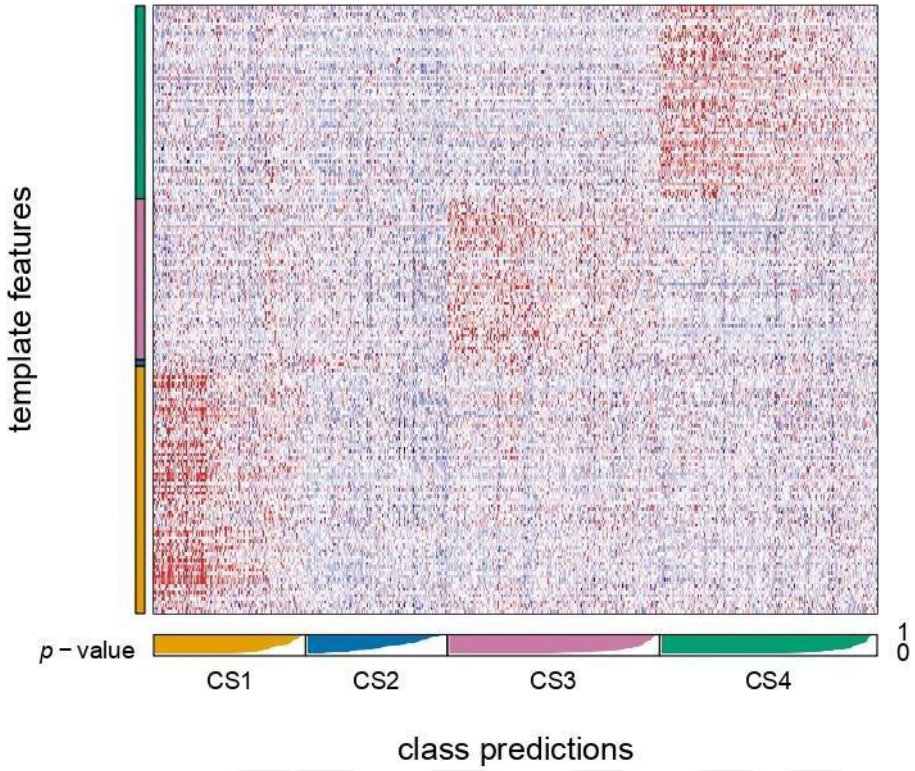


Figure 3.175. Heatmap of NTP in GSE39582 cohort using subtype-specific upregulated biomarkers identified using DESeq2 from TCGA-COAD cohort.

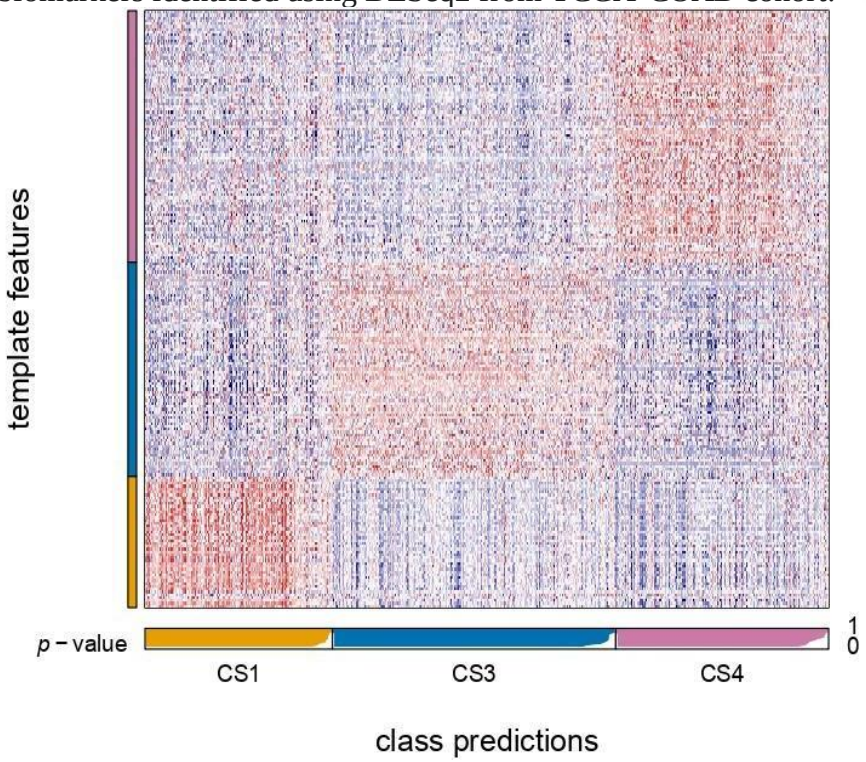


Figure 3.176. Heatmap of NTP in GSE39582 cohort using subtype-specific upregulated biomarkers identified using limma from TCGA-COAD cohort.

Survival analysis based on the results of edgeR, DESeq2 and limma in the GSE39582 cohort showed significant results with edgeR and DESeq2, while no statistically significant results were obtained with limma (Figures 3.177-3.179). For both algorithms, CS1 was the subtype with the worst prognosis.

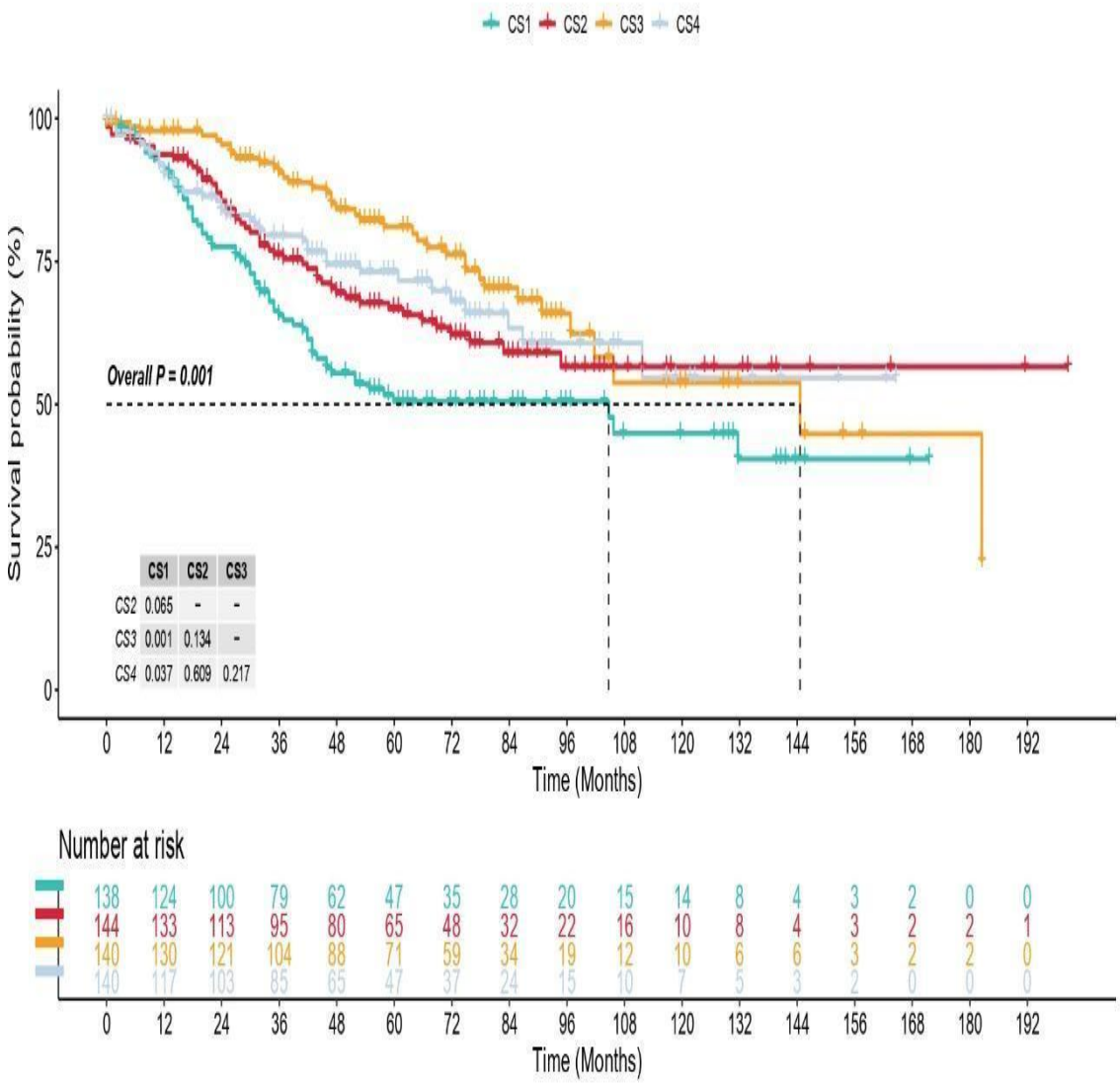


Figure 3.177. Kaplan-Meier survival curve of 4 colon adenocarcinoma subtypes predicted by edgeR in the GSE39582 cohort.

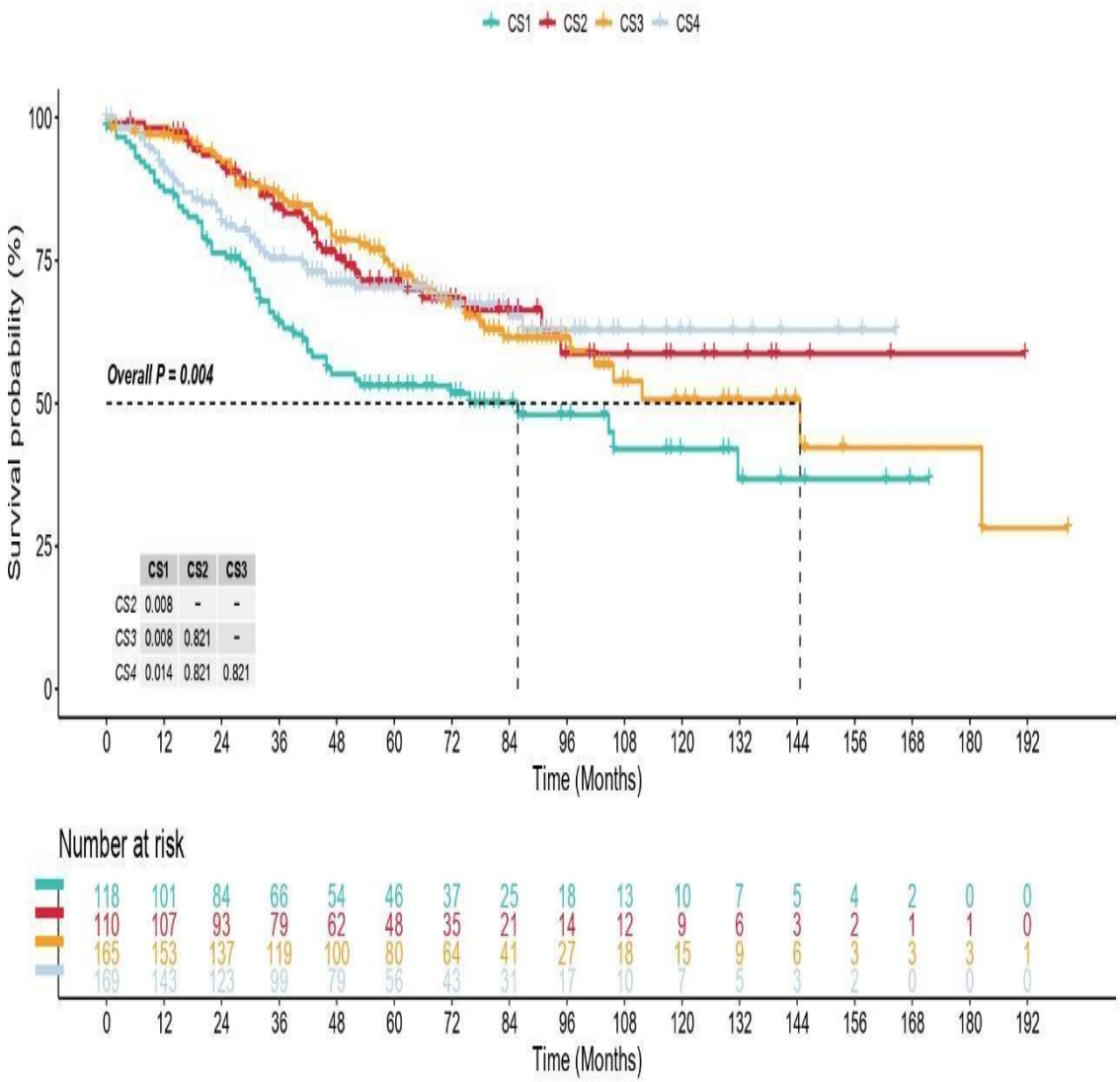


Figure 3.178. Kaplan-Meier survival curve of 4 colon adenocarcinoma subtypes predicted by DESeq2 in the GSE39582 cohort.

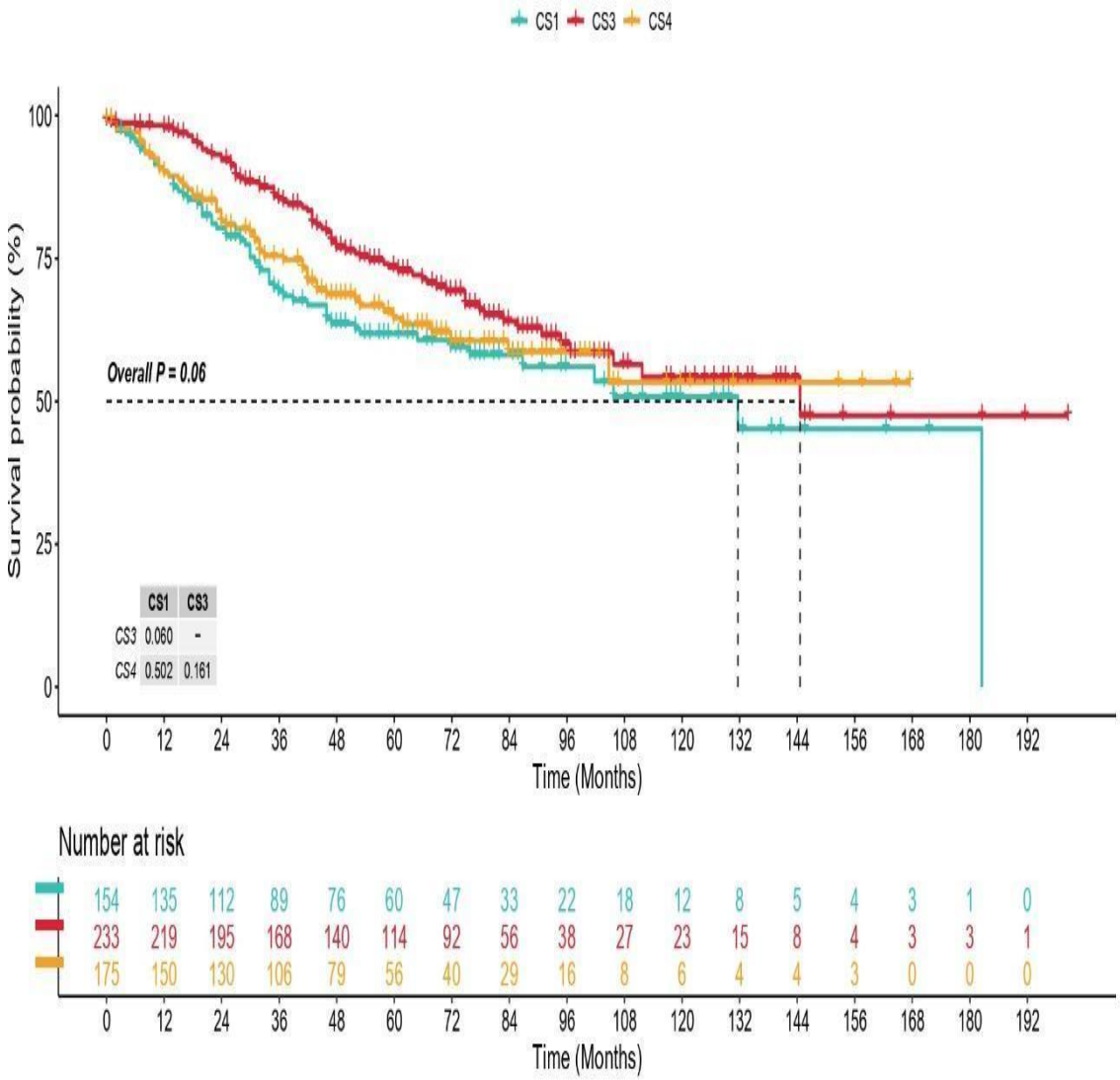


Figure 3.179. Kaplan-Meier survival curve of 4 colon adenocarcinoma subtypes predicted by limma in the GSE39582 cohort.

According to the IGP statistics obtained as a result of the PAM analysis of the GSE39582 cohort, the subtypes obtained between the discovery and validation groups were found to be similar and reproducible (Table 3.9).

According to the results of the three algorithms (Figures 3.180-3.185), the consistency between the subtypes found in the TCGA dataset and those predicted by PAM is much more significant than that predicted by NTP.

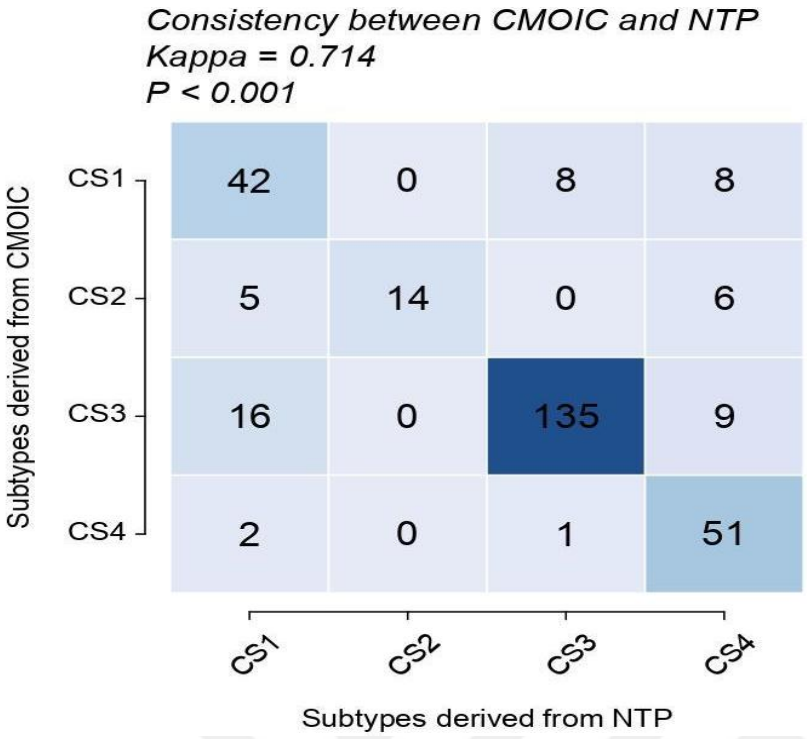


Figure 3.180. Consistency heatmap between current and NTP-predicted Kappa statistics for edgeR results in TCGA-COAD cohort.

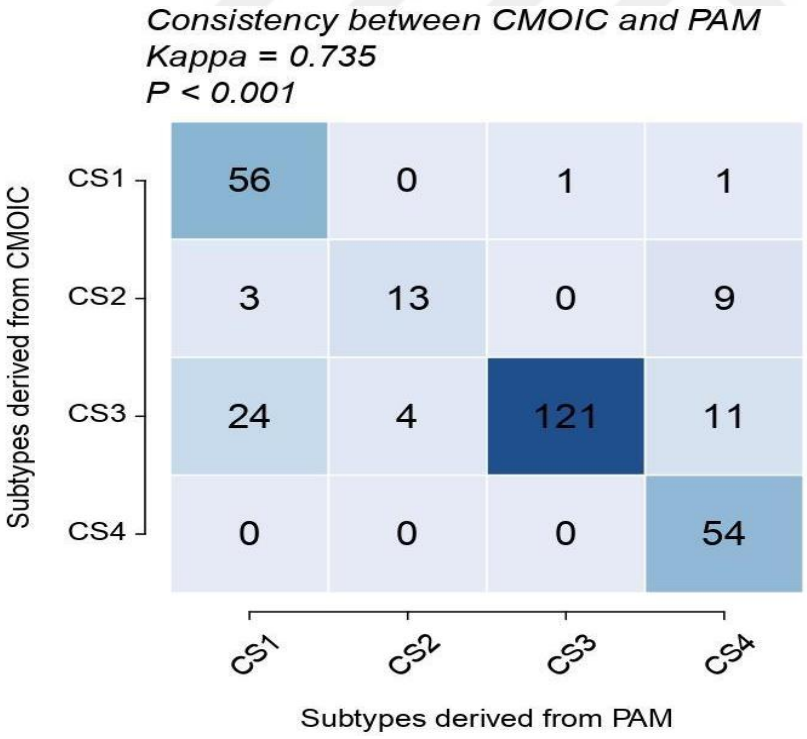


Figure 3.181. Consistency heatmap between current and PAM-predicted Kappa statistics for edgeR results in TCGA-COAD cohort.

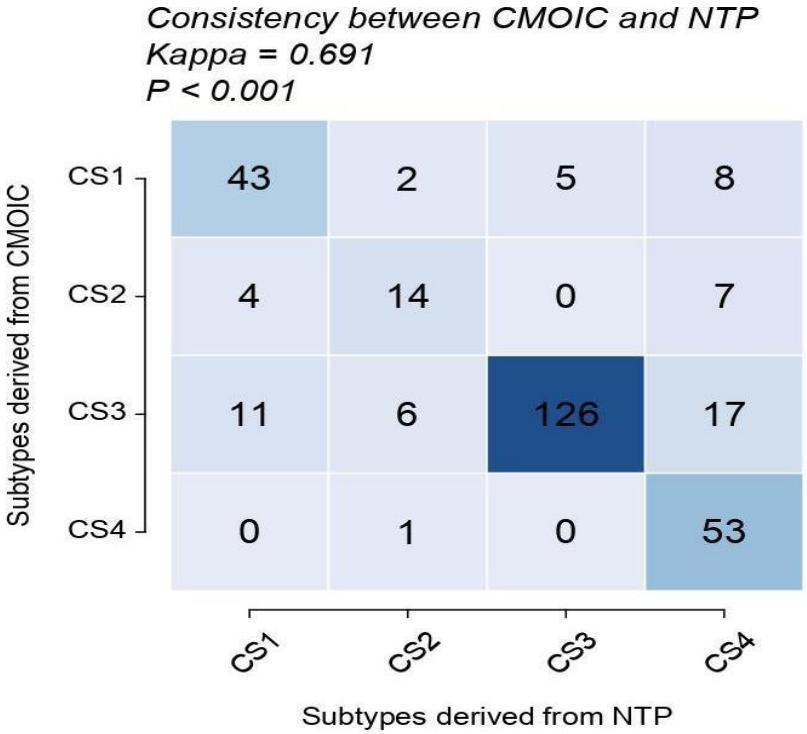


Figure 3.182. Consistency heatmap between current and NTP-predicted Kappa statistics for DESeq2 results in TCGA-COAD cohort.

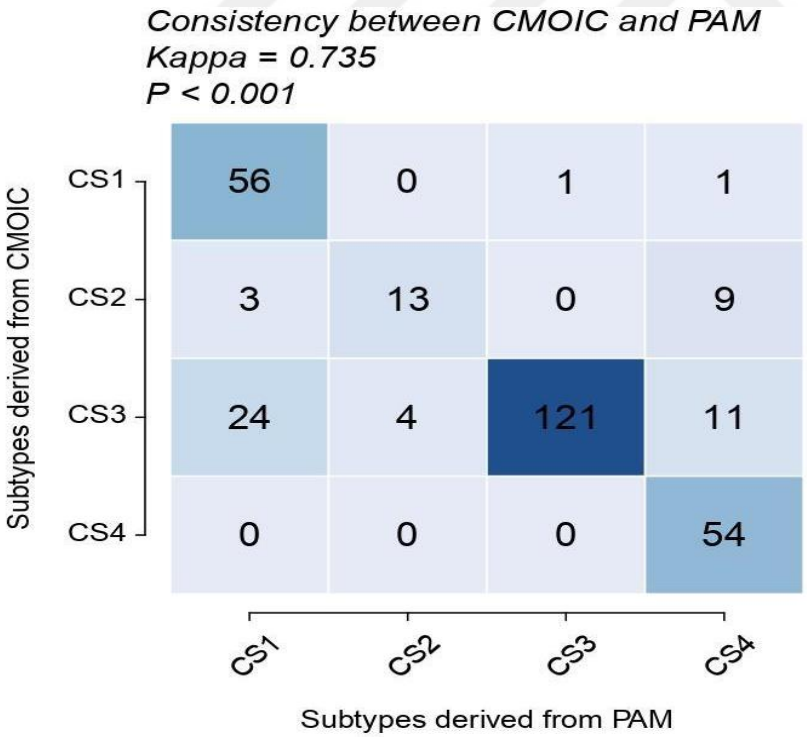


Figure 3.183. Consistency heatmap between current and PAM-predicted Kappa statistics for DESeq2 results in TCGA-COAD cohort.

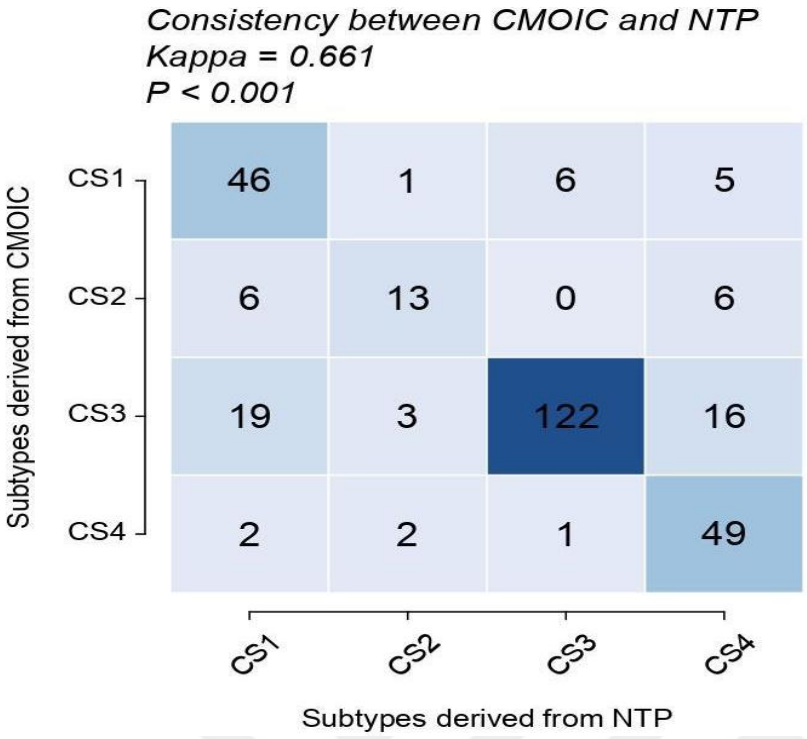


Figure 3.184. Consistency heatmap between current and NTP-predicted Kappa statistics for limma results in TCGA-COAD cohort.

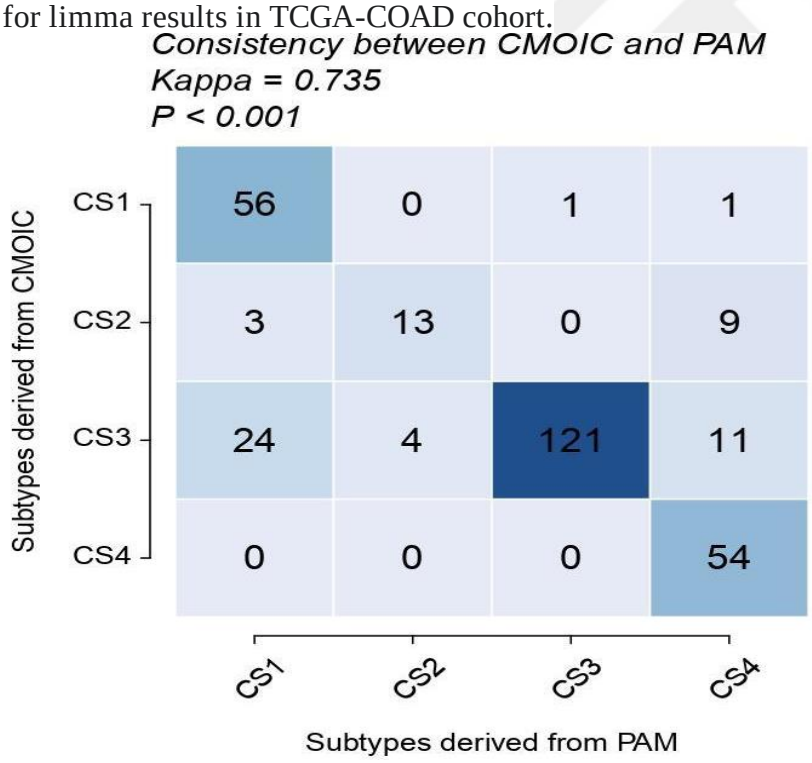


Figure 3.185. Consistency heatmap between current and PAM-predicted Kappa statistics for limma results in TCGA-COAD cohort.

In addition, the consistency results of the subtypes detected by NTP and PAM in the validation data set were best obtained with DESeq2 (0.322 and 0.499 for edgeR and DESeq2, respectively) (Figures 3.186-3.187).

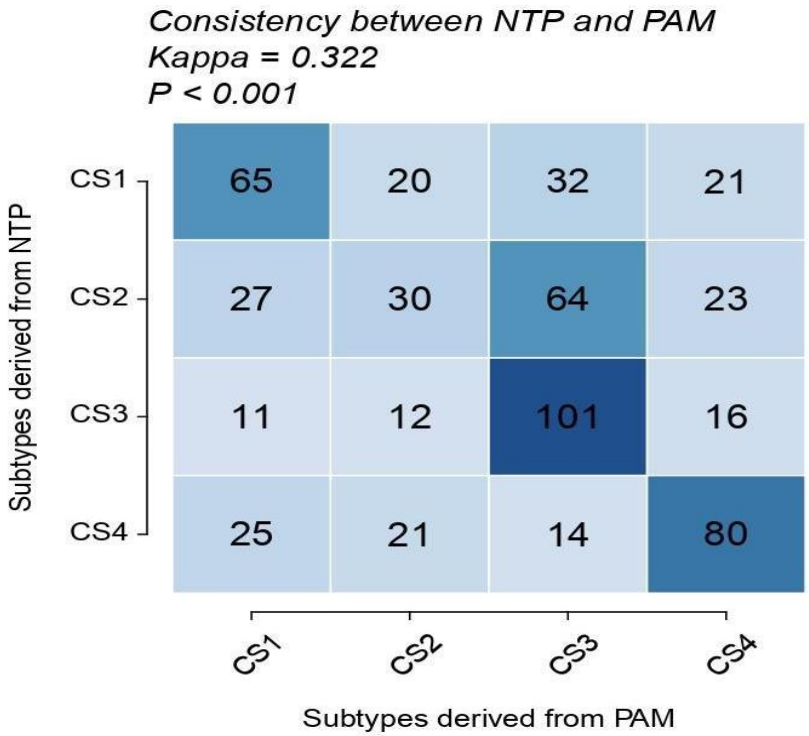


Figure 3.186. Consistency heatmap between NTP and PAM-predicted subtype for edgeR results in GSE39582.

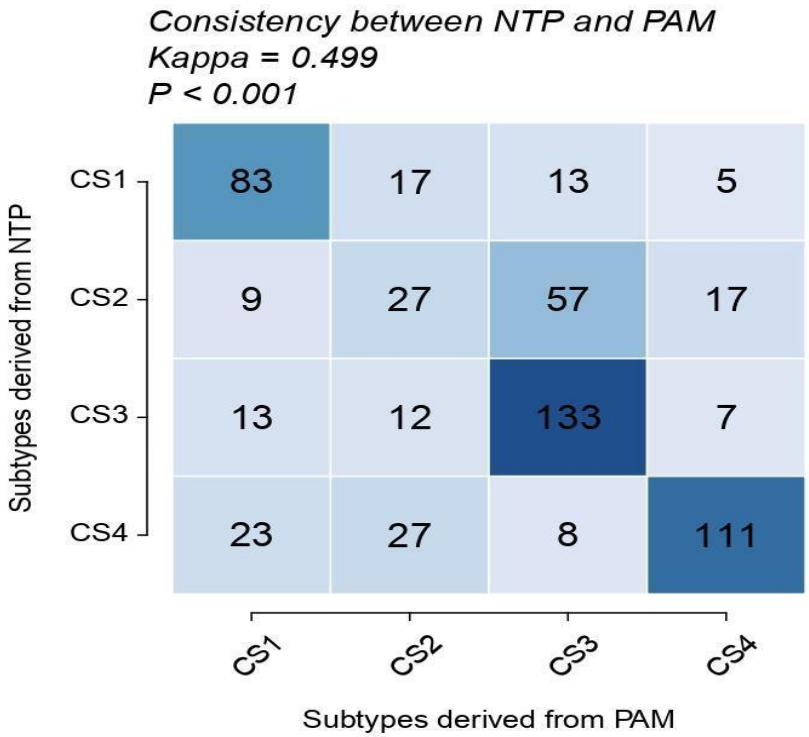


Figure 3.187. Consistency heatmap between NTP and PAM-predicted subtype for DESeq2 results in GSE39582.

To predict subtypes in the GSE1756 cohort, which consists of 177 samples, NTP was performed based on upregulated markers detected with edgeR, DESeq2 and limma in the discovery dataset. However, NTP analysis based on the use of biomarkers predicted with edgeR resulted in no sample in the GSE17536 dataset being assigned to a subspecies (Figure 3.188). On the other hand, NTP analysis using DESeq2 revealed that CS1, CS2, CS3 and CS4 subtypes matched 13, 5, 23 and 27 samples, respectively (Figure 3.189). In addition, NTP analysis with Limma showed that subtypes CS1, CS2, CS3 and CS4 matched 44, 0, 69 and 44 samples, respectively (Figure 3.190).

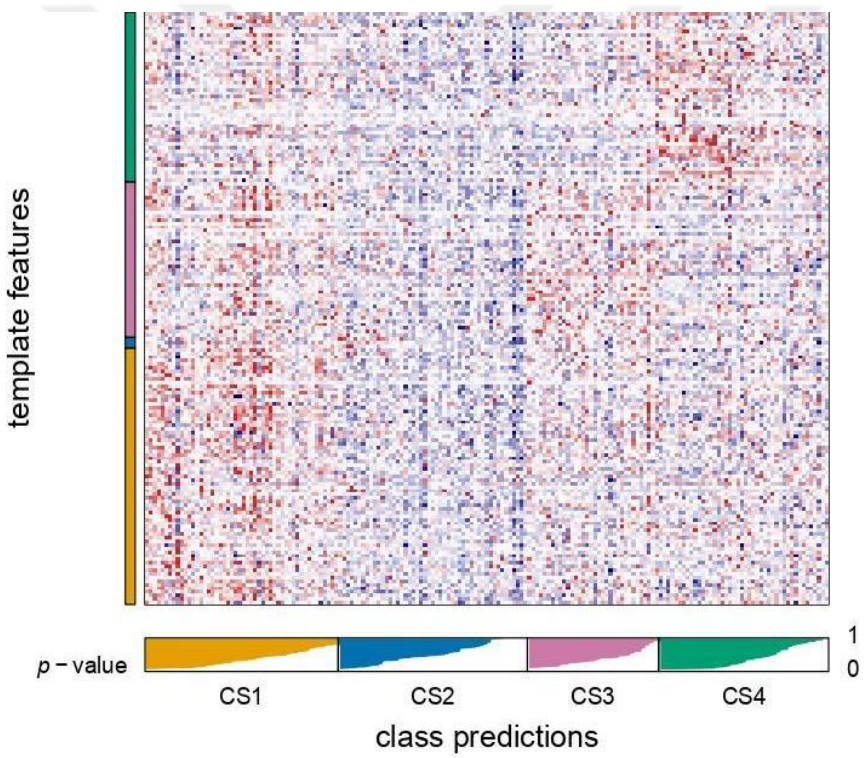


Figure 3.188. Heatmap of NTP in GSE17536 cohort using subtype-specific upregulated biomarkers identified using edgeR from TCGA-COAD cohort.

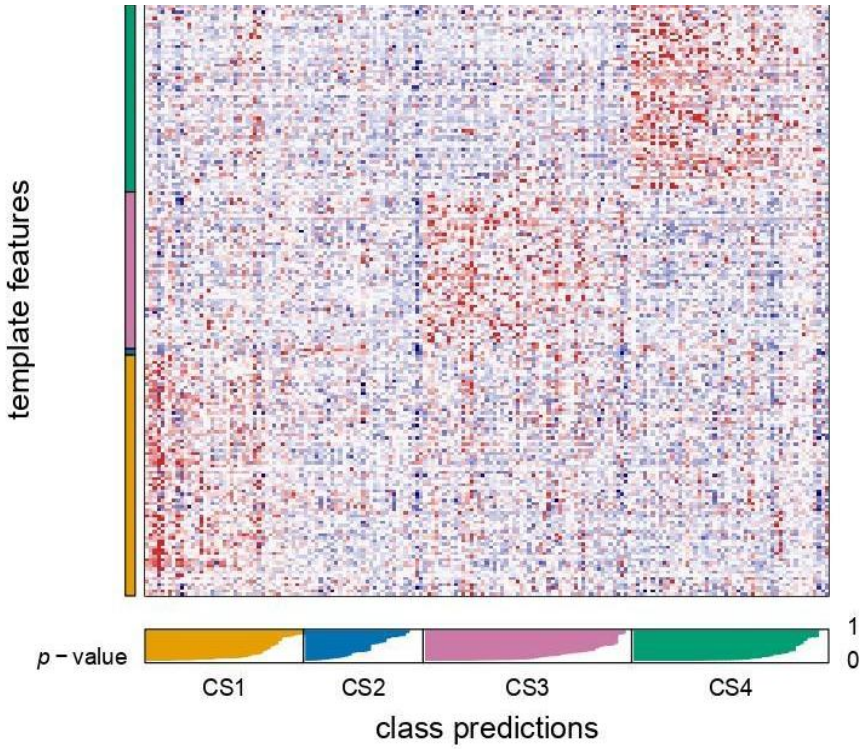


Figure 3.189. Heatmap of NTP in GSE17536 cohort using subtype-specific upregulated biomarkers identified using DESeq2 from TCGA-COAD cohort.

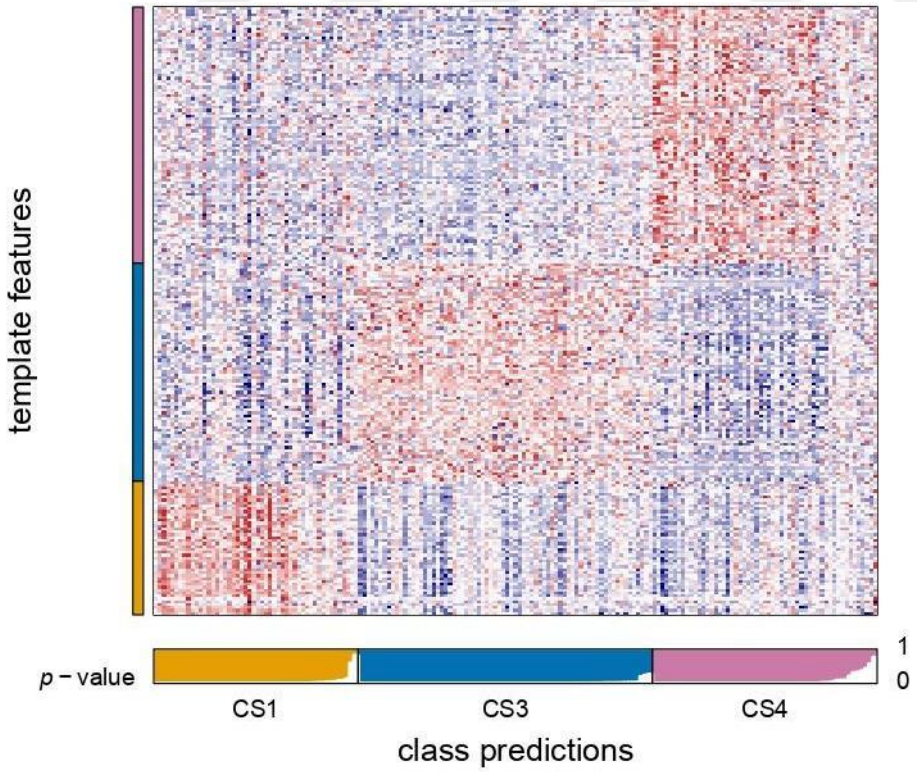


Figure 3.190. Heatmap of NTP in GSE17536 cohort using subtype-specific upregulated biomarkers identified using limma from TCGA-COAD cohort.

As a result of the survival analysis performed with edgeR, DESeq2 and limma in the GSE17536 cohort, a statistically significant difference was found only with limma (Figures 3.191-3.193). CS1 had the poorest prognosis.

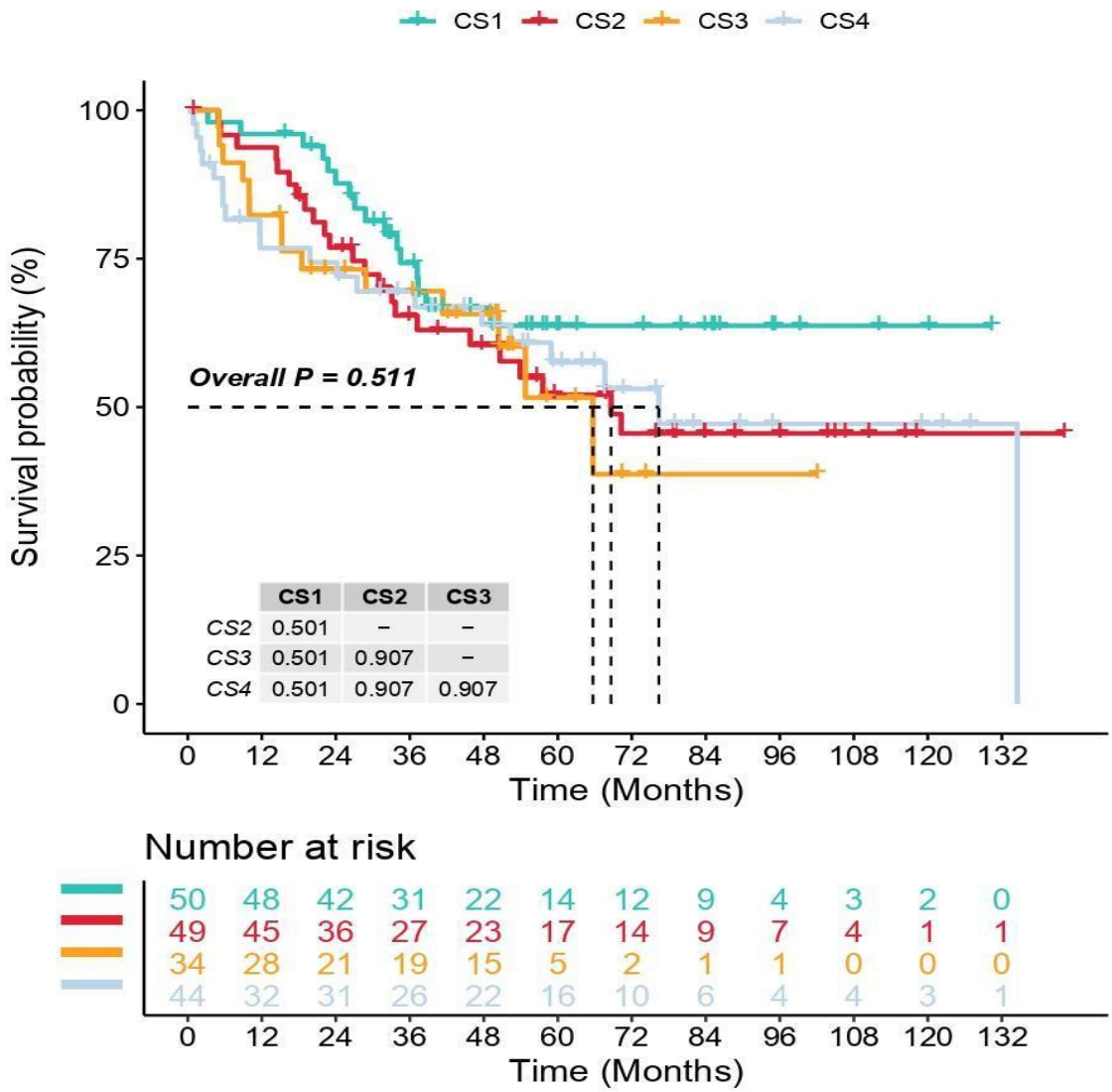


Figure 3.191. Kaplan-Meier survival curve of 4 colon adenocarcinoma subtypes predicted by edgeR in the GSE17536 cohort.

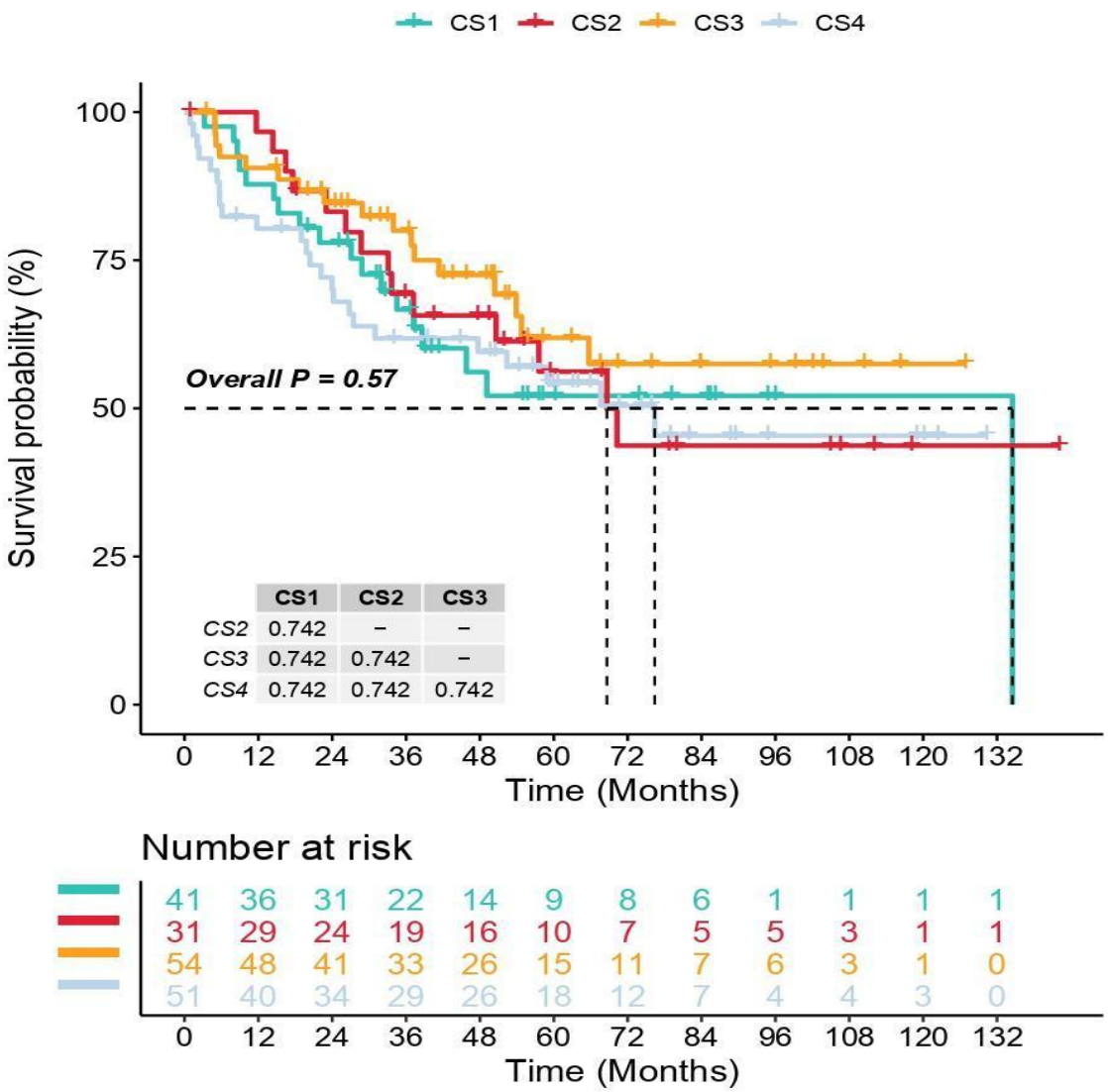


Figure 3.192. Kaplan-Meier survival curve of 4 colon adenocarcinoma subtypes predicted by DESeq2 in the GSE17536 cohort.

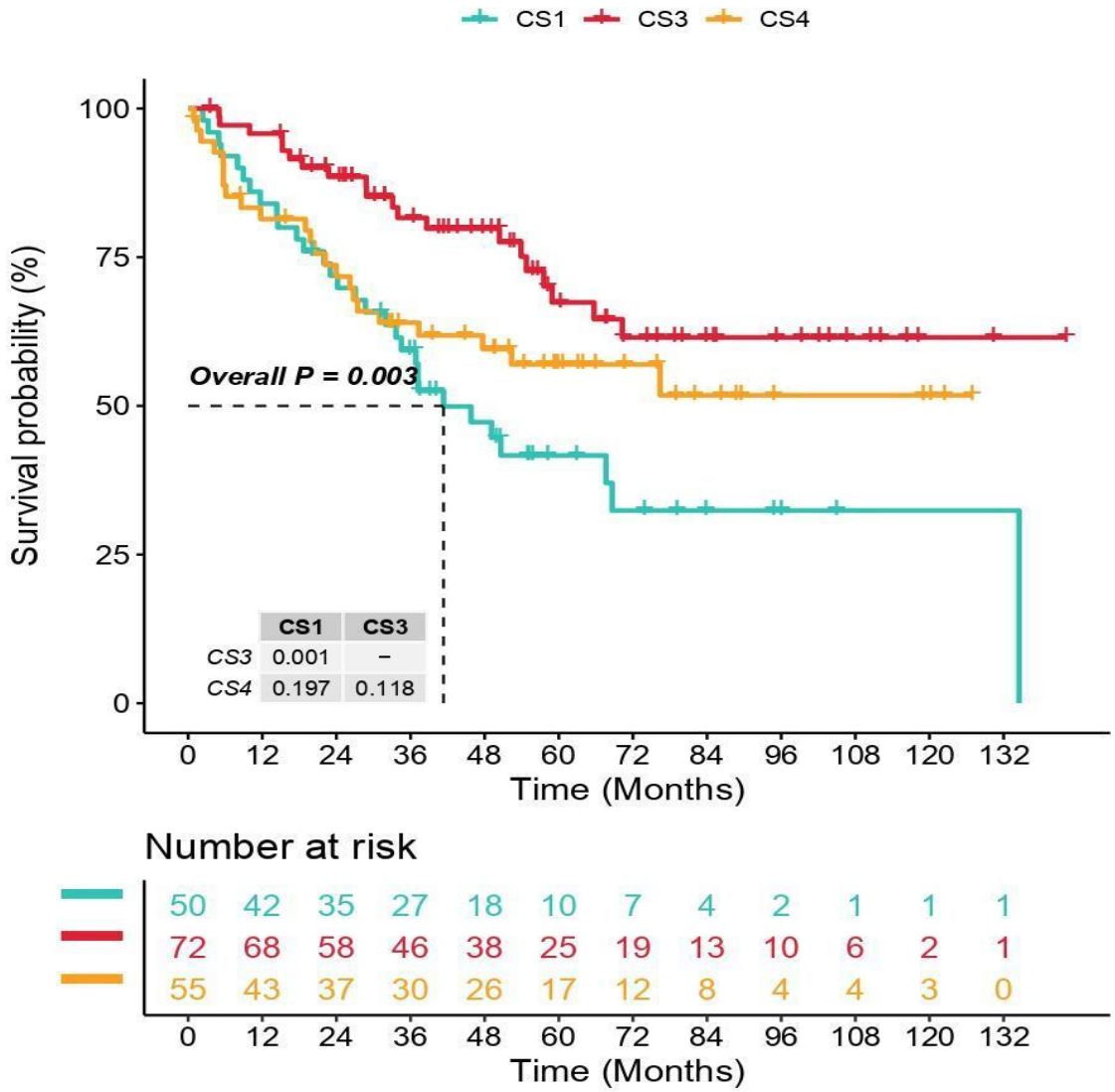


Figure 3.193. Kaplan-Meier survival curve of 4 colon adenocarcinoma subtypes predicted by limma in the GSE17536 cohort.

According to the IGP statistics obtained as a result of the PAM analysis of the GSE17536 cohort, the subtypes obtained between the discovery and validation groups were found to be similar and reproducible (Table 3.9).

According to the results of the three algorithms (Figures 3.194-3.199), the consistency between the subtypes found in the TCGA dataset and those predicted by PAM is much more significant than that predicted by NTP.

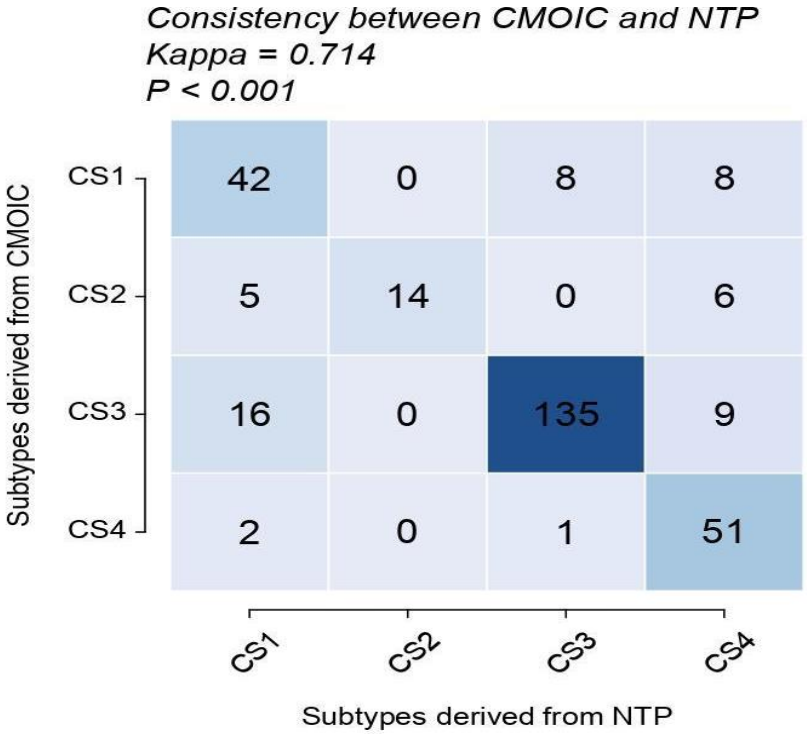


Figure 3.194. Consistency heatmap between current and NTP-predicted Kappa statistics for edgeR results in TCGA-COAD cohort.

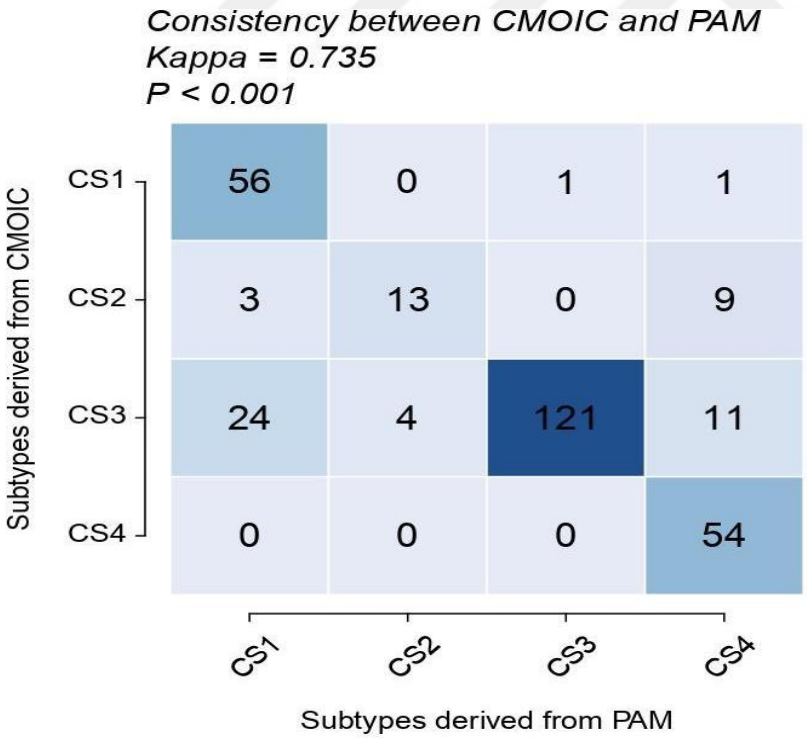


Figure 3.195. Consistency heatmap between current and PAM-predicted Kappa statistics for edgeR results in TCGA-COAD cohort.

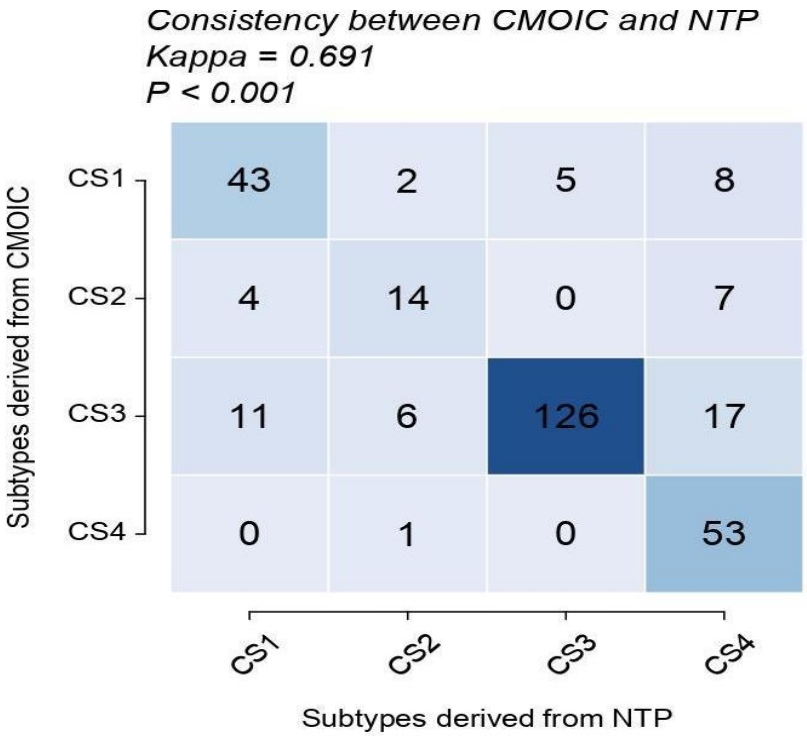


Figure 3.196. Consistency heatmap between current and NTP-predicted Kappa statistics for DESeq2 results in TCGA-COAD cohort.

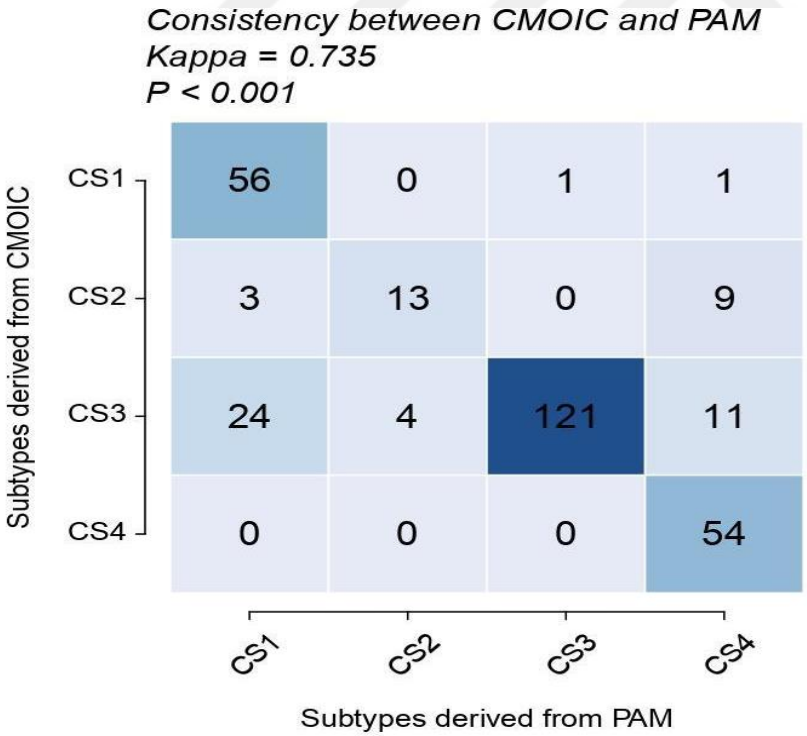


Figure 3.197. Consistency heatmap between current and PAM-predicted Kappa statistics for DESeq2 results in TCGA-COAD cohort.

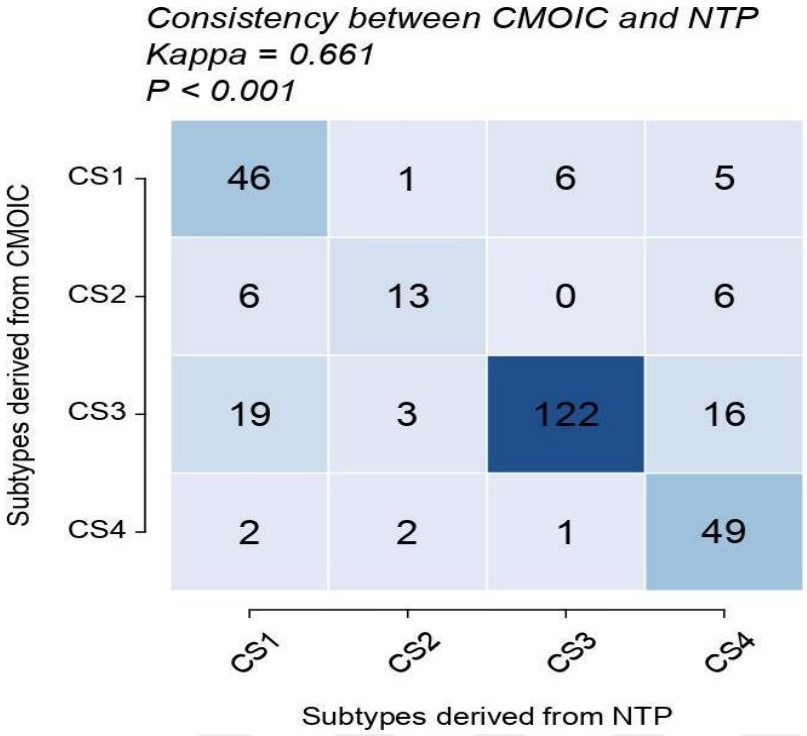


Figure 3.198. Consistency heatmap between current and NTP-predicted Kappa statistics for limma results in TCGA-COAD cohort.

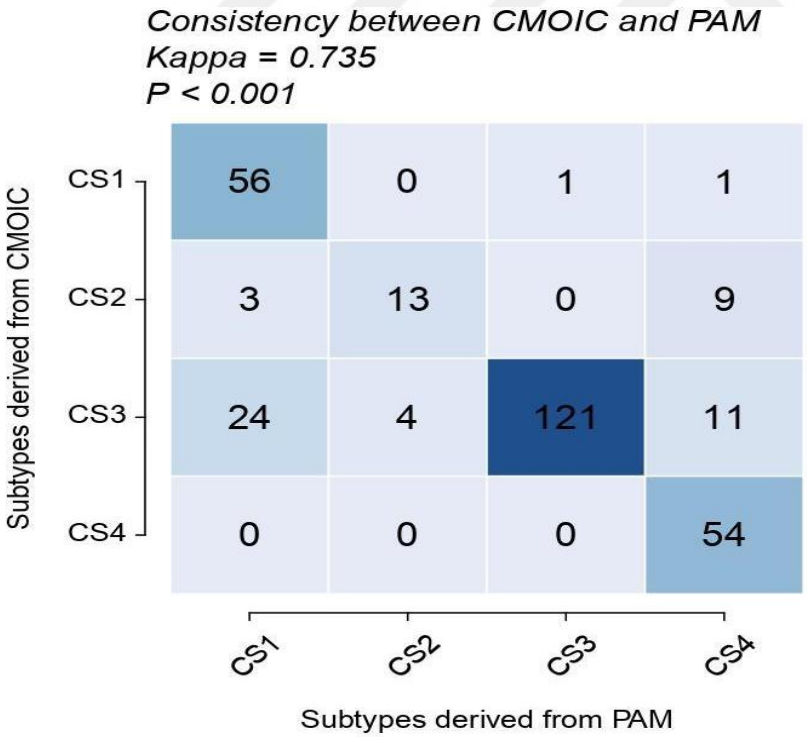


Figure 3.199. Consistency heatmap between current and PAM-predicted Kappa statistics for limma results in TCGA-COAD cohort.

In addition, the consistency results of the subtypes detected by NTP and PAM in the validation data set were best obtained with DESeq2 (0.250 and 0.408 for edgeR and DESeq2, respectively) (Figures 3.200-3.201).

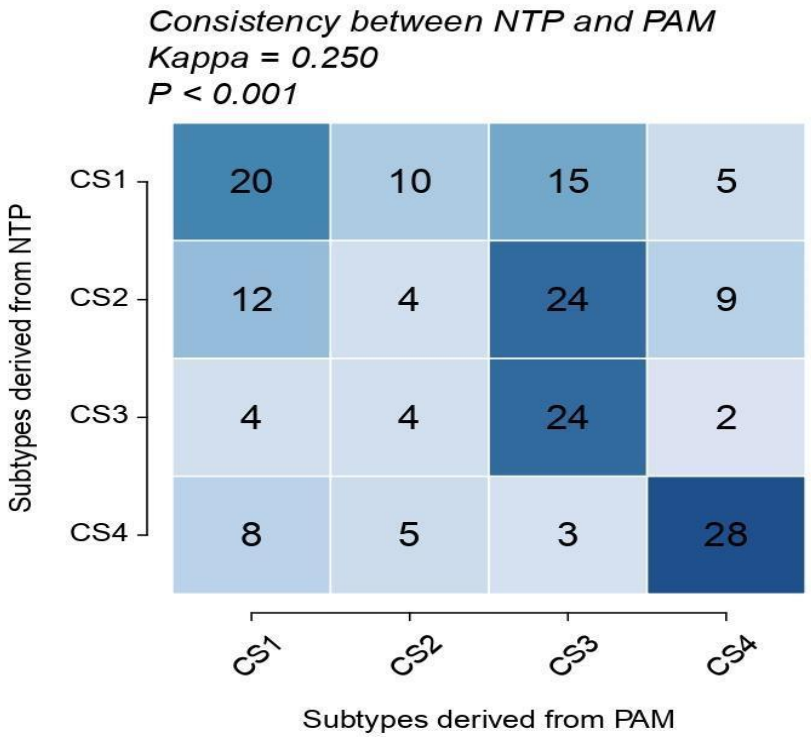


Figure 3.200. Consistency heatmap between NTP and PAM-predicted subtype for edgeR results in GSE17536.

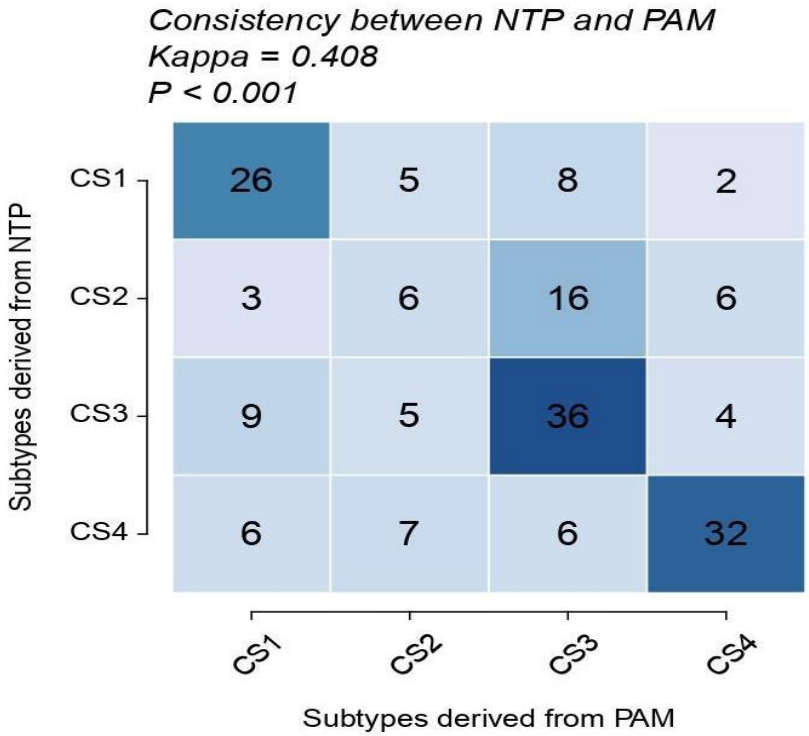


Figure 3.201. Consistency heatmap between NTP and PAM-predicted subtype for DESeq2 results in GSE17536.

To predict subtypes in the GSE17537 cohort, which consists of 55 samples, NTP was performed based on upregulated markers detected with edgeR, DESeq2 and limma in the discovery dataset. However, NTP analysis based on the use of biomarkers predicted with edgeR resulted in no sample in the GSE17536 dataset being assigned to a subspecies (Figure 3.202). On the other hand, NTP analysis using DESeq2 revealed that CS1, CS2, CS3 and CS4 subtypes matched 5, 0, 4 and 9 samples, respectively (Figure 3.203). In addition, NTP analysis with Limma revealed that subtypes CS1, CS2, CS3 and CS4 matched 14, 0, 19 and 16 samples, respectively (Figure 3.204).

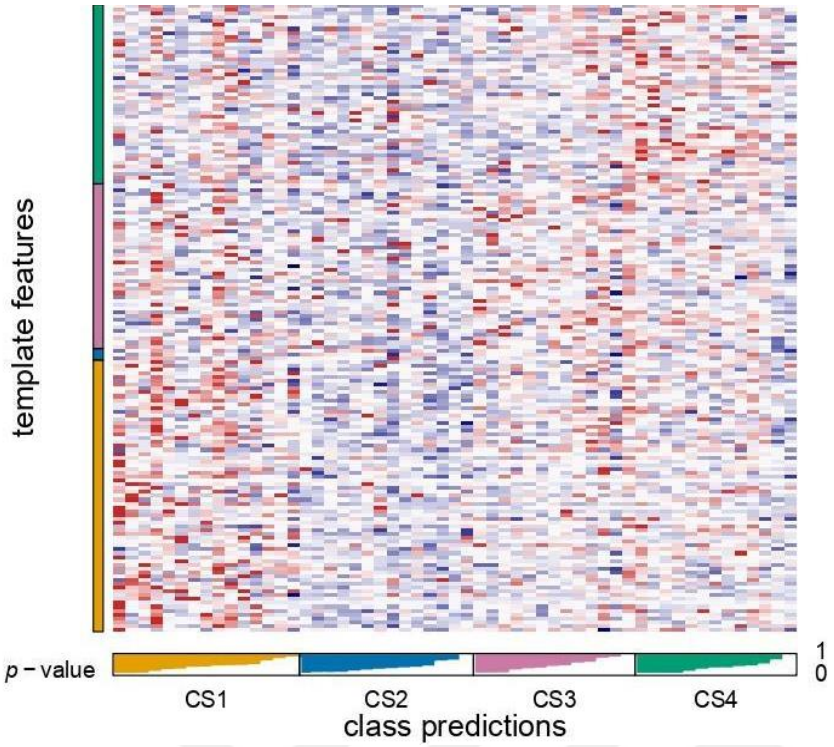


Figure 3.202. Heatmap of NTP in GSE17537 cohort using subtype-specific upregulated biomarkers identified using edgeR from TCGA-COAD cohort.

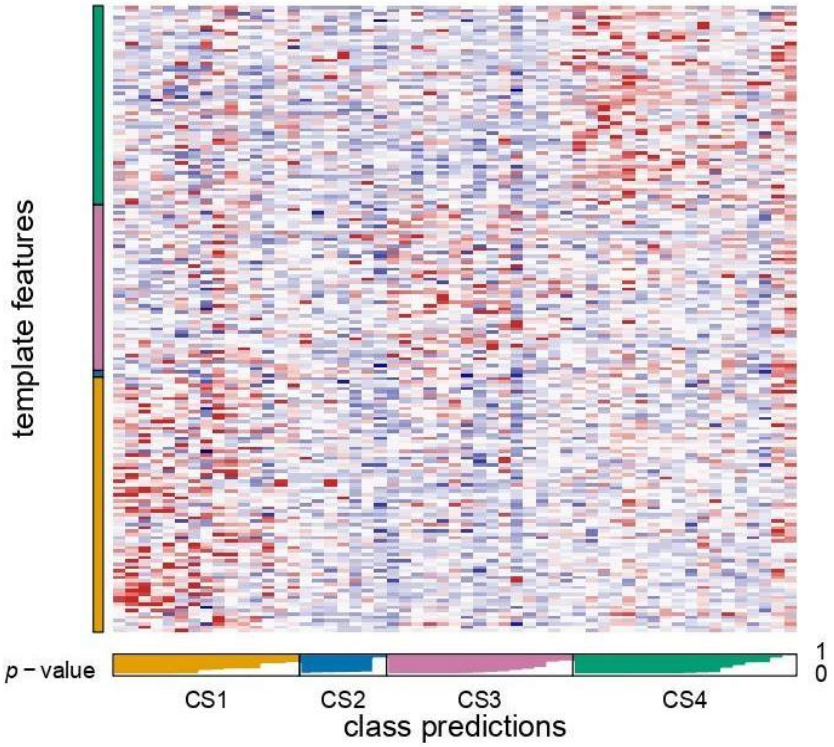


Figure 3.203. Heatmap of NTP in GSE17537 cohort using subtype-specific upregulated biomarkers identified using DESeq2 from TCGA-COAD cohort.

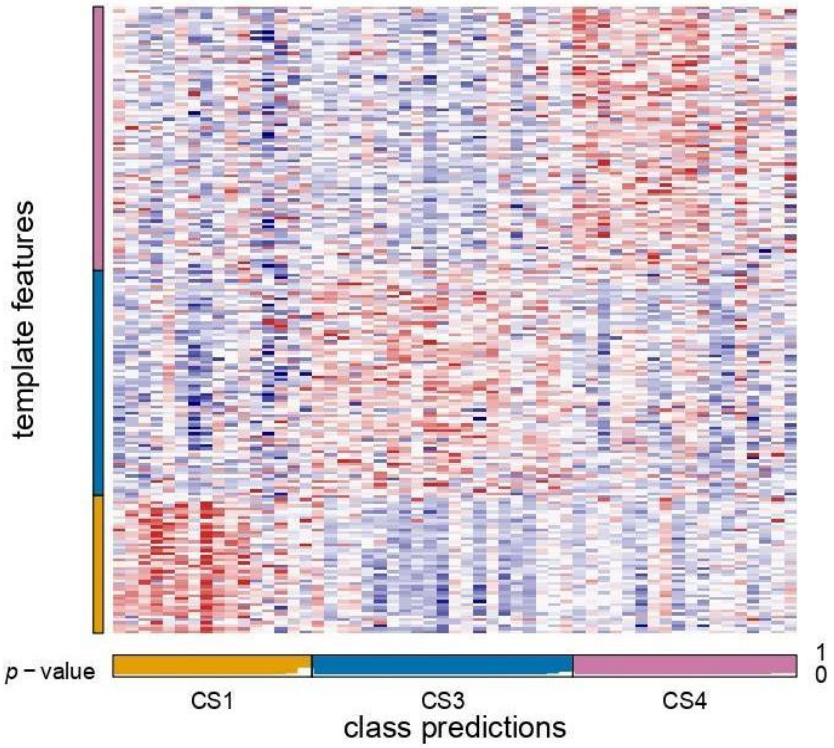


Figure 3.204. Heatmap of NTP in GSE17537 cohort using subtype-specific upregulated biomarkers identified using limma from TCGA-COAD cohort.

In the GSE17537 cohort, a survival analysis of the subtypes obtained by NTP was performed based on the results of edgeR, DESeq2 and limma. The result: While no statistically significant result was obtained with edgeR and DESeq2, a statistically significant result with a p-value of 0.052 was obtained with limma (Figure 3.205-3.207). CS1 showed the worst prognosis among the other subtypes.

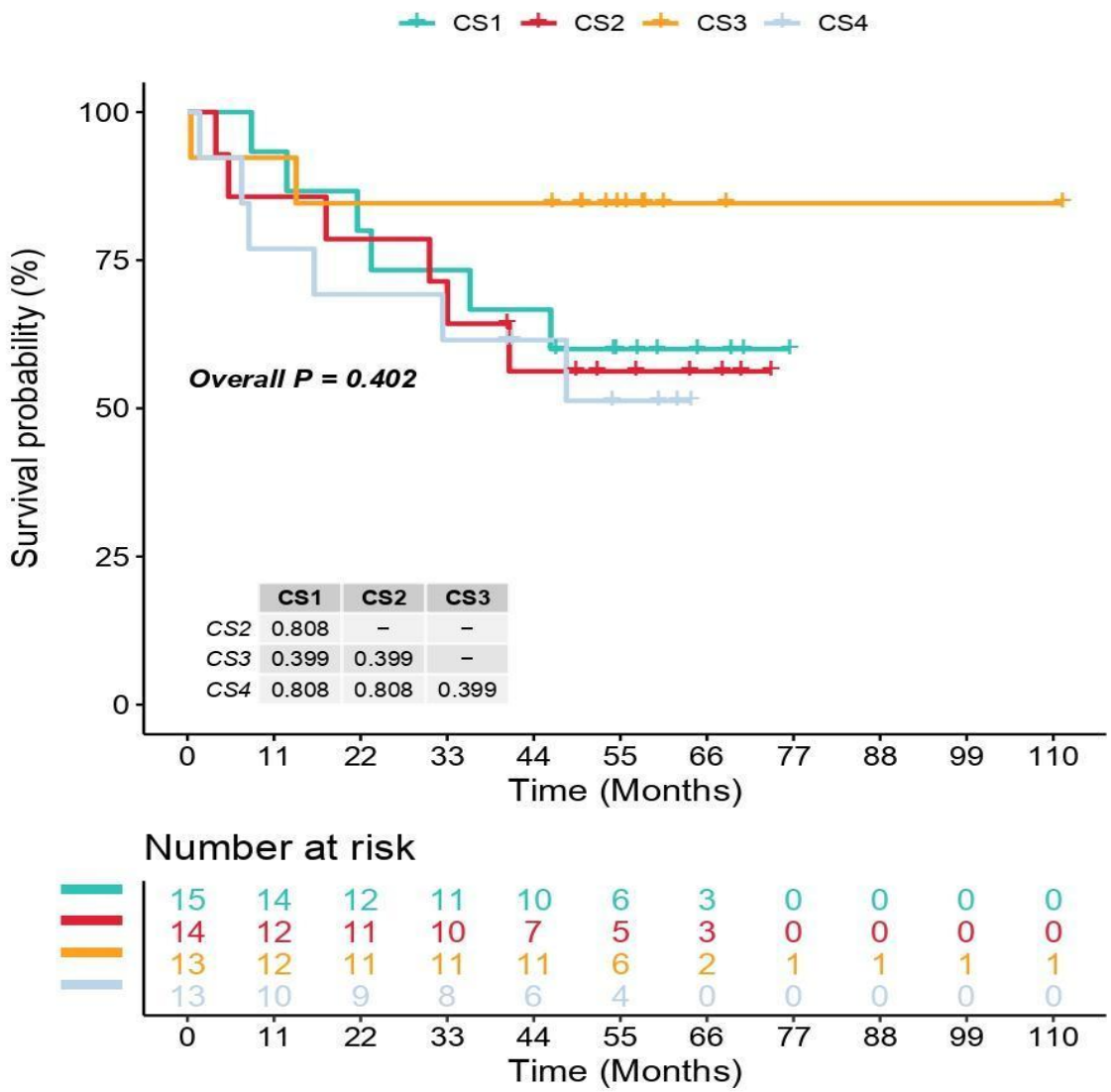


Figure 3.205. Kaplan-Meier survival curve of 4 colon adenocarcinoma subtypes predicted by edgeR in the GSE17537 cohort.

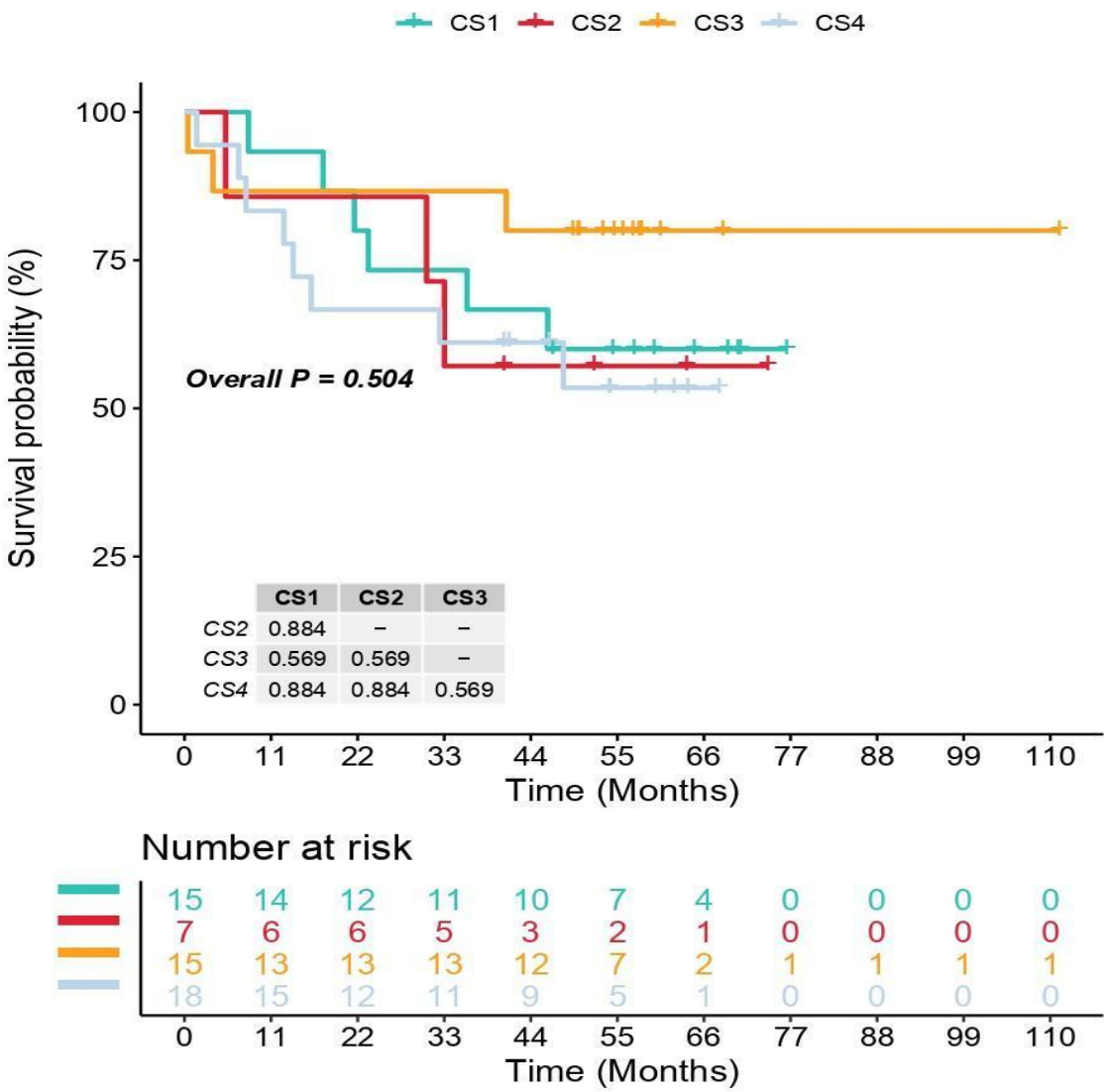


Figure 3.206. Kaplan-Meier survival curve of 4 colon adenocarcinoma subtypes predicted by DESeq2 in the GSE17537 cohort.

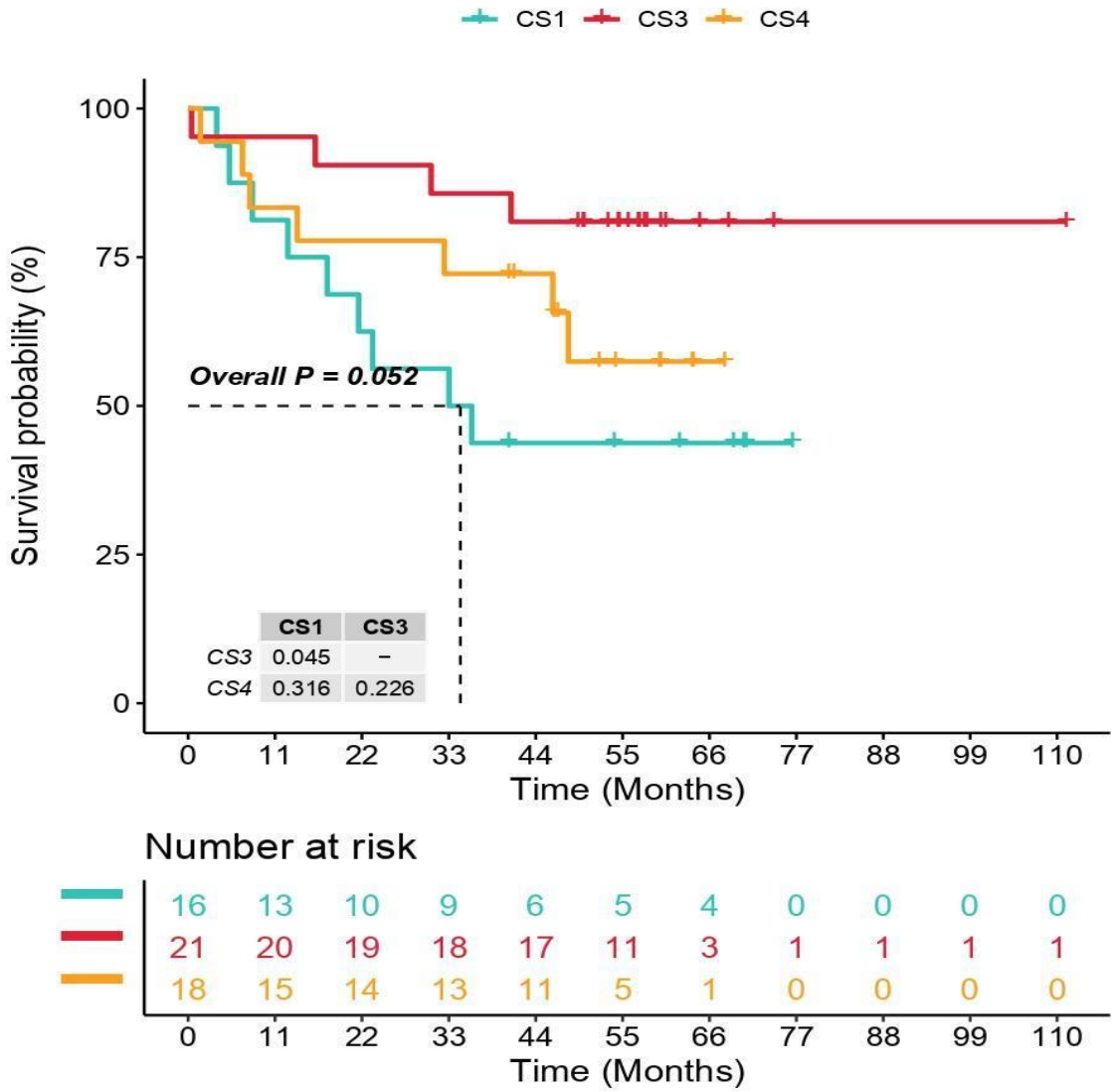


Figure 3.207. Kaplan-Meier survival curve of 4 colon adenocarcinoma subtypes predicted by limma in the GSE17537 cohort.

According to the IGP statistics obtained as a result of the PAM analysis of the GSE17537 cohort, the subtypes obtained between the discovery and validation groups were found to be similar and reproducible (Table 3.9).

According to the results of the three algorithms (Figures 3.208-3.213), the consistency between the subtypes found in the TCGA dataset and those predicted by PAM is much more significant than that predicted by NTP.

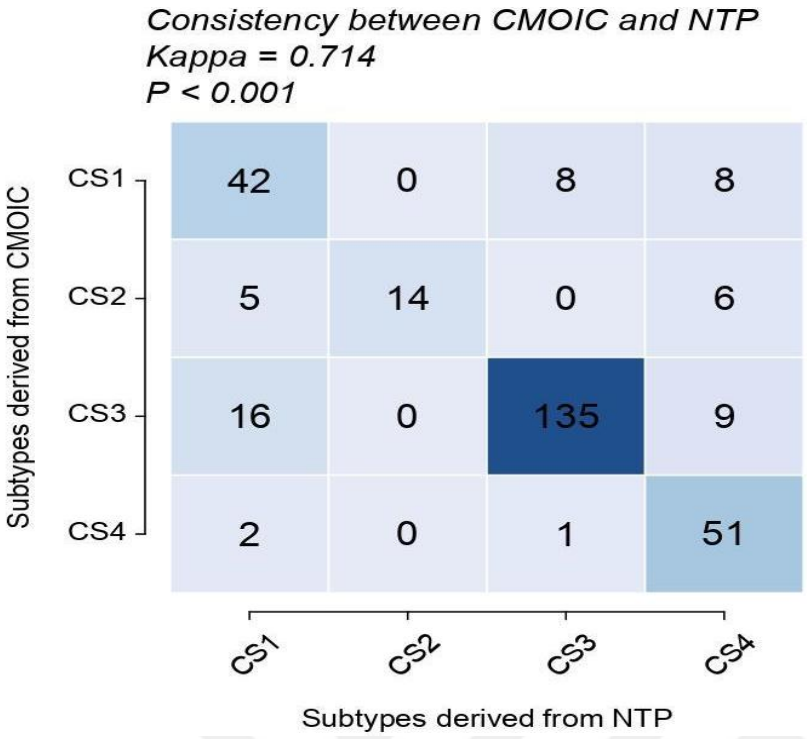


Figure 3.208. Consistency heatmap between current and NTP-predicted Kappa statistics for edgeR results in TCGA-COAD cohort.

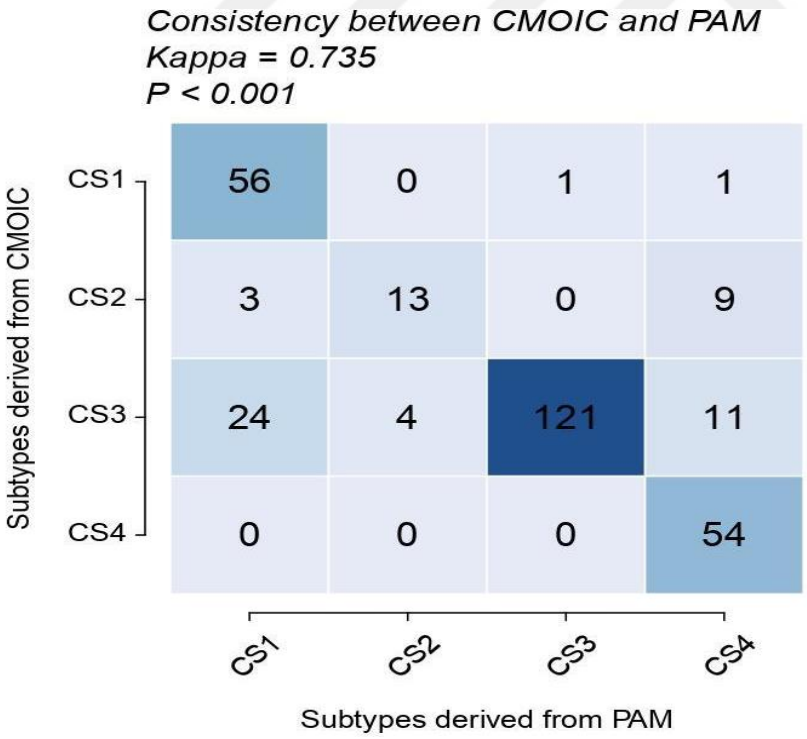


Figure 3.209. Consistency heatmap between current and PAM-predicted Kappa statistics for edgeR results in TCGA-COAD cohort.

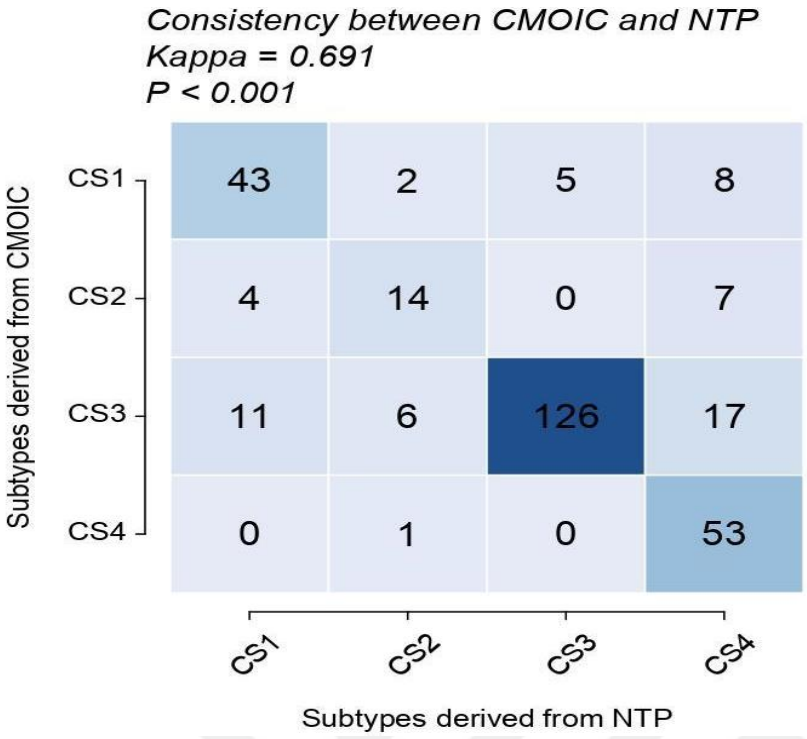


Figure 3.210. Consistency heatmap between current and NTP-predicted Kappa statistics for DESeq2 results in TCGA-COAD cohort.

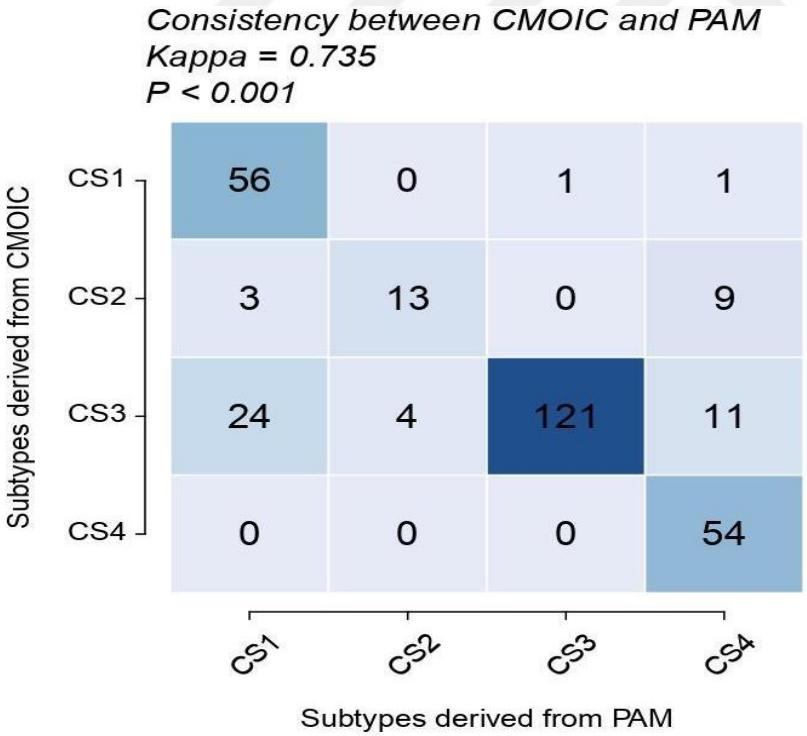


Figure 3.211. Consistency heatmap between current and PAM-predicted Kappa statistics for DESeq2 results in TCGA-COAD cohort.

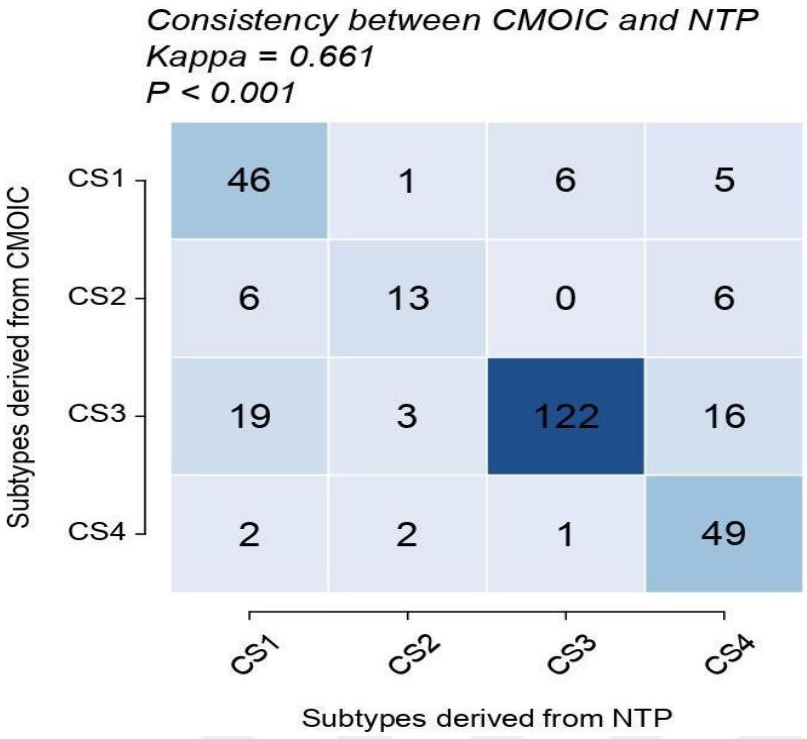


Figure 3.212. Consistency heatmap between current and NTP-predicted Kappa statistics for limma results in TCGA-COAD cohort.

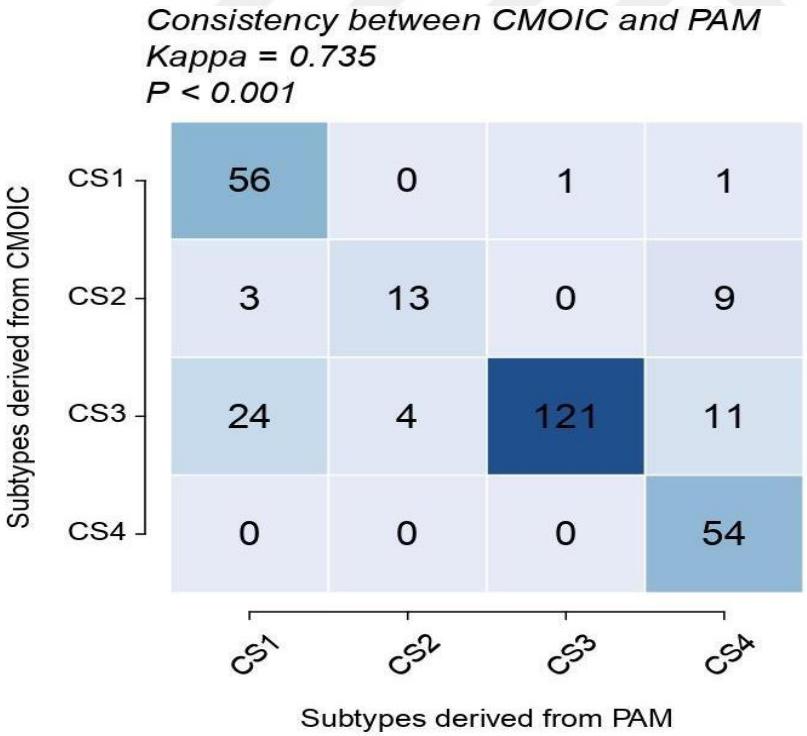


Figure 3.213. Consistency heatmap between current and PAM-predicted Kappa statistics for limma results in TCGA-COAD cohort.

In addition, the consistency results of the subtypes detected by NTP and PAM in the validation data set were best obtained with DESeq2 (0.301 and 0.501 for edgeR and DESeq2, respectively) (Figures 3.214-3.215).

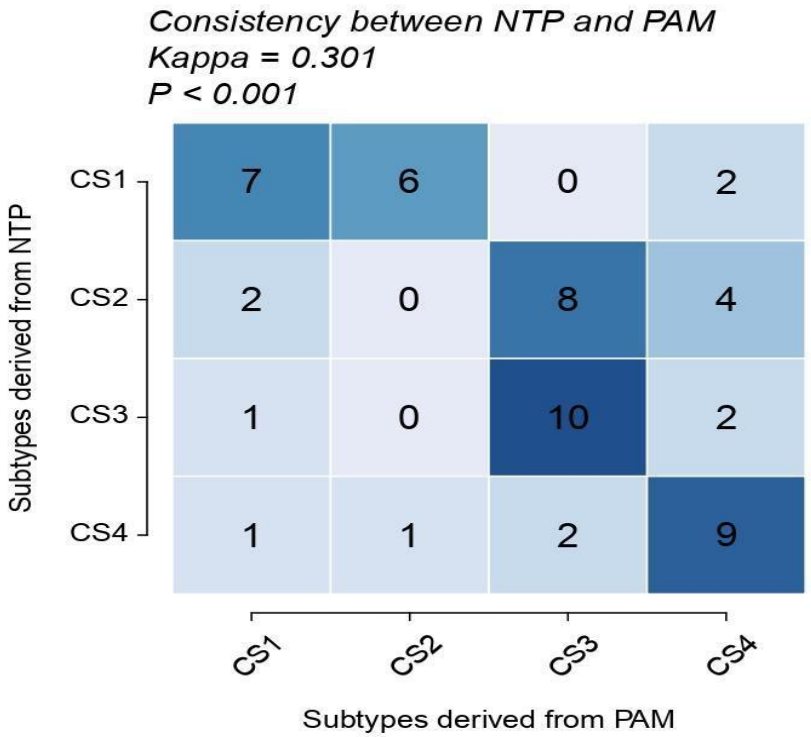


Figure 3.214. Consistency heatmap between NTP and PAM-predicted subtype for edgeR results in GSE17537.

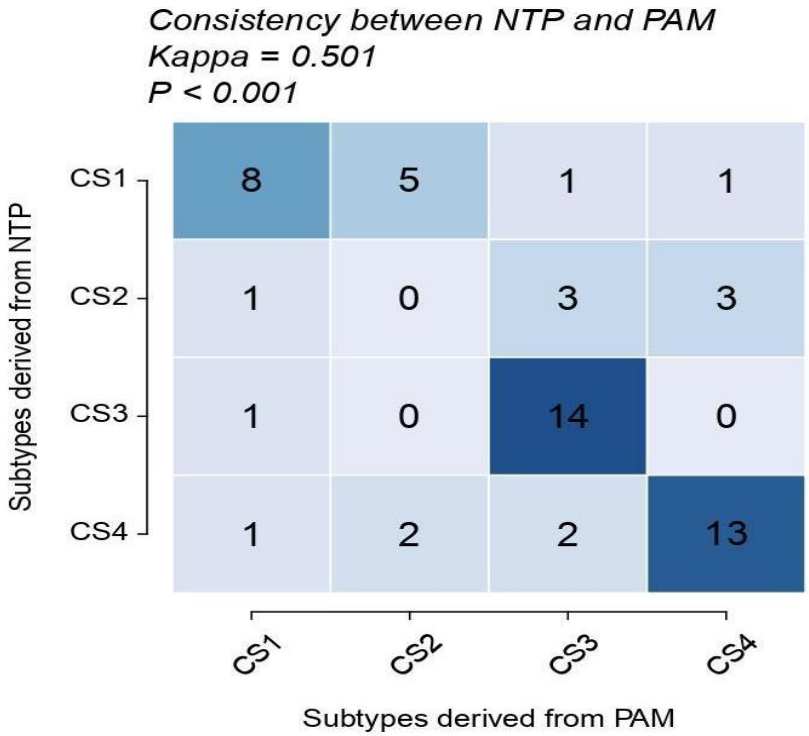


Figure 3.215. Consistency heatmap between NTP and PAM-predicted subtype for DESeq2 results in GSE17537.

4. CONCLUSIONS

The primary objective of this study was to systematically classify colon adenocarcinoma into subtypes using integrated clustering algorithms based on multi-omic data, aiming to comprehensively understand the molecular heterogeneity of the disease and tumorigenesis process, thereby contributing to the development of personalized treatment strategies. The detailed characterization of subtypes derived from the integration of three different omic levels provides valuable insights into the underlying biological mechanisms of colon adenocarcinoma. This approach lays the groundwork for identifying and developing innovative treatment strategies for patients with COAD. Various multi-omic data types, including mRNA, lncRNA, miRNA expressions, DNA methylation, somatic mutations, and copy number alterations, were utilized for comprehensive molecular characterization of colon adenocarcinoma. These data were sourced from extensive databases such as The Cancer Genome Atlas (TCGA) and Gene Expression Omnibus (GEO). In the study, a consensus clustering approach incorporating the "MOVICS" R package and different integrated clustering algorithms was employed to stratify COAD patients into specific subtypes. The obtained subtypes were characterized through extensive analyses, and a detailed investigation was conducted based on identified molecular markers and functional signaling pathways. Additionally, the response of each subtype to approved chemotherapeutic agents was evaluated. Furthermore, an assessment was made on subtypes potentially sensitive to immunotherapy based on mutation rates. These analyses have contributed to the determination of personalized treatment strategies for COAD patients and the development of effective treatment options. Finally, a separate validation cohort was utilized to confirm the discovered subtypes, and the consistency and reproducibility of the obtained results were evaluated.

In the study, clustering analysis was conducted for the subtyping of colon adenocarcinoma, considering both the obtained subtyping results and important conditions of colon cancer while determining the optimal number of clusters. As a result, three different scenarios were considered, examining 2, 3, and 4 subtypes. The results revealed differences in mRNA, lncRNA, miRNA, methylation, and mutation profiles for each subtype in all three scenarios. Particularly, APC mutation emerged as the most

frequent mutation, showing statistically significant differences among subtypes in all scenarios. However, when clinically evaluated, stage-dependent differences were observed only in the scenario with 4 subtyping. Additionally, statistically significant responses to drug treatments such as 5-fluorouracil, cisplatin, paclitaxel, SN-38, rapamycin, and imatinib were observed in all three different scenarios. Validation analyses confirmed the accuracy of the obtained findings.

The findings obtained have significant implications in the diagnosis and treatment process of colon cancer. Determining molecular subtypes serves as a crucial tool in predicting patient prognosis and responses to treatment. These analyses aid in better understanding the underlying biological mechanisms of the disease, facilitating improved disease classification and the development of personalized treatment strategies based on patients' molecular profiles. Moreover, due to the complex nature of colon cancer, conducting molecular subtyping analyses across multiple omic levels enables a better understanding of the disease's complexity and underlying biological mechanisms. Such integrative analyses allow us to examine the interaction between different omic data types and their contribution to the disease process. In particular, the finding of frequent APC mutation and its association with other mutations provides new insights into the pathogenesis of colon cancer and may contribute to the development of targeted treatment approaches. In this study, three different widely used differential expression analysis algorithms were utilized to identify biomarkers across different omic dimensions with high sensitivity, which play a critical role in the diagnosis and treatment process of the disease. Biomarkers in colon cancer play a significant role in diagnosis, prognosis, and treatment processes. They are utilized to better understand the biological characteristics and molecular subtypes of the disease, contributing to the development of personalized treatment strategies. Through biomarkers, treatment responses can be predicted in advance based on specific genetic or molecular characteristics, thereby enabling the identification of more effective treatment options and minimizing side effects. Therefore, the discovery of promising new biomarkers is a valuable tool in disease management, providing valuable information to increase patient survival and improve treatment outcomes from early diagnosis to treatment, they provide valuable information. These findings represent a significant milestone in colon cancer treatment and patient management. Furthermore, investigating the different responses of subtypes to chemotherapeutic drugs plays a

critical role in determining treatment options for patients. The sensitivity of specific subtypes to certain drugs allows for their preference and enhances treatment success. Similarly, examining factors influencing response to immunotherapy plays a crucial role in determining patient sensitivity to this treatment and in developing treatment plans. These findings may lead to better patient response to treatment and more effective disease control, potentially changing the paradigms in colon cancer treatment. Understanding the different responses of specific subtypes to different drugs is crucial for personalizing treatment plans for patients. Examining the effects of different chemotherapeutic drugs on subtypes beyond traditionally used drugs allows for the expansion of treatment options and the development of more specific treatment plans tailored to the patient's molecular characteristics. Similarly, investigating factors influencing response to immunotherapy contributes to the emergence of a new perspective in colon cancer treatment and plays a crucial role in treatment planning. Overall, these findings may contribute to more effective disease control in colon cancer. Identifying specific genetic or molecular characteristics that enhance response to immunotherapy in subtypes may encourage the development of new therapeutic approaches targeting these factors. Therefore, all these findings contribute significantly to determining future directions in colon cancer treatment, enabling the use of more effective treatment options and minimizing side effects in patients with specific subtypes. These findings may lead to the development of new approaches in colon cancer treatment and better treatment of patients.

The findings obtained from the discovery dataset were analyzed using a validation dataset, and it was concluded that the results were repeatable and consistent. The computational validation of the reliability of the findings indicates that the study is based on a robust methodology. Analyses conducted using the validation dataset have increased the reliability of the findings obtained from the discovery dataset. The repeatability of the findings supports the reliability of the study's results and is an important step in confirming the accuracy of the findings obtained during the discovery phase. However, one of the fundamental limitations of the study is that the obtained findings have not been validated in a wet lab environment. This uncertainty regarding the clinical applicability and real-world usability of the findings underscores the need for future research to support the discovered findings with wet lab experiments. Therefore, in future research, validating

the discovered findings with wet lab experiments will be a crucial step towards the clinical usability of the obtained findings.

The topics addressed in this study form an important foundation for future research. Firstly, there is a need for more in-depth analyses on the identification of molecular subtypes and their impact on colon cancer treatment. Particularly, it is important to further examine the biological characteristics of the identified subtypes and their effects on disease prognosis. Additionally, the clinical applicability of the discovered molecular biomarkers needs to be evaluated. Determining the role of these biomarkers in the diagnosis, prognosis, and prediction of response to treatment in colon cancer can facilitate better management and treatment of patients. Finally, more research focusing on the role of immunotherapy in colon cancer treatment is essential. Specifically, identifying factors that influence the response to immunotherapy in different subtypes and gaining a better understanding of sensitivity to this treatment are crucial. This could provide patients with access to more effective and personalized treatment options, ultimately improving treatment outcomes.

In conclusion, this study has contributed to the comprehensive investigation of the complex molecular nature of colon cancer and the identification of personalized treatment options. The findings have provided significant opportunities for managing patients' clinical courses and optimizing therapeutic interventions. Future research should conduct more detailed studies to further advance the clinical applicability of these molecular subtypes and optimize treatment strategies. In this context, the discovery of new biomarkers and therapeutic targets in colon cancer treatment can fill important gaps in disease management and contribute to the development of more effective treatment approaches.

REFERENCES

1. Kahai, P., et al., *Anatomy, Abdomen and Pelvis: Large Intestine,* in *StatPearls*. 2023, StatPearls Publishing

Copyright © 2023, StatPearls Publishing LLC.: Treasure Island (FL).

2. Mishra, J., et al., *Prospective of colon cancer treatments and scope for combinatorial approach to enhanced cancer cell apoptosis.* Crit Rev Oncol Hematol, 2013. 86(3): p. 232-50.

3. Marley, A.R. and H. Nan, *Epidemiology of colorectal cancer.* Int J Mol Epidemiol Genet, 2016. 7(3): p. 105-114.

4. Keum, N. and E. Giovannucci, *Global burden of colorectal cancer: emerging trends, risk factors and prevention strategies.* Nat Rev Gastroenterol Hepatol, 2019. 16(12): p. 713-732.

5. Fleming, M., et al., *Colorectal carcinoma: Pathologic aspects.* J Gastrointest Oncol, 2012. 3(3): p. 153-73.

6. Lotfollahzadeh, S., A. Recio-Boiles, and B. Cagir, *Colon Cancer*, in *StatPearls*. 2023, StatPearls Publishing

Copyright © 2023, StatPearls Publishing LLC.: Treasure Island (FL).

7. Lichtenstein, P., et al., *Environmental and heritable factors in the causation of cancer--analyses of cohorts of twins from Sweden, Denmark, and Finland.* N Engl J Med, 2000. 343(2): p. 78-85.

8. Grady, W.M., *Genetic testing for high-risk colon cancer patients.* Gastroenterology, 2003. 124(6): p. 1574-94.

9. Jasperson, K.W., et al., *Hereditary and familial colon cancer.* Gastroenterology, 2010. 138(6): p. 2044-58.

10. Graff, R.E., et al., *Familial Risk and Heritability of Colorectal Cancer in the Nordic Twin Study of Cancer.* Clin Gastroenterol Hepatol, 2017. 15(8): p. 1256-1264.

11. Conteduca, V., et al., *Precancerous colorectal lesions (Review).* Int J Oncol, 2013. 43(4): p. 973-84.

12. Carethers, J.M. and B.H. Jung, *Genetics and Genetic Biomarkers in Sporadic Colorectal Cancer.* Gastroenterology, 2015. 149(5): p. 1177-1190.e3.

13. Vaseghi Maghvan, P., et al., *Personalized medicine in colorectal cancer.* Gastroenterol Hepatol Bed Bench, 2020. 13(Suppl1): p. S18-s28.

14. Buikhuisen, J.Y., A. Torang, and J.P. Medema, *Exploring and modelling colon cancer inter-tumour heterogeneity: opportunities and challenges.* Oncogenesis, 2020. 9(7): p. 66.

15. Ewing, I., et al., *The molecular genetics of colorectal cancer.* Frontline Gastroenterol, 2014. 5(1): p. 26-30.

16. Dey, A., et al., *Recent Advancements, Limitations, and Future Perspectives of the use of Personalized Medicine in Treatment of Colon Cancer.* Technol Cancer Res Treat, 2023. 22: p. 15330338231178403.

17. Slattery, M.L., *Diet, lifestyle, and colon cancer.* Semin Gastrointest Dis, 2000. 11(3): p. 142-6.

18. Sung, H., et al., *Global Cancer Statistics 2020: GLOBOCAN Estimates of Incidence and Mortality Worldwide for 36 Cancers in 185 Countries.* CA Cancer J Clin, 2021. 71(3): p. 209-249.

19. Xi, Y. and P. Xu, *Global colorectal cancer burden in 2020 and projections to 2040.* Transl Oncol, 2021. 14(10): p. 101174.

20. Siegel, R.L., et al., *Colorectal cancer statistics, 2023.* CA Cancer J Clin, 2023. 73(3): p. 233-254.

21. Rawla, P., T. Sunkara, and A. Barsouk, *Epidemiology of colorectal cancer: incidence, mortality, survival, and risk factors.* Prz Gastroenterol, 2019. 14(2): p. 89-103.

22. Arnold, M., et al., *Global patterns and trends in colorectal cancer incidence and mortality.* Gut, 2017. 66(4): p. 683-691.

23. Koncina, E., et al., *Prognostic and Predictive Molecular Biomarkers for Colorectal Cancer: Updates and Challenges.* Cancers (Basel), 2020. 12(2).

24. Krasteva, N. and M. Georgieva, *Promising Therapeutic Strategies for Colorectal Cancer Treatment Based on Nanomaterials.* Pharmaceutics, 2022. 14(6).

25. Xie, Y.H., Y.X. Chen, and J.Y. Fang, *Comprehensive review of targeted therapy for colorectal cancer.* Signal Transduct Target Ther, 2020. 5(1): p. 22.

26. Young, P.E., et al., *Early detection of colorectal cancer recurrence in patients undergoing surgery with curative intent: current status and challenges.* J Cancer, 2014. 5(4): p. 262-71.

27. Taieb, J. and C. Gallois, *Adjuvant Chemotherapy for Stage III Colon Cancer.* Cancers (Basel), 2020. 12(9).

28. Labianca, R., et al., *Early colon cancer: ESMO Clinical Practice Guidelines for diagnosis, treatment and follow-up.* Ann Oncol, 2013. 24 Suppl 6: p. vi64-72.

29. Tohme, S., R.L. Simmons, and A. Tsung, *Surgery for Cancer: A Trigger for Metastases.* Cancer Res, 2017. 77(7): p. 1548-1552.

30. Aziz, M.A., et al., *Towards personalized medicine of colorectal cancer.* Crit Rev Oncol Hematol, 2017. 118: p. 70-78.

31. Alorda-Clara, M., et al., *Use of Omics Technologies for the Detection of Colorectal Cancer Biomarkers.* Cancers (Basel), 2022. 14(3).

32. Pinu, F.R., et al., *Systems Biology and Multi-Omics Integration: Viewpoints from the Metabolomics Research Community.* Metabolites, 2019. 9(4).

33. Kitano, H., *Systems biology: a brief overview.* Science, 2002. 295(5560): p. 1662-4.

34. Beklen, H., et al., *Systems-level biomarkers identification and drug repositioning in colorectal cancer.* World J Gastrointest Oncol, 2021. 13(7): p. 638-661.

35. Rai, S., U. Raj, and P.K. Varadwaj, *Systems Biology: A Powerful Tool for Drug Development.* Curr Top Med Chem, 2018. 18(20): p. 1745-1754.

36. Zafari, N., et al., *Integrated analysis of multi-omics data for the discovery of biomarkers and therapeutic targets for colorectal cancer.* Comput Biol Med, 2023. 155: p. 106639.

37. Sardo, E., et al., *Multi-Omic Approaches in Colorectal Cancer beyond Genomic Data.* J Pers Med, 2022. 12(2).

38. Lehner, B., *Modelling genotype-phenotype relationships and human disease with genetic interaction networks.* J Exp Biol, 2007. 210(Pt 9): p. 1559-66.

39. Xu, L., et al., *Transcriptome analysis of human colorectal cancer biopsies reveals extensive expression correlations among genes related to cell proliferation, lipid metabolism, immune response and collagen catabolism.* Oncotarget, 2017. 8(43): p. 74703-74719.

40. Kothalawala, W.J. and B. Győrffy, *Transcriptomic and Cellular Content Analysis of Colorectal Cancer by Combining Multiple Independent Cohorts.* Clin Transl Gastroenterol, 2023. 14(2): p. e00517.

41. Pournoor, E., et al., *Identification of Key Components in Colon Adenocarcinoma Using Transcriptome to Interactome Multilayer Framework.* Sci Rep, 2020. 10(1): p. 4991.

42. Li, P., et al., *Comprehensive genomic profiling of colorectal cancer patients reveals differences in mutational landscapes among clinical and pathological subgroups.* Front Oncol, 2022. 12: p. 1000146.

43. Saleem, S., et al., *Proteomics analysis of colon cancer progression.* Clin Proteomics, 2019. 16: p. 44.

44. Zhu, J., et al., *Identification of immunotherapy and chemotherapy-related molecular subtypes in colon cancer by integrated multi-omics data analysis.* Front Immunol, 2023. 14: p. 1142609.

45. Momeni, Z., et al., *A survey on single and multi omics data mining methods in cancer data classification.* J Biomed Inform, 2020. 107: p. 103466.

46. Yao, L., et al., *Functional annotation of colon cancer risk SNPs.* Nat Commun, 2014. 5: p. 5114.

47. Salimy, S., et al., *A deep learning-based framework for predicting survival-associated groups in colon cancer by integrating multi-omics and clinical data.* Heliyon, 2023. 9(7): p. e17653.

48. Hu, F., et al., *Comprehensive Analysis of Subtype-Specific Molecular Characteristics of Colon Cancer: Specific Genes, Driver Genes, Signaling Pathways, and Immunotherapy Responses.* Front Cell Dev Biol, 2021. 9: p. 758776.

49. Sobral, D., et al., *Genetic and microenvironmental intra-tumor heterogeneity impacts colorectal cancer evolution and metastatic development.* Commun Biol, 2022. 5(1): p. 937.

50. Rappoport, N. and R. Shamir, *Multi-omic and multi-view clustering algorithms: review and cancer benchmark.* Nucleic Acids Res, 2018. 46(20): p. 10546-10562.

51. Xu, T., et al., *CancerSubtypes: an R/Bioconductor package for molecular cancer subtype identification, validation and visualization.* Bioinformatics, 2017. 33(19): p. 3131-3133.

52. Duan, R., et al., *CEPICS: A Comparison and Evaluation Platform for Integration Methods in Cancer Subtyping.* Front Genet, 2019. 10: p. 966.

53. Lu, X., et al., *MOVICS: an R package for multi-omics integration and visualization in cancer subtyping.* Bioinformatics, 2021. 36(22-23): p. 5539-5541.

54. Ramazzotti, D., et al., *Multi-omic tumor data reveal diversity of molecular mechanisms that correlate with survival.* Nat Commun, 2018. 9(1): p. 4453.

55. Mo, Q., et al., *A fully Bayesian latent variable model for integrative clustering analysis of multi-type omics data.* Biostatistics, 2018. 19(1): p. 71-86.

56. Meng, C., et al., *moCluster: Identifying Joint Patterns Across Multiple Omics Data Sets.* J Proteome Res, 2016. 15(3): p. 755-65.

57. Hoadley, K.A., et al., *Multiplatform analysis of 12 cancer types reveals molecular classification within and across tissues of origin.* Cell, 2014. 158(4): p. 929-944.

58. Monti, S., Tamayo, P., Mesirov, J. et al., *Consensus Clustering: A Resampling-Based Method for Class Discovery and Visualization of Gene Expression Microarray Data.* Machine Learning, 2003. 52.

59. Chalise, P. and B.L. Fridley, *Integrative clustering of multi-level 'omic data based on non-negative matrix factorization algorithm.* PLoS One, 2017. 12(5): p. e0176278.

60. Wu, D., et al., *Fast dimension reduction and integrative clustering of multi-omics data using low-rank approximation: application to cancer molecular classification.* BMC Genomics, 2015. 16: p. 1022.

61. Rappoport, N. and R. Shamir, *NEMO: cancer subtyping by integration of partial multi-omic data.* Bioinformatics, 2019. 35(18): p. 3348-3356.

62. Nguyen, H., et al., *PINSPlus: a tool for tumor subtype discovery in integrated genomic data.* Bioinformatics, 2019. 35(16): p. 2843-2846.

63. Wang, B., et al., *Similarity network fusion for aggregating data types on a genomic scale.* Nat Methods, 2014. 11(3): p. 333-7.

64. Colaprico, A., et al., *TCGAbiolinks: an R/Bioconductor package for integrative analysis of TCGA data.* Nucleic Acids Res, 2016. 44(8): p. e71.

65. Haunsberger, S.J., N.M. Connolly, and J.H. Prehn, *miRNAmeConverter: an R/bioconductor package for translating mature miRNA names to different miRBase versions.* Bioinformatics, 2017. 33(4): p. 592-593.

66. Marisa, L., et al., *Gene expression classification of colon cancer into molecular subtypes: characterization, validation, and prognostic value.* PLoS Med, 2013. 10(5): p. e1001453.

67. Reid, J.F., et al., *Integrative approach for prioritizing cancer genes in sporadic colon cancer.* Genes Chromosomes Cancer, 2009. 48(11): p. 953-62.

68. Smith, J.J., et al., *Experimentally derived metastasis gene expression profile predicts recurrence and death in patients with colon cancer.* Gastroenterology, 2010. 138(3): p. 958-68.

69. Tibshirani, R., G. Walther, and T. Hastie, *Estimating the Number of Clusters in a Data Set Via the Gap Statistic.* Journal of the Royal Statistical Society Series B: Statistical Methodology, 2002. 63(2): p. 411-423.

70. Robinson, M.D., D.J. McCarthy, and G.K. Smyth, *edgeR: a Bioconductor package for differential expression analysis of digital gene expression data.* Bioinformatics, 2010. 26(1): p. 139-40.

71. McCarthy, D.J., Y. Chen, and G.K. Smyth, *Differential expression analysis of multifactor RNA-Seq experiments with respect to biological variation.* Nucleic Acids Res, 2012. 40(10): p. 4288-97.

72. Love, M.I., W. Huber, and S. Anders, *Moderated estimation of fold change and dispersion for RNA-seq data with DESeq2.* Genome Biol, 2014. 15(12): p. 550.

73. Ritchie, M.E., et al., *limma powers differential expression analyses for RNA-sequencing and microarray studies.* Nucleic Acids Res, 2015. 43(7): p. e47.

74. Barbie, D.A., et al., *Systematic RNA interference reveals that oncogenic KRAS-driven cancers require TBK1.* Nature, 2009. 462(7269): p. 108-12.

75. Hänzelmann, S., R. Castelo, and J. Guinney, *GSVA: gene set variation analysis for microarray and RNA-seq data.* BMC Bioinformatics, 2013. 14: p. 7.

76. Godec, J., et al., *Compendium of Immune Signatures Identifies Conserved and Species-Specific Biology in Response to Inflammation.* Immunity, 2016. 44(1): p. 194-206.

77. Liberzon, A., et al., *Molecular signatures database (MSigDB) 3.0.* Bioinformatics, 2011. 27(12): p. 1739-40.

78. Liberzon, A., et al., *The Molecular Signatures Database (MSigDB) hallmark gene set collection.* Cell Syst, 2015. 1(6): p. 417-425.

79. Cerami, E., et al., *The cBio cancer genomics portal: an open platform for exploring multidimensional cancer genomics data.* Cancer Discov, 2012. 2(5): p. 401-4.

80. Gao, J., et al., *Integrative analysis of complex cancer genomics and clinical profiles using the cBioPortal.* Sci Signal, 2013. 6(269): p. pl1.

81. Mayakonda, A., et al., *Maftools: efficient and comprehensive analysis of somatic variants in cancer.* Genome Res, 2018. 28(11): p. 1747-1756.

82. Yang, W., et al., *Genomics of Drug Sensitivity in Cancer (GDSC): a resource for therapeutic biomarker discovery in cancer cells.* Nucleic Acids Res, 2013. 41(Database issue): p. D955-61.

83. Hoshida, Y., *Nearest template prediction: a single-sample-based flexible class prediction with confidence assessment.* PLoS One, 2010. 5(11): p. e15543.

84. Tibshirani, R., et al., *Diagnosis of multiple cancer types by shrunken centroids of gene expression.* Proc Natl Acad Sci U S A, 2002. 99(10): p. 6567-72.

85. Kapp, A.V. and R. Tibshirani, *Are clusters found in one dataset present in another dataset?* Biostatistics, 2007. 8(1): p. 9-31.

86. Yau, T.O., *Precision treatment in colorectal cancer: Now and the future.* JGH Open, 2019. 3(5): p. 361-369.

87. Singh, M.P., et al., *Molecular subtypes of colorectal cancer: An emerging therapeutic opportunity for personalized medicine.* Genes Dis, 2021. 8(2): p. 133-145.

88. Mohajer, M., K.-H. Englmeier, and Volker, *A comparison of Gap statistic definitions with and without logarithm function.* arXiv pre-print server, 2011.

89. Goder, A. and V. Filkov, *Consensus Clustering Algorithms: Comparison and Refinement*, in *2008 Proceedings of the Workshop on Algorithm Engineering and Experiments (ALENEX)*. p. 109-117.

90. Strehl, A. and J. Ghosh, *Cluster Ensembles --- A Knowledge Reuse Framework for Combining Multiple Partitions.* J. Mach. Learn. Res., 2003. 3: p. 583-617.

91. Nguyen, N.a.C.R., *Consensus Clusterings*, in *Seventh IEEE International Conference on Data Mining*. 2007: Omaha, NE, USA.

92. Rousseeuw, P.J., *Silhouettes: A graphical aid to the interpretation and validation of cluster analysis.* Journal of Computational and Applied Mathematics, 1987. 20: p. 53-65.

93. Zhao, S., et al., *Silhouette Scores for Arbitrary Defined Groups in Gene Expression Data and Insights into Differential Expression Results.* Biol Proced Online, 2018. 20: p. 5.

94. Conesa, A., et al., *A survey of best practices for RNA-seq data analysis.* Genome Biol, 2016. 17: p. 13.

95. Liu, H.Y. and C.J. Zhang, *Identification of differentially expressed genes and their upstream regulators in colorectal cancer.* Cancer Gene Ther, 2017. 24(6): p. 244-250.

96. Rodriguez-Esteban, R. and X. Jiang, *Differential gene expression in disease: a comparison between high-throughput studies and the literature.* BMC Med Genomics, 2017. 10(1): p. 59.

97. Anders, S., et al., *Count-based differential expression analysis of RNA sequencing data using R and Bioconductor.* Nat Protoc, 2013. 8(9): p. 1765-86.

98. Chabanais, J., et al., *POFUT1 as a Promising Novel Biomarker of Colorectal Cancer*. Cancers (Basel), 2018. 10(11).

99. Du, Y., et al., *POFUT1 promotes colorectal cancer development through the activation of Notch1 signaling.* Cell Death Dis, 2018. 9(10): p. 995.

100. Zhu, J., J. Ren, and L. Tang, *Genistein inhibits invasion and migration of colon cancer cells by recovering WIF1 expression.* Mol Med Rep, 2018. 17(5): p. 7265-7273.

101. Chen, Z., S. Downing, and E.S. Tzanakakis, *Four Decades After the Discovery of Regenerating Islet-Derived (Reg) Proteins: Current Understanding and Challenges.* Front Cell Dev Biol, 2019. 7: p. 235.

102. Zhang, J., et al., *The Clinical Significance and Mechanisms of REG4 in Human Cancers.* Front Oncol, 2020. 10: p. 559230.

103. Zito, A., et al., *Gene Set Enrichment Analysis of Interaction Networks Weighted by Node Centrality.* Front Genet, 2021. 12: p. 577623.

104. Subramanian, A., et al., *Gene set enrichment analysis: a knowledge-based approach for interpreting genome-wide expression profiles.* Proc Natl Acad Sci U S A, 2005. 102(43): p. 15545-50.

105. Benjamini, Y., et al., *Controlling the false discovery rate in behavior genetics research.* Behav Brain Res, 2001. 125(1-2): p. 279-84.

106. Reiner, A., D. Yekutieli, and Y. Benjamini, *Identifying differentially expressed genes using false discovery rate controlling procedures.* Bioinformatics, 2003. 19(3): p. 368-75.

107. Waidhauser, J., et al., *Circulating Lymphocytes Reflect the Local Immune Response in Patients with Colorectal Carcinoma.* Diagnostics (Basel), 2022. 12(6).

108. Mlecnik, B., et al., *Histopathologic-based prognostic factors of colorectal cancers are associated with the state of the local immune reaction.* J Clin Oncol, 2011. 29(6): p. 610-8.

109. Bhat, A.A., et al., *Cytokine- and chemokine-induced inflammatory colorectal tumor microenvironment: Emerging avenue for targeted therapy.* Cancer Commun (Lond), 2022. 42(8): p. 689-715.

110. Wang, H., T. Tian, and J. Zhang, *Tumor-Associated Macrophages (TAMs) in Colorectal Cancer (CRC): From Mechanism to Therapy and Prognosis.* Int J Mol Sci, 2021. 22(16).

111. Kori, M., et al., *A Pan-Cancer Atlas of Differentially Interacting Hallmarks of Cancer Proteins.* J Pers Med, 2022. 12(11).

112. Hanahan, D. and R.A. Weinberg, *The hallmarks of cancer.* Cell, 2000. 100(1): p. 57-70.

113. Hanahan, D. and R.A. Weinberg, *Hallmarks of cancer: the next generation.* Cell, 2011. 144(5): p. 646-74.

114. Vu, T. and P.K. Datta, *Regulation of EMT in Colorectal Cancer: A Culprit in Metastasis.* Cancers (Basel), 2017. 9(12).

115. Zhang, N., et al., *Novel therapeutic strategies: targeting epithelial-mesenchymal transition in colorectal cancer.* Lancet Oncol, 2021. 22(8): p. e358-e368.

116. Zhuang, Y., et al., *Multi gene mutation signatures in colorectal cancer patients: predict for the diagnosis, pathological classification, staging and prognosis.* BMC Cancer, 2021. 21(1): p. 380.

117. Tan, E.S., et al., *Copy Number Alterations as Novel Biomarkers and Therapeutic Targets in Colorectal Cancer.* Cancers (Basel), 2022. 14(9).

118. Szvicsek, Z., et al., *Extracellular vesicle release from intestinal organoids is modulated by Apc mutation and other colorectal cancer progression factors.* Cell Mol Life Sci, 2019. 76(12): p. 2463-2476.

119. Turnbull, C.L., et al., *In vitro stability of APC gene sequences and the influence of DNA repair status.* Mutagenesis, 2012. 27(2): p. 233-8.

120. Kwong, L.N. and W.F. Dove, *APC and its modifiers in colon cancer.* Adv Exp Med Biol, 2009. 656: p. 85-106.

121. Li, B., G. Zhang, and X. Xu, *APC mutation correlated with poor response of immunotherapy in colon cancer.* BMC Gastroenterol, 2023. 23(1): p. 95.

122. Fearon, E.R. and B. Vogelstein, *A genetic model for colorectal tumorigenesis.* Cell, 1990. 61(5): p. 759-67.

123. Müller, M.F., A.E. Ibrahim, and M.J. Arends, *Molecular pathological classification of colorectal cancer.* Virchows Arch, 2016. 469(2): p. 125-34.

124. *Comprehensive molecular characterization of human colon and rectal cancer.* Nature, 2012. 487(7407): p. 330-7.

125. Kandoth, C., et al., *Mutational landscape and significance across 12 major cancer types.* Nature, 2013. 502(7471): p. 333-339.

126. Giannakis, M., et al., *Genomic Correlates of Immune-Cell Infiltrates in Colorectal Carcinoma.* Cell Rep, 2016. 15(4): p. 857-865.

127. Olivier, M., M. Hollstein, and P. Hainaut, *TP53 mutations in human cancers: origins, consequences, and clinical use.* Cold Spring Harb Perspect Biol, 2010. 2(1): p. a001008.

128. Iacopetta, B., *TP53 mutation in colorectal cancer.* Hum Mutat, 2003. 21(3): p. 271-6.

129. Zhao, L., et al., *Construction of a TTN Mutation-Based Prognostic Model for Evaluating Immune Microenvironment, Cancer Stemness, and Outcomes of Colorectal Cancer Patients.* Stem Cells Int, 2023. 2023: p. 6079957.

130. Melotte, V., et al., *Spectrin repeat containing nuclear envelope 1 and forkhead box protein E1 are promising markers for the detection of colorectal cancer in blood.* Cancer Prev Res (Phila), 2015. 8(2): p. 157-64.

131. Dinu, D., et al., *Prognostic significance of KRAS gene mutations in colorectal cancer--preliminary study.* J Med Life, 2014. 7(4): p. 581-7.

132. Roth, A.D., et al., *Prognostic role of KRAS and BRAF in stage II and III resected colon cancer: results of the translational study on the PETACC-3, EORTC 40993, SAKK 60-00 trial.* J Clin Oncol, 2010. 28(3): p. 466-74.

133. Dienstmann, R., et al., *Prediction of overall survival in stage II and III colon cancer beyond TNM system: a retrospective, pooled biomarker study.* Ann Oncol, 2017. 28(5): p. 1023-1031.

134. Samuels, Y., et al., *Mutant PIK3CA promotes cell growth and invasion of human cancer cells.* Cancer Cell, 2005. 7(6): p. 561-73.

135. Luo, Q., et al., *KRAS and PIK3CA bi-mutations predict a poor prognosis in colorectal cancer patients: A single-site report.* Transl Oncol, 2020. 13(12): p. 100874.

136. Kato, S., et al., *PIK3CA mutation is predictive of poor survival in patients with colorectal cancer.* Int J Cancer, 2007. 121(8): p. 1771-8.

137. Smith, G., et al., *Mutations in APC, Kirsten-ras, and p53--alternative genetic pathways to colorectal cancer.* Proc Natl Acad Sci U S A, 2002. 99(14): p. 9433-8.

138. Wilson, P.M., M.J. Labonte, and H.J. Lenz, *Molecular markers in the treatment of metastatic colorectal cancer.* Cancer J, 2010. 16(3): p. 262-72.

139. Smith, C.G., et al., *Somatic profiling of the epidermal growth factor receptor pathway in tumors from patients with advanced colorectal cancer treated with chemotherapy ± cetuximab.* Clin Cancer Res, 2013. 19(15): p. 4104-13.

140. Schrock, A.B., et al., *Tumor mutational burden is predictive of response to immune checkpoint inhibitors in MSI-high metastatic colorectal cancer.* Ann Oncol, 2019. 30(7): p. 1096-1103.

141. Zhang, C., et al., *Exploration of the relationships between tumor mutation burden with immune infiltrates in clear cell renal cell carcinoma.* Ann Transl Med, 2019. 7(22): p. 648.

142. Li, Y., et al., *Tumor Mutational Burden Predicting the Efficacy of Immune Checkpoint Inhibitors in Colorectal Cancer: A Systematic Review and Meta-Analysis.* Front Immunol, 2021. 12: p. 751407.

143. Hu, T., et al., *Mechanisms of drug resistance in colon cancer and its therapeutic strategies.* World J Gastroenterol, 2016. 22(30): p. 6876-89.

144. Druzhkova, I.N., et al., *Modern Approaches to Testing Drug Sensitivity of Patients' Tumors (Review).* Sovrem Tekhnologii Med, 2021. 12(4): p. 91-102.

145. Pardini, B., et al., *5-Fluorouracil-based chemotherapy for colorectal cancer and MTHFR/MTRR genotypes.* Br J Clin Pharmacol, 2011. 72(1): p. 162-3.

146. Jiang, W., Yan, Y., Chen, M., Luo, G., Hao, J., Pan, J., Hu, S., Guo, P., Li, W., Wang, R., Zuo, Y., Sun, Y., Sui, S., Yu, W., Pan, Z., Zou, K., Zheng, Z., Deng, W., Wu, X., & Guo, W., *Aspirin enhances the sensitivity of colon cancer cells to cisplatin by abrogating the binding of NF-κB to the COX-2 promoter.* Aging, 2020. 12(1).

147. Pham, D.T., N. Saelim, and W. Tiyaboonchai, *Paclitaxel loaded EDC-crosslinked fibroin nanoparticles: a potential approach for colon cancer treatment.* Drug Deliv Transl Res, 2020. 10(2): p. 413-424.

148. Blagosklonny, M.V., et al., *Taxol-induced apoptosis and phosphorylation of Bcl-2 protein involves c-Raf-1 and represents a novel c-Raf-1 signal transduction pathway.* Cancer Res, 1996. 56(8): p. 1851-4.

149. Murono, K., et al., *SN-38 overcomes chemoresistance of colorectal cancer cells induced by hypoxia, through HIF1alpha.* Anticancer Res, 2012. 32(3): p. 865-72.

150. Okuno, T., et al., *SN-38 Acts as a Radiosensitizer for Colorectal Cancer by Inhibiting the Radiation-induced Up-regulation of HIF-1α.* Anticancer Res, 2018. 38(6): p. 3323-3331.

151. Chen, Y.Q., et al., *Delivery of Rapamycin by Liposomes Synergistically Enhances the Chemotherapy Effect of 5-Fluorouracil on Colorectal Cancer.* Int J Nanomedicine, 2021. 16: p. 269-281.

152. Chao, T.H., et al., *The synergistic effect of rapamycin combined with 5-fluorouracil in BALB/cByJNarl mice bearing CT-26 tumor cells.* Anticancer Res, 2014. 34(7): p. 3329-35.

153. Yang, J.W., Q.H. Zhang, and T. Liu, *Autophagy facilitates anticancer effect of 5-fluorouracil in HCT-116 cells.* J Cancer Res Ther, 2018. 14(Supplement): p. S1141-s1147.

154. Kotlarz, A., et al., *Imatinib inhibits the regrowth of human colon cancer cells after treatment with 5-FU and cooperates with vitamin D analogue PRI-2191 in the downregulation of expression of stemness-related genes in 5-FU refractory cells.* J Steroid Biochem Mol Biol, 2019. 189: p. 48-62.

155. McHugh, M.L., *Interrater reliability: the kappa statistic.* Biochem Med (Zagreb), 2012. 22(3): p. 276-82.

156. Mir, S.M., et al., *The clinical significance of VDR and WIFI downregulation in colorectal cancer tissue.* Gene Reports, 2020. 20: p. 100762.

157. Ho, M.L., et al., *N-acetylgalactosamine-6-sulfatase (GALNS), Similar to Glycodelin, Is a Potential General Biomarker for Multiple Malignancies.* Anticancer Res, 2019. 39(11): p. 6317-6324.

158. Fonseca, A.S., et al., *ETV4 plays a role on the primary events during the adenoma-adenocarcinoma progression in colorectal cancer.* BMC Cancer, 2021. 21(1): p. 207.

159. Xu, H., et al., *Deltex E3 ubiquitin ligase 3 inhibits colorectal cancer cell growth and regulates cell cycle progression via upregulating E2F transcription factor 1.* Mol Biol Rep, 2022. 49(3): p. 1661-1668.

160. Kasprzak, A. and A. Adamek, *Insulin-Like Growth Factor 2 (IGF2) Signaling in Colorectal Cancer-From Basic Research to Potential Clinical Applications.* Int J Mol Sci, 2019. 20(19).

161. Paladhi, A., et al., *Targeting thymidine phosphorylase alleviates resistance to dendritic cell immunotherapy in colorectal cancer and promotes antitumor immunity.* Front Immunol, 2022. 13: p. 988071.

162. Kishani Farahani, R., et al., *PIWIL2 Regulates the Proliferation, Apoptosis and Colony Formation of Colorectal Cancer Cell Line.* Iran J Biotechnol, 2023. 21(1): p. e3176.

163. Zhang, N., et al., *Keratin 23 promotes telomerase reverse transcriptase expression and human colorectal cancer growth.* Cell Death Dis, 2017. 8(7): p. e2961.

164. Bai, Z., et al., *Effects of YAP1 and SFRP2 overexpression on the biological behavior of colorectal cancer cells and their molecular mechanisms.* J Gastrointest Oncol, 2021. 12(4): p. 1601-1612.

165. Astrosini, C., et al., *REG1A expression is a prognostic marker in colorectal cancer and associated with peritoneal carcinomatosis.* Int J Cancer, 2008. 123(2): p. 409-413.

166. Buckens, O.J., et al., *The role of Eph receptors in cancer and how to target them: novel approaches in cancer treatment.* Expert Opin Investig Drugs, 2020. 29(6): p. 567-582.

167. Fromme, J.E., et al., *FGFR3 mRNA overexpression defines a subset of oligometastatic colorectal cancers with worse prognosis.* Oncotarget, 2018. 9(63): p. 32204-32218.

168. Sonvilla, G., et al., *Fibroblast growth factor receptor 3-IIIc mediates colorectal cancer growth and migration.* Br J Cancer, 2010. 102(7): p. 1145-56.

169. Cheng, L., et al., *The role of CRYAB in tumor prognosis and immune infiltration: A Pan-cancer analysis.* Front Surg, 2022. 9: p. 1117307.

170. Binefa, G., et al., *Colorectal cancer: from prevention to personalized medicine.* World J Gastroenterol, 2014. 20(22): p. 6786-808.

171. Park, S.H., et al., *Clinicopathological characteristics of colon cancer diagnosed at primary health care institutions.* Intest Res, 2014. 12(2): p. 131-8.

172. Carethers, J.M., *Racial and ethnic disparities in colorectal cancer incidence and mortality.* Adv Cancer Res, 2021. 151: p. 197-229.

173. Royston, K.J., B. Adedokun, and O.I. Olopade, *Race, the microbiome and colorectal cancer.* World J Gastrointest Oncol, 2019. 11(10): p. 773-787.

174. Butcher, D., et al., *Female gender is a major determinant of changing subsite distribution of colorectal cancer with age.* Cancer, 1985. 56(3): p. 714-6.

175. Kim, S.E., et al., *Sex- and gender-specific disparities in colorectal cancer risk.* World J Gastroenterol, 2015. 21(17): p. 5167-75.

176. White, A., et al., *A review of sex-related differences in colorectal cancer incidence, screening uptake, routes to diagnosis, cancer stage and survival in the UK.* BMC Cancer, 2018. 18(1): p. 906.

177. Maguire, A. and K. Sheahan, *Controversies in the pathological assessment of colorectal cancer.* World J Gastroenterol, 2014. 20(29): p. 9850-61.

178. Compton, C.C. and F.L. Greene, *The staging of colorectal cancer: 2004 and beyond.* CA Cancer J Clin, 2004. 54(6): p. 295-308.

179. Aghabozorgi, A.S., et al., *Role of adenomatous polyposis coli (APC) gene mutations in the pathogenesis of colorectal cancer; current status and perspectives.* Biochimie, 2019. 157: p. 64-71.

180. Zhang, L. and J.W. Shay, *Multiple Roles of APC and its Therapeutic Implications in Colorectal Cancer.* J Natl Cancer Inst, 2017. 109(8).

181. Fu, X., et al., *TFAP2B overexpression contributes to tumor growth and progression of thyroid cancer through the COX-2 signaling pathway.* Cell Death Dis, 2019. 10(6): p. 397.

182. Ji, Y., et al., *ADCK1 activates the β-catenin/TCF signaling pathway to promote the growth and migration of colon cancer cells.* Cell Death Dis, 2021. 12(4): p. 354.

183. Yi, Q., et al., *ACAP1 Deficiency Predicts Inferior Immunotherapy Response in Solid Tumors.* Cancers (Basel), 2022. 14(23).

184. Otani, K., et al., *Adiponectin and colorectal cancer.* Surg Today, 2017. 47(2): p. 151-158.

185. Zeng, Z.L., et al., *Prognostic relevance of melanoma antigen D1 expression in colorectal carcinoma.* J Transl Med, 2012. 10: p. 181.

186. Li, D., et al., *Serine protease PRSS56, a novel cancer-testis antigen activated by DNA hypomethylation, promotes colorectal and gastric cancer progression via PI3K/AKT axis.* Cell Biosci, 2023. 13(1): p. 124.

187. Wei, W., et al., *METTL16 promotes glycolytic metabolism reprogramming and colorectal cancer progression.* J Exp Clin Cancer Res, 2023. 42(1): p. 151.

188. Bovolenta, P., et al., *Beyond Wnt inhibition: new functions of secreted Frizzled-related proteins in development and disease.* J Cell Sci, 2008. 121(Pt 6): p. 737-46.

189. Wood, S.M., et al., *Fatty acid-binding protein 1 is preferentially lost in microsatellite instable colorectal carcinomas and is immune modulated via the interferon γ pathway.* Mod Pathol, 2017. 30(1): p. 123-133.

190. Lawrie, L.C., et al., *Liver fatty acid binding protein expression in colorectal neoplasia.* Br J Cancer, 2004. 90(10): p. 1955-60.

191. Llosa, N.J., et al., *The vigorous immune microenvironment of microsatellite instable colon cancer is balanced by multiple counter-inhibitory checkpoints.* Cancer Discov, 2015. 5(1): p. 43-51.

192. Friedman, K., et al., *Medullary carcinoma of the colon: a distinct morphology reveals a distinctive immunoregulatory microenvironment.* Mod Pathol, 2016. 29(5): p. 528-41.

193. Yoon, J.H., et al., *NOTUM Is Involved in the Progression of Colorectal Cancer.* Cancer Genomics Proteomics, 2018. 15(6): p. 485-497.

194. Bishnupuri, K.S., et al., *Reg4-induced mitogenesis involves Akt-GSK3β-β-Catenin-TCF-4 signaling in human colorectal cancer.* Mol Carcinog, 2014. 53 Suppl 1(0 1): p. E169-80.

195. Provenzano, P.P., et al., *Collagen reorganization at the tumor-stromal interface facilitates local invasion.* BMC Med, 2006. 4(1): p. 38.

196. Naba, A., et al., *Extracellular matrix signatures of human primary metastatic colon cancers and their metastases to liver.* BMC Cancer, 2014. 14: p. 518.

197. Kirkland, S.C., *Type I collagen inhibits differentiation and promotes a stem cell-like phenotype in human colorectal carcinoma cells.* Br J Cancer, 2009. 101(2): p. 320-6.

198. Roussos, E.T., J.S. Condeelis, and A. Patsialou, *Chemotaxis in cancer.* Nat Rev Cancer, 2011. 11(8): p. 573-87.

199. Vicari, A.P. and C. Caux, *Chemokines in cancer.* Cytokine Growth Factor Rev, 2002. 13(2): p. 143-54.

200. Pączek, S., M. Łukaszewicz-Zając, and B. Mroczko, *Chemokines-What Is Their Role in Colorectal Cancer?* Cancer Control, 2020. 27(1): p. 1073274820903384.

201. Zhang, Y.J., et al., *mTOR signaling pathway is a target for the treatment of colorectal cancer.* Ann Surg Oncol, 2009. 16(9): p. 2617-28.

202. Tian, T., X. Li, and J. Zhang, *mTOR Signaling in Cancer and mTOR Inhibitors in Solid Tumor Targeting Therapy.* Int J Mol Sci, 2019. 20(3).

203. Satoh, K., et al., *Global metabolic reprogramming of colorectal cancer occurs at adenoma stage and is induced by MYC.* Proc Natl Acad Sci U S A, 2017. 114(37): p. E7697-e7706.

204. Nakayama, M. and M. Oshima, *Mutant p53 in colon cancer.* J Mol Cell Biol, 2019. 11(4): p. 267-276.

205. Petitjean, A., et al., *TP53 mutations in human cancers: functional selection and impact on cancer prognosis and outcomes.* Oncogene, 2007. 26(15): p. 2157-65.

206. Blondy, S., et al., *5-Fluorouracil resistance mechanisms in colorectal cancer: From classical pathways to promising processes.* Cancer Sci, 2020. 111(9): p. 3142-3154.

207. Longley, D.B., D.P. Harkin, and P.G. Johnston, *5-fluorouracil: mechanisms of action and clinical strategies.* Nat Rev Cancer, 2003. 3(5): p. 330-8.

208. Jiang, W., et al., *Aspirin enhances the sensitivity of colon cancer cells to cisplatin by abrogating the binding of NF-κB to the COX-2 promoter.* Aging (Albany NY), 2020. 12(1): p. 611-627.

209. Galluzzi, L., et al., *Systems biology of cisplatin resistance: past, present and future.* Cell Death Dis, 2014. 5(5): p. e1257.

210. Van Cutsem, E., et al., *ESMO consensus guidelines for the management of patients with metastatic colorectal cancer.* Ann Oncol, 2016. 27(8): p. 1386-422.

211. Cunningham, D., et al., *Cetuximab monotherapy and cetuximab plus irinotecan in irinotecan-refractory metastatic colorectal cancer.* N Engl J Med, 2004. 351(4): p. 337-45.

212. Jonker, D.J., et al., *Cetuximab for the Treatment of Colorectal Cancer.* New England Journal of Medicine, 2007. 357(20): p. 2040-2048.

213. Qu, X., et al., *Integrated genomic analysis of colorectal cancer progression reveals activation of EGFR through demethylation of the EREG promoter.* Oncogene, 2016. 35(50): p. 6403-6415.

214. Ebert, B., et al., *Proteasome inhibitors MG-132 and bortezomib induce AKR1C1, AKR1C3, AKR1B1, and AKR1B10 in human colon cancer cell lines SW-480 and HT-29.* Chem Biol Interact, 2011. 191(1-3): p. 239-49.

215. Ding, W.X., et al., *A coordinated action of Bax, PUMA, and p53 promotes MG132-induced mitochondria activation and apoptosis in colon cancer cells.* Mol Cancer Ther, 2007. 6(3): p. 1062-9.

216. Guo, N. and Z. Peng, *MG132, a proteasome inhibitor, induces apoptosis in tumor cells.* Asia Pac J Clin Oncol, 2013. 9(1): p. 6-11.

APPENDIX A DEGs for All Clusters

Table A.1. The list of the top 100 upregulated DEGs identified in the CS1 subtype using edgeR as a result of two clustering analyzes.

	fc	log2fc	pvalue	padj
WIF1	$5.04x10^{1}$	$5.65x10^{0}$	$4.68x10^{-30}$	$9.46x10^{-28}$
BX322234.2	$4.61x10^{1}$	$5.53x10^{0}$	$1.63x10^{-7}$	$9.53x10^{-7}$
RNA5.8SP5	$3.90x10^{1}$	$5.28x10^{0}$	$2.07x10^{-3}$	$5.35x10^{-3}$
AC152010.1	$3.73x10^{1}$	$5.22x10^{0}$	$5.46x10^{-3}$	$1.27x10^{-2}$
ORM1	$3.02x10^{1}$	$4.92x10^{0}$	$2.02x10^{-18}$	$6.97x10^{-17}$
RNA5SP267	$2.79x10^{1}$	$4.80x10^{0}$	$1.83x10^{-2}$	$3.66x10^{-2}$
RNA5SP211	$2.77x10^{1}$	$4.79x10^{0}$	$2.21x10^{-2}$	$4.29x10^{-2}$
RN7SL618P	$2.65x10^{1}$	$4.73x10^{0}$	$1.44x10^{-2}$	$2.97x10^{-2}$
PTF1A	$2.29x10^{1}$	$4.52x10^{0}$	$6.23x10^{-16}$	$1.47x10^{-14}$
RNA5SP389	$2.15x10^{1}$	$4.42x10^{0}$	$2.16x10^{-2}$	$4.21x10^{-2}$
SFTPC	$2.10x10^{1}$	$4.39x10^{0}$	$2.04x10^{-6}$	$9.73x10^{-6}$
KRT31	$1.83x10^{1}$	$4.20x10^{0}$	$2.95x10^{-12}$	$3.84x10^{-11}$
SOHLH1	$1.62x10^{1}$	$4.02x10^{0}$	$2.38x10^{-10}$	$2.26x10^{-9}$
RN7SL149P	$1.58x10^{1}$	$3.98x10^{0}$	$2.07x10^{-2}$	$4.06x10^{-2}$
AC127459.2	$1.44x10^{1}$	$3.85x10^{0}$	$8.57x10^{-6}$	$3.65x10^{-5}$
AC114291.1	$1.40x10^{1}$	$3.80x10^{0}$	$9.34x10^{-37}$	$5.14x10^{-34}$
AC026336.3	$1.37x10^{1}$	$3.77x10^{0}$	$1.45x10^{-22}$	$9.41x10^{-21}$
LINC01896	$1.36x10^{1}$	$3.77x10^{0}$	$1.29x10^{-3}$	$3.50x10^{-3}$
PRR9	$1.29x10^{1}$	$3.69x10^{0}$	$3.38x10^{-9}$	$2.66x10^{-8}$
RN7SL762P	$1.29x10^{1}$	$3.68x10^{0}$	$1.29x10^{-8}$	$9.18x10^{-8}$
AL356433.1	$1.23x10^{1}$	$3.62x10^{0}$	$3.79x10^{-14}$	$6.69x10^{-13}$
XAGE2	$1.21x10^{1}$	$3.60x10^{0}$	$6.57x10^{-7}$	$3.44x10^{-6}$
GOLGA6L2	$1.14x10^{1}$	$3.52x10^{0}$	$4.68x10^{-20}$	$2.03x10^{-18}$
GALP	$1.13x10^{1}$	$3.49x10^{0}$	$1.14x10^{-3}$	$3.13x10^{-3}$
AC026774.1	$1.09x10^{1}$	$3.44x10^{0}$	$7.53x10^{-18}$	$2.41x10^{-16}$
AC009446.1	$1.08x10^{1}$	$3.44x10^{0}$	$2.40x10^{-3}$	$6.11x10^{-3}$
MAGEB17	$1.08x10^{1}$	$3.43x10^{0}$	$1.10x10^{-17}$	$3.42x10^{-16}$
APOA2	$1.08x10^{1}$	$3.43x10^{0}$	$1.53x10^{-14}$	$2.90x10^{-13}$
PPBP	$1.04x10^{1}$	$3.37x10^{0}$	$2.56x10^{-11}$	$2.85x10^{-10}$
NOTUM	$1.02x10^{1}$	$3.36x10^{0}$	$2.99x10^{-23}$	$2.14x10^{-21}$
PNLIP	$1.02x10^{1}$	$3.35x10^{0}$	$1.88x10^{-2}$	$3.75x10^{-2}$
SLC5A8	$1.01x10^{1}$	$3.33x10^{0}$	$2.42x10^{-7}$	$1.37x10^{-6}$
AC078993.1	$1.00x10^{1}$	$3.32x10^{0}$	$3.95x10^{-20}$	$1.73x10^{-18}$
TKTL1	$9.74x10^{0}$	$3.28x10^{0}$	$2.09x10^{-12}$	$2.81x10^{-11}$
GDF10	$9.36x10^{0}$	$3.23x10^{0}$	$7.81x10^{-15}$	$1.54x10^{-13}$
PRSS56	$9.36x10^{0}$	$3.23x10^{0}$	$2.76x10^{-7}$	$1.55x10^{-6}$
RNA5SP213	$9.33x10^{0}$	$3.22x10^{0}$	$1.36x10^{-2}$	$2.83x10^{-2}$

Table A.1 (continued). The list of the top 100 upregulated DEGs identified in the CS1 subtype using edgeR as a result of two clustering analyzes.

KRT40	$9.18x10^{0}$	$3.20x10^{0}$	$1.44x10^{-16}$	$3.77x10^{-15}$
AP002963.1	$9.17x10^{0}$	$3.20x10^{0}$	$5.21x10^{-3}$	$1.22x10^{-2}$
TUBAP13	$9.06x10^{0}$	$3.18x10^{0}$	$1.74x10^{-17}$	$5.25x10^{-16}$
MAGEB1	$8.93x10^{0}$	$3.16x10^{0}$	$2.11x10^{-2}$	$4.12x10^{-2}$
HSPB3	$8.83x10^{0}$	$3.14x10^{0}$	$4.69x10^{-16}$	$1.13x10^{-14}$
CPN1	$8.79x10^{0}$	$3.14x10^{0}$	$7.07x10^{-17}$	$1.94x10^{-15}$
LINC00661	$8.78x10^{0}$	$3.13x10^{0}$	$5.63x10^{-4}$	$1.66x10^{-3}$
SSX1	$8.76x10^{0}$	$3.13x10^{0}$	$7.29x10^{-4}$	$2.10x10^{-3}$
GPR83	$8.68x10^{0}$	$3.12x10^{0}$	$5.60x10^{-20}$	$2.41x10^{-18}$
AC108865.1	$8.68x10^{0}$	$3.12x10^{0}$	$5.28x10^{-12}$	$6.61x10^{-11}$
TMEM252	$8.52x10^{0}$	$3.09x10^{0}$	$6.43x10^{-23}$	$4.45x10^{-21}$
SLC30A2	$8.41x10^{0}$	$3.07x10^{0}$	$6.06x10^{-27}$	$7.42x10^{-25}$
LY6G6D	$8.27x10^{0}$	$3.05x10^{0}$	$9.38x10^{-16}$	$2.14x10^{-14}$
RN7SL122P	$8.23x10^{0}$	$3.04x10^{0}$	$1.83x10^{-2}$	$3.66x10^{-2}$
LCN15	$8.20x10^{0}$	$3.04x10^{0}$	$2.86x10^{-11}$	$3.16x10^{-10}$
TNNC2	$7.98x10^{0}$	$3.00x10^{0}$	$3.86x10^{-44}$	$7.88x10^{-41}$
AC010255.2	$7.90x10^{0}$	$2.98x10^{0}$	$1.86x10^{-10}$	$1.80x10^{-9}$
MAGEC2	$7.82x10^{0}$	$2.97x10^{0}$	$6.29x10^{-3}$	$1.44x10^{-2}$
BPIFA1	$7.76x10^{0}$	$2.96x10^{0}$	$4.30x10^{-3}$	$1.03x10^{-2}$
SYN3	$7.73x10^{0}$	$2.95x10^{0}$	$4.46x10^{-33}$	$1.42x10^{-30}$
LINC02525	$7.57x10^{0}$	$2.92x10^{0}$	$5.92x10^{-12}$	$7.36x10^{-11}$
AC091304.1	$7.49x10^{0}$	$2.90x10^{0}$	$2.17x10^{-11}$	$2.46x10^{-10}$
HS3ST4	$7.23x10^{0}$	$2.85x10^{0}$	$3.84x10^{-9}$	$2.99x10^{-8}$
KRT37	$7.16x10^{0}$	$2.84x10^{0}$	$6.34x10^{-12}$	$7.85x10^{-11}$
VWA5B1	$7.12x10^{0}$	$2.83x10^{0}$	$4.72x10^{-12}$	$5.96x10^{-11}$
AC132825.1	$7.05x10^{0}$	$2.82x10^{0}$	$6.46x10^{-9}$	$4.84x10^{-8}$
DMRT1	$6.85x10^{0}$	$2.78x10^{0}$	$2.55x10^{-9}$	$2.05x10^{-8}$
CTNNA2.AS 1	$6.78x10^{0}$	$2.76x10^{0}$	$2.51x10^{-5}$	$9.75x10^{-5}$
AL512356.5	$6.78x10^{0}$	$2.76x10^{0}$	$3.74x10^{-10}$	$3.42x10^{-9}$
RNA5SP243	$6.77x10^{0}$	$2.76x10^{0}$	$5.49x10^{-3}$	$1.27x10^{-2}$
SALL3	$6.77x10^{0}$	$2.76x10^{0}$	$1.62x10^{-3}$	$4.30x10^{-3}$
AL354863.1	$6.67x10^{0}$	$2.74x10^{0}$	$2.46x10^{-8}$	$1.67x10^{-7}$
MIR483	$6.63x10^{0}$	$2.73x10^{0}$	$1.05x10^{-4}$	$3.62x10^{-4}$
FGF3	$6.52x10^{0}$	$2.71x10^{0}$	$1.86x10^{-8}$	$1.29x10^{-7}$
RN7SL217P	$6.47x10^{0}$	$2.69x10^{0}$	$1.86x10^{-2}$	$3.71x10^{-2}$
AC079804.2	$6.45x10^{0}$	$2.69x10^{0}$	$1.84x10^{-6}$	$8.84x10^{-6}$
RN7SL253P	$6.44x10^{0}$	$2.69x10^{0}$	$5.71x10^{-4}$	$1.69x10^{-3}$
C6orf15	$6.43x10^{0}$	$2.69x10^{0}$	$2.07x10^{-12}$	$2.78x10^{-11}$
KRT23	$6.37x10^{0}$	$2.67x10^{0}$	$4.94x10^{-23}$	$3.48x10^{-21}$
AL121885.2	$6.35x10^{0}$	$2.67x10^{0}$	$3.86x10^{-13}$	$5.82x10^{-12}$

Table A.1 (continued). The list of the top 100 upregulated DEGs identified in the CS1 subtype using edgeR as a result of two clustering analyzes.

LY6G6F.LY6G6D	$6.35x10^{0}$	$2.67x10^{0}$	$2.72x10^{-12}$	$3.58x10^{-11}$
RPS10.NUDT3	$6.24x10^{0}$	$2.64x10^{0}$	$4.24x10^{-3}$	$1.01x10^{-2}$
AP000851.2	$6.21x10^{0}$	$2.63x10^{0}$	$1.92x10^{-11}$	$2.20x10^{-10}$
TCAP	$6.19x10^{0}$	$2.63x10^{0}$	$2.38x10^{-20}$	$1.09x10^{-18}$
SHISA9	$6.19x10^{0}$	$2.63x10^{0}$	$1.66x10^{-10}$	$1.62x10^{-9}$
AL391650.2	$6.18x10^{0}$	$2.63x10^{0}$	$3.59x10^{-12}$	$4.62x10^{-11}$
MAP7D2	$6.10x10^{0}$	$2.61x10^{0}$	$3.12x10^{-19}$	$1.21x10^{-17}$
SULT2A1	$6.04x10^{0}$	$2.60x10^{0}$	$2.21x10^{-11}$	$2.50x10^{-10}$
OR10G4	$6.04x10^{0}$	$2.59x10^{0}$	$1.83x10^{-4}$	$6.02x10^{-4}$
IGF2	$6.03x10^{0}$	$2.59x10^{0}$	$2.19x10^{-9}$	$1.78x10^{-8}$
SERPINA7	$6.00x10^{0}$	$2.58x10^{0}$	$2.38x10^{-11}$	$2.67x10^{-10}$
BX276092.9	$5.99x10^{0}$	$2.58x10^{0}$	$2.74x10^{-6}$	$1.28x10^{-5}$
AP003774.2	$5.91x10^{0}$	$2.56x10^{0}$	$1.74x10^{-31}$	$4.17x10^{-29}$
GLRA2	$5.90x10^{0}$	$2.56x10^{0}$	$3.37x10^{-15}$	$7.06x10^{-14}$
KRTAP1.1	$5.90x10^{0}$	$2.56x10^{0}$	$6.47x10^{-7}$	$3.39x10^{-6}$
AC016925.3	$5.89x10^{0}$	$2.56x10^{0}$	$1.12x10^{-9}$	$9.52x10^{-9}$
CYP4F8	$5.73x10^{0}$	$2.52x10^{0}$	$1.60x10^{-16}$	$4.15x10^{-15}$
CELP	$5.71x10^{0}$	$2.51x10^{0}$	$3.26x10^{-22}$	$2.00x10^{-20}$
EYA1	$5.69x10^{0}$	$2.51x10^{0}$	$2.32x10^{-15}$	$4.98x10^{-14}$
SFTA3	$5.67x10^{0}$	$2.50x10^{0}$	$6.00x10^{-3}$	$1.38x10^{-2}$
SLC1A7	$5.64x10^{0}$	$2.50x10^{0}$	$4.68x10^{-28}$	$6.80x10^{-26}$
LINC02128	$5.59x10^{0}$	$2.48x10^{0}$	$3.03x10^{-10}$	$2.82x10^{-9}$
AC135388.1	$5.57x10^{0}$	$2.48x10^{0}$	$4.01x10^{-16}$	$9.82x10^{-15}$

Table A.2. The list of the top 100 downregulated DEGs identified in the CS1 subtype using edgeR as a result of two clustering analyzes.

	fc	**log2fc**	**pvalue**	**padj**
RNY4	6.02×10^{-3}	-7.38×10^{0}	4.67×10^{-9}	3.59×10^{-8}
PAEP	7.39×10^{-3}	-7.08×10^{0}	2.59×10^{-63}	1.48×10^{-58}
FBXO40	9.29×10^{-3}	-6.75×10^{0}	5.33×10^{-31}	1.21×10^{-28}
MTND5P32	1.08×10^{-2}	-6.53×10^{0}	5.77×10^{-16}	1.37×10^{-14}
RNU1.28P	1.11×10^{-2}	-6.49×10^{0}	1.22×10^{-6}	6.08×10^{-6}
RNVU1.2	1.14×10^{-2}	-6.46×10^{0}	1.74×10^{-14}	3.24×10^{-13}
CLDN18	1.19×10^{-2}	-6.40×10^{0}	2.72×10^{-58}	7.78×10^{54}
AC066616.2	1.20×10^{-2}	-6.38×10^{0}	6.04×10^{-16}	1.43×10^{-14}
RNU1.52P	1.20×10^{-2}	-6.38×10^{0}	4.68×10^{-9}	3.60×10^{-8}
TFAP2B	1.28×10^{-2}	-6.29×10^{0}	4.78×10^{-16}	1.15×10^{-14}
RNU1.19P	1.29×10^{-2}	-6.27×10^{0}	1.10×10^{-10}	1.10×10^{-9}
RNU1.83P	1.31×10^{-2}	-6.26×10^{0}	4.91×10^{-12}	6.19×10^{-11}

Table A.2 (continued). The list of the top 100 downregulated DEGs identified in the CS1 subtype using edgeR as a result of two clustering analyzes.

RNU1.20P	1.32×10^{-2}	-6.24×10^{0}	1.14×10^{-8}	8.21×10^{-8}

AC090220.1	1.36×10^{-2}	-6.20×10^{0}	3.50×10^{-17}	1.00×10^{-15}
RNVU1.18	1.42×10^{-2}	-6.14×10^{0}	2.01×10^{-7}	1.16×10^{-6}
RNU1.139P	1.45×10^{-2}	-6.10×10^{0}	5.53×10^{-8}	3.53×10^{-7}
MTCYBP23	1.46×10^{-2}	-6.09×10^{0}	4.97×10^{-15}	1.02×10^{-13}
RNU1.46P	1.54×10^{-2}	-6.02×10^{0}	9.51×10^{-9}	6.92×10^{-8}
RNU2.59P	1.56×10^{-2}	-6.00×10^{0}	8.94×10^{-9}	6.54×10^{-8}
Y_RNA.209	1.56×10^{-2}	-6.00×10^{0}	7.92×10^{-8}	4.92×10^{-7}
SERPINB13	1.61×10^{-2}	-5.96×10^{0}	7.19×10^{-13}	1.04×10^{-11}
Y_RNA.241	1.69×10^{-2}	-5.88×10^{0}	4.25×10^{-11}	4.56×10^{-10}
MTCYBP32	1.76×10^{-2}	-5.83×10^{0}	4.67×10^{-10}	4.21×10^{-9}
KRT14	1.83×10^{-2}	-5.77×10^{0}	5.44×10^{-31}	1.23×10^{-28}
MUC6	1.90×10^{-2}	-5.72×10^{0}	1.44×10^{-57}	2.74×10^{-53}
RNU1.88P	1.94×10^{-2}	-5.69×10^{0}	9.47×10^{-9}	6.89×10^{-8}
AL157402.2	2.05×10^{-2}	-5.61×10^{0}	5.35×10^{-15}	1.09×10^{-13}
AL139274.1	2.09×10^{-2}	-5.58×10^{0}	4.34×10^{-11}	4.65×10^{-10}
RNU5A.1	2.19×10^{-2}	-5.51×10^{0}	2.34×10^{-13}	3.67×10^{-12}
MT.TH	2.24×10^{-2}	-5.48×10^{0}	2.24×10^{-16}	5.71×10^{-15}
AL360178.2	2.26×10^{-2}	-5.47×10^{0}	4.64×10^{-12}	5.87×10^{-11}
MTND1P11	2.27×10^{-2}	-5.46×10^{0}	2.29×10^{-17}	6.78×10^{-16}
AC069549.2	2.31×10^{-2}	-5.44×10^{0}	1.18×10^{-20}	5.60×10^{-19}
MSMB	2.32×10^{-2}	-5.43×10^{0}	9.77×10^{-35}	4.05×10^{-32}
AC079316.2	2.34×10^{-2}	-5.41×10^{0}	3.00×10^{-12}	3.91×10^{-11}
Y_RNA.713	2.35×10^{-2}	-5.41×10^{0}	2.58×10^{-9}	2.07×10^{-8}
MTND3P12	2.35×10^{-2}	-5.41×10^{0}	6.82×10^{-10}	6.00×10^{-9}
MTND5P26	2.35×10^{-2}	-5.41×10^{0}	1.78×10^{-8}	1.24×10^{-7}
IFNK	2.39×10^{-2}	-5.39×10^{0}	1.58×10^{-13}	2.54×10^{-12}
RLIMP1	2.40×10^{-2}	-5.38×10^{0}	1.38×10^{-27}	1.86×10^{-25}
Z93020.1	2.44×10^{-2}	-5.35×10^{0}	1.43×10^{-10}	1.42×10^{-9}
AC130895.1	2.45×10^{-2}	-5.35×10^{0}	1.02×10^{-11}	1.22×10^{-10}
AC009951.4	2.51×10^{-2}	-5.32×10^{0}	8.93×10^{-33}	2.68×10^{-30}
RNU2.23P	2.53×10^{-2}	-5.30×10^{0}	7.85×10^{-7}	4.05×10^{-6}
AL359095.1	2.54×10^{-2}	-5.30×10^{0}	2.95×10^{-11}	3.25×10^{-10}
AL035693.1	2.57×10^{-2}	-5.28×10^{0}	1.43×10^{-17}	4.36×10^{-16}
AL138713.1	2.57×10^{-2}	-5.28×10^{0}	6.29×10^{-15}	1.27×10^{-13}
MTCO3P23	2.59×10^{-2}	-5.27×10^{0}	3.51×10^{-11}	3.82×10^{-10}
ANXA10	2.64×10^{-2}	-5.24×10^{0}	6.88×10^{-43}	1.09×10^{-39}
RN7SKP227	2.66×10^{-2}	-5.23×10^{0}	4.28×10^{-3}	1.02×10^{-2}
CRCT1	2.67×10^{-2}	-5.23×10^{0}	1.07×10^{-12}	1.50×10^{-11}
DIAPH1.AS1	2.69×10^{-2}	-5.22×10^{0}	8.55×10^{-23}	5.80×10^{-21}
AC087286.1	2.69×10^{-2}	-5.22×10^{0}	2.21×10^{-12}	2.95×10^{-11}

Table A.2 (continued). The list of the top 100 downregulated DEGs identified in the CS1 subtype using edgeR as a result of two clustering analyzes.

MTND4P14	2.71×10^{-2}	-5.21×10^{0}	1.17×10^{-28}	1.87×10^{-26}
FOXN3.AS2	2.74×10^{-2}	-5.19×10^{0}	8.51×10^{-13}	1.21×10^{-11}

AC107050.1	2.74×10^{-2}	-5.19×10^{0}	3.58×10^{-31}	8.30×10^{-29}
AL356057.1	2.76×10^{-2}	-5.18×10^{0}	1.55×10^{-8}	1.09×10^{-7}
RAD51AP1P1	2.78×10^{-2}	-5.17×10^{0}	3.52×10^{-10}	3.24×10^{-9}
RNU4.6P	2.78×10^{-2}	-5.17×10^{0}	2.26×10^{-9}	1.83×10^{-8}
RNU1.148P	2.83×10^{-2}	-5.14×10^{0}	1.10×10^{-8}	7.91×10^{-8}
LPP.AS1	2.88×10^{-2}	-5.12×10^{0}	2.06×10^{-8}	1.42×10^{-7}
PLCB1.IT1	2.89×10^{-2}	-5.11×10^{0}	9.23×10^{-8}	5.68×10^{-7}
AL391863.2	2.90×10^{-2}	-5.11×10^{0}	8.73×10^{-14}	1.46×10^{-12}
RNU1.42P	2.90×10^{-2}	-5.11×10^{0}	8.44×10^{-9}	6.20×10^{-8}
AL589655.1	2.94×10^{-2}	-5.09×10^{0}	2.64×10^{-7}	1.49×10^{-6}
EIF4E2P1	2.94×10^{-2}	-5.09×10^{0}	3.42×10^{-9}	2.69×10^{-8}
AC022133.2	2.94×10^{-2}	-5.09×10^{0}	2.71×10^{-26}	2.99×10^{-24}
AC008833.1	2.95×10^{-2}	-5.08×10^{0}	6.75×10^{-9}	5.04×10^{-8}
AC120349.2	2.95×10^{-2}	-5.08×10^{0}	4.22×10^{-9}	3.26×10^{-8}
Y_RNA.720	2.97×10^{-2}	-5.07×10^{0}	6.97×10^{-10}	6.12×10^{-9}
AC133106.1	2.98×10^{-2}	-5.07×10^{0}	3.38×10^{-14}	6.02×10^{-13}
AL390318.1	2.99×10^{-2}	-5.06×10^{0}	1.48×10^{-5}	6.00×10^{-5}
AL356785.1	2.99×10^{-2}	-5.06×10^{0}	1.23×10^{-9}	1.04×10^{-8}
VTRNA1.2	3.01×10^{-2}	-5.06×10^{0}	8.28×10^{-28}	1.14×10^{-25}
SNRPGP18	3.03×10^{-2}	-5.04×10^{0}	2.00×10^{-8}	1.38×10^{-7}
AF127577.6	3.09×10^{-2}	-5.02×10^{0}	1.22×10^{-31}	3.04×10^{-29}
MTND1P32	3.09×10^{-2}	-5.01×10^{0}	9.45×10^{-11}	9.57×10^{-10}
AC026124.1	3.10×10^{-2}	-5.01×10^{0}	1.18×10^{-17}	3.64×10^{-16}
MTATP6P11	3.11×10^{-2}	-5.01×10^{0}	2.09×10^{-18}	7.21×10^{-17}
AC125612.1	3.11×10^{-2}	-5.01×10^{0}	2.85×10^{-12}	3.73×10^{-11}
MTCYBP3	3.14×10^{-2}	-5.00×10^{0}	6.57×10^{-21}	3.27×10^{-19}
AC005183.1	3.15×10^{-2}	-4.99×10^{0}	3.53×10^{-24}	2.86×10^{-22}
AL357141.1	3.16×10^{-2}	-4.98×10^{0}	6.12×10^{-20}	2.62×10^{-18}
SOX5.AS1	3.18×10^{-2}	-4.97×10^{0}	6.57×10^{-11}	6.83×10^{-10}
ZBTB20.AS5	3.18×10^{-2}	-4.97×10^{0}	3.92×10^{-12}	5.01×10^{-11}
AL391097.1	3.19×10^{-2}	-4.97×10^{0}	6.43×10^{-11}	6.71×10^{-10}
GP2	3.20×10^{-2}	-4.97×10^{0}	2.01×10^{-34}	8.06×10^{-32}
SNORA70.24	3.22×10^{-2}	-4.96×10^{0}	4.86×10^{-9}	3.72×10^{-8}
RNU1.3	3.23×10^{-2}	-4.95×10^{0}	1.49×10^{-6}	7.29×10^{-6}
RNU5B.1	3.24×10^{-2}	-4.95×10^{0}	8.27×10^{-7}	4.24×10^{-6}
HECW1.IT1	3.25×10^{-2}	-4.94×10^{0}	2.28×10^{-12}	3.04×10^{-11}
TAAR1	3.25×10^{-2}	-4.94×10^{0}	1.27×10^{-25}	1.29×10^{-23}
AC100800.1	3.26×10^{-2}	-4.94×10^{0}	1.32×10^{-8}	9.39×10^{-8}
RNU1.43P	3.27×10^{-2}	-4.94×10^{0}	2.18×10^{-7}	1.25×10^{-6}

Table A.2 (continued). The list of the top 100 downregulated DEGs identified in the CS1 subtype using edgeR as a result of two clustering analyzes.

RNU1.55P	3.27×10^{-2}	-4.93×10^{0}	1.14×10^{-8}	8.16×10^{-8}
AL136320.1	3.27×10^{-2}	-4.93×10^{0}	1.14×10^{-11}	1.35×10^{-10}

ST7.AS2	3.28×10^{-2}	-4.93×10^{0}	2.84×10^{-26}	3.13×10^{-24}
DOCK4.AS1	3.33×10^{-2}	-4.91×10^{0}	2.42×10^{-18}	8.28×10^{-17}
AC016542.2	3.33×10^{-2}	-4.91×10^{0}	4.46×10^{-20}	1.93×10^{-18}
AC100763.1	3.33×10^{-2}	-4.91×10^{0}	7.90×10^{-10}	6.87×10^{-9}

Table A.3. The list of the top 100 upregulated DEGs identified in the CS2 subtype using edgeR as a result of two clustering analyzes.

	fc	**log2fc**	**pvalue**	**padj**
RNY4	1.66×10^{2}	7.38×10^{0}	4.67×10^{-9}	3.59×10^{-8}
PAEP	1.35×10^{2}	7.08×10^{0}	2.59×10^{-63}	1.48×10^{-58}
FBXO40	1.08×10^{2}	6.75×10^{0}	5.33×10^{-31}	1.21×10^{-28}
MTND5P32	9.22×10^{1}	6.53×10^{0}	5.77×10^{-16}	1.37×10^{-14}
RNU1.28P	8.99×10^{1}	6.49×10^{0}	1.22×10^{-6}	6.08×10^{-6}
RNVU1.2	8.80×10^{1}	6.46×10^{0}	1.74×10^{-14}	3.24×10^{-13}
CLDN18	8.42×10^{1}	6.40×10^{0}	2.72×10^{-58}	7.78×10^{54}
AC066616.2	8.36×10^{1}	6.38×10^{0}	6.04×10^{-16}	1.43×10^{-14}
RNU1.52P	8.30×10^{1}	6.38×10^{0}	4.68×10^{-9}	3.60×10^{-8}
TFAP2B	7.80×10^{1}	6.29×10^{0}	4.78×10^{-16}	1.15×10^{-14}
RNU1.19P	7.74×10^{1}	6.27×10^{0}	1.10×10^{-10}	1.10×10^{-9}
RNU1.83P	7.64×10^{1}	6.26×10^{0}	4.91×10^{-12}	6.19×10^{-11}
RNU1.20P	7.58×10^{1}	6.24×10^{0}	1.14×10^{-8}	8.21×10^{-8}
AC090220.1	7.37×10^{1}	6.20×10^{0}	3.50×10^{-17}	1.00×10^{-15}
RNVU1.18	7.04×10^{1}	6.14×10^{0}	2.01×10^{-7}	1.16×10^{-6}
RNU1.139P	6.88×10^{1}	6.10×10^{0}	5.53×10^{-8}	3.53×10^{-7}
MTCYBP23	6.83×10^{1}	6.09×10^{0}	4.97×10^{-15}	1.02×10^{-13}
RNU1.46P	6.51×10^{1}	6.02×10^{0}	9.51×10^{-9}	6.92×10^{-8}
RNU2.59P	6.43×10^{1}	6.01×10^{0}	8.94×10^{-9}	6.54×10^{-8}
Y_RNA.209	6.40×10^{1}	6.00×10^{0}	7.92×10^{-8}	4.92×10^{-7}
SERPINB13	6.22×10^{1}	5.96×10^{0}	7.19×10^{-13}	1.04×10^{-11}
Y_RNA.241	5.90×10^{1}	5.88×10^{0}	4.25×10^{-11}	4.56×10^{-10}
MTCYBP32	5.69×10^{1}	5.83×10^{0}	4.67×10^{-10}	4.21×10^{-9}
KRT14	5.47×10^{1}	5.77×10^{0}	5.44×10^{-31}	1.23×10^{-28}
MUC6	5.27×10^{1}	5.72×10^{0}	1.44×10^{-57}	2.74×10^{-53}
RNU1.88P	5.16×10^{1}	5.69×10^{0}	9.47×10^{-9}	6.89×10^{-8}
AL157402.2	4.89×10^{1}	5.61×10^{0}	5.35×10^{-15}	1.09×10^{-13}
AL139274.1	4.79×10^{1}	5.58×10^{0}	4.34×10^{-11}	4.65×10^{-10}
RNU5A.1	4.57×10^{1}	5.51×10^{0}	2.34×10^{-13}	3.67×10^{-12}
MT.TH	4.46×10^{1}	5.48×10^{0}	2.24×10^{-16}	5.71×10^{-15}
AL360178.2	4.42×10^{1}	5.47×10^{0}	4.64×10^{-12}	5.87×10^{-11}

Table A.3 (continued). The list of the top 100 upregulated DEGs identified in the CS2 subtype using edgeR as a result of two clustering analyzes.

MTND1P11	4.40×10^{1}	5.46×10^{0}	2.29×10^{-17}	6.78×10^{-16}
AC069549.2	4.34×10^{1}	5.44×10^{0}	1.18×10^{-20}	5.60×10^{-19}
MSMB	4.32×10^{1}	5.43×10^{0}	9.77×10^{-35}	4.05×10^{-32}

AC079316.2	4.26×10^{1}	5.41×10^{0}	3.00×10^{-12}	3.91×10^{-11}
Y_RNA.713	4.26×10^{1}	5.41×10^{0}	2.58×10^{-9}	2.07×10^{-8}
MTND3P12	4.25×10^{1}	5.41×10^{0}	6.82×10^{-10}	6.00×10^{-9}
MTND5P26	4.25×10^{1}	5.41×10^{0}	1.78×10^{-8}	1.24×10^{-7}
IFNK	4.19×10^{1}	5.39×10^{0}	1.58×10^{-13}	2.54×10^{-12}
RLIMP1	4.16×10^{1}	5.38×10^{0}	1.38×10^{-27}	1.86×10^{-25}
Z93020.1	4.09×10^{1}	5.35×10^{0}	1.43×10^{-10}	1.42×10^{-9}
AC130895.1	4.08×10^{1}	5.35×10^{0}	1.02×10^{-11}	1.22×10^{-10}
AC009951.4	3.98×10^{1}	5.32×10^{0}	8.93×10^{-33}	2.68×10^{-30}
RNU2.23P	3.95×10^{1}	5.31×10^{0}	7.85×10^{-7}	4.05×10^{-6}
AL359095.1	3.94×10^{1}	5.30×10^{0}	2.95×10^{-11}	3.25×10^{-10}
AL035693.1	3.89×10^{1}	5.28×10^{0}	1.43×10^{-17}	4.36×10^{-16}
AL138713.1	3.89×10^{1}	5.28×10^{0}	6.29×10^{-15}	1.27×10^{-13}
MTCO3P23	3.85×10^{1}	5.27×10^{0}	3.51×10^{-11}	3.82×10^{-10}
ANXA10	3.78×10^{1}	5.24×10^{0}	6.88×10^{-43}	1.09×10^{-39}
RN7SKP227	3.76×10^{1}	5.23×10^{0}	4.28×10^{-3}	1.02×10^{-2}
CRCT1	3.74×10^{1}	5.23×10^{0}	1.07×10^{-12}	1.50×10^{-11}
DIAPH1.AS1	3.72×10^{1}	5.22×10^{0}	8.55×10^{-23}	5.80×10^{-21}
AC087286.1	3.72×10^{1}	5.22×10^{0}	2.21×10^{-12}	2.95×10^{-11}
MTND4P14	3.69×10^{1}	5.21×10^{0}	1.17×10^{-28}	1.87×10^{-26}
FOXN3.AS2	3.65×10^{1}	5.19×10^{0}	8.51×10^{-13}	1.21×10^{-11}
AC107050.1	3.64×10^{1}	5.19×10^{0}	3.58×10^{-31}	8.30×10^{-29}
AL356057.1	3.63×10^{1}	5.18×10^{0}	1.55×10^{-8}	1.09×10^{-7}
RAD51AP1P1	3.60×10^{1}	5.17×10^{0}	3.52×10^{-10}	3.24×10^{-9}
RNU4.6P	3.59×10^{1}	5.17×10^{0}	2.26×10^{-9}	1.83×10^{-8}
RNU1.148P	3.53×10^{1}	5.14×10^{0}	1.10×10^{-8}	7.91×10^{-8}
LPP.AS1	3.48×10^{1}	5.12×10^{0}	2.06×10^{-8}	1.42×10^{-7}
PLCB1.IT1	3.46×10^{1}	5.11×10^{0}	9.23×10^{-8}	5.68×10^{-7}
AL391863.2	3.45×10^{1}	5.11×10^{0}	8.73×10^{-14}	1.46×10^{-12}
RNU1.42P	3.45×10^{1}	5.11×10^{0}	8.44×10^{-9}	6.20×10^{-8}
AL589655.1	3.41×10^{1}	5.09×10^{0}	2.64×10^{-7}	1.49×10^{-6}
EIF4E2P1	3.40×10^{1}	5.09×10^{0}	3.42×10^{-9}	2.69×10^{-8}
AC022133.2	3.40×10^{1}	5.09×10^{0}	2.71×10^{-26}	2.99×10^{-24}
AC008833.1	3.39×10^{1}	5.08×10^{0}	6.75×10^{-9}	5.04×10^{-8}
AC120349.2	3.39×10^{1}	5.08×10^{0}	4.22×10^{-9}	3.26×10^{-8}
Y_RNA.720	3.37×10^{1}	5.07×10^{0}	6.97×10^{-10}	6.12×10^{-9}
AC133106.1	3.35×10^{1}	5.07×10^{0}	3.38×10^{-14}	6.02×10^{-13}
AL390318.1	3.34×10^{1}	5.06×10^{0}	1.48×10^{-5}	6.00×10^{-5}

Table A.3 (continued). The list of the top 100 upregulated DEGs identified in the CS2 subtype using edgeR as a result of two clustering analyzes.

AL356785.1	3.34×10^{1}	5.06×10^{0}	1.23×10^{-9}	1.04×10^{-8}
VTRNA1.2	3.33×10^{1}	5.06×10^{0}	8.28×10^{-28}	1.14×10^{-25}
SNRPGP18	3.30×10^{1}	5.04×10^{0}	2.00×10^{-8}	1.38×10^{-7}

AF127577.6	3.23×10^{1}	5.02×10^{0}	1.22×10^{-31}	3.04×10^{-29}
MTND1P32	3.23×10^{1}	5.01×10^{0}	9.45×10^{-11}	9.57×10^{-10}
AC026124.1	3.23×10^{1}	5.01×10^{0}	1.18×10^{-17}	3.64×10^{-16}
MTATP6P11	3.22×10^{1}	5.01×10^{0}	2.09×10^{-18}	7.21×10^{-17}
AC125612.1	3.21×10^{1}	5.01×10^{0}	2.85×10^{-12}	3.73×10^{-11}
MTCYBP3	3.19×10^{1}	5.00×10^{0}	6.57×10^{-21}	3.27×10^{-19}
AC005183.1	3.17×10^{1}	4.99×10^{0}	3.53×10^{-24}	2.86×10^{-22}
AL357141.1	3.17×10^{1}	4.98×10^{0}	6.12×10^{-20}	2.62×10^{-18}
SOX5.AS1	3.14×10^{1}	4.97×10^{0}	6.57×10^{-11}	6.83×10^{-10}
ZBTB20.AS5	3.14×10^{1}	4.97×10^{0}	3.92×10^{-12}	5.01×10^{-11}
AL391097.1	3.13×10^{1}	4.97×10^{0}	6.43×10^{-11}	6.71×10^{-10}
GP2	3.13×10^{1}	4.97×10^{0}	2.01×10^{-34}	8.06×10^{-32}
SNORA70.24	3.11×10^{1}	4.96×10^{0}	4.86×10^{-9}	3.72×10^{-8}
RNU1.3	3.09×10^{1}	4.95×10^{0}	1.49×10^{-6}	7.29×10^{-6}
RNU5B.1	3.09×10^{1}	4.95×10^{0}	8.27×10^{-7}	4.24×10^{-6}
HECW1.IT1	3.08×10^{1}	4.94×10^{0}	2.28×10^{-12}	3.04×10^{-11}
TAAR1	3.08×10^{1}	4.94×10^{0}	1.27×10^{-25}	1.29×10^{-23}
AC100800.1	3.07×10^{1}	4.94×10^{0}	1.32×10^{-8}	9.39×10^{-8}
RNU1.43P	3.06×10^{1}	4.94×10^{0}	2.18×10^{-7}	1.25×10^{-6}
RNU1.55P	3.06×10^{1}	4.93×10^{0}	1.14×10^{-8}	8.16×10^{-8}
AL136320.1	3.06×10^{1}	4.93×10^{0}	1.14×10^{-11}	1.35×10^{-10}
ST7.AS2	3.05×10^{1}	4.93×10^{0}	2.84×10^{-26}	3.13×10^{-24}
DOCK4.AS1	3.01×10^{1}	4.91×10^{0}	2.42×10^{-18}	8.28×10^{-17}
AC016542.2	3.00×10^{1}	4.91×10^{0}	4.46×10^{-20}	1.93×10^{-18}
AC100763.1	3.00×10^{1}	4.91×10^{0}	7.90×10^{-10}	6.87×10^{-9}

Table A.4. The list of the top 100 downregulated DEGs identified in the CS2 subtype using edgeR as a result of two clustering analyzes.

	fc	**log2fc**	**pvalue**	**padj**
WIF1	1.99×10^{-2}	-5.65×10^{0}	4.68×10^{-30}	9.46×10^{-28}
BX322234.2	2.17×10^{-2}	-5.53×10^{0}	1.63×10^{-7}	9.53×10^{-7}
RNA5.8SP5	2.57×10^{-2}	-5.28×10^{0}	2.07×10^{-3}	5.35×10^{-3}
AC152010.1	2.68×10^{-2}	-5.22×10^{0}	5.46×10^{-3}	1.27×10^{-2}
ORM1	3.31×10^{-2}	-4.92×10^{0}	2.02×10^{-18}	6.97×10^{-17}
RNA5SP267	3.58×10^{-2}	-4.80×10^{0}	1.83×10^{-2}	3.66×10^{-2}
RNA5SP211	3.62×10^{-2}	-4.79×10^{0}	2.21×10^{-2}	4.29×10^{-2}
RN7SL618P	3.78×10^{-2}	-4.73×10^{0}	1.44×10^{-2}	2.97×10^{-2}
PTF1A	4.36×10^{-2}	-4.52×10^{0}	6.23×10^{-16}	1.47×10^{-14}

Table A.4 (continued). The list of the top 100 downregulated DEGs identified in the CS2 subtype using edgeR as a result of two clustering analyzes.

RNA5SP389	4.66×10^{-2}	-4.42×10^{0}	2.16×10^{-2}	4.21×10^{-2}
SFTPC	4.76×10^{-2}	-4.39×10^{0}	2.04×10^{-6}	9.73×10^{-6}
KRT31	5.45×10^{-2}	-4.20×10^{0}	2.95×10^{-12}	3.84×10^{-11}
SOHLH1	6.17×10^{-2}	-4.02×10^{0}	2.38×10^{-10}	2.26×10^{-9}

RN7SL149P	6.33×10^{-2}	-3.98×10^{0}	2.07×10^{-2}	4.06×10^{-2}
AC127459.2	6.92×10^{-2}	-3.85×10^{0}	8.57×10^{-6}	3.65×10^{-5}
AC114291.1	7.16×10^{-2}	-3.80×10^{0}	9.34×10^{-37}	5.14×10^{-34}
AC026336.3	7.32×10^{-2}	-3.77×10^{0}	1.45×10^{-22}	9.41×10^{-21}
LINC01896	7.33×10^{-2}	-3.77×10^{0}	1.29×10^{-3}	3.50×10^{-3}
PRR9	7.76×10^{-2}	-3.69×10^{0}	3.38×10^{-9}	2.66×10^{-8}
RN7SL762P	7.78×10^{-2}	-3.68×10^{0}	1.29×10^{-8}	9.18×10^{-8}
AL356433.1	8.15×10^{-2}	-3.62×10^{0}	3.79×10^{-14}	6.69×10^{-13}
XAGE2	8.26×10^{-2}	-3.60×10^{0}	6.57×10^{-7}	3.44×10^{-6}
GOLGA6L2	8.74×10^{-2}	-3.52×10^{0}	4.68×10^{-20}	2.03×10^{-18}
GALP	8.87×10^{-2}	-3.49×10^{0}	1.14×10^{-3}	3.13×10^{-3}
AC026774.1	9.19×10^{-2}	-3.44×10^{0}	7.53×10^{-18}	2.41×10^{-16}
AC009446.1	9.24×10^{-2}	-3.44×10^{0}	2.40×10^{-3}	6.11×10^{-3}
MAGEB17	9.25×10^{-2}	-3.43×10^{0}	1.10×10^{-17}	3.42×10^{-16}
APOA2	9.30×10^{-2}	-3.43×10^{0}	1.53×10^{-14}	2.90×10^{-13}
PPBP	9.64×10^{-2}	-3.37×10^{0}	2.56×10^{-11}	2.85×10^{-10}
NOTUM	9.76×10^{-2}	-3.36×10^{0}	2.99×10^{-23}	2.14×10^{-21}
PNLIP	9.79×10^{-2}	-3.35×10^{0}	1.88×10^{-2}	3.75×10^{-2}
SLC5A8	9.92×10^{-2}	-3.33×10^{0}	2.42×10^{-7}	1.37×10^{-6}
AC078993.1	9.98×10^{-2}	-3.32×10^{0}	3.95×10^{-20}	1.73×10^{-18}
TKTL1	1.03×10^{-1}	-3.28×10^{0}	2.09×10^{-12}	2.81×10^{-11}
GDF10	1.07×10^{-1}	-3.23×10^{0}	7.81×10^{-15}	1.54×10^{-13}
PRSS56	1.07×10^{-1}	-3.23×10^{0}	2.76×10^{-7}	1.55×10^{-6}
RNA5SP213	1.07×10^{-1}	-3.22×10^{0}	1.36×10^{-2}	2.83×10^{-2}
KRT40	1.09×10^{-1}	-3.20×10^{0}	1.44×10^{-16}	3.77×10^{-15}
AP002963.1	1.09×10^{-1}	-3.20×10^{0}	5.21×10^{-3}	1.22×10^{-2}
TUBAP13	1.10×10^{-1}	-3.18×10^{0}	1.74×10^{-17}	5.25×10^{-16}
MAGEB1	1.12×10^{-1}	-3.16×10^{0}	2.11×10^{-2}	4.12×10^{-2}
HSPB3	1.13×10^{-1}	-3.14×10^{0}	4.69×10^{-16}	1.13×10^{-14}
CPN1	1.14×10^{-1}	-3.14×10^{0}	7.07×10^{-17}	1.94×10^{-15}
LINC00661	1.14×10^{-1}	-3.13×10^{0}	5.63×10^{-4}	1.66×10^{-3}
SSX1	1.14×10^{-1}	-3.13×10^{0}	7.29×10^{-4}	2.10×10^{-3}
GPR83	1.15×10^{-1}	-3.12×10^{0}	5.60×10^{-20}	2.41×10^{-18}
AC108865.1	1.15×10^{-1}	-3.12×10^{0}	5.28×10^{-12}	6.61×10^{-11}
TMEM252	1.17×10^{-1}	-3.09×10^{0}	6.43×10^{-23}	4.45×10^{-21}
SLC30A2	1.19×10^{-1}	-3.07×10^{0}	6.06×10^{-27}	7.42×10^{-25}
LY6G6D	1.21×10^{-1}	-3.05×10^{0}	9.38×10^{-16}	2.14×10^{-14}

Table A.4 (continued). The list of the top 100 downregulated DEGs identified in the CS2 subtype using edgeR as a result of two clustering analyzes.

RN7SL122P	1.21×10^{-1}	-3.04×10^{0}	1.83×10^{-2}	3.66×10^{-2}
LCN15	1.22×10^{-1}	-3.04×10^{0}	2.86×10^{-11}	3.16×10^{-10}
TNNC2	1.25×10^{-1}	-3.00×10^{0}	3.86×10^{-44}	7.88×10^{-41}
AC010255.2	1.27×10^{-1}	-2.98×10^{0}	1.86×10^{-10}	1.80×10^{-9}
MAGEC2	1.28×10^{-1}	-2.97×10^{0}	6.29×10^{-3}	1.44×10^{-2}

BPIFA1	1.29×10^{-1}	-2.96×10^{0}	4.30×10^{-3}	1.03×10^{-2}
SYN3	1.29×10^{-1}	-2.95×10^{0}	4.46×10^{-33}	1.42×10^{-30}
LINC02525	1.32×10^{-1}	-2.92×10^{0}	5.92×10^{-12}	7.36×10^{-11}
AC091304.1	1.34×10^{-1}	-2.90×10^{0}	2.17×10^{-11}	2.46×10^{-10}
HS3ST4	1.38×10^{-1}	-2.85×10^{0}	3.84×10^{-9}	2.99×10^{-8}
KRT37	1.40×10^{-1}	-2.84×10^{0}	6.34×10^{-12}	7.85×10^{-11}
VWA5B1	1.40×10^{-1}	-2.83×10^{0}	4.72×10^{-12}	5.96×10^{-11}
AC132825.1	1.42×10^{-1}	-2.82×10^{0}	6.46×10^{-9}	4.84×10^{-8}
DMRT1	1.46×10^{-1}	-2.78×10^{0}	2.55×10^{-9}	2.05×10^{-8}
CTNNA2.AS1	1.48×10^{-1}	-2.76×10^{0}	2.51×10^{-5}	9.75×10^{-5}
AL512356.5	1.48×10^{-1}	-2.76×10^{0}	3.74×10^{-10}	3.42×10^{-9}
RNA5SP243	1.48×10^{-1}	-2.76×10^{0}	5.49×10^{-3}	1.27×10^{-2}
SALL3	1.48×10^{-1}	-2.76×10^{0}	1.62×10^{-3}	4.30×10^{-3}
AL354863.1	1.50×10^{-1}	-2.74×10^{0}	2.46×10^{-8}	1.67×10^{-7}
MIR483	1.51×10^{-1}	-2.73×10^{0}	1.05×10^{-4}	3.62×10^{-4}
FGF3	1.53×10^{-1}	-2.71×10^{0}	1.86×10^{-8}	1.29×10^{-7}
RN7SL217P	1.55×10^{-1}	-2.69×10^{0}	1.86×10^{-2}	3.71×10^{-2}
AC079804.2	1.55×10^{-1}	-2.69×10^{0}	1.84×10^{-6}	8.84×10^{-6}
RN7SL253P	1.55×10^{-1}	-2.69×10^{0}	5.71×10^{-4}	1.69×10^{-3}
C6orf15	1.55×10^{-1}	-2.69×10^{0}	2.07×10^{-12}	2.78×10^{-11}
KRT23	1.57×10^{-1}	-2.67×10^{0}	4.94×10^{-23}	3.48×10^{-21}
AL121885.2	1.57×10^{-1}	-2.67×10^{0}	3.86×10^{-13}	5.82×10^{-12}
LY6G6F.LY6G6D	1.58×10^{-1}	-2.67×10^{0}	2.72×10^{-12}	3.58×10^{-11}
RPS10.NUDT3	1.60×10^{-1}	-2.64×10^{0}	4.24×10^{-3}	1.01×10^{-2}
AP000851.2	1.61×10^{-1}	-2.63×10^{0}	1.92×10^{-11}	2.20×10^{-10}
TCAP	1.62×10^{-1}	-2.63×10^{0}	2.38×10^{-20}	1.09×10^{-18}
SHISA9	1.62×10^{-1}	-2.63×10^{0}	1.66×10^{-10}	1.62×10^{-9}
AL391650.2	1.62×10^{-1}	-2.63×10^{0}	3.59×10^{-12}	4.62×10^{-11}
MAP7D2	1.64×10^{-1}	-2.61×10^{0}	3.12×10^{-19}	1.21×10^{-17}
SULT2A1	1.65×10^{-1}	-2.60×10^{0}	2.21×10^{-11}	2.50×10^{-10}
OR10G4	1.66×10^{-1}	-2.59×10^{0}	1.83×10^{-4}	6.02×10^{-4}
IGF2	1.66×10^{-1}	-2.59×10^{0}	2.19×10^{-9}	1.78×10^{-8}
SERPINA7	1.67×10^{-1}	-2.58×10^{0}	2.38×10^{-11}	2.67×10^{-10}
BX276092.9	1.67×10^{-1}	-2.58×10^{0}	2.74×10^{-6}	1.28×10^{-5}

Table A.4 (continued). The list of the top 100 downregulated DEGs identified in the CS2 subtype using edgeR as a result of two clustering analyzes.

AP003774.2	1.69×10^{-1}	-2.56×10^{0}	1.74×10^{-31}	4.17×10^{-29}
GLRA2	1.70×10^{-1}	-2.56×10^{0}	3.37×10^{-15}	7.06×10^{-14}
KRTAP1.1	1.70×10^{-1}	-2.56×10^{0}	6.47×10^{-7}	3.39×10^{-6}
AC016925.3	1.70×10^{-1}	-2.56×10^{0}	1.12×10^{-9}	9.52×10^{-9}
CYP4F8	1.75×10^{-1}	-2.52×10^{0}	1.60×10^{-16}	4.15×10^{-15}

CELP	1.75×10^{-1}	-2.51×10^{0}	3.26×10^{-22}	2.00×10^{-20}
EYA1	1.76×10^{-1}	-2.51×10^{0}	2.32×10^{-15}	4.98×10^{-14}
SFTA3	1.76×10^{-1}	-2.50×10^{0}	6.01×10^{-3}	1.38×10^{-2}
SLC1A7	1.77×10^{-1}	-2.50×10^{0}	4.68×10^{-28}	6.80×10^{-26}
LINC02128	1.79×10^{-1}	-2.48×10^{0}	3.03×10^{-10}	2.82×10^{-9}
AC135388.1	1.80×10^{-1}	-2.48×10^{0}	4.01×10^{-16}	9.82×10^{-15}

Table A.5. The list of the top 100 upregulated DEGs identified in the CS1 subtype using DESeq2 as a result of two clustering analyzes.

	fc	**log2fc**	**pvalue**	**padj**
WIF1	4.83×10^{1}	5.59×10^{0}	1.03×10^{-50}	3.02×10^{-47}
PTF1A	2.59×10^{1}	4.69×10^{0}	3.33×10^{-22}	1.34×10^{-20}
PRSS56	2.33×10^{1}	4.54×10^{0}	6.35×10^{-26}	4.62×10^{-24}
IGF2	2.10×10^{1}	4.39×10^{0}	4.96×10^{-34}	1.22×10^{-31}
AL356433.1	1.97×10^{1}	4.30×10^{0}	1.57×10^{-23}	8.02×10^{-22}
LY6G6D	1.77×10^{1}	4.14×10^{0}	3.59×10^{-40}	2.01×10^{-37}
KRT35	1.52×10^{1}	3.93×10^{0}	2.63×10^{-16}	4.21×10^{-15}
AC114291.1	1.35×10^{1}	3.76×10^{0}	3.55×10^{-49}	7.01×10^{-46}
AC026336.3	1.32×10^{1}	3.72×10^{0}	3.64×10^{-31}	5.85×10^{-29}
AC026774.1	1.31×10^{1}	3.71×10^{0}	3.68×10^{-21}	1.26×10^{-19}
LY6G6F.LY6G6D	1.30×10^{1}	3.70×10^{0}	1.08×10^{-30}	1.63×10^{-28}
MAGEB17	1.18×10^{1}	3.56×10^{0}	5.29×10^{-26}	3.92×10^{-24}
GOLGA6L2	1.16×10^{1}	3.53×10^{0}	1.48×10^{-22}	6.27×10^{-21}
KRT43P	1.11×10^{1}	3.47×10^{0}	1.42×10^{-14}	1.73×10^{-13}
NOTUM	1.05×10^{1}	3.39×10^{0}	1.36×10^{-32}	2.82×10^{-30}
LCN15	1.04×10^{1}	3.38×10^{0}	8.61×10^{-21}	2.75×10^{-19}
KRT32	9.98×10^{0}	3.32×10^{0}	1.51×10^{-14}	1.84×10^{-13}
KRT37	9.89×10^{0}	3.31×10^{0}	2.73×10^{-18}	5.89×10^{-17}
CDH9	9.89×10^{0}	3.31×10^{0}	8.97×10^{-6}	2.93×10^{-5}
BX510359.5	9.66×10^{0}	3.27×10^{0}	6.11×10^{-13}	5.87×10^{-12}
BHLHA9	9.49×10^{0}	3.25×10^{0}	2.57×10^{-20}	7.69×10^{-19}
MAGEA4.AS1	8.92×10^{0}	3.16×10^{0}	7.00×10^{-5}	1.98×10^{-4}
SULT2A1	8.84×10^{0}	3.14×10^{0}	1.60×10^{-20}	4.93×10^{-19}
KRT40	8.83×10^{0}	3.14×10^{0}	2.81×10^{-21}	9.79×10^{-20}

Table A.5 (continued). The list of the top 100 upregulated DEGs identified in the CS1 subtype using DESeq2 as a result of two clustering analyzes.

HSPB3	8.75×10^{0}	3.13×10^{0}	2.99×10^{-20}	8.85×10^{-19}
CPN1	8.73×10^{0}	3.13×10^{0}	1.42×10^{-21}	5.15×10^{-20}
VWA5B1	8.63×10^{0}	3.11×10^{0}	1.71×10^{-18}	3.80×10^{-17}
SLC30A2	8.51×10^{0}	3.09×10^{0}	3.56×10^{-36}	1.17×10^{-33}
PRR9	8.27×10^{0}	3.05×10^{0}	5.16×10^{-11}	3.75×10^{-10}
TMEM252	8.25×10^{0}	3.04×10^{0}	3.97×10^{-29}	4.90×10^{-27}

AC003958.2	8.18 x 10^{0}	3.03 x 10^{0}	1.39 x 10^{-16}	2.31 x 10^{-15}
AC078993.1	8.10 x 10^{0}	3.02 x 10^{0}	6.13 x 10^{-22}	2.36 x 10^{-20}
AC108865.1	7.96 x 10^{0}	2.99 x 10^{0}	1.85 x 10^{-14}	2.21 x 10^{-13}
TNNC2	7.79 x 10^{0}	2.96 x 10^{0}	3.17 x 10^{-57}	1.74 x 10^{-53}
SERPINA10	7.63 x 10^{0}	2.93 x 10^{0}	7.47 x 10^{-26}	5.37 x 10^{-24}
NPTX2	7.52 x 10^{0}	2.91 x 10^{0}	5.28 x 10^{-31}	8.31 x 10^{-29}
LINC02864	7.49 x 10^{0}	2.91 x 10^{0}	3.92 x 10^{-9}	2.15 x 10^{-8}
AC110772.2	7.44 x 10^{0}	2.90 x 10^{0}	2.66 x 10^{-16}	4.25 x 10^{-15}
PCSK1N	7.31 x 10^{0}	2.87 x 10^{0}	9.43 x 10^{-21}	3.00 x 10^{-19}
LGALS14	7.31 x 10^{0}	2.87 x 10^{0}	7.38 x 10^{-10}	4.50 x 10^{-9}
TUBAP13	7.15 x 10^{0}	2.84 x 10^{0}	1.15 x 10^{-17}	2.26 x 10^{-16}
KRT41P	7.13 x 10^{0}	2.83 x 10^{0}	8.72 x 10^{-13}	8.19 x 10^{-12}
AL391650.2	7.09 x 10^{0}	2.83 x 10^{0}	2.92 x 10^{-13}	2.94 x 10^{-12}
SLC14A1	7.06 x 10^{0}	2.82 x 10^{0}	1.65 x 10^{-23}	8.38 x 10^{-22}
SYN3	7.05 x 10^{0}	2.82 x 10^{0}	1.61 x 10^{-38}	7.29 x 10^{-36}
SPACA3	6.98 x 10^{0}	2.80 x 10^{0}	3.64 x 10^{-32}	7.02 x 10^{-30}
CLDN10	6.95 x 10^{0}	2.80 x 10^{0}	1.56 x 10^{-15}	2.22 x 10^{-14}
AC108865.2	6.92 x 10^{0}	2.79 x 10^{0}	8.32 x 10^{-11}	5.85 x 10^{-10}
LINC02525	6.73 x 10^{0}	2.75 x 10^{0}	2.73 x 10^{-12}	2.38 x 10^{-11}
C6orf15	6.60 x 10^{0}	2.72 x 10^{0}	1.28 x 10^{-17}	2.49 x 10^{-16}
AL512356.5	6.58 x 10^{0}	2.72 x 10^{0}	5.22 x 10^{-11}	3.79 x 10^{-10}
MAGEA6	6.54 x 10^{0}	2.71 x 10^{0}	2.40 x 10^{-4}	6.19 x 10^{-4}
SERPINA7	6.29 x 10^{0}	2.65 x 10^{0}	1.34 x 10^{-14}	1.65 x 10^{-13}
DLX3	6.24 x 10^{0}	2.64 x 10^{0}	3.05 x 10^{-18}	6.52 x 10^{-17}
KRT23	6.23 x 10^{0}	2.64 x 10^{0}	5.78 x 10^{-29}	6.95 x 10^{-27}
LINC00545	6.19 x 10^{0}	2.63 x 10^{0}	7.20 x 10^{-12}	5.93 x 10^{-11}
ATP12A	5.81 x 10^{0}	2.54 x 10^{0}	4.73 x 10^{-13}	4.62 x 10^{-12}
AL121885.2	5.78 x 10^{0}	2.53 x 10^{0}	4.13 x 10^{-12}	3.51 x 10^{-11}
MAP7D2	5.77 x 10^{0}	2.53 x 10^{0}	4.75 x 10^{-23}	2.24 x 10^{-21}
AP000851.2	5.76 x 10^{0}	2.53 x 10^{0}	7.82 x 10^{-11}	5.52 x 10^{-10}
AC135388.1	5.73 x 10^{0}	2.52 x 10^{0}	1.43 x 10^{-18}	3.23 x 10^{-17}
CELP	5.67 x 10^{0}	2.50 x 10^{0}	1.01 x 10^{-27}	1.01 x 10^{-25}
AP003774.2	5.65 x 10^{0}	2.50 x 10^{0}	2.25 x 10^{-37}	8.68 x 10^{-35}
AC091304.1	5.62 x 10^{0}	2.49 x 10^{0}	6.05 x 10^{-7}	2.38 x 10^{-6}
AC109136.1	5.60 x 10^{0}	2.49 x 10^{0}	8.77 x 10^{-10}	5.30 x 10^{-9}

Table A.5 (continued). The list of the top 100 upregulated DEGs identified in the CS1 subtype using DESeq2 as a result of two clustering analyzes.

GS1.594A7.3	5.58 x 10^{0}	2.48 x 10^{0}	1.14 x 10^{-8}	5.86 x 10^{-8}
MAGEA4	5.56 x 10^{0}	2.48 x 10^{0}	8.35 x 10^{-4}	1.95 x 10^{-3}
KRT31	5.54 x 10^{0}	2.47 x 10^{0}	2.48 x 10^{-8}	1.21 x 10^{-7}
AC110772.1	5.50 x 10^{0}	2.46 x 10^{0}	1.32 x 10^{-9}	7.77 x 10^{-9}
MIR483	5.44 x 10^{0}	2.44 x 10^{0}	1.42 x 10^{-3}	3.16 x 10^{-3}
NEUROD1	5.44 x 10^{0}	2.44 x 10^{0}	3.40 x 10^{-8}	1.63 x 10^{-7}
ORM1	5.42 x 10^{0}	2.44 x 10^{0}	2.11 x 10^{-12}	1.88 x 10^{-11}

SLC1A7	5.33×10^{0}	2.41×10^{0}	2.52×10^{-32}	5.00×10^{-30}
PAGE1	5.28×10^{0}	2.40×10^{0}	3.95×10^{-3}	8.08×10^{-3}
SHISA9	5.23×10^{0}	2.39×10^{0}	6.39×10^{-11}	4.58×10^{-10}
ZP2	5.18×10^{0}	2.37×10^{0}	3.03×10^{-21}	1.05×10^{-19}
LINC02178	5.07×10^{0}	2.34×10^{0}	5.69×10^{-8}	2.63×10^{-7}
ELF5	5.07×10^{0}	2.34×10^{0}	1.04×10^{-9}	6.24×10^{-9}
FGF3	5.04×10^{0}	2.33×10^{0}	5.18×10^{-9}	2.79×10^{-8}
PPBP	5.03×10^{0}	2.33×10^{0}	1.92×10^{-12}	1.71×10^{-11}
LINC02128	5.01×10^{0}	2.32×10^{0}	1.94×10^{-10}	1.29×10^{-9}
MC3R	4.97×10^{0}	2.31×10^{0}	1.78×10^{-8}	8.90×10^{-8}
SLC39A2	4.96×10^{0}	2.31×10^{0}	4.85×10^{-13}	4.72×10^{-12}
LINC00355	4.95×10^{0}	2.31×10^{0}	3.56×10^{-5}	1.06×10^{-4}
AC091839.1	4.95×10^{0}	2.31×10^{0}	1.31×10^{-4}	3.53×10^{-4}
KRT38	4.93×10^{0}	2.30×10^{0}	1.30×10^{-6}	4.85×10^{-6}
PHYHIPL	4.90×10^{0}	2.29×10^{0}	1.39×10^{-14}	1.70×10^{-13}
TGM6	4.90×10^{0}	2.29×10^{0}	4.50×10^{-4}	1.10×10^{-3}
RBP2	4.88×10^{0}	2.29×10^{0}	1.37×10^{-18}	3.11×10^{-17}
AL035252.2	4.88×10^{0}	2.29×10^{0}	1.04×10^{-9}	6.24×10^{-9}
AC079804.2	4.87×10^{0}	2.28×10^{0}	9.89×10^{-6}	3.21×10^{-5}
DRD2	4.85×10^{0}	2.28×10^{0}	2.74×10^{-19}	6.98×10^{-18}
MAGEA11	4.83×10^{0}	2.27×10^{0}	5.88×10^{-5}	1.69×10^{-4}
CTNNA2	4.81×10^{0}	2.27×10^{0}	9.35×10^{-13}	8.73×10^{-12}
AL445205.1	4.81×10^{0}	2.27×10^{0}	6.80×10^{-8}	3.11×10^{-7}
CRAT37	4.79×10^{0}	2.26×10^{0}	6.00×10^{-13}	5.76×10^{-12}
SLC13A3	4.77×10^{0}	2.25×10^{0}	7.71×10^{-21}	2.50×10^{-19}
PAH	4.71×10^{0}	2.24×10^{0}	8.00×10^{-16}	1.19×10^{-14}
AL390334.1	4.67×10^{0}	2.22×10^{0}	4.02×10^{-4}	9.93×10^{-4}
UMODL1	4.67×10^{0}	2.22×10^{0}	2.77×10^{-29}	3.50×10^{-27}

Table A.6. The list of the top 100 downregulated DEGs identified in the CS1 subtype using DESeq2 as a result of two clustering analyzes.

	fc	**log2fc**	**pvalue**	**padj**
RN7SKP227	3.33×10^{-4}	-1.16×10^{1}	2.66×10^{-7}	1.11×10^{-6}
CLDN18	5.37×10^{-3}	-7.54×10^{0}	1.18×10^{-118}	5.16×10^{-114}

Table A.6 (continued). The list of the top 100 downregulated DEGs identified in the CS1 subtype using DESeq2 as a result of two clustering analyzes.

RN7SKP203	7.80×10^{-3}	-7.00×10^{0}	3.10×10^{-15}	4.22×10^{-14}
AL139274.1	8.64×10^{-3}	-6.85×10^{0}	7.13×10^{-17}	1.24×10^{-15}
RNU1.88P	8.91×10^{-3}	-6.81×10^{0}	2.41×10^{-15}	3.33×10^{-14}
MIR3609	1.33×10^{-2}	-6.23×10^{0}	2.44×10^{-27}	2.28×10^{-25}
ANXA10	1.37×10^{-2}	-6.19×10^{0}	5.87×10^{-88}	1.29×10^{-83}
RN7SKP9	1.40×10^{-2}	-6.16×10^{0}	1.56×10^{-29}	2.03×10^{-27}
AL390318.1	1.43×10^{-2}	-6.13×10^{0}	2.90×10^{-5}	8.75×10^{-5}
RN7SKP186	1.48×10^{-2}	-6.07×10^{0}	5.57×10^{-3}	1.10×10^{-2}

RNU1.11P	1.49×10^{-2}	-6.07×10^{0}	4.00×10^{-9}	2.19×10^{-8}
RN7SKP255	1.60×10^{-2}	-5.96×10^{0}	2.48×10^{-11}	1.89×10^{-10}
AL139120.1	1.66×10^{-2}	-5.91×10^{0}	4.41×10^{-9}	2.40×10^{-8}
RAD51AP1P1	1.67×10^{-2}	-5.90×10^{0}	1.00×10^{-8}	5.19×10^{-8}
LPP.AS1	1.67×10^{-2}	-5.90×10^{0}	6.89×10^{-8}	3.14×10^{-7}
IFNK	1.75×10^{-2}	-5.83×10^{0}	1.27×10^{-14}	1.57×10^{-13}
AC010997.6	1.82×10^{-2}	-5.78×10^{0}	2.99×10^{-9}	1.67×10^{-8}
EIF4E2P1	1.86×10^{-2}	-5.75×10^{0}	8.47×10^{-8}	3.81×10^{-7}
AL606517.2	1.87×10^{-2}	-5.74×10^{0}	1.72×10^{-6}	6.30×10^{-6}
AC008533.1	1.92×10^{-2}	-5.70×10^{0}	8.17×10^{-24}	4.33×10^{-22}
CCNJP2	1.95×10^{-2}	-5.68×10^{0}	1.09×10^{-11}	8.72×10^{-11}
MUC6	1.99×10^{-2}	-5.65×10^{0}	4.23×10^{-65}	4.65×10^{-61}
BMP2KL	2.00×10^{-2}	-5.64×10^{0}	3.45×10^{-16}	5.44×10^{-15}
AF107885.2	2.04×10^{-2}	-5.61×10^{0}	8.30×10^{-19}	1.94×10^{-17}
AC016542.2	2.05×10^{-2}	-5.61×10^{0}	4.77×10^{-25}	3.05×10^{-23}
AC064874.1	2.06×10^{-2}	-5.60×10^{0}	4.45×10^{-16}	6.89×10^{-15}
AC009716.2	2.07×10^{-2}	-5.60×10^{0}	6.31×10^{-22}	2.43×10^{-20}
AC125437.3	2.07×10^{-2}	-5.60×10^{0}	3.99×10^{-19}	9.87×10^{-18}
AC096741.1	2.12×10^{-2}	-5.56×10^{0}	5.39×10^{-11}	3.90×10^{-10}
AL589655.1	2.12×10^{-2}	-5.56×10^{0}	7.66×10^{-6}	2.53×10^{-5}
PIGFP2	2.12×10^{-2}	-5.56×10^{0}	6.84×10^{-6}	2.28×10^{-5}
RNVU1.2	2.13×10^{-2}	-5.55×10^{0}	1.70×10^{-12}	1.53×10^{-11}
RN7SL151P	2.15×10^{-2}	-5.54×10^{0}	1.23×10^{-20}	3.86×10^{-19}
MTCYBP32	2.19×10^{-2}	-5.51×10^{0}	7.04×10^{-7}	2.75×10^{-6}
AC022133.2	2.20×10^{-2}	-5.51×10^{0}	1.73×10^{-31}	2.91×10^{-29}
RNU2.59P	2.20×10^{-2}	-5.50×10^{0}	2.08×10^{-7}	8.81×10^{-7}
AL357141.1	2.21×10^{-2}	-5.50×10^{0}	2.87×10^{-30}	4.13×10^{-28}
EDDM3CP	2.24×10^{-2}	-5.48×10^{0}	3.13×10^{-4}	7.91×10^{-4}
AC130895.1	2.27×10^{-2}	-5.46×10^{0}	1.82×10^{-11}	1.42×10^{-10}
AC009682.1	2.28×10^{-2}	-5.45×10^{0}	1.21×10^{-14}	1.49×10^{-13}
AL606517.1	2.30×10^{-2}	-5.45×10^{0}	2.12×10^{-9}	1.21×10^{-8}
Y_RNA.241	2.31×10^{-2}	-5.44×10^{0}	3.57×10^{-8}	1.70×10^{-7}
AC011939.2	2.31×10^{-2}	-5.44×10^{0}	1.58×10^{-16}	2.60×10^{-15}

Table A.6 (continued). The list of the top 100 downregulated DEGs identified in the CS1 subtype using DESeq2 as a result of two clustering analyzes.

RNU2.23P	2.32×10^{-2}	-5.43×10^{0}	2.14×10^{-5}	6.61×10^{-5}
CELF2.AS2	2.32×10^{-2}	-5.43×10^{0}	3.23×10^{-28}	3.44×10^{-26}
RN7SKP8	2.34×10^{-2}	-5.42×10^{0}	7.31×10^{-7}	2.84×10^{-6}
AC087286.1	2.37×10^{-2}	-5.40×10^{0}	5.89×10^{-12}	4.91×10^{-11}
METTL21AP1	2.39×10^{-2}	-5.39×10^{0}	4.36×10^{-9}	2.38×10^{-8}
SCARNA7	2.39×10^{-2}	-5.38×10^{0}	2.79×10^{-51}	8.76×10^{-48}
USP12.AS1	2.40×10^{-2}	-5.38×10^{0}	1.72×10^{-12}	1.54×10^{-11}

RNY1	2.41×10^{-2}	-5.38×10^{0}	4.74×10^{-13}	4.62×10^{-12}
AC100763.1	2.43×10^{-2}	-5.36×10^{0}	3.39×10^{-10}	2.18×10^{-9}
AC023813.2	2.43×10^{-2}	-5.36×10^{0}	3.92×10^{-11}	2.90×10^{-10}
FBXO40	2.49×10^{-2}	-5.33×10^{0}	2.93×10^{-25}	1.95×10^{-23}
AC055733.1	2.50×10^{-2}	-5.32×10^{0}	2.13×10^{-11}	1.64×10^{-10}
AC016542.3	2.50×10^{-2}	-5.32×10^{0}	5.87×10^{-16}	8.91×10^{-15}
AC021236.1	2.50×10^{-2}	-5.32×10^{0}	3.59×10^{-21}	1.22×10^{-19}
Y_RNA.331	2.51×10^{-2}	-5.32×10^{0}	3.59×10^{-4}	8.97×10^{-4}
MTND4P32	2.53×10^{-2}	-5.31×10^{0}	4.97×10^{-10}	3.11×10^{-9}
AL603824.1	2.53×10^{-2}	-5.30×10^{0}	1.52×10^{-15}	2.17×10^{-14}
MTND2P2	2.53×10^{-2}	-5.30×10^{0}	2.07×10^{-7}	8.78×10^{-7}
Z93020.1	2.54×10^{-2}	-5.30×10^{0}	1.03×10^{-9}	6.15×10^{-9}
RNU2.61P	2.54×10^{-2}	-5.30×10^{0}	4.76×10^{-3}	9.57×10^{-3}
AL136320.1	2.55×10^{-2}	-5.30×10^{0}	1.59×10^{-12}	1.44×10^{-11}
X7SK.1	2.56×10^{-2}	-5.29×10^{0}	6.10×10^{-6}	2.05×10^{-5}
AL360178.2	2.58×10^{-2}	-5.28×10^{0}	2.20×10^{-7}	9.30×10^{-7}
AC018398.2	2.59×10^{-2}	-5.27×10^{0}	1.32×10^{-11}	1.04×10^{-10}
ADAD1P2	2.59×10^{-2}	-5.27×10^{0}	1.40×10^{-4}	3.76×10^{-4}
RN7SL141P	2.60×10^{-2}	-5.26×10^{0}	2.62×10^{-8}	1.27×10^{-7}
SNRPGP18	2.61×10^{-2}	-5.26×10^{0}	3.45×10^{-7}	1.42×10^{-6}
H2BC3	2.62×10^{-2}	-5.26×10^{0}	4.27×10^{-22}	1.69×10^{-20}
TMEM14EP	2.63×10^{-2}	-5.25×10^{0}	5.21×10^{-32}	9.65×10^{-30}
AC007736.1	2.67×10^{-2}	-5.23×10^{0}	1.55×10^{-11}	1.21×10^{-10}
AC105224.1	2.68×10^{-2}	-5.22×10^{0}	3.02×10^{-5}	9.08×10^{-5}
AC092910.2	2.70×10^{-2}	-5.21×10^{0}	1.99×10^{-8}	9.86×10^{-8}
AC022537.1	2.70×10^{-2}	-5.21×10^{0}	8.77×10^{-5}	2.44×10^{-4}
ZBTB20.AS5	2.70×10^{-2}	-5.21×10^{0}	3.81×10^{-14}	4.37×10^{-13}
AC008833.1	2.71×10^{-2}	-5.21×10^{0}	2.52×10^{-5}	7.68×10^{-5}
RPL23AP23	2.71×10^{-2}	-5.20×10^{0}	8.76×10^{-21}	2.79×10^{-19}
AC016549.1	2.72×10^{-2}	-5.20×10^{0}	5.21×10^{-14}	5.86×10^{-13}
AC022022.2	2.75×10^{-2}	-5.19×10^{0}	4.15×10^{-6}	1.43×10^{-5}
RNU5D.1	2.75×10^{-2}	-5.19×10^{0}	1.28×10^{-21}	4.67×10^{-20}
AC087257.1	2.77×10^{-2}	-5.17×10^{0}	3.66×10^{-23}	1.76×10^{-21}

Table A.6 (continued). The list of the top 100 downregulated DEGs identified in the CS1 subtype using DESeq2 as a result of two clustering analyzes.

AC090220.1	2.79×10^{-2}	-5.16×10^{0}	6.52×10^{-12}	5.40×10^{-11}
AC012555.2	2.80×10^{-2}	-5.16×10^{0}	1.56×10^{-12}	1.41×10^{-11}
AP004289.2	2.82×10^{-2}	-5.15×10^{0}	7.43×10^{-9}	3.91×10^{-8}
FOXN3.AS2	2.82×10^{-2}	-5.15×10^{0}	3.61×10^{-8}	1.72×10^{-7}
AC002381.1	2.83×10^{-2}	-5.14×10^{0}	6.63×10^{-10}	4.07×10^{-9}
STX18.IT1	2.84×10^{-2}	-5.14×10^{0}	2.65×10^{-15}	3.64×10^{-14}
PDHA1P1	2.84×10^{-2}	-5.14×10^{0}	3.89×10^{-17}	7.04×10^{-16}
AC104332.1	2.85×10^{-2}	-5.13×10^{0}	2.85×10^{-14}	3.32×10^{-13}
PSAPL1	2.85×10^{-2}	-5.13×10^{0}	5.91×10^{-40}	3.09×10^{-37}

AC010480.1	2.85×10^{-2}	-5.13×10^{0}	8.81×10^{-17}	1.51×10^{-15}
AC092910.1	2.86×10^{-2}	-5.13×10^{0}	1.27×10^{-22}	5.46×10^{-21}
DPRXP1	2.86×10^{-2}	-5.13×10^{0}	2.53×10^{-13}	2.57×10^{-12}
RN7SKP48	2.87×10^{-2}	-5.12×10^{0}	2.19×10^{-3}	4.70×10^{-3}
RN7SL683P	2.87×10^{-2}	-5.12×10^{0}	7.08×10^{-7}	2.76×10^{-6}
AL356776.1	2.87×10^{-2}	-5.12×10^{0}	3.28×10^{-11}	2.45×10^{-10}
AL158801.1	2.88×10^{-2}	-5.12×10^{0}	5.98×10^{-32}	1.10×10^{-29}
AL391863.2	2.89×10^{-2}	-5.11×10^{0}	9.49×10^{-15}	1.19×10^{-13}

Table A.7. The list of the top 100 upregulated DEGs identified in the CS2 subtype using DESeq2 as a result of two clustering analyzes.

	fc	**log2fc**	**pvalue**	**padj**
RN7SKP227	2.99×10^{3}	1.16×10^{1}	2.66×10^{-7}	1.11×10^{-6}
CLDN18	1.86×10^{2}	7.54×10^{0}	1.18×10^{-118}	5.16×10^{-114}
RN7SKP203	1.28×10^{2}	7.00×10^{0}	3.10×10^{-15}	4.22×10^{-14}
AL139274.1	1.16×10^{2}	6.85×10^{0}	7.13×10^{-17}	1.24×10^{-15}
RNU1.88P	1.12×10^{2}	6.81×10^{0}	2.41×10^{-15}	3.34×10^{-14}
MIR3609	7.52×10^{1}	6.23×10^{0}	2.44×10^{-27}	2.28×10^{-25}
ANXA10	7.31×10^{1}	6.19×10^{0}	5.87×10^{-88}	1.29×10^{-83}
RN7SKP9	7.16×10^{1}	6.16×10^{0}	1.56×10^{-29}	2.03×10^{-27}
AL390318.1	7.00×10^{1}	6.13×10^{0}	2.90×10^{-5}	8.75×10^{-5}
RN7SKP186	6.74×10^{1}	6.07×10^{0}	5.57×10^{-3}	1.10×10^{-2}
RNU1.11P	6.73×10^{1}	6.07×10^{0}	4.00×10^{-9}	2.19×10^{-8}
RN7SKP255	6.24×10^{1}	5.96×10^{0}	2.48×10^{-11}	1.89×10^{-10}
AL139120.1	6.02×10^{1}	5.91×10^{0}	4.41×10^{-9}	2.40×10^{-8}
RAD51AP1P1	5.97×10^{1}	5.90×10^{0}	1.00×10^{-8}	5.19×10^{-8}
LPP.AS1	5.97×10^{1}	5.90×10^{0}	6.89×10^{-8}	3.14×10^{-7}
IFNK	5.71×10^{1}	5.83×10^{0}	1.27×10^{-14}	1.57×10^{-13}
AC010997.6	5.48×10^{1}	5.78×10^{0}	2.99×10^{-9}	1.67×10^{-8}
EIF4E2P1	5.37×10^{1}	5.75×10^{0}	8.47×10^{-8}	3.81×10^{-7}
AL606517.2	5.33×10^{1}	5.74×10^{0}	1.72×10^{-6}	6.30×10^{-6}
AC008533.1	5.21×10^{1}	5.70×10^{0}	8.17×10^{-24}	4.33×10^{-22}

Table A.7 (continued). The list of the top 100 upregulated DEGs identified in the CS2 subtype using DESeq2 as a result of two clustering analyzes.

CCNJP2	5.12×10^{1}	5.68×10^{0}	1.09×10^{-11}	8.72×10^{-11}
MUC6	5.02×10^{1}	5.65×10^{0}	4.24×10^{-65}	4.66×10^{-61}
BMP2KL	4.99×10^{1}	5.64×10^{0}	3.45×10^{-16}	5.44×10^{-15}
AF107885.2	4.89×10^{1}	5.61×10^{0}	8.30×10^{-19}	1.95×10^{-17}
AC016542.2	4.88×10^{1}	5.61×10^{0}	4.77×10^{-25}	3.06×10^{-23}
AC064874.1	4.86×10^{1}	5.60×10^{0}	4.45×10^{-16}	6.89×10^{-15}
AC009716.2	4.84×10^{1}	5.60×10^{0}	6.31×10^{-22}	2.43×10^{-20}
AC125437.3	4.84×10^{1}	5.60×10^{0}	3.99×10^{-19}	9.87×10^{-18}
AC096741.1	4.73×10^{1}	5.56×10^{0}	5.39×10^{-11}	3.90×10^{-10}

AL589655.1	4.71×10^{1}	5.56×10^{0}	7.66×10^{-6}	2.53×10^{-5}
PIGFP2	4.71×10^{1}	5.56×10^{0}	6.84×10^{-6}	2.28×10^{-5}
RNVU1.2	4.69×10^{1}	5.55×10^{0}	1.70×10^{-12}	1.53×10^{-11}
RN7SL151P	4.66×10^{1}	5.54×10^{0}	1.23×10^{-20}	3.86×10^{-19}
MTCYBP32	4.56×10^{1}	5.51×10^{0}	7.04×10^{-7}	2.75×10^{-6}
AC022133.2	4.55×10^{1}	5.51×10^{0}	1.73×10^{-31}	2.91×10^{-29}
RNU2.59P	4.54×10^{1}	5.50×10^{0}	2.08×10^{-7}	8.81×10^{-7}
AL357141.1	4.53×10^{1}	5.50×10^{0}	2.87×10^{-30}	4.13×10^{-28}
EDDM3CP	4.46×10^{1}	5.48×10^{0}	3.13×10^{-4}	7.91×10^{-4}
AC130895.1	4.41×10^{1}	5.46×10^{0}	1.82×10^{-11}	1.42×10^{-10}
AC009682.1	4.38×10^{1}	5.45×10^{0}	1.21×10^{-14}	1.50×10^{-13}
AL606517.1	4.36×10^{1}	5.44×10^{0}	2.12×10^{-9}	1.21×10^{-8}
Y_RNA.241	4.33×10^{1}	5.44×10^{0}	3.57×10^{-8}	1.70×10^{-7}
AC011939.2	4.33×10^{1}	5.44×10^{0}	1.58×10^{-16}	2.61×10^{-15}
RNU2.23P	4.31×10^{1}	5.43×10^{0}	2.14×10^{-5}	6.61×10^{-5}
CELF2.AS2	4.31×10^{1}	5.43×10^{0}	3.22×10^{-28}	3.44×10^{-26}
RN7SKP8	4.28×10^{1}	5.42×10^{0}	7.31×10^{-7}	2.84×10^{-6}
AC087286.1	4.22×10^{1}	5.40×10^{0}	5.89×10^{-12}	4.91×10^{-11}
METTL21AP1	4.19×10^{1}	5.39×10^{0}	4.36×10^{-9}	2.38×10^{-8}
SCARNA7	4.18×10^{1}	5.38×10^{0}	2.81×10^{-51}	8.81×10^{-48}
USP12.AS1	4.17×10^{1}	5.38×10^{0}	1.72×10^{-12}	1.54×10^{-11}
RNY1	4.15×10^{1}	5.38×10^{0}	4.74×10^{-13}	4.63×10^{-12}
AC100763.1	4.12×10^{1}	5.36×10^{0}	3.39×10^{-10}	2.18×10^{-9}
AC023813.2	4.12×10^{1}	5.36×10^{0}	3.92×10^{-11}	2.90×10^{-10}
FBXO40	4.01×10^{1}	5.33×10^{0}	2.93×10^{-25}	1.95×10^{-23}
AC055733.1	4.00×10^{1}	5.32×10^{0}	2.13×10^{-11}	1.64×10^{-10}
AC016542.3	4.00×10^{1}	5.32×10^{0}	5.87×10^{-16}	8.91×10^{-15}
AC021236.1	4.00×10^{1}	5.32×10^{0}	3.59×10^{-21}	1.23×10^{-19}
Y_RNA.331	3.98×10^{1}	5.32×10^{0}	3.59×10^{-4}	8.97×10^{-4}
MTND4P32	3.96×10^{1}	5.31×10^{0}	4.97×10^{-10}	3.11×10^{-9}
AL603824.1	3.95×10^{1}	5.30×10^{0}	1.52×10^{-15}	2.17×10^{-14}

Table A.7 (continued). The list of the top 100 upregulated DEGs identified in the CS2 subtype using DESeq2 as a result of two clustering analyzes.

MTND2P2	3.95×10^{1}	5.30×10^{0}	2.07×10^{-7}	8.78×10^{-7}
Z93020.1	3.94×10^{1}	5.30×10^{0}	1.03×10^{-9}	6.15×10^{-9}
RNU2.61P	3.94×10^{1}	5.30×10^{0}	4.76×10^{-3}	9.57×10^{-3}
AL136320.1	3.93×10^{1}	5.30×10^{0}	1.59×10^{-12}	1.44×10^{-11}
X7SK.1	3.91×10^{1}	5.29×10^{0}	6.10×10^{-6}	2.05×10^{-5}
AL360178.2	3.88×10^{1}	5.28×10^{0}	2.20×10^{-7}	9.30×10^{-7}
AC018398.2	3.87×10^{1}	5.27×10^{0}	1.32×10^{-11}	1.04×10^{-10}
ADAD1P2	3.86×10^{1}	5.27×10^{0}	1.40×10^{-4}	3.76×10^{-4}
RN7SL141P	3.84×10^{1}	5.26×10^{0}	2.62×10^{-8}	1.27×10^{-7}
SNRPGP18	3.84×10^{1}	5.26×10^{0}	3.45×10^{-7}	1.42×10^{-6}

H2BC3	3.82×10^{1}	5.26×10^{0}	4.27×10^{-22}	1.69×10^{-20}
TMEM14EP	3.80×10^{1}	5.25×10^{0}	5.21×10^{-32}	9.65×10^{-30}
AC007736.1	3.75×10^{1}	5.23×10^{0}	1.55×10^{-11}	1.21×10^{-10}
AC105224.1	3.72×10^{1}	5.22×10^{0}	3.02×10^{-5}	9.08×10^{-5}
AC092910.2	3.71×10^{1}	5.21×10^{0}	1.99×10^{-8}	9.86×10^{-8}
AC022537.1	3.71×10^{1}	5.21×10^{0}	8.77×10^{-5}	2.44×10^{-4}
ZBTB20.AS5	3.70×10^{1}	5.21×10^{0}	3.81×10^{-14}	4.37×10^{-13}
AC008833.1	3.70×10^{1}	5.21×10^{0}	2.52×10^{-5}	7.68×10^{-5}
RPL23AP23	3.69×10^{1}	5.20×10^{0}	8.76×10^{-21}	2.79×10^{-19}
AC016549.1	3.68×10^{1}	5.20×10^{0}	5.21×10^{-14}	5.86×10^{-13}
AC022022.2	3.64×10^{1}	5.19×10^{0}	4.15×10^{-6}	1.43×10^{-5}
RNU5D.1	3.64×10^{1}	5.19×10^{0}	1.28×10^{-21}	4.68×10^{-20}
AC087257.1	3.61×10^{1}	5.17×10^{0}	3.66×10^{-23}	1.76×10^{-21}
AC090220.1	3.58×10^{1}	5.16×10^{0}	6.52×10^{-12}	5.40×10^{-11}
AC012555.2	3.57×10^{1}	5.16×10^{0}	1.56×10^{-12}	1.41×10^{-11}
AP004289.2	3.54×10^{1}	5.15×10^{0}	7.43×10^{-9}	3.91×10^{-8}
FOXN3.AS2	3.54×10^{1}	5.15×10^{0}	3.61×10^{-8}	1.72×10^{-7}
AC002381.1	3.53×10^{1}	5.14×10^{0}	6.63×10^{-10}	4.07×10^{-9}
STX18.IT1	3.52×10^{1}	5.14×10^{0}	2.65×10^{-15}	3.64×10^{-14}
PDHA1P1	3.52×10^{1}	5.14×10^{0}	3.89×10^{-17}	7.04×10^{-16}
AC104332.1	3.51×10^{1}	5.13×10^{0}	2.85×10^{-14}	3.32×10^{-13}
PSAPL1	3.51×10^{1}	5.13×10^{0}	5.91×10^{-40}	3.09×10^{-37}
AC010480.1	3.50×10^{1}	5.13×10^{0}	8.81×10^{-17}	1.51×10^{-15}
AC092910.1	3.50×10^{1}	5.13×10^{0}	1.27×10^{-22}	5.47×10^{-21}
DPRXP1	3.49×10^{1}	5.13×10^{0}	2.53×10^{-13}	2.57×10^{-12}
RN7SKP48	3.49×10^{1}	5.12×10^{0}	2.19×10^{-3}	4.69×10^{-3}
RN7SL683P	3.48×10^{1}	5.12×10^{0}	7.08×10^{-7}	2.76×10^{-6}
AL356776.1	3.48×10^{1}	5.12×10^{0}	3.27×10^{-11}	2.45×10^{-10}
AL158801.1	3.48×10^{1}	5.12×10^{0}	5.98×10^{-32}	1.10×10^{-29}
AL391863.2	3.46×10^{1}	5.11×10^{0}	9.49×10^{-15}	1.19×10^{-13}

Table A.8. The list of the top 100 downregulated DEGs identified in the CS2 subtype using DESeq2 as a result of two clustering analyzes.

	fc	**log2fc**	**pvalue**	**padj**
WIF1	2.07×10^{-2}	5.59×10^{0}	1.03×10^{-50}	3.02×10^{-47}
PTF1A	3.86×10^{-2}	4.69×10^{0}	3.33×10^{-22}	1.34×10^{-20}
PRSS56	4.29×10^{-2}	4.54×10^{0}	6.35×10^{-26}	4.63×10^{-24}
IGF2	4.77×10^{-2}	4.39×10^{0}	4.95×10^{-34}	1.22×10^{-31}
AL356433.1	5.09×10^{-2}	4.30×10^{0}	1.57×10^{-23}	8.04×10^{-22}
LY6G6D	5.65×10^{-2}	4.14×10^{0}	3.59×10^{-40}	2.01×10^{-37}
KRT35	6.56×10^{-2}	3.93×10^{0}	2.63×10^{-16}	4.22×10^{-15}
AC114291.1	7.39×10^{-2}	3.76×10^{0}	3.55×10^{-49}	7.01×10^{-46}
AC026336.3	7.57×10^{-2}	3.72×10^{0}	3.64×10^{-31}	5.85×10^{-29}
AC026774.1	7.65×10^{-2}	3.71×10^{0}	3.68×10^{-21}	1.26×10^{-19}

LY6G6F.LY6G6D	7.71×10^{-2}	3.70×10^{0}	1.08×10^{-30}	1.63×10^{-28}
MAGEB17	8.45×10^{-2}	3.56×10^{0}	5.29×10^{-26}	3.93×10^{-24}
GOLGA6L2	8.65×10^{-2}	3.53×10^{0}	1.48×10^{-22}	6.27×10^{-21}
KRT43P	9.01×10^{-2}	3.47×10^{0}	1.42×10^{-14}	1.73×10^{-13}
NOTUM	9.53×10^{-2}	3.39×10^{0}	1.36×10^{-32}	2.82×10^{-30}
LCN15	9.63×10^{-2}	3.38×10^{0}	8.61×10^{-21}	2.76×10^{-19}
KRT32	1.00×10^{-1}	3.32×10^{0}	1.51×10^{-14}	1.84×10^{-13}
KRT37	1.01×10^{-1}	3.31×10^{0}	2.73×10^{-18}	5.89×10^{-17}
CDH9	1.01×10^{-1}	3.31×10^{0}	8.97×10^{-6}	2.93×10^{-5}
BX510359.5	1.03×10^{-1}	3.27×10^{0}	6.11×10^{-13}	5.87×10^{-12}
BHLHA9	1.05×10^{-1}	3.25×10^{0}	2.57×10^{-20}	7.69×10^{-19}
MAGEA4.AS1	1.12×10^{-1}	3.16×10^{0}	7.00×10^{-5}	1.98×10^{-4}
SULT2A1	1.13×10^{-1}	3.14×10^{0}	1.60×10^{-20}	4.93×10^{-19}
KRT40	1.13×10^{-1}	3.14×10^{0}	2.81×10^{-21}	9.80×10^{-20}
HSPB3	1.14×10^{-1}	3.13×10^{0}	2.99×10^{-20}	8.85×10^{-19}
CPN1	1.15×10^{-1}	3.12×10^{0}	1.42×10^{-21}	5.15×10^{-20}
VWA5B1	1.16×10^{-1}	3.11×10^{0}	1.71×10^{-18}	3.80×10^{-17}
SLC30A2	1.17×10^{-1}	3.09×10^{0}	3.56×10^{-36}	1.17×10^{-33}
PRR9	1.21×10^{-1}	3.05×10^{0}	5.16×10^{-11}	3.75×10^{-10}
TMEM252	1.21×10^{-1}	3.04×10^{0}	3.97×10^{-29}	4.90×10^{-27}
AC003958.2	1.22×10^{-1}	3.03×10^{0}	1.39×10^{-16}	2.31×10^{-15}
AC078993.1	1.24×10^{-1}	3.02×10^{0}	6.13×10^{-22}	2.37×10^{-20}
AC108865.1	1.26×10^{-1}	2.99×10^{0}	1.85×10^{-14}	2.22×10^{-13}
TNNC2	1.28×10^{-1}	2.96×10^{0}	3.17×10^{-57}	1.74×10^{-53}
SERPINA10	1.31×10^{-1}	2.93×10^{0}	7.47×10^{-26}	5.38×10^{-24}
NPTX2	1.33×10^{-1}	2.91×10^{0}	5.28×10^{-31}	8.31×10^{-29}
LINC02864	1.33×10^{-1}	-2.91×10^{0}	3.92×10^{-9}	2.15×10^{-8}
AC110772.2	1.34×10^{-1}	-2.90×10^{0}	2.66×10^{-16}	4.26×10^{-15}

Table A.8 (continued). The list of the top 100 downregulated DEGs identified in the CS2 subtype using DESeq2 as a result of two clustering analyzes.

PCSK1N	1.37×10^{-1}	-2.87×10^{0}	9.43×10^{-21}	3.00×10^{-19}
LGALS14	1.37×10^{-1}	-2.87×10^{0}	7.38×10^{-10}	4.50×10^{-9}
TUBAP13	1.40×10^{-1}	-2.84×10^{0}	1.15×10^{-17}	2.26×10^{-16}
KRT41P	1.40×10^{-1}	-2.83×10^{0}	8.72×10^{-13}	8.19×10^{-12}
AL391650.2	1.41×10^{-1}	-2.83×10^{0}	2.92×10^{-13}	2.94×10^{-12}
SLC14A1	1.42×10^{-1}	-2.82×10^{0}	1.65×10^{-23}	8.40×10^{-22}
SYN3	1.42×10^{-1}	-2.82×10^{0}	1.61×10^{-38}	7.29×10^{-36}
SPACA3	1.43×10^{-1}	-2.80×10^{0}	3.64×10^{-32}	7.02×10^{-30}
CLDN10	1.44×10^{-1}	-2.80×10^{0}	1.56×10^{-15}	2.22×10^{-14}
AC108865.2	1.44×10^{-1}	-2.79×10^{0}	8.32×10^{-11}	5.85×10^{-10}
LINC02525	1.49×10^{-1}	-2.75×10^{0}	2.73×10^{-12}	2.38×10^{-11}
C6orf15	1.52×10^{-1}	-2.72×10^{0}	1.28×10^{-17}	2.49×10^{-16}

AL512356.5	1.52×10^{-1}	-2.72×10^{0}	5.22×10^{-11}	3.79×10^{-10}
MAGEA6	1.53×10^{-1}	-2.71×10^{0}	2.40×10^{-4}	6.19×10^{-4}
SERPINA7	1.59×10^{-1}	-2.65×10^{0}	1.34×10^{-14}	1.65×10^{-13}
DLX3	1.60×10^{-1}	-2.64×10^{0}	3.05×10^{-18}	6.53×10^{-17}
KRT23	1.60×10^{-1}	-2.64×10^{0}	5.78×10^{-29}	6.95×10^{-27}
LINC00545	1.61×10^{-1}	-2.63×10^{0}	7.20×10^{-12}	5.93×10^{-11}
ATP12A	1.72×10^{-1}	-2.54×10^{0}	4.73×10^{-13}	4.62×10^{-12}
AL121885.2	1.73×10^{-1}	-2.53×10^{0}	4.13×10^{-12}	3.51×10^{-11}
MAP7D2	1.73×10^{-1}	-2.53×10^{0}	4.75×10^{-23}	2.25×10^{-21}
AP000851.2	1.74×10^{-1}	-2.53×10^{0}	7.82×10^{-11}	5.52×10^{-10}
AC135388.1	1.74×10^{-1}	-2.52×10^{0}	1.43×10^{-18}	3.24×10^{-17}
CELP	1.76×10^{-1}	-2.50×10^{0}	1.01×10^{-27}	1.01×10^{-25}
AP003774.2	1.77×10^{-1}	-2.50×10^{0}	2.25×10^{-37}	8.68×10^{-35}
AC091304.1	1.78×10^{-1}	-2.49×10^{0}	6.05×10^{-7}	2.38×10^{-6}
AC109136.1	1.78×10^{-1}	-2.48×10^{0}	8.77×10^{-10}	5.30×10^{-9}
GS1.594A7.3	1.79×10^{-1}	-2.48×10^{0}	1.14×10^{-8}	5.86×10^{-8}
MAGEA4	1.79×10^{-1}	-2.48×10^{0}	8.35×10^{-4}	1.95×10^{-3}
KRT31	1.81×10^{-1}	-2.47×10^{0}	2.48×10^{-8}	1.21×10^{-7}
AC110772.1	1.82×10^{-1}	-2.46×10^{0}	1.32×10^{-9}	7.77×10^{-9}
MIR483	1.84×10^{-1}	-2.44×10^{0}	1.42×10^{-3}	3.17×10^{-3}
NEUROD1	1.84×10^{-1}	-2.44×10^{0}	3.40×10^{-8}	1.63×10^{-7}
ORM1	1.84×10^{-1}	-2.44×10^{0}	2.11×10^{-12}	1.88×10^{-11}
SLC1A7	1.88×10^{-1}	-2.41×10^{0}	2.52×10^{-32}	5.00×10^{-30}
PAGE1	1.89×10^{-1}	-2.40×10^{0}	3.95×10^{-3}	8.08×10^{-3}
SHISA9	1.91×10^{-1}	-2.39×10^{0}	6.39×10^{-11}	4.58×10^{-10}
ZP2	1.93×10^{-1}	-2.37×10^{0}	3.03×10^{-21}	1.05×10^{-19}
LINC02178	1.97×10^{-1}	-2.34×10^{0}	5.69×10^{-8}	2.63×10^{-7}
ELF5	1.97×10^{-1}	-2.34×10^{0}	1.04×10^{-9}	6.24×10^{-9}
FGF3	1.99×10^{-1}	-2.33×10^{0}	5.18×10^{-9}	2.79×10^{-8}

Table A.8 (continued). The list of the top 100 downregulated DEGs identified in the CS2 subtype using DESeq2 as a result of two clustering analyzes.

PPBP	1.99×10^{-1}	-2.33×10^{0}	1.92×10^{-12}	1.71×10^{-11}
LINC02128	2.00×10^{-1}	-2.32×10^{0}	1.94×10^{-10}	1.29×10^{-9}
MC3R	2.01×10^{-1}	-2.31×10^{0}	1.78×10^{-8}	8.90×10^{-8}
SLC39A2	2.02×10^{-1}	-2.31×10^{0}	4.85×10^{-13}	4.72×10^{-12}
LINC00355	2.02×10^{-1}	-2.31×10^{0}	3.56×10^{-5}	1.06×10^{-4}
AC091839.1	2.02×10^{-1}	-2.31×10^{0}	1.31×10^{-4}	3.53×10^{-4}
KRT38	2.03×10^{-1}	-2.30×10^{0}	1.30×10^{-6}	4.85×10^{-6}
PHYHIPL	2.04×10^{-1}	-2.29×10^{0}	1.39×10^{-14}	1.70×10^{-13}
TGM6	2.04×10^{-1}	-2.29×10^{0}	4.50×10^{-4}	1.10×10^{-3}
RBP2	2.05×10^{-1}	-2.29×10^{0}	1.37×10^{-18}	3.11×10^{-17}
AL035252.2	2.05×10^{-1}	-2.29×10^{0}	1.04×10^{-9}	6.23×10^{-9}
AC079804.2	2.06×10^{-1}	-2.28×10^{0}	9.89×10^{-6}	3.21×10^{-5}
DRD2	2.06×10^{-1}	-2.28×10^{0}	2.74×10^{-19}	6.99×10^{-18}

MAGEA11	2.07×10^{-1}	-2.27×10^{0}	5.88×10^{-5}	1.69×10^{-4}
CTNNA2	2.08×10^{-1}	-2.27×10^{0}	9.35×10^{-13}	8.73×10^{-12}
AL445205.1	2.08×10^{-1}	-2.27×10^{0}	6.80×10^{-8}	3.11×10^{-7}
CRAT37	2.09×10^{-1}	-2.26×10^{0}	6.00×10^{-13}	5.76×10^{-12}
SLC13A3	2.10×10^{-1}	-2.25×10^{0}	7.71×10^{-21}	2.50×10^{-19}
PAH	2.12×10^{-1}	-2.24×10^{0}	8.00×10^{-16}	1.19×10^{-14}
AL390334.1	2.14×10^{-1}	-2.22×10^{0}	4.02×10^{-4}	9.93×10^{-4}
UMODL1	2.14×10^{-1}	-2.22×10^{0}	2.77×10^{-29}	3.50×10^{-27}

Table A.9. The list of the top 100 upregulated DEGs identified in the CS1 subtype using limma as a result of two clustering analyzes.

	fc	**log2fc**	**pvalue**	**padj**
TNNC2	9.77×10^{0}	3.29×10^{0}	1.27×10^{-47}	7.28×10^{-43}
AP003774.2	7.71×10^{0}	2.95×10^{0}	4.49×10^{-40}	1.28×10^{-35}
CEL	7.68×10^{0}	2.94×10^{0}	7.42×10^{-24}	4.04×10^{-21}
C10orf99	7.48×10^{0}	2.90×10^{0}	2.02×10^{-23}	1.01×10^{-20}
KRT23	6.47×10^{0}	2.69×10^{0}	9.17×10^{-22}	3.26×10^{-19}
QPRT	6.01×10^{0}	2.59×10^{0}	1.71×10^{-36}	1.22×10^{-32}
NOTUM	5.38×10^{0}	2.43×10^{0}	1.57×10^{-15}	1.49×10^{-13}
GNG4	5.37×10^{0}	2.43×10^{0}	2.78×10^{-22}	1.13×10^{-19}
CDHR1	5.22×10^{0}	2.38×10^{0}	1.19×10^{-24}	7.64×10^{-22}
ASCL2	5.13×10^{0}	2.36×10^{0}	2.14×10^{-31}	5.33×10^{-28}
DPEP1	5.06×10^{0}	2.34×10^{0}	1.80×10^{-17}	2.56×10^{-15}
SLC26A3	5.00×10^{0}	2.32×10^{0}	1.72×10^{-11}	6.46×10^{-10}
SLC39A5	4.78×10^{0}	2.26×10^{0}	1.55×10^{-30}	3.07×10^{-27}
TDGF1	4.58×10^{0}	2.19×10^{0}	1.64×10^{-32}	5.51×10^{-29}
Y_RNA.244	4.46×10^{0}	2.16×10^{0}	6.98×10^{-25}	4.65×10^{-22}
FABP1	4.38×10^{0}	2.13×10^{0}	9.65×10^{-11}	3.10×10^{-9}

Table A.9 (continued). The list of the top 100 upregulated DEGs identified in the CS1 subtype using limma as a result of two clustering analyzes.

VAV3	4.30×10^{0}	2.10×10^{0}	4.32×10^{-32}	1.18×10^{-28}
CYP2B6	4.25×10^{0}	2.09×10^{0}	1.67×10^{-25}	1.31×10^{-22}
CXCL14	4.20×10^{0}	2.07×10^{0}	1.20×10^{-16}	1.43×10^{-14}
CYP2W1	4.20×10^{0}	2.07×10^{0}	2.95×10^{-13}	1.68×10^{-11}
CELP	4.03×10^{0}	2.01×10^{0}	3.91×10^{-34}	1.72×10^{-30}
AL117382.1	4.03×10^{0}	2.01×10^{0}	1.25×10^{-37}	1.16×10^{-33}
PLA2G12B	3.98×10^{0}	1.99×10^{0}	3.79×10^{-18}	6.00×10^{-16}
RUBCNL	3.95×10^{0}	1.98×10^{0}	8.38×10^{-31}	1.71×10^{-27}
LEFTY1	3.89×10^{0}	1.96×10^{0}	2.70×10^{-11}	9.76×10^{-10}
EREG	3.84×10^{0}	1.94×10^{0}	2.61×10^{-14}	1.89×10^{-12}
ENPP3	3.84×10^{0}	1.94×10^{0}	2.25×10^{-18}	3.79×10^{-16}
GPR143	3.83×10^{0}	1.94×10^{0}	3.56×10^{-29}	5.99×10^{-26}
IHH	3.74×10^{0}	1.90×10^{0}	3.75×10^{-30}	7.16×10^{-27}
LY6G6D	3.59×10^{0}	1.84×10^{0}	3.32×10^{-24}	1.98×10^{-21}

AXIN2	3.58×10^{0}	1.84×10^{0}	2.49×10^{-29}	4.31×10^{-26}
NKD1	3.50×10^{0}	1.81×10^{0}	3.84×10^{-19}	7.66×10^{-17}
GRM8	3.50×10^{0}	1.81×10^{0}	1.06×10^{-24}	6.87×10^{-22}
RPL39P40	3.48×10^{0}	1.80×10^{0}	5.81×10^{-23}	2.62×10^{-20}
MEP1A	3.40×10^{0}	1.77×10^{0}	5.57×10^{-14}	3.74×10^{-12}
FABP6	3.39×10^{0}	1.76×10^{0}	1.37×10^{-18}	2.44×10^{-16}
LINC02441	3.31×10^{0}	1.73×10^{0}	2.36×10^{-24}	1.44×10^{-21}
RBP2	3.27×10^{0}	1.71×10^{0}	1.11×10^{-12}	5.46×10^{-11}
MOGAT3	3.26×10^{0}	1.70×10^{0}	8.47×10^{-28}	9.51×10^{-25}
APCDD1	3.25×10^{0}	1.70×10^{0}	3.25×10^{-16}	3.49×10^{-14}
AIFM3	3.22×10^{0}	1.69×10^{0}	4.17×10^{-27}	4.19×10^{-24}
LINC02418	3.21×10^{0}	1.68×10^{0}	1.21×10^{-14}	9.47×10^{-13}
NOX1	3.17×10^{0}	1.66×10^{0}	9.75×10^{-17}	1.18×10^{-14}
R3HDML	3.15×10^{0}	1.65×10^{0}	4.30×10^{-34}	1.76×10^{-30}
CDX2	3.13×10^{0}	1.65×10^{0}	5.87×10^{-29}	8.61×10^{-26}
PLCB4	3.13×10^{0}	1.64×10^{0}	3.07×10^{-18}	4.93×10^{-16}
AC114291.1	3.11×10^{0}	1.64×10^{0}	1.92×10^{-21}	6.18×10^{-19}
GGT7	3.11×10^{0}	1.64×10^{0}	9.32×10^{-29}	1.30×10^{-25}
HMGCS2	3.11×10^{0}	1.64×10^{0}	8.01×10^{-8}	1.33×10^{-6}
MAB21L4	3.11×10^{0}	1.64×10^{0}	2.14×10^{-23}	1.03×10^{-20}
MIR3131	3.11×10^{0}	1.64×10^{0}	3.85×10^{-18}	6.08×10^{-16}
XPNPEP2	3.10×10^{0}	1.63×10^{0}	6.75×10^{-14}	4.47×10^{-12}
RNF43	3.10×10^{0}	1.63×10^{0}	1.56×10^{-39}	2.97×10^{-35}
SATB2.AS1	3.09×10^{0}	1.63×10^{0}	1.79×10^{-27}	1.93×10^{-24}
MUC12	3.09×10^{0}	1.63×10^{0}	5.25×10^{-13}	2.78×10^{-11}
CHP2	3.08×10^{0}	1.62×10^{0}	1.42×10^{-10}	4.38×10^{-9}
MAP7D2	3.06×10^{0}	1.61×10^{0}	1.07×10^{-13}	6.76×10^{-12}

Table A.9 (continued). The list of the top 100 upregulated DEGs identified in the CS1 subtype using limma as a result of two clustering analyzes.

ISX	3.05×10^{0}	1.61×10^{0}	1.12×10^{-16}	1.34×10^{-14}
PPP1R14D	3.01×10^{0}	1.59×10^{0}	6.54×10^{-21}	1.89×10^{-18}
DIO3OS	2.98×10^{0}	1.58×10^{0}	3.69×10^{-23}	1.75×10^{-20}
HUNK	2.90×10^{0}	1.54×10^{0}	3.34×10^{-20}	8.45×10^{-18}
TUSC8	2.90×10^{0}	1.53×10^{0}	3.72×10^{-20}	9.38×10^{-18}
CYP4F2	2.89×10^{0}	1.53×10^{0}	8.51×10^{-16}	8.37×10^{-14}
CFTR	2.88×10^{0}	1.53×10^{0}	5.26×10^{-17}	6.78×10^{-15}
WNT11	2.88×10^{0}	1.52×10^{0}	4.91×10^{-12}	2.08×10^{-10}
AC124067.4	2.85×10^{0}	1.51×10^{0}	1.26×10^{-23}	6.48×10^{-21}
PTPRO	2.85×10^{0}	1.51×10^{0}	7.70×10^{-15}	6.20×10^{-13}
ANO9	2.84×10^{0}	1.50×10^{0}	1.80×10^{-31}	4.67×10^{-28}
SELENBP1	2.82×10^{0}	1.50×10^{0}	1.63×10^{-17}	2.33×10^{-15}
BEX2	2.82×10^{0}	1.49×10^{0}	2.34×10^{-11}	8.58×10^{-10}
TINAG	2.81×10^{0}	1.49×10^{0}	9.74×10^{-21}	2.71×10^{-18}
SLC13A2	2.80×10^{0}	1.49×10^{0}	1.88×10^{-13}	1.13×10^{-11}

AL162413.1	2.78×10^{0}	1.47×10^{0}	2.31×10^{-8}	4.40×10^{-7}
COL9A3	2.76×10^{0}	1.47×10^{0}	9.78×10^{-13}	4.87×10^{-11}
AC108865.1	2.75×10^{0}	1.46×10^{0}	6.82×10^{-8}	1.15×10^{-6}
NKD2	2.72×10^{0}	1.45×10^{0}	5.84×10^{-17}	7.43×10^{-15}
URAD	2.72×10^{0}	1.44×10^{0}	5.39×10^{-8}	9.38×10^{-7}
AL354743.2	2.71×10^{0}	1.44×10^{0}	1.66×10^{-18}	2.88×10^{-16}
DDC	2.69×10^{0}	1.43×10^{0}	1.47×10^{-15}	1.40×10^{-13}
CAB39L	2.67×10^{0}	1.42×10^{0}	1.07×10^{-21}	3.73×10^{-19}
PPP1R14C	2.67×10^{0}	1.42×10^{0}	1.65×10^{-15}	1.55×10^{-13}
ENGASE	2.67×10^{0}	1.42×10^{0}	3.71×10^{-32}	1.06×10^{-28}
TMEM176A	2.66×10^{0}	1.41×10^{0}	7.63×10^{-21}	2.13×10^{-18}
SLC30A2	2.66×10^{0}	1.41×10^{0}	3.18×10^{-21}	9.75×10^{-19}
PRR15	2.65×10^{0}	1.41×10^{0}	5.25×10^{-33}	1.88×10^{-29}
TSPAN6	2.65×10^{0}	1.41×10^{0}	4.38×10^{-38}	5.01×10^{-34}
AC005050.2	2.64×10^{0}	1.40×10^{0}	1.51×10^{-26}	1.40×10^{-23}
TMEM252	2.63×10^{0}	1.39×10^{0}	3.86×10^{-13}	2.13×10^{-11}
WIF1	2.62×10^{0}	1.39×10^{0}	3.61×10^{-11}	1.26×10^{-9}
NR1I2	2.62×10^{0}	1.39×10^{0}	1.14×10^{-22}	4.95×10^{-20}
SYT7	2.61×10^{0}	1.39×10^{0}	6.32×10^{-22}	2.35×10^{-19}
AC078993.1	2.58×10^{0}	1.37×10^{0}	1.59×10^{-13}	9.72×10^{-12}
CTTNBP2	2.58×10^{0}	1.37×10^{0}	1.35×10^{-22}	5.73×10^{-20}
SLC35D3	2.58×10^{0}	1.37×10^{0}	1.32×10^{-12}	6.33×10^{-11}
AC055717.2	2.58×10^{0}	1.37×10^{0}	3.64×10^{-17}	4.86×10^{-15}
FGFR4	2.55×10^{0}	1.35×10^{0}	1.16×10^{-21}	3.99×10^{-19}
TLE2	2.55×10^{0}	1.35×10^{0}	2.01×10^{-17}	2.83×10^{-15}
SLC39A2	2.54×10^{0}	1.35×10^{0}	2.71×10^{-9}	6.34×10^{-8}

Table A.9 (continued). The list of the top 100 upregulated DEGs identified in the CS1 subtype using limma as a result of two clustering analyzes.

CYCSP6	2.54×10^{0}	1.35×10^{0}	2.14×10^{-9}	5.11×10^{-8}
NXPE4	2.54×10^{0}	1.35×10^{0}	2.09×10^{-6}	2.39×10^{-5}

Table A.10. The list of the top 100 downregulated DEGs identified in the CS1 subtype using limma as a result of two clustering analyzes.

	fc	**log2fc**	**pvalue**	**padj**
REG4	9.27×10^{-2}	-3.43×10^{0}	1.42×10^{-16}	1.65×10^{-14}
CTSE	1.44×10^{-1}	-2.80×10^{0}	2.55×10^{-19}	5.28×10^{-17}
PLA2G2A	1.87×10^{-1}	-2.42×10^{0}	3.16×10^{-13}	1.77×10^{-11}
CLDN18	1.92×10^{-1}	-2.38×10^{0}	4.82×10^{-20}	1.17×10^{-17}
DUSP4	2.02×10^{-1}	-2.31×10^{0}	1.99×10^{-35}	1.26×10^{-31}
GJB5	2.57×10^{-1}	-1.96×10^{0}	4.14×10^{-18}	6.50×10^{-16}
MUC2	2.59×10^{-1}	-1.95×10^{0}	6.37×10^{-8}	1.09×10^{-6}
MUC5AC	2.64×10^{-1}	-1.92×10^{0}	9.37×10^{-17}	1.14×10^{-14}
LYZ	2.68×10^{-1}	-1.90×10^{0}	8.39×10^{-14}	5.45×10^{-12}
TCN1	2.73×10^{-1}	-1.87×10^{0}	3.81×10^{-10}	1.08×10^{-8}

CXCL13	2.74×10^{-1}	-1.87×10^{0}	1.38×10^{-19}	3.08×10^{-17}
RAMP1	2.76×10^{-1}	-1.86×10^{0}	1.32×10^{-14}	1.02×10^{-12}
REG1A	2.81×10^{-1}	-1.83×10^{0}	7.78×10^{-5}	4.91×10^{-4}
VNN1	2.83×10^{-1}	-1.82×10^{0}	1.31×10^{-21}	4.50×10^{-19}
TFF2	2.84×10^{-1}	-1.82×10^{0}	1.49×10^{-10}	4.55×10^{-9}
TNNT1	2.88×10^{-1}	-1.80×10^{0}	1.04×10^{-19}	2.35×10^{-17}
RAB27B	2.99×10^{-1}	-1.74×10^{0}	1.42×10^{-37}	1.16×10^{-33}
CCL18	3.02×10^{-1}	-1.73×10^{0}	4.96×10^{-11}	1.69×10^{-9}
CXCL9	3.14×10^{-1}	-1.67×10^{0}	1.69×10^{-13}	1.02×10^{-11}
TRNP1	3.19×10^{-1}	-1.65×10^{0}	4.52×10^{-21}	1.33×10^{-18}
SDR16C5	3.23×10^{-1}	-1.63×10^{0}	1.99×10^{-14}	1.49×10^{-12}
ANXA10	3.28×10^{-1}	-1.61×10^{0}	7.19×10^{-21}	2.04×10^{-18}
RARRES1	3.34×10^{-1}	-1.58×10^{0}	2.18×10^{-19}	4.58×10^{-17}
SPINK4	3.39×10^{-1}	-1.56×10^{0}	1.08×10^{-4}	6.44×10^{-4}
TNFSF9	3.39×10^{-1}	-1.56×10^{0}	1.55×10^{-18}	2.74×10^{-16}
TRIM7	3.39×10^{-1}	-1.56×10^{0}	9.19×10^{-35}	4.78×10^{-31}
MUC6	3.41×10^{-1}	-1.55×10^{0}	3.00×10^{-14}	2.13×10^{-12}
SPON1	3.44×10^{-1}	-1.54×10^{0}	2.25×10^{-16}	2.50×10^{-14}
TM4SF4	3.55×10^{-1}	-1.49×10^{0}	9.23×10^{-11}	2.98×10^{-9}
CXCL10	3.56×10^{-1}	-1.49×10^{0}	8.21×10^{-12}	3.33×10^{-10}
GBP4	3.58×10^{-1}	-1.48×10^{0}	1.62×10^{-18}	2.83×10^{-16}
SERPINB5	3.59×10^{-1}	-1.48×10^{0}	4.30×10^{-10}	1.20×10^{-8}
SPP1	3.60×10^{-1}	-1.47×10^{0}	3.39×10^{-7}	4.80×10^{-6}
MT1E	3.60×10^{-1}	-1.47×10^{0}	9.86×10^{-12}	3.92×10^{-10}
GZMA	3.61×10^{-1}	-1.47×10^{0}	4.38×10^{-20}	1.08×10^{-17}

Table A.10 (continued). The list of the top 100 downregulated DEGs identified in the CS1 subtype using limma as a result of two clustering analyzes.

ADGRG6	3.63×10^{-1}	-1.46×10^{0}	3.03×10^{-27}	3.16×10^{-24}
IL1RN	3.63×10^{-1}	-1.46×10^{0}	1.53×10^{-16}	1.78×10^{-14}
MUC5B	3.65×10^{-1}	-1.45×10^{0}	7.48×10^{-7}	9.60×10^{-6}
TRIB2	3.67×10^{-1}	-1.45×10^{0}	5.09×10^{-33}	1.88×10^{-29}
FCGR3A	3.68×10^{-1}	-1.44×10^{0}	2.13×10^{-13}	1.26×10^{-11}
GNLY	3.68×10^{-1}	-1.44×10^{0}	3.57×10^{-21}	1.07×10^{-18}
PRSS2	3.71×10^{-1}	-1.43×10^{0}	3.04×10^{-5}	2.31×10^{-4}
PLA2G4A	3.72×10^{-1}	-1.43×10^{0}	6.51×10^{-15}	5.33×10^{-13}
CD109	3.73×10^{-1}	-1.42×10^{0}	4.88×10^{-19}	9.56×10^{-17}
CCL5	3.74×10^{-1}	-1.42×10^{0}	2.26×10^{-17}	3.16×10^{-15}
MUC17	3.78×10^{-1}	-1.40×10^{0}	7.02×10^{-8}	1.18×10^{-6}
GCNT3	3.79×10^{-1}	-1.40×10^{0}	1.13×10^{-10}	3.58×10^{-9}
GABRP	3.80×10^{-1}	-1.40×10^{0}	1.86×10^{-12}	8.68×10^{-11}
CA9	3.82×10^{-1}	-1.39×10^{0}	1.31×10^{-6}	1.57×10^{-5}
DAPK1	3.88×10^{-1}	-1.37×10^{0}	1.73×10^{-21}	5.64×10^{-19}
SPDEF	3.88×10^{-1}	-1.36×10^{0}	2.83×10^{-8}	5.28×10^{-7}
PLAAT4	3.89×10^{-1}	-1.36×10^{0}	1.50×10^{-14}	1.15×10^{-12}

FCGBP	3.91×10^{-1}	-1.36×10^{0}	3.44×10^{-5}	2.55×10^{-4}
AQP3	3.92×10^{-1}	-1.35×10^{0}	1.27×10^{-11}	4.94×10^{-10}
AQP5	3.93×10^{-1}	-1.35×10^{0}	6.51×10^{-8}	1.11×10^{-6}
NKG7	3.97×10^{-1}	-1.33×10^{0}	2.84×10^{-16}	3.09×10^{-14}
MYRF	3.99×10^{-1}	-1.33×10^{0}	1.97×10^{-16}	2.22×10^{-14}
CXCL8	3.99×10^{-1}	-1.33×10^{0}	6.77×10^{-9}	1.45×10^{-7}
CXCR4	4.00×10^{-1}	-1.32×10^{0}	3.36×10^{-19}	6.75×10^{-17}
AGR2	4.00×10^{-1}	-1.32×10^{0}	1.40×10^{-15}	1.34×10^{-13}
AFAP1.AS1	4.02×10^{-1}	-1.32×10^{0}	1.80×10^{-14}	1.35×10^{-12}
CREB3L1	4.02×10^{-1}	-1.32×10^{0}	8.11×10^{-12}	3.29×10^{-10}
IGHG1	4.02×10^{-1}	-1.31×10^{0}	5.17×10^{-5}	3.52×10^{-4}
SAMD9L	4.03×10^{-1}	-1.31×10^{0}	1.82×10^{-23}	9.20×10^{-21}
TFAP2A	4.03×10^{-1}	-1.31×10^{0}	3.56×10^{-28}	4.33×10^{-25}
ZIC2	4.07×10^{-1}	-1.30×10^{0}	9.45×10^{-10}	2.45×10^{-8}
SECTM1	4.08×10^{-1}	-1.30×10^{0}	1.81×10^{-15}	1.67×10^{-13}
PTMAP4	4.08×10^{-1}	-1.29×10^{0}	1.57×10^{-21}	5.27×10^{-19}
HLA.DRA	4.09×10^{-1}	-1.29×10^{0}	1.18×10^{-12}	5.75×10^{-11}
OAS2	4.11×10^{-1}	-1.28×10^{0}	1.15×10^{-14}	9.00×10^{-13}
AGR3	4.12×10^{-1}	-1.28×10^{0}	1.25×10^{-7}	1.99×10^{-6}
VNN2	4.12×10^{-1}	-1.28×10^{0}	8.18×10^{-24}	4.38×10^{-21}
GBP5	4.13×10^{-1}	-1.28×10^{0}	2.25×10^{-16}	2.50×10^{-14}
FFAR4	4.15×10^{-1}	-1.27×10^{0}	1.93×10^{-10}	5.81×10^{-9}
IGLV3.1	4.16×10^{-1}	-1.27×10^{0}	1.41×10^{-4}	7.98×10^{-4}
KRT7	4.16×10^{-1}	-1.27×10^{0}	6.53×10^{-16}	6.54×10^{-14}

Table A.10 (continued). The list of the top 100 downregulated DEGs identified in the CS1 subtype using limma as a result of two clustering analyzes.

PRDM8	4.16×10^{-1}	-1.27×10^{0}	2.24×10^{-32}	7.12×10^{-29}
EVI2B	4.17×10^{-1}	-1.26×10^{0}	4.36×10^{-19}	8.61×10^{-17}
CD163	4.18×10^{-1}	-1.26×10^{0}	2.21×10^{-11}	8.11×10^{-10}
IGHV2.70	4.18×10^{-1}	-1.26×10^{0}	4.91×10^{-6}	5.02×10^{-5}
IGHV1.69	4.19×10^{-1}	-1.26×10^{0}	1.16×10^{-5}	1.04×10^{-4}
PTAFR	4.20×10^{-1}	-1.25×10^{0}	2.79×10^{-19}	5.73×10^{-17}
MMP1	4.22×10^{-1}	-1.25×10^{0}	2.01×10^{-6}	2.30×10^{-5}
GFI1	4.22×10^{-1}	-1.24×10^{0}	5.80×10^{-28}	6.92×10^{-25}
IDO1	4.22×10^{-1}	-1.24×10^{0}	3.11×10^{-10}	8.97×10^{-9}
IGHV1.69.2	4.22×10^{-1}	-1.24×10^{0}	1.56×10^{-5}	1.34×10^{-4}
CXCL11	4.23×10^{-1}	-1.24×10^{0}	1.52×10^{-8}	3.02×10^{-7}
SRGN	4.27×10^{-1}	-1.23×10^{0}	1.95×10^{-14}	1.46×10^{-12}
HLA.DPA1	4.27×10^{-1}	-1.23×10^{0}	2.41×10^{-11}	8.78×10^{-10}
GZMH	4.27×10^{-1}	-1.23×10^{0}	1.36×10^{-16}	1.60×10^{-14}
SEMG1	4.28×10^{-1}	-1.23×10^{0}	2.19×10^{-13}	1.29×10^{-11}
IL1R2	4.29×10^{-1}	-1.22×10^{0}	9.91×10^{-15}	7.85×10^{-13}
SFRP2	4.31×10^{-1}	-1.22×10^{0}	2.16×10^{-4}	1.13×10^{-3}
IGHV1.24	4.31×10^{-1}	-1.21×10^{0}	9.32×10^{-5}	5.69×10^{-4}

KCTD12	4.32×10^{-1}	-1.21×10^{0}	8.56×10^{-14}	5.55×10^{-12}
HLA.DQA1	4.32×10^{-1}	-1.21×10^{0}	1.13×10^{-11}	4.43×10^{-10}
CCL4	4.33×10^{-1}	-1.21×10^{0}	3.91×10^{-17}	5.15×10^{-15}
PTPRC	4.34×10^{-1}	-1.21×10^{0}	3.69×10^{-14}	2.57×10^{-12}
PLEK	4.34×10^{-1}	-1.20×10^{0}	1.25×10^{-12}	6.09×10^{-11}
BCL2A1	4.35×10^{-1}	-1.20×10^{0}	5.33×10^{-14}	3.60×10^{-12}

Table A.11. The list of the top 100 upregulated DEGs identified in the CS2 subtype using limma as a result of two clustering analyzes.

	fc	**log2fc**	**pvalue**	**padj**
REG4	1.08×10^{1}	3.43×10^{0}	1.42×10^{-16}	1.65×10^{-14}
CTSE	6.95×10^{0}	2.80×10^{0}	2.55×10^{-19}	5.28×10^{-17}
PLA2G2A	5.36×10^{0}	2.42×10^{0}	3.16×10^{-13}	1.77×10^{-11}
CLDN18	5.22×10^{0}	2.38×10^{0}	4.82×10^{-20}	1.17×10^{-17}
DUSP4	4.95×10^{0}	2.31×10^{0}	1.99×10^{-35}	1.26×10^{-31}
GJB5	3.90×10^{0}	1.96×10^{0}	4.14×10^{-18}	6.50×10^{-16}
MUC2	3.86×10^{0}	1.95×10^{0}	6.37×10^{-8}	1.09×10^{-6}
MUC5AC	3.78×10^{0}	1.92×10^{0}	9.37×10^{-17}	1.14×10^{-14}
LYZ	3.74×10^{0}	1.90×10^{0}	8.39×10^{-14}	5.45×10^{-12}
TCN1	3.66×10^{0}	1.87×10^{0}	3.81×10^{-10}	1.08×10^{-8}
CXCL13	3.66×10^{0}	1.87×10^{0}	1.38×10^{-19}	3.08×10^{-17}
RAMP1	3.62×10^{0}	1.86×10^{0}	1.32×10^{-14}	1.02×10^{-12}
REG1A	3.56×10^{0}	1.83×10^{0}	7.78×10^{-5}	4.91×10^{-4}

Table A.11 (continued). The list of the top 100 upregulated DEGs identified in the CS2 subtype using limma as a result of two clustering analyzes.

VNN1	3.54×10^{0}	1.82×10^{0}	1.31×10^{-21}	4.50×10^{-19}
TFF2	3.52×10^{0}	1.82×10^{0}	1.49×10^{-10}	4.55×10^{-9}
TNNT1	3.48×10^{0}	1.80×10^{0}	1.04×10^{-19}	2.35×10^{-17}
RAB27B	3.34×10^{0}	1.74×10^{0}	1.42×10^{-37}	1.16×10^{-33}
CCL18	3.31×10^{0}	1.73×10^{0}	4.96×10^{-11}	1.69×10^{-9}
CXCL9	3.19×10^{0}	1.67×10^{0}	1.69×10^{-13}	1.02×10^{-11}
TRNP1	3.13×10^{0}	1.65×10^{0}	4.52×10^{-21}	1.33×10^{-18}
SDR16C5	3.10×10^{0}	1.63×10^{0}	1.99×10^{-14}	1.49×10^{-12}
ANXA10	3.05×10^{0}	1.61×10^{0}	7.19×10^{-21}	2.04×10^{-18}
RARRES1	3.00×10^{0}	1.58×10^{0}	2.18×10^{-19}	4.58×10^{-17}
SPINK4	2.95×10^{0}	1.56×10^{0}	1.08×10^{-4}	6.44×10^{-4}
TNFSF9	2.95×10^{0}	1.56×10^{0}	1.55×10^{-18}	2.74×10^{-16}
TRIM7	2.95×10^{0}	1.56×10^{0}	9.19×10^{-35}	4.78×10^{-31}
MUC6	2.93×10^{0}	1.55×10^{0}	3.00×10^{-14}	2.13×10^{-12}
SPON1	2.91×10^{0}	1.54×10^{0}	2.25×10^{-16}	2.50×10^{-14}
TM4SF4	2.82×10^{0}	1.49×10^{0}	9.23×10^{-11}	2.98×10^{-9}
CXCL10	2.81×10^{0}	1.49×10^{0}	8.21×10^{-12}	3.33×10^{-10}
GBP4	2.79×10^{0}	1.48×10^{0}	1.62×10^{-18}	2.83×10^{-16}
SERPINB5	2.79×10^{0}	1.48×10^{0}	4.30×10^{-10}	1.20×10^{-8}

SPP1	2.78×10^{0}	1.47×10^{0}	3.39×10^{-7}	4.80×10^{-6}
MT1E	2.78×10^{0}	1.47×10^{0}	9.86×10^{-12}	3.92×10^{-10}
GZMA	2.77×10^{0}	1.47×10^{0}	4.38×10^{-20}	1.08×10^{-17}
ADGRG6	2.76×10^{0}	1.46×10^{0}	3.03×10^{-27}	3.16×10^{-24}
IL1RN	2.76×10^{0}	1.46×10^{0}	1.53×10^{-16}	1.78×10^{-14}
MUC5B	2.74×10^{0}	1.45×10^{0}	7.48×10^{-7}	9.60×10^{-6}
TRIB2	2.72×10^{0}	1.45×10^{0}	5.09×10^{-33}	1.88×10^{-29}
FCGR3A	2.72×10^{0}	1.44×10^{0}	2.13×10^{-13}	1.26×10^{-11}
GNLY	2.72×10^{0}	1.44×10^{0}	3.57×10^{-21}	1.07×10^{-18}
PRSS2	2.70×10^{0}	1.43×10^{0}	3.04×10^{-5}	2.31×10^{-4}
PLA2G4A	2.69×10^{0}	1.43×10^{0}	6.51×10^{-15}	5.33×10^{-13}
CD109	2.68×10^{0}	1.42×10^{0}	4.88×10^{-19}	9.56×10^{-17}
CCL5	2.68×10^{0}	1.42×10^{0}	2.26×10^{-17}	3.16×10^{-15}
MUC17	2.65×10^{0}	1.40×10^{0}	7.02×10^{-8}	1.18×10^{-6}
GCNT3	2.64×10^{0}	1.40×10^{0}	1.13×10^{-10}	3.58×10^{-9}
GABRP	2.63×10^{0}	1.40×10^{0}	1.86×10^{-12}	8.68×10^{-11}
CA9	2.62×10^{0}	1.39×10^{0}	1.31×10^{-6}	1.57×10^{-5}
DAPK1	2.58×10^{0}	1.37×10^{0}	1.73×10^{-21}	5.64×10^{-19}
SPDEF	2.57×10^{0}	1.36×10^{0}	2.83×10^{-8}	5.28×10^{-7}
PLAAT4	2.57×10^{0}	1.36×10^{0}	1.50×10^{-14}	1.15×10^{-12}
FCGBP	2.56×10^{0}	1.36×10^{0}	3.44×10^{-5}	2.55×10^{-4}
AQP3	2.55×10^{0}	1.35×10^{0}	1.27×10^{-11}	4.94×10^{-10}

Table A.11 (continued). The list of the top 100 upregulated DEGs identified in the CS2 subtype using limma as a result of two clustering analyzes.

AQP5	2.55×10^{0}	1.35×10^{0}	6.51×10^{-8}	1.11×10^{-6}
NKG7	2.52×10^{0}	1.33×10^{0}	2.84×10^{-16}	3.09×10^{-14}
MYRF	2.51×10^{0}	1.33×10^{0}	1.97×10^{-16}	2.22×10^{-14}
CXCL8	2.51×10^{0}	1.33×10^{0}	6.77×10^{-9}	1.45×10^{-7}
CXCR4	2.50×10^{0}	1.32×10^{0}	3.36×10^{-19}	6.75×10^{-17}
AGR2	2.50×10^{0}	1.32×10^{0}	1.40×10^{-15}	1.34×10^{-13}
AFAP1.AS1	2.49×10^{0}	1.32×10^{0}	1.80×10^{-14}	1.35×10^{-12}
CREB3L1	2.49×10^{0}	1.32×10^{0}	8.11×10^{-12}	3.29×10^{-10}
IGHG1	2.48×10^{0}	1.31×10^{0}	5.17×10^{-5}	3.52×10^{-4}
SAMD9L	2.48×10^{0}	1.31×10^{0}	1.82×10^{-23}	9.20×10^{-21}
TFAP2A	2.48×10^{0}	1.31×10^{0}	3.56×10^{-28}	4.33×10^{-25}
ZIC2	2.46×10^{0}	1.30×10^{0}	9.45×10^{-10}	2.45×10^{-8}
SECTM1	2.45×10^{0}	1.30×10^{0}	1.81×10^{-15}	1.67×10^{-13}
PTMAP4	2.45×10^{0}	1.29×10^{0}	1.57×10^{-21}	5.27×10^{-19}
HLA.DRA	2.45×10^{0}	1.29×10^{0}	1.18×10^{-12}	5.75×10^{-11}
OAS2	2.43×10^{0}	1.28×10^{0}	1.15×10^{-14}	9.00×10^{-13}
AGR3	2.43×10^{0}	1.28×10^{0}	1.25×10^{-7}	1.99×10^{-6}
VNN2	2.43×10^{0}	1.28×10^{0}	8.18×10^{-24}	4.38×10^{-21}
GBP5	2.42×10^{0}	1.28×10^{0}	2.25×10^{-16}	2.50×10^{-14}
FFAR4	2.41×10^{0}	1.27×10^{0}	1.93×10^{-10}	5.81×10^{-9}

IGLV3.1	2.41×10^{0}	1.27×10^{0}	1.41×10^{-4}	7.98×10^{-4}
KRT7	2.41×10^{0}	1.27×10^{0}	6.53×10^{-16}	6.54×10^{-14}
PRDM8	2.40×10^{0}	1.27×10^{0}	2.24×10^{-32}	7.12×10^{-29}
EVI2B	2.40×10^{0}	1.26×10^{0}	4.36×10^{-19}	8.61×10^{-17}
CD163	2.39×10^{0}	1.26×10^{0}	2.21×10^{-11}	8.11×10^{-10}
IGHV2.70	2.39×10^{0}	1.26×10^{0}	4.91×10^{-6}	5.02×10^{-5}
IGHV1.69	2.39×10^{0}	1.26×10^{0}	1.16×10^{-5}	1.04×10^{-4}
PTAFR	2.38×10^{0}	1.25×10^{0}	2.79×10^{-19}	5.73×10^{-17}
MMP1	2.37×10^{0}	1.25×10^{0}	2.01×10^{-6}	2.30×10^{-5}
GFI1	2.37×10^{0}	1.24×10^{0}	5.80×10^{-28}	6.92×10^{-25}
IDO1	2.37×10^{0}	1.24×10^{0}	3.11×10^{-10}	8.97×10^{-9}
IGHV1.69.2	2.37×10^{0}	1.24×10^{0}	1.56×10^{-5}	1.34×10^{-4}
CXCL11	2.36×10^{0}	1.24×10^{0}	1.52×10^{-8}	3.02×10^{-7}
SRGN	2.34×10^{0}	1.23×10^{0}	1.95×10^{-14}	1.46×10^{-12}
HLA.DPA1	2.34×10^{0}	1.23×10^{0}	2.41×10^{-11}	8.78×10^{-10}
GZMH	2.34×10^{0}	1.23×10^{0}	1.36×10^{-16}	1.60×10^{-14}
SEMG1	2.34×10^{0}	1.23×10^{0}	2.19×10^{-13}	1.29×10^{-11}
IL1R2	2.33×10^{0}	1.22×10^{0}	9.91×10^{-15}	7.85×10^{-13}
SFRP2	2.32×10^{0}	1.22×10^{0}	2.16×10^{-4}	1.13×10^{-3}
IGHV1.24	2.32×10^{0}	1.21×10^{0}	9.32×10^{-5}	5.69×10^{-4}
KCTD12	2.32×10^{0}	1.21×10^{0}	8.56×10^{-14}	5.55×10^{-12}

Table A.11 (continued). The list of the top 100 upregulated DEGs identified in the CS2 subtype using limma as a result of two clustering analyzes.

HLA.DQA1	2.32×10^{0}	1.21×10^{0}	1.13×10^{-11}	4.43×10^{-10}
CCL4	2.31×10^{0}	1.21×10^{0}	3.91×10^{-17}	5.15×10^{-15}
PTPRC	2.31×10^{0}	1.21×10^{0}	3.69×10^{-14}	2.57×10^{-12}
PLEK	2.30×10^{0}	1.20×10^{0}	1.25×10^{-12}	6.09×10^{-11}
BCL2A1	2.30×10^{0}	1.20×10^{0}	5.33×10^{-14}	3.60×10^{-12}

Table A.12. The list of the top 100 downregulated DEGs identified in the CS2 subtype using limma as a result of two clustering analyzes.

	fc	**log2fc**	**pvalue**	**padj**
TNNC2	1.02×10^{-1}	-3.29×10^{0}	1.27×10^{-47}	7.28×10^{-43}
AP003774.2	1.30×10^{-1}	-2.95×10^{0}	4.49×10^{-40}	1.28×10^{-35}
CEL	1.30×10^{-1}	-2.94×10^{0}	7.42×10^{-24}	4.04×10^{-21}
C10orf99	1.34×10^{-1}	-2.90×10^{0}	2.02×10^{-23}	1.01×10^{-20}
KRT23	1.55×10^{-1}	-2.69×10^{0}	9.17×10^{-22}	3.26×10^{-19}
QPRT	1.67×10^{-1}	-2.59×10^{0}	1.71×10^{-36}	1.22×10^{-32}
NOTUM	1.86×10^{-1}	-2.43×10^{0}	1.57×10^{-15}	1.49×10^{-13}
GNG4	1.86×10^{-1}	-2.43×10^{0}	2.78×10^{-22}	1.13×10^{-19}
CDHR1	1.92×10^{-1}	-2.38×10^{0}	1.19×10^{-24}	7.64×10^{-22}
ASCL2	1.95×10^{-1}	-2.36×10^{0}	2.14×10^{-31}	5.33×10^{-28}
DPEP1	1.98×10^{-1}	-2.34×10^{0}	1.80×10^{-17}	2.56×10^{-15}
SLC26A3	2.00×10^{-1}	-2.32×10^{0}	1.72×10^{-11}	6.46×10^{-10}

SLC39A5	2.09×10^{-1}	-2.26×10^{0}	1.55×10^{-30}	3.07×10^{-27}
TDGF1	2.19×10^{-1}	-2.19×10^{0}	1.64×10^{-32}	5.51×10^{-29}
Y_RNA.244	2.24×10^{-1}	-2.16×10^{0}	6.98×10^{-25}	4.65×10^{-22}
FABP1	2.28×10^{-1}	-2.13×10^{0}	9.65×10^{-11}	3.10×10^{-9}
VAV3	2.33×10^{-1}	-2.10×10^{0}	4.32×10^{-32}	1.18×10^{-28}
CYP2B6	2.35×10^{-1}	-2.09×10^{0}	1.67×10^{-25}	1.31×10^{-22}
CXCL14	2.38×10^{-1}	-2.07×10^{0}	1.20×10^{-16}	1.43×10^{-14}
CYP2W1	2.38×10^{-1}	-2.07×10^{0}	2.95×10^{-13}	1.68×10^{-11}
CELP	2.48×10^{-1}	-2.01×10^{0}	3.91×10^{-34}	1.72×10^{-30}
AL117382.1	2.48×10^{-1}	-2.01×10^{0}	1.25×10^{-37}	1.16×10^{-33}
PLA2G12B	2.51×10^{-1}	-1.99×10^{0}	3.79×10^{-18}	6.00×10^{-16}
RUBCNL	2.53×10^{-1}	-1.98×10^{0}	8.38×10^{-31}	1.71×10^{-27}
LEFTY1	2.57×10^{-1}	-1.96×10^{0}	2.70×10^{-11}	9.76×10^{-10}
EREG	2.60×10^{-1}	-1.94×10^{0}	2.61×10^{-14}	1.89×10^{-12}
ENPP3	2.61×10^{-1}	-1.94×10^{0}	2.25×10^{-18}	3.79×10^{-16}
GPR143	2.61×10^{-1}	-1.94×10^{0}	3.56×10^{-29}	5.99×10^{-26}
IHH	2.68×10^{-1}	-1.90×10^{0}	3.75×10^{-30}	7.16×10^{-27}
LY6G6D	2.79×10^{-1}	-1.84×10^{0}	3.32×10^{-24}	1.98×10^{-21}
AXIN2	2.80×10^{-1}	-1.84×10^{0}	2.49×10^{-29}	4.31×10^{-26}
NKD1	2.85×10^{-1}	-1.81×10^{0}	3.84×10^{-19}	7.66×10^{-17}

Table A.12 (continued). The list of the top 100 downregulated DEGs identified in the CS2 subtype using limma as a result of two clustering analyzes.

GRM8	2.86×10^{-1}	-1.81×10^{0}	1.06×10^{-24}	6.87×10^{-22}
RPL39P40	2.88×10^{-1}	-1.80×10^{0}	5.81×10^{-23}	2.62×10^{-20}
MEP1A	2.94×10^{-1}	-1.77×10^{0}	5.57×10^{-14}	3.74×10^{-12}
FABP6	2.95×10^{-1}	-1.76×10^{0}	1.37×10^{-18}	2.44×10^{-16}
LINC02441	3.02×10^{-1}	-1.73×10^{0}	2.36×10^{-24}	1.44×10^{-21}
RBP2	3.06×10^{-1}	-1.71×10^{0}	1.11×10^{-12}	5.46×10^{-11}
MOGAT3	3.07×10^{-1}	-1.70×10^{0}	8.47×10^{-28}	9.51×10^{-25}
APCDD1	3.08×10^{-1}	-1.70×10^{0}	3.25×10^{-16}	3.49×10^{-14}
AIFM3	3.10×10^{-1}	-1.69×10^{0}	4.17×10^{-27}	4.19×10^{-24}
LINC02418	3.12×10^{-1}	-1.68×10^{0}	1.21×10^{-14}	9.47×10^{-13}
NOX1	3.15×10^{-1}	-1.66×10^{0}	9.75×10^{-17}	1.18×10^{-14}
R3HDML	3.18×10^{-1}	-1.65×10^{0}	4.30×10^{-34}	1.76×10^{-30}
CDX2	3.19×10^{-1}	-1.65×10^{0}	5.87×10^{-29}	8.61×10^{-26}
PLCB4	3.20×10^{-1}	-1.64×10^{0}	3.07×10^{-18}	4.93×10^{-16}
AC114291.1	3.21×10^{-1}	-1.64×10^{0}	1.92×10^{-21}	6.18×10^{-19}
GGT7	3.21×10^{-1}	-1.64×10^{0}	9.32×10^{-29}	1.30×10^{-25}
HMGCS2	3.21×10^{-1}	-1.64×10^{0}	8.01×10^{-8}	1.33×10^{-6}
MAB21L4	3.22×10^{-1}	-1.64×10^{0}	2.14×10^{-23}	1.03×10^{-20}
MIR3131	3.22×10^{-1}	-1.64×10^{0}	3.85×10^{-18}	6.08×10^{-16}
XPNPEP2	3.22×10^{-1}	-1.63×10^{0}	6.75×10^{-14}	4.47×10^{-12}
RNF43	3.23×10^{-1}	-1.63×10^{0}	1.56×10^{-39}	2.97×10^{-35}
SATB2.AS1	3.23×10^{-1}	-1.63×10^{0}	1.79×10^{-27}	1.93×10^{-24}

MUC12	3.23×10^{-1}	-1.63×10^{0}	5.25×10^{-13}	2.78×10^{-11}
CHP2	3.25×10^{-1}	-1.62×10^{0}	1.42×10^{-10}	4.38×10^{-9}
MAP7D2	3.27×10^{-1}	-1.61×10^{0}	1.07×10^{-13}	6.76×10^{-12}
ISX	3.28×10^{-1}	-1.61×10^{0}	1.12×10^{-16}	1.34×10^{-14}
PPP1R14D	3.32×10^{-1}	-1.59×10^{0}	6.54×10^{-21}	1.89×10^{-18}
DIO3OS	3.35×10^{-1}	-1.58×10^{0}	3.69×10^{-23}	1.75×10^{-20}
HUNK	3.44×10^{-1}	-1.54×10^{0}	3.34×10^{-20}	8.45×10^{-18}
TUSC8	3.45×10^{-1}	-1.53×10^{0}	3.72×10^{-20}	9.38×10^{-18}
CYP4F2	3.47×10^{-1}	-1.53×10^{0}	8.51×10^{-16}	8.37×10^{-14}
CFTR	3.47×10^{-1}	-1.53×10^{0}	5.26×10^{-17}	6.78×10^{-15}
WNT11	3.48×10^{-1}	-1.52×10^{0}	4.91×10^{-12}	2.08×10^{-10}
AC124067.4	3.51×10^{-1}	-1.51×10^{0}	1.26×10^{-23}	6.48×10^{-21}
PTPRO	3.51×10^{-1}	-1.51×10^{0}	7.70×10^{-15}	6.20×10^{-13}
ANO9	3.52×10^{-1}	-1.50×10^{0}	1.80×10^{-31}	4.67×10^{-28}
SELENBP1	3.54×10^{-1}	-1.50×10^{0}	1.63×10^{-17}	2.33×10^{-15}
BEX2	3.55×10^{-1}	-1.49×10^{0}	2.34×10^{-11}	8.58×10^{-10}
TINAG	3.55×10^{-1}	-1.49×10^{0}	9.74×10^{-21}	2.71×10^{-18}
SLC13A2	3.57×10^{-1}	-1.49×10^{0}	1.88×10^{-13}	1.13×10^{-11}
AL162413.1	3.60×10^{-1}	-1.47×10^{0}	2.31×10^{-8}	4.40×10^{-7}

Table A.12 (continued). The list of the top 100 downregulated DEGs identified in the CS2 subtype using limma as a result of two clustering analyzes.

COL9A3	3.62×10^{-1}	-1.47×10^{0}	9.78×10^{-13}	4.87×10^{-11}
AC108865.1	3.63×10^{-1}	-1.46×10^{0}	6.82×10^{-8}	1.15×10^{-6}
NKD2	3.67×10^{-1}	-1.45×10^{0}	5.84×10^{-17}	7.43×10^{-15}
URAD	3.68×10^{-1}	-1.44×10^{0}	5.39×10^{-8}	9.38×10^{-7}
AL354743.2	3.69×10^{-1}	-1.44×10^{0}	1.66×10^{-18}	2.88×10^{-16}
DDC	3.72×10^{-1}	-1.43×10^{0}	1.47×10^{-15}	1.40×10^{-13}
CAB39L	3.74×10^{-1}	-1.42×10^{0}	1.07×10^{-21}	3.73×10^{-19}
PPP1R14C	3.74×10^{-1}	-1.42×10^{0}	1.65×10^{-15}	1.55×10^{-13}
ENGASE	3.75×10^{-1}	-1.42×10^{0}	3.71×10^{-32}	1.06×10^{-28}
TMEM176A	3.75×10^{-1}	-1.41×10^{0}	7.63×10^{-21}	2.13×10^{-18}
SLC30A2	3.77×10^{-1}	-1.41×10^{0}	3.18×10^{-21}	9.75×10^{-19}
PRR15	3.77×10^{-1}	-1.41×10^{0}	5.25×10^{-33}	1.88×10^{-29}
TSPAN6	3.77×10^{-1}	-1.41×10^{0}	4.38×10^{-38}	5.01×10^{-34}
AC005050.2	3.78×10^{-1}	-1.40×10^{0}	1.51×10^{-26}	1.40×10^{-23}
TMEM252	3.80×10^{-1}	-1.39×10^{0}	3.86×10^{-13}	2.13×10^{-11}
WIF1	3.81×10^{-1}	-1.39×10^{0}	3.61×10^{-11}	1.26×10^{-9}
NR1I2	3.82×10^{-1}	-1.39×10^{0}	1.14×10^{-22}	4.95×10^{-20}
SYT7	3.83×10^{-1}	-1.39×10^{0}	6.32×10^{-22}	2.35×10^{-19}
AC078993.1	3.87×10^{-1}	-1.37×10^{0}	1.59×10^{-13}	9.72×10^{-12}
CTTNBP2	3.88×10^{-1}	-1.37×10^{0}	1.35×10^{-22}	5.73×10^{-20}
SLC35D3	3.88×10^{-1}	-1.37×10^{0}	1.32×10^{-12}	6.33×10^{-11}
AC055717.2	3.88×10^{-1}	-1.37×10^{0}	3.64×10^{-17}	4.86×10^{-15}
FGFR4	3.92×10^{-1}	-1.35×10^{0}	1.16×10^{-21}	3.99×10^{-19}

TLE2	3.93×10^{-1}	-1.35×10^{0}	2.01×10^{-17}	2.83×10^{-15}
SLC39A2	3.93×10^{-1}	-1.35×10^{0}	2.71×10^{-9}	6.34×10^{-8}
CYCSP6	3.93×10^{-1}	-1.35×10^{0}	2.14×10^{-9}	5.11×10^{-8}
NXPE4	3.93×10^{-1}	-1.35×10^{0}	2.09×10^{-6}	2.39×10^{-5}

Table A.13. The list of the top 100 upregulated DEGs identified in the CS1 subtype using edgeR as a result of three clustering analyzes.

	fc	**log2fc**	**pvalue**	**padj**
BX322234.2	4.93×10^{1}	5.62×10^{0}	5.19×10^{-8}	2.92×10^{-7}
WIF1	4.68×10^{1}	5.55×10^{0}	1.41×10^{-30}	1.59×10^{-28}
RNA5.8SP5	4.02×10^{1}	5.33×10^{0}	1.54×10^{-3}	3.91×10^{-3}
AC152010.1	3.87×10^{1}	5.27×10^{0}	4.21×10^{-3}	9.65×10^{-3}
RNA5SP267	2.94×10^{1}	4.88×10^{0}	1.48×10^{-2}	2.93×10^{-2}
RNA5SP211	2.69×10^{1}	4.75×10^{0}	2.08×10^{-2}	3.96×10^{-2}
RNA5SP389	2.25×10^{1}	4.49×10^{0}	1.75×10^{-2}	3.41×10^{-2}
SFTPC	2.23×10^{1}	4.48×10^{0}	7.99×10^{-7}	3.71×10^{-6}
SOHLH1	1.70×10^{1}	4.08×10^{0}	4.89×10^{-11}	4.37×10^{-10}
KRT31	1.66×10^{1}	4.05×10^{0}	4.92×10^{-12}	5.12×10^{-11}

Table A.13 (continued). The list of the top 100 upregulated DEGs identified in the CS1 subtype using edgeR as a result of three clustering analyzes.

AC127459.2	1.50×10^{1}	3.91×10^{0}	3.77×10^{-6}	1.57×10^{-5}
LINC01896	1.42×10^{1}	3.83×10^{0}	7.61×10^{-4}	2.07×10^{-3}
PRR9	1.17×10^{1}	3.55×10^{0}	5.55×10^{-9}	3.64×10^{-8}
AC114291.1	1.14×10^{1}	3.51×10^{0}	1.17×10^{-32}	1.68×10^{-30}
AC009446.1	1.14×10^{1}	3.51×10^{0}	1.47×10^{-3}	3.75×10^{-3}
PTF1A	1.14×10^{1}	3.51×10^{0}	1.46×10^{-10}	1.22×10^{-9}
XAGE2	1.14×10^{1}	3.51×10^{0}	7.55×10^{-7}	3.52×10^{-6}
GALP	1.10×10^{1}	3.46×10^{0}	1.06×10^{-3}	2.80×10^{-3}
PNLIP	1.09×10^{1}	3.45×10^{0}	1.39×10^{-2}	2.79×10^{-2}
SLC5A8	1.07×10^{1}	3.42×10^{0}	7.22×10^{-8}	3.97×10^{-7}
NOTUM	1.06×10^{1}	3.41×10^{0}	5.93×10^{-25}	3.53×10^{-23}
AC026774.1	1.03×10^{1}	3.36×10^{0}	7.16×10^{-18}	1.72×10^{-16}
TKTL1	1.03×10^{1}	3.36×10^{0}	2.35×10^{-13}	2.96×10^{-12}
PRSS56	9.97×10^{0}	3.32×10^{0}	7.87×10^{-8}	4.31×10^{-7}
AC026336.3	9.94×10^{0}	3.31×10^{0}	1.57×10^{-18}	4.13×10^{-17}
GDF10	9.92×10^{0}	3.31×10^{0}	4.33×10^{-16}	8.12×10^{-15}
MAGEB17	9.61×10^{0}	3.26×10^{0}	8.06×10^{-17}	1.66×10^{-15}
RNA5SP213	9.61×10^{0}	3.26×10^{0}	1.10×10^{-2}	2.26×10^{-2}
LINC00661	9.48×10^{0}	3.24×10^{0}	2.60×10^{-4}	7.76×10^{-4}
AC078993.1	9.46×10^{0}	3.24×10^{0}	5.23×10^{-20}	1.67×10^{-18}
MAGEB1	9.29×10^{0}	3.22×10^{0}	1.55×10^{-2}	3.07×10^{-2}
SSX1	8.97×10^{0}	3.17×10^{0}	4.93×10^{-4}	1.39×10^{-3}
TUBAP13	8.83×10^{0}	3.14×10^{0}	8.06×10^{-18}	1.92×10^{-16}
LCN15	8.63×10^{0}	3.11×10^{0}	4.13×10^{-12}	4.36×10^{-11}

CPN1	8.63×10^{0}	3.11×10^{0}	2.68×10^{-17}	5.95×10^{-16}
GPR83	8.62×10^{0}	3.11×10^{0}	1.20×10^{-20}	4.19×10^{-19}
AP002963.1	8.60×10^{0}	3.10×10^{0}	6.67×10^{-3}	1.46×10^{-2}
BPIFA1	8.29×10^{0}	3.05×10^{0}	2.69×10^{-3}	6.48×10^{-3}
LY6G6D	8.21×10^{0}	3.04×10^{0}	2.78×10^{-16}	5.35×10^{-15}
KRT40	8.20×10^{0}	3.03×10^{0}	1.10×10^{-15}	1.96×10^{-14}
HS3ST4	7.55×10^{0}	2.92×10^{0}	8.90×10^{-10}	6.61×10^{-9}
MAGEC2	7.36×10^{0}	2.88×10^{0}	6.84×10^{-3}	1.49×10^{-2}
AL356433.1	7.27×10^{0}	2.86×10^{0}	9.01×10^{-10}	6.69×10^{-9}
HSPB3	7.24×10^{0}	2.86×10^{0}	4.58×10^{-14}	6.42×10^{-13}
TMEM252	7.24×10^{0}	2.86×10^{0}	1.53×10^{-20}	5.31×10^{-19}
AC091304.1	7.16×10^{0}	2.84×10^{0}	2.68×10^{-11}	2.50×10^{-10}
TNNC2	7.05×10^{0}	2.82×10^{0}	4.72×10^{-40}	1.54×10^{-37}
RNA5SP243	7.02×10^{0}	2.81×10^{0}	3.86×10^{-3}	8.94×10^{-3}
MIR483	6.99×10^{0}	2.81×10^{0}	4.37×10^{-5}	1.52×10^{-4}
AC132825.1	6.92×10^{0}	2.79×10^{0}	4.69×10^{-9}	3.11×10^{-8}
SALL3	6.86×10^{0}	2.78×10^{0}	1.24×10^{-3}	3.21×10^{-3}

Table A.13 (continued). The list of the top 100 upregulated DEGs identified in the CS1 subtype using edgeR as a result of three clustering analyzes.

LINC02525	6.83×10^{0}	2.77×10^{0}	2.52×10^{-11}	2.36×10^{-10}
DMRT1	6.77×10^{0}	2.76×10^{0}	1.54×10^{-9}	1.10×10^{-8}
CTNNA2.AS1	6.76×10^{0}	2.76×10^{0}	1.75×10^{-5}	6.53×10^{-5}
AL354863.1	6.70×10^{0}	2.74×10^{0}	1.18×10^{-8}	7.39×10^{-8}
GOLGA6L2	6.63×10^{0}	2.73×10^{0}	7.09×10^{-13}	8.34×10^{-12}
SLC30A2	6.62×10^{0}	2.73×10^{0}	3.43×10^{-22}	1.47×10^{-20}
AL391336.1	6.48×10^{0}	2.70×10^{0}	5.52×10^{-3}	1.23×10^{-2}
IGF2	6.42×10^{0}	2.68×10^{0}	3.23×10^{-10}	2.56×10^{-9}
RPS10.NUDT3	6.39×10^{0}	2.68×10^{0}	3.36×10^{-3}	7.89×10^{-3}
C6orf15	6.32×10^{0}	2.66×10^{0}	1.25×10^{-12}	1.42×10^{-11}
TCAP	6.31×10^{0}	2.66×10^{0}	1.51×10^{-21}	5.92×10^{-20}
OR10G4	6.19×10^{0}	2.63×10^{0}	1.11×10^{-4}	3.57×10^{-4}
KRT37	6.16×10^{0}	2.62×10^{0}	9.50×10^{-11}	8.16×10^{-10}
BX276092.9	6.14×10^{0}	2.62×10^{0}	1.29×10^{-6}	5.81×10^{-6}
LY6G6F.LY6G6D	6.07×10^{0}	2.60×10^{0}	3.37×10^{-12}	3.60×10^{-11}
SHISA9	6.06×10^{0}	2.60×10^{0}	1.21×10^{-10}	1.03×10^{-9}
SYN3	6.02×10^{0}	2.59×10^{0}	2.82×10^{-26}	1.95×10^{-24}
SULT2A1	6.00×10^{0}	2.58×10^{0}	1.10×10^{-11}	1.08×10^{-10}
KRTAP1.1	5.99×10^{0}	2.58×10^{0}	2.95×10^{-7}	1.47×10^{-6}
AP000851.2	5.98×10^{0}	2.58×10^{0}	1.93×10^{-11}	1.83×10^{-10}
INSL5	5.94×10^{0}	2.57×10^{0}	1.07×10^{-7}	5.74×10^{-7}
SFTA3	5.89×10^{0}	2.56×10^{0}	4.30×10^{-3}	9.84×10^{-3}

MAP7D2	5.81×10^{0}	2.54×10^{0}	6.08×10^{-19}	1.69×10^{-17}
KRTAP13.2	5.80×10^{0}	2.54×10^{0}	1.71×10^{-5}	6.40×10^{-5}
AP003774.2	5.77×10^{0}	2.53×10^{0}	6.64×10^{-32}	8.74×10^{-30}
AC108865.1	5.74×10^{0}	2.52×10^{0}	8.19×10^{-9}	5.24×10^{-8}
FGF3	5.72×10^{0}	2.52×10^{0}	9.05×10^{-8}	4.91×10^{-7}
OR7A1P	5.66×10^{0}	2.50×10^{0}	3.40×10^{-3}	7.97×10^{-3}
CELP	5.64×10^{0}	2.50×10^{0}	9.17×10^{-23}	4.24×10^{-21}
CYP4F8	5.64×10^{0}	2.50×10^{0}	7.58×10^{-17}	1.57×10^{-15}
CPA1	5.61×10^{0}	2.49×10^{0}	7.79×10^{-5}	2.57×10^{-4}
PCSK1N	5.61×10^{0}	2.49×10^{0}	7.94×10^{-13}	9.26×10^{-12}
AC073176.2	5.58×10^{0}	2.48×10^{0}	2.50×10^{-2}	4.63×10^{-2}
AL391650.2	5.49×10^{0}	2.46×10^{0}	3.40×10^{-11}	3.12×10^{-10}
KCNC2	5.49×10^{0}	2.46×10^{0}	7.15×10^{-6}	2.84×10^{-5}
SLC6A2	5.48×10^{0}	2.45×10^{0}	2.12×10^{-7}	1.08×10^{-6}
AC135388.1	5.48×10^{0}	2.45×10^{0}	1.76×10^{-16}	3.48×10^{-15}
SERPINA7	5.47×10^{0}	2.45×10^{0}	1.00×10^{-10}	8.57×10^{-10}
ELF5	5.46×10^{0}	2.45×10^{0}	6.20×10^{-9}	4.04×10^{-8}

Table A.13 (continued). The list of the top 100 upregulated DEGs identified in the CS1 subtype using edgeR as a result of three clustering analyzes.

PHYHIPL	5.46×10^{0}	2.45×10^{0}	5.95×10^{-14}	8.21×10^{-13}
TCHH	5.45×10^{0}	2.45×10^{0}	2.53×10^{-18}	6.48×10^{-17}
AL139327.1	5.41×10^{0}	2.44×10^{0}	1.16×10^{-2}	2.37×10^{-2}
KRT23	5.41×10^{0}	2.44×10^{0}	5.13×10^{-20}	1.64×10^{-18}
LINC02128	5.38×10^{0}	2.43×10^{0}	3.48×10^{-10}	2.74×10^{-9}
SLC1A7	5.35×10^{0}	2.42×10^{0}	2.25×10^{-27}	1.74×10^{-25}
STRIT1	5.28×10^{0}	2.40×10^{0}	6.30×10^{-6}	2.52×10^{-5}
AC016925.3	5.26×10^{0}	2.40×10^{0}	6.20×10^{-9}	4.04×10^{-8}
MYBPHL	5.24×10^{0}	2.39×10^{0}	4.21×10^{-12}	4.43×10^{-11}
IGDCC3	5.18×10^{0}	2.37×10^{0}	1.19×10^{-8}	7.44×10^{-8}

Table A.14. The list of the top 100 downregulated DEGs identified in the CS1 subtype using edgeR as a result of three clustering analyzes.

	fc	**log2fc**	**pvalue**	**padj**
RN7SKP227	3.14×10^{-3}	-8.32×10^{0}	2.56×10^{-13}	3.21×10^{-12}
RNU1.28P	3.51×10^{-3}	-8.15×10^{0}	3.30×10^{-14}	4.72×10^{-13}
RN7SKP203	4.66×10^{-3}	-7.75×10^{0}	1.58×10^{-16}	3.14×10^{-15}
RNU1.88P	4.99×10^{-3}	-7.65×10^{0}	3.66×10^{-17}	7.97×10^{-16}
MIR3609	5.02×10^{-3}	-7.64×10^{0}	4.36×10^{-31}	5.17×10^{-29}
RNY4	5.31×10^{-3}	-7.56×10^{0}	5.67×10^{-10}	4.34×10^{-9}
H2BC3	5.37×10^{-3}	-7.54×10^{0}	4.44×10^{-28}	3.67×10^{-26}
RNY1	5.45×10^{-3}	-7.52×10^{0}	7.83×10^{-18}	1.87×10^{-16}
SCARNA5	5.70×10^{-3}	-7.45×10^{0}	1.60×10^{-67}	6.54×10^{-64}
RNU5B.1	5.80×10^{-3}	-7.43×10^{0}	2.00×10^{-13}	2.55×10^{-12}
RNVU1.18	6.25×10^{-3}	-7.32×10^{0}	7.34×10^{-14}	1.00×10^{-12}

RN7SKP255	6.49×10^{-3}	-7.27×10^{0}	6.83×10^{-14}	9.36×10^{-13}
RNU2.59P	6.54×10^{-3}	-7.26×10^{0}	5.36×10^{-15}	8.61×10^{-14}
RN7SL149P	6.82×10^{-3}	-7.20×10^{0}	6.89×10^{-13}	8.12×10^{-12}
RNU1.11P	7.00×10^{-3}	-7.16×10^{0}	1.71×10^{-11}	1.64×10^{-10}
RN7SKP9	7.06×10^{-3}	-7.15×10^{0}	4.02×10^{-31}	4.82×10^{-29}
RNU5A.1	7.39×10^{-3}	-7.08×10^{0}	8.84×10^{-21}	3.16×10^{-19}
AL139274.1	7.69×10^{-3}	-7.02×10^{0}	3.58×10^{-20}	1.17×10^{-18}
RN7SKP186	8.25×10^{-3}	-6.92×10^{0}	5.33×10^{-14}	7.41×10^{-13}
AL356057.1	8.82×10^{-3}	-6.83×10^{0}	1.59×10^{-18}	4.18×10^{-17}
SCARNA7	8.93×10^{-3}	-6.81×10^{0}	8.47×10^{-58}	1.67×10^{-54}
RNU2.61P	9.27×10^{-3}	-6.75×10^{0}	1.68×10^{-13}	2.16×10^{-12}
SNORA49	9.34×10^{-3}	-6.74×10^{0}	4.02×10^{-38}	1.08×10^{-35}
H4C3	9.44×10^{-3}	-6.73×10^{0}	5.99×10^{-74}	5.71×10^{-70}
Y_RNA.241	9.53×10^{-3}	-6.71×10^{0}	6.24×10^{-17}	1.31×10^{-15}
RNU1.19P	9.93×10^{-3}	-6.65×10^{0}	1.05×10^{-13}	1.40×10^{-12}
RN7SL507P	1.01×10^{-2}	-6.63×10^{0}	9.06×10^{-19}	2.47×10^{-17}

Table A.14 (continued). The list of the top 100 downregulated DEGs identified in the CS1 subtype using edgeR as a result of three clustering analyzes.

AC100800.1	1.06×10^{-2}	-6.56×10^{0}	7.02×10^{-20}	2.20×10^{-18}
RNVU1.2A	1.06×10^{-2}	-6.56×10^{0}	2.35×10^{-13}	2.97×10^{-12}
RNU2.23P	1.08×10^{-2}	-6.53×10^{0}	7.53×10^{-14}	1.03×10^{-12}
RNY3	1.09×10^{-2}	-6.52×10^{0}	1.20×10^{-8}	7.47×10^{-8}
CELF2.AS2	1.09×10^{-2}	-6.51×10^{0}	9.51×10^{-34}	1.53×10^{-31}
SNORA74A	1.10×10^{-2}	-6.51×10^{0}	6.41×10^{-59}	1.36×10^{-55}
RNU1.83P	1.10×10^{-2}	-6.50×10^{0}	7.10×10^{-14}	9.70×10^{-13}
MTCYBP32	1.11×10^{-2}	-6.49×10^{0}	8.39×10^{-15}	1.31
AC092139.1	1.12×10^{-2}	-6.48×10^{0}	3.87×10^{-25}	2.35×10^{-23}
H2BC10	1.12×10^{-2}	-6.48×10^{0}	1.04×10^{-54}	1.36×10^{-51}
AC064872.1	1.12×10^{-2}	-6.47×10^{0}	6.66×10^{-10}	5.04×10^{-9}
AL390318.1	1.13×10^{-2}	-6.47×10^{0}	1.53×10^{-13}	1.99×10^{-12}
AC096741.1	1.13×10^{-2}	-6.46×10^{0}	2.20×10^{-20}	7.43×10^{-19}
H1.5	1.19×10^{-2}	-6.40×10^{0}	4.37×10^{-77}	6.25×10^{-73}
AC130895.1	1.22×10^{-2}	-6.36×10^{0}	2.69×10^{-19}	7.79×10^{-18}
AC241520.1	1.22×10^{-2}	-6.35×10^{0}	2.31×10^{-24}	1.29×10^{-22}
AL391863.2	1.24×10^{-2}	-6.34×10^{0}	4.18×10^{-24}	2.27×10^{-22}
MTND5P26	1.24×10^{-2}	-6.33×10^{0}	1.63×10^{-14}	2.43×10^{-13}
RNU1.52P	1.26×10^{-2}	-6.31×10^{0}	1.33×10^{-8}	8.25×10^{-8}
ZBTB20.AS5	1.27×10^{-2}	-6.30×10^{0}	2.34×10^{-22}	1.03×10^{-20}
CLDN18	1.27×10^{-2}	-6.30×10^{0}	6.22×10^{-55}	8.28×10^{-52}
Z93020.1	1.27×10^{-2}	-6.30×10^{0}	1.55×10^{-16}	3.08×10^{-15}
RN7SKP8	1.28×10^{-2}	-6.29×10^{0}	2.79×10^{-14}	4.03×10^{-13}
RNU1.139P	1.29×10^{-2}	-6.28×10^{0}	1.13×10^{-9}	8.25×10^{-9}
H4C13	1.30×10^{-2}	-6.27×10^{0}	3.07×10^{-30}	3.30×10^{-28}
IFNK	1.32×10^{-2}	-6.25×10^{0}	9.76×10^{-21}	3.46×10^{-19}

AL139120.1	1.32×10^{-2}	-6.25×10^{0}	8.86×10^{-16}	1.60×10^{-14}
LPP.AS1	1.33×10^{-2}	-6.22×10^{0}	6.97×10^{-17}	1.45×10^{-15}
SNORA53	1.38×10^{-2}	-6.17×10^{0}	2.40×10^{-78}	6.87×10^{-74}
RNU1.20P	1.39×10^{-2}	-6.17×10^{0}	3.77×10^{-8}	2.18×10^{-7}
H3C2	1.39×10^{-2}	-6.17×10^{0}	3.97×10^{-72}	3.25×10^{-68}
RN7SL38P	1.40×10^{-2}	-6.16×10^{0}	3.00×10^{-13}	3.73×10^{-12}
Y_RNA.209	1.43×10^{-2}	-6.13×10^{0}	3.50×10^{-9}	2.36×10^{-8}
AC087286.1	1.43×10^{-2}	-6.13×10^{0}	8.83×10^{-20}	2.73×10^{-18}
RN7SL7P	1.44×10^{-2}	-6.12×10^{0}	5.33×10^{-13}	6.40×10^{-12}
AC018398.2	1.44×10^{-2}	-6.11×10^{0}	2.55×10^{-21}	9.76×10^{-20}
RNU1.89P	1.45×10^{-2}	-6.10×10^{0}	2.30×10^{-12}	2.51×10^{-11}
RNU4.2	1.46×10^{-2}	-6.10×10^{0}	7.64×10^{-39}	2.20×10^{-36}
SCARNA1	1.46×10^{-2}	-6.09×10^{0}	1.12×10^{-31}	1.44×10^{-29}
SNRPGP18	1.47×10^{-2}	-6.09×10^{0}	9.20×10^{-15}	1.42×10^{-13}
BMP2KL	1.47×10^{-2}	-6.09×10^{0}	2.19×10^{-17}	4.92×10^{-16}

Table A.14 (continued). The list of the top 100 downregulated DEGs identified in the CS1 subtype using edgeR as a result of three clustering analyzes.

SNORA23	1.47×10^{-2}	-6.09×10^{0}	5.48×10^{-56}	7.84×10^{-53}
AL157402.2	1.47×10^{-2}	-6.09×10^{0}	7.02×10^{-20}	2.20×10^{-18}
RN7SL618P	1.47×10^{-2}	-6.08×10^{0}	1.12×10^{-6}	5.07×10^{-6}
AL589655.1	1.49×10^{-2}	-6.07×10^{0}	1.58×10^{-13}	2.04×10^{-12}
H4C4	1.50×10^{-2}	-6.06×10^{0}	2.79×10^{-70}	1.60×10^{-66}
AC010997.6	1.51×10^{-2}	-6.05×10^{0}	6.46×10^{-14}	8.88×10^{-13}
RN7SL151P	1.51×10^{-2}	-6.05×10^{0}	2.99×10^{-24}	1.65×10^{-22}
RAD51AP1P1	1.52×10^{-2}	-6.04×10^{0}	4.65×10^{-18}	1.14×10^{-16}
RNU1.46P	1.52×10^{-2}	-6.04×10^{0}	9.26×10^{-10}	6.86×10^{-9}
ZNF75BP	1.54×10^{-2}	-6.02×10^{0}	1.53×10^{-13}	1.99×10^{-12}
EIF4E2P1	1.55×10^{-2}	-6.02×10^{0}	3.44×10^{-17}	7.52×10^{-16}
AC022022.2	1.55×10^{-2}	-6.01×10^{0}	2.44×10^{-15}	4.13×10^{-14}
RNU5D.1	1.55×10^{-2}	-6.01×10^{0}	3.17×10^{-25}	1.95×10^{-23}
SNORA73B	1.55×10^{-2}	-6.01×10^{0}	2.14×10^{-81}	1.22×10^{-76}
EDDM3CP	1.58×10^{-2}	-5.99×10^{0}	1.72×10^{-13}	2.22×10^{-12}
RN7SL296P	1.62×10^{-2}	-5.95×10^{0}	5.25×10^{-22}	2.19×10^{-20}
RN7SL116P	1.63×10^{-2}	-5.94×10^{0}	1.55×10^{-22}	6.95×10^{-21}
H1.3	1.64×10^{-2}	-5.93×10^{0}	7.74×10^{-76}	8.86×10^{-72}
CACNA1C.AS4	1.65×10^{-2}	-5.92×10^{0}	1.25×10^{-19}	3.76×10^{-18}
AC104332.1	1.66×10^{-2}	-5.91×10^{0}	2.62×10^{-23}	1.29×10^{-21}
AC022537.1	1.66×10^{-2}	-5.91×10^{0}	2.36×10^{-13}	2.98×10^{-12}
RN7SL564P	1.67×10^{-2}	-5.90×10^{0}	8.05×10^{-17}	1.66×10^{-15}
H2AC21	1.67×10^{-2}	-5.90×10^{0}	3.65×10^{-46}	2.13×10^{-43}
AC100763.1	1.68×10^{-2}	-5.89×10^{0}	1.96×10^{-16}	3.84×10^{-15}
AL136320.1	1.68×10^{-2}	-5.89×10^{0}	1.15×10^{-18}	3.10×10^{-17}

AL034349.1	1.73×10^{-2}	-5.85×10^{0}	2.52×10^{-25}	1.58×10^{-23}
RN7SL141P	1.77×10^{-2}	-5.82×10^{0}	2.09×10^{-16}	4.08×10^{-15}
AC008833.1	1.77×10^{-2}	-5.82×10^{0}	4.61×10^{-16}	8.60×10^{-15}
AC009682.1	1.79×10^{-2}	-5.80×10^{0}	3.23×10^{-22}	1.38×10^{-20}
AP003086.3	1.84×10^{-2}	-5.77×10^{0}	1.45×10^{-23}	7.35×10^{-22}
AC023813.2	1.84×10^{-2}	-5.76×10^{0}	2.51×10^{-18}	6.44×10^{-17}
AC120349.2	1.85×10^{-2}	-5.76×10^{0}	2.99×10^{-14}	4.30×10^{-13}

Table A.15. The list of the top 100 upregulated DEGs identified in the CS2 subtype using edgeR as a result of three clustering analyzes.

	fc	**log2fc**	**pvalue**	**padj**
RNY4	2.84×10^{2}	8.15×10^{0}	1.62×10^{-16}	1.81×10^{-15}
PAEP	2.04×10^{2}	7.67×10^{0}	1.48×10^{-94}	2.12×10^{-90}
FBXO40	1.99×10^{2}	7.63×10^{0}	5.97×10^{-60}	4.27×10^{-57}
RNU1.28P	1.74×10^{2}	7.44×10^{0}	9.62×10^{-11}	5.70×10^{-10}

Table A.15 (continued). The list of the top 100 upregulated DEGs identified in the CS2 subtype using edgeR as a result of three clustering analyzes.

RNVU1.2	1.67×10^{2}	7.39×10^{0}	2.05×10^{-24}	5.11×10^{-23}
MTND5P32	1.48×10^{2}	7.20×10^{0}	2.85×10^{-27}	9.33×10^{-26}
AC066616.2	1.41×10^{2}	7.14×10^{0}	2.47×10^{-29}	9.92×10^{-28}
RNU1.19P	1.37×10^{2}	7.10×10^{0}	7.00×10^{-20}	1.09×10^{-18}
RNVU1.18	1.34×10^{2}	7.07×10^{0}	1.08×10^{-12}	7.97×10^{-12}
RNU1.20P	1.33×10^{2}	7.05×10^{0}	5.85×10^{-16}	6.18×10^{-15}
TFAP2B	1.30×10^{2}	7.02×10^{0}	3.53×10^{-27}	1.14×10^{-25}
RNU1.83P	1.28×10^{2}	7.00×10^{0}	3.76×10^{-21}	6.67×10^{-20}
AC090220.1	1.27×10^{2}	6.99×10^{0}	1.57×10^{-30}	7.04×10^{-29}
RNU2.59P	1.26×10^{2}	6.98×10^{0}	4.90×10^{-15}	4.70×10^{-14}
RNU1.52P	1.23×10^{2}	6.94×10^{0}	2.97×10^{-12}	2.09×10^{-11}
RNU1.139P	1.18×10^{2}	6.89×10^{0}	3.67×10^{-14}	3.20×10^{-13}
SERPINB13	1.17×10^{2}	6.88×10^{0}	1.01×10^{-22}	2.10×10^{-21}
MTCYBP23	1.12×10^{2}	6.81×10^{0}	5.16×10^{-26}	1.49×10^{-24}
RNU1.46P	1.12×10^{2}	6.81×10^{0}	3.02×10^{-16}	3.28×10^{-15}
Y_RNA.241	1.09×10^{2}	6.77×10^{0}	6.93×10^{-20}	1.08×10^{-18}
Y_RNA.209	1.07×10^{2}	6.74×10^{0}	3.76×10^{-13}	2.92×10^{-12}
KRT14	1.05×10^{2}	6.71×10^{0}	6.38×10^{-49}	1.48×10^{-46}
MTCYBP32	1.04×10^{2}	6.69×10^{0}	2.84×10^{-18}	3.78×10^{-17}
RNU1.88P	1.02×10^{2}	6.68×10^{0}	8.25×10^{-14}	6.89×10^{-13}
AL139274.1	9.48×10^{1}	6.57×10^{0}	6.49×10^{-19}	9.22×10^{-18}
RNU5A.1	9.39×10^{1}	6.55×10^{0}	1.66×10^{-20}	2.75×10^{-19}
AL157402.2	8.72×10^{1}	6.45×10^{0}	1.76×10^{-27}	5.87×10^{-26}
AC079316.2	8.48×10^{1}	6.41×10^{0}	3.15×10^{-24}	7.67×10^{-23}
MTND5P26	8.00×10^{1}	6.32×10^{0}	3.74×10^{-15}	3.63×10^{-14}
Z93020.1	7.87×10^{1}	6.30×10^{0}	1.54×10^{-18}	2.12×10^{-17}
RLIMP1	7.84×10^{1}	6.29×10^{0}	2.68×10^{-48}	5.86×10^{-46}

AL360178.2	7.79×10^{1}	6.28×10^{0}	1.90×10^{-21}	3.47×10^{-20}
AC069549.2	7.78×10^{1}	6.28×10^{0}	6.78×10^{-37}	5.54×10^{-35}
RN7SKP227	7.61×10^{1}	6.25×10^{0}	1.77×10^{-4}	4.60×10^{-4}
MT.TH	7.57×10^{1}	6.24×10^{0}	4.13×10^{-25}	1.10×10^{-23}
IFNK	7.50×10^{1}	6.23×10^{0}	2.50×10^{-23}	5.56×10^{-22}
RNU2.23P	7.50×10^{1}	6.23×10^{0}	1.09×10^{-11}	7.19×10^{-11}
AC009951.4	7.49×10^{1}	6.23×10^{0}	5.01×10^{-59}	3.30×10^{-56}
AC130895.1	7.41×10^{1}	6.21×10^{0}	5.60×10^{-20}	8.82×10^{-19}
MTND3P12	7.27×10^{1}	6.18×10^{0}	1.24×10^{-18}	1.71×10^{-17}
AL035693.1	7.22×10^{1}	6.17×10^{0}	7.91×10^{-29}	3.02×10^{-27}
Y_RNA.713	7.15×10^{1}	6.16×10^{0}	7.40×10^{-17}	8.58×10^{-16}
MTND1P11	7.09×10^{1}	6.15×10^{0}	1.42×10^{-28}	5.27×10^{-27}
AL356057.1	6.98×10^{1}	6.12×10^{0}	3.39×10^{-14}	2.97×10^{-13}
DIAPH1.AS1	6.86×10^{1}	6.10×10^{0}	2.91×10^{-38}	2.77×10^{-36}

Table A.15 (continued). The list of the top 100 upregulated DEGs identified in the CS2 subtype using edgeR as a result of three clustering analyzes.

AL359095.1	6.85×10^{1}	6.10×10^{0}	1.85×10^{-21}	3.39×10^{-20}
AC087286.1	6.83×10^{1}	6.09×10^{0}	1.21×10^{-21}	2.25×10^{-20}
MTCO3P23	6.78×10^{1}	6.08×10^{0}	4.46×10^{-21}	7.84×10^{-20}
AL589655.1	6.70×10^{1}	6.07×10^{0}	3.36×10^{-13}	2.63×10^{-12}
AC107050.1	6.68×10^{1}	6.06×10^{0}	3.18×10^{-54}	1.23×10^{-51}
LPP.AS1	6.58×10^{1}	6.04×10^{0}	6.58×10^{-15}	6.23×10^{-14}
AL391863.2	6.42×10^{1}	6.00×10^{0}	2.77×10^{-23}	6.11×10^{-22}
AL390318.1	6.42×10^{1}	6.00×10^{0}	2.16×10^{-9}	1.09×10^{-8}
AL138713.1	6.40×10^{1}	6.00×10^{0}	1.12×10^{-24}	2.86×10^{-23}
RNU5B.1	6.36×10^{1}	5.99×10^{0}	4.43×10^{-10}	2.43×10^{-9}
SNRPGP18	6.34×10^{1}	5.99×10^{0}	9.87×10^{-15}	9.17×10^{-14}
FOXN3.AS2	6.27×10^{1}	5.97×10^{0}	1.62×10^{-22}	3.30×10^{-21}
AC120349.2	6.26×10^{1}	5.97×10^{0}	6.69×10^{-16}	7.02×10^{-15}
AC133106.1	6.20×10^{1}	5.96×10^{0}	2.18×10^{-26}	6.58×10^{-25}
RAD51AP1P1	6.18×10^{1}	5.95×10^{0}	9.46×10^{-17}	1.09×10^{-15}
Y_RNA.720	6.14×10^{1}	5.94×10^{0}	1.86×10^{-17}	2.29×10^{-16}
PLCB1.IT1	6.13×10^{1}	5.94×10^{0}	7.13×10^{-14}	6.00×10^{-13}
RNU4.6P	6.09×10^{1}	5.93×10^{0}	1.44×10^{-17}	1.78×10^{-16}
AC022133.2	6.07×10^{1}	5.92×10^{0}	2.62×10^{-46}	4.80×10^{-44}
AC005183.1	6.02×10^{1}	5.91×10^{0}	2.24×10^{-41}	2.75×10^{-39}
RNU1.148P	6.00×10^{1}	5.91×10^{0}	7.27×10^{-16}	7.61×10^{-15}
AF127577.6	6.00×10^{1}	5.91×10^{0}	6.71×10^{-55}	2.85×10^{-52}
AL357141.1	5.97×10^{1}	5.90×10^{0}	3.78×10^{-33}	2.19×10^{-31}
MTND1P32	5.96×10^{1}	5.90×10^{0}	6.44×10^{-19}	9.15×10^{-18}
MTND2P2	5.94×10^{1}	5.89×10^{0}	4.46×10^{-14}	3.85×10^{-13}
ZBTB20.AS5	5.90×10^{1}	5.88×10^{0}	2.40×10^{-20}	3.91×10^{-19}
DOCK4.AS1	5.83×10^{1}	5.87×10^{0}	5.93×10^{-35}	4.03×10^{-33}

AC026124.1	5.79×10^{1}	5.85×10^{0}	7.38×10^{-31}	3.46×10^{-29}
AL356785.1	5.78×10^{1}	5.85×10^{0}	3.45×10^{-16}	3.72×10^{-15}
AL136320.1	5.77×10^{1}	5.85×10^{0}	3.72×10^{-20}	5.96×10^{-19}
AC008833.1	5.76×10^{1}	5.85×10^{0}	1.75×10^{-14}	1.58×10^{-13}
RNU1.11P	5.71×10^{1}	5.83×10^{0}	5.59×10^{-8}	2.38×10^{-7}
AC100763.1	5.70×10^{1}	5.83×10^{0}	4.29×10^{-17}	5.10×10^{-16}
AC092139.1	5.68×10^{1}	5.83×10^{0}	1.02×10^{-21}	1.93×10^{-20}
RN7SKP186	5.67×10^{1}	5.83×10^{0}	1.17×10^{-5}	3.64×10^{-5}
SNORA70.24	5.67×10^{1}	5.82×10^{0}	1.85×10^{-16}	2.06×10^{-15}
AC100800.1	5.66×10^{1}	5.82×10^{0}	4.56×10^{-14}	3.93×10^{-13}
EIF4E2P1	5.66×10^{1}	5.82×10^{0}	1.91×10^{-14}	1.71×10^{-13}
ST7.AS2	5.66×10^{1}	5.82×10^{0}	3.50×10^{-46}	6.30×10^{-44}
AC125612.1	5.65×10^{1}	5.82×10^{0}	6.62×10^{-21}	1.14×10^{-19}
RNU1.42P	5.61×10^{1}	5.81×10^{0}	2.28×10^{-14}	2.03×10^{-13}

Table A.15 (continued). The list of the top 100 upregulated DEGs identified in the CS2 subtype using edgeR as a result of three clustering analyzes.

LINC02411	5.58×10^{1}	5.80×10^{0}	3.88×10^{-14}	3.38×10^{-13}
RNU6ATAC	5.57×10^{1}	5.80×10^{0}	8.39×10^{-25}	2.17×10^{-23}
AC241520.1	5.52×10^{1}	5.79×10^{0}	6.41×10^{-21}	1.11×10^{-19}
RNU1.3	5.50×10^{1}	5.78×10^{0}	2.30×10^{-11}	1.46×10^{-10}
AC022022.2	5.50×10^{1}	5.78×10^{0}	3.16×10^{-13}	2.48×10^{-12}
MTCYBP3	5.49×10^{1}	5.78×10^{0}	2.02×10^{-36}	1.56×10^{-34}
MTND4P14	5.46×10^{1}	5.77×10^{0}	1.83×10^{-45}	3.15×10^{-43}
AL606517.2	5.45×10^{1}	5.77×10^{0}	6.28×10^{-13}	4.76×10^{-12}
AL139120.1	5.44×10^{1}	5.77×10^{0}	1.01×10^{-12}	7.47×10^{-12}
RNVU1.28	5.40×10^{1}	5.75×10^{0}	7.95×10^{-13}	5.95×10^{-12}
AC010480.1	5.33×10^{1}	5.74×10^{0}	5.04×10^{-36}	3.79×10^{-34}
AL391097.1	5.33×10^{1}	5.74×10^{0}	1.14×10^{-18}	1.58×10^{-17}
HECW1.IT1	5.32×10^{1}	5.73×10^{0}	9.61×10^{-22}	1.81×10^{-20}
RNU6.1188P	5.29×10^{1}	5.72×10^{0}	1.97×10^{-11}	1.26×10^{-10}

Table A.16. The list of the top 100 downregulated DEGs identified in the CS2 subtype using edgeR as a result of three clustering analyzes.

	fc	**log2fc**	**pvalue**	**padj**
RNA5.8SP5	3.34×10^{-2}	-4.90×10^{0}	2.48×10^{-2}	4.18×10^{-2}
CLEC2A	4.82×10^{-2}	-4.37×10^{0}	4.83×10^{-4}	1.16×10^{-3}
RPL35P2	4.93×10^{-2}	-4.34×10^{0}	3.39×10^{-6}	1.14×10^{-5}
ALB	5.73×10^{-2}	-4.13×10^{0}	5.41×10^{-10}	2.93×10^{-9}
ORM1	5.83×10^{-2}	-4.10×10^{0}	9.71×10^{-9}	4.56×10^{-8}
FP236383.7	7.76×10^{-2}	-3.69×10^{0}	1.31×10^{-2}	2.36×10^{-2}
AC079804.2	7.89×10^{-2}	-3.66×10^{0}	6.28×10^{-7}	2.34×10^{-6}
BHLHA9	7.92×10^{-2}	-3.66×10^{0}	3.54×10^{-11}	2.20×10^{-10}
AC018695.1	8.04×10^{-2}	-3.64×10^{0}	8.43×10^{-9}	3.99×10^{-8}
APOA2	8.25×10^{-2}	-3.60×10^{0}	6.14×10^{-10}	3.30×10^{-9}

DEFA6	9.44×10^{-2}	-3.41×10^{0}	5.25×10^{-9}	2.54×10^{-8}
AL049830.1	1.03×10^{-1}	-3.28×10^{0}	5.95×10^{-9}	2.86×10^{-8}
SRIP3	1.07×10^{-1}	-3.23×10^{0}	1.01×10^{-4}	2.72×10^{-4}
AC074085.2	1.11×10^{-1}	-3.17×10^{0}	1.12×10^{-11}	7.39×10^{-11}
ATP12A	1.13×10^{-1}	-3.15×10^{0}	4.81×10^{-8}	2.07×10^{-7}
GALP	1.20×10^{-1}	-3.05×10^{0}	2.92×10^{-2}	4.84×10^{-2}
AC087612.1	1.25×10^{-1}	-3.00×10^{0}	1.20×10^{-4}	3.20×10^{-4}
AC244102.3	1.26×10^{-1}	-2.98×10^{0}	2.19×10^{-2}	3.74×10^{-2}
SNHG25	1.28×10^{-1}	-2.97×10^{0}	2.08×10^{-12}	1.49×10^{-11}
RPS5P8	1.28×10^{-1}	-2.97×10^{0}	3.84×10^{-8}	1.67×10^{-7}
SLC25A6P2	1.35×10^{-1}	-2.89×10^{0}	1.03×10^{-8}	4.83×10^{-8}
AL589182.1	1.35×10^{-1}	-2.89×10^{0}	9.40×10^{-3}	1.75×10^{-2}
AC091839.1	1.38×10^{-1}	-2.86×10^{0}	8.94×10^{-4}	2.06×10^{-3}

Table A.16 (continued). The list of the top 100 downregulated DEGs identified in the CS2 subtype using edgeR as a result of three clustering analyzes.

RNA5SP243	1.41×10^{-1}	-2.83×10^{0}	2.22×10^{-2}	3.77×10^{-2}
RPL37AP8	1.48×10^{-1}	-2.76×10^{0}	3.80×10^{-8}	1.65×10^{-7}
RPL35AP21	1.53×10^{-1}	-2.71×10^{0}	2.55×10^{-6}	8.73×10^{-6}
NKX6.3	1.60×10^{-1}	-2.65×10^{0}	1.46×10^{-3}	3.21×10^{-3}
IGLJ3	1.60×10^{-1}	-2.65×10^{0}	8.13×10^{-5}	2.23×10^{-4}
RPL13P2	1.63×10^{-1}	-2.62×10^{0}	4.89×10^{-11}	2.99×10^{-10}
RPL38P2	1.64×10^{-1}	-2.61×10^{0}	2.54×10^{-8}	1.13×10^{-7}
MIF	1.66×10^{-1}	-2.59×10^{0}	4.09×10^{-5}	1.18×10^{-4}
LGALS14	1.67×10^{-1}	-2.59×10^{0}	2.42×10^{-5}	7.20×10^{-5}
APOA4	1.67×10^{-1}	-2.58×10^{0}	1.12×10^{-2}	2.04×10^{-2}
AC036111.1	1.71×10^{-1}	-2.55×10^{0}	3.59×10^{-3}	7.31×10^{-3}
IGLJ2	1.78×10^{-1}	-2.49×10^{0}	2.06×10^{-5}	6.21×10^{-5}
BOLA2P1	1.79×10^{-1}	-2.48×10^{0}	3.66×10^{-4}	9.00×10^{-4}
AC023906.1	1.79×10^{-1}	-2.48×10^{0}	1.19×10^{-7}	4.86×10^{-7}
FAM238B	1.80×10^{-1}	-2.47×10^{0}	3.73×10^{-3}	7.58×10^{-3}
AC005307.1	1.82×10^{-1}	-2.46×10^{0}	3.40×10^{-7}	1.31×10^{-6}
AC095059.2	1.82×10^{-1}	-2.46×10^{0}	3.03×10^{-6}	1.03×10^{-5}
CYP4F2	1.83×10^{-1}	-2.45×10^{0}	4.07×10^{-15}	3.93×10^{-14}
GGT4P	1.83×10^{-1}	-2.45×10^{0}	8.81×10^{-13}	6.56×10^{-12}
PPBP	1.88×10^{-1}	-2.41×10^{0}	7.66×10^{-5}	2.11×10^{-4}
AC005165.2	1.88×10^{-1}	-2.41×10^{0}	4.68×10^{-7}	1.77×10^{-6}
OR7A1P	1.88×10^{-1}	-2.41×10^{0}	2.51×10^{-2}	4.22×10^{-2}
AC091179.1	1.90×10^{-1}	-2.40×10^{0}	6.55×10^{-4}	1.54×10^{-3}
CNN2P4	1.90×10^{-1}	-2.39×10^{0}	9.06×10^{-4}	2.08×10^{-3}
EIF3IP1	1.90×10^{-1}	-2.39×10^{0}	1.79×10^{-5}	5.43×10^{-5}
AC106806.1	1.91×10^{-1}	-2.39×10^{0}	2.14×10^{-6}	7.40×10^{-6}
GABRA4	1.93×10^{-1}	-2.38×10^{0}	3.38×10^{-8}	1.48×10^{-7}
RPS10.NUDT3	1.93×10^{-1}	-2.38×10^{0}	2.81×10^{-2}	4.67×10^{-2}

OR7E121P	1.93×10^{-1}	-2.37×10^{0}	2.10×10^{-6}	7.28×10^{-6}
AC012618.1	1.96×10^{-1}	-2.35×10^{0}	1.01×10^{-8}	4.73×10^{-8}
AL138785.1	1.97×10^{-1}	-2.35×10^{0}	1.22×10^{-8}	5.69×10^{-8}
MIR8075	1.99×10^{-1}	-2.33×10^{0}	1.34×10^{-3}	2.97×10^{-3}
IZUMO2	2.00×10^{-1}	-2.32×10^{0}	4.43×10^{-8}	1.91×10^{-7}
RAB5IF	2.01×10^{-1}	-2.31×10^{0}	2.38×10^{-13}	1.90×10^{-12}
SCYGR6	2.04×10^{-1}	-2.30×10^{0}	6.78×10^{-6}	2.19×10^{-5}
C17orf77	2.04×10^{-1}	-2.29×10^{0}	1.40×10^{-7}	5.67×10^{-7}
DBET	2.09×10^{-1}	-2.26×10^{0}	2.52×10^{-5}	7.46×10^{-5}
AC108725.1	2.10×10^{-1}	-2.25×10^{0}	1.10×10^{-6}	3.97×10^{-6}
HMGA1P5	2.11×10^{-1}	-2.24×10^{0}	2.24×10^{-6}	7.74×10^{-6}
RPL31P61	2.13×10^{-1}	-2.23×10^{0}	2.13×10^{-7}	8.40×10^{-7}

Table A.16 (continued). The list of the top 100 downregulated DEGs identified in the CS2 subtype using edgeR as a result of three clustering analyzes.

AC008026.2	2.13×10^{-1}	-2.23×10^{0}	1.21×10^{-6}	4.33×10^{-6}
AC009362.1	2.16×10^{-1}	-2.21×10^{0}	1.02×10^{-7}	4.23×10^{-7}
URAD	2.16×10^{-1}	-2.21×10^{0}	4.90×10^{-8}	2.10×10^{-7}
GS1.594A7.3	2.17×10^{-1}	-2.21×10^{0}	2.84×10^{-5}	8.34×10^{-5}
REN	2.18×10^{-1}	-2.20×10^{0}	1.05×10^{-9}	5.49×10^{-9}
ALDOAP2	2.19×10^{-1}	-2.19×10^{0}	2.47×10^{-6}	8.50×10^{-6}
EIF3KP3	2.20×10^{-1}	-2.18×10^{0}	1.60×10^{-2}	2.84×10^{-2}
RPS6P26	2.21×10^{-1}	-2.18×10^{0}	2.76×10^{-8}	1.22×10^{-7}
TDGF1P3	2.22×10^{-1}	-2.17×10^{0}	8.59×10^{-12}	5.73×10^{-11}
PNLIPRP2	2.23×10^{-1}	-2.17×10^{0}	4.35×10^{-10}	2.38×10^{-9}
AC021074.1	2.23×10^{-1}	-2.16×10^{0}	1.83×10^{-9}	9.36×10^{-9}
LYZL2	2.24×10^{-1}	-2.16×10^{0}	2.37×10^{-5}	7.07×10^{-5}
RPL34P31	2.25×10^{-1}	-2.15×10^{0}	6.18×10^{-7}	2.30×10^{-6}
LINC02022	2.25×10^{-1}	-2.15×10^{0}	1.75×10^{-2}	3.07×10^{-2}
SRXN1	2.25×10^{-1}	-2.15×10^{0}	3.21×10^{-6}	1.09×10^{-5}
RPS4XP8	2.26×10^{-1}	-2.14×10^{0}	2.33×10^{-8}	1.04×10^{-7}
RPL38P6	2.27×10^{-1}	-2.14×10^{0}	5.06×10^{-4}	1.21×10^{-3}
REG3A	2.28×10^{-1}	-2.14×10^{0}	1.34×10^{-4}	3.54×10^{-4}
HSD3B1	2.30×10^{-1}	-2.12×10^{0}	2.30×10^{-9}	1.16×10^{-8}
C10orf99	2.31×10^{-1}	-2.11×10^{0}	1.73×10^{-13}	1.40×10^{-12}
AL122020.1	2.34×10^{-1}	-2.09×10^{0}	7.16×10^{-11}	4.30×10^{-10}
KRTCAP2P1	2.35×10^{-1}	-2.09×10^{0}	1.46×10^{-5}	4.49×10^{-5}
KRTAP5.5	2.35×10^{-1}	-2.09×10^{0}	5.60×10^{-12}	3.82×10^{-11}
RPL30P4	2.36×10^{-1}	-2.08×10^{0}	1.88×10^{-8}	8.52×10^{-8}
RPL35AP34	2.38×10^{-1}	-2.07×10^{0}	1.02×10^{-3}	2.32×10^{-3}
F11	2.39×10^{-1}	-2.06×10^{0}	1.35×10^{-6}	4.81×10^{-6}
AC011753.1	2.41×10^{-1}	-2.05×10^{0}	1.69×10^{-2}	2.97×10^{-2}
CALCB	2.41×10^{-1}	-2.05×10^{0}	3.78×10^{-3}	7.67×10^{-3}
AL358472.1	2.43×10^{-1}	-2.04×10^{0}	6.31×10^{-6}	2.05×10^{-5}
MYL6P3	2.43×10^{-1}	-2.04×10^{0}	2.75×10^{-5}	8.10×10^{-5}

PRAP1	2.47×10^{-1}	-2.02×10^{0}	6.10×10^{-16}	6.43×10^{-15}
PRSS1	2.48×10^{-1}	-2.01×10^{0}	4.26×10^{-5}	1.22×10^{-4}
LINC01996	2.49×10^{-1}	-2.01×10^{0}	3.32×10^{-10}	1.85×10^{-9}
F2	2.50×10^{-1}	-2.00×10^{0}	2.71×10^{-10}	1.53×10^{-9}
HSPD1P21	2.50×10^{-1}	-2.00×10^{0}	2.74×10^{-2}	4.56×10^{-2}
AC093817.2	2.51×10^{-1}	-1.99×10^{0}	4.87×10^{-5}	1.38×10^{-4}
CNN2P6	2.51×10^{-1}	-1.99×10^{0}	6.93×10^{-8}	2.92×10^{-7}

Table A.17. The list of the top 100 upregulated DEGs identified in the CS3 subtype using edgeR as a result of three clustering analyzes.

	fc	**log2fc**	**pvalue**	**padj**
RN7SL618P	1.22×10^{2}	6.93×10^{0}	5.37×10^{-8}	1.92×10^{-6}
RN7SL149P	1.15×10^{2}	6.85×10^{0}	2.25×10^{-10}	2.10×10^{-8}
RN7SL783P	4.79×10^{1}	5.58×10^{0}	7.17×10^{-7}	1.71×10^{-5}
RN7SL822P	4.51×10^{1}	5.49×10^{0}	1.62×10^{-6}	3.40×10^{-5}
RN7SL122P	4.48×10^{1}	5.49×10^{0}	8.84×10^{-10}	6.22×10^{-8}
RN7SL7P	4.08×10^{1}	5.35×10^{0}	1.09×10^{-8}	5.07×10^{-7}
RN7SL762P	4.05×10^{1}	5.34×10^{0}	1.13×10^{-33}	2.16×10^{-29}
RN7SL837P	3.99×10^{1}	5.32×10^{0}	1.22×10^{-7}	3.82×10^{-6}
RN7SL217P	3.88×10^{1}	5.28×10^{0}	2.82×10^{-12}	5.37×10^{-10}
RN7SL507P	3.61×10^{1}	5.17×10^{0}	1.96×10^{-10}	1.88×10^{-8}
RN7SL546P	3.14×10^{1}	4.97×10^{0}	7.22×10^{-31}	6.88×10^{-27}
RN7SL253P	3.00×10^{1}	4.91×10^{0}	8.55×10^{-19}	1.36×10^{-15}
GP2	2.99×10^{1}	4.90×10^{0}	6.31×10^{-33}	9.04×10^{-29}
RN7SL792P	2.66×10^{1}	4.73×10^{0}	6.97×10^{-12}	1.18×10^{-9}
RN7SL126P	2.57×10^{1}	4.68×10^{0}	1.71×10^{-6}	3.55×10^{-5}
RN7SL575P	2.39×10^{1}	4.57×10^{0}	2.38×10^{-6}	4.65×10^{-5}
RN7SL714P	2.31×10^{1}	4.53×10^{0}	6.68×10^{-5}	7.52×10^{-4}
RN7SL14P	2.28×10^{1}	4.51×10^{0}	2.39×10^{-6}	4.67×10^{-5}
RN7SL498P	2.01×10^{1}	4.33×10^{0}	8.10×10^{-8}	2.69×10^{-6}
LINC01790	1.92×10^{1}	4.26×10^{0}	6.34×10^{-4}	4.67×10^{-3}
AC092435.4	1.89×10^{1}	4.24×10^{0}	2.66×10^{-7}	7.44×10^{-6}
RN7SL635P	1.86×10^{1}	4.22×10^{0}	9.31×10^{-5}	9.90×10^{-4}
DEFA11P	1.83×10^{1}	4.20×10^{0}	1.59×10^{-7}	4.76×10^{-6}
AL136442.1	1.78×10^{1}	4.16×10^{0}	5.00×10^{-5}	5.91×10^{-4}
RN7SL516P	1.75×10^{1}	4.13×10^{0}	1.77×10^{-3}	1.07×10^{-2}
COX8C	1.71×10^{1}	4.10×10^{0}	2.28×10^{-23}	6.54×10^{-20}
LIPF	1.68×10^{1}	4.07×10^{0}	5.77×10^{-13}	1.47×10^{-10}
RN7SL659P	1.66×10^{1}	4.06×10^{0}	5.12×10^{-24}	1.73×10^{-20}
CYP1A1	1.64×10^{1}	4.04×10^{0}	4.01×10^{-17}	4.09×10^{-14}
IRGM	1.61×10^{1}	4.01×10^{0}	9.00×10^{-39}	2.58×10^{-34}
RN7SL555P	1.60×10^{1}	4.00×10^{0}	2.35×10^{-5}	3.17×10^{-4}
AC092435.1	1.59×10^{1}	3.99×10^{0}	1.45×10^{-8}	6.48×10^{-7}

RN7SL769P	1.58×10^{1}	3.98×10^{0}	1.55×10^{-6}	3.26×10^{-5}
RN7SL228P	1.58×10^{1}	3.98×10^{0}	5.79×10^{-6}	9.73×10^{-5}
UGT2B4	1.57×10^{1}	3.97×10^{0}	2.15×10^{-16}	1.78×10^{-13}
RN7SL680P	1.56×10^{1}	3.96×10^{0}	3.08×10^{-4}	2.63×10^{-3}
RPS17P1	1.53×10^{1}	3.94×10^{0}	8.81×10^{-19}	1.36×10^{-15}
RN7SL266P	1.51×10^{1}	3.92×10^{0}	5.00×10^{-7}	1.26×10^{-5}
RN7SL480P	1.51×10^{1}	3.91×10^{0}	9.98×10^{-6}	1.55×10^{-4}
RN7SL177P	1.49×10^{1}	3.90×10^{0}	1.03×10^{-3}	6.95×10^{-3}

Table A.17 (continued). The list of the top 100 upregulated DEGs identified in the CS3 subtype using edgeR as a result of three clustering analyzes.

AC126323.1	1.48×10^{1}	3.89×10^{0}	2.05×10^{-11}	2.88×10^{-9}
RN7SL499P	1.46×10^{1}	3.87×10^{0}	3.90×10^{-4}	3.18×10^{-3}
RN7SL314P	1.46×10^{1}	3.87×10^{0}	7.49×10^{-4}	5.35×10^{-3}
ANXA10	1.44×10^{1}	3.84×10^{0}	1.67×10^{-19}	3.08×10^{-16}
BCAR4	1.43×10^{1}	3.84×10^{0}	8.54×10^{-29}	6.11×10^{-25}
RN7SL18P	1.39×10^{1}	3.80×10^{0}	2.18×10^{-6}	4.31×10^{-5}
H4C6	1.37×10^{1}	3.78×10^{0}	3.08×10^{-8}	1.20×10^{-6}
RN7SL183P	1.36×10^{1}	3.77×10^{0}	5.83×10^{-4}	4.38×10^{-3}
RN7SL554P	1.34×10^{1}	3.74×10^{0}	1.87×10^{-3}	1.11×10^{-2}
CIB4	1.32×10^{1}	3.72×10^{0}	1.18×10^{-26}	6.73×10^{-23}
RN7SL617P	1.30×10^{1}	3.70×10^{0}	5.23×10^{-9}	2.75×10^{-7}
PRSS2	1.30×10^{1}	3.70×10^{0}	1.03×10^{-17}	1.28×10^{-14}
TTC29	1.24×10^{1}	3.63×10^{0}	1.48×10^{-10}	1.49×10^{-8}
RN7SL300P	1.23×10^{1}	3.62×10^{0}	2.02×10^{-5}	2.81×10^{-4}
RN7SL280P	1.23×10^{1}	3.62×10^{0}	9.27×10^{-12}	1.50×10^{-9}
Metazoa_SRP.84	1.22×10^{1}	3.61×10^{0}	8.60×10^{-8}	2.83×10^{-6}
AC010983.1	1.18×10^{1}	3.57×10^{0}	8.85×10^{-11}	9.95×10^{-9}
MAGEB10	1.15×10^{1}	3.52×10^{0}	1.06×10^{-6}	2.37×10^{-5}
RN7SL130P	1.14×10^{1}	3.51×10^{0}	3.31×10^{-53}	1.89×10^{-48}
RN7SL836P	1.12×10^{1}	3.48×10^{0}	1.88×10^{-10}	1.81×10^{-8}
RN7SL342P	1.11×10^{1}	3.48×10^{0}	4.13×10^{-3}	2.07×10^{-2}
AC092435.3	1.09×10^{1}	3.45×10^{0}	4.12×10^{-4}	3.32×10^{-3}
RN7SL118P	1.09×10^{1}	3.44×10^{0}	2.56×10^{-16}	2.04×10^{-13}
RN7SL666P	1.07×10^{1}	3.42×10^{0}	1.61×10^{-5}	2.31×10^{-4}
RN7SL570P	1.07×10^{1}	3.41×10^{0}	2.89×10^{-6}	2.49×10^{-3}
MAGEB2	1.04×10^{1}	3.38×10^{0}	1.62×10^{-4}	1.56×10^{-3}
RN7SL359P	1.03×10^{1}	3.36×10^{0}	2.68×10^{-5}	3.53×10^{-4}
RN7SL408P	1.03×10^{1}	3.36×10^{0}	8.33×10^{-4}	5.83×10^{-3}
RN7SL260P	1.02×10^{1}	3.35×10^{0}	1.63×10^{-3}	1.00×10^{-2}
IRX4.AS1	1.00×10^{1}	3.33×10^{0}	1.68×10^{-5}	2.39×10^{-4}
RN7SL597P	9.91×10^{0}	3.31×10^{0}	2.88×10^{-7}	7.94×10^{-6}
RN7SL329P	9.86×10^{0}	3.30×10^{0}	1.69×10^{-5}	2.41×10^{-4}
LIPC	9.85×10^{0}	3.30×10^{0}	3.69×10^{-27}	2.35×10^{-23}

Metazoa_SRP.95	9.77×10^{0}	3.29×10^{0}	1.02×10^{-3}	6.86×10^{-3}
GUSBP7	9.66×10^{0}	3.27×10^{0}	2.81×10^{-9}	1.64×10^{-7}
AC009078.1	9.52×10^{0}	3.25×10^{0}	3.89×10^{-8}	1.46×10^{-6}
TM4SF4	9.49×10^{0}	3.25×10^{0}	5.16×10^{-22}	1.34×10^{-18}
AP005902.1	9.43×10^{0}	3.24×10^{0}	2.09×10^{-4}	1.91×10^{-3}
AC111149.2	9.09×10^{0}	3.18×10^{0}	5.09×10^{-20}	1.01×10^{-16}

Table A.17 (continued). The list of the top 100 upregulated DEGs identified in the CS3 subtype using edgeR as a result of three clustering analyzes.

RN7SL297P	9.06×10^{0}	3.18×10^{0}	2.67×10^{-4}	2.33×10^{-3}
RN7SL451P	9.05×10^{0}	3.18×10^{0}	2.76×10^{-4}	2.39×10^{-3}
RN7SL712P	9.02×10^{0}	3.17×10^{0}	1.28×10^{-3}	8.26×10^{-3}
RN7SL664P	8.87×10^{0}	3.15×10^{0}	1.03×10^{-10}	1.12×10^{-8}
RN7SL494P	8.73×10^{0}	3.13×10^{0}	3.94×10^{-10}	3.28×10^{-8}
RMST	8.68×10^{0}	3.12×10^{0}	3.06×10^{-8}	1.20×10^{-6}
IGFALS	8.64×10^{0}	3.11×10^{0}	2.12×10^{-23}	6.39×10^{-20}
AL356313.1	8.54×10^{0}	3.09×10^{0}	6.26×10^{-5}	7.13×10^{-4}
RNA5SP107	8.25×10^{0}	3.05×10^{0}	5.57×10^{-6}	9.41×10^{-5}
CTSE	8.24×10^{0}	3.04×10^{0}	4.49×10^{-21}	9.88×10^{-18}
RN7SL660P	8.23×10^{0}	3.04×10^{0}	4.07×10^{-6}	7.21×10^{-5}
ESX1	8.14×10^{0}	3.03×10^{0}	6.09×10^{-4}	4.52×10^{-3}
RN7SL236P	8.12×10^{0}	3.02×10^{0}	5.99×10^{-16}	4.19×10^{-13}
CPS1	8.07×10^{0}	3.01×10^{0}	8.76×10^{-19}	1.36×10^{-15}
RBP3	8.00×10^{0}	3.00×10^{0}	4.73×10^{-19}	8.20×10^{-16}
RN7SL402P	7.97×10^{0}	2.99×10^{0}	3.62×10^{-4}	2.99×10^{-3}
RN7SL483P	7.94×10^{0}	2.99×10^{0}	1.65×10^{-3}	1.01×10^{-2}
ALPG	7.89×10^{0}	2.98×10^{0}	6.21×10^{-18}	8.67×10^{-15}
INSL4	7.87×10^{0}	2.98×10^{0}	4.92×10^{-5}	5.84×10^{-4}
MUC5AC	7.84×10^{0}	2.97×10^{0}	5.11×10^{-16}	3.72×10^{-13}
LINC02620	7.84×10^{0}	2.97×10^{0}	1.93×10^{-6}	3.92×10^{-5}

Table A.18. The list of the top 100 downregulated DEGs identified in the CS3 subtype using edgeR as a result of three clustering analyzes.

	fc	**log2fc**	**pvalue**	**padj**
PNMA5	5.86×10^{-3}	-7.41×10^{0}	1.46×10^{-10}	1.48×10^{-8}
PAGE1	1.49×10^{-2}	-6.07×10^{0}	2.61×10^{-4}	2.29×10^{-3}
MAGEA3	2.12×10^{-2}	-5.56×10^{0}	8.80×10^{-5}	9.44×10^{-4}
MAGEA4	2.19×10^{-2}	-5.51×10^{0}	1.45×10^{-4}	1.43×10^{-3}
COL2A1	2.38×10^{-2}	-5.39×10^{0}	6.01×10^{-16}	4.19×10^{-13}
MAGEA12	2.80×10^{-2}	-5.16×10^{0}	1.36×10^{-4}	1.36×10^{-3}
CSAG1	2.97×10^{-2}	-5.07×10^{0}	4.67×10^{-6}	8.10×10^{-5}
CDH9	3.57×10^{-2}	-4.81×10^{0}	1.25×10^{-4}	1.27×10^{-3}
CIDEA	3.91×10^{-2}	-4.68×10^{0}	6.18×10^{-5}	7.05×10^{-4}
MAGEA10	4.17×10^{-2}	-4.59×10^{0}	9.06×10^{-5}	9.67×10^{-4}

LINC02864	4.33×10^{-2}	-4.53×10^{0}	1.94×10^{-6}	3.93×10^{-5}
MAGEA4.AS1	4.34×10^{-2}	-4.53×10^{0}	1.00×10^{-4}	1.05×10^{-3}
TMEM132D.AS1	4.77×10^{-2}	-4.39×10^{0}	5.89×10^{-4}	4.41×10^{-3}
LINC01419	4.79×10^{-2}	-4.38×10^{0}	1.18×10^{-5}	1.78×10^{-4}

Table A.18 (continued). The list of the top 100 downregulated DEGs identified in the CS3 subtype using edgeR as a result of three clustering analyzes.

MAGEA6	5.10×10^{-2}	-4.29×10^{0}	1.50×10^{-3}	9.35×10^{-3}
SALL3	5.30×10^{-2}	-4.24×10^{0}	1.26×10^{-3}	8.15×10^{-3}
SFTPA1	5.52×10^{-2}	-4.18×10^{0}	2.17×10^{-5}	2.97×10^{-4}
GABRA3	5.55×10^{-2}	-4.17×10^{0}	1.39×10^{-9}	8.97×10^{-8}
AC009446.1	5.59×10^{-2}	-4.16×10^{0}	1.66×10^{-3}	1.01×10^{-2}
AC244102.4	5.65×10^{-2}	-4.14×10^{0}	6.70×10^{-3}	3.02×10^{-2}
AC090809.1	5.75×10^{-2}	-4.12×10^{0}	3.23×10^{-6}	5.95×10^{-5}
CTAG2	5.97×10^{-2}	-4.07×10^{0}	9.65×10^{-3}	4.01×10^{-2}
MAGEA9B	6.07×10^{-2}	-4.04×10^{0}	4.50×10^{-3}	2.22×10^{-2}
MIR548XHG	6.20×10^{-2}	-4.01×10^{0}	4.01×10^{-3}	2.03×10^{-2}
LINC00355	6.36×10^{-2}	-3.98×10^{0}	1.51×10^{-5}	2.19×10^{-4}
AL589787.2	6.40×10^{-2}	-3.96×10^{0}	4.42×10^{-4}	3.51×10^{-3}
LINC02476	6.52×10^{-2}	-3.94×10^{0}	4.33×10^{-3}	2.15×10^{-2}
RIMS2	6.57×10^{-2}	-3.93×10^{0}	7.72×10^{-10}	5.58×10^{-8}
MAGEA9	6.87×10^{-2}	-3.86×10^{0}	1.82×10^{-3}	1.09×10^{-2}
BPIFA1	6.88×10^{-2}	-3.86×10^{0}	1.17×10^{-2}	4.65×10^{-2}
AL137001.2	7.36×10^{-2}	-3.76×10^{0}	1.24×10^{-2}	4.89×10^{-2}
OR1N2	7.37×10^{-2}	-3.76×10^{0}	7.22×10^{-3}	3.20×10^{-2}
SSX1	7.58×10^{-2}	-3.72×10^{0}	4.59×10^{-3}	2.25×10^{-2}
SOHLH2	7.70×10^{-2}	-3.70×10^{0}	3.46×10^{-6}	6.27×10^{-5}
VSTM2B	7.71×10^{-2}	-3.70×10^{0}	3.89×10^{-6}	6.95×10^{-5}
AL589743.3	8.12×10^{-2}	-3.62×10^{0}	3.19×10^{-9}	1.83×10^{-7}
RIPPLY2	8.16×10^{-2}	-3.62×10^{0}	3.17×10^{-6}	5.88×10^{-5}
CHRND	8.24×10^{-2}	-3.60×10^{0}	6.94×10^{-6}	1.14×10^{-4}
AMBN	8.25×10^{-2}	-3.60×10^{0}	3.49×10^{-4}	2.90×10^{-3}
AL049828.2	8.30×10^{-2}	-3.59×10^{0}	1.11×10^{-3}	7.36×10^{-3}
EMX2	8.75×10^{-2}	-3.51×10^{0}	1.38×10^{-7}	4.23×10^{-6}
FAM230C	8.78×10^{-2}	-3.51×10^{0}	7.44×10^{-3}	3.27×10^{-2}
ZNF663P	8.91×10^{-2}	-3.49×10^{0}	9.01×10^{-8}	2.95×10^{-6}
SFTA3	9.02×10^{-2}	-3.47×10^{0}	1.02×10^{-2}	4.19×10^{-2}
COX7B2	9.17×10^{-2}	-3.45×10^{0}	9.58×10^{-3}	3.99×10^{-2}
LINCALD	9.18×10^{-2}	-3.45×10^{0}	6.35×10^{-3}	2.90×10^{-2}
AL035467.2	9.26×10^{-2}	-3.43×10^{0}	2.20×10^{-4}	1.99×10^{-3}
EZHIP	9.27×10^{-2}	-3.43×10^{0}	6.89×10^{-4}	4.99×10^{-3}
TMEM132C	9.31×10^{-2}	-3.42×10^{0}	1.09×10^{-8}	5.08×10^{-7}
G2E3.AS1	9.74×10^{-2}	-3.36×10^{0}	7.75×10^{-4}	5.50×10^{-3}

ZIC1	9.95×10^{-2}	-3.33×10^{0}	2.28×10^{-4}	2.05×10^{-3}
AL450345.2	1.01×10^{-1}	-3.31×10^{0}	1.07×10^{-4}	1.11×10^{-3}
AC096759.2	1.01×10^{-1}	-3.31×10^{0}	4.10×10^{-5}	5.01×10^{-4}
TMPRSS11E	1.04×10^{-1}	-3.26×10^{0}	1.75×10^{-5}	2.48×10^{-4}
SFTPB	1.05×10^{-1}	-3.25×10^{0}	7.40×10^{-8}	2.50×10^{-6}

Table A.18 (continued). The list of the top 100 downregulated DEGs identified in the CS3 subtype using edgeR as a result of three clustering analyzes.

PHF2P2	1.07×10^{-1}	-3.23×10^{0}	1.55×10^{-6}	3.26×10^{-5}
CD300LG	1.07×10^{-1}	-3.23×10^{0}	8.66×10^{-8}	2.85×10^{-6}
H2BW1	1.07×10^{-1}	-3.22×10^{0}	4.09×10^{-3}	2.06×10^{-2}
RSPO4	1.07×10^{-1}	-3.22×10^{0}	5.49×10^{-10}	4.21×10^{-8}
AP3B2	1.07×10^{-1}	-3.22×10^{0}	6.68×10^{-12}	1.14×10^{-9}
KRT35	1.07×10^{-1}	-3.22×10^{0}	4.82×10^{-5}	5.73×10^{-4}
AL139327.1	1.08×10^{-1}	-3.21×10^{0}	2.52×10^{-3}	1.41×10^{-2}
CENPVL3	1.09×10^{-1}	-3.20×10^{0}	5.03×10^{-5}	5.93×10^{-4}
CACNG6	1.10×10^{-1}	-3.19×10^{0}	2.75×10^{-5}	3.62×10^{-4}
LINC02820	1.10×10^{-1}	-3.18×10^{0}	2.55×10^{-5}	3.39×10^{-4}
AL031686.1	1.11×10^{-1}	-3.17×10^{0}	5.28×10^{-8}	1.89×10^{-6}
AC106799.3	1.11×10^{-1}	-3.17×10^{0}	4.90×10^{-3}	2.37×10^{-2}
NKX2.1	1.14×10^{-1}	-3.13×10^{0}	1.26×10^{-3}	8.12×10^{-3}
EMX2OS	1.15×10^{-1}	-3.12×10^{0}	2.82×10^{-9}	1.65×10^{-7}
KRT38	1.17×10^{-1}	-3.10×10^{0}	7.09×10^{-5}	7.89×10^{-4}
SAGE1	1.18×10^{0}	-3.08×10^{0}	1.82×10^{-3}	1.09×10^{-2}
SPANXB1	1.19×10^{0}	-3.07×10^{0}	1.23×10^{-2}	4.83×10^{-2}
AL391336.1	1.19×10^{0}	-3.07×10^{0}	5.11×10^{-3}	2.45×10^{-2}
HSPB6	1.20×10^{0}	-3.06×10^{0}	1.27×10^{-15}	8.29×10^{-13}
SLC18A3	1.20×10^{0}	-3.05×10^{0}	6.66×10^{-6}	1.10×10^{-4}
HTR2C	1.21×10^{0}	-3.05×10^{0}	1.18×10^{-2}	4.70×10^{-2}
GABRG3	1.21×10^{0}	-3.05×10^{0}	6.47×10^{-5}	7.32×10^{-4}
CDH12	1.23×10^{0}	-3.03×10^{0}	6.73×10^{-4}	4.90×10^{-3}
AL591501.1	1.23×10^{0}	-3.02×10^{0}	1.83×10^{-5}	2.58×10^{-4}
TUBA3C	1.24×10^{0}	-3.01×10^{0}	2.58×10^{-3}	1.44×10^{-2}
TGM6	1.24×10^{0}	-3.01×10^{0}	5.78×10^{-3}	2.69×10^{-2}
MTATP8P2	1.25×10^{0}	-3.00×10^{0}	1.52×10^{-7}	4.57×10^{-6}
AL162511.1	1.26×10^{0}	-2.98×10^{0}	6.12×10^{-5}	6.99×10^{-4}
CSAG3	1.26×10^{0}	-2.98×10^{0}	3.93×10^{-3}	1.99×10^{-2}
IRX6	1.26×10^{0}	-2.98×10^{0}	4.42×10^{-6}	7.73×10^{-5}
LINC01193	1.29×10^{0}	-2.95×10^{0}	2.74×10^{-3}	1.51×10^{-2}
AL117329.1	1.30×10^{0}	-2.95×10^{0}	6.58×10^{-6}	1.08×10^{-4}
AC108865.2	1.31×10^{0}	-2.93×10^{0}	4.56×10^{-5}	5.47×10^{-4}
LMX1A	1.31×10^{0}	-2.93×10^{0}	8.67×10^{-7}	2.00×10^{-5}
RPTN	1.34×10^{0}	-2.90×10^{0}	5.88×10^{-3}	2.73×10^{-2}
LINC01726	1.37×10^{0}	-2.87×10^{0}	5.69×10^{-4}	4.29×10^{-3}
CR392039.3	1.39×10^{0}	-2.84×10^{0}	6.41×10^{-3}	2.92×10^{-2}

ALX1	1.39×10^{0}	-2.84×10^{0}	1.99×10^{-4}	1.84×10^{-3}
MUC15	1.40×10^{0}	-2.84×10^{0}	9.43×10^{-4}	6.45×10^{-3}
SLC7A10	1.40×10^{0}	-2.84×10^{0}	6.27×10^{-9}	3.23×10^{-7}
PDYN	1.40×10^{0}	-2.84×10^{0}	8.54×10^{-3}	3.65×10^{-2}

Table A.18 (continued). The list of the top 100 downregulated DEGs identified in the CS3 subtype using edgeR as a result of three clustering analyzes.

AC010970.1	1.40×10^{0}	-2.84×10^{0}	7.12×10^{-5}	7.92×10^{-4}
WASF3	1.41×10^{0}	-2.82×10^{0}	4.26×10^{-20}	8.70×10^{-17}
AC012213.1	1.42×10^{0}	-2.81×10^{0}	1.15×10^{-2}	4.58×10^{-2}
FP325330.2	1.43×10^{0}	-2.81×10^{0}	2.48×10^{-3}	1.39×10^{-2}

Table A.19. The list of the top 100 upregulated DEGs identified in the CS1 subtype using DESeq2 as a result of three clustering analyzes.

	fc	**log2fc**	**pvalue**	**padj**
WIF1	4.37×10^{1}	5.45×10^{0}	2.86×10^{-49}	3.92×10^{-46}
PTF1A	2.66×10^{1}	4.74×10^{0}	3.00×10^{-23}	1.12×10^{-21}
PRSS56	2.25×10^{1}	4.49×10^{0}	5.39×10^{-26}	3.01×10^{-24}
IGF2	2.18×10^{1}	4.45×10^{0}	7.08×10^{-36}	1.78×10^{-33}
LY6G6D	1.59×10^{1}	3.99×10^{0}	3.99×10^{-38}	1.36×10^{-35}
AC026774.1	1.20×10^{1}	3.58×10^{0}	2.42×10^{-20}	5.74×10^{-19}
KRT35	1.13×10^{1}	3.50×10^{0}	2.73×10^{-13}	2.47×10^{-12}
AL356433.1	1.12×10^{1}	3.48×10^{0}	2.45×10^{-16}	3.33×10^{-15}
LY6G6F.LY6G6D	1.10×10^{1}	3.46×10^{0}	2.77×10^{-27}	1.92×10^{-25}
NOTUM	1.09×10^{1}	3.44×10^{0}	1.60×10^{-34}	3.21×10^{-32}
AC114291.1	1.07×10^{1}	3.41×10^{0}	2.09×10^{-40}	9.46×10^{-38}
GOLGA6L2	1.05×10^{1}	3.39×10^{0}	1.10×10^{-21}	3.22×10^{-20}
LCN15	9.89×10^{0}	3.31×10^{0}	8.16×10^{-20}	1.78×10^{-18}
CDH9	9.56×10^{0}	3.26×10^{0}	9.52×10^{-6}	3.00×10^{-5}
MAGEA4.AS1	9.44×10^{0}	3.24×10^{0}	3.37×10^{-5}	9.73×10^{-5}
BHLHA9	9.24×10^{0}	3.21×10^{0}	1.46×10^{-20}	3.60×10^{-19}
AC026336.3	9.16×10^{0}	3.20×10^{0}	6.82×10^{-23}	2.43×10^{-21}
HSPB3	8.92×10^{0}	3.16×10^{0}	3.25×10^{-21}	8.87×10^{-20}
CPN1	8.47×10^{0}	3.08×10^{0}	1.69×10^{-21}	4.83×10^{-20}
SULT2A1	8.31×10^{0}	3.05×10^{0}	8.20×10^{-20}	1.79×10^{-18}
KRT43P	8.01×10^{0}	3.00×10^{0}	2.36×10^{-11}	1.64×10^{-10}
LINC02864	7.99×10^{0}	2.99×10^{0}	7.15×10^{-10}	4.05×10^{-9}
PCSK1N	7.85×10^{0}	2.97×10^{0}	7.66×10^{-23}	2.71×10^{-21}
AC078993.1	7.67×10^{0}	2.94×10^{0}	2.95×10^{-21}	8.15×10^{-20}
MAGEB17	7.67×10^{0}	2.94×10^{0}	1.02×10^{-17}	1.67×10^{-16}
KRT40	7.64×10^{0}	2.93×10^{0}	7.16×10^{-19}	1.38×10^{-17}
LGALS14	7.59×10^{0}	2.92×10^{0}	1.63×10^{-10}	1.01×10^{-9}
BX510359.5	7.29×10^{0}	2.87×10^{0}	2.05×10^{-10}	1.25×10^{-9}

SERPINA10	7.20×10^{0}	2.85×10^{0}	7.01×10^{-25}	3.38×10^{-23}
KRT32	7.18×10^{0}	2.84×10^{0}	2.96×10^{-11}	2.03×10^{-10}
MAGEA11	7.17×10^{0}	2.84×10^{0}	2.46×10^{-7}	9.82×10^{-7}

Table A.19 (continued). The list of the top 100 upregulated DEGs identified in the CS1 subtype using DESeq2 as a result of three clustering analyzes.

NPTX2	7.10×10^{0}	2.83×10^{0}	8.08×10^{-30}	8.49×10^{-28}
TUBAP13	7.06×10^{0}	2.82×10^{0}	7.48×10^{-18}	1.26×10^{-16}
CLDN10	6.96×10^{0}	2.80×10^{0}	6.59×10^{-16}	8.48×10^{-15}
SLC14A1	6.91×10^{0}	2.79×10^{0}	1.79×10^{-23}	6.92×10^{-22}
TMEM252	6.76×10^{0}	2.76×10^{0}	5.01×10^{-24}	2.13×10^{-22}
TNNC2	6.68×10^{0}	2.74×10^{0}	5.60×10^{-48}	6.83×10^{-45}
PRR9	6.61×10^{0}	2.73×10^{0}	3.88×10^{-9}	1.99×10^{-8}
KRT41P	6.55×10^{0}	2.71×10^{0}	5.20×10^{-12}	3.95×10^{-11}
DLX3	6.52×10^{0}	2.70×10^{0}	1.40×10^{-19}	2.97×10^{-18}
SLC30A2	6.29×10^{0}	2.65×10^{0}	3.05×10^{-26}	1.77×10^{-24}
C6orf15	6.26×10^{0}	2.65×10^{0}	5.48×10^{-17}	8.19×10^{-16}
KRT37	6.13×10^{0}	2.62×10^{0}	6.14×10^{-13}	5.29×10^{-12}
LINC02525	6.09×10^{0}	2.61×10^{0}	2.16×10^{-11}	1.51×10^{-10}
VWA5B1	5.99×10^{0}	2.58×10^{0}	4.39×10^{-13}	3.86×10^{-12}
AC108865.2	5.89×10^{0}	2.56×10^{0}	2.26×10^{-9}	1.20×10^{-8}
AL391650.2	5.88×10^{0}	2.56×10^{0}	2.16×10^{-11}	1.51×10^{-10}
MAGEA4	5.82×10^{0}	2.54×10^{0}	5.15×10^{-4}	1.22×10^{-3}
MIR483	5.71×10^{0}	2.51×10^{0}	8.61×10^{-4}	1.96×10^{-3}
NEUROD1	5.66×10^{0}	2.50×10^{0}	1.02×10^{-8}	4.90×10^{-8}
SERPINA7	5.64×10^{0}	2.50×10^{0}	3.22×10^{-13}	2.88×10^{-12}
AC091304.1	5.59×10^{0}	2.48×10^{0}	4.49×10^{-7}	1.73×10^{-6}
AC135388.1	5.57×10^{0}	2.48×10^{0}	1.78×10^{-18}	3.26×10^{-17}
PAGE1	5.55×10^{0}	2.47×10^{0}	2.61×10^{-3}	5.43×10^{-3}
CELP	5.53×10^{0}	2.47×10^{0}	1.67×10^{-27}	1.19×10^{-25}
AP003774.2	5.49×10^{0}	2.46×10^{0}	6.40×10^{-37}	1.78×10^{-34}
AC109136.1	5.48×10^{0}	2.45×10^{0}	8.27×10^{-10}	4.64×10^{-9}
AC003958.2	5.43×10^{0}	2.44×10^{0}	1.82×10^{-11}	1.28×10^{-10}
AP000851.2	5.41×10^{0}	2.44×10^{0}	1.84×10^{-10}	1.13×10^{-9}
ELF5	5.39×10^{0}	2.43×10^{0}	1.36×10^{-10}	8.49×10^{-10}
MAP7D2	5.33×10^{0}	2.41×10^{0}	2.30×10^{-21}	6.45×10^{-20}
SYN3	5.33×10^{0}	2.41×10^{0}	1.26×10^{-27}	9.16×10^{-26}
AL121885.2	5.31×10^{0}	2.41×10^{0}	1.62×10^{-11}	1.16×10^{-10}
PPBP	5.27×10^{0}	2.40×10^{0}	2.18×10^{-13}	2.00×10^{-12}
FGF3	5.19×10^{0}	2.38×10^{0}	1.46×10^{-9}	7.91×10^{-9}
KRT23	5.17×10^{0}	2.37×10^{0}	2.06×10^{-23}	7.89×10^{-22}
PHYHIPL	5.17×10^{0}	2.37×10^{0}	6.79×10^{-16}	8.72×10^{-15}
INSL5	5.09×10^{0}	2.35×10^{0}	4.71×10^{-8}	2.07×10^{-7}
SHISA9	5.08×10^{0}	2.35×10^{0}	8.73×10^{-11}	5.60×10^{-10}
AC108865.1	5.07×10^{0}	2.34×10^{0}	2.79×10^{-9}	1.46×10^{-8}

SLC22A11	5.05×10^{0}	2.34×10^{0}	1.84×10^{-21}	5.24×10^{-20}
MC3R	5.03×10^{0}	2.33×10^{0}	7.77×10^{-9}	3.81×10^{-8}

Table A.19 (continued). The list of the top 100 upregulated DEGs identified in the CS1 subtype using DESeq2 as a result of three clustering analyzes.

AC091839.1	5.03×10^{0}	2.33×10^{0}	9.05×10^{-5}	2.44×10^{-4}
DRD2	5.00×10^{0}	2.32×10^{0}	1.51×10^{-20}	3.69×10^{-19}
SLC1A7	5.00×10^{0}	2.32×10^{0}	2.43×10^{-30}	2.76×10^{-28}
LINC00355	4.97×10^{0}	2.31×10^{0}	2.76×10^{-5}	8.11×10^{-5}
CTNNA2	4.95×10^{0}	2.31×10^{0}	1.60×10^{-13}	1.49×10^{-12}
KRT31	4.90×10^{0}	2.29×10^{0}	1.71×10^{-7}	6.96×10^{-7}
ATP12A	4.89×10^{0}	2.29×10^{0}	6.04×10^{-11}	3.97×10^{-10}
MAGEA6	4.79×10^{0}	2.26×10^{0}	2.18×10^{-3}	4.59×10^{-3}
LINC02128	4.76×10^{0}	2.25×10^{0}	4.77×10^{-10}	2.77×10^{-9}
VENTX	4.74×10^{0}	2.24×10^{0}	8.92×10^{-20}	1.94×10^{-18}
PKLR	4.73×10^{0}	2.24×10^{0}	1.81×10^{-17}	2.87×10^{-16}
SLC39A2	4.69×10^{0}	2.23×10^{0}	1.99×10^{-12}	1.60×10^{-11}
AC090809.1	4.67×10^{0}	2.22×10^{0}	1.64×10^{-5}	4.99×10^{-5}
ISM2	4.66×10^{0}	2.22×10^{0}	1.97×10^{-16}	2.71×10^{-15}
KRTAP13.2	4.66×10^{0}	2.22×10^{0}	1.73×10^{-4}	4.45×10^{-4}
AC004233.4	4.61×10^{0}	2.21×10^{0}	1.28×10^{-10}	8.07×10^{-10}
SLC38A3	4.61×10^{0}	2.21×10^{0}	1.00×10^{-16}	1.44×10^{-15}
RBP2	4.58×10^{0}	2.20×10^{0}	1.75×10^{-17}	2.78×10^{-16}
SERPINA6	4.58×10^{0}	2.20×10^{0}	1.33×10^{-15}	1.63×10^{-14}
UMODL1	4.56×10^{0}	2.19×10^{0}	5.28×10^{-29}	4.89×10^{-27}
ZP2	4.52×10^{0}	2.18×10^{0}	3.13×10^{-18}	5.54×10^{-17}
AC036111.1	4.48×10^{0}	2.16×10^{0}	2.98×10^{-3}	6.13×10^{-3}
TRIM54	4.47×10^{0}	2.16×10^{0}	5.93×10^{-14}	5.88×10^{-13}
AL035252.2	4.45×10^{0}	2.16×10^{0}	6.38×10^{-9}	3.16×10^{-8}
FOLR1	4.33×10^{0}	2.11×10^{0}	2.22×10^{-15}	2.66×10^{-14}
QPRT	4.33×10^{0}	2.11×10^{0}	5.31×10^{-43}	3.64×10^{-40}
LPO	4.32×10^{0}	2.11×10^{0}	1.26×10^{-15}	1.55×10^{-14}
CTNNA2.AS1	4.29×10^{0}	2.10×10^{0}	1.17×10^{-3}	2.60×10^{-3}

Table A.20. The list of the top 100 downregulated DEGs identified in the CS1 subtype using DESeq2 as a result of three clustering analyzes.

	fc	**log2fc**	**pvalue**	**padj**
RN7SKP227	3.14×10^{-4}	-1.16×10^{1}	3.98×10^{-9}	2.04×10^{-8}
CLDN18	5.71×10^{-3}	-7.45×10^{0}	1.09×10^{-114}	4.77×10^{-110}
AL139274.1	6.89×10^{-3}	-7.18×10^{0}	3.03×10^{-19}	6.16×10^{-18}
AL390318.1	1.10×10^{-2}	-6.51×10^{0}	2.25×10^{-6}	7.81×10^{-6}
AL139120.1	1.24×10^{-2}	-6.34×10^{0}	3.42×10^{-11}	2.32×10^{-10}
ANXA10	1.38×10^{-2}	-6.18×10^{0}	2.50×10^{-87}	5.50×10^{-83}
RN7SKP186	1.47×10^{-2}	-6.09×10^{0}	1.56×10^{-3}	3.37×10^{-3}

AC096741.1	1.47×10^{-2}	-6.09×10^{0}	3.92×10^{-14}	3.97×10^{-13}
LPP.AS1	1.52×10^{-2}	-6.04×10^{0}	1.01×10^{-8}	4.85×10^{-8}

Table A.20 (continued). The list of the top 100 downregulated DEGs identified in the CS1 subtype using DESeq2 as a result of three clustering analyzes.

RAD51AP1P1	1.60×10^{-2}	-5.97×10^{0}	2.25×10^{-9}	1.19×10^{-8}
AC010997.6	1.61×10^{-2}	-5.96×10^{0}	3.07×10^{-10}	1.82×10^{-9}
EIF4E2P1	1.77×10^{-2}	-5.82×10^{0}	2.06×10^{-8}	9.53×10^{-8}
EDDM3CP	1.83×10^{-2}	-5.77×10^{0}	5.67×10^{-5}	1.58×10^{-4}
AL606517.2	1.85×10^{-2}	-5.76×10^{0}	6.84×10^{-7}	2.56×10^{-6}
RNY3	1.85×10^{-2}	-5.76×10^{0}	5.36×10^{-5}	1.50×10^{-4}
AL136320.1	1.86×10^{-2}	-5.75×10^{0}	6.15×10^{-16}	7.95×10^{-15}
AC018398.2	1.87×10^{-2}	-5.74×10^{0}	8.54×10^{-15}	9.48×10^{-14}
METTL21AP1	1.88×10^{-2}	-5.74×10^{0}	5.68×10^{-11}	3.75×10^{-10}
AL589655.1	1.92×10^{-2}	-5.70×10^{0}	1.67×10^{-6}	5.90×10^{-6}
PIGFP2	1.93×10^{-2}	-5.69×10^{0}	1.57×10^{-6}	5.59×10^{-6}
AC055733.1	1.97×10^{-2}	-5.67×10^{0}	1.82×10^{-13}	1.68×10^{-12}
AC023813.2	1.98×10^{-2}	-5.66×10^{0}	4.05×10^{-13}	3.58×10^{-12}
RN7SL683P	1.99×10^{-2}	-5.65×10^{0}	1.09×10^{-8}	5.26×10^{-8}
Y_RNA.241	2.01×10^{-2}	-5.64×10^{0}	2.86×10^{-9}	1.49×10^{-8}
MUC6	2.03×10^{-2}	-5.62×10^{0}	6.18×10^{-65}	5.42×10^{-61}
AC105224.1	2.03×10^{-2}	-5.62×10^{0}	1.85×10^{-6}	6.48×10^{-6}
AC130895.1	2.06×10^{-2}	-5.60×10^{0}	1.41×10^{-12}	1.15×10^{-11}
RNU2.23P	2.08×10^{-2}	-5.59×10^{0}	4.94×10^{-6}	1.62×10^{-5}
MTCYBP32	2.11×10^{-2}	-5.56×10^{0}	2.28×10^{-7}	9.16×10^{-7}
Z93020.1	2.11×10^{-2}	-5.56×10^{0}	2.81×10^{-11}	1.93×10^{-10}
SNRPGP18	2.11×10^{-2}	-5.56×10^{0}	1.72×10^{-8}	8.04×10^{-8}
RN7SKP8	2.13×10^{-2}	-5.55×10^{0}	1.09×10^{-7}	4.57×10^{-7}
AC104332.1	2.19×10^{-2}	-5.51×10^{0}	1.33×10^{-17}	2.15×10^{-16}
X7SK.3	2.19×10^{-2}	-5.51×10^{0}	1.21×10^{-11}	8.73×10^{-11}
X7SK.1	2.20×10^{-2}	-5.51×10^{0}	7.61×10^{-7}	2.83×10^{-6}
AC100763.1	2.20×10^{-2}	-5.51×10^{0}	3.34×10^{-11}	2.28×10^{-10}
RNU2.61P	2.23×10^{-2}	-5.49×10^{0}	1.17×10^{-3}	2.59×10^{-3}
AC100800.1	2.25×10^{-2}	-5.47×10^{0}	1.23×10^{-10}	7.76×10^{-10}
CHCHD4P5	2.27×10^{-2}	-5.46×10^{0}	8.29×10^{-10}	4.66×10^{-9}
MTND4P32	2.27×10^{-2}	-5.46×10^{0}	4.14×10^{-11}	2.79×10^{-10}
AC092910.2	2.28×10^{-2}	-5.46×10^{0}	9.27×10^{-10}	5.16×10^{-9}
ADAD1P2	2.28×10^{-2}	-5.45×10^{0}	3.32×10^{-5}	9.60×10^{-5}
AC012555.2	2.29×10^{-2}	-5.45×10^{0}	7.03×10^{-15}	7.88×10^{-14}
RN7SL57P	2.29×10^{-2}	-5.45×10^{0}	2.35×10^{-18}	4.23×10^{-17}
Y_RNA.331	2.31×10^{-2}	-5.44×10^{0}	1.26×10^{-4}	3.31×10^{-4}
AL360178.2	2.37×10^{-2}	-5.40×10^{0}	7.48×10^{-8}	3.21×10^{-7}
AL391863.1	2.39×10^{-2}	-5.39×10^{0}	2.42×10^{-22}	7.86×10^{-21}

MTND2P2	2.41×10^{-2}	-5.37×10^{0}	5.88×10^{-8}	2.56×10^{-7}
AC125612.1	2.42×10^{-2}	-5.37×10^{0}	5.12×10^{-11}	3.40×10^{-10}

Table A.20 (continued). The list of the top 100 downregulated DEGs identified in the CS1 subtype using DESeq2 as a result of three clustering analyzes.

AC097639.2	2.43×10^{-2}	-5.36×10^{0}	1.86×10^{-10}	1.14×10^{-9}
RN7SKP48	2.43×10^{-2}	-5.36×10^{0}	4.62×10^{-4}	1.10×10^{-3}
ZNF75BP	2.44×10^{-2}	-5.36×10^{0}	4.87×10^{-7}	1.87×10^{-6}
AC022022.2	2.44×10^{-2}	-5.36×10^{0}	7.58×10^{-7}	2.82×10^{-6}
MTND1P32	2.46×10^{-2}	-5.34×10^{0}	8.31×10^{-10}	4.67×10^{-9}
AC022537.1	2.50×10^{-2}	-5.32×10^{0}	3.34×10^{-5}	9.66×10^{-5}
AC009951.5	2.51×10^{-2}	-5.32×10^{0}	2.70×10^{-10}	1.62×10^{-9}
RN7SL116P	2.52×10^{-2}	-5.31×10^{0}	1.02×10^{-16}	1.47×10^{-15}
Y_RNA.341	2.53×10^{-2}	-5.31×10^{0}	3.15×10^{-13}	2.82×10^{-12}
RNU2.59P	2.57×10^{-2}	-5.28×10^{0}	1.35×10^{-7}	5.60×10^{-7}
AC003989.1	2.57×10^{-2}	-5.28×10^{0}	2.72×10^{-14}	2.82×10^{-13}
RNVU1.2A	2.58×10^{-2}	-5.28×10^{0}	2.17×10^{-6}	7.54×10^{-6}
FOXN3.AS2	2.59×10^{-2}	-5.27×10^{0}	1.01×10^{-8}	4.88×10^{-8}
AP004289.2	2.62×10^{-2}	-5.25×10^{0}	1.35×10^{-9}	7.35×10^{-9}
RPAP2P1	2.66×10^{-2}	-5.23×10^{0}	1.10×10^{-17}	1.79×10^{-16}
RNVU1.18	2.66×10^{-2}	-5.23×10^{0}	3.75×10^{-6}	1.26×10^{-5}
AC008833.1	2.67×10^{-2}	-5.23×10^{0}	1.18×10^{-5}	3.66×10^{-5}
MIR3140	2.69×10^{-2}	-5.22×10^{0}	3.70×10^{-5}	1.06×10^{-4}
Y_RNA.326	2.71×10^{-2}	-5.21×10^{0}	3.45×10^{-6}	1.16×10^{-5}
RPL17P17	2.74×10^{-2}	-5.19×10^{0}	1.70×10^{-11}	1.21×10^{-10}
RN7SL38P	2.76×10^{-2}	-5.18×10^{0}	1.40×10^{-5}	4.32×10^{-5}
AL356057.1	2.77×10^{-2}	-5.18×10^{0}	4.88×10^{-9}	2.46×10^{-8}
KCTD9P5	2.77×10^{-2}	-5.17×10^{0}	6.85×10^{-10}	3.89×10^{-9}
PSAPL1	2.80×10^{-2}	-5.16×10^{0}	1.19×10^{-40}	5.63×10^{-38}
AC004865.1	2.82×10^{-2}	-5.15×10^{0}	3.23×10^{-13}	2.88×10^{-12}
RNU6.681P	2.82×10^{-2}	-5.15×10^{0}	9.82×10^{-6}	3.09×10^{-5}
AL391097.1	2.85×10^{-2}	-5.13×10^{0}	2.04×10^{-7}	8.22×10^{-7}
ZBTB8OSP1	2.87×10^{-2}	-5.12×10^{0}	6.85×10^{-15}	7.68×10^{-14}
AC005104.2	2.89×10^{-2}	-5.11×10^{0}	9.21×10^{-23}	3.20×10^{-21}
AC124069.1	2.89×10^{-2}	-5.11×10^{0}	2.86×10^{-24}	1.27×10^{-22}
AC069079.1	2.90×10^{-2}	-5.11×10^{0}	5.67×10^{-7}	2.15×10^{-6}
AC005920.2	2.90×10^{-2}	-5.11×10^{0}	6.26×10^{-17}	9.25×10^{-16}
SND1.IT1	2.92×10^{-2}	-5.10×10^{0}	2.77×10^{-29}	2.70×10^{-27}
AL354794.1	2.94×10^{-2}	-5.09×10^{0}	2.90×10^{-10}	1.73×10^{-9}
AC010359.1	2.95×10^{-2}	-5.08×10^{0}	1.13×10^{-5}	3.53×10^{-5}
AL355531.1	2.96×10^{-2}	-5.08×10^{0}	2.14×10^{-16}	2.93×10^{-15}
AC009303.3	2.96×10^{-2}	-5.08×10^{0}	3.13×10^{-14}	3.22×10^{-13}
AL118556.2	2.96×10^{-2}	-5.08×10^{0}	2.36×10^{-8}	1.08×10^{-7}
AC009509.3	2.97×10^{-2}	-5.07×10^{0}	2.67×10^{-8}	1.22×10^{-7}
AC079316.2	2.98×10^{-2}	-5.07×10^{0}	7.32×10^{-10}	4.14×10^{-9}

AL357054.1	3.01×10^{-2}	-5.05×10^{0}	4.92×10^{-11}	3.27×10^{-10}

Table A.20 (continued). The list of the top 100 downregulated DEGs identified in the CS1 subtype using DESeq2 as a result of three clustering analyzes.

AC092139.1	3.04×10^{-2}	-5.04×10^{0}	2.67×10^{-18}	4.77×10^{-17}
RNU7.80P	3.05×10^{-2}	-5.04×10^{0}	5.48×10^{-5}	1.53×10^{-4}
RNU6.268P	3.05×10^{-2}	-5.03×10^{0}	1.12×10^{-5}	3.50×10^{-5}
USP12P2	3.06×10^{-2}	-5.03×10^{0}	1.31×10^{-9}	7.15×10^{-9}
H4C13	3.07×10^{-2}	-5.03×10^{0}	5.96×10^{-26}	3.33×10^{-24}
RNY4	3.07×10^{-2}	-5.02×10^{0}	7.20×10^{-4}	1.66×10^{-3}
AC099845.1	3.08×10^{-2}	-5.02×10^{0}	1.53×10^{-32}	2.42×10^{-30}
RNU6.251P	3.11×10^{-2}	-5.01×10^{0}	1.28×10^{-8}	6.12×10^{-8}
ATG10.AS1	3.11×10^{-2}	-5.01×10^{0}	3.52×10^{-4}	8.57×10^{-4}
AC055733.3	3.12×10^{-2}	-5.00×10^{0}	1.01×10^{-11}	7.38×10^{-11}

Table A.21. The list of the top 100 upregulated DEGs identified in the CS2 subtype using DESeq2 as a result of three clustering analyzes.

	fc	**log2fc**	**pvalue**	**padj**
RNU1.88P	8.61×10^{2}	9.75×10^{0}	6.85×10^{-29}	2.01×10^{-27}
RN7SKP203	6.76×10^{2}	9.40×10^{0}	6.26×10^{-27}	1.50×10^{-25}
RNU2.59P	5.33×10^{2}	9.06×10^{0}	3.20×10^{-17}	2.98×10^{-16}
RNU2.23P	5.12×10^{2}	9.00×10^{0}	2.22×10^{-12}	1.28×10^{-11}
MTND5P26	4.88×10^{2}	8.93×10^{0}	1.03×10^{-14}	7.51×10^{-14}
RNY3	4.50×10^{2}	8.81×10^{0}	4.92×10^{-10}	2.23×10^{-9}
MTCYBP32	4.28×10^{2}	8.74×10^{0}	2.14×10^{-14}	1.51×10^{-13}
AC022537.1	4.16×10^{2}	8.70×10^{0}	4.55×10^{-11}	2.30×10^{-10}
RN7SKP255	3.82×10^{2}	8.58×10^{0}	3.27×10^{-22}	4.93×10^{-21}
RNVU1.2A	3.69×10^{2}	8.53×10^{0}	4.01×10^{-13}	2.49×10^{-12}
AC010997.6	3.27×10^{2}	8.35×10^{0}	4.50×10^{-17}	4.12×10^{-16}
ZNF75BP	3.14×10^{2}	8.29×10^{0}	3.73×10^{-14}	2.57×10^{-13}
RN7SKP186	3.08×10^{2}	8.27×10^{0}	2.70×10^{-5}	7.16×10^{-5}
RNVU1.2	3.06×10^{2}	8.26×10^{0}	1.01×10^{-22}	1.60×10^{-21}
AC100800.1	2.92×10^{2}	8.19×10^{0}	8.70×10^{-19}	9.42×10^{-18}
AC090220.1	2.71×10^{2}	8.08×10^{0}	5.06×10^{-24}	9.08×10^{-23}
SCARNA5	2.70×10^{2}	8.08×10^{0}	8.01×10^{-109}	1.94×10^{-104}
RNU5A.1	2.66×10^{2}	8.05×10^{0}	2.44×10^{-32}	1.00×10^{-30}
AL391863.2	2.57×10^{2}	8.00×10^{0}	1.87×10^{-31}	7.07×10^{-30}
AL360178.2	2.54×10^{2}	7.99×10^{0}	2.97×10^{-14}	2.06×10^{-13}
SCARNA1	2.50×10^{2}	7.97×10^{0}	2.80×10^{-54}	1.06×10^{-51}
Y_RNA.241	2.43×10^{2}	7.93×10^{0}	6.21×10^{-15}	4.62×10^{-14}
RNU1.11P	2.40×10^{2}	7.91×10^{0}	6.62×10^{-12}	3.64×10^{-11}
RNU6.82P	2.39×10^{2}	7.90×10^{0}	2.86×10^{-16}	2.41×10^{-15}
AL157402.2	2.34×10^{2}	7.87×10^{0}	1.35×10^{-19}	1.58×10^{-18}
SNORA49	2.25×10^{2}	7.81×10^{0}	3.84×10^{-61}	2.55×10^{-58}

Table A.21 (continued). The list of the top 100 upregulated DEGs identified in the CS2 subtype using DESeq2 as a result of three clustering analyzes.

CACNA1C.AS4	2.16×10^{2}	7.75×10^{0}	7.98×10^{-28}	2.10×10^{-26}
AC241520.1	2.08×10^{2}	7.70×10^{0}	1.06×10^{-28}	3.02×10^{-27}
AC079316.2	2.01×10^{2}	7.65×10^{0}	2.57×10^{-18}	2.65×10^{-17}
RSU1P3	1.98×10^{2}	7.63×10^{0}	1.02×10^{-18}	1.09×10^{-17}
RNU4.2	1.94×10^{2}	7.60×10^{0}	2.80×10^{-61}	1.91×10^{-58}
AC027279.4	1.83×10^{2}	7.52×10^{0}	6.16×10^{-19}	6.76×10^{-18}
AP003086.3	1.78×10^{2}	7.48×10^{0}	2.69×10^{-33}	1.22×10^{-31}
Y_RNA.720	1.76×10^{2}	7.46×10^{0}	1.96×10^{-11}	1.03×10^{-10}
AC133106.1	1.73×10^{2}	7.44×10^{0}	2.25×10^{-20}	2.83×10^{-19}
AC120349.2	1.63×10^{2}	7.35×10^{0}	1.93×10^{-10}	9.13×10^{-10}
MTND1P11	1.62×10^{2}	7.34×10^{0}	4.31×10^{-24}	7.78×10^{-23}
RAD17P2	1.62×10^{2}	7.34×10^{0}	1.28×10^{-30}	4.41×10^{-29}
AL139274.1	1.58×10^{2}	7.31×10^{0}	7.19×10^{-16}	5.82×10^{-15}
CELF2.AS2	1.53×10^{2}	7.26×10^{0}	2.14×10^{-37}	1.47×10^{-35}
RN7SKP8	1.53×10^{2}	7.26×10^{0}	1.70×10^{-10}	8.08×10^{-10}
AC069549.2	1.53×10^{2}	7.26×10^{0}	4.67×10^{-33}	2.07×10^{-31}
RAD51AP1P1	1.51×10^{2}	7.24×10^{0}	2.40×10^{-11}	1.25×10^{-10}
Z93020.1	1.49×10^{2}	7.22×10^{0}	1.90×10^{-14}	1.35×10^{-13}
SNORA23	1.49×10^{2}	7.22×10^{0}	1.95×10^{-90}	1.35×10^{-86}
MTND1P32	1.48×10^{2}	7.21×10^{0}	1.02×10^{-13}	6.73×10^{-13}
RNU5D.1	1.44×10^{2}	7.18×10^{0}	4.75×10^{-37}	3.16×10^{-35}
LPP.AS1	1.44×10^{2}	7.17×10^{0}	3.72×10^{-10}	1.71×10^{-9}
IFNK	1.43×10^{2}	7.16×10^{0}	4.66×10^{-18}	4.68×10^{-17}
AC130895.1	1.42×10^{2}	7.15×10^{0}	1.50×10^{-15}	1.18×10^{-14}
AL589655.1	1.42×10^{2}	7.15×10^{0}	4.90×10^{-9}	2.00×10^{-8}
UHRF2P1	1.41×10^{2}	7.14×10^{0}	6.25×10^{-52}	1.79×10^{-49}
BIRC6.AS1	1.38×10^{2}	7.11×10^{0}	1.34×10^{-21}	1.89×10^{-20}
AC009951.5	1.37×10^{2}	7.09×10^{0}	7.41×10^{-16}	5.99×10^{-15}
AC110769.3	1.36×10^{2}	7.09×10^{0}	4.01×10^{-41}	3.98×10^{-39}
BMP2KL	1.36×10^{2}	7.09×10^{0}	1.63×10^{-18}	1.71×10^{-17}
AC087286.1	1.35×10^{2}	7.07×10^{0}	1.50×10^{-16}	1.30×10^{-15}
AL390318.1	1.33×10^{2}	7.06×10^{0}	4.11×10^{-6}	1.21×10^{-5}
AC125612.1	1.32×10^{2}	7.05×10^{0}	4.02×10^{-15}	3.04×10^{-14}
EIF4E2P1	1.32×10^{2}	7.05×10^{0}	7.37×10^{-10}	3.29×10^{-9}
RNVU1.31	1.29×10^{2}	7.01×10^{0}	3.56×10^{-57}	1.67×10^{-54}
AC013410.1	1.28×10^{2}	7.00×10^{0}	1.02×10^{-27}	2.66×10^{-26}
AL606517.2	1.28×10^{2}	7.00×10^{0}	9.96×10^{-9}	3.93×10^{-8}
RLIMP1	1.27×10^{2}	6.99×10^{0}	5.42×10^{-43}	6.54×10^{-41}
SNRPGP18	1.26×10^{2}	6.98×10^{0}	6.77×10^{-11}	3.35×10^{-10}
AC009951.4	1.25×10^{2}	6.96×10^{0}	3.52×10^{-53}	1.16×10^{-50}

Table A.21 (continued). The list of the top 100 upregulated DEGs identified in the CS2 subtype using DESeq2 as a result of three clustering analyzes.

RNY1	1.23×10^{2}	6.94×10^{0}	2.11×10^{-17}	1.99×10^{-16}
RN7SKP227	1.23×10^{2}	6.94×10^{0}	9.30×10^{-4}	2.01×10^{-3}
AC069431.2	1.23×10^{2}	6.94×10^{0}	2.04×10^{-33}	9.37×10^{-32}
AC010480.1	1.22×10^{2}	6.94×10^{0}	1.52×10^{-29}	4.77×10^{-28}
AL356057.1	1.22×10^{12}	6.93×10^{0}	2.51×10^{-11}	1.30×10^{-10}
AC114802.1	1.20×10^{12}	6.91×10^{0}	3.48×10^{-17}	3.22×10^{-16}
MTND2P2	1.19×10^{12}	6.90×10^{0}	1.38×10^{-10}	6.63×10^{-10}
MTCYBP3	1.19×10^{12}	6.89×10^{0}	5.51×10^{-32}	2.20×10^{-30}
MTND4P14	1.19×10^{12}	6.89×10^{0}	9.06×10^{-40}	7.75×10^{-38}
AL158195.1	1.18×10^{12}	6.89×10^{0}	9.44×10^{-29}	2.72×10^{-27}
AL138713.1	1.16×10^{12}	6.86×10^{0}	1.79×10^{-17}	1.70×10^{-16}
AC022022.2	1.15×10^{12}	6.84×10^{0}	3.38×10^{-9}	1.41×10^{-8}
AC026124.1	1.13×10^{12}	6.82×10^{0}	2.66×10^{-27}	6.64×10^{-26}
DOCK4.AS1	1.11×10^{12}	6.79×10^{0}	1.49×10^{-30}	5.13×10^{-29}
AC107050.1	1.10×10^{12}	6.79×10^{0}	3.69×10^{-49}	8.33×10^{-47}
AC005920.2	1.10×10^{12}	6.79×10^{0}	6.50×10^{-26}	1.41×10^{-24}
AL035693.1	1.10×10^{12}	6.78×10^{0}	9.38×10^{-26}	2.00×10^{-24}
AC069228.1	1.10×10^{12}	6.78×10^{0}	4.21×10^{-25}	8.41×10^{-24}
AC100763.1	1.10×10^{12}	6.78×10^{0}	7.31×10^{-13}	4.43×10^{-12}
AC022133.2	1.09×10^{12}	6.76×10^{0}	5.66×10^{-41}	5.56×10^{-39}
DIAPH1.AS1	1.08×10^{12}	6.76×10^{0}	9.40×10^{-34}	4.44×10^{-32}
SNORA73B	1.06×10^{12}	6.72×10^{0}	1.24×10^{-125}	5.99×10^{-121}
AL445223.1	1.06×10^{12}	6.72×10^{0}	5.84×10^{-26}	1.27×10^{-24}
AL136320.1	1.05×10^{12}	6.71×10^{0}	1.73×10^{-16}	1.49×10^{-15}
AP000919.2	1.05×10^{12}	6.71×10^{0}	8.14×10^{-35}	4.31×10^{-33}
RNA5SP33	1.04×10^{12}	6.70×10^{0}	1.72×10^{-15}	1.34×10^{-14}
H3C2	1.03×10^{12}	6.69×10^{0}	1.15×10^{-102}	1.39×10^{-98}
MTND4P32	1.03×10^{12}	6.68×10^{0}	2.64×10^{-12}	1.51×10^{-11}
ZBTB20.AS5	1.01×10^{12}	6.67×10^{0}	8.71×10^{-17}	7.73×10^{-16}
PIGFP2	1.01×10^{12}	6.66×10^{0}	2.10×10^{-7}	7.15×10^{-7}
PPP1R9A.AS1	9.99×10^{11}	6.64×10^{0}	3.37×10^{-25}	6.80×10^{-24}
AL139120.1	9.91×10^{11}	6.63×10^{0}	1.54×10^{-9}	6.63×10^{-9}
AL606517.1	9.76×10^{11}	6.61×10^{0}	9.00×10^{-12}	4.89×10^{-11}
AL731559.1	9.66×10^{11}	6.59×10^{0}	7.58×10^{-69}	1.02×10^{-65}

Table A.22. The list of the top 100 downregulated DEGs identified in the CS2 subtype using DESeq2 as a result of three clustering analyzes.

	fc	**log2fc**	**pvalue**	**padj**
AC079804.2	5.63×10^{-2}	-4.15×10^{0}	1.16×10^{-11}	6.21×10^{-11}
RPL35P2	7.11×10^{-2}	-3.81×10^{0}	7.37×10^{-9}	2.95×10^{-8}

Table A.22 (continued). The list of the top 100 downregulated DEGs identified in the CS2 subtype using DESeq2 as a result of three clustering analyzes.

FP236383.5	7.41×10^{-2}	-3.75×10^{0}	1.68×10^{-2}	2.95×10^{-2}
SRIP3	1.06×10^{-1}	-3.24×10^{0}	1.69×10^{-5}	4.60×10^{-5}
RPL35AP21	1.23×10^{-1}	-3.02×10^{0}	1.85×10^{-8}	7.11×10^{-8}
MAGEB2	1.27×10^{-1}	-2.98×10^{0}	8.49×10^{-4}	1.84×10^{-3}
MIF	1.36×10^{-1}	-2.87×10^{0}	6.74×10^{-7}	2.17×10^{-6}
BOLA2P1	1.53×10^{-1}	-2.71×10^{0}	1.01×10^{-4}	2.49×10^{-4}
CNN2P4	1.55×10^{-1}	-2.69×10^{0}	6.52×10^{-5}	1.65×10^{-4}
RETNLB	1.61×10^{-1}	-2.64×10^{0}	9.12×10^{-17}	8.08×10^{-16}
DEFA6	1.70×10^{-1}	-2.56×10^{0}	1.35×10^{-9}	5.84×10^{-9}
DEFA5	1.70×10^{-1}	-2.56×10^{0}	4.94×10^{-9}	2.02×10^{-8}
EIF3IP1	1.74×10^{-1}	-2.52×10^{0}	2.16×10^{-6}	6.57×10^{-6}
AL138785.1	1.75×10^{-1}	-2.52×10^{0}	6.82×10^{-15}	5.06×10^{-14}
RPL35AP34	1.76×10^{-1}	-2.51×10^{0}	7.98×10^{-5}	1.99×10^{-4}
GGT4P	1.77×10^{-1}	-2.50×10^{0}	1.79×10^{-16}	1.53×10^{-15}
OR7E121P	1.81×10^{-1}	-2.47×10^{0}	2.25×10^{-6}	6.83×10^{-6}
EIF3KP3	1.81×10^{-1}	-2.46×10^{0}	8.16×10^{-3}	1.52×10^{-2}
MT.TY	1.88×10^{-1}	-2.41×10^{0}	1.19×10^{-12}	7.04×10^{-12}
AC008026.2	1.89×10^{-1}	-2.40×10^{0}	6.66×10^{-8}	2.40×10^{-7}
AC095059.2	1.89×10^{-1}	-2.40×10^{0}	6.72×10^{-7}	2.16×10^{-6}
RAB5IF	1.92×10^{-1}	-2.38×10^{0}	5.00×10^{-22}	7.42×10^{-21}
AC091179.1	1.92×10^{-1}	-2.38×10^{0}	6.48×10^{-5}	1.64×10^{-4}
LYPD8	1.93×10^{-1}	-2.38×10^{0}	8.53×10^{-15}	6.26×10^{-14}
AC106806.1	1.95×10^{-1}	-2.35×10^{0}	2.32×10^{-7}	7.86×10^{-7}
SLC5A8	1.98×10^{-1}	-2.34×10^{0}	3.64×10^{-5}	9.50×10^{-5}
AC005307.1	1.99×10^{-1}	-2.33×10^{0}	1.93×10^{-8}	7.40×10^{-8}
AC021074.1	2.01×10^{-1}	-2.31×10^{0}	8.64×10^{-16}	6.95×10^{-15}
AC074085.2	2.04×10^{-1}	-2.29×10^{0}	3.81×10^{-11}	1.94×10^{-10}
GS1.594A7.3	2.06×10^{-1}	-2.28×10^{0}	2.10×10^{-5}	5.64×10^{-5}
SLC25A6P2	2.06×10^{-1}	-2.28×10^{0}	9.23×10^{-10}	4.08×10^{-9}
CLEC2A	2.06×10^{-1}	-2.28×10^{0}	7.11×10^{-3}	1.34×10^{-2}
AC108725.1	2.08×10^{-1}	-2.26×10^{0}	7.54×10^{-6}	2.14×10^{-5}
AL049830.1	2.10×10^{-1}	-2.25×10^{0}	9.16×10^{-8}	3.25×10^{-7}
UPK3A	2.10×10^{-1}	-2.25×10^{0}	1.48×10^{-15}	1.16×10^{-14}
RPL38P6	2.12×10^{-1}	-2.24×10^{0}	8.64×10^{-4}	1.87×10^{-3}
CYP4F2	2.13×10^{-1}	-2.23×10^{0}	3.66×10^{-17}	3.38×10^{-16}
AC036111.1	2.13×10^{-1}	-2.23×10^{0}	1.34×10^{-2}	2.40×10^{-2}
ZG16	2.13×10^{-1}	-2.23×10^{0}	2.19×10^{-8}	8.34×10^{-8}
URAD	2.14×10^{-1}	-2.23×10^{0}	1.42×10^{-10}	6.80×10^{-10}
MYL6P3	2.17×10^{-1}	-2.21×10^{0}	2.06×10^{-6}	6.28×10^{-6}
ALDOAP2	2.18×10^{-1}	-2.19×10^{0}	1.30×10^{-8}	5.08×10^{-8}
C17orf77	2.19×10^{-1}	-2.19×10^{0}	3.58×10^{-9}	1.49×10^{-8}

Table A.22 (continued). The list of the top 100 downregulated DEGs identified in the CS2 subtype using DESeq2 as a result of three clustering analyzes.

KRTCAP2P1	2.20×10^{-1}	-2.18×10^{0}	1.60×10^{-6}	4.95×10^{-6}
RPL37AP8	2.21×10^{-1}	-2.18×10^{0}	1.24×10^{-7}	4.34×10^{-7}
SELENOWP1	2.22×10^{-1}	-2.17×10^{0}	1.15×10^{-4}	2.81×10^{-4}
RPS5P8	2.24×10^{-1}	-2.16×10^{0}	3.23×10^{-7}	1.08×10^{-6}
RPL30P4	2.24×10^{-1}	-2.16×10^{0}	2.71×10^{-10}	1.26×10^{-9}
KRT8P36	2.26×10^{-1}	-2.15×10^{0}	1.06×10^{-11}	5.71×10^{-11}
AL161636.2	2.30×10^{-1}	-2.12×10^{0}	3.22×10^{-9}	1.34×10^{-8}
AC104823.1	2.32×10^{-1}	-2.11×10^{0}	3.40×10^{-9}	1.41×10^{-8}
AC018695.1	2.32×10^{-1}	-2.11×10^{0}	2.75×10^{-6}	8.27×10^{-6}
RPL8P1	2.32×10^{-1}	-2.11×10^{0}	1.85×10^{-10}	8.78×10^{-10}
AL391883.1	2.33×10^{-1}	-2.10×10^{0}	7.00×10^{-9}	2.81×10^{-8}
HSD3B1	2.33×10^{-1}	-2.10×10^{0}	2.04×10^{-11}	1.07×10^{-10}
PPP1R14BP4	2.36×10^{-1}	-2.08×10^{0}	6.35×10^{-6}	1.82×10^{-5}
AC026316.1	2.37×10^{-1}	-2.08×10^{0}	1.13×10^{-4}	2.77×10^{-4}
RPL38P2	2.38×10^{-1}	-2.07×10^{0}	1.71×10^{-7}	5.90×10^{-7}
APOA4	2.38×10^{-1}	-2.07×10^{0}	1.34×10^{-2}	2.40×10^{-2}
C10orf99	2.39×10^{-1}	-2.07×10^{0}	4.33×10^{-17}	3.97×10^{-16}
SRXN1	2.39×10^{-1}	-2.06×10^{0}	3.28×10^{-7}	1.10×10^{-6}
RPL18P13	2.40×10^{-1}	-2.06×10^{0}	2.56×10^{-7}	8.65×10^{-7}
KRTAP5.5	2.41×10^{-1}	-2.05×10^{0}	5.83×10^{-14}	3.94×10^{-13}
IZUMO2	2.44×10^{-1}	-2.03×10^{0}	4.86×10^{-8}	1.78×10^{-7}
HCRT	2.44×10^{-1}	-2.03×10^{0}	2.83×10^{-12}	1.62×10^{-11}
PNLIPRP2	2.47×10^{-1}	-2.02×10^{0}	1.63×10^{-11}	8.61×10^{-11}
IGLJ3	2.49×10^{-1}	-2.00×10^{0}	2.59×10^{-4}	6.04×10^{-4}
ATP5MC2P2	2.50×10^{-1}	-2.00×10^{0}	7.18×10^{-6}	2.04×10^{-5}
REN	2.50×10^{-1}	-2.00×10^{0}	2.15×10^{-11}	1.12×10^{-10}
AL122020.1	2.51×10^{-1}	-1.99×10^{0}	1.48×10^{-14}	1.06×10^{-13}
LYZL2	2.53×10^{-1}	-1.98×10^{0}	7.19×10^{-4}	1.58×10^{-3}
ATP5MGP3	2.53×10^{-1}	-1.98×10^{0}	9.54×10^{-6}	2.68×10^{-5}
PRAP1	2.54×10^{-1}	-1.98×10^{0}	1.17×10^{-18}	1.25×10^{-17}
NKX6.3	2.61×10^{-1}	-1.94×10^{0}	2.43×10^{-3}	4.94×10^{-3}
FABP1	2.61×10^{-1}	-1.94×10^{0}	2.01×10^{-12}	1.17×10^{-11}
IHH	2.63×10^{-1}	-1.93×10^{0}	1.33×10^{-37}	9.36×10^{-36}
RPS19P1	2.64×10^{-1}	-1.92×10^{0}	5.12×10^{-11}	2.57×10^{-10}
AP00102.4.1	2.65×10^{-1}	-1.92×10^{0}	6.70×10^{-12}	3.69×10^{-11}
F2	2.66×10^{-1}	-1.91×10^{0}	2.59×10^{-11}	1.34×10^{-10}
AC00936.2.1	2.66×10^{-1}	-1.91×10^{0}	9.80×10^{-8}	3.47×10^{-7}
LSM3P3	2.66×10^{-1}	-1.91×10^{0}	5.98×10^{-5}	1.52×10^{-4}
LINC01996	2.67×10^{-1}	-1.91×10^{0}	3.38×10^{-11}	1.73×10^{-10}
HPN	2.67×10^{-1}	-1.91×10^{0}	6.90×10^{-9}	2.77×10^{-8}
AL136981.4	2.68×10^{-1}	-1.90×10^{0}	1.10×10^{-2}	2.00×10^{-2}

Table A.22 (continued). The list of the top 100 downregulated DEGs identified in the CS2 subtype using DESeq2 as a result of three clustering analyzes.

AC11744.1	2.69×10^{-1}	-1.89×10^{0}	6.72×10^{-3}	1.27×10^{-2}
RPS6P26	2.70×10^{-1}	-1.89×10^{0}	2.93×10^{-8}	1.10×10^{-7}
TUFMP1	2.71×10^{-1}	-1.88×10^{0}	5.87×10^{-7}	1.90×10^{-6}
COX7A2P2	2.71×10^{-1}	-1.88×10^{0}	1.70×10^{-5}	4.62×10^{-5}
ATP5PFP1	2.71×10^{-1}	-1.88×10^{0}	1.09×10^{-3}	2.33×10^{-3}
RPLP1P5	2.71×10^{-1}	-1.88×10^{0}	1.34×10^{-5}	3.69×10^{-5}
AQP8	2.72×10^{-1}	-1.88×10^{0}	1.08×10^{-6}	3.39×10^{-6}
AC108114.1	2.72×10^{-1}	-1.88×10^{0}	5.41×10^{-6}	1.56×10^{-5}
AC012618.1	2.72×10^{-1}	-1.88×10^{0}	1.19×10^{-9}	5.17×10^{-9}
AL355309.1	2.75×10^{-1}	-1.86×10^{0}	3.81×10^{-7}	1.26×10^{-6}
DPEP1	2.75×10^{-1}	-1.86×10^{0}	9.74×10^{-15}	7.11×10^{-14}
CKB	2.76×10^{-1}	-1.86×10^{0}	4.21×10^{-16}	3.49×10^{-15}
HSPD1P2	2.76×10^{-1}	-1.86×10^{0}	3.95×10^{-6}	1.16×10^{-5}
PRSS41	2.77×10^{-1}	-1.85×10^{0}	5.48×10^{-11}	2.74×10^{-10}
COX4I1P1	2.77×10^{-1}	-1.85×10^{0}	1.47×10^{-4}	3.54×10^{-4}
AC099670.1	2.78×10^{-1}	-1.85×10^{0}	1.02×10^{-3}	2.18×10^{-3}

Table A.23. The list of the top 100 upregulated DEGs identified in the CS3 subtype using DESeq2 as a result of three clustering analyzes.

	fc	**log2fc**	**pvalue**	**padj**
GP2	3.02×10^{1}	4.92×10^{0}	1.27×10^{-22}	5.18×10^{-19}
TTC29	2.22×10^{1}	4.47×10^{0}	6.03×10^{-12}	5.80×10^{-10}
RN7SL507P	1.14×10^{1}	3.51×10^{0}	6.87×10^{-6}	9.41×10^{-5}
TM4SF4	1.01×10^{1}	3.34×10^{0}	8.68×10^{-17}	5.18×10^{-14}
FGL1	9.61×10^{0}	3.27×10^{0}	8.73×10^{-9}	2.98×10^{-7}
CYP1A1	9.53×10^{0}	3.25×10^{0}	1.93×10^{-9}	8.19×10^{-8}
LINC02620	8.93×10^{0}	3.16×10^{0}	1.13×10^{-3}	6.62×10^{-3}
IGFALS	8.77×10^{0}	3.13×10^{0}	5.67×10^{-17}	3.42×10^{-14}
RBP3	8.57×10^{0}	3.10×10^{0}	1.68×10^{-14}	4.03×10^{-12}
CTSE	8.34×10^{0}	3.06×10^{0}	1.88×10^{-15}	6.45×10^{-13}
AC009078.1	8.23×10^{0}	3.04×10^{0}	1.48×10^{-4}	1.24×10^{-3}
AC253536.4	8.23×10^{0}	3.04×10^{0}	6.96×10^{-10}	3.39×10^{-8}
EIF3KP3	8.23×10^{0}	3.04×10^{0}	1.63×10^{-3}	8.96×10^{-3}
AC092435.1	8.11×10^{0}	3.02×10^{0}	3.12×10^{-3}	1.52×10^{-2}
MUC5AC	7.78×10^{0}	2.96×10^{0}	1.19×10^{-11}	1.04×10^{-9}
AC021534.1	7.52×10^{0}	2.91×10^{0}	7.37×10^{-7}	1.39×10^{-5}
IRX4.AS1	7.38×10^{0}	2.88×10^{0}	6.49×10^{-3}	2.76×10^{-2}
TFF1	6.76×10^{0}	2.76×10^{0}	2.96×10^{-19}	3.94×10^{-16}
AC009517.1	6.74×10^{0}	2.75×10^{0}	9.48×10^{-6}	1.23×10^{-4}
ALPG	6.63×10^{0}	2.73×10^{0}	7.59×10^{-14}	1.47×10^{-11}
VNN1	6.55×10^{0}	2.71×10^{0}	7.14×10^{-19}	8.13×10^{-16}

Table A.23 (continued). The list of the top 100 upregulated DEGs identified in the CS3 subtype using DESeq2 as a result of three clustering analyzes.

PRSS2	6.54×10^{0}	2.71×10^{0}	3.73×10^{-8}	1.06×10^{-6}
REG4	6.39×10^{0}	2.68×10^{0}	6.58×10^{-11}	4.50×10^{-9}
AL122008.2	5.94×10^{0}	2.57×10^{0}	4.72×10^{-5}	4.79×10^{-4}
NBPF7	5.74×10^{0}	2.52×10^{0}	7.18×10^{-9}	2.52×10^{-7}
REG1A	5.70×10^{0}	2.51×10^{0}	2.28×10^{-7}	5.07×10^{-6}
CPS1	5.59×10^{0}	2.48×10^{0}	1.61×10^{-11}	1.35×10^{-9}
GSTT4	5.52×10^{0}	2.46×10^{0}	2.98×10^{-7}	6.39×10^{-6}
REG1CP	5.37×10^{0}	2.43×10^{0}	1.24×10^{-4}	1.07×10^{-3}
SLC18A1	5.25×10^{0}	2.39×10^{0}	7.75×10^{-11}	5.14×10^{-9}
LINC02826	5.23×10^{0}	2.39×10^{0}	1.04×10^{-9}	4.84×10^{-8}
RPS6P20	5.13×10^{0}	2.36×10^{0}	1.92×10^{-3}	1.02×10^{-2}
SPINK4	5.08×10^{0}	2.35×10^{0}	2.11×10^{-8}	6.50×10^{-7}
CYMP	5.03×10^{0}	2.33×10^{0}	3.36×10^{-3}	1.61×10^{-2}
ANPEP	4.99×10^{0}	2.32×10^{0}	7.80×10^{-14}	1.50×10^{-11}
LINC00520	4.86×10^{0}	2.28×10^{0}	1.59×10^{-13}	2.62×10^{-11}
AC107890.1	4.82×10^{0}	2.27×10^{0}	1.01×10^{-2}	3.96×10^{-2}
RPSAP28	4.76×10^{0}	2.25×10^{0}	4.95×10^{-6}	7.12×10^{-5}
AP006565.1	4.69×10^{0}	2.23×10^{0}	1.12×10^{-6}	1.98×10^{-5}
ASS1P4	4.68×10^{0}	2.23×10^{0}	8.38×10^{-6}	1.11×10^{-4}
AC087612.1	4.66×10^{0}	2.22×10^{0}	6.12×10^{-6}	8.53×10^{-5}
COX5AP1	4.65×10^{0}	2.22×10^{0}	1.56×10^{-5}	1.88×10^{-4}
UGT2B4	4.65×10^{0}	2.22×10^{0}	4.36×10^{-6}	6.39×10^{-5}
AP002498.1	4.55×10^{0}	2.19×10^{0}	1.92×10^{-9}	8.17×10^{-8}
SEMG1	4.45×10^{0}	2.15×10^{0}	8.75×10^{-6}	1.15×10^{-4}
ATP5PBP6	4.43×10^{0}	2.15×10^{0}	1.42×10^{-5}	1.73×10^{-4}
NEUROG3	4.40×10^{0}	2.14×10^{0}	1.33×10^{-6}	2.29×10^{-5}
AP000894.1	4.39×10^{0}	2.14×10^{0}	1.58×10^{-3}	8.71×10^{-3}
LINC02404	4.38×10^{0}	2.13×10^{0}	6.56×10^{-4}	4.23×10^{-3}
LY6D	4.33×10^{0}	2.11×10^{0}	4.65×10^{-6}	6.74×10^{-5}
PNKDP1	4.29×10^{0}	2.10×10^{0}	3.80×10^{-5}	3.97×10^{-4}
AC112236.1	4.22×10^{0}	2.08×10^{0}	3.49×10^{-7}	7.31×10^{-6}
KRT89P	4.21×10^{0}	2.07×10^{0}	5.09×10^{-8}	1.38×10^{-6}
LINC01913	4.16×10^{0}	2.06×10^{0}	2.78×10^{-5}	3.05×10^{-4}
C11orf86	4.16×10^{0}	2.06×10^{0}	1.83×10^{-8}	5.75×10^{-7}
AC107373.2	4.14×10^{0}	2.05×10^{0}	8.89×10^{-3}	3.58×10^{-2}
TCN1	4.13×10^{0}	2.05×10^{0}	4.31×10^{-7}	8.76×10^{-6}
PFN1P9	4.07×10^{0}	2.03×10^{0}	1.18×10^{-6}	2.06×10^{-5}
INSM1	4.06×10^{0}	2.02×10^{0}	1.08×10^{-7}	2.68×10^{-6}
RPA2P2	4.06×10^{0}	2.02×10^{0}	4.97×10^{-3}	2.22×10^{-2}
AC005256.1	4.03×10^{0}	2.01×10^{0}	5.62×10^{-11}	3.92×10^{-9}
RPL18AP15	3.99×10^{0}	2.00×10^{0}	7.19×10^{-11}	4.82×10^{-9}

Table A.23 (continued). The list of the top 100 upregulated DEGs identified in the CS3 subtype using DESeq2 as a result of three clustering analyzes.

CCL25	3.99×10^{0}	2.00×10^{0}	8.67×10^{-7}	1.59×10^{-5}
AC108751.5	3.98×10^{0}	1.99×10^{0}	1.46×10^{-11}	1.24×10^{-9}
SI	3.95×10^{0}	1.98×10^{0}	1.99×10^{-7}	4.52×10^{-6}
KLK12	3.94×10^{0}	1.98×10^{0}	2.13×10^{-8}	6.55×10^{-7}
ATP5PBP3	3.94×10^{0}	1.98×10^{0}	7.96×10^{-5}	7.40×10^{-4}
AC009163.6	3.92×10^{0}	1.97×10^{0}	5.29×10^{-8}	1.43×10^{-6}
AL022316.1	3.91×10^{0}	1.97×10^{0}	1.21×10^{-13}	2.11×10^{-11}
WFDC21P	3.87×10^{0}	1.95×10^{0}	1.23×10^{-14}	3.03×10^{-12}
RPLP0P11	3.83×10^{0}	1.94×10^{0}	1.16×10^{-3}	6.78×10^{-3}
MUC2	3.82×10^{0}	1.93×10^{0}	1.77×10^{-7}	4.09×10^{-6}
LINC00261	3.81×10^{0}	1.93×10^{0}	1.92×10^{-10}	1.11×10^{-8}
KLK11	3.80×10^{0}	1.93×10^{0}	2.98×10^{-10}	1.61×10^{-8}
ACNATP	3.80×10^{0}	1.92×10^{0}	9.61×10^{-4}	5.81×10^{-3}
LINC01713	3.80×10^{0}	1.92×10^{0}	5.40×10^{-4}	3.60×10^{-3}
RPS2P48	3.79×10^{0}	1.92×10^{0}	4.05×10^{-16}	1.74×10^{-13}
PCSK1	3.78×10^{0}	1.92×10^{0}	4.45×10^{-6}	6.51×10^{-5}
KIF19	3.77×10^{0}	1.92×10^{0}	2.09×10^{-8}	6.44×10^{-7}
OAZ1P1	3.76×10^{0}	1.91×10^{0}	1.33×10^{-4}	1.13×10^{-3}
CEACAM20	3.76×10^{0}	1.91×10^{0}	4.88×10^{-7}	9.75×10^{-6}
ALDH1L1	3.74×10^{0}	1.90×10^{0}	1.72×10^{-8}	5.47×10^{-7}
AGR2	3.74×10^{0}	1.90×10^{0}	1.01×10^{-25}	7.24×10^{-22}
C17orf78	3.73×10^{0}	1.90×10^{0}	1.85×10^{-5}	2.17×10^{-4}
AC046168.2	3.72×10^{0}	1.89×10^{0}	6.61×10^{-9}	2.35×10^{-7}
LINC02683	3.70×10^{0}	1.89×10^{0}	1.63×10^{-3}	8.94×10^{-3}
COX4I1P1	3.70×10^{0}	1.89×10^{0}	7.89×10^{-5}	7.34×10^{-4}
CLCA1	3.68×10^{0}	1.88×10^{0}	5.33×10^{-5}	5.30×10^{-4}
FAM177B	3.66×10^{0}	1.87×10^{0}	2.26×10^{-9}	9.39×10^{-8}
AC004224.1	3.65×10^{0}	1.87×10^{0}	5.45×10^{-7}	1.07×10^{-5}
CRIP1P4	3.65×10^{0}	1.87×10^{0}	8.29×10^{-4}	5.14×10^{-3}
CA8	3.64×10^{0}	1.86×10^{0}	9.36×10^{-10}	4.43×10^{-8}
RPL38P6	3.64×10^{0}	1.86×10^{0}	7.80×10^{-3}	3.22×10^{-2}
HSD17B2	3.63×10^{0}	1.86×10^{0}	6.79×10^{-14}	1.34×10^{-11}
CIB4	3.63×10^{0}	1.86×10^{0}	4.42×10^{-6}	6.47×10^{-5}
BOLA2P1	3.61×10^{0}	1.85×10^{0}	1.24×10^{-2}	4.70×10^{-2}
PYDC1	3.61×10^{0}	1.85×10^{0}	1.81×10^{-4}	1.46×10^{-3}
CA9	3.61×10^{0}	1.85×10^{0}	5.22×10^{-9}	1.92×10^{-7}
L1TD1	3.59×10^{0}	1.84×10^{0}	3.33×10^{-6}	5.08×10^{-5}
SPDEF	3.58×10^{0}	1.84×10^{0}	3.41×10^{-10}	1.80×10^{-8}

Table A.24. The list of the top 100 downregulated DEGs identified in the CS3 subtype using DESeq2 as a result of three clustering analyzes.

	fc	log2fc	pvalue	padj
AC244102.4	2.96×10^{-2}	-5.08×10^{0}	6.16×10^{-5}	5.99×10^{-4}
TMEM132D.AS1	4.01×10^{-2}	-4.64×10^{0}	3.29×10^{-7}	6.95×10^{-6}
MAGEA3	4.54×10^{-2}	-4.46×10^{0}	3.21×10^{-6}	4.93×10^{-5}
AC244102.3	4.64×10^{-2}	-4.43×10^{0}	2.92×10^{-5}	3.19×10^{-4}
LINC00491	4.96×10^{-2}	-4.33×10^{0}	7.64×10^{-6}	1.03×10^{-4}
MAGEA4	5.19×10^{-2}	-4.27×10^{0}	1.74×10^{-5}	2.06×10^{-4}
CSAG1	5.48×10^{-2}	-4.19×10^{0}	1.27×10^{-8}	4.17×10^{-7}
MTND1P23	5.51×10^{-2}	-4.18×10^{0}	2.84×10^{-20}	6.02×10^{-17}
LINC00355	5.51×10^{-2}	-4.18×10^{0}	3.19×10^{-8}	9.30×10^{-7}
VSTM2B	5.67×10^{-2}	-4.14×10^{0}	4.81×10^{-10}	2.44×10^{-8}
AC090809.1	5.92×10^{-2}	-4.08×10^{0}	9.35×10^{-9}	3.17×10^{-7}
HTR2C	6.22×10^{-2}	-4.01×10^{0}	6.33×10^{-5}	6.13×10^{-4}
GABRA3	6.25×10^{-2}	-4.00×10^{0}	1.06×10^{-14}	2.70×10^{-12}
HAND1	6.48×10^{-2}	-3.95×10^{0}	9.88×10^{-15}	2.56×10^{-12}
MAGEA12	6.51×10^{-2}	-3.94×10^{0}	1.17×10^{-5}	1.47×10^{-4}
CIDEA	6.78×10^{-2}	-3.88×10^{0}	4.61×10^{-6}	6.70×10^{-5}
AL591501.1	6.94×10^{-2}	-3.85×10^{0}	1.54×10^{-11}	1.29×10^{-9}
AL589787.2	7.51×10^{-2}	-3.73×10^{0}	2.53×10^{-6}	4.00×10^{-5}
AC090578.1	7.54×10^{-2}	-3.73×10^{0}	2.21×10^{-15}	7.30×10^{-13}
AL589743.3	7.80×10^{-2}	-3.68×10^{0}	1.00×10^{-11}	8.97×10^{-10}
G2E3.AS1	7.98×10^{-2}	-3.65×10^{0}	4.03×10^{-5}	4.18×10^{-4}
AC016044.1	8.02×10^{-2}	-3.64×10^{0}	4.39×10^{-6}	6.44×10^{-5}
AL110505.1	8.04×10^{-2}	-3.64×10^{0}	9.87×10^{-6}	1.27×10^{-4}
EMX2	8.04×10^{-2}	-3.64×10^{0}	3.10×10^{-13}	4.66×10^{-11}
TRARG1	8.89×10^{-2}	-3.49×10^{0}	1.26×10^{-9}	5.70×10^{-8}
LINC02820	9.11×10^{-2}	-3.46×10^{0}	1.70×10^{-7}	3.95×10^{-6}
PAGE1	9.11×10^{-2}	-3.46×10^{0}	1.69×10^{-3}	9.20×10^{-3}
WT1.AS	9.21×10^{-2}	-3.44×10^{0}	3.43×10^{-9}	1.33×10^{-7}
TGM6	9.47×10^{-2}	-3.40×10^{0}	1.32×10^{-4}	1.12×10^{-3}
AL031686.1	9.56×10^{-2}	-3.39×10^{0}	8.20×10^{-11}	5.37×10^{-9}
PWWP3B	9.70×10^{-2}	-3.37×10^{0}	8.46×10^{-18}	7.02×10^{-15}
COL2A1	9.85×10^{-2}	-3.34×10^{0}	2.63×10^{-21}	7.92×10^{-18}
LINC01980	9.92×10^{-2}	-3.33×10^{0}	3.51×10^{-7}	7.34×10^{-6}
EMX2OS	1.00×10^{-1}	-3.32×10^{0}	3.52×10^{-16}	1.57×10^{-13}
AL117329.1	1.01×10^{-1}	-3.30×10^{0}	4.12×10^{-10}	2.13×10^{-8}
TBX5	1.03×10^{-1}	-3.28×10^{0}	2.54×10^{-7}	5.56×10^{-6}
GABRR1	1.06×10^{-1}	-3.24×10^{0}	1.33×10^{-10}	8.10×10^{-9}
AL390334.1	1.07×10^{-1}	-3.23×10^{0}	1.70×10^{-4}	1.39×10^{-3}
CT83	1.09×10^{-1}	-3.20×10^{0}	5.32×10^{-3}	2.35×10^{-2}

Table A.24 (continued). The list of the top 100 downregulated DEGs identified in the CS3 subtype using DESeq2 as a result of three clustering analyzes.

PAK5	1.10×10^{-1}	-3.18×10^{0}	3.00×10^{-5}	3.26×10^{-4}

AL139023.1	1.12×10^{-1}	-3.16×10^{0}	1.60×10^{-3}	8.81×10^{-3}
ALX1	1.13×10^{-1}	-3.14×10^{0}	2.59×10^{-6}	4.08×10^{-5}
PNMA5	1.15×10^{-1}	-3.12×10^{0}	3.15×10^{-9}	1.25×10^{-7}
PLIN4	1.16×10^{-1}	-3.11×10^{0}	1.47×10^{-17}	1.11×10^{-14}
KCNC2	1.17×10^{-1}	-3.09×10^{0}	2.61×10^{-6}	4.11×10^{-5}
CLEC3A	1.18×10^{-1}	-3.09×10^{0}	1.35×10^{-6}	2.31×10^{-5}
HSPB6	1.19×10^{-1}	-3.07×10^{0}	6.49×10^{-24}	3.71×10^{-20}
AC010595.1	1.21×10^{-1}	-3.05×10^{0}	1.78×10^{-4}	1.44×10^{-3}
IRX6	1.24×10^{-1}	-3.01×10^{0}	8.57×10^{-7}	1.58×10^{-5}
FOXG1	1.29×10^{-1}	-2.96×10^{0}	1.34×10^{-4}	1.14×10^{-3}
VWDE	1.32×10^{-1}	-2.92×10^{0}	8.04×10^{-14}	1.53×10^{-11}
AL049828.2	1.33×10^{-1}	-2.91×10^{0}	1.28×10^{-2}	4.84×10^{-2}
SLC18A3	1.34×10^{-1}	-2.90×10^{0}	9.71×10^{-7}	1.76×10^{-5}
AC138123.2	1.34×10^{-1}	-2.90×10^{0}	1.25×10^{-11}	1.08×10^{-9}
AC096759.2	1.35×10^{-1}	-2.89×10^{0}	3.09×10^{-4}	2.27×10^{-3}
FGF19	1.35×10^{-1}	-2.89×10^{0}	3.57×10^{-14}	7.59×10^{-12}
LINC00470	1.36×10^{-1}	-2.87×10^{0}	4.51×10^{-6}	6.57×10^{-5}
AC012501.2	1.37×10^{-1}	-2.87×10^{0}	2.12×10^{-7}	4.77×10^{-6}
WASF3	1.40×10^{-1}	-2.83×10^{0}	1.01×10^{-29}	1.93×10^{-25}
U91319.1	1.41×10^{-1}	-2.82×10^{0}	1.96×10^{-5}	2.28×10^{-4}
AC091646.1	1.42×10^{-1}	-2.81×10^{0}	2.65×10^{-7}	5.77×10^{-6}
AL356274.2	1.43×10^{-1}	-2.81×10^{0}	7.58×10^{-6}	1.02×10^{-4}
LINC01239	1.44×10^{-1}	-2.79×10^{0}	2.70×10^{-8}	8.07×10^{-7}
NKX2.1	1.45×10^{-1}	-2.79×10^{0}	9.01×10^{-5}	8.20×10^{-4}
LINC01139	1.45×10^{-1}	-2.79×10^{0}	5.23×10^{-7}	1.04×10^{-5}
LINC00607	1.46×10^{-1}	-2.78×10^{0}	9.47×10^{-16}	3.74×10^{-13}
CHRND	1.48×10^{-1}	-2.76×10^{0}	4.04×10^{-7}	8.28×10^{-6}
DCAF12L2	1.48×10^{-1}	-2.75×10^{0}	2.17×10^{-9}	9.06×10^{-8}
CNTNAP5	1.49×10^{-1}	-2.74×10^{0}	1.28×10^{-6}	2.22×10^{-5}
ZNF716	1.52×10^{-1}	-2.72×10^{0}	5.17×10^{-3}	2.30×10^{-2}
AL358335.2	1.52×10^{-1}	-2.72×10^{0}	1.30×10^{-2}	4.89×10^{-2}
ZIC4	1.52×10^{-1}	-2.71×10^{0}	9.16×10^{-4}	5.59×10^{-3}
AL022151.1	1.54×10^{-1}	-2.70×10^{0}	1.11×10^{-5}	1.41×10^{-4}
AC013457.1	1.55×10^{-1}	-2.69×10^{0}	5.73×10^{-5}	5.63×10^{-4}
MUC15	1.56×10^{-1}	-2.68×10^{0}	5.63×10^{-5}	5.54×10^{-4}
LINC01230	1.57×10^{-1}	-2.67×10^{0}	8.23×10^{-6}	1.09×10^{-4}
Z93403.1	1.57×10^{-1}	-2.67×10^{0}	1.01×10^{-6}	1.81×10^{-5}
AL035467.2	1.57×10^{-1}	-2.67×10^{0}	4.07×10^{-3}	1.89×10^{-2}
AL033530.1	1.57×10^{-1}	-2.67×10^{0}	9.03×10^{-4}	5.52×10^{-3}
AC092969.1	1.58×10^{-1}	-2.66×10^{0}	4.63×10^{-8}	1.28×10^{-6}

Table A.24 (continued). The list of the top 100 downregulated DEGs identified in the CS3 subtype using DESeq2 as a result of three clustering analyzes.

SALL3	1.61×10^{-1}	-2.64×10^{0}	5.49×10^{-3}	2.41×10^{-2}
CARTPT	1.63×10^{-1}	-2.62×10^{0}	4.60×10^{-8}	1.27×10^{-6}

MIR483	1.63×10^{-1}	-2.61×10^{0}	1.11×10^{-2}	4.30×10^{-2}
FAM83C	1.64×10^{-1}	-2.61×10^{0}	3.94×10^{-10}	2.05×10^{-8}
FMN2	1.64×10^{-1}	-2.61×10^{0}	3.35×10^{-12}	3.59×10^{-10}
AF064858.2	1.64×10^{-1}	-2.61×10^{0}	4.47×10^{-14}	9.27×10^{-12}
L1CAM	1.64×10^{-1}	-2.60×10^{0}	1.30×10^{-16}	6.97×10^{-14}
AL121949.1	1.67×10^{-1}	-2.58×10^{0}	3.24×10^{-5}	3.48×10^{-4}
LINC02327	1.67×10^{-1}	-2.58×10^{0}	7.85×10^{-3}	3.23×10^{-2}
DES	1.68×10^{-1}	-2.57×10^{0}	1.75×10^{-12}	2.08×10^{-10}
SMYD1	1.72×10^{-1}	-2.54×10^{0}	1.69×10^{-10}	9.95×10^{-9}
AC138649.1	1.73×10^{-1}	-2.53×10^{0}	1.69×10^{-12}	2.01×10^{-10}
MKRN7P	1.74×10^{-1}	-2.52×10^{0}	4.14×10^{-4}	2.90×10^{-3}
LINC00954	1.74×10^{-1}	-2.52×10^{0}	9.38×10^{-28}	1.34×10^{-23}
LINC02302	1.75×10^{-1}	-2.51×10^{0}	8.26×10^{-4}	5.13×10^{-3}
LINC02466	1.76×10^{-1}	-2.50×10^{0}	1.63×10^{-3}	8.95×10^{-3}
WNT6	1.77×10^{-1}	-2.50×10^{0}	8.61×10^{-15}	2.32×10^{-12}
CSAG3	1.77×10^{-1}	-2.50×10^{0}	4.96×10^{-3}	2.22×10^{-2}
TOMM40P1	1.80×10^{-1}	-2.48×10^{0}	2.28×10^{-10}	1.28×10^{-8}
AL450345.2	1.80×10^{-1}	-2.48×10^{0}	2.65×10^{-4}	1.99×10^{-3}

Table A.25. The list of the top 100 upregulated DEGs identified in the CS1 subtype using limma as a result of three clustering analyzes.

	fc	**log2fc**	**pvalue**	**padj**
TNNC2	9.38×10^{0}	3.23×10^{0}	1.74×10^{-46}	9.96×10^{-42}
CEL	7.63×10^{0}	2.93×10^{0}	3.71×10^{-24}	2.28×10^{-21}
AP003774.2	7.58×10^{0}	2.92×10^{0}	3.60×10^{-40}	1.03×10^{-35}
C10orf99	7.10×10^{0}	2.83×10^{0}	1.51×10^{-22}	6.71×10^{-20}
KRT23	6.04×10^{0}	2.59×10^{0}	1.81×10^{-20}	5.12×10^{-18}
QPRT	6.00×10^{0}	2.58×10^{0}	2.68×10^{-37}	3.07×10^{-33}
GNG4	5.78×10^{0}	2.53×10^{0}	5.42×10^{-25}	4.25×10^{-22}
NOTUM	5.46×10^{0}	2.45×10^{0}	4.05×10^{-16}	4.73×10^{-14}
DPEP1	5.06×10^{0}	2.34×10^{0}	8.59×10^{-18}	1.45×10^{-15}
ASCL2	5.05×10^{0}	2.34×10^{0}	2.16×10^{-31}	5.62×10^{-28}
CDHR1	4.99×10^{0}	2.32×10^{0}	1.03×10^{-23}	5.91×10^{-21}
SLC26A3	4.98×10^{0}	2.32×10^{0}	1.22×10^{-11}	5.22×10^{-10}
SLC39A5	4.78×10^{0}	2.26×10^{0}	2.87×10^{-31}	6.84×10^{-28}
TDGF1	4.57×10^{0}	2.19×10^{0}	3.07×10^{-33}	1.25×10^{-29}
Y_RNA.244	4.36×10^{0}	2.13×10^{0}	1.29×10^{-24}	9.50×10^{-22}
CXCL14	4.28×10^{0}	2.10×10^{0}	2.11×10^{-17}	3.25×10^{-15}
CYP2B6	4.27×10^{0}	2.09×10^{0}	3.09×10^{-26}	2.99×10^{-23}

Table A.25 (continued). The list of the top 100 upregulated DEGs identified in the CS1 subtype using limma as a result of three clustering analyzes.

CYP2W1	4.25×10^{0}	2.09×10^{0}	9.50×10^{-14}	6.55×10^{-12}
FABP1	4.24×10^{0}	2.08×10^{0}	1.82×10^{-10}	6.05×10^{-9}
VAV3	4.15×10^{0}	2.05×10^{0}	6.09×10^{-31}	1.34×10^{-27}

CELP	4.11×10^{0}	2.04×10^{0}	4.49×10^{-36}	4.29×10^{-32}
PLA2G12B	4.00×10^{0}	2.00×10^{0}	1.19×10^{-18}	2.37×10^{-16}
LEFTY1	3.91×10^{0}	1.97×10^{0}	1.44×10^{-11}	6.03×10^{-10}
RUBCNL	3.90×10^{0}	1.96×10^{0}	9.99×10^{-31}	2.04×10^{-27}
AL117382.1	3.83×10^{0}	1.94×10^{0}	3.96×10^{-35}	3.24×10^{-31}
EREG	3.78×10^{0}	1.92×10^{0}	3.14×10^{-14}	2.45×10^{-12}
ENPP3	3.76×10^{0}	1.91×10^{0}	4.20×10^{-18}	7.55×10^{-16}
IHH	3.60×10^{0}	1.85×10^{0}	7.21×10^{-29}	1.06×10^{-25}
LY6G6D	3.58×10^{0}	1.84×10^{0}	1.58×10^{-24}	1.12×10^{-21}
AXIN2	3.48×10^{0}	1.80×10^{0}	1.73×10^{-28}	2.47×10^{-25}
GPR143	3.44×10^{0}	1.78×10^{0}	1.44×10^{-24}	1.04×10^{-21}
MEP1A	3.40×10^{0}	1.76×10^{0}	3.33×10^{-14}	2.59×10^{-12}
NKD1	3.39×10^{0}	1.76×10^{0}	1.77×10^{-18}	3.32×10^{-16}
RPL39P40	3.35×10^{0}	1.75×10^{0}	5.87×10^{-22}	2.28×10^{-19}
GRM8	3.27×10^{0}	1.71×10^{0}	2.34×10^{-22}	1.01×10^{-19}
LINC02441	3.27×10^{0}	1.71×10^{0}	2.90×10^{-24}	1.89×10^{-21}
APCDD1	3.26×10^{0}	1.71×10^{0}	1.23×10^{-16}	1.59×10^{-14}
LINC02418	3.21×10^{0}	1.68×10^{0}	6.08×10^{-15}	5.44×10^{-13}
FABP6	3.19×10^{0}	1.67×10^{0}	4.37×10^{-17}	6.18×10^{-15}
MOGAT3	3.19×10^{0}	1.67×10^{0}	3.68×10^{-27}	4.50×10^{-24}
MAP7D2	3.17×10^{0}	1.67×10^{0}	6.81×10^{-15}	6.03×10^{-13}
RBP2	3.16×10^{0}	1.66×10^{0}	3.02×10^{-12}	1.49×10^{-10}
GGT7	3.14×10^{0}	1.65×10^{0}	5.47×10^{-30}	9.20×10^{-27}
MAB21L4	3.14×10^{0}	1.65×10^{0}	2.58×10^{-24}	1.70×10^{-21}
CDX2	3.13×10^{0}	1.64×10^{0}	1.70×10^{-29}	2.70×10^{-26}
AIFM3	3.11×10^{0}	1.64×10^{0}	9.64×10^{-26}	8.49×10^{-23}
MUC12	3.08×10^{0}	1.62×10^{0}	3.93×10^{-13}	2.33×10^{-11}
RNF43	3.08×10^{0}	1.62×10^{0}	6.25×10^{-40}	1.19×10^{-35}
CHP2	3.07×10^{0}	1.62×10^{0}	1.09×10^{-10}	3.77×10^{-9}
HMGCS2	3.05×10^{0}	1.61×10^{0}	1.08×10^{-7}	1.81×10^{-6}
XPNPEP2	3.03×10^{0}	1.60×10^{0}	1.31×10^{-13}	8.77×10^{-12}
SATB2.AS1	3.03×10^{0}	1.60×10^{0}	6.76×10^{-27}	7.90×10^{-24}
AC114291.1	3.03×10^{0}	1.60×10^{0}	1.01×10^{-20}	3.09×10^{-18}
PPP1R14D	3.01×10^{0}	1.59×10^{0}	2.26×10^{-21}	7.92×10^{-19}
ISX	3.01×10^{0}	1.59×10^{0}	1.55×10^{-16}	1.98×10^{-14}
R3HDML	3.00×10^{0}	1.59×10^{0}	1.67×10^{-31}	4.79×10^{-28}
MIR3131	2.96×10^{0}	1.57×10^{0}	6.48×10^{-17}	8.83×10^{-15}
TUSC8	2.95×10^{0}	1.56×10^{0}	2.30×10^{-21}	8.03×10^{-19}

Table A.25 (continued). The list of the top 100 upregulated DEGs identified in the CS1 subtype using limma as a result of three clustering analyzes.

HUNK	2.91×10^{0}	1.54×10^{0}	9.97×10^{-21}	3.07×10^{-18}
NOX1	2.91×10^{0}	1.54×10^{0}	1.43×10^{-14}	1.19×10^{-12}
SLC13A2	2.88×10^{0}	1.53×10^{0}	1.96×10^{-14}	1.59×10^{-12}
URAD	2.88×10^{0}	1.53×10^{0}	5.85×10^{-9}	1.35×10^{-7}

PLCB4	2.87×10^{0}	1.52×10^{0}	7.85×10^{-16}	8.51×10^{-14}
DIO3OS	2.86×10^{0}	1.51×10^{0}	1.26×10^{-21}	4.67×10^{-19}
COL9A3	2.85×10^{0}	1.51×10^{0}	9.86×10^{-14}	6.76×10^{-12}
PTPRO	2.84×10^{0}	1.50×10^{0}	5.37×10^{-15}	4.85×10^{-13}
ANO9	2.83×10^{0}	1.50×10^{0}	5.90×10^{-32}	1.88×10^{-28}
BEX2	2.82×10^{0}	1.49×10^{0}	1.43×10^{-11}	6.01×10^{-10}
SELENBP1	2.80×10^{0}	1.49×10^{0}	1.38×10^{-17}	2.21×10^{-15}
AC124067.4	2.79×10^{0}	1.48×10^{0}	4.52×10^{-23}	2.31×10^{-20}
WNT11	2.77×10^{0}	1.47×10^{0}	2.16×10^{-11}	8.76×10^{-10}
AL162413.1	2.76×10^{0}	1.47×10^{0}	1.95×10^{-8}	3.95×10^{-7}
CFTR	2.75×10^{0}	1.46×10^{0}	7.33×10^{-16}	8.02×10^{-14}
CAB39L	2.73×10^{0}	1.45×10^{0}	3.01×10^{-23}	1.59×10^{-20}
TINAG	2.73×10^{0}	1.45×10^{0}	6.95×10^{-20}	1.78×10^{-17}
PPP1R14C	2.72×10^{0}	1.44×10^{0}	2.14×10^{-16}	2.67×10^{-14}
CYP4F2	2.71×10^{0}	1.44×10^{0}	3.12×10^{-14}	2.43×10^{-12}
PRAC1	2.69×10^{0}	1.43×10^{0}	5.79×10^{-4}	2.36×10^{-3}
AL354743.2	2.69×10^{0}	1.43×10^{0}	1.52×10^{-18}	2.92×10^{-16}
ENGASE	2.68×10^{0}	1.42×10^{0}	2.49×10^{-33}	1.09×10^{-29}
TMEM176A	2.68×10^{0}	1.42×10^{0}	1.52×10^{-21}	5.54×10^{-19}
WIF1	2.64×10^{0}	1.40×10^{0}	1.54×10^{-11}	6.40×10^{-10}
AC005050.2	2.63×10^{0}	1.39×10^{0}	9.97×10^{-27}	1.06×10^{-23}
NKD2	2.61×10^{0}	1.39×10^{0}	6.99×10^{-16}	7.69×10^{-14}
SYT7	2.61×10^{0}	1.39×10^{0}	2.26×10^{-22}	9.78×10^{-20}
DDC	2.61×10^{0}	1.38×10^{0}	7.18×10^{-15}	6.32×10^{-13}
SLC30A2	2.59×10^{0}	1.37×10^{0}	1.56×10^{-20}	4.51×10^{-18}
PRR15	2.59×10^{0}	1.37×10^{0}	8.35×10^{-32}	2.51×10^{-28}
SLC39A2	2.57×10^{0}	1.36×10^{0}	1.20×10^{-9}	3.24×10^{-8}
AC078993.1	2.57×10^{0}	1.36×10^{0}	1.33×10^{-13}	8.85×10^{-12}
FGFR4	2.56×10^{0}	1.36×10^{0}	2.55×10^{-22}	1.07×10^{-19}
TMEM252	2.54×10^{0}	1.35×10^{0}	1.70×10^{-12}	8.73×10^{-11}
BOLA3P3	2.54×10^{0}	1.34×10^{0}	1.13×10^{-21}	4.23×10^{-19}
AC055717.2	2.53×10^{0}	1.34×10^{0}	7.62×10^{-17}	1.03×10^{-14}
TSPAN6	2.53×10^{0}	1.34×10^{0}	2.35×10^{-34}	1.34×10^{-30}
PRDX5	2.52×10^{0}	1.34×10^{0}	1.01×10^{-25}	8.79×10^{-23}
HOXB9	2.52×10^{0}	1.34×10^{0}	2.02×10^{-10}	6.62×10^{-9}
CKMT2	2.52×10^{0}	1.33×10^{0}	9.23×10^{-8}	1.57×10^{-6}
TLE2	2.52×10^{0}	1.33×10^{0}	2.75×10^{-17}	4.13×10^{-15}

Table A.25 (continued). The list of the top 100 upregulated DEGs identified in the CS1 subtype using limma as a result of three clustering analyzes.

CTTNBP2	2.51×10^{0}	1.33×10^{0}	1.11×10^{-21}	4.19×10^{-19}

Table A.26. The list of the top 100 downregulated DEGs identified in the CS1 subtype using limma as a result of three clustering analyzes.

	fc	**log2fc**	**pvalue**	**padj**

REG4	1.03×10^{-1}	-3.28×10^{0}	2.14×10^{-15}	2.12×10^{-13}
CTSE	1.50×10^{-1}	-2.74×10^{0}	7.97×10^{-19}	1.66×10^{-16}
CLDN18	2.07×10^{-1}	-2.27×10^{0}	1.83×10^{-18}	3.42×10^{-16}
PLA2G2A	2.14×10^{-1}	-2.22×10^{0}	1.95×10^{-11}	7.98×10^{-10}
DUSP4	2.16×10^{-1}	-2.21×10^{0}	1.11×10^{-32}	4.25×10^{-29}
GJB5	2.62×10^{-1}	-1.93×10^{0}	7.88×10^{-18}	1.34×10^{-15}
MUC5AC	2.71×10^{-1}	-1.88×10^{0}	2.22×10^{-16}	2.74×10^{-14}
TCN1	2.76×10^{-1}	-1.86×10^{0}	3.81×10^{-10}	1.17×10^{-8}
LYZ	2.77×10^{-1}	-1.85×10^{0}	2.26×10^{-13}	1.43×10^{-11}
MUC2	2.80×10^{-1}	-1.84×10^{0}	2.89×10^{-7}	4.28×10^{-6}
CXCL13	2.84×10^{-1}	-1.82×10^{0}	8.93×10^{-19}	1.83×10^{-16}
REG1A	2.91×10^{-1}	-1.78×10^{0}	1.03×10^{-4}	5.55×10^{-4}
TNNT1	2.96×10^{-1}	-1.76×10^{0}	3.52×10^{-19}	7.81×10^{-17}
RAMP1	3.01×10^{-1}	-1.73×10^{0}	5.48×10^{-13}	3.16×10^{-11}
TFF2	3.02×10^{-1}	-1.73×10^{0}	8.71×10^{-10}	2.44×10^{-8}
RAB27B	3.14×10^{-1}	-1.67×10^{0}	9.77×10^{-35}	6.99×10^{-31}
VNN1	3.14×10^{-1}	-1.67×10^{0}	2.82×10^{-18}	5.14×10^{-16}
CCL18	3.25×10^{-1}	-1.62×10^{0}	5.26×10^{-10}	1.56×10^{-8}
TRNP1	3.29×10^{-1}	-1.60×10^{0}	3.23×10^{-20}	8.67×10^{-18}
CXCL9	3.37×10^{-1}	-1.57×10^{0}	4.03×10^{-12}	1.92×10^{-10}
SDR16C5	3.38×10^{-1}	-1.56×10^{0}	1.61×10^{-13}	1.05×10^{-11}
ANXA10	3.42×10^{-1}	-1.55×10^{0}	1.26×10^{-19}	3.05×10^{-17}
TNFSF9	3.50×10^{-1}	-1.51×10^{0}	9.77×10^{-18}	1.63×10^{-15}
MUC6	3.51×10^{-1}	-1.51×10^{0}	8.85×10^{-14}	6.15×10^{-12}
TRIM7	3.52×10^{-1}	-1.51×10^{0}	1.36×10^{-32}	4.85×10^{-29}
SERPINB5	3.60×10^{-1}	-1.47×10^{0}	3.23×10^{-10}	1.01×10^{-8}
CXCL10	3.66×10^{-1}	-1.45×10^{0}	2.04×10^{-11}	8.31×10^{-10}
SPON1	3.67×10^{-1}	-1.45×10^{0}	1.08×10^{-14}	9.13×10^{-13}
TM4SF4	3.67×10^{-1}	-1.45×10^{0}	2.66×10^{-10}	8.46×10^{-9}
RARRES1	3.69×10^{-1}	-1.44×10^{0}	3.36×10^{-16}	4.00×10^{-14}
SPINK4	3.69×10^{-1}	-1.44×10^{0}	3.32×10^{-4}	1.48×10^{-3}
GBP4	3.74×10^{-1}	-1.42×10^{0}	2.81×10^{-17}	4.19×10^{-15}
MUC17	3.77×10^{-1}	-1.41×10^{0}	4.93×10^{-8}	8.95×10^{-7}
PRSS2	3.78×10^{-1}	-1.40×10^{0}	3.73×10^{-5}	2.40×10^{-4}
CD109	3.81×10^{-1}	-1.39×10^{0}	1.52×10^{-18}	2.92×10^{-16}
ADGRG6	3.82×10^{-1}	-1.39×10^{0}	1.27×10^{-24}	9.41×10^{-22}

Table A.26 (continued). The list of the top 100 downregulated DEGs identified in the CS1 subtype using limma as a result of three clustering analyzes.

SPP1	3.83×10^{-1}	-1.38×10^{0}	1.45×10^{-6}	1.72×10^{-5}
SPDEF	3.86×10^{-1}	-1.37×10^{0}	1.69×10^{-8}	3.49×10^{-7}
PLA2G4A	3.88×10^{-1}	-1.37×10^{0}	6.35×10^{-14}	4.61×10^{-12}
IL1RN	3.89×10^{-1}	-1.36×10^{0}	1.26×10^{-14}	1.06×10^{-12}
TRIB2	3.90×10^{-1}	-1.36×10^{0}	4.74×10^{-29}	7.14×10^{-26}
GZMA	3.92×10^{-1}	-1.35×10^{0}	3.46×10^{-17}	5.07×10^{-15}

GNLY	3.93×10^{-1}	-1.35×10^{0}	1.09×10^{-18}	2.20×10^{-16}
FCGR3A	3.94×10^{-1}	-1.35×10^{0}	6.54×10^{-12}	2.99×10^{-10}
MT1E	3.95×10^{-1}	-1.34×10^{0}	5.49×10^{-10}	1.61×10^{-8}
CA9	3.96×10^{-1}	-1.33×10^{0}	2.70×10^{-6}	2.90×10^{-5}
MUC5B	3.99×10^{-1}	-1.32×10^{0}	5.73×10^{-6}	5.33×10^{-5}
CCL5	4.01×10^{-1}	-1.32×10^{0}	3.45×10^{-15}	3.25×10^{-13}
FCGBP	4.06×10^{-1}	-1.30×10^{0}	6.09×10^{-5}	3.58×10^{-4}
GABRP	4.06×10^{-1}	-1.30×10^{0}	4.29×10^{-11}	1.61×10^{-9}
DAPK1	4.10×10^{-1}	-1.29×10^{0}	2.85×10^{-19}	6.43×10^{-17}
PLAAT4	4.13×10^{-1}	-1.28×10^{0}	5.41×10^{-13}	3.13×10^{-11}
ZIC2	4.13×10^{-1}	-1.27×10^{0}	1.32×10^{-9}	3.54×10^{-8}
GCNT3	4.14×10^{-1}	-1.27×10^{0}	3.88×10^{-9}	9.32×10^{-8}
TFAP2A	4.14×10^{-1}	-1.27×10^{0}	7.77×10^{-27}	8.89×10^{-24}
PTMAP4	4.15×10^{-1}	-1.27×10^{0}	4.43×10^{-21}	1.46×10^{-18}
AFAP1.AS1	4.16×10^{-1}	-1.27×10^{0}	1.18×10^{-13}	7.97×10^{-12}
SAMD9L	4.19×10^{-1}	-1.25×10^{0}	8.86×10^{-22}	3.38×10^{-19}
AQP3	4.20×10^{-1}	-1.25×10^{0}	2.92×10^{-10}	9.16×10^{-9}
AGR2	4.22×10^{-1}	-1.25×10^{0}	3.84×10^{-14}	2.95×10^{-12}
AQP5	4.22×10^{-1}	-1.25×10^{0}	5.11×10^{-7}	7.05×10^{-6}
MYRF	4.22×10^{-1}	-1.24×10^{0}	1.01×10^{-14}	8.67×10^{-13}
HLA.DRA	4.22×10^{-1}	-1.24×10^{0}	5.58×10^{-12}	2.58×10^{-10}
OAS2	4.27×10^{-1}	-1.23×10^{0}	1.20×10^{-13}	8.05×10^{-12}
CXCR4	4.28×10^{-1}	-1.23×10^{0}	1.04×10^{-16}	1.37×10^{-14}
IL1R2	4.28×10^{-1}	-1.23×10^{0}	4.30×10^{-15}	3.95×10^{-13}
PRDM8	4.30×10^{-1}	-1.22×10^{0}	2.75×10^{-30}	5.08×10^{-27}
FFAR4	4.30×10^{-1}	-1.22×10^{0}	7.77×10^{-10}	2.19×10^{-8}
KRT7	4.30×10^{-1}	-1.22×10^{0}	5.97×10^{-15}	5.36×10^{-13}
KLK11	4.33×10^{-1}	-1.21×10^{0}	9.43×10^{-9}	2.07×10^{-7}
RN7SL3	4.33×10^{-1}	-1.21×10^{0}	3.95×10^{-7}	5.61×10^{-6}
CXCL11	4.33×10^{-1}	-1.21×10^{0}	2.97×10^{-8}	5.72×10^{-7}
NKG7	4.33×10^{-1}	-1.21×10^{0}	1.50×10^{-13}	9.89×10^{-12}
VNN2	4.34×10^{-1}	-1.20×10^{0}	2.84×10^{-21}	9.74×10^{-19}
GBP5	4.35×10^{-1}	-1.20×10^{0}	8.33×10^{-15}	7.26×10^{-13}
ANO1	4.35×10^{-1}	-1.20×10^{0}	3.66×10^{-14}	2.82×10^{-12}
GFI1	4.35×10^{-1}	-1.20×10^{0}	2.78×10^{-26}	2.79×10^{-23}

Table A.26 (continued). The list of the top 100 downregulated DEGs identified in the CS1 subtype using limma as a result of three clustering analyzes.

CXCL8	4.38×10^{-1}	-1.19×10^{0}	1.69×10^{-7}	2.67×10^{-6}
CREB3L1	4.39×10^{-1}	-1.19×10^{0}	6.03×10^{-10}	1.75×10^{-8}
HLA.DPA1	4.40×10^{-1}	-1.18×10^{0}	9.21×10^{-11}	3.23×10^{-9}
PTAFR	4.41×10^{-1}	-1.18×10^{0}	2.16×10^{-17}	3.32×10^{-15}
IGHG1	4.42×10^{-1}	-1.18×10^{0}	2.55×10^{-4}	1.18×10^{-3}
KCTD12	4.44×10^{-1}	-1.17×10^{0}	3.90×10^{-13}	2.32×10^{-11}
SPRR1A	4.44×10^{-1}	-1.17×10^{0}	2.29×10^{-6}	2.54×10^{-5}

HLA.DQA1	4.45×10^{-1}	-1.17×10^{0}	4.18×10^{-11}	1.58×10^{-9}
LINC02041	4.45×10^{-1}	-1.17×10^{0}	3.12×10^{-15}	2.97×10^{-13}
EVI2B	4.46×10^{-1}	-1.17×10^{0}	1.54×10^{-16}	1.98×10^{-14}
IGHV2.70	4.46×10^{-1}	-1.17×10^{0}	2.00×10^{-5}	1.45×10^{-4}
IDO1	4.46×10^{-1}	-1.17×10^{0}	3.07×10^{-9}	7.58×10^{-8}
AGR3	4.47×10^{-1}	-1.16×10^{0}	1.41×10^{-6}	1.68×10^{-5}
PTPRC	4.47×10^{-1}	-1.16×10^{0}	2.23×10^{-13}	1.41×10^{-11}
SEMG1	4.49×10^{-1}	-1.15×10^{0}	3.83×10^{-12}	1.84×10^{-10}
MMP12	4.53×10^{-1}	-1.14×10^{0}	1.83×10^{-7}	2.87×10^{-6}
SRGN	4.55×10^{-1}	-1.14×10^{0}	1.20×10^{-12}	6.34×10^{-11}
AP002498.1	4.55×10^{-1}	-1.14×10^{0}	1.38×10^{-10}	4.71×10^{-9}
IGLV3.1	4.55×10^{-1}	-1.14×10^{0}	5.78×10^{-4}	2.36×10^{-3}
IGHV1.69.2	4.55×10^{-1}	-1.14×10^{0}	7.02×10^{-5}	4.03×10^{-4}
LCK	4.56×10^{-1}	-1.13×10^{0}	2.27×10^{-14}	1.81×10^{-12}
AL121761.1	4.57×10^{-1}	-1.13×10^{0}	7.00×10^{-12}	3.17×10^{-10}
MMP1	4.57×10^{-1}	-1.13×10^{0}	1.47×10^{-5}	1.13×10^{-4}

Table A.27. The list of the top 100 upregulated DEGs identified in the CS2 subtype using limma as a result of three clustering analyzes.

	fc	**log2fc**	**pvalue**	**padj**
SFRP2	7.52×10^{0}	2.91×10^{0}	3.30×10^{-15}	1.11×10^{-13}
CCL18	6.55×10^{0}	2.71×10^{0}	7.54×10^{-20}	5.77×10^{-18}
CXCL13	5.83×10^{0}	2.54×10^{0}	2.62×10^{-27}	8.14×10^{-25}
CXCL9	5.38×10^{0}	2.43×10^{0}	5.27×10^{-21}	4.95×10^{-19}
IGHG1	4.85×10^{0}	2.28×10^{0}	1.04×10^{-9}	1.03×10^{-8}
COL10A1	4.79×10^{0}	2.26×10^{0}	1.62×10^{-14}	4.88×10^{-13}
CD163	4.78×10^{0}	2.26×10^{0}	1.26×10^{-27}	4.05×10^{-25}
FCGR3A	4.77×10^{0}	2.25×10^{0}	2.01×10^{-24}	3.53×10^{-22}
MRC1	4.58×10^{0}	2.19×10^{0}	6.87×10^{-29}	2.93×10^{-26}
GREM1	4.45×10^{0}	2.16×10^{0}	2.37×10^{-19}	1.68×10^{-17}
GPNMB	4.41×10^{0}	2.14×10^{0}	6.28×10^{-21}	5.83×10^{-19}
IGLV3.1	4.34×10^{0}	2.12×10^{0}	3.50×10^{-8}	2.28×10^{-7}
IGHV1.24	4.30×10^{0}	2.10×10^{0}	4.05×10^{-9}	3.36×10^{-8}
SPP1	4.28×10^{0}	2.10×10^{0}	3.56×10^{-10}	4.11×10^{-9}

Table A.27 (continued). The list of the top 100 upregulated DEGs identified in the CS2 subtype using limma as a result of three clustering analyzes.

POSTN	4.26×10^{0}	2.09×10^{0}	3.86×10^{-17}	1.84×10^{-15}
GAS1	4.25×10^{0}	2.09×10^{0}	1.14×10^{-23}	1.69×10^{-21}
GBP5	4.24×10^{0}	2.08×10^{0}	1.76×10^{-34}	2.96×10^{-31}
PTPRC	4.20×10^{0}	2.07×10^{0}	1.52×10^{-32}	1.53×10^{-29}
CYBB	4.18×10^{0}	2.06×10^{0}	4.97×10^{-28}	1.78×10^{-25}
ADAM12	4.17×10^{0}	2.06×10^{0}	6.61×10^{-26}	1.59×10^{-23}
IGHV1.69	4.17×10^{0}	2.06×10^{0}	4.13×10^{-10}	4.66×10^{-9}
THBS2	4.17×10^{0}	2.06×10^{0}	2.30×10^{-14}	6.70×10^{-13}

CCDC80	4.14×10^{0}	2.05×10^{0}	1.02×10^{-23}	1.53×10^{-21}
HLA.DQA1	4.13×10^{0}	2.05×10^{0}	7.82×10^{-25}	1.50×10^{-22}
IGHV5.51	4.11×10^{0}	2.04×10^{0}	1.42×10^{-7}	8.00×10^{-7}
GBP4	4.08×10^{0}	2.03×10^{0}	3.79×10^{-26}	9.73×10^{-24}
FN1	4.07×10^{0}	2.03×10^{0}	1.35×10^{-14}	4.11×10^{-13}
IGHV1.2	4.06×10^{0}	2.02×10^{0}	9.07×10^{-8}	5.35×10^{-7}
IGHV4.39	4.04×10^{0}	2.02×10^{0}	1.68×10^{-7}	9.31×10^{-7}
IGHV3.21	4.02×10^{0}	2.01×10^{0}	9.12×10^{-8}	5.37×10^{-7}
IGHV1.18	4.02×10^{0}	2.01×10^{0}	1.06×10^{-7}	6.13×10^{-7}
IGHV1.69D	4.01×10^{0}	2.00×10^{0}	1.66×10^{-8}	1.18×10^{-7}
SULF1	4.00×10^{0}	2.00×10^{0}	2.87×10^{-18}	1.68×10^{-16}
IGHV2.70	3.98×10^{0}	1.99×10^{0}	3.19×10^{-10}	3.75×10^{-9}
IGHV3.33	3.97×10^{0}	1.99×10^{0}	8.56×10^{-9}	6.55×10^{-8}
SPOCK1	3.96×10^{0}	1.98×10^{0}	7.32×10^{-20}	5.63×10^{-18}
FNDC1	3.94×10^{0}	1.98×10^{0}	4.16×10^{-16}	1.66×10^{-14}
IGLV3.19	3.93×10^{0}	1.98×10^{0}	7.06×10^{-8}	4.27×10^{-7}
CYP1B1	3.91×10^{0}	1.97×10^{0}	8.19×10^{-28}	2.76×10^{-25}
C3	3.91×10^{0}	1.97×10^{0}	2.22×10^{-14}	6.50×10^{-13}
IGHG3	3.90×10^{0}	1.96×10^{0}	1.59×10^{-8}	1.13×10^{-7}
MARCO	3.88×10^{0}	1.96×10^{0}	1.05×10^{-14}	3.28×10^{-13}
HLA.DOA	3.87×10^{0}	1.95×10^{0}	2.94×10^{-26}	7.64×10^{-24}
FPR3	3.86×10^{0}	1.95×10^{0}	6.70×10^{-25}	1.31×10^{-22}
IGHV3.30	3.84×10^{0}	1.94×10^{0}	4.54×10^{-8}	2.87×10^{-7}
IGHV2.5	3.80×10^{0}	1.93×10^{0}	2.84×10^{-7}	1.49×10^{-6}
IGLV3.25	3.80×10^{0}	1.93×10^{0}	3.54×10^{-7}	1.82×10^{-6}
IGLV2.14	3.79×10^{0}	1.92×10^{0}	4.24×10^{-7}	2.15×10^{-6}
CXCL10	3.78×10^{0}	1.92×10^{0}	2.95×10^{-14}	8.44×10^{-13}
CD109	3.78×10^{0}	1.92×10^{0}	7.63×10^{-26}	1.81×10^{-23}
OLR1	3.77×10^{0}	1.91×10^{0}	5.32×10^{-22}	5.98×10^{-20}
IGHV4.31	3.76×10^{0}	1.91×10^{0}	2.20×10^{-8}	1.51×10^{-7}
COL11A1	3.74×10^{0}	1.90×10^{0}	1.20×10^{-15}	4.40×10^{-14}
CCL13	3.73×10^{0}	1.90×10^{0}	1.15×10^{-18}	7.26×10^{-17}
IGLV3.21	3.73×10^{0}	1.90×10^{0}	5.47×10^{-7}	2.71×10^{-6}

Table A.27 (continued). The list of the top 100 upregulated DEGs identified in the CS2 subtype using limma as a result of three clustering analyzes.

PLEK	3.71×10^{0}	1.89×10^{0}	3.78×10^{-23}	5.06×10^{-21}
IGHV2.26	3.70×10^{0}	1.89×10^{0}	2.29×10^{-9}	2.05×10^{-8}
CCL19	3.68×10^{0}	1.88×10^{0}	2.07×10^{-13}	5.08×10^{-12}
MSR1	3.67×10^{0}	1.88×10^{0}	5.89×10^{-26}	1.43×10^{-23}
IGHV4.34	3.67×10^{0}	1.88×10^{0}	4.42×10^{-8}	2.81×10^{-7}
CD53	3.65×10^{0}	1.87×10^{0}	6.77×10^{-26}	1.62×10^{-23}
F13A1	3.64×10^{0}	1.86×10^{0}	7.71×10^{-19}	5.01×10^{-17}
HLA.DPA1	3.61×10^{0}	1.85×10^{0}	9.06×10^{-19}	5.84×10^{-17}
VSIG4	3.61×10^{0}	1.85×10^{0}	3.57×10^{-20}	2.89×10^{-18}

CILP	3.59×10^{0}	1.84×10^{0}	3.11×10^{-21}	3.01×10^{-19}
SRGN	3.58×10^{0}	1.84×10^{0}	3.11×10^{-24}	5.14×10^{-22}
IGHV3.11	3.56×10^{0}	1.83×10^{0}	3.64×10^{-7}	1.87×10^{-6}
PRRX1	3.55×10^{0}	1.83×10^{0}	9.64×10^{-26}	2.24×10^{-23}
IGHGP	3.55×10^{0}	1.83×10^{0}	5.31×10^{-7}	2.64×10^{-6}
PLN	3.54×10^{0}	1.82×10^{0}	4.13×10^{-18}	2.33×10^{-16}
EVI2B	3.53×10^{0}	1.82×10^{0}	2.03×10^{-30}	1.21×10^{-27}
SELL	3.49×10^{0}	1.80×10^{0}	9.23×10^{-28}	3.07×10^{-25}
IGLV6.57	3.46×10^{0}	1.79×10^{0}	1.31×10^{-6}	6.00×10^{-6}
FBN1	3.45×10^{0}	1.79×10^{0}	6.53×10^{-21}	6.03×10^{-19}
IGHV1.46	3.45×10^{0}	1.78×10^{0}	2.86×10^{-7}	1.50×10^{-6}
CCL21	3.44×10^{0}	1.78×10^{0}	3.18×10^{-9}	2.72×10^{-8}
IGHV1.69.2	3.44×10^{0}	1.78×10^{0}	9.69×10^{-8}	5.67×10^{-7}
COMP	3.44×10^{0}	1.78×10^{0}	1.11×10^{-8}	8.23×10^{-8}
SFRP4	3.43×10^{0}	1.78×10^{0}	1.43×10^{-8}	1.03×10^{-7}
VCAN	3.43×10^{0}	1.78×10^{0}	5.42×10^{-20}	4.24×10^{-18}
MS4A7	3.42×10^{0}	1.77×10^{0}	7.61×10^{-31}	5.01×10^{-28}
TNC	3.42×10^{0}	1.77×10^{0}	2.43×10^{-14}	7.05×10^{-13}
MPEG1	3.41×10^{0}	1.77×10^{0}	2.61×10^{-23}	3.61×10^{-21}
RAB31	3.41×10^{0}	1.77×10^{0}	3.61×10^{-22}	4.14×10^{-20}
IGHG4	3.40×10^{0}	1.77×10^{0}	2.21×10^{-6}	9.67×10^{-6}
IGHV3.23	3.38×10^{0}	1.76×10^{0}	2.27×10^{-6}	9.88×10^{-6}
IGKV1.12	3.38×10^{0}	1.76×10^{0}	7.16×10^{-8}	4.33×10^{-7}
COL8A1	3.38×10^{0}	1.76×10^{0}	2.05×10^{-16}	8.63×10^{-15}
COL6A3	3.37×10^{0}	1.75×10^{0}	3.54×10^{-18}	2.02×10^{-16}
IGKV4.1	3.37×10^{0}	1.75×10^{0}	4.39×10^{-6}	1.81×10^{-5}
CD84	3.37×10^{0}	1.75×10^{0}	3.22×10^{-35}	8.00×10^{-32}
LCP1	3.37×10^{0}	1.75×10^{0}	2.58×10^{-23}	3.58×10^{-21}
CSF2RB	3.36×10^{0}	1.75×10^{0}	3.51×10^{-27}	1.06×10^{-24}
PLXDC2	3.35×10^{0}	1.75×10^{0}	5.47×10^{-24}	8.66×10^{-22}
FYB1	3.34×10^{0}	1.74×10^{0}	1.50×10^{-35}	4.29×10^{-32}
MAFB	3.34×10^{0}	1.74×10^{0}	7.57×10^{-26}	1.80×10^{-23}

Table A.27 (continued). The list of the top 100 upregulated DEGs identified in the CS2 subtype using limma as a result of three clustering analyzes.

ASPN	3.34×10^{0}	1.74×10^{0}	1.82×10^{-12}	3.74×10^{-11}
IGKV3.15	3.33×10^{0}	1.74×10^{0}	1.24×10^{-6}	5.69×10^{-6}
HLA.DRA	3.33×10^{0}	1.74×10^{0}	1.10×10^{-16}	4.86×10^{-15}
FCGR2A	3.32×10^{0}	1.73×10^{0}	7.37×10^{-29}	3.12×10^{-26}

Table A.28. The list of the top 100 downregulated DEGs identified in the CS2 subtype using limma as a result of three clustering analyzes.

	fc	**log2fc**	**pvalue**	**padj**
FABP1	1.34×10^{-1}	-2.90×10^{0}	2.21×10^{-14}	6.49×10^{-13}
IHH	2.03×10^{-1}	-2.30×10^{0}	1.37×10^{-32}	1.42×10^{-29}

MEP1A	2.11×10^{-1}	-2.24×10^{0}	1.93×10^{-16}	8.19×10^{-15}
HMGCS2	2.19×10^{-1}	-2.19×10^{0}	6.49×10^{-10}	6.92×10^{-9}
PPP1R14D	2.26×10^{-1}	-2.15×10^{0}	8.24×10^{-29}	3.47×10^{-26}
FABP6	2.62×10^{-1}	-1.93×10^{0}	2.72×10^{-16}	1.12×10^{-14}
LYPD8	2.65×10^{-1}	-1.92×10^{0}	3.22×10^{-9}	2.75×10^{-8}
CDX2	2.66×10^{-1}	-1.91×10^{0}	1.87×10^{-28}	7.23×10^{-26}
DEFA6	2.68×10^{-1}	-1.90×10^{0}	1.80×10^{-5}	6.55×10^{-5}
PHGR1	2.70×10^{-1}	-1.89×10^{0}	4.92×10^{-20}	3.89×10^{-18}
DDC	2.70×10^{-1}	-1.89×10^{0}	4.53×10^{-20}	3.59×10^{-18}
NOX1	2.76×10^{-1}	-1.86×10^{0}	3.11×10^{-15}	1.05×10^{-13}
KRT20	2.78×10^{-1}	-1.85×10^{0}	3.17×10^{-10}	3.73×10^{-9}
CLDN3	2.83×10^{-1}	-1.82×10^{0}	3.23×10^{-25}	6.88×10^{-23}
AL354743.2	2.97×10^{-1}	-1.75×10^{0}	3.79×10^{-20}	3.06×10^{-18}
CHP2	3.02×10^{-1}	-1.73×10^{0}	6.39×10^{-9}	5.03×10^{-8}
SELENBP1	3.03×10^{-1}	-1.72×10^{0}	5.99×10^{-17}	2.75×10^{-15}
SPINK1	3.07×10^{-1}	-1.71×10^{0}	3.33×10^{-10}	3.89×10^{-9}
ISX	3.10×10^{-1}	-1.69×10^{0}	1.95×10^{-13}	4.80×10^{-12}
CKB	3.12×10^{-1}	-1.68×10^{0}	2.38×10^{-9}	2.11×10^{-8}
AC124067.4	3.23×10^{-1}	-1.63×10^{0}	7.27×10^{-20}	5.60×10^{-18}
FAM3D	3.28×10^{-1}	-1.61×10^{0}	1.48×10^{-13}	3.71×10^{-12}
GJB1	3.28×10^{-1}	-1.61×10^{0}	1.07×10^{-22}	1.34×10^{-20}
ARSL	3.28×10^{-1}	-1.61×10^{0}	1.69×10^{-11}	2.85×10^{-10}
PRR15	3.36×10^{-1}	-1.57×10^{0}	1.78×10^{-29}	8.50×10^{-27}
PRDX5	3.43×10^{-1}	-1.54×10^{0}	1.56×10^{-24}	2.82×10^{-22}
AZGP1	3.45×10^{-1}	-1.54×10^{0}	1.86×10^{-13}	4.60×10^{-12}
AL365226.1	3.47×10^{-1}	-1.53×10^{0}	1.72×10^{-5}	6.28×10^{-5}
URAD	3.48×10^{-1}	-1.52×10^{0}	1.03×10^{-6}	4.80×10^{-6}
OLFM4	3.48×10^{-1}	-1.52×10^{0}	3.25×10^{-3}	7.24×10^{-3}
HOXB9	3.51×10^{-1}	-1.51×10^{0}	1.18×10^{-9}	1.15×10^{-8}
HSD11B2	3.53×10^{-1}	-1.50×10^{0}	1.48×10^{-21}	1.53×10^{-19}
CDX1	3.53×10^{-1}	-1.50×10^{0}	9.25×10^{-22}	9.93×10^{-20}

Table A.28 (continued). The list of the top 100 downregulated DEGs identified in the CS2 subtype using limma as a result of three clustering analyzes.

CYP4F2	3.57×10^{-1}	-1.49×10^{0}	5.29×10^{-11}	7.91×10^{-10}
CEACAM7	3.58×10^{-1}	-1.48×10^{0}	5.32×10^{-5}	1.76×10^{-4}
GPX2	3.62×10^{-1}	-1.46×10^{0}	3.43×10^{-20}	2.79×10^{-18}
NR1I2	3.63×10^{-1}	-1.46×10^{0}	4.06×10^{-18}	2.30×10^{-16}
ID1	3.66×10^{-1}	-1.45×10^{0}	5.32×10^{-11}	7.94×10^{-10}
RETNLB	3.69×10^{-1}	-1.44×10^{0}	5.55×10^{-6}	2.24×10^{-5}
DEFA5	3.73×10^{-1}	-1.42×10^{0}	2.90×10^{-3}	6.54×10^{-3}
SLC39A4	3.75×10^{-1}	-1.41×10^{0}	4.86×10^{-19}	3.28×10^{-17}
SCAND1	3.77×10^{-1}	-1.41×10^{0}	1.36×10^{-18}	8.47×10^{-17}
RBBP8NL	3.79×10^{-1}	-1.40×10^{0}	1.16×10^{-24}	2.15×10^{-22}
SGK2	3.79×10^{-1}	-1.40×10^{0}	2.06×10^{-18}	1.24×10^{-16}

GUCA2A	3.80×10^{-1}	-1.40×10^{0}	1.05×10^{-5}	4.01×10^{-5}
FAM3B	3.80×10^{-1}	-1.39×10^{0}	4.71×10^{-6}	1.93×10^{-5}
ROMO1	3.80×10^{-1}	-1.39×10^{0}	1.97×10^{-20}	1.65×10^{-18}
SMIM24	3.82×10^{-1}	-1.39×10^{0}	7.24×10^{-12}	1.33×10^{-10}
STYXL2	3.83×10^{-1}	-1.38×10^{0}	6.52×10^{-4}	1.71×10^{-3}
AL162413.1	3.85×10^{-1}	-1.38×10^{0}	9.80×10^{-6}	3.76×10^{-5}
C4orf48	3.85×10^{-1}	-1.38×10^{0}	5.63×10^{-15}	1.84×10^{-13}
CDHR5	3.87×10^{-1}	-1.37×10^{0}	2.31×10^{-15}	8.06×10^{-14}
AC097493.3	3.89×10^{-1}	-1.36×10^{0}	1.04×10^{-11}	1.85×10^{-10}
DUOXA2	3.89×10^{-1}	-1.36×10^{0}	2.40×10^{-5}	8.51×10^{-5}
MUC20P1	3.89×10^{-1}	-1.36×10^{0}	3.28×10^{-15}	1.11×10^{-13}
NXPE4	3.92×10^{-1}	-1.35×10^{0}	5.11×10^{-5}	1.69×10^{-4}
AOC1	3.92×10^{-1}	-1.35×10^{0}	3.26×10^{-17}	1.59×10^{-15}
KCNQ1	3.93×10^{-1}	-1.35×10^{0}	1.71×10^{-16}	7.34×10^{-15}
AC124067.2	3.97×10^{-1}	-1.33×10^{0}	4.52×10^{-16}	1.80×10^{-14}
SMIM22	4.01×10^{-1}	-1.32×10^{0}	1.84×10^{-23}	2.65×10^{-21}
KIF12	4.02×10^{-1}	-1.31×10^{0}	8.83×10^{-14}	2.30×10^{-12}
LINC02747	4.03×10^{-1}	-1.31×10^{0}	2.01×10^{-16}	8.49×10^{-15}
SNHG18	4.07×10^{-1}	-1.30×10^{0}	2.52×10^{-18}	1.48×10^{-16}
SHD	4.07×10^{-1}	-1.30×10^{0}	3.39×10^{-23}	4.58×10^{-21}
MUC20	4.07×10^{-1}	-1.30×10^{0}	1.65×10^{-17}	8.36×10^{-16}
TM4SF5	4.07×10^{-1}	-1.30×10^{0}	5.27×10^{-11}	7.88×10^{-10}
PRSS8	4.07×10^{-1}	-1.30×10^{0}	3.00×10^{-20}	2.46×10^{-18}
DEFB1	4.11×10^{-1}	-1.28×10^{0}	1.68×10^{-7}	9.31×10^{-7}
TFF3	4.12×10^{-1}	-1.28×10^{0}	6.14×10^{-8}	3.76×10^{-7}
CDH17	4.12×10^{-1}	-1.28×10^{0}	6.01×10^{-17}	2.75×10^{-15}
WNK4	4.12×10^{-1}	-1.28×10^{0}	2.55×10^{-15}	8.82×10^{-14}
PPDPF	4.12×10^{-1}	-1.28×10^{0}	1.71×10^{-18}	1.04×10^{-16}
RNF186	4.13×10^{-1}	-1.28×10^{0}	7.40×10^{-10}	7.75×10^{-9}
GGT6	4.14×10^{-1}	-1.27×10^{0}	3.86×10^{-9}	3.22×10^{-8}

Table A.28 (continued). The list of the top 100 downregulated DEGs identified in the CS2 subtype using limma as a result of three clustering analyzes.

TRAPPC6A	4.15×10^{-1}	-1.27×10^{0}	5.38×10^{-21}	5.04×10^{-19}
RXFP4	4.21×10^{-1}	-1.25×10^{0}	5.14×10^{-20}	4.04×10^{-18}
PIGZ	4.24×10^{-1}	-1.24×10^{0}	7.75×10^{-14}	2.05×10^{-12}
AL035661.1	4.25×10^{-1}	-1.24×10^{0}	5.00×10^{-16}	1.98×10^{-14}
H2AJ	4.25×10^{-1}	-1.23×10^{0}	1.39×10^{-16}	5.99×10^{-15}
GUCY2C	4.27×10^{-1}	-1.23×10^{0}	2.91×10^{-14}	8.33×10^{-13}
B3GNT8	4.30×10^{-1}	-1.22×10^{0}	2.31×10^{-18}	1.37×10^{-16}
COMTD1	4.30×10^{-1}	-1.22×10^{0}	4.04×10^{-19}	2.77×10^{-17}
LGALS4	4.34×10^{-1}	-1.21×10^{0}	3.36×10^{-17}	1.63×10^{-15}
PPP1R1B	4.34×10^{-1}	-1.20×10^{0}	2.24×10^{-17}	1.12×10^{-15}
PLA2G4F	4.35×10^{-1}	-1.20×10^{0}	2.78×10^{-16}	1.14×10^{-14}
AL390719.2	4.37×10^{-1}	-1.20×10^{0}	2.20×10^{-13}	5.36×10^{-12}

MRPL12	4.37×10^{-1}	-1.19×10^{0}	7.35×10^{-14}	1.95×10^{-12}
AC103702.2	4.37×10^{-1}	-1.19×10^{0}	9.64×10^{-10}	9.68×10^{-9}
AC106876.1	4.39×10^{-1}	-1.19×10^{0}	1.83×10^{-24}	3.25×10^{-22}
FAAH	4.40×10^{-1}	-1.18×10^{0}	1.83×10^{-24}	3.25×10^{-22}
EPS8L3	4.41×10^{-1}	-1.18×10^{0}	1.21×10^{-20}	1.06×10^{-18}
TMEM211	4.41×10^{-1}	-1.18×10^{0}	6.15×10^{-8}	3.77×10^{-7}
CCL20	4.41×10^{-1}	-1.18×10^{0}	4.97×10^{-8}	3.12×10^{-7}
PNLIPRP2	4.42×10^{-1}	-1.18×10^{0}	1.81×10^{-8}	1.27×10^{-7}
GPA33	4.42×10^{-1}	-1.18×10^{0}	2.75×10^{-11}	4.43×10^{-10}
AL137785.1	4.45×10^{-1}	-1.17×10^{0}	8.82×10^{-11}	1.23×10^{-9}
SPIRE2	4.45×10^{-1}	-1.17×10^{0}	4.66×10^{-26}	1.18×10^{-23}
EXOSC5	4.46×10^{-1}	-1.16×10^{0}	1.23×10^{-20}	1.08×10^{-18}
DUOX2	4.48×10^{-1}	-1.16×10^{0}	3.78×10^{-4}	1.04×10^{-3}
ALKBH7	4.48×10^{-1}	-1.16×10^{0}	1.71×10^{-16}	7.35×10^{-15}

Table A.29. The list of the top 65 upregulated DEGs identified in the CS3 subtype using limma as a result of three clustering analyzes.

	fc	**log2fc**	**pvalue**	**padj**
REG1A	6.59×10^{0}	2.72×10^{0}	5.35×10^{-6}	1.55×10^{-4}
TFF1	6.45×10^{0}	2.69×10^{0}	6.41×10^{-13}	8.73×10^{-10}
SPINK4	5.69×10^{0}	2.51×10^{0}	1.36×10^{-6}	5.24×10^{-5}
TFF2	4.91×10^{0}	2.30×10^{0}	4.28×10^{-10}	1.03×10^{-7}
MUC2	4.87×10^{0}	2.28×10^{0}	1.16×10^{-6}	4.62×10^{-5}
REG3A	4.51×10^{0}	2.17×10^{0}	1.04×10^{-5}	2.62×10^{-4}
FCGBP	4.34×10^{0}	2.12×10^{0}	5.05×10^{-7}	2.43×10^{-5}
SPDEF	4.25×10^{0}	2.09×10^{0}	3.57×10^{-11}	1.53×10^{-8}
CA9	3.82×10^{0}	1.93×10^{0}	1.81×10^{-7}	1.11×10^{-5}
PIGR	3.78×10^{0}	1.92×10^{0}	8.91×10^{-5}	1.46×10^{-3}
TM4SF4	3.77×10^{0}	1.91×10^{0}	1.62×10^{-10}	4.95×10^{-8}

Table A.29 (continued). The list of the top 65 upregulated DEGs identified in the CS3 subtype using limma as a result of three clustering analyzes.

AGR3	3.69×10^{0}	1.88×10^{0}	1.48×10^{-9}	2.73×10^{-7}
AGR2	3.54×10^{0}	1.82×10^{0}	1.01×10^{-17}	2.88×10^{-13}
REG1B	3.46×10^{0}	1.79×10^{0}	7.71×10^{-5}	1.30×10^{-3}
FFAR4	3.29×10^{0}	1.72×10^{0}	2.60×10^{-11}	1.21×10^{-8}
KLK11	3.14×10^{0}	1.65×10^{0}	1.74×10^{-9}	3.07×10^{-7}
KLK12	2.95×10^{0}	1.56×10^{0}	7.24×10^{-10}	1.58×10^{-7}
PRSS2	2.92×10^{0}	1.55×10^{0}	5.35×10^{-4}	6.13×10^{-3}
GP2	2.90×10^{0}	1.53×10^{0}	2.56×10^{-11}	1.21×10^{-8}
CREB3L1	2.88×10^{0}	1.53×10^{0}	1.30×10^{-9}	2.47×10^{-7}
GCNT3	2.84×10^{0}	1.51×10^{0}	1.11×10^{-7}	7.66×10^{-6}
MLPH	2.82×10^{0}	1.50×10^{0}	3.17×10^{-10}	8.10×10^{-8}
DMBT1	2.71×10^{0}	1.44×10^{0}	7.82×10^{-4}	8.31×10^{-3}
MUC5B	2.70×10^{0}	1.43×10^{0}	1.95×10^{-4}	2.77×10^{-3}

BARX2	2.65×10^{0}	1.41×10^{0}	6.85×10^{-11}	2.63×10^{-8}
ATOH1	2.65×10^{0}	1.41×10^{0}	1.16×10^{-5}	2.85×10^{-4}
LCN2	2.58×10^{0}	1.37×10^{0}	4.60×10^{-5}	8.61×10^{-4}
L1TD1	2.57×10^{0}	1.36×10^{0}	2.73×10^{-4}	3.60×10^{-3}
HYAL1	2.55×10^{0}	1.35×10^{0}	2.77×10^{-8}	2.66×10^{-6}
RAB26	2.54×10^{0}	1.34×10^{0}	3.81×10^{-12}	3.07×10^{-9}
ZBTB7C	2.50×10^{0}	1.32×10^{0}	4.63×10^{-10}	1.09×10^{-7}
HEPACAM2	2.47×10^{0}	1.30×10^{0}	5.10×10^{-5}	9.36×10^{-4}
SPRR1A	2.44×10^{0}	1.29×10^{0}	8.01×10^{-5}	1.34×10^{-3}
SMIM31	2.43×10^{0}	1.28×10^{0}	2.34×10^{-11}	1.16×10^{-8}
AC005256.1	2.36×10^{0}	1.24×10^{0}	2.85×10^{-13}	4.29×10^{-10}
PLAC8	2.36×10^{0}	1.24×10^{0}	3.38×10^{-6}	1.08×10^{-4}
AKR1B10	2.35×10^{0}	1.23×10^{0}	5.94×10^{-5}	1.05×10^{-3}
LINC02489	2.34×10^{0}	1.23×10^{0}	2.86×10^{-12}	2.55×10^{-9}
ST6GALNAC1	2.31×10^{0}	1.21×10^{0}	3.45×10^{-6}	1.10×10^{-4}
LINC00261	2.31×10^{0}	1.21×10^{0}	1.83×10^{-5}	4.10×10^{-4}
B3GNT6	2.27×10^{0}	1.18×10^{0}	6.45×10^{-4}	7.11×10^{-3}
TSPAN1	2.26×10^{0}	1.17×10^{0}	7.02×10^{-9}	9.09×10^{-7}
NOS2	2.25×10^{0}	1.17×10^{0}	4.90×10^{-5}	9.07×10^{-4}
LRRC26	2.24×10^{0}	1.16×10^{0}	3.43×10^{-6}	1.10×10^{-4}
TFF3	2.24×10^{0}	1.16×10^{0}	1.06×10^{-5}	2.66×10^{-4}
CHST4	2.21×10^{0}	1.14×10^{0}	5.88×10^{-6}	1.68×10^{-4}
ALDH1L1	2.21×10^{0}	1.14×10^{0}	6.51×10^{-7}	2.94×10^{-5}
ANG	2.20×10^{0}	1.14×10^{0}	1.78×10^{-14}	3.77×10^{-11}
RHOV	2.19×10^{0}	1.13×10^{0}	3.01×10^{-8}	2.82×10^{-6}
RAP1GAP	2.17×10^{0}	1.12×10^{0}	1.36×10^{-7}	8.95×10^{-6}
AKR7A3	2.16×10^{0}	1.11×10^{0}	2.07×10^{-12}	2.21×10^{-9}

Table A.29 (continued). The list of the top 65 upregulated DEGs identified in the CS3 subtype using limma as a result of three clustering analyzes.

CAPN9	2.14×10^{0}	1.10×10^{0}	1.66×10^{-5}	3.79×10^{-4}
S100A14	2.14×10^{0}	1.10×10^{0}	3.65×10^{-10}	9.03×10^{-8}
S100P	2.10×10^{0}	1.07×10^{0}	2.65×10^{-6}	9.04×10^{-5}
C4BPB	2.09×10^{0}	1.06×10^{0}	1.00×10^{-8}	1.20×10^{-6}
C11orf86	2.09×10^{0}	1.06×10^{0}	1.86×10^{-5}	4.13×10^{-4}
DEGS2	2.09×10^{0}	1.06×10^{0}	2.90×10^{-8}	2.75×10^{-6}
KLK1	2.08×10^{0}	1.06×10^{0}	9.49×10^{-6}	2.44×10^{-4}
PDZK1IP1	2.06×10^{0}	1.05×10^{0}	8.56×10^{-7}	3.64×10^{-5}
NEURL1	2.06×10^{0}	1.04×10^{0}	5.44×10^{-6}	1.57×10^{-4}
SERPINA1	2.06×10^{0}	1.04×10^{0}	2.70×10^{-4}	3.57×10^{-3}
FABP2	2.05×10^{0}	1.04×10^{0}	1.17×10^{-4}	1.83×10^{-3}
MRAP2	2.03×10^{0}	1.02×10^{0}	2.27×10^{-7}	1.32×10^{-5}
HSD17B2	2.02×10^{0}	1.02×10^{0}	1.85×10^{-8}	1.95×10^{-6}
C2CD4A	2.01×10^{0}	1.01×10^{0}	9.36×10^{-6}	2.41×10^{-4}

Table A.30. The list of the top 100 downregulated DEGs identified in the CS3 subtype using limma as a result of three clustering analyzes.

	fc	log2fc	pvalue	padj
SFRP4	2.22×10^{-1}	-2.17×10^{0}	3.00×10^{-10}	7.82×10^{-8}
COMP	2.37×10^{-1}	-2.08×10^{0}	1.62×10^{-9}	2.93×10^{-7}
CES1	2.77×10^{-1}	-1.85×10^{0}	1.97×10^{-9}	3.38×10^{-7}
PRELP	3.40×10^{-1}	-1.56×10^{0}	5.15×10^{-9}	6.98×10^{-7}
DES	3.43×10^{-1}	-1.55×10^{0}	3.72×10^{-4}	4.61×10^{-3}
MPP1	3.47×10^{-1}	-1.53×10^{0}	1.11×10^{-16}	1.06×10^{-12}
CCL21	3.51×10^{-1}	-1.51×10^{0}	7.93×10^{-6}	2.13×10^{-4}
MYH11	3.56×10^{-1}	-1.49×10^{0}	2.78×10^{-6}	9.33×10^{-5}
ASPN	3.58×10^{-1}	-1.48×10^{0}	1.03×10^{-7}	7.26×10^{-6}
FBLN1	3.65×10^{-1}	-1.45×10^{0}	3.18×10^{-9}	4.78×10^{-7}
ELN	3.66×10^{-1}	-1.45×10^{0}	6.59×10^{-11}	2.55×10^{-8}
EFEMP1	3.66×10^{-1}	-1.45×10^{0}	1.22×10^{-9}	2.35×10^{-7}
SRPX2	3.71×10^{-1}	-1.43×10^{0}	8.47×10^{-11}	3.00×10^{-8}
NPTX2	3.74×10^{-1}	-1.42×10^{0}	9.50×10^{-6}	2.44×10^{-4}
CHRDL1	3.74×10^{-1}	-1.42×10^{0}	1.04×10^{-7}	7.29×10^{-6}
PTGIS	3.74×10^{-1}	-1.42×10^{0}	9.80×10^{-10}	2.01×10^{-7}
RBP1	3.75×10^{-1}	-1.42×10^{0}	4.03×10^{-8}	3.49×10^{-6}
MFAP4	3.78×10^{-1}	-1.40×10^{0}	3.13×10^{-8}	2.90×10^{-6}
ZCCHC24	3.84×10^{-1}	-1.38×10^{0}	8.75×10^{-15}	2.51×10^{-11}
HSPB6	3.86×10^{-1}	-1.37×10^{0}	1.54×10^{-9}	2.81×10^{-7}
SLC6A6	3.88×10^{-1}	-1.37×10^{0}	3.64×10^{-18}	2.08×10^{-13}
TIMP3	3.93×10^{-1}	-1.35×10^{0}	2.25×10^{-10}	6.32×10^{-8}
IGFBP5	3.96×10^{-1}	-1.34×10^{0}	4.74×10^{-8}	3.93×10^{-6}

Table A.30 (continued). The list of the top 100 downregulated DEGs identified in the CS3 subtype using limma as a result of three clustering analyzes.

SMOC2	4.00×10^{-1}	-1.32×10^{0}	7.08×10^{-7}	3.14×10^{-5}
MGP	4.02×10^{-1}	-1.32×10^{0}	2.01×10^{-7}	1.21×10^{-5}
CHRDL2	4.02×10^{-1}	-1.31×10^{0}	8.63×10^{-6}	2.27×10^{-4}
ZNF853	4.03×10^{-1}	-1.31×10^{0}	1.08×10^{-15}	4.77×10^{-12}
ST6GAL1	4.09×10^{-1}	-1.29×10^{0}	2.58×10^{-11}	1.21×10^{-8}
ANTXR1	4.11×10^{-1}	-1.28×10^{0}	2.02×10^{-7}	1.21×10^{-5}
RAI2	4.15×10^{-1}	-1.27×10^{0}	2.82×10^{-11}	1.28×10^{-8}
STRA6	4.16×10^{-1}	-1.27×10^{0}	6.25×10^{-10}	1.40×10^{-7}
TMEM150C	4.20×10^{-1}	-1.25×10^{0}	4.15×10^{-12}	3.21×10^{-9}
CPE	4.20×10^{-1}	-1.25×10^{0}	1.46×10^{-6}	5.54×10^{-5}
APOD	4.27×10^{-1}	-1.23×10^{0}	1.29×10^{-5}	3.10×10^{-4}
CST1	4.27×10^{-1}	-1.23×10^{0}	9.17×10^{-4}	9.41×10^{-3}
CNN1	4.35×10^{-1}	-1.20×10^{0}	5.60×10^{-5}	1.01×10^{-3}
HSPB7	4.36×10^{-1}	-1.20×10^{0}	4.02×10^{-7}	2.05×10^{-5}
KLF7	4.36×10^{-1}	-1.20×10^{0}	5.19×10^{-17}	8.69×10^{-13}
ACTG2	4.37×10^{-1}	-1.20×10^{0}	1.12×10^{-4}	1.77×10^{-3}

FARP1	4.37×10^{-1}	-1.19×10^{0}	6.07×10^{-17}	8.69×10^{-13}
NINL	4.37×10^{-1}	-1.19×10^{0}	1.39×10^{-10}	4.39×10^{-8}
INHBB	4.39×10^{-1}	-1.19×10^{0}	3.77×10^{-8}	3.37×10^{-6}
COL14A1	4.39×10^{-1}	-1.19×10^{0}	4.33×10^{-8}	3.68×10^{-6}
APOLD1	4.39×10^{-1}	-1.19×10^{0}	7.95×10^{-8}	5.92×10^{-6}
SLC26A2	4.40×10^{-1}	-1.18×10^{0}	1.51×10^{-5}	3.51×10^{-4}
NES	4.41×10^{-1}	-1.18×10^{0}	6.25×10^{-12}	4.43×10^{-9}
PODN	4.42×10^{-1}	-1.18×10^{0}	5.99×10^{-9}	7.98×10^{-7}
SYNM	4.43×10^{-1}	-1.18×10^{0}	2.67×10^{-6}	9.08×10^{-5}
LRRC15	4.43×10^{-1}	-1.17×10^{0}	6.08×10^{-8}	4.78×10^{-6}
FIBIN	4.43×10^{-1}	-1.17×10^{0}	8.30×10^{-9}	1.03×10^{-6}
SYNPO2	4.44×10^{-1}	-1.17×10^{0}	1.47×10^{-6}	5.59×10^{-5}
LMOD1	4.44×10^{-1}	-1.17×10^{0}	1.95×10^{-6}	7.03×10^{-5}
MOXD1	4.45×10^{-1}	-1.17×10^{0}	4.71×10^{-10}	1.11×10^{-7}
MYL9	4.48×10^{-1}	-1.16×10^{0}	4.07×10^{-7}	2.07×10^{-5}
THBS4	4.48×10^{-1}	-1.16×10^{0}	5.02×10^{-6}	1.48×10^{-4}
MMP11	4.48×10^{-1}	-1.16×10^{0}	1.22×10^{-5}	2.96×10^{-4}
ISLR	4.49×10^{-1}	-1.16×10^{0}	3.44×10^{-6}	1.10×10^{-4}
SORBS1	4.49×10^{-1}	-1.15×10^{0}	6.56×10^{-10}	1.45×10^{-7}
ARL11	4.51×10^{-1}	-1.15×10^{0}	8.48×10^{-11}	3.00×10^{-8}
ALKAL1	4.54×10^{-1}	-1.14×10^{0}	7.74×10^{-9}	9.81×10^{-7}
DPT	4.55×10^{-1}	-1.14×10^{0}	2.88×10^{-7}	1.58×10^{-5}
SALL4	4.55×10^{-1}	-1.14×10^{0}	6.72×10^{-13}	8.95×10^{-10}
CARD11	4.55×10^{-1}	-1.14×10^{0}	3.51×10^{-6}	1.11×10^{-4}
EMB	4.58×10^{-1}	-1.13×10^{0}	2.44×10^{-6}	8.43×10^{-5}

Table A.30 (continued). The list of the top 100 downregulated DEGs identified in the CS3 subtype using limma as a result of three clustering analyzes.

COL8A2	4.58×10^{-1}	-1.13×10^{0}	1.74×10^{-8}	1.84×10^{-6}
VSTM2L	4.58×10^{-1}	-1.13×10^{0}	2.87×10^{-6}	9.57×10^{-5}
L1CAM	4.58×10^{-1}	-1.13×10^{0}	1.38×10^{-6}	5.30×10^{-5}
SSC5D	4.59×10^{-1}	-1.12×10^{0}	1.12×10^{-7}	7.72×10^{-6}
AEBP1	4.61×10^{-1}	-1.12×10^{0}	1.48×10^{-5}	3.46×10^{-4}
RBMS1	4.62×10^{-1}	-1.11×10^{0}	7.05×10^{-12}	4.76×10^{-9}
PLTP	4.63×10^{-1}	-1.11×10^{0}	3.53×10^{-7}	1.85×10^{-5}
PCDHGC3	4.64×10^{-1}	-1.11×10^{0}	9.89×10^{-11}	3.41×10^{-8}
NFATC2	4.64×10^{-1}	-1.11×10^{0}	6.94×10^{-15}	2.21×10^{-11}
MYLK	4.65×10^{-1}	-1.10×10^{0}	1.41×10^{-7}	9.22×10^{-6}
FNBP1	4.67×10^{-1}	-1.10×10^{0}	1.48×10^{-14}	3.52×10^{-11}
C1S	4.67×10^{-1}	-1.10×10^{0}	5.19×10^{-7}	2.49×10^{-5}
PALM	4.67×10^{-1}	-1.10×10^{0}	1.45×10^{-10}	4.51×10^{-8}
OLFML3	4.67×10^{-1}	-1.10×10^{0}	4.88×10^{-9}	6.73×10^{-7}
RGS5	4.68×10^{-1}	-1.10×10^{0}	2.12×10^{-9}	3.50×10^{-7}
EPM2AIP1	4.68×10^{-1}	-1.09×10^{0}	2.36×10^{-13}	3.85×10^{-10}

TSPOAP1.AS1	4.69×10^{-1}	-1.09×10^{0}	1.53×10^{-11}	8.65×10^{-9}
ISM1	4.70×10^{-1}	-1.09×10^{0}	2.59×10^{-9}	4.09×10^{-7}
ANKRD10.IT1	4.71×10^{-1}	-1.09×10^{0}	3.27×10^{-8}	3.01×10^{-6}
ACKR1	4.71×10^{-1}	-1.09×10^{0}	3.50×10^{-5}	6.88×10^{-4}
MAB21L2	4.74×10^{-1}	-1.08×10^{0}	4.14×10^{-8}	3.56×10^{-6}
PLA1A	4.75×10^{-1}	-1.08×10^{0}	3.10×10^{-9}	4.69×10^{-7}
DAB2	4.76×10^{-1}	-1.07×10^{0}	1.54×10^{-14}	3.52×10^{-11}
PDE3A	4.76×10^{-1}	-1.07×10^{0}	2.95×10^{-8}	2.78×10^{-6}
SMO	4.78×10^{-1}	-1.07×10^{0}	2.48×10^{-10}	6.75×10^{-8}
ITGA11	4.78×10^{-1}	-1.07×10^{0}	7.30×10^{-7}	3.21×10^{-5}
RTL8C	4.79×10^{-1}	-1.06×10^{0}	2.06×10^{-8}	2.13×10^{-6}
IGF2	4.80×10^{-1}	-1.06×10^{0}	6.33×10^{-4}	7.01×10^{-3}
CAMK1D	4.81×10^{-1}	-1.06×10^{0}	1.16×10^{-9}	2.26×10^{-7}
CAPN6	4.81×10^{-1}	-1.05×10^{0}	5.96×10^{-4}	6.69×10^{-3}
DCN	4.82×10^{-1}	-1.05×10^{0}	8.53×10^{-6}	2.25×10^{-4}
PIP4P2	4.82×10^{-1}	-1.05×10^{0}	1.05×10^{-16}	1.06×10^{-12}
SHISA4	4.83×10^{-1}	-1.05×10^{0}	1.19×10^{-11}	7.17×10^{-9}
FRG1CP	4.83×10^{-1}	-1.05×10^{0}	7.63×10^{-7}	3.32×10^{-5}
HCG11	4.86×10^{-1}	-1.04×10^{0}	2.73×10^{-10}	7.27×10^{-8}
CYP27A1	4.86×10^{-1}	-1.04×10^{0}	2.97×10^{-8}	2.80×10^{-6}

Table A.31. The list of the top 100 upregulated DEGs identified in the CS1 subtype using edgeR as a result of four clustering analyzes.

	fc	**log2fc**	**pvalue**	**padj**
KRT14	1.13×10^{2}	6.82×10^{0}	3.53×10^{-51}	8.15×10^{-48}
TFAP2B	9.77×10^{1}	6.61×10^{0}	5.16×10^{-21}	2.39×10^{-19}
SERPINB13	5.52×10^{1}	5.79×10^{0}	9.98×10^{-13}	2.40×10^{-11}
CRCT1	5.18×10^{1}	5.69×10^{0}	9.57×10^{-17}	3.13×10^{-15}
SPRR2C	4.16×10^{1}	5.38×10^{0}	1.02×10^{-10}	2.04×10^{-9}
UNCX	4.09×10^{1}	5.36×10^{0}	1.46×10^{-13}	3.74×10^{-12}
SPRR2E	4.02×10^{1}	5.33×10^{0}	5.75×10^{-17}	1.92×10^{-15}
KRTAP4.6	3.58×10^{1}	5.16×10^{0}	8.50×10^{-8}	1.17×10^{-6}
KRT78	3.31×10^{1}	5.05×10^{0}	4.58×10^{-32}	5.71×10^{-30}
SPRR2B	2.91×10^{1}	4.86×10^{0}	4.13×10^{-6}	3.97×10^{-5}
NEUROD4	2.56×10^{1}	4.68×10^{0}	7.06×10^{-7}	8.17×10^{-6}
SBK2	2.53×10^{1}	4.66×10^{0}	8.30×10^{-24}	4.79×10^{-22}
TFAP2D	2.50×10^{1}	4.65×10^{0}	1.06×10^{-5}	9.11×10^{-5}
LEP	2.41×10^{1}	4.59×10^{0}	2.78×10^{-41}	1.10×10^{-38}
LHX3	2.38×10^{1}	4.57×10^{0}	4.42×10^{-30}	4.55×10^{-28}
HRH3	2.29×10^{1}	4.52×10^{0}	2.35×10^{-24}	1.45×10^{-22}
TRARG1	2.29×10^{1}	4.51×10^{0}	6.97×10^{-24}	4.09×10^{-22}

LINC00661	2.28×10^{1}	4.51×10^{0}	5.48×10^{-11}	1.13×10^{-9}
CNGA3	2.26×10^{1}	4.50×10^{0}	7.44×10^{-70}	2.13×10^{-65}
ANXA8	2.15×10^{1}	4.43×10^{0}	1.54×10^{-34}	2.49×10^{-32}
CRNN	2.14×10^{1}	4.42×10^{0}	2.03×10^{-7}	2.61×10^{-6}
ADIPOQ	2.03×10^{1}	4.34×10^{0}	3.57×10^{-12}	8.19×10^{-11}
ANXA8L1	1.99×10^{1}	4.31×10^{0}	5.47×10^{-23}	2.98×10^{-21}
LCE3D	1.85×10^{1}	4.21×10^{0}	3.06×10^{-5}	2.31×10^{-4}
PSG9	1.81×10^{1}	4.18×10^{0}	1.90×10^{-13}	4.82×10^{-12}
PPP1R17	1.81×10^{1}	4.18×10^{0}	6.28×10^{-14}	1.66×10^{-12}
LINC01831	1.77×10^{1}	4.14×10^{0}	1.69×10^{-3}	7.08×10^{-3}
NNAT	1.76×10^{1}	4.14×10^{0}	4.01×10^{-81}	2.30×10^{-76}
FABP4	1.69×10^{1}	4.08×10^{0}	1.15×10^{-40}	4.18×10^{-38}
KRT5	1.67×10^{1}	4.06×10^{0}	2.51×10^{-23}	1.39×10^{-21}
KRT6A	1.63×10^{1}	4.03×10^{0}	2.52×10^{-29}	2.39×10^{-27}
PCSK2	1.62×10^{1}	4.02×10^{0}	6.93×10^{-41}	2.61×10^{-38}
CHST8	1.61×10^{1}	4.01×10^{0}	1.73×10^{-52}	4.95×10^{-49}
CACNG7	1.61×10^{1}	4.01×10^{0}	1.59×10^{-37}	3.78×10^{-35}
IL36A	1.61×10^{1}	4.01×10^{0}	5.66×10^{-16}	1.76×10^{-14}
ARHGAP36	1.55×10^{1}	3.96×10^{0}	4.37×10^{-28}	3.71×10^{-26}
TBX5.AS1	1.48×10^{1}	3.89×10^{0}	3.13×10^{-24}	1.90×10^{-22}
CIDEA	1.42×10^{1}	3.82×10^{0}	1.34×10^{-9}	2.39×10^{-8}
MYOC	1.40×10^{1}	3.80×10^{0}	3.99×10^{-25}	2.64×10^{-23}
LCE3E	1.35×10^{1}	3.75×10^{0}	3.98×10^{-6}	3.85×10^{-5}

Table A.31 (continued). The list of the top 100 upregulated DEGs identified in the CS1 subtype using edgeR as a result of four clustering analyzes.

PROK1	1.34×10^{1}	3.74×10^{0}	4.69×10^{-21}	2.18×10^{-19}
PLIN4	1.31×10^{1}	3.71×10^{0}	5.53×10^{-41}	2.11×10^{-38}
C8orf86	1.28×10^{1}	3.68×10^{0}	5.09×10^{-9}	8.39×10^{-8}
KRT6C	1.28×10^{1}	3.67×10^{0}	4.05×10^{-21}	1.89×10^{-19}
GPR50	1.26×10^{1}	3.65×10^{0}	2.22×10^{-9}	3.84×10^{-8}
ATP2B3	1.24×10^{1}	3.64×10^{0}	1.34×10^{-35}	2.41×10^{-33}
IVL	1.24×10^{1}	3.63×10^{0}	1.98×10^{-9}	3.45×10^{-8}
ARL14EPL	1.23×10^{1}	3.62×10^{0}	1.09×10^{-12}	2.61×10^{-11}
DPYSL5	1.21×10^{1}	3.59×10^{0}	1.49×10^{-34}	2.42×10^{-32}
PLIN1	1.18×10^{1}	3.56×10^{0}	1.43×10^{-42}	6.67×10^{-40}
TCF23	1.17×10^{1}	3.55×10^{0}	1.33×10^{-40}	4.74×10^{-38}
CER1	1.13×10^{1}	3.50×10^{0}	2.56×10^{-17}	8.83×10^{-16}
KRT24	1.11×10^{1}	3.48×10^{0}	4.24×10^{-7}	5.14×10^{-6}
GAGE12J	1.10×10^{1}	3.45×10^{0}	2.73×10^{-3}	1.05×10^{-2}
AC034213.1	1.08×10^{1}	3.43×10^{0}	6.69×10^{-28}	5.53×10^{-26}
IGFL1	1.08×10^{1}	3.43×10^{0}	5.02×10^{-19}	1.97×10^{-17}
TCEAL2	1.08×10^{1}	3.43×10^{0}	9.87×10^{-32}	1.19×10^{-29}
LINC02500	1.07×10^{1}	3.42×10^{0}	1.95×10^{-3}	7.96×10^{-3}
ERICH3	1.06×10^{1}	3.41×10^{0}	7.24×10^{-29}	6.64×10^{-27}

BPIFB4	1.06×10^{1}	3.41×10^{0}	7.99×10^{-10}	1.46×10^{-8}
KRT16	1.05×10^{1}	3.40×10^{0}	1.23×10^{-26}	9.13×10^{-25}
BX119904.1	1.04×10^{1}	3.38×10^{0}	3.66×10^{-5}	2.71×10^{-4}
THSD7B	1.02×10^{1}	3.34×10^{0}	3.05×10^{-36}	5.90×10^{-34}
SPOCK3	1.01×10^{1}	3.34×10^{0}	3.83×10^{-23}	2.10×10^{-21}
SYNGR4	9.94×10^{0}	3.31×10^{0}	2.41×10^{-33}	3.35×10^{-31}
NCAN	9.90×10^{0}	3.31×10^{0}	2.26×10^{-29}	2.16×10^{-27}
TCEAL5	9.76×10^{0}	3.29×10^{0}	1.28×10^{-37}	3.10×10^{-35}
SLC7A14	9.72×10^{0}	3.28×10^{0}	6.99×10^{-27}	5.29×10^{-25}
SFRP1	9.70×10^{0}	3.28×10^{0}	6.12×10^{-42}	2.59×10^{-39}
KC877982.1	9.69×10^{0}	3.28×10^{0}	1.81×10^{-6}	1.90×10^{-5}
Y_RNA.302	9.60×10^{0}	3.26×10^{0}	2.90×10^{-6}	2.91×10^{-5}
TP63	9.58×10^{0}	3.26×10^{0}	1.50×10^{-49}	2.60×10^{-46}
NPTX1	9.49×10^{0}	3.25×10^{0}	1.17×10^{-45}	9.45×10^{-43}
UTS2B	9.35×10^{0}	3.23×10^{0}	2.22×10^{-37}	5.09×10^{-35}
KIF1A	9.35×10^{0}	3.23×10^{0}	8.12×10^{-31}	8.85×10^{-29}
ADH1B	9.29×10^{0}	3.22×10^{0}	2.74×10^{-28}	2.35×10^{-26}
NGB	9.28×10^{0}	3.21×10^{0}	7.96×10^{-22}	3.92×10^{-20}
WNT7A	9.28×10^{0}	3.21×10^{0}	3.38×10^{-17}	1.15×10^{-15}
GPR1.AS	9.27×10^{0}	3.21×10^{0}	1.64×10^{-9}	2.89×10^{-8}
SLITRK1	9.22×10^{0}	3.20×10^{0}	1.27×10^{-11}	2.79×10^{-10}
PENK	9.11×10^{0}	3.19×10^{0}	5.77×10^{-26}	4.09×10^{-24}

Table A.31 (continued). The list of the top 100 upregulated DEGs identified in the CS1 subtype using edgeR as a result of four clustering analyzes.

CLCA2	9.03×10^{0}	3.17×10^{0}	5.88×10^{-18}	2.13×10^{-16}
PRIMA1	8.94×10^{0}	3.16×10^{0}	1.57×10^{-33}	2.24×10^{-31}
LINC02434	8.93×10^{0}	3.16×10^{0}	1.49×10^{-3}	6.36×10^{-3}
SHISA7	8.85×10^{0}	3.15×10^{0}	3.68×10^{-32}	4.65×10^{-30}
FCER2	8.83×10^{0}	3.14×10^{0}	1.16×10^{-29}	1.14×10^{-27}
KRT13	8.81×10^{0}	3.14×10^{0}	3.32×10^{-21}	1.56×10^{-19}
PGM5.AS1	8.72×10^{0}	3.12×10^{0}	2.60×10^{-24}	1.59×10^{-22}
CHGB	8.71×10^{0}	3.12×10^{0}	1.50×10^{-19}	6.15×10^{-18}
ASTN1	8.61×10^{0}	3.11×10^{0}	6.76×10^{-31}	7.47×10^{-29}
GIP	8.61×10^{0}	3.11×10^{0}	5.95×10^{-9}	9.71×10^{-8}
EEF1A2	8.58×10^{0}	3.10×10^{0}	7.55×10^{-30}	7.62×10^{-28}
CCL19	8.57×10^{0}	3.10×10^{0}	1.06×10^{-42}	5.08×10^{-40}
SCRT2	8.57×10^{0}	3.10×10^{0}	6.10×10^{-7}	7.15×10^{-6}
NFE4	8.55×10^{0}	3.10×10^{0}	1.26×10^{-21}	6.14×10^{-20}
CHRDL2	8.52×10^{0}	3.09×10^{0}	1.03×10^{-31}	1.23×10^{-29}
MIR4432HG	8.52×10^{0}	3.09×10^{0}	9.33×10^{-24}	5.35×10^{-22}
CADM3	8.50×10^{0}	3.09×10^{0}	8.89×10^{-40}	2.84×10^{-37}
NLGN1	8.49×10^{0}	3.09×10^{0}	5.03×10^{-35}	8.65×10^{-33}
LINCADL	8.37×10^{0}	3.07×10^{0}	3.02×10^{-4}	1.65×10^{-3}

Table A.32. The list of the top 100 downregulated DEGs identified in the CS1 subtype using edgeR as a result of four clustering analyzes.

	fc	log2fc	pvalue	padj
PNLIP	2.12×10^{-2}	-5.56×10^{0}	4.49×10^{-3}	1.60×10^{-2}
ZNF479	4.86×10^{-2}	-4.36×10^{0}	8.85×10^{-3}	2.78×10^{-2}
GALP	5.27×10^{-2}	-4.25×10^{0}	2.17×10^{-4}	1.25×10^{-3}
CLEC2A	5.32×10^{-2}	-4.23×10^{0}	1.27×10^{-3}	5.57×10^{-3}
FAM238B	7.27×10^{-2}	-3.78×10^{0}	4.91×10^{-5}	3.50×10^{-4}
AL390961.1	7.58×10^{-2}	-3.72×10^{0}	8.27×10^{-4}	3.89×10^{-3}
RN7SL314P	7.71×10^{-2}	-3.70×10^{0}	2.03×10^{-3}	8.23×10^{-3}
RN7SL837P	8.03×10^{-2}	-3.64×10^{0}	1.66×10^{-2}	4.63×10^{-2}
RN7SL791P	8.38×10^{-2}	-3.58×10^{0}	1.21×10^{-3}	5.36×10^{-3}
OR10G4	8.82×10^{-2}	-3.50×10^{0}	1.23×10^{-4}	7.68×10^{-4}
RN7SL321P	9.49×10^{-2}	-3.40×10^{0}	2.51×10^{-3}	9.79×10^{-3}
RN7SL414P	9.93×10^{-2}	-3.33×10^{0}	7.35×10^{-4}	3.52×10^{-3}
AP002963.1	9.99×10^{-2}	-3.32×10^{0}	1.44×10^{-2}	4.11×10^{-2}
AC073530.2	1.01×10^{-1}	-3.30×10^{0}	1.21×10^{-3}	5.35×10^{-3}
SNORA35B	1.03×10^{-1}	-3.28×10^{0}	2.87×10^{-3}	1.10×10^{-2}
AC073176.2	1.05×10^{-1}	-3.25×10^{0}	1.74×10^{-2}	4.80×10^{-2}
OR8D4	1.09×10^{-1}	-3.20×10^{0}	1.69×10^{-5}	1.38×10^{-3}
RN7SL210P	1.10×10^{-1}	-3.19×10^{0}	5.13×10^{-4}	2.60×10^{-3}

Table A.32 (continued). The list of the top 100 downregulated DEGs identified in the CS1 subtype using edgeR as a result of four clustering analyzes.

RN7SL764P	1.11×10^{-1}	-3.17×10^{0}	8.18×10^{-5}	5.42×10^{-4}
RN7SKP217	1.14×10^{-1}	-3.13×10^{0}	1.12×10^{-2}	3.36×10^{-2}
NKX6.3	1.18×10^{-1}	-3.08×10^{0}	5.58×10^{-4}	2.79×10^{-3}
RN7SL214P	1.20×10^{-1}	-3.06×10^{0}	4.27×10^{-3}	1.53×10^{-2}
RN7SL865P	1.21×10^{-1}	-3.05×10^{0}	1.23×10^{-2}	3.64×10^{-2}
AP002001.1	1.23×10^{-1}	-3.02×10^{0}	8.08×10^{-3}	2.58×10^{-2}
RN7SL174P	1.26×10^{-1}	-2.99×10^{0}	2.97×10^{-3}	1.13×10^{-2}
DSCAM.AS1	1.28×10^{-1}	-2.97×10^{0}	1.42×10^{-2}	4.06×10^{-2}
NDUFB1P1	1.28×10^{-1}	-2.97×10^{0}	3.35×10^{-9}	5.67×10^{-8}
RN7SL451P	1.28×10^{-1}	-2.96×10^{0}	6.93×10^{-3}	2.28×10^{-2}
OR7A1P	1.29×10^{-1}	-2.96×10^{0}	6.35×10^{-3}	2.12×10^{-2}
RN7SL643P	1.32×10^{-1}	-2.92×10^{0}	1.24×10^{-3}	5.47×10^{-3}
RN7SL795P	1.36×10^{-1}	-2.88×10^{0}	1.07×10^{-2}	3.23×10^{-2}
AC010997.1	1.41×10^{-1}	-2.83×10^{0}	5.81×10^{-3}	1.97×10^{-2}
LINC00293	1.45×10^{-1}	-2.79×10^{0}	4.02×10^{-3}	1.45×10^{-2}
RN7SL666P	1.47×10^{-1}	-2.77×10^{0}	4.80×10^{-3}	1.69×10^{-2}
AC026402.1	1.49×10^{-1}	-2.75×10^{0}	4.55×10^{-4}	2.34×10^{-3}
RN7SKP178	1.49×10^{-1}	-2.75×10^{0}	2.74×10^{-3}	1.06×10^{-2}
RN7SL712P	1.50×10^{-1}	-2.73×10^{0}	2.87×10^{-3}	1.10×10^{-2}
RN7SL326P	1.52×10^{-1}	-2.72×10^{0}	3.50×10^{-5}	2.60×10^{-4}
RN7SL394P	1.52×10^{-1}	-2.72×10^{0}	3.12×10^{-4}	1.70×10^{-3}

RN7SL518P	1.52×10^{-1}	-2.72×10^{0}	1.76×10^{-2}	4.85×10^{-2}
RN7SL786P	1.53×10^{-1}	-2.71×10^{0}	1.49×10^{-3}	6.36×10^{-3}
RNA5SP497	1.54×10^{-1}	-2.70×10^{0}	1.21×10^{-2}	3.58×10^{-2}
PRDX2P1	1.55×10^{-1}	-2.69×10^{0}	4.66×10^{-7}	5.59×10^{-6}
RN7SL402P	1.57×10^{-1}	-2.68×10^{0}	1.35×10^{-2}	3.90×10^{-2}
AC091839.1	1.57×10^{-1}	-2.67×10^{0}	3.08×10^{-3}	1.17×10^{-2}
RN7SL713P	1.60×10^{-1}	-2.65×10^{0}	1.13×10^{-2}	3.39×10^{-2}
SRIP3	1.65×10^{-1}	-2.60×10^{0}	2.70×10^{-3}	1.04×10^{-2}
ANKRD20A9P	1.65×10^{-1}	-2.60×10^{0}	4.85×10^{-4}	2.48×10^{-3}
RPL11P3	1.71×10^{-1}	-2.55×10^{0}	3.80×10^{-10}	7.19×10^{-9}
LINC01427	1.72×10^{-1}	-2.54×10^{0}	3.95×10^{-3}	1.43×10^{-2}
AL591846.1	1.73×10^{-1}	-2.53×10^{0}	2.52×10^{-10}	4.87×10^{-9}
RN7SL266P	1.73×10^{-1}	-2.53×10^{0}	7.10×10^{-3}	2.32×10^{-2}
RNVU1.23	1.75×10^{-1}	-2.51×10^{0}	7.88×10^{-5}	5.26×10^{-4}
MTCO1P45	1.78×10^{-1}	-2.49×10^{0}	8.28×10^{-3}	2.64×10^{-2}
RNA5SP48	1.78×10^{-1}	-2.49×10^{0}	1.73×10^{-2}	4.77×10^{-2}
MYADML	1.80×10^{-1}	-2.48×10^{0}	1.29×10^{-3}	5.66×10^{-3}
RN7SL702P	1.81×10^{-1}	-2.46×10^{0}	3.36×10^{-3}	1.25×10^{-2}

Table A.32 (continued). The list of the top 100 downregulated DEGs identified in the CS1 subtype using edgeR as a result of four clustering analyzes.

Metazoa_SRP.90	1.82×10^{-1}	-2.46×10^{0}	8.50×10^{-3}	2.69×10^{-2}
AC009035.1	1.82×10^{-1}	-2.46×10^{0}	9.99×10^{-3}	3.07×10^{-2}
RN7SL715P	1.84×10^{-1}	-2.44×10^{0}	7.54×10^{-3}	2.44×10^{-2}
AC140076.1	1.87×10^{-1}	-2.42×10^{0}	1.17×10^{-4}	7.38×10^{-4}
CUL1P1	1.88×10^{-1}	-2.41×10^{0}	3.01×10^{-6}	3.01×10^{-5}
AC134508.1	1.90×10^{-1}	-2.39×10^{0}	5.54×10^{-3}	1.90×10^{-2}
AC016716.1	1.92×10^{-1}	-2.38×10^{0}	2.32×10^{-4}	1.32×10^{-3}
AP001531.1	1.92×10^{-1}	-2.38×10^{0}	1.79×10^{-2}	4.92×10^{-2}
KRTAP10.11	1.92×10^{-1}	-2.38×10^{0}	2.34×10^{-3}	9.24×10^{-3}
AC012618.1	1.95×10^{-1}	-2.36×10^{0}	4.24×10^{-8}	6.11×10^{-7}
KRTCAP2P1	1.96×10^{-1}	-2.35×10^{0}	4.81×10^{-6}	4.55×10^{-5}
RN7SL413P	1.97×10^{-1}	-2.34×10^{0}	5.89×10^{-3}	1.99×10^{-2}
AC098591.3	1.98×10^{-1}	-2.33×10^{0}	4.82×10^{-9}	7.97×10^{-8}
RN7SL97P	2.01×10^{-1}	-2.32×10^{0}	1.91×10^{-4}	1.12×10^{-3}
MIR8075	2.02×10^{-1}	-2.31×10^{0}	2.68×10^{-3}	1.04×10^{-2}
RN7SL598P	2.02×10^{-1}	-2.31×10^{0}	4.38×10^{-3}	1.56×10^{-2}
LINC01639	2.03×10^{-1}	-2.30×10^{0}	1.79×10^{-2}	4.91×10^{-2}
AL353662.1	2.03×10^{-1}	-2.30×10^{0}	3.59×10^{-10}	6.81×10^{-9}
ATP5F1AP2	2.03×10^{-1}	-2.30×10^{0}	6.50×10^{-6}	5.94×10^{-5}
LINC02484	2.03×10^{-1}	-2.30×10^{0}	1.63×10^{-2}	4.56×10^{-2}
AC109481.1	2.04×10^{-1}	-2.29×10^{0}	4.80×10^{-4}	2.45×10^{-3}
RN7SL472P	2.04×10^{-1}	-2.29×10^{0}	2.57×10^{-5}	1.99×10^{-4}

ATP5PBP7	2.04×10^{-1}	-2.29×10^{0}	8.93×10^{-4}	4.15×10^{-3}
PRELID3BP3	2.05×10^{-1}	-2.28×10^{0}	1.19×10^{-2}	3.53×10^{-2}
AL358472.1	2.05×10^{-1}	-2.28×10^{0}	2.29×10^{-6}	2.35×10^{-5}
RN7SL33P	2.05×10^{-1}	-2.28×10^{0}	1.28×10^{-2}	3.74×10^{-2}
RPS14P7	2.05×10^{-1}	-2.28×10^{0}	7.60×10^{-3}	2.46×10^{-2}
UBQLN3	2.08×10^{-1}	-2.27×10^{0}	1.60×10^{-2}	4.48×10^{-2}
RN7SL108P	2.08×10^{-1}	-2.26×10^{0}	2.62×10^{-3}	1.02×10^{-2}
AC073626.2	2.09×10^{-1}	-2.26×10^{0}	1.76×10^{-4}	1.04×10^{-3}
PMPCAP1	2.11×10^{-1}	-2.25×10^{0}	1.11×10^{-4}	7.07×10^{-4}
RN7SL447P	2.14×10^{-1}	-2.22×10^{0}	9.82×10^{-3}	3.03×10^{-2}
EPPIN	2.14×10^{-1}	-2.22×10^{0}	1.02×10^{-3}	4.63×10^{-3}
AC108052.1	2.17×10^{-1}	-2.20×10^{0}	6.09×10^{-3}	2.05×10^{-2}
AC010329.1	2.18×10^{-1}	-2.20×10^{0}	4.68×10^{-5}	3.35×10^{-4}
AC099654.1	2.19×10^{-1}	-2.19×10^{0}	1.01×10^{-2}	3.10×10^{-2}
EIF3IP1	2.19×10^{-1}	-2.19×10^{0}	1.84×10^{-4}	1.08×10^{-3}
MIF	2.20×10^{-1}	-2.19×10^{0}	8.65×10^{-4}	4.04×10^{-3}
AL442128.1	2.21×10^{-1}	-2.18×10^{0}	8.60×10^{-5}	5.67×10^{-4}
HSPD1P21	2.23×10^{-1}	-2.17×10^{0}	1.71×10^{-2}	4.73×10^{-2}

Table A.32 (continued). The list of the top 100 downregulated DEGs identified in the CS1 subtype using edgeR as a result of four clustering analyzes.

OR10G7	2.25×10^{-1}	-2.15×10^{0}	5.88×10^{-3}	1.99×10^{-2}
RPL37P3	2.25×10^{-1}	-2.15×10^{0}	1.45×10^{-3}	6.24×10^{-3}
RPL18P13	2.27×10^{-1}	-2.14×10^{0}	1.47×10^{-5}	1.22×10^{-4}

Table A.33. The list of the top 100 upregulated DEGs identified in the CS2 subtype using edgeR as a result of four clustering analyzes.

	fc	**log2fc**	**pvalue**	**padj**
RNU1.28P	9.68×10^{2}	9.92×10^{0}	1.29×10^{-50}	2.92×10^{-49}
RNY4	7.74×10^{2}	9.60×10^{0}	3.10×10^{-40}	4.99×10^{-39}
AL139274.1	5.82×10^{2}	9.18×10^{0}	1.21×10^{-107}	1.79×10^{-105}
RNVU1.2	5.60×10^{2}	9.13×10^{0}	1.06×10^{-58}	3.16×10^{-57}
FBXO40	4.55×10^{2}	8.83×10^{0}	5.89×10^{-129}	1.66×10^{-126}
PAEP	4.43×10^{2}	8.79×10^{0}	4.85×10^{-138}	1.79×10^{-135}
AC090220.1	4.25×10^{2}	8.73×10^{0}	5.29×10^{-106}	7.55×10^{-104}
RNU1.88P	4.19×10^{2}	8.71×10^{0}	7.51×10^{-31}	8.76×10^{-30}
RNU1.19P	4.10×10^{2}	8.68×10^{0}	2.99×10^{-57}	8.48×10^{-56}
RNVU1.18	4.07×10^{2}	8.67×10^{0}	2.42×10^{-27}	2.52×10^{-26}
RNU1.83P	4.05×10^{2}	8.66×10^{0}	2.28×10^{-66}	8.95×10^{-65}
RNU2.59P	4.05×10^{2}	8.66×10^{0}	9.39×10^{-34}	1.21×10^{-32}
Y_RNA.241	3.93×10^{2}	8.62×10^{0}	2.16×10^{-67}	8.71×10^{-66}
RNU5A.1	3.93×10^{2}	8.62×10^{0}	4.46×10^{-37}	6.46×10^{-36}
MTND5P32	3.88×10^{2}	8.60×10^{0}	1.85×10^{-62}	6.41×10^{-61}
MTCYBP32	3.83×10^{2}	8.58×10^{0}	6.03×10^{-71}	2.75×10^{-69}

AC092139.1	3.60×10^{2}	8.49×10^{0}	6.37×10^{-91}	5.49×10^{-89}
AL356057.1	3.45×10^{2}	8.43×10^{0}	6.28×10^{-53}	1.53×10^{-51}
RN7SKP227	3.40×10^{2}	8.41×10^{0}	6.18×10^{-10}	2.88×10^{-9}
AL035693.1	3.38×10^{2}	8.40×10^{0}	1.44×10^{-94}	1.42×10^{-92}
AC066616.2	3.38×10^{2}	8.40×10^{0}	2.16×10^{-61}	7.22×10^{-60}
AC130895.1	3.34×10^{2}	8.39×10^{0}	4.45×10^{-90}	3.74×10^{-88}
Z93020.1	3.34×10^{2}	8.39×10^{0}	2.70×10^{-70}	1.20×10^{-68}
RNU1.20P	3.31×10^{2}	8.37×10^{0}	9.31×10^{-34}	1.20×10^{-32}
RNU1.139P	3.26×10^{2}	8.35×10^{0}	4.70×10^{-42}	8.02×10^{-41}
MTND5P26	3.25×10^{2}	8.34×10^{0}	5.11×10^{-61}	1.68×10^{-59}
RNU1.52P	3.24×10^{2}	8.34×10^{0}	9.00×10^{-30}	1.02×10^{-28}
DIAPH1.AS1	3.05×10^{2}	8.25×10^{0}	1.70×10^{-131}	5.14×10^{-129}
RNU5B.1	3.05×10^{2}	8.25×10^{0}	1.43×10^{-18}	1.09×10^{-17}
IFNK	3.02×10^{2}	8.24×10^{0}	8.97×10^{-93}	8.23×10^{-91}
ZBTB20.AS5	3.00×10^{2}	8.23×10^{0}	3.43×10^{-86}	2.54×10^{-84}
AL391863.2	2.99×10^{2}	8.22×10^{0}	1.21×10^{-90}	1.04×10^{-88}
RNU1.46P	2.99×10^{2}	8.22×10^{0}	3.46×10^{-46}	6.71×10^{-45}
AC010997.6	2.97×10^{2}	8.21×10^{0}	1.24×10^{-61}	4.17×10^{-60}

Table A.33 (continued). The list of the top 100 upregulated DEGs identified in the CS2 subtype using edgeR as a result of four clustering analyzes.

RNU1.28P	9.68×10^{2}	9.92×10^{0}	1.29×10^{-50}	2.92×10^{-49}
RNY4	7.74×10^{2}	9.60×10^{0}	3.10×10^{-40}	4.99×10^{-39}
AL139274.1	5.82×10^{2}	9.18×10^{0}	1.21×10^{-107}	1.79×10^{-105}
RNVU1.2	5.60×10^{2}	9.13×10^{0}	1.06×10^{-58}	3.16×10^{-57}
FBXO40	4.55×10^{2}	8.83×10^{0}	5.89×10^{-129}	1.66×10^{-126}
PAEP	4.43×10^{2}	8.79×10^{0}	4.85×10^{-138}	1.79×10^{-135}
AC090220.1	4.25×10^{2}	8.73×10^{0}	5.29×10^{-106}	7.55×10^{-104}
RNU1.88P	4.19×10^{2}	8.71×10^{0}	7.51×10^{-31}	8.76×10^{-30}
RNU1.19P	4.10×10^{2}	8.68×10^{0}	2.99×10^{-57}	8.48×10^{-56}
RNVU1.18	4.07×10^{2}	8.67×10^{0}	2.42×10^{-27}	2.52×10^{-26}
RNU1.83P	4.05×10^{2}	8.66×10^{0}	2.28×10^{-66}	8.95×10^{-65}
RNU2.59P	4.05×10^{2}	8.66×10^{0}	9.39×10^{-34}	1.21×10^{-32}
Y_RNA.241	3.93×10^{2}	8.62×10^{0}	2.16×10^{-67}	8.71×10^{-66}
RNU5A.1	3.93×10^{2}	8.62×10^{0}	4.46×10^{-37}	6.46×10^{-36}
MTND5P32	3.88×10^{2}	8.60×10^{0}	1.85×10^{-62}	6.41×10^{-61}
MTCYBP32	3.83×10^{2}	8.58×10^{0}	6.03×10^{-71}	2.75×10^{-69}
AC092139.1	3.60×10^{2}	8.49×10^{0}	6.37×10^{-91}	5.49×10^{-89}
AL356057.1	3.45×10^{2}	8.43×10^{0}	6.28×10^{-53}	1.53×10^{-51}
RN7SKP227	3.40×10^{2}	8.41×10^{0}	6.18×10^{-10}	2.88×10^{-9}
AL035693.1	3.38×10^{2}	8.40×10^{0}	1.44×10^{-94}	1.42×10^{-92}
AC066616.2	3.38×10^{2}	8.40×10^{0}	2.16×10^{-61}	7.22×10^{-60}
AC130895.1	3.34×10^{2}	8.39×10^{0}	4.45×10^{-90}	3.74×10^{-88}
Z93020.1	3.34×10^{2}	8.39×10^{0}	2.70×10^{-70}	1.20×10^{-68}
RNU1.20P	3.31×10^{2}	8.37×10^{0}	9.31×10^{-34}	1.20×10^{-32}

RNU1.139P	3.26×10^{2}	8.35×10^{0}	4.70×10^{-42}	8.02×10^{-41}
MTND5P26	3.25×10^{2}	8.34×10^{0}	5.11×10^{-61}	1.68×10^{-59}
RNU1.52P	3.24×10^{2}	8.34×10^{0}	9.00×10^{-30}	1.02×10^{-28}
DIAPH1.AS1	3.05×10^{2}	8.25×10^{0}	1.70×10^{-131}	5.14×10^{-129}
RNU5B.1	3.05×10^{2}	8.25×10^{0}	1.43×10^{-18}	1.09×10^{-17}
IFNK	3.02×10^{2}	8.24×10^{0}	8.97×10^{-93}	8.23×10^{-91}
ZBTB20.AS5	3.00×10^{2}	8.23×10^{0}	3.43×10^{-86}	2.54×10^{-84}
AL391863.2	2.99×10^{2}	8.22×10^{0}	1.21×10^{-90}	1.04×10^{-88}
RNU1.46P	2.99×10^{2}	8.22×10^{0}	3.46×10^{-46}	6.71×10^{-45}
AC010997.6	2.97×10^{2}	8.21×10^{0}	1.24×10^{-61}	4.17×10^{-60}
AL136320.1	2.20×10^{2}	7.78×10^{0}	4.95×10^{-61}	1.63×10^{-59}
AC008833.1	2.19×10^{2}	7.78×10^{0}	2.27×10^{-72}	1.08×10^{-70}
AP003086.3	2.19×10^{2}	7.77×10^{0}	2.19×10^{-92}	1.98×10^{-90}
AF127577.6	2.17×10^{2}	7.76×10^{0}	2.12×10^{-160}	1.64×10^{-157}
AL360178.2	2.17×10^{2}	7.76×10^{0}	2.27×10^{-59}	6.93×10^{-58}
UHRF2P1	2.16×10^{2}	7.76×10^{0}	1.66×10^{-121}	3.59×10^{-119}
Y_RNA.720	2.15×10^{2}	7.75×10^{0}	7.08×10^{-75}	3.66×10^{-73}

Table A.33 (continued). The list of the top 100 upregulated DEGs identified in the CS2 subtype using edgeR as a result of four clustering analyzes.

AC027279.4	2.15×10^{2}	7.75×10^{0}	1.00×10^{-60}	3.25×10^{-59}
BMP2KL	2.14×10^{2}	7.74×10^{0}	1.02×10^{-40}	1.67×10^{-39}
AC018359.1	2.13×10^{2}	7.74×10^{0}	3.16×10^{-37}	4.59×10^{-36}
AC064874.1	2.11×10^{2}	7.72×10^{0}	7.42×10^{-98}	8.22×10^{-96}
PIGFP2	2.11×10^{2}	7.72×10^{0}	4.83×10^{-53}	1.18×10^{-51}
EDDM3CP	2.11×10^{2}	7.72×10^{0}	3.53×10^{-35}	4.81×10^{-34}
AC023813.2	2.10×10^{2}	7.71×10^{0}	7.26×10^{-71}	3.29×10^{-69}
AC018398.2	2.09×10^{2}	7.70×10^{0}	5.74×10^{-60}	1.79×10^{-58}
RNU1.11P	2.07×10^{2}	7.70×10^{0}	2.44×10^{-14}	1.54×10^{-13}
AF107885.2	2.07×10^{2}	7.70×10^{0}	2.65×10^{-98}	2.96×10^{-96}
AL034349.1	2.07×10^{2}	7.69×10^{0}	2.06×10^{-89}	1.70×10^{-87}
RN7SKP186	2.07×10^{2}	7.69×10^{0}	2.55×10^{-11}	1.33×10^{-10}
Y_RNA.331	2.06×10^{2}	7.68×10^{0}	1.15×10^{-49}	2.52×10^{-48}
MTND1P32	2.03×10^{2}	7.67×10^{0}	1.98×10^{-63}	7.10×10^{-62}
RNY1	2.03×10^{2}	7.66×10^{0}	1.05×10^{-19}	8.43×10^{-19}
AC016549.1	2.03×10^{2}	7.66×10^{0}	1.83×10^{-75}	9.63×10^{-74}
PRSS48	2.02×10^{2}	7.66×10^{0}	1.24×10^{-183}	2.15×10^{-180}
ST7.AS2	1.98×10^{2}	7.63×10^{0}	5.56×10^{-135}	1.87×10^{-132}
RAD17P2	1.97×10^{2}	7.62×10^{0}	1.01×10^{-88}	8.14×10^{-87}
AC011933.2	1.96×10^{2}	7.62×10^{0}	3.80×10^{-137}	1.36×10^{-134}
MTND4P32	1.96×10^{2}	7.62×10^{0}	1.86×10^{-64}	6.86×10^{-63}
AC104332.1	1.95×10^{2}	7.61×10^{0}	8.21×10^{-72}	3.84×10^{-70}
RNU6ATAC	1.94×10^{2}	7.60×10^{0}	9.68×10^{-48}	1.99×10^{-46}
AL606517.1	1.94×10^{2}	7.60×10^{0}	5.46×10^{-59}	1.65×10^{-57}
AL138713.1	1.93×10^{2}	7.59×10^{0}	3.39×10^{-70}	1.51×10^{-68}

Table A.34. The list of the top 100 downregulated DEGs identified in the CS2 subtype using edgeR as a result of four clustering analyzes.

	fc	log2fc	pvalue	padj
PPBP	4.96×10^{-3}	-7.65×10^{0}	3.83×10^{-9}	1.66×10^{-8}
AC247036.1	1.89×10^{-2}	-5.73×10^{0}	8.69×10^{-3}	1.60×10^{-2}
SPRR2F	3.15×10^{-2}	-4.99×10^{0}	1.39×10^{-2}	2.46×10^{-2}
SP9	3.22×10^{-2}	-4.96×10^{0}	5.56×10^{-4}	1.27×10^{-3}
LCN15	4.04×10^{-2}	-4.63×10^{0}	5.49×10^{-6}	1.69×10^{-5}
IGHA2	4.12×10^{-2}	-4.60×10^{0}	1.28×10^{-10}	6.28×10^{-10}
SERPINA11	4.87×10^{-2}	-4.36×10^{0}	2.06×10^{-5}	5.89×10^{-5}
MS4A12	5.23×10^{-2}	-4.26×10^{0}	5.61×10^{-7}	1.95×10^{-6}
VGLL1	5.39×10^{-2}	-4.21×10^{0}	2.09×10^{-5}	5.97×10^{-5}
FABP1	5.87×10^{-2}	-4.09×10^{0}	8.51×10^{-13}	4.89×10^{-12}
HPN	5.92×10^{-2}	-4.08×10^{0}	1.73×10^{-8}	7.09×10^{-8}
GUCA2A	6.14×10^{-2}	-4.03×10^{0}	3.70×10^{-11}	1.90×10^{-10}

Table A.34 (continued). The list of the top 100 downregulated DEGs identified in the CS2 subtype using edgeR as a result of four clustering analyzes.

PYY	6.39×10^{-2}	-3.97×10^{0}	2.85×10^{-8}	1.14×10^{-7}
GUCA2B	6.77×10^{-2}	-3.89×10^{0}	1.07×10^{-6}	3.63×10^{-6}
CALCA	7.52×10^{-2}	-3.73×10^{0}	5.97×10^{-7}	2.07×10^{-6}
SCNN1B	7.78×10^{-2}	-3.68×10^{0}	6.17×10^{-11}	3.12×10^{-10}
AC021146.12	8.24×10^{-2}	-3.60×10^{0}	2.57×10^{-2}	4.29×10^{-2}
DEFB1	8.29×10^{-2}	-3.59×10^{0}	2.79×10^{-13}	1.66×10^{-12}
REN	8.37×10^{-2}	-3.58×10^{0}	9.83×10^{-9}	4.12×10^{-8}
VSIG2	8.57×10^{-2}	-3.55×10^{0}	1.94×10^{-9}	8.68×10^{-9}
AC012213.4	9.25×10^{-2}	-3.43×10^{0}	1.16×10^{-2}	2.09×10^{-2}
RPL10P9	9.72×10^{-2}	-3.36×10^{0}	1.72×10^{-9}	7.72×10^{-9}
HOXC12	9.92×10^{-2}	-3.33×10^{0}	9.49×10^{-3}	1.73×10^{-2}
RTN4RL1	9.92×10^{-2}	-3.33×10^{0}	8.96×10^{-8}	3.40×10^{-7}
VSTM2L	1.04×10^{-1}	-3.27×10^{0}	1.46×10^{-8}	6.01×10^{-8}
KCNH6	1.05×10^{-1}	-3.25×10^{0}	1.55×10^{-8}	6.36×10^{-8}
NKX2.1	1.06×10^{-1}	-3.24×10^{0}	1.70×10^{-2}	2.95×10^{-2}
LINC02672	1.08×10^{-1}	-3.21×10^{0}	1.74×10^{-5}	5.01×10^{-5}
FAM189A1	1.12×10^{-1}	-3.16×10^{0}	3.15×10^{-8}	1.25×10^{-7}
PKP1	1.13×10^{-1}	-3.15×10^{0}	3.59×10^{-11}	1.85×10^{-10}
SLC7A4	1.13×10^{-1}	-3.14×10^{0}	8.57×10^{-13}	4.92×10^{-12}
TBX4	1.13×10^{-1}	-3.14×10^{0}	2.85×10^{-5}	8.00×10^{-5}
SOX1	1.13×10^{-1}	-3.14×10^{0}	2.08×10^{-4}	5.13×10^{-4}
BPIFB2	1.14×10^{-1}	-3.14×10^{0}	1.60×10^{-2}	2.79×10^{-2}
CCKBR	1.14×10^{-1}	-3.13×10^{0}	1.26×10^{-3}	2.73×10^{-3}
AQP8	1.15×10^{-1}	-3.12×10^{0}	6.86×10^{-5}	1.81×10^{-4}
LINC00404	1.20×10^{-1}	-3.06×10^{0}	1.01×10^{-3}	2.22×10^{-3}
UCN3	1.23×10^{-1}	-3.02×10^{0}	1.06×10^{-6}	3.57×10^{-6}
TBC1D3D	1.23×10^{-1}	-3.02×10^{0}	1.41×10^{-2}	2.50×10^{-2}

TTR	1.24×10^{-1}	-3.02×10^{0}	6.01×10^{-6}	1.84×10^{-5}
DSC3	1.24×10^{-1}	-3.01×10^{0}	1.65×10^{-6}	5.46×10^{-6}
FAM155B	1.25×10^{-1}	-3.00×10^{0}	5.98×10^{-6}	1.84×10^{-5}
AC091179.1	1.25×10^{-1}	-2.99×10^{0}	9.27×10^{-3}	1.70×10^{-2}
AC012354.2	1.27×10^{-1}	-2.98×10^{0}	1.96×10^{-4}	4.84×10^{-4}
AC004080.1	1.28×10^{-1}	-2.97×10^{0}	2.71×10^{-5}	7.64×10^{-5}
ADH1C	1.28×10^{-1}	-2.97×10^{0}	5.23×10^{-8}	2.04×10^{-7}
UGT2B7	1.28×10^{-1}	-2.96×10^{0}	2.20×10^{-7}	8.03×10^{-7}
MRPL23.AS1	1.28×10^{-1}	-2.96×10^{0}	6.16×10^{-5}	1.64×10^{-4}
TBXT	1.29×10^{-1}	-2.96×10^{0}	1.50×10^{-2}	2.63×10^{-2}
BRINP3	1.29×10^{-1}	-2.95×10^{0}	2.15×10^{-3}	4.48×10^{-3}
NUPR2	1.33×10^{-1}	-2.92×10^{0}	2.37×10^{-3}	4.89×10^{-3}
ARHGDIG	1.37×10^{-1}	-2.86×10^{0}	2.39×10^{-7}	8.67×10^{-7}
UGT1A8	1.38×10^{-1}	-2.86×10^{0}	8.37×10^{-8}	3.19×10^{-7}

Table A.34 (continued). The list of the top 100 downregulated DEGs identified in the CS2 subtype using edgeR as a result of four clustering analyzes.

SST	1.38×10^{-1}	-2.85×10^{0}	1.69×10^{-4}	4.23×10^{-4}
MTTP	1.40×10^{-1}	-2.84×10^{0}	1.09×10^{-4}	2.79×10^{-4}
WNT11	1.45×10^{-1}	-2.79×10^{0}	1.76×10^{-8}	7.21×10^{-8}
SH2D6	1.45×10^{-1}	-2.79×10^{0}	8.68×10^{-8}	3.31×10^{-7}
IGLJ2	1.46×10^{-1}	-2.78×10^{0}	3.15×10^{-3}	6.32×10^{-3}
RPL10P6	1.47×10^{-1}	-2.77×10^{0}	2.14×10^{-6}	6.97×10^{-6}
OPRD1	1.47×10^{-1}	-2.76×10^{0}	1.23×10^{-6}	4.12×10^{-6}
VAX1	1.52×10^{-1}	-2.72×10^{0}	2.96×10^{-2}	4.87×10^{-2}
DUOX2	1.52×10^{-1}	-2.72×10^{0}	1.60×10^{-6}	5.27×10^{-6}
KRTAP3.1	1.52×10^{-1}	-2.72×10^{0}	1.31×10^{-3}	2.82×10^{-3}
AC136443.1	1.53×10^{-1}	-2.71×10^{0}	1.29×10^{-3}	2.79×10^{-3}
TMEM229A	1.57×10^{-1}	-2.67×10^{0}	1.89×10^{-2}	3.25×10^{-2}
TMIGD1	1.58×10^{-1}	-2.66×10^{0}	1.57×10^{-3}	3.34×10^{-3}
LINC01219	1.60×10^{-1}	-2.65×10^{0}	2.01×10^{-4}	4.95×10^{-4}
AC091932.1	1.61×10^{-1}	-2.64×10^{0}	8.80×10^{-3}	1.62×10^{-2}
VGF	1.62×10^{-1}	-2.63×10^{0}	7.25×10^{-6}	2.20×10^{-5}
SLITRK6	1.62×10^{-1}	-2.63×10^{0}	9.72×10^{-5}	2.51×10^{-4}
MEP1A	1.63×10^{-1}	-2.62×10^{0}	3.95×10^{-10}	1.88×10^{-9}
IGHA1	1.63×10^{-1}	-2.61×10^{0}	4.08×10^{-6}	1.28×10^{-5}
AL162739.1	1.68×10^{-1}	-2.57×10^{0}	4.69×10^{-3}	9.06×10^{-3}
IGKV1D.27	1.70×10^{-1}	-2.56×10^{0}	6.66×10^{-4}	1.51×10^{-3}
HTR3C	1.70×10^{-1}	-2.56×10^{0}	5.48×10^{-3}	1.05×10^{-2}
ECHDC3	1.73×10^{-1}	-2.54×10^{0}	2.49×10^{-6}	8.03×10^{-6}
C5orf52	1.76×10^{-1}	-2.50×10^{0}	4.22×10^{-11}	2.16×10^{-10}
TCL6	1.77×10^{-1}	-2.49×10^{0}	5.95×10^{-4}	1.35×10^{-3}
AP004550.1	1.83×10^{-1}	-2.45×10^{0}	4.37×10^{-4}	1.02×10^{-3}
CCL25	1.84×10^{-1}	-2.44×10^{0}	9.94×10^{-3}	1.81×10^{-2}

EVX1	1.84×10^{-1}	-2.44×10^{0}	2.88×10^{-6}	9.24×10^{-6}
LYPD8	1.86×10^{-1}	-2.43×10^{0}	3.15×10^{-5}	8.79×10^{-5}
AC012653.2	1.86×10^{-1}	-2.43×10^{0}	1.32×10^{-2}	2.34×10^{-2}
RPL35AP21	1.87×10^{-1}	-2.42×10^{0}	7.90×10^{-3}	1.47×10^{-2}
FAM3B	1.88×10^{-1}	-2.41×10^{0}	1.21×10^{-5}	3.57×10^{-5}
UGT1A10	1.91×10^{-1}	-2.39×10^{0}	5.76×10^{-8}	2.24×10^{-7}
PRDM13	1.92×10^{-1}	-2.38×10^{0}	1.22×10^{-3}	2.65×10^{-3}
OR2W3	1.93×10^{-1}	-2.38×10^{0}	5.01×10^{-5}	1.35×10^{-4}
EVX1.AS	1.94×10^{-1}	-2.37×10^{0}	1.96×10^{-4}	4.85×10^{-4}
SFTA2	2.01×10^{-1}	-2.32×10^{0}	6.30×10^{-6}	1.93×10^{-5}
CRABP1	2.01×10^{-1}	-2.32×10^{0}	2.78×10^{-4}	6.71×10^{-4}
NXPE4	2.02×10^{-1}	-2.31×10^{0}	6.57×10^{-5}	1.74×10^{-4}
KRTAP5.5	2.02×10^{-1}	-2.30×10^{0}	3.20×10^{-6}	1.02×10^{-5}
AL022318.1	2.03×10^{-1}	-2.30×10^{0}	3.79×10^{-5}	1.04×10^{-4}

Table A.34 (continued). The list of the top 100 downregulated DEGs identified in the CS2 subtype using edgeR as a result of four clustering analyzes.

LGALS9B	2.03×10^{-1}	-2.30×10^{0}	6.59×10^{-7}	2.28×10^{-6}
SCNN1G	2.04×10^{-1}	-2.29×10^{0}	8.63×10^{-4}	1.92×10^{-3}
AL953883.1	2.05×10^{-1}	-2.29×10^{0}	3.91×10^{-4}	9.18×10^{-4}
CWH43	2.06×10^{-1}	-2.28×10^{0}	3.63×10^{-4}	8.59×10^{-4}
NEFLP1	2.06×10^{-1}	-2.28×10^{0}	5.24×10^{-3}	1.00×10^{-2}
IGKJ1	2.06×10^{-1}	-2.28×10^{0}	9.16×10^{-4}	2.03×10^{-3}

Table A.35. The list of the top 100 upregulated DEGs identified in the CS3 subtype using edgeR as a result of four clustering analyzes.

	fc	**log2fc**	**pvalue**	**padj**
BX322234.2	6.48×10^{1}	6.02×10^{0}	1.40×10^{-10}	1.44×10^{-9}
AC152010.1	4.63×10^{1}	5.53×10^{0}	3.15×10^{-4}	1.01×10^{-3}
RN7SL618P	3.42×10^{1}	5.10×10^{0}	3.84×10^{-3}	9.56×10^{-3}
SFTPC	2.92×10^{1}	4.87×10^{0}	5.86×10^{-9}	4.56×10^{-8}
RNA5SP267	2.46×10^{1}	4.62×10^{0}	1.37×10^{-2}	2.94×10^{-2}
RNA5SP211	2.26×10^{1}	4.50×10^{0}	1.83×10^{-2}	3.77×10^{-2}
SOHLH1	2.01×10^{1}	4.33×10^{0}	1.97×10^{-14}	3.86×10^{-13}
RNA5SP389	1.86×10^{1}	4.22×10^{0}	1.86×10^{-2}	3.82×10^{-2}
AC127459.2	1.84×10^{1}	4.20×10^{0}	3.72×10^{-8}	2.50×10^{-7}
RN7SL149P	1.73×10^{1}	4.11×10^{0}	7.91×10^{-3}	1.82×10^{-2}
GALP	1.46×10^{1}	3.87×10^{0}	3.90×10^{-5}	1.50×10^{-4}
PNLIP	1.46×10^{1}	3.87×10^{0}	2.91×10^{-3}	7.46×10^{-3}
RN7SL762P	1.38×10^{1}	3.79×10^{0}	5.92×10^{-11}	6.48×10^{-10}
AC009446.1	1.34×10^{1}	3.75×10^{0}	1.92×10^{-4}	6.40×10^{-4}
SLC5A8	1.30×10^{1}	3.70×10^{0}	3.05×10^{-10}	2.97×10^{-9}
KRT31	1.23×10^{1}	3.62×10^{0}	1.52×10^{-11}	1.84×10^{-10}
PRSS56	1.15×10^{1}	3.52×10^{0}	9.14×10^{-10}	8.18×10^{-9}
GTF2IP11	1.14×10^{1}	3.51×10^{0}	1.61×10^{-2}	3.39×10^{-2}

MAGEB1	1.12×10^{1}	3.49×10^{0}	3.34×10^{-3}	8.45×10^{-3}
BPIFA1	1.12×10^{1}	3.48×10^{0}	2.03×10^{-4}	6.72×10^{-4}
RN7SL837P	1.11×10^{1}	3.47×10^{0}	1.43×10^{-2}	3.04×10^{-2}
PRR9	1.07×10^{1}	3.42×10^{0}	1.06×10^{-9}	9.44×10^{-9}
AP002963.1	1.05×10^{1}	3.39×10^{0}	9.46×10^{-4}	2.73×10^{-3}
RN7SL822P	1.03×10^{1}	3.36×10^{0}	2.44×10^{-2}	4.82×10^{-2}
TKTL1	1.02×10^{1}	3.35×10^{0}	2.03×10^{-15}	4.77×10^{-14}
SSX1	1.02×10^{1}	3.35×10^{0}	5.91×10^{-5}	2.19×10^{-4}
RN7SL122P	1.00×10^{1}	3.33×10^{0}	4.25×10^{-3}	1.05×10^{-2}
RNA5SP213	9.73×10^{0}	3.28×10^{0}	1.03×10^{-2}	2.29×10^{-2}
GPR83	9.66×10^{0}	3.27×10^{0}	9.77×10^{-27}	1.76×10^{-24}
AC132825.1	9.16×10^{0}	3.19×10^{0}	5.55×10^{-13}	8.57×10^{-12}
AL354863.1	8.83×10^{0}	3.14×10^{0}	9.70×10^{-13}	1.44×10^{-11}

Table A.35 (continued). The list of the top 100 upregulated DEGs identified in the CS3 subtype using edgeR as a result of four clustering analyzes.

RN7SL253P	8.31×10^{0}	3.05×10^{0}	1.42×10^{-5}	5.93×10^{-5}
AC010255.2	8.28×10^{0}	3.05×10^{0}	6.09×10^{-13}	9.35×10^{-12}
TRIM49B	7.94×10^{0}	2.99×10^{0}	2.41×10^{-2}	4.77×10^{-2}
NOTUM	7.63×10^{0}	2.93×10^{0}	6.38×10^{-22}	4.41×10^{-20}
DMRT1	7.51×10^{0}	2.91×10^{0}	5.92×10^{-12}	7.63×10^{-11}
NKX6.3	7.43×10^{0}	2.89×10^{0}	1.92×10^{-6}	9.47×10^{-6}
STRIT1	7.36×10^{0}	2.88×10^{0}	4.65×10^{-9}	3.68×10^{-8}
AC073176.2	7.35×10^{0}	2.88×10^{0}	4.70×10^{-3}	1.15×10^{-2}
OR7A1P	7.33×10^{0}	2.87×10^{0}	2.18×10^{-4}	7.20×10^{-4}
RPS10.NUDT3	7.25×10^{0}	2.86×10^{0}	1.15×10^{-27}	2.49×10^{-25}
RN7SL7P	7.13×10^{0}	2.83×10^{0}	1.24×10^{-2}	2.69×10^{-2}
TCAP	6.91×10^{0}	2.79×10^{0}	1.15×10^{-27}	2.49×10^{-25}
LINC00508	6.61×10^{0}	2.73×10^{0}	1.01×10^{-3}	2.89×10^{-3}
SYCN	6.51×10^{0}	2.70×10^{0}	2.51×10^{-2}	4.94×10^{-2}
TGM6	6.44×10^{0}	2.69×10^{0}	8.77×10^{-5}	3.14×10^{-4}
CPA1	6.39×10^{0}	2.68×10^{0}	5.55×10^{-6}	2.51×10^{-5}
AL356433.1	6.38×10^{0}	2.67×10^{0}	7.83×10^{-10}	7.10×10^{-9}
HSPB3	6.34×10^{0}	2.67×10^{0}	3.01×10^{-14}	5.72×10^{-13}
FGFR3P6	6.30×10^{0}	2.65×10^{0}	2.15×10^{-2}	4.32×10^{-2}
MAGEB6	6.13×10^{0}	2.62×10^{0}	1.01×10^{-4}	3.58×10^{-4}
AC114291.1	6.12×10^{0}	2.61×10^{0}	5.67×10^{-21}	3.34×10^{-19}
APOA2	6.02×10^{0}	2.59×10^{0}	1.10×10^{-10}	1.15×10^{-9}
AC244102.3	6.01×10^{0}	2.59×10^{0}	5.44×10^{-3}	1.31×10^{-2}
TMEM252	6.00×10^{0}	2.59×10^{0}	1.21×10^{-19}	5.57×10^{-18}
AL139327.1	5.94×10^{0}	2.57×10^{0}	4.51×10^{-3}	1.11×10^{-2}
PTF1A	5.92×10^{0}	2.57×10^{0}	4.20×10^{-7}	2.35×10^{-6}
LINC01419	5.90×10^{0}	2.56×10^{0}	1.56×10^{-5}	6.49×10^{-5}
GDF10	5.77×10^{0}	2.53×10^{0}	1.47×10^{-11}	1.78×10^{-10}

AC104809.1	5.74×10^{0}	2.52×10^{0}	3.18×10^{-6}	1.51×10^{-5}
RN7SL659P	5.71×10^{0}	2.51×10^{0}	1.33×10^{-7}	8.09×10^{-7}
AC078993.1	5.70×10^{0}	2.51×10^{0}	1.88×10^{-14}	3.69×10^{-13}
MAGEB17	5.58×10^{0}	2.48×10^{0}	7.44×10^{-12}	9.43×10^{-11}
AC108865.1	5.57×10^{0}	2.48×10^{0}	1.25×10^{-9}	1.10×10^{-8}
CTNNA2.AS1	5.54×10^{0}	2.47×10^{0}	4.60×10^{-5}	1.74×10^{-4}
KRT40	5.47×10^{0}	2.45×10^{0}	2.59×10^{-12}	3.55×10^{-11}
CPN1	5.43×10^{0}	2.44×10^{0}	1.05×10^{-12}	1.55×10^{-11}
RN7SL792P	5.34×10^{0}	2.42×10^{0}	3.19×10^{-3}	8.12×10^{-3}
AC090386.1	5.29×10^{0}	2.40×10^{0}	2.52×10^{-2}	4.97×10^{-2}
RN7SL217P	5.27×10^{0}	2.40×10^{0}	2.47×10^{-2}	4.87×10^{-2}
KRTAP9.8	5.25×10^{0}	2.39×10^{0}	2.07×10^{-3}	5.51×10^{-3}

Table A.35 (continued). The list of the top 100 upregulated DEGs identified in the CS3 subtype using edgeR as a result of four clustering analyzes.

ATP12A	5.22×10^{0}	2.38×10^{0}	4.17×10^{-9}	3.34×10^{-8}
SFTA3	5.22×10^{0}	2.38×10^{0}	4.42×10^{-3}	1.08×10^{-2}
LINC01533	5.20×10^{0}	2.38×10^{0}	1.23×10^{-3}	3.46×10^{-3}
C20orf85	5.20×10^{0}	2.38×10^{0}	2.85×10^{-8}	1.96×10^{-7}
AC093523.1	5.19×10^{0}	2.37×10^{0}	1.12×10^{-11}	1.38×10^{-10}
SLC39A2	5.12×10^{0}	2.36×10^{0}	6.36×10^{-13}	9.73×10^{-12}
FGF6	5.12×10^{0}	2.36×10^{0}	1.90×10^{-3}	5.11×10^{-3}
SFTPA1	5.05×10^{0}	2.34×10^{0}	5.02×10^{-5}	1.89×10^{-4}
KRTAP1.1	5.01×10^{0}	2.32×10^{0}	9.93×10^{-7}	5.17×10^{-6}
AC087386.2	4.94×10^{0}	2.30×10^{0}	4.45×10^{-3}	1.09×10^{-2}
SERPINA7	4.91×10^{0}	2.30×10^{0}	8.90×10^{-11}	9.47×10^{-10}
OR10G4	4.89×10^{0}	2.29×10^{0}	3.55×10^{-4}	1.12×10^{-3}
OBP2B	4.88×10^{0}	2.29×10^{0}	3.69×10^{-8}	2.48×10^{-7}
TMCO2	4.88×10^{0}	2.29×10^{0}	5.61×10^{-9}	4.38×10^{-8}
AC026336.3	4.87×10^{0}	2.28×10^{0}	6.87×10^{-11}	7.45×10^{-10}
LY6G6D	4.86×10^{0}	2.28×10^{0}	3.98×10^{-11}	4.48×10^{-10}
CHRNA2	4.86×10^{0}	2.28×10^{0}	7.42×10^{-7}	3.96×10^{-6}
IGDCC3	4.85×10^{0}	2.28×10^{0}	4.63×10^{-9}	3.67×10^{-8}
TCHH	4.85×10^{0}	2.28×10^{0}	2.73×10^{-18}	1.02×10^{-16}
CTRB2	4.83×10^{0}	2.27×10^{0}	2.48×10^{-7}	1.45×10^{-6}
ZP2	4.82×10^{0}	2.27×10^{0}	1.44×10^{-20}	7.88×10^{-19}
AC011303.1	4.82×10^{0}	2.27×10^{0}	1.56×10^{-3}	4.26×10^{-3}
GLYATL2	4.79×10^{0}	2.26×10^{0}	3.20×10^{-17}	1.01×10^{-15}
FGF3	4.76×10^{0}	2.25×10^{0}	2.96×10^{-7}	1.70×10^{-6}
MIR8075	4.73×10^{0}	2.24×10^{0}	2.00×10^{-4}	6.65×10^{-4}
AC016925.3	4.69×10^{0}	2.23×10^{0}	7.57×10^{-9}	5.76×10^{-8}
PAX7	4.67×10^{0}	2.22×10^{0}	1.75×10^{-4}	5.90×10^{-4}
AL445205.1	4.67×10^{0}	2.22×10^{0}	6.88×10^{-9}	5.28×10^{-8}
LINC01487	4.66×10^{0}	2.22×10^{0}	1.34×10^{-2}	2.89×10^{-2}

Table A.36. The list of the top 100 downregulated DEGs identified in the CS3 subtype using edgeR as a result of four clustering analyzes.

	fc	log2fc	pvalue	padj
CLDN18	1.63×10^{-2}	-5.94×10^{0}	2.28×10^{-42}	1.09×10^{-38}
INSL4	1.71×10^{-2}	-5.87×10^{0}	1.09×10^{-18}	4.36×10^{-17}
MSMB	2.81×10^{-2}	-5.15×10^{0}	3.37×10^{-26}	5.35×10^{-24}
DLGAP1.AS5	2.85×10^{-2}	-5.13×10^{0}	5.57×10^{-26}	8.48×10^{-24}
AL136442.1	3.30×10^{-2}	-4.92×10^{0}	8.49×10^{-11}	9.07×10^{-10}
TAAR1	3.65×10^{-2}	-4.78×10^{0}	3.85×10^{-20}	1.93×10^{-18}
RNU1.29P	4.21×10^{-2}	-4.57×10^{0}	2.97×10^{-6}	1.42×10^{-5}
LCE3D	5.04×10^{-2}	-4.31×10^{0}	4.92×10^{-6}	2.25×10^{-5}

Table A.36 (continued). The list of the top 100 downregulated DEGs identified in the CS3 subtype using edgeR as a result of four clustering analyzes.

SPRR2C	5.18×10^{-2}	-4.27×10^{0}	1.21×10^{-5}	5.13×10^{-5}
MUC5AC	5.55×10^{-2}	-4.17×10^{0}	5.15×10^{-36}	4.61×10^{-33}
LINC01790	5.71×10^{-2}	-4.13×10^{0}	6.90×10^{-5}	2.52×10^{-4}
AC013437.1	5.89×10^{-2}	-4.09×10^{0}	1.74×10^{-10}	1.75×10^{-9}
PSAPL1	5.96×10^{-2}	-4.07×10^{0}	2.09×10^{-18}	8.02×10^{-17}
RNU1.104P	6.13×10^{-2}	-4.03×10^{0}	2.50×10^{-6}	1.21×10^{-5}
TFAP2D	6.36×10^{-2}	-3.97×10^{0}	9.18×10^{-6}	3.99×10^{-5}
MAGEA1	6.41×10^{-2}	-3.96×10^{0}	1.47×10^{-4}	5.03×10^{-4}
MIR548K	6.44×10^{-2}	-3.96×10^{0}	1.25×10^{-8}	9.13×10^{-8}
Y_RNA.291	6.55×10^{-2}	-3.93×10^{0}	6.90×10^{-5}	2.52×10^{-4}
NEUROD4	6.56×10^{-2}	-3.93×10^{0}	5.87×10^{-5}	2.18×10^{-4}
AC093001.1	6.78×10^{-2}	-3.88×10^{0}	1.35×10^{-18}	5.33×10^{-17}
CDY4P	6.88×10^{-2}	-3.86×10^{0}	5.44×10^{-6}	2.47×10^{-5}
RPL12P20	6.92×10^{-2}	-3.85×10^{0}	2.83×10^{-11}	3.26×10^{-10}
KRTAP4.6	6.99×10^{-2}	-3.84×10^{0}	7.52×10^{-4}	2.22×10^{-3}
AC011242.1	7.09×10^{-2}	-3.82×10^{0}	2.29×10^{-9}	1.92×10^{-8}
ELMO1.AS1	7.13×10^{-2}	-3.81×10^{0}	1.35×10^{-6}	6.88×10^{-6}
AC108451.2	7.23×10^{-2}	-3.79×10^{0}	1.25×10^{-22}	9.76×10^{-21}
TRPV6	7.26×10^{-2}	-3.78×10^{0}	3.88×10^{-33}	2.29×10^{-30}
AC129492.2	7.44×10^{-2}	-3.75×10^{0}	4.70×10^{-17}	1.45×10^{-15}
TMPRSS11D	7.53×10^{-2}	-3.73×10^{0}	1.83×10^{-16}	5.10×10^{-15}
Y_RNA.643	7.62×10^{-2}	-3.71×10^{0}	8.97×10^{-6}	3.90×10^{-5}
AC011139.1	7.64×10^{-2}	-3.71×10^{0}	2.24×10^{-8}	1.57×10^{-7}
RNU1.78P	7.64×10^{-2}	-3.71×10^{0}	3.70×10^{-3}	9.24×10^{-3}
MTATP6P15	7.69×10^{-2}	-3.70×10^{0}	7.78×10^{-7}	4.13×10^{-6}
RNU6ATAC10P	7.75×10^{-2}	-3.69×10^{0}	1.11×10^{-7}	6.88×10^{-7}
Z98742.2	7.96×10^{-2}	-3.65×10^{0}	1.12×10^{-8}	8.21×10^{-8}
RNU6.979P	8.17×10^{-2}	-3.61×10^{0}	1.27×10^{-7}	7.80×10^{-7}
LINC02303	8.33×10^{-2}	-3.59×10^{0}	2.67×10^{-12}	3.65×10^{-11}

OR13H1	8.40×10^{-2}	-3.57×10^{0}	2.36×10^{-7}	1.38×10^{-6}
KRT24	8.44×10^{-2}	-3.57×10^{0}	1.41×10^{-7}	8.57×10^{-7}
AC004549.1	8.48×10^{-2}	-3.56×10^{0}	2.25×10^{-8}	1.57×10^{-7}
AL450003.1	8.50×10^{-2}	-3.56×10^{0}	4.50×10^{-7}	2.50×10^{-6}
LINC01831	8.55×10^{-2}	-3.55×10^{0}	1.70×10^{-3}	4.62×10^{-3}
AL391097.3	8.63×10^{-2}	-3.53×10^{0}	4.02×10^{-11}	4.52×10^{-10}
SPRR1B	8.65×10^{-2}	-3.53×10^{0}	1.49×10^{-13}	2.53×10^{-12}
RNU6.425P	8.74×10^{-2}	-3.52×10^{0}	3.50×10^{-7}	1.98×10^{-6}
PRLHR	8.75×10^{-2}	-3.51×10^{0}	2.30×10^{-14}	4.45×10^{-13}
RNU6.14P	8.78×10^{-2}	-3.51×10^{0}	6.08×10^{-5}	2.25×10^{-4}
RNU5D.2P	8.79×10^{-2}	-3.51×10^{0}	1.18×10^{-5}	5.03×10^{-5}

Table A.36 (continued). The list of the top 100 downregulated DEGs identified in the CS3 subtype using edgeR as a result of four clustering analyzes.

HS6ST2.AS1	8.99×10^{-2}	-3.47×10^{0}	3.21×10^{-10}	3.11×10^{-9}
AC008764.1	9.01×10^{-2}	-3.47×10^{0}	2.93×10^{-7}	1.68×10^{-6}
AL139193.2	9.12×10^{-2}	-3.45×10^{0}	1.37×10^{-7}	8.33×10^{-7}
AC026782.1	9.19×10^{-2}	-3.44×10^{0}	8.69×10^{-7}	4.58×10^{-6}
KRT6C	9.22×10^{-2}	-3.44×10^{0}	4.53×10^{-18}	1.65×10^{-16}
MTCO1P4	9.36×10^{-2}	-3.42×10^{0}	1.58×10^{-7}	9.52×10^{-7}
RMST	9.37×10^{-2}	-3.42×10^{0}	5.21×10^{-12}	6.77×10^{-11}
SERPINB7	9.37×10^{-2}	-3.42×10^{0}	3.83×10^{-23}	3.31×10^{-21}
AL357793.1	9.52×10^{-2}	-3.39×10^{0}	2.05×10^{-8}	1.45×10^{-7}
SFXN4P1	9.54×10^{-2}	-3.39×10^{0}	7.19×10^{-9}	5.49×10^{-8}
HINT1P2	9.58×10^{-2}	-3.38×10^{0}	4.23×10^{-6}	1.96×10^{-5}
CRNN	9.85×10^{-2}	-3.34×10^{0}	3.23×10^{-4}	1.03×10^{-3}
AL391097.2	9.85×10^{-2}	-3.34×10^{0}	6.28×10^{-12}	8.05×10^{-11}
Y_RNA.488	9.87×10^{-2}	-3.34×10^{0}	1.97×10^{-5}	8.02×10^{-5}
AP000248.1	9.96×10^{-2}	-3.33×10^{0}	6.54×10^{-7}	3.53×10^{-6}
LINC02775	9.98×10^{-2}	-3.33×10^{0}	1.57×10^{-11}	1.89×10^{-10}
RNU1.117P	1.00×10^{-1}	-3.31×10^{0}	4.27×10^{-4}	1.33×10^{-3}
MYOCD.AS1	1.01×10^{-1}	-3.31×10^{0}	1.30×10^{-5}	5.48×10^{-5}
SOD2P1	1.01×10^{-1}	-3.31×10^{0}	1.46×10^{-8}	1.05×10^{-7}
Y_RNA.323	1.03×10^{-1}	-3.28×10^{0}	1.69×10^{-4}	5.69×10^{-4}
AC022929.1	1.03×10^{-1}	-3.27×10^{0}	5.84×10^{-7}	3.18×10^{-6}
ACTBL2	1.03×10^{-1}	-3.27×10^{0}	3.50×10^{-24}	3.77×10^{-22}
RNU1.130P	1.04×10^{0}	-3.27×10^{0}	7.04×10^{-4}	2.09×10^{-3}
MIR5706	1.04×10^{0}	-3.27×10^{0}	5.80×10^{-6}	2.62×10^{-5}
SNORD113.1	1.04×10^{0}	-3.27×10^{0}	7.97×10^{-6}	3.50×10^{-5}
AC108861.1	1.04×10^{0}	-3.26×10^{0}	3.05×10^{-9}	2.50×10^{-8}
CDH12	1.07×10^{0}	-3.23×10^{0}	3.28×10^{-10}	3.17×10^{-9}
AC104126.1	1.07×10^{0}	-3.23×10^{0}	8.29×10^{-9}	6.25×10^{-8}
AL050343.1	1.07×10^{0}	-3.22×10^{0}	1.26×10^{-7}	7.70×10^{-7}
AL360157.1	1.08×10^{0}	-3.21×10^{0}	1.08×10^{-3}	3.07×10^{-3}

RNU6ATAC2P	1.08×10^{0}	-3.21×10^{0}	3.45×10^{-5}	1.34×10^{-4}
Y_RNA.211	1.08×10^{0}	-3.21×10^{0}	1.26×10^{-6}	6.44×10^{-6}
PAPPA.AS2	1.08×10^{0}	-3.21×10^{0}	2.92×10^{-9}	2.40×10^{-8}
MAP1LC3P	1.09×10^{0}	-3.20×10^{0}	7.21×10^{-12}	9.15×10^{-11}
RNU6.31P	1.09×10^{0}	-3.20×10^{0}	5.36×10^{-5}	2.01×10^{-4}
ARHGAP16P	1.09×10^{0}	-3.20×10^{0}	1.71×10^{-4}	5.78×10^{-4}
AP001172.1	1.09×10^{0}	-3.19×10^{0}	3.22×10^{-7}	1.84×10^{-6}
MIR626	1.11×10^{0}	-3.17×10^{0}	1.92×10^{-5}	7.83×10^{-5}
UGT3A1	1.12×10^{0}	-3.16×10^{0}	8.79×10^{-6}	3.83×10^{-5}
CCDC83	1.12×10^{0}	-3.16×10^{0}	9.45×10^{-22}	6.38×10^{-20}

Table A.36 (continued). The list of the top 100 downregulated DEGs identified in the CS3 subtype using edgeR as a result of four clustering analyzes.

UST.AS1	1.12×10^{0}	-3.16×10^{0}	7.43×10^{-11}	8.00×10^{-10}
CYP1A1	1.12×10^{0}	-3.16×10^{0}	7.27×10^{-11}	7.85×10^{-10}
AC090960.1	1.13×10^{0}	-3.15×10^{0}	3.25×10^{-5}	1.27×10^{-4}
AC107029.2	1.14×10^{0}	-3.13×10^{0}	1.47×10^{-7}	8.89×10^{-7}
FAM167A.AS1	1.15×10^{0}	-3.12×10^{0}	6.77×10^{-11}	7.35×10^{-10}
RNU6ATAC7P	1.15×10^{0}	-3.12×10^{0}	1.04×10^{-6}	5.38×10^{-6}
AL731575.1	1.16×10^{0}	-3.11×10^{0}	7.84×10^{-8}	5.00×10^{-7}
MIR4308	1.16×10^{0}	-3.11×10^{0}	7.81×10^{-8}	4.98×10^{-7}
HPR	1.16×10^{0}	-3.10×10^{0}	1.05×10^{-18}	4.20×10^{-17}
RNA5.8SN3	1.17×10^{0}	-3.09×10^{0}	3.50×10^{-4}	1.11×10^{-3}
AP006248.3	1.17×10^{0}	-3.09×10^{0}	2.14×10^{-6}	1.05×10^{-5}
AC104350.1	1.18×10^{0}	-3.08×10^{0}	2.31×10^{-7}	1.35×10^{-6}

Table A.37. The list of the top 100 upregulated DEGs identified in the CS4 subtype using edgeR as a result of four clustering analyzes.

	fc	**log2fc**	**pvalue**	**padj**
GP2	3.82×10^{1}	5.26×10^{0}	1.98×10^{-40}	5.67×10^{-36}
MLN	2.29×10^{1}	4.52×10^{0}	4.47×10^{-19}	1.77×10^{-16}
TTC29	2.16×10^{1}	4.43×10^{0}	3.68×10^{-17}	8.50×10^{-15}
COX8C	1.61×10^{1}	4.01×10^{0}	8.47×10^{-23}	6.83×10^{-20}
AL136442.1	1.60×10^{1}	4.00×10^{0}	8.72×10^{-5}	5.94×10^{-4}
LIPF	1.59×10^{1}	3.99×10^{0}	8.58×10^{-13}	6.49×10^{-11}
CIB4	1.56×10^{1}	3.96×10^{0}	1.06×10^{-33}	1.35×10^{-29}
ANXA10	1.56×10^{1}	3.96×10^{0}	1.18×10^{-21}	8.21×10^{-19}
CYP1A1	1.46×10^{1}	3.87×10^{0}	4.98×10^{-16}	8.56×10^{-14}
SEMG2	1.45×10^{1}	3.86×10^{0}	7.87×10^{-15}	9.90×10^{-13}
RPS17P1	1.39×10^{1}	3.80×10^{0}	1.39×10^{-17}	3.61×10^{-15}
IRGM	1.38×10^{1}	3.78×10^{0}	1.18×10^{-33}	1.35×10^{-29}
PRSS2	1.36×10^{1}	3.77×10^{0}	4.14×10^{-19}	1.65×10^{-16}
AC126323.1	1.34×10^{1}	3.74×10^{0}	8.39×10^{-11}	3.62×10^{-9}

UGT2B4	1.30×10^{1}	3.70×10^{0}	2.08×10^{-14}	2.35×10^{-12}
BCAR4	1.30×10^{1}	3.70×10^{0}	9.10×10^{-27}	2.17×10^{-23}
FGL1	1.26×10^{1}	3.66×10^{0}	1.48×10^{-15}	2.21×10^{-13}
DEFA11P	1.24×10^{1}	3.63×10^{0}	3.80×10^{-4}	2.05×10^{-3}
CTSE	1.17×10^{1}	3.55×10^{0}	2.19×10^{-32}	1.79×10^{-28}
TM4SF4	1.13×10^{1}	3.49×10^{0}	1.50×10^{-27}	4.52×10^{-24}
IGFALS	1.09×10^{1}	3.45×10^{0}	5.49×10^{-32}	3.93×10^{-28}
MUC5AC	1.06×10^{1}	3.41×10^{0}	4.94×10^{-23}	4.41×10^{-20}
GUSBP7	1.05×10^{1}	3.39×10^{0}	7.17×10^{-11}	3.15×10^{-9}

Table A.37 (continued). The list of the top 100 upregulated DEGs identified in the CS4 subtype using edgeR as a result of four clustering analyzes.

MAGEB10	1.02×10^{1}	3.35×10^{0}	4.44×10^{-6}	4.62×10^{-5}
AC024597.1	1.01×10^{1}	3.34×10^{0}	3.22×10^{-5}	2.54×10^{-4}
RBP3	9.46×10^{0}	3.24×10^{0}	1.03×10^{-24}	1.25×10^{-21}
MAGEB2	9.22×10^{0}	3.21×10^{0}	2.95×10^{-4}	1.66×10^{-3}
AC009078.1	8.96×10^{0}	3.16×10^{0}	5.36×10^{-8}	1.02×10^{-6}
LIPC	8.96×10^{0}	3.16×10^{0}	1.64×10^{-25}	2.40×10^{-22}
AC111149.2	8.87×10^{0}	3.15×10^{0}	1.97×10^{-20}	1.11×10^{-17}
AP005902.1	8.87×10^{0}	3.15×10^{0}	1.66×10^{-4}	1.02×10^{-3}
IRX4.AS1	8.79×10^{0}	3.14×10^{0}	4.83×10^{-5}	3.58×10^{-4}
REG4	8.67×10^{0}	3.12×10^{0}	1.14×10^{-21}	8.08×10^{-19}
LINC02620	8.49×10^{0}	3.09×10^{0}	9.63×10^{-8}	1.69×10^{-6}
ALPG	8.19×10^{0}	3.03×10^{0}	1.39×10^{-19}	6.38×10^{-17}
PGC	7.98×10^{0}	2.99×10^{0}	2.41×10^{-24}	2.66×10^{-21}
CPS1	7.96×10^{0}	2.99×10^{0}	2.35×10^{-19}	9.95×10^{-17}
LINC01477	7.94×10^{0}	2.99×10^{0}	8.99×10^{-8}	1.60×10^{-6}
RMST	7.91×10^{0}	2.98×10^{0}	8.66×10^{-8}	1.55×10^{-6}
INSL4	7.76×10^{0}	2.96×10^{0}	3.76×10^{-5}	2.89×10^{-4}
AL356313.1	7.56×10^{0}	2.92×10^{0}	1.40×10^{-4}	8.81×10^{-4}
RNA5SP107	7.47×10^{0}	2.90×10^{0}	1.51×10^{-5}	1.32×10^{-4}
TCN1	7.46×10^{0}	2.90×10^{0}	8.53×10^{-20}	4.10×10^{-17}
ARX	7.40×10^{0}	2.89×10^{0}	1.54×10^{-23}	1.45×10^{-20}
AC021534.1	7.33×10^{0}	2.87×10^{0}	2.92×10^{-10}	1.07×10^{-8}
FP671120.6	7.29×10^{0}	2.87×10^{0}	2.99×10^{-4}	1.68×10^{-3}
PRSS3P1	7.22×10^{0}	2.85×10^{0}	9.04×10^{-13}	6.76×10^{-11}
CLCA1	7.20×10^{0}	2.85×10^{0}	1.79×10^{-13}	1.63×10^{-11}
CYP3A4	7.10×10^{0}	2.83×10^{0}	3.73×10^{-25}	5.08×10^{-22}
NBPF7	6.98×10^{0}	2.80×10^{0}	4.36×10^{-16}	7.58×10^{-14}
SPINK4	6.95×10^{0}	2.80×10^{0}	7.84×10^{-17}	1.69×10^{-14}
AC008514.1	6.71×10^{0}	2.75×10^{0}	4.71×10^{-17}	1.06×10^{-14}
LRRC26	6.68×10^{0}	2.74×10^{0}	8.37×10^{-19}	3.11×10^{-16}
GUSBP10	6.64×10^{0}	2.73×10^{0}	1.23×10^{-3}	5.44×10^{-3}
AC099654.5	6.62×10^{0}	2.73×10^{0}	4.25×10^{-4}	2.25×10^{-3}
ESX1	6.58×10^{0}	2.72×10^{0}	2.31×10^{-3}	9.14×10^{-3}

VSIG1	6.58×10^{0}	2.72×10^{0}	3.39×10^{-24}	3.66×10^{-21}
PRSS41	6.57×10^{0}	2.72×10^{0}	7.90×10^{-23}	6.64×10^{-20}
TFF1	6.56×10^{0}	2.71×10^{0}	1.06×10^{-26}	2.34×10^{-23}
LINC00261	6.50×10^{0}	2.70×10^{0}	1.73×10^{-31}	1.10×10^{-27}
ADAM2	6.50×10^{0}	2.70×10^{0}	1.09×10^{-7}	1.89×10^{-6}
LINC02826	6.43×10^{0}	2.68×10^{0}	1.17×10^{-17}	3.11×10^{-15}
LINC02575	6.42×10^{0}	2.68×10^{0}	1.30×10^{-15}	2.01×10^{-13}
SLURP1	6.38×10^{0}	2.67×10^{0}	1.98×10^{-9}	5.74×10^{-8}

Table A.37 (continued). The list of the top 100 upregulated DEGs identified in the CS4 subtype using edgeR as a result of four clustering analyzes.

SLC18A1	6.37×10^{0}	2.67×10^{0}	1.91×10^{-19}	8.35×10^{-17}
ANPEP	6.32×10^{0}	2.66×10^{0}	1.01×10^{-26}	2.32×10^{-23}
CYMP.AS1	6.32×10^{0}	2.66×10^{0}	1.28×10^{-8}	2.91×10^{-7}
MAGEA1	6.31×10^{0}	2.66×10^{0}	1.63×10^{-2}	4.48×10^{-2}
LINC00469	6.30×10^{0}	2.66×10^{0}	7.90×10^{-8}	1.43×10^{-6}
AC009154.1	6.29×10^{0}	2.65×10^{0}	3.14×10^{-7}	4.68×10^{-6}
FGFR1OP2P1	6.29×10^{0}	2.65×10^{0}	5.60×10^{-3}	1.89×10^{-2}
CA7	6.21×10^{0}	2.64×10^{0}	2.58×10^{-26}	5.09×10^{-23}
AC253536.4	6.21×10^{0}	2.63×10^{0}	4.63×10^{-13}	3.74×10^{-11}
NXPH4	6.19×10^{0}	2.63×10^{0}	2.56×10^{-21}	1.68×10^{-18}
AP001531.1	6.04×10^{0}	2.59×10^{0}	1.88×10^{-3}	7.73×10^{-3}
AC020637.1	5.99×10^{0}	2.58×10^{0}	9.61×10^{-9}	2.27×10^{-7}
AP002498.1	5.98×10^{0}	2.58×10^{0}	3.77×10^{-19}	1.51×10^{-16}
CYMP	5.96×10^{0}	2.57×10^{0}	2.86×10^{-13}	2.46×10^{-11}
AC009055.2	5.91×10^{0}	2.56×10^{0}	2.89×10^{-8}	5.91×10^{-7}
AC093001.1	5.89×10^{0}	2.56×10^{0}	9.21×10^{-7}	1.18×10^{-5}
AC126564.1	5.85×10^{0}	2.55×10^{0}	9.95×10^{-18}	2.69×10^{-15}
AC100826.1	5.84×10^{0}	2.55×10^{0}	1.11×10^{-9}	3.40×10^{-8}
AFM	5.76×10^{0}	2.53×10^{0}	1.85×10^{-8}	4.00×10^{-7}
RFX6	5.73×10^{0}	2.52×10^{0}	6.01×10^{-12}	3.58×10^{-10}
AL132775.1	5.71×10^{0}	2.51×10^{0}	5.17×10^{-12}	3.16×10^{-10}
LINC02113	5.71×10^{0}	2.51×10^{0}	8.35×10^{-6}	7.95×10^{-5}
ATP5MC1P5	5.68×10^{0}	2.51×10^{0}	4.14×10^{-10}	1.44×10^{-8}
DHRS2	5.53×10^{0}	2.47×10^{0}	7.16×10^{-23}	6.12×10^{-20}
HEPACAM2	5.49×10^{0}	2.46×10^{0}	1.70×10^{-18}	5.65×10^{-16}
MKRN6P	5.48×10^{0}	2.45×10^{0}	1.90×10^{-8}	4.11×10^{-7}
QRFPR	5.47×10^{0}	2.45×10^{0}	8.02×10^{-9}	1.94×10^{-7}
AC107892.1	5.46×10^{0}	2.45×10^{0}	6.28×10^{-4}	3.11×10^{-3}
AC129492.2	5.44×10^{0}	2.44×10^{0}	1.18×10^{-5}	1.07×10^{-4}
AC009055.1	5.40×10^{0}	2.43×10^{0}	2.47×10^{-3}	9.66×10^{-3}
AC010998.3	5.39×10^{0}	2.43×10^{0}	1.00×10^{-10}	4.17×10^{-9}
NEUROG3	5.34×10^{0}	2.42×10^{0}	3.34×10^{-11}	1.60×10^{-9}
PIK3C2G	5.31×10^{0}	2.41×10^{0}	9.17×10^{-10}	2.88×10^{-8}

PSLNR	5.28×10^{0}	2.40×10^{0}	2.28×10^{-3}	9.06×10^{-3}
ALOXE3P1	5.28×10^{0}	2.40×10^{0}	3.71×10^{-9}	9.92×10^{-8}
MUC2	5.25×10^{0}	2.39×10^{0}	2.29×10^{-15}	3.26×10^{-13}

Table A.38. The list of the top 100 downregulated DEGs identified in the CS4 subtype using edgeR as a result of four clustering analyzes.

	fc	**log2fc**	**pvalue**	**padj**
TMEM132D.AS1	1.40×10^{-2}	-6.16×10^{0}	2.45×10^{-6}	2.77×10^{-5}
PTF1A	2.42×10^{-2}	-5.37×10^{0}	2.23×10^{-10}	8.47×10^{-9}
CDH9	2.51×10^{-2}	-5.32×10^{0}	3.12×10^{-6}	3.41×10^{-5}
AC152010.1	2.59×10^{-2}	-5.27×10^{0}	1.25×10^{-2}	3.63×10^{-2}
RN7SL618P	2.76×10^{-2}	-5.18×10^{0}	1.30×10^{-2}	3.74×10^{-2}
RNA5.8SP5	2.98×10^{-2}	-5.07×10^{0}	1.36×10^{-2}	3.88×10^{-2}
MAGEA10	3.76×10^{-2}	-4.73×10^{0}	2.24×10^{-5}	1.86×10^{-4}
CT45A1	3.84×10^{-2}	-4.70×10^{0}	1.43×10^{-2}	4.05×10^{-2}
RN7SL783P	3.96×10^{-2}	-4.66×10^{0}	6.17×10^{-3}	2.05×10^{-2}
CHRND	4.05×10^{-2}	-4.63×10^{0}	5.65×10^{-9}	1.43×10^{-7}
MAGEA4.AS1	4.14×10^{-2}	-4.59×10^{0}	2.92×10^{-5}	2.33×10^{-4}
LINC02128	4.37×10^{-2}	-4.52×10^{0}	4.18×10^{-14}	4.38×10^{-12}
OR1N2	4.52×10^{-2}	-4.47×10^{0}	8.04×10^{-5}	5.54×10^{-4}
RNA5SP225	4.84×10^{-2}	-4.37×10^{0}	1.36×10^{-2}	3.88×10^{-2}
EYA1	5.36×10^{-2}	-4.22×10^{0}	3.71×10^{-19}	1.50×10^{-16}
MAGEA9B	5.40×10^{-2}	-4.21×10^{0}	1.75×10^{-3}	7.28×10^{-3}
LINC01419	5.67×10^{-2}	-4.14×10^{0}	1.15×10^{-5}	1.05×10^{-4}
AL589787.2	5.70×10^{-2}	-4.13×10^{0}	1.31×10^{-4}	8.38×10^{-4}
AL110505.1	5.75×10^{-2}	-4.12×10^{0}	2.25×10^{-6}	2.58×10^{-5}
AC110772.2	6.01×10^{-2}	-4.06×10^{0}	1.07×10^{-11}	5.87×10^{-10}
KRT38	6.04×10^{-2}	-4.05×10^{0}	1.12×10^{-7}	1.93×10^{-6}
BPIFA1	6.27×10^{-2}	-4.00×10^{0}	6.24×10^{-3}	2.07×10^{-2}
CHRNA4	6.54×10^{-2}	-3.93×10^{0}	1.25×10^{-5}	1.12×10^{-4}
MAGEC2	6.74×10^{-2}	-3.89×10^{0}	1.16×10^{-2}	3.43×10^{-2}
MAGEA9	6.74×10^{-2}	-3.89×10^{0}	9.47×10^{-4}	4.37×10^{-3}
AC090809.1	6.82×10^{-2}	-3.87×10^{0}	3.32×10^{-6}	3.60×10^{-5}
KCNC2	6.92×10^{-2}	-3.85×10^{0}	1.65×10^{-6}	1.97×10^{-5}
AMBN	6.95×10^{-2}	-3.85×10^{0}	6.31×10^{-5}	4.50×10^{-4}
CTNNA2.AS1	7.10×10^{-2}	-3.82×10^{0}	1.48×10^{-5}	1.30×10^{-4}
RN7SL635P	7.15×10^{-2}	-3.81×10^{0}	1.69×10^{-2}	4.63×10^{-2}
MIR483	7.18×10^{-2}	-3.80×10^{0}	5.27×10^{-6}	5.35×10^{-5}

AL035252.2	7.27×10^{-2}	-3.78×10^{0}	5.54×10^{-11}	2.51×10^{-9}
LINCADL	7.28×10^{-2}	-3.78×10^{0}	9.51×10^{-4}	4.38×10^{-3}
AC012501.2	7.28×10^{-2}	-3.78×10^{0}	5.92×10^{-12}	3.53×10^{-10}
ASB5	7.30×10^{-2}	-3.78×10^{0}	5.16×10^{-8}	9.86×10^{-7}
VSTM2B	7.30×10^{-2}	-3.78×10^{0}	7.20×10^{-7}	9.64×10^{-6}
PHF2P2	7.42×10^{-2}	-3.75×10^{0}	9.45×10^{-9}	2.23×10^{-7}
GRPR	7.48×10^{-2}	-3.74×10^{0}	1.92×10^{-20}	1.09×10^{-17}

Table A.38 (continued). The list of the top 100 downregulated DEGs identified in the CS4 subtype using edgeR as a result of four clustering analyzes.

CTNNA2	7.77×10^{-2}	-3.69×10^{0}	2.05×10^{-11}	1.04×10^{-9}
AL033539.2	7.83×10^{-2}	-3.67×10^{0}	7.87×10^{-9}	1.91×10^{-7}
SAGE1	7.85×10^{-2}	-3.67×10^{0}	1.24×10^{-4}	7.99×10^{-4}
AC025839.1	7.97×10^{-2}	-3.65×10^{0}	2.05×10^{-7}	3.26×10^{-6}
RNA5SP161	8.06×10^{-2}	-3.63×10^{0}	1.18×10^{-2}	3.48×10^{-2}
AL358335.2	8.07×10^{-2}	-3.63×10^{0}	9.33×10^{-5}	6.29×10^{-4}
AP000428.2	8.11×10^{-2}	-3.62×10^{0}	2.90×10^{-3}	1.10×10^{-2}
RN7SL14P	8.26×10^{-2}	-3.60×10^{0}	1.64×10^{-2}	4.52×10^{-2}
LINC00607	8.28×10^{-2}	-3.59×10^{0}	3.73×10^{-16}	6.64×10^{-14}
GLRA2	8.45×10^{-2}	-3.56×10^{0}	3.81×10^{-14}	4.03×10^{-12}
SFTA3	8.45×10^{-2}	-3.56×10^{0}	5.73×10^{-3}	1.93×10^{-2}
AL137001.2	8.50×10^{-2}	-3.56×10^{0}	1.53×10^{-2}	4.27×10^{-2}
COX7B2	8.55×10^{-2}	-3.55×10^{0}	5.12×10^{-3}	1.76×10^{-2}
EZHIP	8.57×10^{-2}	-3.54×10^{0}	2.30×10^{-4}	1.34×10^{-3}
AL035467.2	8.80×10^{-2}	-3.51×10^{0}	6.61×10^{-5}	4.69×10^{-4}
RN7SL191P	9.10×10^{-2}	-3.46×10^{0}	1.03×10^{-3}	4.70×10^{-3}
ZNF663P	9.12×10^{-2}	-3.46×10^{0}	2.19×10^{-8}	4.66×10^{-7}
AC090578.1	9.35×10^{-2}	-3.42×10^{0}	8.34×10^{-12}	4.74×10^{-10}
AL033397.1	9.36×10^{-2}	-3.42×10^{0}	1.39×10^{-10}	5.60×10^{-9}
AL031686.1	9.40×10^{-2}	-3.41×10^{0}	9.72×10^{-10}	3.03×10^{-8}
U95743.1	9.41×10^{-2}	-3.41×10^{0}	7.36×10^{-5}	5.14×10^{-4}
AL583808.1	9.44×10^{-2}	-3.40×10^{0}	7.72×10^{-6}	7.43×10^{-5}
EMX2	9.68×10^{-2}	-3.37×10^{0}	8.97×10^{-8}	1.59×10^{-6}
AL022151.1	9.80×10^{-2}	-3.35×10^{0}	5.13×10^{-6}	5.23×10^{-5}
AC096759.2	9.92×10^{-2}	-3.33×10^{0}	1.29×10^{-5}	1.16×10^{-4}
TRPM3	1.00×10^{-1}	-3.32×10^{0}	6.33×10^{-14}	6.31×10^{-12}
VWDE	1.01×10^{-1}	-3.31×10^{0}	3.62×10^{-13}	3.04×10^{-11}
WT1.AS	1.01×10^{-1}	-3.31×10^{0}	7.39×10^{-8}	1.35×10^{-6}
AC019330.1	1.02×10^{-1}	-3.29×10^{0}	8.60×10^{-17}	1.82×10^{-14}
SALL3	1.03×10^{-1}	-3.28×10^{0}	7.22×10^{-3}	2.33×10^{-2}
ZIC1	1.03×10^{-1}	-3.27×10^{0}	1.35×10^{-4}	8.56×10^{-4}
H2BW1	1.04×10^{-1}	-3.27×10^{0}	2.05×10^{-3}	8.30×10^{-3}
LINC02525	1.04×10^{-1}	-3.27×10^{0}	8.51×10^{-8}	1.52×10^{-6}
AL355922.4	1.05×10^{-1}	-3.26×10^{0}	5.52×10^{-8}	1.05×10^{-6}
CACNG6	1.06×10^{-1}	-3.24×10^{0}	7.68×10^{-6}	7.40×10^{-5}

G2E3.AS1	1.08×10^{-1}	-3.22×10^{0}	6.94×10^{-4}	3.38×10^{-3}
LINC00508	1.09×10^{-1}	-3.20×10^{0}	6.19×10^{-3}	2.05×10^{-2}
EMX2OS	1.11×10^{-1}	-3.17×10^{0}	2.29×10^{-10}	8.65×10^{-9}
CENPVL3	1.13×10^{-1}	-3.14×10^{0}	2.97×10^{-5}	2.36×10^{-4}
AL121757.2	1.16×10^{-1}	-3.10×10^{0}	5.06×10^{-13}	4.06×10^{-11}
AC091646.1	1.16×10^{-1}	-3.10×10^{0}	1.13×10^{-7}	1.94×10^{-6}

Table A.38 (continued). The list of the top 100 downregulated DEGs identified in the CS4 subtype using edgeR as a result of four clustering analyzes.

RN7SL107P	1.16×10^{-1}	-3.10×10^{0}	4.67×10^{-3}	1.63×10^{-2}
RNA5SP145	1.17×10^{-1}	-3.10×10^{0}	1.35×10^{-2}	3.88×10^{-2}
STXBP5L	1.17×10^{-1}	-3.10×10^{0}	3.90×10^{-13}	3.22×10^{-11}
AL592043.1	1.17×10^{-1}	-3.09×10^{0}	7.44×10^{-6}	7.20×10^{-5}
NEUROG2.AS1	1.17×10^{-1}	-3.09×10^{0}	1.17×10^{-7}	2.00×10^{-6}
SPACA3	1.19×10^{-1}	-3.07×10^{0}	6.48×10^{-15}	8.40×10^{-13}
RN7SL457P	1.20×10^{-1}	-3.05×10^{0}	3.94×10^{-3}	1.42×10^{-2}
AL139327.1	1.20×10^{-1}	-3.05×10^{0}	8.19×10^{-3}	2.58×10^{-2}
PCDH19	1.20×10^{-1}	-3.05×10^{0}	6.33×10^{-15}	8.26×10^{-13}
KRT39	1.21×10^{-1}	-3.05×10^{0}	3.52×10^{-10}	1.26×10^{-8}
ERVH.1	1.21×10^{-1}	-3.04×10^{0}	1.77×10^{-10}	6.91×10^{-9}
LY6G6F	1.21×10^{-1}	-3.04×10^{0}	2.06×10^{-17}	5.07×10^{-15}
AL121885.2	1.22×10^{-1}	-3.04×10^{0}	1.32×10^{-8}	2.98×10^{-7}
LINC02251	1.22×10^{-1}	-3.04×10^{0}	1.53×10^{-16}	2.97×10^{-14}
AL391650.2	1.23×10^{-1}	-3.03×10^{0}	3.39×10^{-8}	6.81×10^{-7}
GABRG3	1.23×10^{-1}	-3.02×10^{0}	3.02×10^{-5}	2.40×10^{-4}
AL450345.2	1.24×10^{-1}	-3.02×10^{0}	1.74×10^{-4}	1.06×10^{-3}
TUBA3C	1.24×10^{-1}	-3.01×10^{0}	1.56×10^{-3}	6.61×10^{-3}
DUX4L34	1.24×10^{-1}	-3.01×10^{0}	1.15×10^{-3}	5.14×10^{-3}
FGF19	1.25×10^{-1}	-3.00×10^{0}	1.24×10^{-9}	3.76×10^{-8}
AC012213.1	1.25×10^{-1}	-3.00×10^{0}	4.32×10^{-3}	1.53×10^{-2}

Table A.39. The list of the top 100 upregulated DEGs identified in the CS1 subtype using DESeq2 as a result of four clustering analyzes.

	fc	**log2fc**	**pvalue**	**padj**
TRARG1	2.40×10^{1}	4.59×10^{0}	3.11×10^{-18}	1.33×10^{-16}
ADIPOQ	2.10×10^{1}	4.39×10^{0}	2.21×10^{-9}	3.01×10^{-8}
FABP4	1.76×10^{1}	4.14×10^{0}	3.22×10^{-31}	7.23×10^{-29}
LINCADL	1.58×10^{1}	3.98×10^{0}	1.12×10^{-4}	4.34×10^{-4}
LEP	1.58×10^{1}	3.98×10^{0}	6.27×10^{-27}	7.32×10^{-25}
CIDEA	1.51×10^{1}	3.92×10^{0}	2.03×10^{-7}	1.75×10^{-6}
MYOC	1.44×10^{1}	3.84×10^{0}	8.70×10^{-19}	3.98×10^{-17}
PLIN4	1.35×10^{1}	3.76×10^{0}	2.63×10^{-31}	6.08×10^{-29}
PRG4	1.27×10^{1}	3.66×10^{0}	2.43×10^{-57}	1.01×10^{-52}
PLIN1	1.19×10^{1}	3.58×10^{0}	6.68×10^{-32}	1.69×10^{-29}

TCF23	1.12×10^{1}	3.48×10^{0}	9.38×10^{-28}	1.23×10^{-25}
TCEAL2	1.08×10^{1}	3.44×10^{0}	1.52×10^{-23}	1.17×10^{-21}
NGB	1.08×10^{1}	3.44×10^{0}	2.07×10^{-17}	8.02×10^{-16}
TCEAL5	1.08×10^{1}	3.43×10^{0}	2.31×10^{-28}	3.34×10^{-26}
THSD7B	1.06×10^{1}	3.40×10^{0}	1.01×10^{-26}	1.14×10^{-24}

Table A.39 (continued). The list of the top 100 upregulated DEGs identified in the CS1 subtype using DESeq2 as a result of four clustering analyzes.

SPOCK3	1.05×10^{1}	3.39×10^{0}	7.57×10^{-17}	2.75×10^{-15}
NPTX1	9.76×10^{0}	3.29×10^{0}	1.14×10^{-34}	5.47×10^{-32}
SLC7A14	9.60×10^{0}	3.26×10^{0}	2.14×10^{-18}	9.32×10^{-17}
PROK1	9.46×10^{0}	3.24×10^{0}	1.05×10^{-11}	2.09×10^{-10}
FCER2	9.31×10^{0}	3.22×10^{0}	3.68×10^{-23}	2.69×10^{-21}
ADH1B	9.23×10^{0}	3.21×10^{0}	3.60×10^{-21}	2.16×10^{-19}
PENK	9.22×10^{0}	3.20×10^{0}	7.55×10^{-20}	3.86×10^{-18}
PGM5.AS1	9.21×10^{0}	3.20×10^{0}	1.21×10^{-18}	5.42×10^{-17}
SFRP1	9.12×10^{0}	3.19×10^{0}	6.67×10^{-29}	1.05×10^{-26}
ASTN1	8.99×10^{0}	3.17×10^{0}	5.22×10^{-23}	3.76×10^{-21}
PRIMA1	8.97×10^{0}	3.17×10^{0}	2.22×10^{-25}	2.21×10^{-23}
KRT24	8.84×10^{0}	3.14×10^{0}	2.57×10^{-5}	1.20×10^{-4}
CCL19	8.77×10^{0}	3.13×10^{0}	4.75×10^{-33}	1.57×10^{-30}
CADM3	8.70×10^{0}	3.12×10^{0}	7.12×10^{-31}	1.52×10^{-28}
CHRDL2	8.65×10^{0}	3.11×10^{0}	1.20×10^{-24}	1.07×10^{-22}
KRT14	8.61×10^{0}	3.11×10^{0}	1.78×10^{-14}	4.98×10^{-13}
IGLV3.22	8.61×10^{0}	3.11×10^{0}	6.80×10^{-10}	1.02×10^{-8}
THRSP	8.51×10^{0}	3.09×10^{0}	5.19×10^{-21}	3.05×10^{-19}
ATCAY	8.45×10^{0}	3.08×10^{0}	5.40×10^{-29}	8.66×10^{-27}
CD300LG	8.29×10^{0}	3.05×10^{0}	1.69×10^{-13}	4.29×10^{-12}
TRARG1	2.40×10^{1}	4.59×10^{0}	3.11×10^{-18}	1.33×10^{-16}
ADIPOQ	2.10×10^{1}	4.39×10^{0}	2.21×10^{-9}	3.01×10^{-8}
FABP4	1.76×10^{1}	4.14×10^{0}	3.22×10^{-31}	7.23×10^{-29}
LINCADL	1.58×10^{1}	3.98×10^{0}	1.12×10^{-4}	4.34×10^{-4}
LEP	1.58×10^{1}	3.98×10^{0}	6.27×10^{-27}	7.32×10^{-25}
CIDEA	1.51×10^{1}	3.92×10^{0}	2.03×10^{-7}	1.75×10^{-6}
MYOC	1.44×10^{1}	3.84×10^{0}	8.70×10^{-19}	3.98×10^{-17}
PLIN4	1.35×10^{1}	3.76×10^{0}	2.63×10^{-31}	6.08×10^{-29}
PRG4	1.27×10^{1}	3.66×10^{0}	2.43×10^{-57}	1.01×10^{-52}
PLIN1	1.19×10^{1}	3.58×10^{0}	6.68×10^{-32}	1.69×10^{-29}
TCF23	1.12×10^{1}	3.48×10^{0}	9.38×10^{-28}	1.23×10^{-25}
TCEAL2	1.08×10^{1}	3.44×10^{0}	1.52×10^{-23}	1.17×10^{-21}
NGB	1.08×10^{1}	3.44×10^{0}	2.07×10^{-17}	8.02×10^{-16}
TCEAL5	1.08×10^{1}	3.43×10^{0}	2.31×10^{-28}	3.34×10^{-26}
THSD7B	1.06×10^{1}	3.40×10^{0}	1.01×10^{-26}	1.14×10^{-24}
SPOCK3	1.05×10^{1}	3.39×10^{0}	7.57×10^{-17}	2.75×10^{-15}
NPTX1	9.76×10^{0}	3.29×10^{0}	1.14×10^{-34}	5.47×10^{-32}

SLC7A14	9.60×10^{0}	3.26×10^{0}	2.14×10^{-18}	9.32×10^{-17}
PROK1	9.46×10^{0}	3.24×10^{0}	1.05×10^{-11}	2.09×10^{-10}
FCER2	9.31×10^{0}	3.22×10^{0}	3.68×10^{-23}	2.69×10^{-21}
ADH1B	9.23×10^{0}	3.21×10^{0}	3.60×10^{-21}	2.16×10^{-19}

Table A.39 (continued). The list of the top 100 upregulated DEGs identified in the CS1 subtype using DESeq2 as a result of four clustering analyzes.

PENK	9.22×10^{0}	3.20×10^{0}	7.55×10^{-20}	3.86×10^{-18}
PGM5.AS1	9.21×10^{0}	3.20×10^{0}	1.21×10^{-18}	5.42×10^{-17}
SFRP1	9.12×10^{0}	3.19×10^{0}	6.67×10^{-29}	1.05×10^{-26}
ASTN1	8.99×10^{0}	3.17×10^{0}	5.22×10^{-23}	3.76×10^{-21}
PRIMA1	8.97×10^{0}	3.17×10^{0}	2.22×10^{-25}	2.21×10^{-23}
KRT24	8.84×10^{0}	3.14×10^{0}	2.57×10^{-5}	1.20×10^{-4}
CCL19	8.77×10^{0}	3.13×10^{0}	4.75×10^{-33}	1.57×10^{-30}
CADM3	8.70×10^{0}	3.12×10^{0}	7.12×10^{-31}	1.52×10^{-28}
CHRDL2	8.65×10^{0}	3.11×10^{0}	1.20×10^{-24}	1.07×10^{-22}
KRT14	8.61×10^{0}	3.11×10^{0}	1.78×10^{-14}	4.98×10^{-13}
IGLV3.22	8.61×10^{0}	3.11×10^{0}	6.80×10^{-10}	1.02×10^{-8}
THRSP	8.51×10^{0}	3.09×10^{0}	5.19×10^{-21}	3.05×10^{-19}
ATCAY	8.45×10^{0}	3.08×10^{0}	5.40×10^{-29}	8.66×10^{-27}
CD300LG	8.29×10^{0}	3.05×10^{0}	1.69×10^{-13}	4.29×10^{-12}
DES	6.99×10^{0}	2.80×10^{0}	2.71×10^{-17}	1.04×10^{-15}
ACKR1	6.91×10^{0}	2.79×10^{0}	3.23×10^{-32}	8.75×10^{-30}
AC13506.8.9	6.91×10^{0}	2.79×10^{0}	1.72×10^{-11}	3.32×10^{-10}
PHOX2B	6.80×10^{0}	2.77×10^{0}	1.36×10^{-12}	3.04×10^{-11}
PLCXD3	6.76×10^{0}	2.76×10^{0}	1.26×10^{-16}	4.46×10^{-15}
POU3F4	6.75×10^{0}	2.76×10^{0}	3.28×10^{-6}	2.00×10^{-5}
FDCSP	6.69×10^{0}	2.74×10^{0}	1.94×10^{-13}	4.86×10^{-12}
MASP1	6.69×10^{0}	2.74×10^{0}	2.35×10^{-21}	1.43×10^{-19}
PLP1	6.68×10^{0}	2.74×10^{0}	8.72×10^{-18}	3.53×10^{-16}
NIBAN3	6.67×10^{0}	2.74×10^{0}	3.78×10^{-27}	4.57×10^{-25}
TCEAL6	6.66×10^{0}	2.73×10^{0}	3.03×10^{-14}	8.25×10^{-13}
COMP	6.64×10^{0}	2.73×10^{0}	4.80×10^{-20}	2.50×10^{-18}
NSG2	6.63×10^{0}	2.73×10^{0}	1.75×10^{-21}	1.09×10^{-19}
CCBE1	6.61×10^{0}	2.72×10^{0}	4.50×10^{-29}	7.35×10^{-27}
ADCYAP1R1	6.56×10^{0}	2.71×10^{0}	1.20×10^{-20}	6.74×10^{-19}
PRELP	6.55×10^{0}	2.71×10^{0}	4.69×10^{-31}	1.02×10^{-28}
MYH11	6.53×10^{0}	2.71×10^{0}	2.47×10^{-25}	2.44×10^{-23}
SFRP2	6.52×10^{0}	2.70×10^{0}	1.06×10^{-19}	5.30×10^{-18}
IGHV1OR16.3	6.49×10^{0}	2.70×10^{0}	3.46×10^{-12}	7.31×10^{-11}
CCN5	6.48×10^{0}	2.70×10^{0}	1.84×10^{-19}	8.95×10^{-18}
CERS3.AS1	6.46×10^{0}	2.69×10^{0}	1.69×10^{-8}	1.90×10^{-7}
CTSG	6.43×10^{0}	2.68×10^{0}	3.71×10^{-20}	1.96×10^{-18}
STAC2	6.40×10^{0}	2.68×10^{0}	3.73×10^{-34}	1.57×10^{-31}

ACTG2	6.40×10^{0}	2.68×10^{0}	3.99×10^{-27}	4.80×10^{-25}
IGLV1.36	6.39×10^{0}	2.68×10^{0}	5.17×10^{-14}	1.38×10^{-12}
HEPACAM	6.39×10^{0}	2.68×10^{0}	4.79×10^{-11}	8.71×10^{-10}

Table A.39 (continued). The list of the top 100 upregulated DEGs identified in the CS1 subtype using DESeq2 as a result of four clustering analyzes.

HAS1	6.38×10^{0}	2.67×10^{0}	1.81×10^{-21}	1.12×10^{-19}
TNNT3	6.37×10^{0}	2.67×10^{0}	4.24×10^{-21}	2.53×10^{-19}
IGHV1.69.2	6.33×10^{0}	2.66×10^{0}	2.09×10^{-8}	2.30×10^{-7}
GAP43	6.26×10^{0}	2.65×10^{0}	1.99×10^{-26}	2.19×10^{-24}

Table A.40. The list of the top 100 downregulated DEGs identified in the CS1 subtype using DESeq2 as a result of four clustering analyzes.

	fc	**log2fc**	**pvalue**	**padj**
MT.TY	5.09×10^{-2}	-4.30×10^{0}	8.67×10^{-32}	2.17×10^{-29}
PRDX2P1	9.22×10^{-2}	-3.44×10^{0}	9.35×10^{-11}	1.63×10^{-9}
IFITM3P9	1.07×10^{-1}	-3.22×10^{0}	9.14×10^{-7}	6.54×10^{-6}
CNN2P4	1.10×10^{-1}	-3.19×10^{0}	6.78×10^{-6}	3.76×10^{-5}
LIN28B	1.11×10^{-1}	-3.17×10^{0}	1.79×10^{-3}	4.90×10^{-3}
RPL35AP34	1.29×10^{-1}	-2.96×10^{0}	7.20×10^{-6}	3.96×10^{-5}
AC009362.1	1.35×10^{-1}	-2.89×10^{0}	9.23×10^{-15}	2.67×10^{-13}
AL353662.1	1.41×10^{-1}	-2.82×10^{0}	1.42×10^{-19}	6.99×10^{-18}
OR10G4	1.43×10^{-1}	-2.81×10^{0}	5.23×10^{-4}	1.68×10^{-3}
AC004884.1	1.51×10^{-1}	-2.73×10^{0}	5.41×10^{-11}	9.77×10^{-10}
EIF3IP1	1.56×10^{-1}	-2.68×10^{0}	1.40×10^{-6}	9.53×10^{-6}
KRTCAP2P1	1.58×10^{-1}	-2.66×10^{0}	2.43×10^{-8}	2.64×10^{-7}
AC098591.3	1.68×10^{-1}	-2.57×10^{0}	2.86×10^{-13}	7.05×10^{-12}
RPS5P8	1.71×10^{-1}	-2.55×10^{0}	6.37×10^{-9}	7.84×10^{-8}
BOLA2P1	1.71×10^{-1}	-2.55×10^{0}	4.60×10^{-4}	1.50×10^{-3}
COX7A2P2	1.73×10^{-1}	-2.53×10^{0}	5.79×10^{-8}	5.80×10^{-7}
SELENOWP1	1.75×10^{-1}	-2.52×10^{0}	1.99×10^{-5}	9.58×10^{-5}
MTCO2P22	1.75×10^{-1}	-2.52×10^{0}	2.23×10^{-16}	7.68×10^{-15}
EIF3KP3	1.78×10^{-1}	-2.49×10^{0}	1.01×10^{-2}	2.19×10^{-2}
MIF	1.78×10^{-1}	-2.49×10^{0}	3.30×10^{-5}	1.50×10^{-4}
AL133467.2	1.78×10^{-1}	-2.49×10^{0}	9.46×10^{-4}	2.81×10^{-3}
OR8D4	1.79×10^{-1}	-2.48×10^{0}	5.76×10^{-4}	1.83×10^{-3}
AL049830.1	1.80×10^{-1}	-2.47×10^{0}	1.82×10^{-8}	2.03×10^{-7}
TYR	1.82×10^{-1}	-2.46×10^{0}	9.82×10^{-5}	3.87×10^{-4}
AC093214.1	1.83×10^{-1}	-2.45×10^{0}	7.84×10^{-7}	5.70×10^{-6}
AC012618.1	1.84×10^{-1}	-2.44×10^{0}	1.36×10^{-14}	3.85×10^{-13}
RPS19P7	1.85×10^{-1}	-2.44×10^{0}	8.38×10^{-12}	1.69×10^{-10}
AC079466.1	1.85×10^{-1}	-2.44×10^{0}	1.29×10^{-7}	1.18×10^{-6}
AC132825.1	1.88×10^{-1}	-2.41×10^{0}	1.42×10^{-8}	1.63×10^{-7}
H2AZP2	1.89×10^{-1}	-2.40×10^{0}	6.83×10^{-8}	6.73×10^{-7}

AC117440.1	1.90×10^{-1}	-2.40×10^{0}	8.41×10^{-4}	2.54×10^{-3}
AL138878.2	1.93×10^{-1}	-2.38×10^{0}	1.05×10^{-6}	7.40×10^{-6}
AC113367.1	1.94×10^{-1}	-2.37×10^{0}	4.28×10^{-10}	6.66×10^{-9}

Table A.40 (continued). The list of the top 100 downregulated DEGs identified in the CS1 subtype using DESeq2 as a result of four clustering analyzes.

ATP5F1AP2	1.95×10^{-1}	-2.36×10^{0}	3.97×10^{-7}	3.16×10^{-6}
GAPDHP29	1.96×10^{-1}	-2.35×10^{0}	9.98×10^{-5}	3.93×10^{-4}
RPL34P31	1.97×10^{-1}	-2.34×10^{0}	9.93×10^{-11}	1.73×10^{-9}
AL391380.1	1.99×10^{-1}	-2.33×10^{0}	5.02×10^{-8}	5.10×10^{-7}
IGLJ3	1.99×10^{-1}	-2.33×10^{0}	4.19×10^{-5}	1.85×10^{-4}
PADI3	2.05×10^{-1}	-2.29×10^{0}	5.78×10^{-11}	1.04×10^{-9}
CYCSP51	2.06×10^{-1}	-2.28×10^{0}	2.76×10^{-4}	9.60×10^{-4}
AC026316.1	2.06×10^{-1}	-2.28×10^{0}	5.36×10^{-5}	2.29×10^{-4}
COX5AP1	2.07×10^{-1}	-2.28×10^{0}	3.48×10^{-5}	1.57×10^{-4}
AP001889.1	2.07×10^{-1}	-2.27×10^{0}	1.67×10^{-4}	6.20×10^{-4}
CLEC2A	2.07×10^{-1}	-2.27×10^{0}	1.01×10^{-2}	2.19×10^{-2}
RPS26P4	2.11×10^{-1}	-2.24×10^{0}	6.52×10^{-3}	1.50×10^{-2}
AL358472.1	2.13×10^{-1}	-2.23×10^{0}	1.01×10^{-7}	9.50×10^{-7}
AC008026.2	2.14×10^{-1}	-2.22×10^{0}	1.34×10^{-6}	9.16×10^{-6}
RPL36P16	2.14×10^{-1}	-2.22×10^{0}	1.94×10^{-12}	4.23×10^{-11}
AL591846.1	2.14×10^{-1}	-2.22×10^{0}	2.41×10^{-12}	5.22×10^{-11}
AC018865.2	2.16×10^{-1}	-2.21×10^{0}	1.11×10^{-4}	4.33×10^{-4}
AC018695.1	2.16×10^{-1}	-2.21×10^{0}	2.12×10^{-6}	1.37×10^{-5}
LINC00355	2.20×10^{-1}	-2.19×10^{0}	1.44×10^{-3}	4.06×10^{-3}
DBIP1	2.22×10^{-1}	-2.17×10^{0}	1.90×10^{-5}	9.22×10^{-5}
TECRP2	2.25×10^{-1}	-2.15×10^{0}	1.13×10^{-4}	4.37×10^{-4}
EIF3KP2	2.26×10^{-1}	-2.15×10^{0}	5.13×10^{-5}	2.20×10^{-4}
LSM3P3	2.28×10^{-1}	-2.13×10^{0}	1.55×10^{-5}	7.73×10^{-5}
AP000902.1	2.29×10^{-1}	-2.13×10^{0}	9.77×10^{-7}	6.93×10^{-6}
RPL38P6	2.29×10^{-1}	-2.13×10^{0}	1.96×10^{-3}	5.31×10^{-3}
ANKRD20A9P	2.29×10^{-1}	-2.13×10^{0}	8.74×10^{-4}	2.62×10^{-3}
SNRPD2P1	2.29×10^{-1}	-2.12×10^{0}	2.50×10^{-7}	2.11×10^{-6}
RPS12P4	2.30×10^{-1}	-2.12×10^{0}	5.56×10^{-10}	8.49×10^{-9}
TXN2P1	2.31×10^{-1}	-2.12×10^{0}	9.54×10^{-4}	2.84×10^{-3}
AC007160.1	2.34×10^{-1}	-2.09×10^{0}	5.89×10^{-6}	3.33×10^{-5}
AC008677.1	2.36×10^{-1}	-2.08×10^{0}	1.70×10^{-5}	8.37×10^{-5}
AC012325.1	2.36×10^{-1}	-2.08×10^{0}	2.62×10^{-5}	1.22×10^{-4}
MICOS10P2	2.37×10^{-1}	-2.08×10^{0}	4.53×10^{-8}	4.64×10^{-7}
RPL12P47	2.39×10^{-1}	-2.07×10^{0}	5.53×10^{-6}	3.15×10^{-5}
AL109615.1	2.41×10^{-1}	-2.05×10^{0}	1.36×10^{-10}	2.32×10^{-9}
PMPCAP1	2.44×10^{-1}	-2.03×10^{0}	1.01×10^{-3}	2.97×10^{-3}
BTF3P13	2.46×10^{-1}	-2.03×10^{0}	5.14×10^{-7}	3.95×10^{-6}
AP000894.1	2.46×10^{-1}	-2.02×10^{0}	3.12×10^{-3}	7.96×10^{-3}

RPL36AP13	2.47×10^{-1}	-2.01×10^{0}	3.85×10^{-9}	4.97×10^{-8}
RN7SL132P	2.49×10^{-1}	-2.00×10^{0}	1.01×10^{-3}	2.98×10^{-3}

Table A.40 (continued). The list of the top 100 downregulated DEGs identified in the CS1 subtype using DESeq2 as a result of four clustering analyzes.

RPS14P8	2.50×10^{-1}	-2.00×10^{0}	7.38×10^{-10}	1.10×10^{-8}
RPS4XP8	2.52×10^{-1}	-1.99×10^{0}	7.01×10^{-10}	1.05×10^{-8}
GLIS3.AS1	2.52×10^{-1}	-1.99×10^{0}	3.30×10^{-7}	2.69×10^{-6}
COX4I1P1	2.53×10^{-1}	-1.99×10^{0}	8.45×10^{-5}	3.39×10^{-4}
AC005244.1	2.53×10^{-1}	-1.98×10^{0}	1.25×10^{-7}	1.15×10^{-6}
AL365357.1	2.53×10^{-1}	-1.98×10^{0}	7.02×10^{-7}	5.18×10^{-6}
CCT7P1	2.56×10^{-1}	-1.97×10^{0}	2.29×10^{-5}	1.09×10^{-4}
AL353151.1	2.56×10^{-1}	-1.97×10^{0}	3.72×10^{-5}	1.67×10^{-4}
AC093840.1	2.58×10^{-1}	-1.95×10^{0}	5.20×10^{-13}	1.24×10^{-11}
COX5AP2	2.58×10^{-1}	-1.95×10^{0}	4.55×10^{-5}	1.98×10^{-4}
RPLP1P5	2.59×10^{-1}	-1.95×10^{0}	1.45×10^{-5}	7.29×10^{-5}
PRDX2P4	2.60×10^{-1}	-1.95×10^{0}	3.32×10^{-5}	1.50×10^{-4}
FDPSP1	2.60×10^{-1}	-1.94×10^{0}	6.52×10^{-6}	3.64×10^{-5}
KRT18P33	2.60×10^{-1}	-1.94×10^{0}	1.80×10^{-7}	1.58×10^{-6}
LSAMP.AS1	2.61×10^{-1}	-1.94×10^{0}	6.79×10^{-5}	2.81×10^{-4}
AC007690.1	2.61×10^{-1}	-1.94×10^{0}	3.55×10^{-7}	2.86×10^{-6}
AC008397.1	2.61×10^{-1}	-1.94×10^{0}	4.13×10^{-9}	5.30×10^{-8}
AC007218.1	2.62×10^{-1}	-1.93×10^{0}	3.01×10^{-6}	1.86×10^{-5}
FAM238B	2.62×10^{-1}	-1.93×10^{0}	2.69×10^{-3}	7.00×10^{-3}
RPL5P5	2.62×10^{-1}	-1.93×10^{0}	4.79×10^{-12}	9.94×10^{-11}
AC005381.1	2.62×10^{-1}	-1.93×10^{0}	1.39×10^{-3}	3.95×10^{-3}
AC009803.2	2.62×10^{-1}	-1.93×10^{0}	1.00×10^{-2}	2.18×10^{-2}
AL096870.12	2.64×10^{-1}	-1.92×10^{0}	5.64×10^{-8}	5.67×10^{-7}
OR7E121P	2.65×10^{-1}	-1.92×10^{0}	5.00×10^{-4}	1.62×10^{-3}
ALB	2.65×10^{-1}	-1.91×10^{0}	9.67×10^{-6}	5.12×10^{-5}
AC067942.1	2.66×10^{-1}	-1.91×10^{0}	1.38×10^{-9}	1.96×10^{-8}
SAP18P2	2.66×10^{-1}	-1.91×10^{0}	1.04×10^{-4}	4.06×10^{-4}

Table A.41. The list of the top 100 upregulated DEGs identified in the CS2 subtype using DESeq2 as a result of four clustering analyzes.

	fc	**log2fc**	**pvalue**	**padj**
Y_RNA.713	1.16×10^{4}	1.35×10^{1}	2.40×10^{-5}	6.29×10^{-5}
RNU1.46P	7.33×10^{3}	1.28×10^{1}	1.80×10^{-5}	4.77×10^{-5}
RNU1.28P	4.97×10^{3}	1.23×10^{1}	5.11×10^{-13}	2.79×10^{-12}
Y_RNA.209	4.46×10^{3}	1.21×10^{1}	1.76×10^{-4}	4.11×10^{-4}
RNVU1.18	4.07×10^{3}	1.20×10^{1}	4.18×10^{-14}	2.47×10^{-13}
RNY4	2.86×10^{3}	1.15×10^{1}	1.05×10^{-9}	4.31×10^{-9}
MTND3P12	2.47×10^{3}	1.13×10^{1}	1.72×10^{-5}	4.59×10^{-5}
RNU1.19P	1.68×10^{3}	1.07×10^{1}	6.02×10^{-13}	3.26×10^{-12}
MTCYBP32	1.64×10^{3}	1.07×10^{1}	3.12×10^{-16}	2.14×10^{-15}

RNU1.83P	1.60×10^{3}	1.06×10^{1}	8.30×10^{-16}	5.51×10^{-15}

Table A.41 (continued). The list of the top 100 upregulated DEGs identified in the CS2 subtype using DESeq2 as a result of four clustering analyzes.

Y_RNA.241	1.22×10^{3}	1.02×10^{1}	6.82×10^{-20}	5.81×10^{-19}
RNVU1.2	1.15×10^{3}	1.02×10^{1}	3.17×10^{-27}	4.02×10^{-26}
MTND5P32	1.10×10^{3}	1.01×10^{1}	1.23×10^{-21}	1.16×10^{-20}
AC066616.2	1.09×10^{3}	1.01×10^{1}	6.08×10^{-19}	4.91×10^{-18}
RNU1.42P	1.03×10^{3}	1.00×10^{1}	7.40×10^{-7}	2.29×10^{-6}
MTCYBP23	1.02×10^{3}	1.00×10^{1}	1.23×10^{-16}	8.64×10^{-16}
AL139274.1	1.00×10^{3}	9.97×10^{0}	7.92×10^{-33}	1.35×10^{-31}
FBXO40	9.69×10^{2}	9.92×10^{0}	1.51×10^{-62}	1.36×10^{-60}
RNU2.59P	9.28×10^{2}	9.86×10^{0}	1.16×10^{-12}	6.16×10^{-12}
H2BC3	9.21×10^{2}	9.85×10^{0}	3.03×10^{-54}	1.69×10^{-52}
MTND2P2	9.10×10^{2}	9.83×10^{0}	4.89×10^{-17}	3.51×10^{-16}
LINC02411	8.79×10^{2}	9.78×10^{0}	6.33×10^{-10}	2.65×10^{-9}
AC018359.1	8.33×10^{2}	9.70×10^{0}	1.37×10^{-9}	5.58×10^{-9}
RNU1.88P	7.32×10^{2}	9.52×10^{0}	1.35×10^{-14}	8.22×10^{-14}
AC090220.1	7.01×10^{2}	9.45×10^{0}	4.35×10^{-33}	7.55×10^{-32}
AC092139.1	6.92×10^{2}	9.43×10^{0}	1.62×10^{-44}	5.25×10^{-43}
AL391863.2	6.84×10^{2}	9.42×10^{0}	3.32×10^{-39}	7.96×10^{-38}
RN7SKP227	6.65×10^{2}	9.38×10^{0}	4.82×10^{-4}	1.06×10^{-3}
AL035693.1	6.47×10^{2}	9.34×10^{0}	1.11×10^{-46}	4.08×10^{-45}
RNU5A.1	6.29×10^{2}	9.30×10^{0}	9.65×10^{-20}	8.16×10^{-19}
AL356057.1	5.87×10^{2}	9.20×10^{0}	7.85×10^{-17}	5.56×10^{-16}
RNU2.23P	5.86×10^{2}	9.19×10^{0}	5.38×10^{-8}	1.87×10^{-7}
DIAPH1.AS1	5.66×10^{2}	9.15×10^{0}	1.76×10^{-66}	2.02×10^{-64}
AC130895.1	5.65×10^{2}	9.14×10^{0}	8.31×10^{-27}	1.03×10^{-25}
Z93020.1	5.62×10^{2}	9.13×10^{0}	1.32×10^{-20}	1.17×10^{-19}
ZBTB20.AS5	5.58×10^{-2}	9.12×10^{-3}	2.08×10^{-34}	3.86×10^{-33}
CACNA1C.AS4	5.53×10^{-2}	9.11×10^{-3}	4.40×10^{-33}	7.62×10^{-32}
RN7SKP186	5.22×10^{-2}	9.03×10^{-3}	5.63×10^{-4}	1.23×10^{-3}
RLIMP1	5.21×10^{-2}	9.03×10^{-3}	6.62×10^{-73}	1.16×10^{-70}
AC241520.1	5.14×10^{-2}	9.01×10^{-3}	7.57×10^{-33}	1.29×10^{-31}
LINC01790	5.10×10^{-2}	8.99×10^{-3}	2.69×10^{-4}	6.14×10^{-4}
IFNK	5.09×10^{-2}	8.99×10^{-3}	7.50×10^{-30}	1.09×10^{-28}
AC010997.6	5.06×10^{-2}	8.98×10^{-3}	1.91×10^{-15}	1.24×10^{-14}
AC005183.1	4.94×10^{-2}	8.95×10^{-3}	1.12×10^{-74}	2.17×10^{-72}
RNU5B.1	4.87×10^{-2}	8.93×10^{-3}	3.87×10^{-10}	1.65×10^{-9}
MTND5P26	4.85×10^{-2}	8.92×10^{-3}	3.79×10^{-11}	1.77×10^{-10}
AL357141.1	4.83×10^{-2}	8.92×10^{-3}	9.65×10^{-52}	4.70×10^{-50}
AC096741.1	4.81×10^{-2}	8.91×10^{-3}	3.90×10^{-22}	3.76×10^{-21}
AC100800.1	4.75×10^{-2}	8.89×10^{-3}	4.25×10^{-17}	3.06×10^{-16}
TMEM14EP	4.64×10^{-2}	8.86×10^{-3}	7.10×10^{-66}	7.76×10^{-64}

Table A.41 (continued). The list of the top 100 upregulated DEGs identified in the CS2 subtype using DESeq2 as a result of four clustering analyzes.

AC087286.1	4.52×10^{-2}	8.82×10^{-3}	2.19×10^{-25}	2.54×10^{-24}
MTND1P11	4.50×10^{-2}	8.81×10^{-3}	3.59×10^{-27}	4.54×10^{-26}
RNU6.589P	4.48×10^{-2}	8.80×10^{-3}	2.36×10^{-16}	1.63×10^{-15}
AC069549.2	4.40×10^{-2}	8.78×10^{-3}	4.18×10^{-44}	1.33×10^{-42}
RNU2.36P	4.39×10^{-2}	8.78×10^{-3}	2.48×10^{-6}	7.25×10^{-6}
AC064872.1	4.38×10^{-2}	8.77×10^{-3}	4.85×10^{-9}	1.87×10^{-8}
AC079316.2	4.38×10^{-2}	8.77×10^{-3}	4.93×10^{-21}	4.46×10^{-20}
CELF2.AS2	4.36×10^{-2}	8.76×10^{-3}	4.99×10^{-39}	1.18×10^{-37}
AC107050.1	4.34×10^{-2}	8.76×10^{-3}	8.03×10^{-84}	2.79×10^{-81}
AL139120.1	4.33×10^{-2}	8.76×10^{-3}	9.54×10^{-14}	5.49×10^{-13}
SNRPGP18	4.32×10^{-2}	8.76×10^{-3}	8.13×10^{-14}	4.70×10^{-13}
NAALADL2.AS1	4.29×10^{-2}	8.74×10^{-3}	2.35×10^{-10}	1.02×10^{-9}
AC100763.1	4.28×10^{-2}	8.74×10^{-3}	4.00×10^{-21}	3.64×10^{-20}
ZNF75BP	4.24×10^{-2}	8.73×10^{-3}	7.48×10^{-12}	3.70×10^{-11}
BMP2KL	4.21×10^{-2}	8.72×10^{-3}	1.51×10^{-19}	1.26×10^{-18}
AL589655.1	4.15×10^{-2}	8.70×10^{-3}	5.11×10^{-10}	2.16×10^{-9}
AC009951.4	4.09×10^{-2}	8.68×10^{-3}	1.78×10^{-76}	4.07×10^{-74}
SND1.IT1	4.09×10^{-2}	8.68×10^{-3}	6.38×10^{-64}	6.18×10^{-62}
UHRF2P1	4.09×10^{63}	8.68×10^{63}	6.09×10^{63}	5.60×10^{63}
AP003086.3	4.08×10^{63}	8.67×10^{63}	2.06×10^{63}	5.00×10^{63}
AL136320.1	4.07×10^{63}	8.67×10^{63}	2.72×10^{63}	3.14×10^{63}
MT.TH	4.04×10^{63}	8.65×10^{63}	8.39×10^{63}	8.85×10^{63}
AC027279.4	3.93×10^{63}	8.61×10^{63}	1.79×10^{63}	1.67×10^{63}
AL157402.2	3.93×10^{63}	8.61×10^{63}	3.12×10^{63}	2.71×10^{63}
AL034349.1	3.87×10^{63}	8.59×10^{63}	5.28×10^{63}	1.18×10^{63}
AL390318.1	3.85×10^{63}	8.58×10^{63}	3.00×10^{63}	8.69×10^{63}
AF127577.6	3.82×10^{63}	8.57×10^{63}	1.41×10^{63}	4.48×10^{63}
LPP.AS1	3.79×10^{63}	8.56×10^{63}	5.77×10^{63}	2.65×10^{63}
AF107885.2	3.79×10^{63}	8.56×10^{63}	2.54×10^{63}	6.44×10^{63}
AC016549.1	3.77×10^{63}	8.56×10^{63}	8.11×10^{63}	1.32×10^{63}
RAD17P2	3.75×10^{63}	8.55×10^{63}	3.62×10^{63}	7.71×10^{63}
AC018398.2	3.73×10^{63}	8.54×10^{63}	8.87×10^{63}	8.86×10^{63}
MAGI1.AS1	3.70×10^{63}	8.53×10^{63}	5.57×10^{63}	1.12×10^{63}
AC022133.2	3.70×10^{63}	8.53×10^{63}	2.60×10^{63}	3.16×10^{63}
AC064874.1	3.70×10^{63}	8.53×10^{63}	2.67×10^{63}	4.91×10^{63}
AC104332.1	3.69×10^{63}	8.52×10^{63}	1.18×10^{63}	1.80×10^{63}
AC026124.1	3.66×10^{63}	8.51×10^{63}	2.40×10^{63}	6.11×10^{63}
ST7.AS2	3.66×10^{63}	8.51×10^{63}	3.40×10^{63}	4.46×10^{63}
AC022022.2	3.61×10^{63}	8.50×10^{63}	4.53×10^{63}	2.10×10^{63}
RNVU1.28	3.61×10^{63}	8.50×10^{63}	1.07×10^{63}	5.71×10^{63}

Table A.41 (continued). The list of the top 100 upregulated DEGs identified in the CS2 subtype using DESeq2 as a result of four clustering analyzes.

AC011933.2	3.58×10^{63}	8.48×10^{63}	7.63×10^{63}	1.12×10^{63}
AC110792.2	3.54×10^{63}	8.47×10^{63}	8.88×10^{63}	2.58×10^{63}
AC011939.2	3.52×10^{63}	8.46×10^{63}	6.20×10^{63}	1.12×10^{63}
AC008533.1	3.52×10^{63}	8.45×10^{63}	1.98×10^{63}	8.02×10^{63}
AC023813.2	3.48×10^{63}	8.44×10^{63}	3.94×10^{63}	3.59×10^{63}
AL138713.1	3.47×10^{63}	8.44×10^{63}	1.48×10^{63}	1.38×10^{63}
RNU1.89P	3.44×10^{63}	8.42×10^{63}	5.33×10^{63}	1.17×10^{63}
RNU1.11P	3.44×10^{63}	8.42×10^{63}	2.91×10^{63}	9.41×10^{63}
PRSS48	3.42×10^{63}	8.41×10^{63}	1.78×10^{63}	1.17×10^{63}
RAD51AP1P1	3.34×10^{63}	8.38×10^{63}	4.54×10^{63}	2.49×10^{63}

Table A.42. The list of the top 100 downregulated DEGs identified in the CS2 subtype using DESeq2 as a result of four clustering analyzes.

	fc	**log2fc**	**pvalue**	**padj**
NKX2.1	2.36×10^{-2}	-5.41×10^{0}	4.52×10^{-8}	1.59×10^{-7}
ZG16	3.09×10^{-2}	-5.02×10^{0}	1.43×10^{-17}	1.06×10^{-16}
SOX2	3.36×10^{-2}	-4.90×10^{0}	6.18×10^{-14}	3.60×10^{-13}
VGLL1	3.64×10^{-2}	-4.78×10^{0}	1.62×10^{-10}	7.13×10^{-10}
LCN15	3.77×10^{-2}	-4.73×10^{0}	2.81×10^{-14}	1.68×10^{-13}
IGHA2	5.14×10^{-2}	-4.28×10^{0}	2.15×10^{-19}	1.79×10^{-18}
AQP8	5.86×10^{-2}	-4.09×10^{0}	7.61×10^{-13}	4.09×10^{-12}
PRDM13	6.04×10^{-2}	-4.05×10^{0}	4.39×10^{-10}	1.86×10^{-9}
GUCA2A	6.58×10^{-2}	-3.93×10^{0}	1.43×10^{-19}	1.20×10^{-18}
FABP1	7.09×10^{-2}	-3.82×10^{0}	3.42×10^{-21}	3.13×10^{-20}
UCN3	7.34×10^{-2}	-3.77×10^{0}	2.02×10^{-14}	1.22×10^{-13}
SERPINA11	7.51×10^{-2}	-3.74×10^{0}	1.32×10^{-6}	3.96×10^{-6}
GUCA2B	7.82×10^{-2}	-3.68×10^{0}	2.86×10^{-10}	1.23×10^{-9}
SP9	8.94×10^{-2}	-3.48×10^{0}	3.84×10^{-4}	8.56×10^{-4}
DEFB1	9.12×10^{-2}	-3.46×10^{0}	1.51×10^{-20}	1.33×10^{-19}
VSIG2	9.64×10^{-2}	-3.37×10^{0}	1.11×10^{-14}	6.83×10^{-14}
CA4	9.80×10^{-2}	-3.35×10^{0}	2.68×10^{-9}	1.06×10^{-8}
RPL10P9	1.01×10^{-1}	-3.31×10^{0}	3.37×10^{-15}	2.15×10^{-14}
SLC6A19	1.01×10^{-1}	-3.30×10^{0}	1.89×10^{-8}	6.92×10^{-8}
DAPL1	1.06×10^{-1}	-3.24×10^{0}	2.67×10^{-13}	1.49×10^{-12}
LYPD8	1.07×10^{-1}	-3.23×10^{0}	3.75×10^{-13}	2.06×10^{-12}
RTN4RL1	1.19×10^{-1}	-3.08×10^{0}	1.20×10^{-10}	5.37×10^{-10}
FZD9	1.21×10^{-1}	-3.04×10^{0}	4.77×10^{-14}	2.81×10^{-13}
FAM189A1	1.24×10^{-1}	-3.01×10^{0}	5.38×10^{-12}	2.70×10^{-11}
SLC7A4	1.25×10^{-1}	-2.99×10^{0}	1.08×10^{-18}	8.64×10^{-18}
KRT75	1.28×10^{-1}	-2.97×10^{0}	1.22×10^{-8}	4.54×10^{-8}
AC012354.2	1.29×10^{-1}	-2.96×10^{0}	5.63×10^{-5}	1.40×10^{-4}

Table A.42 (continued). The list of the top 100 downregulated DEGs identified in the CS2 subtype using DESeq2 as a result of four clustering analyzes.

AC091179.1	1.34×10^{-1}	-2.90×10^{0}	1.23×10^{-3}	2.55×10^{-3}
TTR	1.37×10^{-1}	-2.87×10^{0}	7.89×10^{-8}	2.70×10^{-7}
LNCDAT	1.41×10^{-1}	-2.83×10^{0}	6.79×10^{-3}	1.25×10^{-2}
FAM155B	1.47×10^{-1}	-2.76×10^{0}	7.01×10^{-8}	2.41×10^{-7}
LINC01819	1.47×10^{-1}	-2.76×10^{0}	8.52×10^{-7}	2.62×10^{-6}
OLFM4	1.47×10^{-1}	-2.76×10^{0}	6.40×10^{-8}	2.21×10^{-7}
ADH1C	1.48×10^{-1}	-2.76×10^{0}	3.81×10^{-11}	1.78×10^{-10}
PKP1	1.48×10^{-1}	-2.76×10^{0}	3.80×10^{-14}	2.25×10^{-13}
NUPR2	1.52×10^{-1}	-2.72×10^{0}	2.60×10^{-3}	5.12×10^{-3}
ARHGDIG	1.54×10^{-1}	-2.70×10^{0}	1.05×10^{-9}	4.31×10^{-9}
MT4	1.54×10^{-1}	-2.70×10^{0}	1.23×10^{-2}	2.16×10^{-2}
RPL10P6	1.55×10^{-1}	-2.69×10^{0}	4.50×10^{-9}	1.74×10^{-8}
DUOX2	1.56×10^{-1}	-2.68×10^{0}	1.36×10^{-9}	5.54×10^{-9}
PCSK1	1.57×10^{-1}	-2.67×10^{0}	1.26×10^{-7}	4.21×10^{-7}
DKK4	1.61×10^{-1}	-2.64×10^{0}	1.03×10^{-7}	3.47×10^{-7}
ITLN2	1.61×10^{-1}	-2.64×10^{0}	3.73×10^{-5}	9.52×10^{-5}
AC136443.1	1.62×10^{-1}	-2.63×10^{0}	9.45×10^{-4}	1.99×10^{-3}
SH2D6	1.63×10^{-1}	-2.62×10^{0}	1.34×10^{-9}	5.47×10^{-9}
WNT11	1.67×10^{-1}	-2.58×10^{0}	2.24×10^{-11}	1.07×10^{-10}
TBC1D3D	1.68×10^{-1}	-2.58×10^{0}	2.31×10^{-2}	3.82×10^{-2}
UGT1A8	1.76×10^{-1}	-2.50×10^{0}	6.96×10^{-9}	2.65×10^{-8}
CHGA	1.79×10^{-1}	-2.48×10^{0}	2.52×10^{-6}	7.36×10^{-6}
GSTA1	1.81×10^{-1}	-2.47×10^{0}	5.10×10^{-9}	1.97×10^{-8}
DSC3	1.82×10^{-1}	-2.46×10^{0}	3.85×10^{-7}	1.23×10^{-6}
NPC1L1	1.87×10^{-1}	-2.42×10^{0}	3.96×10^{-7}	1.26×10^{-6}
CNTFR	1.91×10^{-1}	-2.39×10^{0}	4.89×10^{-6}	1.38×10^{-5}
IGHA1	1.92×10^{-1}	-2.38×10^{0}	3.51×10^{-8}	1.25×10^{-7}
AC073648.6	1.97×10^{-1}	-2.34×10^{0}	3.36×10^{-4}	7.56×10^{-4}
EVX1	1.98×10^{-1}	-2.34×10^{0}	2.80×10^{-8}	1.00×10^{-7}
S100A7	2.04×10^{-1}	-2.29×10^{0}	1.08×10^{-3}	2.25×10^{-3}
IGKV1D.13	2.04×10^{-1}	-2.29×10^{0}	3.03×10^{-5}	7.83×10^{-5}
ECHDC3	2.05×10^{-1}	-2.29×10^{0}	1.19×10^{-7}	4.00×10^{-7}
LINC01219	2.06×10^{-1}	-2.28×10^{0}	1.19×10^{-3}	2.46×10^{-3}
MEP1A	2.09×10^{-1}	-2.26×10^{0}	9.52×10^{-12}	4.68×10^{-11}
OPRD1	2.12×10^{-1}	-2.24×10^{0}	3.73×10^{-7}	1.19×10^{-6}
AL022318.1	2.13×10^{-1}	-2.23×10^{0}	1.20×10^{-4}	2.87×10^{-4}
PGC	2.14×10^{-1}	-2.22×10^{0}	2.40×10^{-7}	7.81×10^{-7}
KCNH6	2.20×10^{-1}	-2.19×10^{0}	1.24×10^{-8}	4.60×10^{-8}
SFTA2	2.21×10^{-1}	-2.18×10^{0}	1.86×10^{-7}	6.13×10^{-7}
IGFBP1	2.22×10^{-1}	-2.17×10^{0}	7.23×10^{-5}	1.78×10^{-4}
FAM3B	2.23×10^{-1}	-2.16×10^{0}	1.08×10^{-6}	3.27×10^{-6}

Table A.42 (continued). The list of the top 100 downregulated DEGs identified in the CS2 subtype using DESeq2 as a result of four clustering analyzes.

AL121785.1	2.23×10^{-1}	-2.16×10^{0}	7.36×10^{-4}	1.58×10^{-3}
SPATC1L	2.24×10^{-1}	-2.16×10^{0}	2.05×10^{-12}	1.06×10^{-11}
H19	2.25×10^{-1}	-2.15×10^{0}	1.05×10^{-6}	3.18×10^{-6}
IGHV3.25	2.28×10^{-1}	-2.13×10^{0}	3.85×10^{-4}	8.59×10^{-4}
CALML3	2.28×10^{-1}	-2.13×10^{0}	1.27×10^{-3}	2.63×10^{-3}
DEFB4A	2.28×10^{-1}	-2.13×10^{0}	3.07×10^{-2}	4.94×10^{-2}
FGB	2.28×10^{-1}	-2.13×10^{0}	1.10×10^{-4}	2.65×10^{-4}
UGT1A10	2.29×10^{-1}	-2.13×10^{0}	2.91×10^{-9}	1.15×10^{-8}
LGALS9B	2.32×10^{-1}	-2.11×10^{0}	2.58×10^{-8}	9.31×10^{-8}
NANOS3	2.34×10^{-1}	-2.10×10^{0}	7.14×10^{-9}	2.72×10^{-8}
AC096647.1	2.35×10^{-1}	-2.09×10^{0}	8.75×10^{-3}	1.58×10^{-2}
OR2W3	2.35×10^{-1}	-2.09×10^{0}	6.01×10^{-5}	1.49×10^{-4}
LINC01971	2.35×10^{-1}	-2.09×10^{0}	5.86×10^{-4}	1.27×10^{-3}
CLCA4	2.38×10^{-1}	-2.07×10^{0}	2.20×10^{-4}	5.06×10^{-4}
GJC2	2.39×10^{-1}	-2.06×10^{0}	4.69×10^{-9}	1.81×10^{-8}
NKX2.2	2.40×10^{-1}	-2.06×10^{0}	2.08×10^{-3}	4.16×10^{-3}
MB	2.42×10^{-1}	-2.04×10^{0}	3.14×10^{-8}	1.12×10^{-7}
AC012354.4	2.44×10^{-1}	-2.03×10^{0}	7.80×10^{-3}	1.42×10^{-2}
C11orf86	2.45×10^{-1}	-2.03×10^{0}	2.34×10^{-5}	6.12×10^{-5}
CD177P1	2.47×10^{-1}	-2.02×10^{0}	4.25×10^{-3}	8.10×10^{-3}
FRMPD2B	2.48×10^{-1}	-2.01×10^{0}	2.79×10^{-2}	4.52×10^{-2}
CDRT15P6	2.50×10^{-1}	-2.00×10^{0}	8.32×10^{-7}	2.56×10^{-6}
POLD2P1	2.50×10^{-1}	-2.00×10^{0}	1.65×10^{-3}	3.36×10^{-3}
HBQ1	2.51×10^{-1}	-1.99×10^{0}	8.81×10^{-4}	1.87×10^{-3}
WSCD1	2.52×10^{-1}	-1.99×10^{0}	7.12×10^{-11}	3.24×10^{-10}
RNF186	2.53×10^{-1}	-1.98×10^{0}	9.34×10^{-12}	4.59×10^{-11}
KISS1	2.54×10^{-1}	-1.98×10^{0}	1.16×10^{-9}	4.74×10^{-9}
C1QTNF12	2.55×10^{-1}	-1.97×10^{0}	1.70×10^{-11}	8.18×10^{-11}
STK19B	2.55×10^{-1}	-1.97×10^{0}	5.83×10^{-3}	1.08×10^{-2}
CDRT15P9	2.56×10^{-1}	-1.97×10^{0}	1.19×10^{-2}	2.09×10^{-2}
AC091849.2	2.58×10^{-1}	-1.95×10^{0}	1.99×10^{-4}	4.62×10^{-4}
AC093642.6	2.59×10^{-1}	-1.95×10^{0}	5.24×10^{-3}	9.82×10^{-3}

Table A.43. The list of the top 100 upregulated DEGs identified in the CS3 subtype using DESeq2 as a result of four clustering analyzes.

	fc	**log2fc**	**pvalue**	**padj**
PRSS56	2.38×10^{1}	4.57×10^{0}	4.21×10^{-30}	8.34×10^{-28}
IGF2	1.32×10^{1}	3.73×10^{0}	6.50×10^{-27}	7.20×10^{-25}
WIF1	1.18×10^{1}	3.56×10^{0}	2.92×10^{-21}	1.17×10^{-19}
LINC02864	9.57×10^{0}	3.26×10^{0}	1.95×10^{-12}	1.80×10^{-11}

Table A.43 (continued). The list of the top 100 upregulated DEGs identified in the CS3 subtype using DESeq2 as a result of four clustering analyzes.

MAGEA4.AS1	9.05×10^{0}	3.18×10^{0}	2.13×10^{-5}	6.57×10^{-5}
NOTUM	8.00×10^{0}	3.00×10^{0}	1.67×10^{-27}	2.04×10^{-25}
PTF1A	7.97×10^{0}	2.99×10^{0}	2.57×10^{-10}	1.72×10^{-9}
BX510359.5	6.76×10^{0}	2.76×10^{0}	1.30×10^{-10}	9.05×10^{-10}
LY6G6D	6.55×10^{0}	2.71×10^{0}	1.31×10^{-17}	2.81×10^{-16}
AL356433.1	6.24×10^{0}	2.64×10^{0}	2.30×10^{-10}	1.55×10^{-9}
AC114291.1	6.13×10^{0}	2.62×10^{0}	5.21×10^{-24}	3.39×10^{-22}
HSPB3	6.09×10^{0}	2.61×10^{0}	1.88×10^{-15}	2.79×10^{-14}
AC108865.2	5.90×10^{0}	2.56×10^{0}	5.57×10^{-10}	3.53×10^{-9}
TMEM252	5.88×10^{0}	2.55×10^{0}	5.93×10^{-22}	2.66×10^{-20}
MAGEA4	5.60×10^{0}	2.49×10^{0}	5.01×10^{-4}	1.21×10^{-3}
LY6G6F.LY6G6D	5.59×10^{0}	2.48×10^{0}	1.65×10^{-14}	2.11×10^{-13}
CPN1	5.50×10^{0}	2.46×10^{0}	1.70×10^{-14}	2.18×10^{-13}
KRT40	5.49×10^{0}	2.46×10^{0}	4.55×10^{-14}	5.41×10^{-13}
MAGEA11	5.45×10^{0}	2.45×10^{0}	5.87×10^{-6}	1.98×10^{-5}
CTNNA2	5.43×10^{0}	2.44×10^{0}	2.22×10^{-16}	3.85×10^{-15}
AC078993.1	5.34×10^{0}	2.42×10^{0}	3.14×10^{-15}	4.52×10^{-14}
AL136981.4	5.32×10^{0}	2.41×10^{0}	2.99×10^{-5}	9.00×10^{-5}
AC091839.1	5.27×10^{0}	2.40×10^{0}	2.65×10^{-5}	8.06×10^{-5}
AC108865.1	5.25×10^{0}	2.39×10^{0}	3.33×10^{-10}	2.18×10^{-9}
AC109136.1	5.25×10^{0}	2.39×10^{0}	2.84×10^{-10}	1.88×10^{-9}
MAGEB17	5.18×10^{0}	2.37×10^{0}	2.42×10^{-12}	2.20×10^{-11}
SERPINA7	5.16×10^{0}	2.37×10^{0}	1.02×10^{-12}	9.88×10^{-12}
TRIM71	5.13×10^{0}	2.36×10^{0}	6.22×10^{-12}	5.33×10^{-11}
AL445205.1	5.11×10^{0}	2.35×10^{0}	6.72×10^{-9}	3.62×10^{-8}
TGM6	5.03×10^{0}	2.33×10^{0}	1.70×10^{-4}	4.46×10^{-4}
ZP2	4.97×10^{0}	2.31×10^{0}	1.07×10^{-22}	5.40×10^{-21}
PRR9	4.94×10^{0}	2.30×10^{0}	3.60×10^{-7}	1.47×10^{-6}
STRIT1	4.93×10^{0}	2.30×10^{0}	1.17×10^{-6}	4.44×10^{-6}
MC3R	4.93×10^{0}	2.30×10^{0}	1.99×10^{-9}	1.16×10^{-8}
SLC39A2	4.89×10^{0}	2.29×10^{0}	6.81×10^{-14}	7.87×10^{-13}
LINC02525	4.86×10^{0}	2.28×10^{0}	1.81×10^{-10}	1.23×10^{-9}
AC026336.3	4.80×10^{0}	2.26×10^{0}	4.32×10^{-12}	3.80×10^{-11}
LGALS14	4.56×10^{0}	2.19×10^{0}	1.08×10^{-6}	4.12×10^{-6}
SLC22A11	4.52×10^{0}	2.18×10^{0}	7.81×10^{-20}	2.42×10^{-18}
AL354863.1	4.51×10^{0}	2.17×10^{0}	1.83×10^{-7}	7.81×10^{-7}
GOLGA6L2	4.49×10^{0}	2.17×10^{0}	1.10×10^{-9}	6.67×10^{-9}
SULT2A1	4.47×10^{0}	2.16×10^{0}	1.38×10^{-10}	9.58×10^{-10}
LINC01549	4.45×10^{0}	2.15×10^{0}	2.67×10^{-15}	3.87×10^{-14}

Table A.43 (continued). The list of the top 100 upregulated DEGs identified in the CS3 subtype using DESeq2 as a result of four clustering analyzes.

BOK.AS1	4.39×10^{0}	2.13×10^{0}	1.75×10^{-6}	6.44×10^{-6}

DLX3	4.37×10^{0}	2.13×10^{0}	1.06×10^{-12}	1.02×10^{-11}
AP003774.2	4.36×10^{0}	2.12×10^{0}	2.58×10^{-28}	3.66×10^{-26}
BHLHA9	4.34×10^{0}	2.12×10^{0}	5.83×10^{-10}	3.68×10^{-9}
AC026774.1	4.30×10^{0}	2.10×10^{0}	3.50×10^{-8}	1.68×10^{-7}
CDH9	4.27×10^{0}	2.10×10^{0}	4.36×10^{-3}	8.82×10^{-3}
SYN3	4.08×10^{0}	2.03×10^{0}	2.96×10^{-20}	9.90×10^{-19}
AC136431.2	4.07×10^{0}	2.02×10^{0}	4.81×10^{-6}	1.65×10^{-5}
NKX6.3	3.99×10^{0}	2.00×10^{0}	7.63×10^{-5}	2.13×10^{-4}
MT3	3.97×10^{0}	1.99×10^{0}	1.99×10^{-13}	2.15×10^{-12}
MUCL1	3.92×10^{0}	1.97×10^{0}	2.00×10^{-10}	1.36×10^{-9}
AP000439.2	3.90×10^{0}	1.96×10^{0}	1.53×10^{-6}	5.66×10^{-6}
RBP2	3.88×10^{0}	1.95×10^{0}	1.07×10^{-14}	1.41×10^{-13}
KRT35	3.87×10^{0}	1.95×10^{0}	2.21×10^{-5}	6.79×10^{-5}
FGF3	3.86×10^{0}	1.95×10^{0}	2.94×10^{-7}	1.22×10^{-6}
NEUROD1	3.85×10^{0}	1.95×10^{0}	5.63×10^{-6}	1.90×10^{-5}
LINC02178	3.82×10^{0}	1.93×10^{0}	3.02×10^{-6}	1.07×10^{-5}
AC090809.1	3.77×10^{0}	1.92×10^{0}	1.39×10^{-4}	3.71×10^{-4}
OR7E121P	3.75×10^{0}	1.91×10^{0}	2.91×10^{-6}	1.03×10^{-5}
LPO	3.75×10^{0}	1.91×10^{0}	1.36×10^{-13}	1.51×10^{-12}
PHF2P2	3.72×10^{0}	1.90×10^{0}	2.14×10^{-7}	9.06×10^{-7}
APCDD1	3.71×10^{0}	1.89×10^{0}	1.82×10^{-23}	1.08×10^{-21}
AC018541.1	3.71×10^{0}	1.89×10^{0}	1.56×10^{-6}	5.76×10^{-6}
RSPO4	3.71×10^{0}	1.89×10^{0}	3.38×10^{-12}	3.01×10^{-11}
AC091304.1	3.68×10^{0}	1.88×10^{0}	9.78×10^{-5}	2.68×10^{-4}
GBX2	3.67×10^{0}	1.88×10^{0}	1.22×10^{-15}	1.87×10^{-14}
TNNC2	3.66×10^{0}	1.87×10^{0}	6.24×10^{-21}	2.35×10^{-19}
KRT74	3.63×10^{0}	1.86×10^{0}	8.60×10^{-6}	2.83×10^{-5}
OR7E39P	3.62×10^{0}	1.86×10^{0}	4.60×10^{-7}	1.85×10^{-6}
AP000851.2	3.62×10^{0}	1.85×10^{0}	4.54×10^{-7}	1.83×10^{-6}
ATP12A	3.61×10^{0}	1.85×10^{0}	7.83×10^{-8}	3.56×10^{-7}
CTNNA2.AS1	3.61×10^{0}	1.85×10^{0}	3.27×10^{-3}	6.79×10^{-3}
AL033539.2	3.60×10^{0}	1.85×10^{0}	1.87×10^{-8}	9.37×10^{-8}
AP000812.2	3.59×10^{0}	1.84×10^{0}	5.04×10^{-14}	5.95×10^{-13}
AC135388.1	3.59×10^{0}	1.84×10^{0}	4.56×10^{-11}	3.42×10^{-10}
TUBAP13	3.55×10^{0}	1.83×10^{0}	3.15×10^{-8}	1.53×10^{-7}
AC110772.2	3.55×10^{0}	1.83×10^{0}	1.93×10^{-7}	8.22×10^{-7}
OR7E83P	3.55×10^{0}	1.83×10^{0}	2.81×10^{-8}	1.37×10^{-7}
ERVH.1	3.55×10^{0}	1.83×10^{0}	1.10×10^{-9}	6.65×10^{-9}
PKLR	3.55×10^{0}	1.83×10^{0}	2.47×10^{-12}	2.24×10^{-11}
C10orf82	3.52×10^{0}	1.81×10^{0}	1.34×10^{-11}	1.09×10^{-10}

Table A.43 (continued). The list of the top 100 upregulated DEGs identified in the CS3 subtype using DESeq2 as a result of four clustering analyzes.

AC004080.1	3.51×10^{0}	1.81×10^{0}	1.75×10^{-10}	1.20×10^{-9}

SLC30A2	3.51×10^{0}	1.81×10^{0}	1.04×10^{-12}	1.01×10^{-11}
CELP	3.51×10^{0}	1.81×10^{0}	4.11×10^{-15}	5.78×10^{-14}
CELF3	3.51×10^{0}	1.81×10^{0}	3.83×10^{-18}	8.96×10^{-17}
PRAC1	3.50×10^{0}	1.81×10^{0}	1.33×10^{-4}	3.56×10^{-4}
SLC13A2	3.49×10^{0}	1.80×10^{0}	1.10×10^{-12}	1.06×10^{-11}
RN7SL272P	3.48×10^{0}	1.80×10^{0}	6.96×10^{-10}	4.34×10^{-9}
VENTX	3.48×10^{0}	1.80×10^{0}	1.86×10^{-13}	2.02×10^{-12}
KRT39	3.45×10^{0}	1.79×10^{0}	6.71×10^{-9}	3.62×10^{-8}
AL049777.1	3.44×10^{0}	1.78×10^{0}	1.00×10^{-2}	1.88×10^{-2}
SLC38A3	3.43×10^{0}	1.78×10^{0}	1.26×10^{-11}	1.02×10^{-10}
TEKT5	3.42×10^{0}	1.77×10^{0}	3.59×10^{-22}	1.66×10^{-20}
IZUMO2	3.41×10^{0}	1.77×10^{0}	3.56×10^{-9}	2.00×10^{-8}
AL391650.2	3.40×10^{0}	1.77×10^{0}	1.22×10^{-6}	4.60×10^{-6}
SLC1A7	3.37×10^{0}	1.75×10^{0}	1.61×10^{-17}	3.43×10^{-16}
KRT31	3.36×10^{0}	1.75×10^{0}	4.31×10^{-5}	1.26×10^{-4}

Table A.44. The list of the top 100 downregulated DEGs identified in the CS3 subtype using DESeq2 as a result of four clustering analyzes.

	fc	**log2fc**	**pvalue**	**padj**
RN7SKP227	1.38×10^{-2}	-6.18×10^{0}	5.63×10^{-3}	1.11×10^{-2}
AL390318.1	1.55×10^{-2}	-6.01×10^{0}	5.76×10^{-5}	1.65×10^{-4}
RN7SKP186	2.22×10^{-2}	-5.49×10^{0}	1.17×10^{-2}	2.16×10^{-2}
DLGAP1.AS5	2.52×10^{-2}	-5.31×10^{0}	8.04×10^{-39}	6.37×10^{-36}
RNU2.61P	3.03×10^{-2}	-5.04×10^{0}	4.65×10^{-3}	9.35×10^{-3}
EDDM3CP	3.23×10^{-2}	-4.95×10^{0}	1.12×10^{-3}	2.56×10^{-3}
AC008833.1	3.25×10^{-2}	-4.94×10^{0}	4.26×10^{-5}	1.25×10^{-4}
AL589655.1	3.30×10^{-2}	-4.92×10^{0}	7.44×10^{-5}	2.08×10^{-4}
RN7SKP48	3.36×10^{-2}	-4.90×10^{0}	2.27×10^{-3}	4.86×10^{-3}
ATG10.AS1	3.70×10^{-2}	-4.76×10^{0}	7.34×10^{-4}	1.73×10^{-3}
RNU6.52P	3.93×10^{-2}	-4.67×10^{0}	1.36×10^{-3}	3.04×10^{-3}
TRPV6	4.43×10^{-2}	-4.50×10^{0}	1.45×10^{-59}	2.07×10^{-55}
MIR3140	4.53×10^{-2}	-4.46×10^{0}	6.69×10^{-4}	1.58×10^{-3}
RN7SKP189	4.66×10^{-2}	-4.42×10^{0}	4.81×10^{-3}	9.65×10^{-3}
RN7SKP133	4.80×10^{-2}	-4.38×10^{0}	1.11×10^{-2}	2.05×10^{-2}
Y_RNA.93	4.83×10^{-2}	-4.37×10^{0}	2.53×10^{-3}	5.37×10^{-3}
AL158832.1	4.88×10^{-2}	-4.36×10^{0}	9.65×10^{-5}	2.65×10^{-4}
AL358333.2	5.10×10^{-2}	-4.29×10^{0}	1.16×10^{-4}	3.13×10^{-4}
RN7SKP56	5.11×10^{-2}	-4.29×10^{0}	1.20×10^{-4}	3.23×10^{-4}
AL117341.1	5.17×10^{-2}	-4.27×10^{0}	3.00×10^{-4}	7.57×10^{-4}
AC136424.1	5.25×10^{-2}	-4.25×10^{0}	2.90×10^{-4}	7.32×10^{-4}

Table A.44 (continued). The list of the top 100 downregulated DEGs identified in the CS3 subtype using DESeq2 as a result of four clustering analyzes.

INSL4	5.27×10^{-2}	-4.25×10^{0}	7.99×10^{-19}	2.10×10^{-17}

MIR548U	5.28×10^{-2}	-4.24×10^{0}	4.33×10^{-3}	8.77×10^{-3}
AP000897.1	5.33×10^{-2}	-4.23×10^{0}	3.37×10^{-3}	6.97×10^{-3}
AC012404.1	5.42×10^{-2}	-4.21×10^{0}	5.55×10^{-4}	1.33×10^{-3}
RNY3	5.43×10^{-2}	-4.20×10^{0}	4.15×10^{-3}	8.43×10^{-3}
SNORD63.1	5.48×10^{-2}	-4.19×10^{0}	2.09×10^{-2}	3.64×10^{-2}
AC103706.2	5.62×10^{-2}	-4.15×10^{0}	3.79×10^{-5}	1.12×10^{-4}
RNA5SP104	5.65×10^{-2}	-4.15×10^{0}	3.81×10^{-4}	9.42×10^{-4}
RNU6.1188P	5.66×10^{-2}	-4.14×10^{0}	1.14×10^{-2}	2.10×10^{-2}
AC019278.1	5.72×10^{-2}	-4.13×10^{0}	5.54×10^{-3}	1.10×10^{-2}
RNU6ATAC23P	5.83×10^{-2}	-4.10×10^{0}	1.26×10^{-2}	2.30×10^{-2}
CTD.2350J17.1	5.85×10^{-2}	-4.10×10^{0}	1.67×10^{-3}	3.67×10^{-3}
AC104232.2	5.91×10^{-2}	-4.08×10^{0}	4.83×10^{-4}	1.17×10^{-3}
AL359095.1	5.99×10^{-2}	-4.06×10^{0}	1.03×10^{-3}	2.35×10^{-3}
AL512326.1	6.00×10^{-2}	-4.06×10^{0}	7.59×10^{-4}	1.78×10^{-3}
ELMO1.AS1	6.01×10^{-2}	-4.06×10^{0}	7.58×10^{-4}	1.78×10^{-3}
Y_RNA.714	6.23×10^{-2}	-4.00×10^{0}	4.32×10^{-4}	1.06×10^{-3}
AC113398.2	6.25×10^{-2}	-4.00×10^{0}	1.04×10^{-3}	2.37×10^{-3}
SUMO2P14	6.44×10^{-2}	-3.96×10^{0}	4.43×10^{-3}	8.94×10^{-3}
RNU6.1237P	6.48×10^{-2}	-3.95×10^{0}	2.15×10^{-4}	5.54×10^{-4}
AC129492.2	6.49×10^{-2}	-3.95×10^{0}	1.45×10^{-15}	2.19×10^{-14}
Y_RNA.600	6.52×10^{-2}	-3.94×10^{0}	2.21×10^{-3}	4.74×10^{-3}
RNU1.109P	6.54×10^{-2}	-3.93×10^{0}	2.10×10^{-4}	5.43×10^{-4}
AL133384.1	6.55×10^{-2}	-3.93×10^{0}	5.04×10^{-4}	1.22×10^{-3}
RN7SKP193	6.55×10^{-2}	-3.93×10^{0}	1.98×10^{-3}	4.29×10^{-3}
AL357793.2	6.60×10^{-2}	-3.92×10^{0}	4.09×10^{-3}	8.32×10^{-3}
AL513185.1	6.63×10^{-2}	-3.92×10^{0}	3.81×10^{-4}	9.43×10^{-4}
AP000462.2	6.69×10^{-2}	-3.90×10^{0}	1.08×10^{-2}	2.02×10^{-2}
AP002967.1	6.69×10^{-2}	-3.90×10^{0}	3.21×10^{-4}	8.06×10^{-4}
RNU6.272P	6.80×10^{-2}	-3.88×10^{0}	3.89×10^{-4}	9.61×10^{-4}
RNU6.1034P	6.80×10^{-2}	-3.88×10^{0}	4.47×10^{-3}	9.02×10^{-3}
AC011139.1	6.82×10^{-2}	-3.87×10^{0}	1.30×10^{-4}	3.50×10^{-4}
RNU6.874P	6.89×10^{-2}	-3.86×10^{0}	3.85×10^{-4}	9.50×10^{-4}
AC022467.2	6.94×10^{-2}	-3.85×10^{0}	1.92×10^{-4}	5.00×10^{-4}
AC013437.1	6.98×10^{-2}	-3.84×10^{0}	5.91×10^{-4}	1.41×10^{-3}
Y_RNA.598	6.99×10^{-2}	-3.84×10^{0}	1.82×10^{-2}	3.20×10^{-2}
RNA5SP363	7.02×10^{-2}	-3.83×10^{0}	1.34×10^{-3}	2.99×10^{-3}
MUCL3	7.02×10^{-2}	-3.83×10^{0}	2.87×10^{-38}	2.12×10^{-35}
Y_RNA.219	7.04×10^{-2}	-3.83×10^{0}	3.48×10^{-3}	7.17×10^{-3}

Table A.44 (continued). The list of the top 100 downregulated DEGs identified in the CS3 subtype using DESeq2 as a result of four clustering analyzes.

RNU6.613P	7.05×10^{-2}	-3.83×10^{0}	1.99×10^{-3}	4.30×10^{-3}
RNU1.89P	7.12×10^{-2}	-3.81×10^{0}	2.41×10^{-2}	4.14×10^{-2}

AC021766.1	7.17×10^{-2}	-3.80×10^{0}	5.13×10^{-4}	1.24×10^{-3}
ZBTB20.AS3	7.18×10^{-2}	-3.80×10^{0}	1.31×10^{-3}	2.93×10^{-3}
PLCB1.IT1	7.24×10^{-2}	-3.79×10^{0}	1.46×10^{-2}	2.63×10^{-2}
SLC9A9.AS1	7.29×10^{-2}	-3.78×10^{0}	4.91×10^{-4}	1.19×10^{-3}
Y_RNA.560	7.29×10^{-2}	-3.78×10^{0}	3.21×10^{-3}	6.67×10^{-3}
AC110603.1	7.31×10^{-2}	-3.77×10^{0}	1.88×10^{-2}	3.30×10^{-2}
RN7SL464P	7.32×10^{-2}	-3.77×10^{0}	2.87×10^{-3}	6.02×10^{-3}
RBM22P4	7.37×10^{-2}	-3.76×10^{0}	1.21×10^{-3}	2.73×10^{-3}
AP002453.1	7.39×10^{-2}	-3.76×10^{0}	4.58×10^{-4}	1.12×10^{-3}
Y_RNA.299	7.42×10^{-2}	-3.75×10^{0}	6.77×10^{-4}	1.60×10^{-3}
AC006566.2	7.43×10^{-2}	-3.75×10^{0}	1.95×10^{-4}	5.07×10^{-4}
RNU6.1190P	7.46×10^{-2}	-3.75×10^{0}	4.49×10^{-4}	1.10×10^{-3}
RN7SKP118	7.50×10^{-2}	-3.74×10^{0}	2.38×10^{-3}	5.08×10^{-3}
AL160159.1	7.54×10^{-2}	-3.73×10^{0}	6.15×10^{-3}	1.21×10^{-2}
RNU2.48P	7.55×10^{-2}	-3.73×10^{0}	2.17×10^{-2}	3.77×10^{-2}
MIR548K	7.56×10^{-2}	-3.73×10^{0}	6.15×10^{-4}	1.47×10^{-3}
AC013549.2	7.62×10^{-2}	-3.71×10^{0}	3.14×10^{-4}	7.89×10^{-4}
RN7SL350P	7.64×10^{-2}	-3.71×10^{0}	1.94×10^{-3}	4.21×10^{-3}
CCK	7.68×10^{-2}	-3.70×10^{0}	5.72×10^{-25}	4.41×10^{-23}
SERPINB3	7.74×10^{-2}	-3.69×10^{0}	1.16×10^{-12}	1.11×10^{-11}
AL133485.2	7.78×10^{-2}	-3.68×10^{0}	1.16×10^{-4}	3.13×10^{-4}
MIR4320	7.81×10^{-2}	-3.68×10^{0}	1.47×10^{-3}	3.26×10^{-3}
AL132992.1	7.89×10^{-2}	-3.66×10^{0}	8.42×10^{-4}	1.96×10^{-3}
RN7SKP184	7.89×10^{-2}	-3.66×10^{0}	5.60×10^{-3}	1.11×10^{-2}
AL356785.1	7.90×10^{-2}	-3.66×10^{0}	4.77×10^{-4}	1.16×10^{-3}
RN7SKP103	7.90×10^{-2}	-3.66×10^{0}	1.66×10^{-3}	3.65×10^{-3}
AC011242.1	7.92×10^{-2}	-3.66×10^{0}	1.95×10^{-4}	5.07×10^{-4}
AC008873.1	7.95×10^{-2}	-3.65×10^{0}	5.37×10^{-3}	1.07×10^{-2}
AP000897.2	7.97×10^{-2}	-3.65×10^{0}	4.31×10^{-4}	1.06×10^{-3}
RN7SKP130	7.99×10^{-2}	-3.65×10^{0}	5.94×10^{-4}	1.42×10^{-3}
AL662889.1	8.02×10^{-2}	-3.64×10^{0}	5.38×10^{-3}	1.07×10^{-2}
MIR4676	8.07×10^{-2}	-3.63×10^{0}	1.58×10^{-3}	3.49×10^{-3}
Y_RNA.175	8.08×10^{-2}	-3.63×10^{0}	1.62×10^{-3}	3.57×10^{-3}
MTCO3P23	8.17×10^{-2}	-3.61×10^{0}	1.36×10^{-3}	3.03×10^{-3}
RNU7.10P	8.20×10^{-2}	-3.61×10^{0}	4.58×10^{-4}	1.12×10^{-3}
TCF4.AS2	8.20×10^{-2}	-3.61×10^{0}	1.08×10^{-2}	2.01×10^{-2}
RN7SKP217	8.23×10^{-2}	-3.60×10^{0}	5.55×10^{-3}	1.10×10^{-2}
U4	8.24×10^{-2}	-3.60×10^{0}	2.23×10^{-4}	5.74×10^{-4}

Table A.45. The list of the top 100 upregulated DEGs identified in the CS4 subtype using DESeq2 as a result of four clustering analyzes.

	fc	**log2fc**	**pvalue**	**padj**
GP2	3.78×10^{1}	5.24×10^{0}	6.05×10^{-29}	7.04×10^{-26}
TTC29	2.95×10^{1}	4.88×10^{0}	1.38×10^{-15}	8.61×10^{-14}
TFF2	1.67×10^{1}	4.06×10^{0}	1.21×10^{-29}	1.55×10^{-26}

ANXA10	1.56×10^{1}	3.96×10^{0}	1.13×10^{-15}	7.23×10^{-14}
SEMG2	1.42×10^{1}	3.82×10^{0}	3.52×10^{-10}	6.46×10^{-9}
FGL1	1.34×10^{1}	3.74×10^{0}	1.13×10^{-11}	3.00×10^{-10}
GUSBP7	1.21×10^{1}	3.59×10^{0}	3.63×10^{-7}	3.02×10^{-6}
TM4SF4	1.17×10^{1}	3.55×10^{0}	6.14×10^{-21}	1.25×10^{-18}
CTSE	1.15×10^{1}	3.53×10^{0}	3.32×10^{-23}	1.14×10^{-20}
IGFALS	1.10×10^{1}	3.46×10^{0}	2.47×10^{-23}	8.79×10^{-21}
MUC5AC	1.03×10^{1}	3.36×10^{0}	2.16×10^{-16}	1.60×10^{-14}
RBP3	1.00×10^{1}	3.32×10^{0}	1.15×10^{-18}	1.48×10^{-16}
LINC02620	9.39×10^{0}	3.23×10^{0}	4.64×10^{-4}	1.50×10^{-3}
REG4	8.69×10^{0}	3.12×10^{0}	3.72×10^{-16}	2.64×10^{-14}
REG1A	8.35×10^{0}	3.06×10^{0}	1.93×10^{-11}	4.82×10^{-10}
MUC6	8.26×10^{0}	3.05×10^{0}	3.42×10^{-10}	6.31×10^{-9}
NKX2.2	8.17×10^{0}	3.03×10^{0}	6.94×10^{-12}	1.94×10^{-10}
PRSS2	7.89×10^{0}	2.98×10^{0}	1.83×10^{-10}	3.59×10^{-9}
AC021534.1	7.81×10^{0}	2.97×10^{0}	1.18×10^{-7}	1.12×10^{-6}
SPRR1A	7.81×10^{0}	2.97×10^{0}	8.44×10^{-8}	8.31×10^{-7}
AC009078.1	7.73×10^{0}	2.95×10^{0}	1.44×10^{-4}	5.50×10^{-4}
ALPG	7.70×10^{0}	2.95×10^{0}	9.30×10^{-18}	9.67×10^{-16}
AC253536.4	7.67×10^{0}	2.94×10^{0}	1.04×10^{-9}	1.70×10^{-8}
CLCA1	7.60×10^{0}	2.93×10^{0}	8.91×10^{-11}	1.87×10^{-9}
TCN1	7.46×10^{0}	2.90×10^{0}	5.88×10^{-15}	3.16×10^{-13}
SPINK4	7.33×10^{0}	2.87×10^{0}	2.03×10^{-13}	7.92×10^{-12}
RFX6	7.24×10^{0}	2.86×10^{0}	2.09×10^{-12}	6.50×10^{-11}
ARX	7.22×10^{0}	2.85×10^{0}	5.83×10^{-17}	5.04×10^{-15}
LRRC26	6.89×10^{0}	2.78×10^{0}	1.88×10^{-14}	9.07×10^{-13}
MSMB	6.75×10^{0}	2.75×10^{0}	6.29×10^{-8}	6.46×10^{-7}
NBPF7	6.69×10^{0}	2.74×10^{0}	2.45×10^{-11}	5.94×10^{-10}
LINC00261	6.64×10^{0}	2.73×10^{0}	1.81×10^{-24}	8.84×10^{-22}
TFF1	6.61×10^{0}	2.73×10^{0}	2.44×10^{-20}	4.55×10^{-18}
SLC18A1	6.53×10^{0}	2.71×10^{0}	4.28×10^{-15}	2.36×10^{-13}
IRX4.AS1	6.40×10^{0}	2.68×10^{0}	9.45×10^{-3}	2.02×10^{-2}
MUCL3	6.31×10^{0}	2.66×10^{0}	3.83×10^{-10}	6.95×10^{-9}
LINC02826	6.29×10^{0}	2.65×10^{0}	5.13×10^{-13}	1.82×10^{-11}
ANPEP	6.20×10^{0}	2.63×10^{0}	7.05×10^{-20}	1.17×10^{-17}
AC009517.1	6.20×10^{0}	2.63×10^{0}	1.38×10^{-5}	7.28×10^{-5}
LINC01351	6.16×10^{0}	2.62×10^{0}	2.55×10^{-5}	1.23×10^{-4}

Table A.45 (continued). The list of the top 100 upregulated DEGs identified in the CS4 subtype using DESeq2 as a result of four clustering analyzes.

MLN	6.12×10^{0}	2.61×10^{0}	2.02×10^{-5}	1.01×10^{-4}
NXPH4	5.99×10^{0}	2.58×10^{0}	8.82×10^{-16}	5.73×10^{-14}
AC126564.1	5.96×10^{0}	2.58×10^{0}	1.03×10^{-13}	4.26×10^{-12}
SPRR1B	5.94×10^{0}	2.57×10^{0}	5.43×10^{-7}	4.29×10^{-6}
CPS1	5.94×10^{0}	2.57×10^{0}	2.63×10^{-13}	1.00×10^{-11}

AP002498.1	5.93×10^{0}	2.57×10^{0}	3.67×10^{-14}	1.67×10^{-12}
BRINP3	5.92×10^{0}	2.57×10^{0}	3.41×10^{-8}	3.76×10^{-7}
AC093001.1	5.88×10^{0}	2.56×10^{0}	3.71×10^{-8}	4.04×10^{-7}
SEMG1	5.81×10^{0}	2.54×10^{0}	2.80×10^{-8}	3.16×10^{-7}
REG1CP	5.73×10^{0}	2.52×10^{0}	2.86×10^{-5}	1.36×10^{-4}
AL122008.2	5.55×10^{0}	2.47×10^{0}	5.49×10^{-5}	2.39×10^{-4}
HEPACAM2	5.54×10^{0}	2.47×10^{0}	1.43×10^{-14}	7.08×10^{-13}
AC010998.3	5.50×10^{0}	2.46×10^{0}	1.85×10^{-8}	2.18×10^{-7}
INSL4	5.43×10^{0}	2.44×10^{0}	3.54×10^{-4}	1.19×10^{-3}
AC125421.1	5.34×10^{0}	2.42×10^{0}	7.43×10^{-5}	3.10×10^{-4}
NEUROG3	5.29×10^{0}	2.40×10^{0}	8.94×10^{-9}	1.14×10^{-7}
ALOXE3P1	5.24×10^{0}	2.39×10^{0}	7.03×10^{-7}	5.38×10^{-6}
AC129492.2	5.24×10^{0}	2.39×10^{0}	7.08×10^{-4}	2.17×10^{-3}
AC009163.6	5.21×10^{0}	2.38×10^{0}	6.80×10^{-13}	2.34×10^{-11}
MUC2	5.19×10^{0}	2.38×10^{0}	8.03×10^{-12}	2.21×10^{-10}
KIF19	5.11×10^{0}	2.35×10^{0}	1.47×10^{-13}	5.94×10^{-12}
CIB4	5.02×10^{0}	2.33×10^{0}	4.45×10^{-10}	7.96×10^{-9}
EIF3KP3	5.01×10^{0}	2.32×10^{0}	1.70×10^{-2}	3.35×10^{-2}
AC008443.3	4.99×10^{0}	2.32×10^{0}	3.05×10^{-11}	7.22×10^{-10}
AP003062.2	4.97×10^{0}	2.31×10^{0}	1.08×10^{-4}	4.29×10^{-4}
NXF3	4.96×10^{0}	2.31×10^{0}	2.86×10^{-9}	4.17×10^{-8}
CCL26	4.90×10^{0}	2.29×10^{0}	8.29×10^{-23}	2.69×10^{-20}
TMEM210	4.87×10^{0}	2.28×10^{0}	2.55×10^{-7}	2.22×10^{-6}
AC004009.1	4.85×10^{0}	2.28×10^{0}	1.52×10^{-6}	1.06×10^{-5}
CA8	4.83×10^{0}	2.27×10^{0}	7.67×10^{-16}	5.06×10^{-14}
COX5AP1	4.82×10^{0}	2.27×10^{0}	3.87×10^{-6}	2.38×10^{-5}
INSM1	4.82×10^{0}	2.27×10^{0}	3.06×10^{-10}	5.72×10^{-9}
B3GNT6	4.78×10^{0}	2.26×10^{0}	2.23×10^{-8}	2.59×10^{-7}
AL121761.1	4.78×10^{0}	2.26×10^{0}	2.47×10^{-12}	7.57×10^{-11}
FAM177B	4.74×10^{0}	2.25×10^{0}	1.19×10^{-14}	5.95×10^{-13}
LINC00520	4.73×10^{0}	2.24×10^{0}	4.66×10^{-14}	2.08×10^{-12}
KRT89P	4.71×10^{0}	2.24×10^{0}	4.85×10^{-10}	8.60×10^{-9}
PCSK1	4.65×10^{0}	2.22×10^{0}	2.29×10^{-8}	2.64×10^{-7}
AC087612.1	4.65×10^{0}	2.22×10^{0}	2.58×10^{-6}	1.68×10^{-5}
CCK	4.64×10^{0}	2.21×10^{0}	1.26×10^{-5}	6.70×10^{-5}
AL079303.1	4.64×10^{0}	2.21×10^{0}	4.13×10^{-4}	1.36×10^{-3}

Table A.45 (continued). The list of the top 100 upregulated DEGs identified in the CS4 subtype using DESeq2 as a result of four clustering analyzes.

AC008514.1	4.63×10^{0}	2.21×10^{0}	4.38×10^{-11}	9.97×10^{-10}
TMEM61	4.62×10^{0}	2.21×10^{0}	9.97×10^{-22}	2.48×10^{-19}
GALNT8	4.61×10^{0}	2.21×10^{0}	6.57×10^{-17}	5.61×10^{-15}
SI	4.61×10^{0}	2.20×10^{0}	1.16×10^{-9}	1.86×10^{-8}
KLK12	4.55×10^{0}	2.19×10^{0}	6.33×10^{-11}	1.39×10^{-9}
AGR2	4.54×10^{0}	2.18×10^{0}	7.69×10^{-43}	9.83×10^{-39}

RPSAP28	4.52×10^{0}	2.18×10^{0}	5.40×10^{-6}	3.20×10^{-5}
MUC5B	4.51×10^{0}	2.17×10^{0}	1.15×10^{-11}	3.05×10^{-10}
SPDEF	4.51×10^{0}	2.17×10^{0}	1.62×10^{-15}	9.94×10^{-14}
NMUR2	4.51×10^{0}	2.17×10^{0}	8.87×10^{-6}	4.93×10^{-5}
IL1R2	4.48×10^{0}	2.17×10^{0}	5.98×10^{-27}	4.50×10^{-24}
GJB5	4.47×10^{0}	2.16×10^{0}	2.99×10^{-10}	5.61×10^{-9}
ALDH1L1	4.42×10^{0}	2.14×10^{0}	1.89×10^{-11}	4.74×10^{-10}
C17orf78	4.42×10^{0}	2.14×10^{0}	8.79×10^{-7}	6.54×10^{-6}
ATOH1	4.39×10^{0}	2.13×10^{0}	3.61×10^{-12}	1.07×10^{-10}
AC108751.5	4.38×10^{0}	2.13×10^{0}	2.05×10^{-14}	9.75×10^{-13}
CLDN18	4.38×10^{0}	2.13×10^{0}	7.90×10^{-5}	3.26×10^{-4}
HSD17B2	4.36×10^{0}	2.12×10^{0}	2.38×10^{-20}	4.45×10^{-18}
CYP1A1	4.35×10^{0}	2.12×10^{0}	3.91×10^{-5}	1.78×10^{-4}

Table A.46. The list of the top 100 downregulated DEGs identified in the CS4 subtype using DESeq2 as a result of four clustering analyzes.

	fc	**log2fc**	**pvalue**	**padj**
SHISA9	1.48×10^{-2}	-6.08×10^{0}	1.87×10^{-40}	1.79×10^{-36}
LINC02128	3.57×10^{-2}	-4.81×10^{0}	9.23×10^{-22}	2.31×10^{-19}
U91319.1	3.68×10^{-2}	-4.76×10^{0}	5.26×10^{-14}	2.32×10^{-12}
TMEM132D.AS1	3.75×10^{-2}	-4.74×10^{0}	3.17×10^{-8}	3.54×10^{-7}
LINC00491	5.32×10^{-2}	-4.23×10^{0}	5.49×10^{-6}	3.25×10^{-5}
AC110772.2	6.16×10^{-2}	-4.02×10^{0}	1.04×10^{-18}	1.35×10^{-16}
EYA1	6.27×10^{-2}	-4.00×10^{0}	4.34×10^{-31}	6.93×10^{-28}
PWWP3B	6.42×10^{-2}	-3.96×10^{0}	1.09×10^{-25}	6.31×10^{-23}
KRT35	6.58×10^{-2}	-3.93×10^{0}	1.51×10^{-9}	2.37×10^{-8}
TUBAP13	6.64×10^{-2}	-3.91×10^{0}	1.44×10^{-19}	2.26×10^{-17}
AL589787.2	6.70×10^{-2}	-3.90×10^{0}	2.61×10^{-7}	2.27×10^{-6}
MAGEA4.AS1	6.81×10^{-2}	-3.88×10^{0}	1.43×10^{-4}	5.46×10^{-4}
AC016044.1	6.84×10^{-2}	-3.87×10^{0}	3.11×10^{-7}	2.63×10^{-6}
GABRA3	6.87×10^{-2}	-3.86×10^{0}	1.54×10^{-15}	9.48×10^{-14}
AC090809.1	7.06×10^{-2}	-3.82×10^{0}	1.58×10^{-8}	1.89×10^{-7}
AL035252.2	7.09×10^{-2}	-3.82×10^{0}	1.77×10^{-14}	8.59×10^{-13}

Table A.46 (continued). The list of the top 100 downregulated DEGs identified in the CS4 subtype using DESeq2 as a result of four clustering analyzes.

CDH9	7.24×10^{-2}	-3.79×10^{0}	8.82×10^{-5}	3.60×10^{-4}
AC012501.2	7.46×10^{-2}	-3.74×10^{0}	5.31×10^{-13}	1.87×10^{-11}
ZNF663P	7.52×10^{-2}	-3.73×10^{0}	4.09×10^{-11}	9.40×10^{-10}
AC090578.1	7.57×10^{-2}	-3.72×10^{0}	7.57×10^{-17}	6.31×10^{-15}
AL031686.1	7.60×10^{-2}	-3.72×10^{0}	1.18×10^{-13}	4.87×10^{-12}
AL110505.1	7.70×10^{-2}	-3.70×10^{0}	2.59×10^{-6}	1.69×10^{-5}
WT1.AS	8.11×10^{-2}	-3.62×10^{0}	8.07×10^{-11}	1.72×10^{-9}

G2E3.AS1	8.12×10^{-2}	-3.62×10^{0}	2.04×10^{-5}	1.02×10^{-4}
MAGEA3	8.20×10^{-2}	-3.61×10^{0}	7.74×10^{-5}	3.20×10^{-4}
GLRA2	8.28×10^{-2}	-3.59×10^{0}	9.79×10^{-23}	3.10×10^{-20}
AC003958.2	9.11×10^{-2}	-3.46×10^{0}	1.31×10^{-11}	3.40×10^{-10}
AL390334.1	9.15×10^{-2}	-3.45×10^{0}	2.25×10^{-5}	1.11×10^{-4}
KRT38	9.17×10^{-2}	-3.45×10^{0}	3.20×10^{-8}	3.56×10^{-7}
VWDE	9.28×10^{-2}	-3.43×10^{0}	4.51×10^{-20}	8.01×10^{-18}
CT83	9.62×10^{-2}	-3.38×10^{0}	2.10×10^{-3}	5.55×10^{-3}
EMX2OS	1.00×10^{-1}	-3.33×10^{0}	8.32×10^{-18}	8.74×10^{-16}
AL121885.2	1.01×10^{-1}	-3.31×10^{0}	5.31×10^{-11}	1.18×10^{-9}
AL592043.1	1.01×10^{-1}	-3.30×10^{0}	4.02×10^{-7}	3.30×10^{-6}
GABRR1	1.02×10^{-1}	-3.29×10^{0}	8.92×10^{-12}	2.42×10^{-10}
NEUROG2.AS1	1.02×10^{-1}	-3.29×10^{0}	5.65×10^{-10}	9.87×10^{-9}
TRPM3	1.07×10^{-1}	-3.22×10^{0}	1.33×10^{-19}	2.11×10^{-17}
EMX2	1.08×10^{-1}	-3.21×10^{0}	6.55×10^{-12}	1.84×10^{-10}
LY6G6F	1.09×10^{-1}	-3.20×10^{0}	3.68×10^{-22}	1.03×10^{-19}
LINC00607	1.10×10^{-1}	-3.18×10^{0}	2.78×10^{-21}	6.12×10^{-19}
AL391650.2	1.12×10^{-1}	-3.15×10^{0}	2.02×10^{-9}	3.06×10^{-8}
AC092969.1	1.13×10^{-1}	-3.15×10^{0}	2.24×10^{-11}	5.50×10^{-10}
AC011370.1	1.14×10^{-1}	-3.13×10^{0}	4.43×10^{-5}	1.98×10^{-4}
LY6G6E	1.15×10^{-1}	-3.12×10^{0}	3.28×10^{-21}	7.10×10^{-19}
SLC22A12	1.16×10^{-1}	-3.11×10^{0}	6.56×10^{-9}	8.71×10^{-8}
AL583808.1	1.17×10^{-1}	-3.10×10^{0}	6.37×10^{-6}	3.71×10^{-5}
SLC6A4	1.17×10^{-1}	-3.09×10^{0}	7.25×10^{-27}	5.35×10^{-24}
LINC02251	1.18×10^{-1}	-3.09×10^{0}	1.35×10^{-23}	5.35×10^{-21}
AC025839.1	1.22×10^{-1}	-3.04×10^{0}	1.80×10^{-6}	1.23×10^{-5}
FREM2	1.23×10^{-1}	-3.03×10^{0}	6.32×10^{-20}	1.06×10^{-17}
PCDH19	1.24×10^{-1}	-3.01×10^{0}	1.98×10^{-27}	1.69×10^{-24}
PAGE1	1.24×10^{-1}	-3.01×10^{0}	3.31×10^{-3}	8.20×10^{-3}
LINC02820	1.25×10^{-1}	-2.99×10^{0}	1.79×10^{-6}	1.22×10^{-5}
RNU1.22P	1.26×10^{-1}	-2.99×10^{0}	1.36×10^{-11}	3.51×10^{-10}
SLC13A3	1.27×10^{-1}	-2.97×10^{0}	1.45×10^{-22}	4.40×10^{-20}
AC096759.2	1.27×10^{-1}	-2.97×10^{0}	1.04×10^{-4}	4.16×10^{-4}

Table A.46 (continued). The list of the top 100 downregulated DEGs identified in the CS4 subtype using DESeq2 as a result of four clustering analyzes.

CHRND	1.27×10^{-1}	-2.97×10^{0}	1.11×10^{-8}	1.38×10^{-7}
LGALS14	1.28×10^{-1}	-2.96×10^{0}	1.70×10^{-6}	1.17×10^{-5}
Z93403.1	1.30×10^{-1}	-2.95×10^{0}	1.76×10^{-8}	2.09×10^{-7}
AC091646.1	1.30×10^{-1}	-2.95×10^{0}	2.80×10^{-8}	3.16×10^{-7}
KRT32	1.31×10^{-1}	-2.93×10^{0}	5.98×10^{-7}	4.68×10^{-6}
CNTNAP5	1.34×10^{-1}	-2.90×10^{0}	8.04×10^{-8}	7.96×10^{-7}
AC021683.1	1.35×10^{-1}	-2.89×10^{0}	2.40×10^{-16}	1.77×10^{-14}
CLEC3A	1.36×10^{-1}	-2.88×10^{0}	2.29×10^{-6}	1.51×10^{-5}

SLC6A2	1.38×10^{-1}	-2.86×10^{0}	1.50×10^{-8}	1.80×10^{-7}
AOAH.IT1	1.38×10^{-1}	-2.86×10^{0}	6.33×10^{-15}	3.37×10^{-13}
AL358335.2	1.38×10^{-1}	-2.85×10^{0}	5.89×10^{-3}	1.34×10^{-2}
ZNF492	1.40×10^{-1}	-2.84×10^{0}	1.58×10^{-11}	4.05×10^{-10}
ZIC4	1.41×10^{-1}	-2.83×10^{0}	3.00×10^{-4}	1.03×10^{-3}
AL445205.1	1.41×10^{-1}	-2.83×10^{0}	2.65×10^{-7}	2.30×10^{-6}
REEP1	1.41×10^{-1}	-2.83×10^{0}	7.33×10^{-32}	1.41×10^{-28}
AL049828.2	1.42×10^{-1}	-2.82×10^{0}	1.21×10^{-2}	2.50×10^{-2}
AL121949.1	1.42×10^{-1}	-2.82×10^{0}	2.26×10^{-6}	1.49×10^{-5}
LINC00954	1.42×10^{-1}	-2.81×10^{0}	1.14×10^{-38}	7.28×10^{-35}
AC107419.1	1.44×10^{-1}	-2.80×10^{0}	3.10×10^{-7}	2.62×10^{-6}
CTNNA2.AS1	1.46×10^{-1}	-2.78×10^{0}	9.08×10^{-4}	2.69×10^{-3}
AC138649.1	1.47×10^{-1}	-2.76×10^{0}	1.27×10^{-15}	7.98×10^{-14}
AL035467.2	1.49×10^{-1}	-2.74×10^{0}	2.06×10^{-3}	5.46×10^{-3}
AL589743.3	1.50×10^{-1}	-2.73×10^{0}	4.84×10^{-8}	5.11×10^{-7}
AC021683.2	1.51×10^{-1}	-2.73×10^{0}	5.80×10^{-16}	3.95×10^{-14}
AL591222.1	1.52×10^{-1}	-2.72×10^{0}	2.74×10^{-10}	5.18×10^{-9}
SV2C	1.53×10^{-1}	-2.71×10^{0}	1.19×10^{-19}	1.91×10^{-17}
AF064858.3	1.53×10^{-1}	-2.71×10^{0}	6.58×10^{-11}	1.43×10^{-9}
EREG	1.53×10^{-1}	-2.70×10^{0}	2.53×10^{-23}	8.91×10^{-21}
AC096589.1	1.54×10^{-1}	-2.70×10^{0}	6.21×10^{-6}	3.62×10^{-5}
FMN2	1.54×10^{-1}	-2.70×10^{0}	4.70×10^{-14}	2.09×10^{-12}
CA5A	1.54×10^{-1}	-2.70×10^{0}	3.79×10^{-11}	8.76×10^{-10}
AF064858.2	1.54×10^{-1}	-2.70×10^{0}	2.72×10^{-16}	1.99×10^{-14}
AL022151.1	1.55×10^{-1}	-2.69×10^{0}	4.81×10^{-6}	2.89×10^{-5}
AL356274.2	1.56×10^{-1}	-2.69×10^{0}	7.60×10^{-6}	4.32×10^{-5}
AL390726.5	1.56×10^{-1}	-2.68×10^{0}	2.65×10^{-18}	3.17×10^{-16}
MIR483	1.57×10^{-1}	-2.67×10^{0}	6.68×10^{-3}	1.50×10^{-2}
LINC02327	1.57×10^{-1}	-2.67×10^{0}	4.00×10^{-3}	9.67×10^{-3}
GCM1	1.58×10^{-1}	-2.66×10^{0}	3.51×10^{-13}	1.30×10^{-11}
NPBWR1	1.58×10^{-1}	-2.66×10^{0}	2.31×10^{-11}	5.64×10^{-10}
LIPI	1.59×10^{-1}	-2.66×10^{0}	1.47×10^{-10}	2.95×10^{-9}
TRAV33	1.59×10^{-1}	-2.65×10^{0}	3.65×10^{-7}	3.04×10^{-6}

Table A.46 (continued). The list of the top 100 downregulated DEGs identified in the CS4 subtype using DESeq2 as a result of four clustering analyzes.

CDH26	1.60×10^{-1}	-2.65×10^{0}	6.33×10^{-32}	1.28×10^{-28}
CRAT37	1.60×10^{-1}	-2.64×10^{0}	1.49×10^{-10}	2.98×10^{-9}
WNT7A	1.61×10^{-1}	-2.63×10^{0}	1.51×10^{-8}	1.82×10^{-7}

Table A.47. The list of the top 100 upregulated DEGs identified in the CS1 subtype using limma as a result of four clustering analyzes.

	fc	**log2fc**	**pvalue**	**padj**
SFRP2	1.36×10^{1}	3.77×10^{0}	2.51×10^{-24}	2.22×10^{-22}

COMP	8.15×10^{0}	3.03×10^{0}	5.55×10^{-23}	4.11×10^{-21}
CCL21	7.91×10^{0}	2.98×10^{0}	6.45×10^{-24}	5.37×10^{-22}
SFRP4	7.61×10^{0}	2.93×10^{0}	4.04×10^{-21}	2.42×10^{-19}
DES	7.40×10^{0}	2.89×10^{0}	1.95×10^{-13}	5.41×10^{-12}
IGHG1	6.99×10^{0}	2.80×10^{0}	1.98×10^{-13}	5.47×10^{-12}
PRELP	6.87×10^{0}	2.78×10^{0}	2.74×10^{-34}	2.66×10^{-31}
C3	6.81×10^{0}	2.77×10^{0}	1.60×10^{-27}	2.42×10^{-25}
FNDC1	6.79×10^{0}	2.76×10^{0}	5.77×10^{-31}	1.83×10^{-28}
CCL19	6.75×10^{0}	2.76×10^{0}	7.77×10^{-28}	1.27×10^{-25}
IGLV3.25	6.73×10^{0}	2.75×10^{0}	8.03×10^{-13}	2.11×10^{-11}
IGHV4.39	6.68×10^{0}	2.74×10^{0}	2.98×10^{-12}	7.39×10^{-11}
IGHG4	6.68×10^{0}	2.74×10^{0}	3.84×10^{-13}	1.04×10^{-11}
IGHV5.51	6.64×10^{0}	2.73×10^{0}	4.61×10^{-12}	1.12×10^{-10}
IGLV1.40	6.39×10^{0}	2.68×10^{0}	6.66×10^{-12}	1.59×10^{-10}
IGHV4.34	6.32×10^{0}	2.66×10^{0}	1.92×10^{-14}	5.89×10^{-13}
THBS2	6.30×10^{0}	2.65×10^{0}	1.33×10^{-22}	9.34×10^{-21}
IGHV3.15	6.28×10^{0}	2.65×10^{0}	7.30×10^{-12}	1.73×10^{-10}
IGLV6.57	6.24×10^{0}	2.64×10^{0}	2.01×10^{-12}	5.09×10^{-11}
IGLV3.21	6.21×10^{0}	2.63×10^{0}	9.36×10^{-12}	2.19×10^{-10}
IGHV1.24	6.21×10^{0}	2.63×10^{0}	5.91×10^{-13}	1.58×10^{-11}
FABP4	6.19×10^{0}	2.63×10^{0}	4.62×10^{-25}	4.57×10^{-23}
IGHV1.2	6.13×10^{0}	2.62×10^{0}	1.30×10^{-11}	2.99×10^{-10}
CNN1	6.13×10^{0}	2.62×10^{0}	1.07×10^{-23}	8.68×10^{-22}
IGLV3.1	6.10×10^{0}	2.61×10^{0}	3.55×10^{-11}	7.90×10^{-10}
MGP	6.07×10^{0}	2.60×10^{0}	1.44×10^{-33}	1.07×10^{-30}
MYH11	6.07×10^{0}	2.60×10^{0}	3.45×10^{-20}	1.86×10^{-18}
IGHV1.18	5.97×10^{0}	2.58×10^{0}	2.40×10^{-11}	5.44×10^{-10}
IGHV4.59	5.93×10^{0}	2.57×10^{0}	3.29×10^{-12}	8.10×10^{-11}
IGLV2.23	5.87×10^{0}	2.55×10^{0}	1.98×10^{-11}	4.52×10^{-10}
ACKR1	5.83×10^{0}	2.54×10^{0}	9.57×10^{-30}	2.33×10^{-27}
IGLV3.19	5.73×10^{0}	2.52×10^{0}	1.87×10^{-11}	4.26×10^{-10}
IGLV1.44	5.72×10^{0}	2.52×10^{0}	3.25×10^{-12}	8.00×10^{-11}
IGHV3.21	5.71×10^{0}	2.51×10^{0}	6.67×10^{-11}	1.44×10^{-9}

Table A.47 (continued). The list of the top 100 upregulated DEGs identified in the CS1 subtype using limma as a result of four clustering analyzes.

IGHV3.11	5.67×10^{0}	2.50×10^{0}	9.09×10^{-12}	2.13×10^{-10}
IGHV1.46	5.65×10^{0}	2.50×10^{0}	1.64×10^{-12}	4.19×10^{-11}
IGHV2.5	5.60×10^{0}	2.49×10^{0}	9.95×10^{-11}	2.11×10^{-9}
IGKV3.20	5.58×10^{0}	2.48×10^{0}	4.88×10^{-11}	1.07×10^{-9}
FN1	5.49×10^{0}	2.46×10^{0}	3.88×10^{-20}	2.08×10^{-18}
IGHV1.69D	5.48×10^{0}	2.45×10^{0}	1.60×10^{-11}	3.67×10^{-10}
AEBP1	5.46×10^{0}	2.45×10^{0}	2.73×10^{-28}	4.85×10^{-26}
IGKV4.1	5.42×10^{0}	2.44×10^{0}	4.23×10^{-10}	8.42×10^{-9}
IGHG3	5.39×10^{0}	2.43×10^{0}	8.20×10^{-12}	1.93×10^{-10}

APOE	5.33×10^{0}	2.42×10^{0}	5.02×10^{-19}	2.34×10^{-17}
CHRDL2	5.32×10^{0}	2.41×10^{0}	4.01×10^{-20}	2.14×10^{-18}
IGHV4.31	5.30×10^{0}	2.41×10^{0}	5.97×10^{-12}	1.43×10^{-10}
IGKV3.15	5.29×10^{0}	2.40×10^{0}	4.83×10^{-11}	1.06×10^{-9}
IGLV2.14	5.29×10^{0}	2.40×10^{0}	7.52×10^{-10}	1.46×10^{-8}
IGHV3.30	5.27×10^{0}	2.40×10^{0}	4.70×10^{-11}	1.03×10^{-9}
LMOD1	5.25×10^{0}	2.39×10^{0}	1.20×10^{-29}	2.84×10^{-27}
IGHV3.48	5.23×10^{0}	2.39×10^{0}	1.18×10^{-10}	2.48×10^{-9}
IGLV1.47	5.21×10^{0}	2.38×10^{0}	6.88×10^{-11}	1.48×10^{-9}
IGHGP	5.20×10^{0}	2.38×10^{0}	1.88×10^{-10}	3.88×10^{-9}
AOC3	5.18×10^{0}	2.37×10^{0}	3.00×10^{-35}	4.09×10^{-32}
IGKV3.11	5.14×10^{0}	2.36×10^{0}	3.23×10^{-10}	6.51×10^{-9}
TAGLN	5.13×10^{0}	2.36×10^{0}	4.15×10^{-29}	8.80×10^{-27}
PTGIS	5.12×10^{0}	2.36×10^{0}	5.66×10^{-32}	2.42×10^{-29}
COL1A1	5.06×10^{0}	2.34×10^{0}	1.45×10^{-22}	1.01×10^{-20}
FDCSP	5.01×10^{0}	2.33×10^{0}	2.92×10^{-17}	1.16×10^{-15}
IGHV5.10.1	5.01×10^{0}	2.32×10^{0}	3.21×10^{-9}	5.83×10^{-8}
IGKV1.12	5.00×10^{0}	2.32×10^{0}	3.12×10^{-12}	7.69×10^{-11}
IGHV3.23	4.98×10^{0}	2.32×10^{0}	1.22×10^{-9}	2.32×10^{-8}
FBLN2	4.98×10^{0}	2.32×10^{0}	3.79×10^{-24}	3.27×10^{-22}
IGHV1.69	4.95×10^{0}	2.31×10^{0}	1.10×10^{-11}	2.56×10^{-10}
IGHG2	4.93×10^{0}	2.30×10^{0}	4.12×10^{-10}	8.19×10^{-9}
IGLV3.9	4.91×10^{0}	2.30×10^{0}	9.05×10^{-13}	2.37×10^{-11}
MFAP4	4.90×10^{0}	2.29×10^{0}	1.09×10^{-24}	1.02×10^{-22}
EFEMP1	4.89×10^{0}	2.29×10^{0}	4.57×10^{-28}	7.83×10^{-26}
CHRDL1	4.89×10^{0}	2.29×10^{0}	4.41×10^{-22}	2.94×10^{-20}
IGLC3	4.88×10^{0}	2.29×10^{0}	1.33×10^{-10}	2.78×10^{-9}
IGHV3.33	4.87×10^{0}	2.28×10^{0}	1.36×10^{-10}	2.84×10^{-9}
SPARCL1	4.83×10^{0}	2.27×10^{0}	2.38×10^{-35}	3.32×10^{-32}
IGHV2.26	4.83×10^{0}	2.27×10^{0}	2.43×10^{-12}	6.07×10^{-11}
IGLV2.11	4.82×10^{0}	2.27×10^{0}	6.10×10^{-9}	1.08×10^{-7}
BGN	4.78×10^{0}	2.26×10^{0}	2.31×10^{-25}	2.40×10^{-23}

Table A.47 (continued). The list of the top 100 upregulated DEGs identified in the CS1 subtype using limma as a result of four clustering analyzes.

C7	4.75×10^{0}	2.25×10^{0}	5.98×10^{-28}	9.96×10^{-26}
IGHV4.4	4.75×10^{0}	2.25×10^{0}	9.14×10^{-10}	1.76×10^{-8}
MFAP5	4.74×10^{0}	2.25×10^{0}	3.53×10^{-29}	7.63×10^{-27}
IGLC2	4.74×10^{0}	2.24×10^{0}	2.27×10^{-10}	4.65×10^{-9}
SSC5D	4.72×10^{0}	2.24×10^{0}	8.25×10^{-36}	1.43×10^{-32}
IGHV3.74	4.71×10^{0}	2.24×10^{0}	2.31×10^{-10}	4.72×10^{-9}
ACTG2	4.69×10^{0}	2.23×10^{0}	1.10×10^{-15}	3.75×10^{-14}
COL1A2	4.68×10^{0}	2.23×10^{0}	2.60×10^{-24}	2.29×10^{-22}
IGKV1.9	4.67×10^{0}	2.22×10^{0}	1.98×10^{-9}	3.67×10^{-8}
IGKC	4.67×10^{0}	2.22×10^{0}	2.17×10^{-9}	4.01×10^{-8}

FBLN1	4.66×10^{0}	2.22×10^{0}	1.53×10^{-24}	1.40×10^{-22}
COL8A1	4.65×10^{0}	2.22×10^{0}	5.98×10^{-25}	5.76×10^{-23}
COL3A1	4.64×10^{0}	2.22×10^{0}	1.11×10^{-24}	1.04×10^{-22}
THBS4	4.61×10^{0}	2.21×10^{0}	4.39×10^{-23}	3.30×10^{-21}
SERPING1	4.61×10^{0}	2.20×10^{0}	1.87×10^{-32}	9.49×10^{-30}
MMP2	4.58×10^{0}	2.19×10^{0}	1.41×10^{-25}	1.53×10^{-23}
IGHV3.7	4.58×10^{0}	2.19×10^{0}	3.82×10^{-9}	6.90×10^{-8}
IGKV1.17	4.57×10^{0}	2.19×10^{0}	5.07×10^{-10}	1.00×10^{-8}
DCN	4.55×10^{0}	2.19×10^{0}	1.60×10^{-26}	2.04×10^{-24}
IGLV4.69	4.55×10^{0}	2.19×10^{0}	2.15×10^{-9}	3.97×10^{-8}
IGKV1.5	4.55×10^{0}	2.19×10^{0}	9.41×10^{-9}	1.62×10^{-7}
C1S	4.54×10^{0}	2.18×10^{0}	2.27×10^{-31}	8.21×10^{-29}
IGHV3.64D	4.48×10^{0}	2.16×10^{0}	2.10×10^{-9}	3.89×10^{-8}
LUM	4.46×10^{0}	2.16×10^{0}	6.50×10^{-23}	4.74×10^{-21}
MYL9	4.46×10^{0}	2.16×10^{0}	1.71×10^{-27}	2.57×10^{-25}

Table A.48. The list of the top 6 downregulated DEGs identified in the CS1 subtype using limma as a result of four clustering analyzes.

	fc	**log2fc**	**pvalue**	**padj**
MT.TY	4.12×10^{-1}	-1.28×10^{0}	2.59×10^{-4}	2.44×10^{-3}
STYXL2	4.27×10^{-1}	-1.23×10^{0}	3.60×10^{-3}	2.48×10^{-2}
SNHG25	4.43×10^{-1}	-1.17×10^{0}	3.47×10^{-6}	4.45×10^{-5}
MT.TC	4.62×10^{-1}	-1.11×10^{0}	7.32×10^{-4}	6.22×10^{-3}
MT.TL1	4.93×10^{-1}	-1.02×10^{0}	1.02×10^{-4}	1.05×10^{-3}
RNU4.1	4.96×10^{-1}	-1.01×10^{0}	5.44×10^{-3}	3.50×10^{-2}

Table A.49. The list of the top 100 upregulated DEGs identified in the CS2 subtype using limma as a result of four clustering analyzes.

	fc	**log2fc**	**pvalue**	**padj**
RNU4.2	4.52×10^{1}	5.50×10^{0}	4.21×10^{-24}	5.73×10^{-23}
RNU4.1	3.33×10^{1}	5.06×10^{0}	2.79×10^{-26}	4.61×10^{-25}

Table A.49 (continued). The list of the top 100 upregulated DEGs identified in the CS2 subtype using limma as a result of four clustering analyzes.

RNY1	3.33×10^{1}	5.06×10^{0}	6.95×10^{-27}	1.22×10^{-25}
MIR3609	2.94×10^{1}	4.88×10^{0}	2.98×10^{-35}	1.67×10^{-33}
RNU5B.1	2.94×10^{1}	4.88×10^{0}	8.62×10^{-29}	1.84×10^{-27}
SNORA73B	2.87×10^{1}	4.85×10^{0}	2.70×10^{-32}	8.87×10^{-31}
SCARNA7	2.79×10^{1}	4.80×10^{0}	2.10×10^{-35}	1.22×10^{-33}
RNU5A.1	2.66×10^{1}	4.73×10^{0}	4.50×10^{-26}	7.31×10^{-25}
SCARNA5	2.55×10^{1}	4.67×10^{0}	3.36×10^{-31}	9.59×10^{-30}
RN7SL3	2.07×10^{1}	4.37×10^{0}	2.65×10^{-30}	6.73×10^{-29}
SNORA23	1.89×10^{1}	4.24×10^{0}	3.47×10^{-32}	1.13×10^{-30}
SNORA74A	1.83×10^{1}	4.19×10^{0}	3.81×10^{-34}	1.70×10^{-32}
SNORA12	1.68×10^{1}	4.07×10^{0}	4.19×10^{-32}	1.35×10^{-30}

H4C3	1.64×10^{1}	4.04×10^{0}	2.47×10^{-35}	1.41×10^{-33}
SNORD13	1.63×10^{1}	4.03×10^{0}	3.98×10^{-21}	4.29×10^{-20}
SNORA53	1.61×10^{1}	4.01×10^{0}	2.12×10^{-33}	8.27×10^{-32}
SNORA49	1.51×10^{1}	3.91×10^{0}	7.15×10^{-32}	2.23×10^{-30}
SCARNA21	1.50×10^{1}	3.91×10^{0}	8.37×10^{-33}	2.98×10^{-31}
RNU1.88P	1.49×10^{1}	3.90×10^{0}	1.80×10^{-36}	1.36×10^{-34}
SNORA79B	1.46×10^{1}	3.87×10^{0}	1.34×10^{-28}	2.79×10^{-27}
RNVU1.31	1.43×10^{1}	3.84×10^{0}	6.79×10^{-25}	9.90×10^{-24}
SNORA54	1.42×10^{1}	3.83×10^{0}	2.33×10^{-30}	5.95×10^{-29}
H4C4	1.38×10^{1}	3.79×10^{0}	2.30×10^{-34}	1.07×10^{-32}
H1.4	1.36×10^{1}	3.77×10^{0}	2.19×10^{-32}	7.29×10^{-31}
RNU1.11P	1.33×10^{1}	3.74×10^{0}	1.98×10^{-36}	1.47×10^{-34}
SNORA74D	1.33×10^{1}	3.73×10^{0}	3.80×10^{-36}	2.62×10^{-34}
RNU6ATAC	1.32×10^{1}	3.72×10^{0}	5.15×10^{-30}	1.25×10^{-28}
RN7SKP9	1.30×10^{1}	3.70×10^{0}	6.89×10^{-37}	5.77×10^{-35}
SNORD15B	1.28×10^{1}	3.68×10^{0}	4.68×10^{-28}	9.16×10^{-27}
H3C2	1.24×10^{1}	3.63×10^{0}	2.26×10^{-32}	7.51×10^{-31}
MALAT1	1.23×10^{1}	3.61×10^{0}	1.65×10^{-26}	2.78×10^{-25}
RNVU1.2	1.20×10^{1}	3.59×10^{0}	2.47×10^{-35}	1.41×10^{-33}
SNORD17	1.19×10^{1}	3.58×10^{0}	1.02×10^{-23}	1.35×10^{-22}
SNORA74B	1.18×10^{1}	3.56×10^{0}	5.34×10^{-32}	1.70×10^{-30}
H1.5	1.10×10^{1}	3.46×10^{0}	1.09×10^{-28}	2.29×10^{-27}
RN7SL4P	1.10×10^{1}	3.46×10^{0}	6.51×10^{-26}	1.04×10^{-24}
SCARNA6	1.10×10^{1}	3.45×10^{0}	7.89×10^{-25}	1.14×10^{-23}
RN7SL1	1.09×10^{1}	3.45×10^{0}	4.77×10^{-20}	4.72×10^{-19}
RNVU1.7	1.09×10^{1}	3.44×10^{0}	5.35×10^{-31}	1.49×10^{-29}
RN7SKP203	1.09×10^{1}	3.44×10^{0}	1.02×10^{-34}	5.09×10^{-33}
RN7SKP255	1.08×10^{1}	3.43×10^{0}	7.04×10^{-35}	3.61×10^{-33}
SCARNA1	1.06×10^{1}	3.41×10^{0}	5.41×10^{-38}	6.36×10^{-36}
Y_RNA.241	1.02×10^{1}	3.35×10^{0}	5.13×10^{-39}	9.11×10^{-37}

Table A.49 (continued). The list of the top 100 upregulated DEGs identified in the CS2 subtype using limma as a result of four clustering analyzes.

RNU5D.1	9.95×10^{0}	3.31×10^{0}	3.71×10^{-33}	1.39×10^{-31}
H1.3	9.91×10^{0}	3.31×10^{0}	1.72×10^{-31}	5.14×10^{-30}
SNORD3A	9.41×10^{0}	3.23×10^{0}	1.92×10^{-17}	1.54×10^{-16}
H4C2	9.40×10^{0}	3.23×10^{0}	2.77×10^{-31}	8.01×10^{-30}
H2BC17	9.26×10^{0}	3.21×10^{0}	6.00×10^{-32}	1.89×10^{-30}
H2AC12	9.13×10^{0}	3.19×10^{0}	2.76×10^{-31}	7.99×10^{-30}
RNY3	9.10×10^{0}	3.19×10^{0}	1.80×10^{-29}	4.11×10^{-28}
RN7SL674P	9.10×10^{0}	3.19×10^{0}	7.40×10^{-30}	1.77×10^{-28}
SNORA22	8.91×10^{0}	3.16×10^{0}	3.84×10^{-24}	5.24×10^{-23}
H2AC14	8.85×10^{0}	3.15×10^{0}	1.98×10^{-32}	6.63×10^{-31}
RN7SL648P	8.71×10^{0}	3.12×10^{0}	6.69×10^{-32}	2.09×10^{-30}
SNORA38	8.63×10^{0}	3.11×10^{0}	5.91×10^{-30}	1.43×10^{-28}

H2BC10	8.47×10^{0}	3.08×10^{0}	1.30×10^{-31}	3.93×10^{-30}
RNU5F.1	8.46×10^{0}	3.08×10^{0}	9.70×10^{-29}	2.06×10^{-27}
RNU2.59P	8.24×10^{0}	3.04×10^{0}	5.54×10^{-36}	3.69×10^{-34}
SNORA28	8.00×10^{0}	3.00×10^{0}	2.58×10^{-27}	4.69×10^{-26}
H2AC13	7.83×10^{0}	2.97×10^{0}	1.36×10^{-25}	2.10×10^{-24}
RN7SKP227	7.81×10^{0}	2.97×10^{0}	2.08×10^{-36}	1.54×10^{-34}
SCARNA3	7.81×10^{0}	2.96×10^{0}	2.71×10^{-35}	1.53×10^{-33}
SNORA37	7.72×10^{0}	2.95×10^{0}	1.41×10^{-30}	3.69×10^{-29}
RN7SL396P	7.72×10^{0}	2.95×10^{0}	5.16×10^{-31}	1.44×10^{-29}
RNU7.124P	7.60×10^{0}	2.93×10^{0}	7.96×10^{-39}	1.29×10^{-36}
SNORA22C	7.55×10^{0}	2.92×10^{0}	9.35×10^{-30}	2.20×10^{-28}
RNU6.681P	7.53×10^{0}	2.91×10^{0}	4.91×10^{-40}	1.50×10^{-37}
RNU6.942P	7.45×10^{0}	2.90×10^{0}	7.68×10^{-40}	2.07×10^{-37}
RNU6.82P	7.43×10^{0}	2.89×10^{0}	3.82×10^{-38}	4.82×10^{-36}
AL732366.1	7.40×10^{0}	2.89×10^{0}	5.55×10^{-25}	8.17×10^{-24}
SNRPGP18	7.39×10^{0}	2.89×10^{0}	2.43×10^{-42}	4.22×10^{-39}
AL035693.1	7.33×10^{0}	2.87×10^{0}	1.57×10^{-43}	1.05×10^{-39}
MIR3679	7.30×10^{0}	2.87×10^{0}	1.38×10^{-37}	1.42×10^{-35}
AL158801.1	7.25×10^{0}	2.86×10^{0}	1.96×10^{-41}	1.22×10^{-38}
VTRNA1.1	7.20×10^{0}	2.85×10^{0}	2.43×10^{-24}	3.37×10^{-23}
RNU7.80P	7.15×10^{0}	2.84×10^{0}	9.37×10^{-41}	4.08×10^{-38}
H2AC20	7.11×10^{0}	2.83×10^{0}	1.23×10^{-29}	2.84×10^{-28}
H4C5	7.10×10^{0}	2.83×10^{0}	1.37×10^{-25}	2.12×10^{-24}
H2BC13	7.07×10^{0}	2.82×10^{0}	3.80×10^{-30}	9.41×10^{-29}
Y_RNA.439	6.96×10^{0}	2.80×10^{0}	1.46×10^{-40}	5.91×10^{-38}
RNU6.107P	6.96×10^{0}	2.80×10^{0}	3.72×10^{-33}	1.40×10^{-31}
RNU6.638P	6.90×10^{0}	2.79×10^{0}	1.77×10^{-27}	3.26×10^{-26}
H2BC14	6.88×10^{0}	2.78×10^{0}	1.10×10^{-31}	3.35×10^{-30}
RNVU1.2A	6.82×10^{0}	2.77×10^{0}	1.65×10^{-34}	7.88×10^{-33}

Table A.49 (continued). The list of the top 100 upregulated DEGs identified in the CS2 subtype using limma as a result of four clustering analyzes.

H2AC21	6.82×10^{0}	2.77×10^{0}	1.23×10^{-33}	5.00×10^{-32}
SNORA7B	6.80×10^{0}	2.76×10^{0}	3.09×10^{-21}	3.36×10^{-20}
RN7SL752P	6.78×10^{0}	2.76×10^{0}	4.54×10^{-25}	6.72×10^{-24}
SNORD56B	6.76×10^{0}	2.76×10^{0}	2.01×10^{-39}	4.34×10^{-37}
Y_RNA.720	6.76×10^{0}	2.76×10^{0}	8.47×10^{-40}	2.24×10^{-37}
SNORA70G	6.75×10^{0}	2.76×10^{0}	3.04×10^{-37}	2.79×10^{-35}
SCARNA18	6.75×10^{0}	2.76×10^{0}	3.90×10^{-35}	2.12×10^{-33}
RN7SL5P	6.75×10^{0}	2.76×10^{0}	5.66×10^{-26}	9.12×10^{-25}
MIR3140	6.74×10^{0}	2.75×10^{0}	7.45×10^{-39}	1.23×10^{-36}
RNVU1.15	6.71×10^{0}	2.75×10^{0}	2.49×10^{-30}	6.34×10^{-29}
RNA5SP33	6.70×10^{0}	2.74×10^{0}	1.85×10^{-35}	1.09×10^{-33}
PRSS48	6.68×10^{0}	2.74×10^{0}	1.50×10^{-40}	6.06×10^{-38}
Y_RNA.341	6.68×10^{0}	2.74×10^{0}	6.51×10^{-40}	1.85×10^{-37}

RNU4ATAC	6.64×10^{0}	2.73×10^{0}	6.35×10^{-19}	5.75×10^{-18}
RNU1.67P	6.64×10^{0}	2.73×10^{0}	2.20×10^{-22}	2.61×10^{-21}
RNU6.998P	6.57×10^{0}	2.72×10^{0}	1.18×10^{-42}	2.60×10^{-39}

Table A.50. The list of the top 100 downregulated DEGs identified in the CS2 subtype using limma as a result of four clustering analyzes.

	fc	**log2fc**	**pvalue**	**padj**
FABP1	1.02×10^{-1}	-3.29×10^{0}	1.05×10^{-8}	3.95×10^{-8}
DEFA6	1.22×10^{-1}	-3.03×10^{0}	3.52×10^{-6}	9.90×10^{-6}
HMGCS2	1.33×10^{-1}	-2.91×10^{0}	3.42×10^{-8}	1.21×10^{-7}
CLCA1	1.41×10^{-1}	-2.83×10^{0}	9.37×10^{-5}	2.20×10^{-4}
CLDN3	1.43×10^{-1}	-2.81×10^{0}	1.19×10^{-27}	2.24×10^{-26}
AC090498.1	1.45×10^{-1}	-2.79×10^{0}	1.94×10^{-17}	1.55×10^{-16}
RPL41P1	1.45×10^{-1}	-2.79×10^{0}	1.77×10^{-5}	4.55×10^{-5}
IGHA2	1.49×10^{-1}	-2.75×10^{0}	2.38×10^{-5}	6.05×10^{-5}
OLFM4	1.58×10^{-1}	-2.66×10^{0}	4.82×10^{-4}	1.03×10^{-3}
GUCA2A	1.59×10^{-1}	-2.65×10^{0}	1.07×10^{-8}	4.01×10^{-8}
MEP1A	1.66×10^{-1}	-2.59×10^{0}	3.33×10^{-10}	1.45×10^{-9}
CKB	1.66×10^{-1}	-2.59×10^{0}	5.00×10^{-10}	2.14×10^{-9}
DEFA5	1.72×10^{-1}	-2.54×10^{0}	3.16×10^{-4}	6.91×10^{-4}
SCAND1	1.73×10^{-1}	-2.53×10^{0}	1.90×10^{-28}	3.88×10^{-27}
DEFB1	1.82×10^{-1}	-2.46×10^{0}	5.35×10^{-12}	2.74×10^{-11}
WFDC2	1.86×10^{-1}	-2.43×10^{0}	1.75×10^{-8}	6.40×10^{-8}
PPDPF	1.90×10^{-1}	-2.40×10^{0}	2.27×10^{-31}	6.66×10^{-30}
IGFBP2	1.92×10^{-1}	-2.38×10^{0}	2.54×10^{-9}	1.02×10^{-8}
C4orf48	1.94×10^{-1}	-2.37×10^{0}	2.08×10^{-20}	2.12×10^{-19}
TFF3	1.96×10^{-1}	-2.35×10^{0}	1.04×10^{-11}	5.20×10^{-11}
RETNLB	2.02×10^{-1}	-2.31×10^{0}	8.05×10^{-7}	2.45×10^{-6}

Table A.50 (continued). The list of the top 100 downregulated DEGs identified in the CS2 subtype using limma as a result of four clustering analyzes.

VSIG2	2.02×10^{-1}	-2.30×10^{0}	3.98×10^{-6}	1.11×10^{-5}
ITLN1	2.06×10^{-1}	-2.28×10^{0}	6.35×10^{-4}	1.34×10^{-3}
SMIM24	2.18×10^{-1}	-2.20×10^{0}	1.71×10^{-13}	9.97×10^{-13}
TRAPPC6A	2.18×10^{-1}	-2.19×10^{0}	7.68×10^{-30}	1.83×10^{-28}
ALKBH7	2.19×10^{-1}	-2.19×10^{0}	4.89×10^{-28}	9.51×10^{-27}
HSD11B2	2.25×10^{-1}	-2.15×10^{0}	4.38×10^{-20}	4.35×10^{-19}
AOC1	2.27×10^{-1}	-2.14×10^{0}	8.36×10^{-20}	8.12×10^{-19}
LYPD8	2.28×10^{-1}	-2.13×10^{0}	1.17×10^{-5}	3.09×10^{-5}
SLC52A2	2.30×10^{-1}	-2.12×10^{0}	1.92×10^{-26}	3.22×10^{-25}
CCDC85B	2.35×10^{-1}	-2.09×10^{0}	1.98×10^{-17}	1.58×10^{-16}
SLC39A4	2.39×10^{-1}	-2.06×10^{0}	1.96×10^{-18}	1.71×10^{-17}
ROMO1	2.39×10^{-1}	-2.06×10^{0}	2.25×10^{-20}	2.29×10^{-19}
AC097493.3	2.40×10^{-1}	-2.06×10^{0}	3.59×10^{-12}	1.87×10^{-11}
RPL41P5	2.41×10^{-1}	-2.05×10^{0}	1.25×10^{-13}	7.36×10^{-13}

REG3A	2.41×10^{-1}	-2.05×10^{0}	2.01×10^{-3}	3.88×10^{-3}
NOX1	2.41×10^{-1}	-2.05×10^{0}	9.35×10^{-9}	3.53×10^{-8}
GPAA1	2.47×10^{-1}	-2.02×10^{0}	1.97×10^{-25}	3.01×10^{-24}
NDUFB7	2.49×10^{-1}	-2.01×10^{0}	4.03×10^{-25}	5.99×10^{-24}
CHCHD2P9	2.49×10^{-1}	-2.00×10^{0}	1.76×10^{-12}	9.38×10^{-12}
ENTPD2	2.50×10^{-1}	-2.00×10^{0}	2.46×10^{-16}	1.80×10^{-15}
TM4SF5	2.52×10^{-1}	-1.99×10^{0}	8.76×10^{-12}	4.40×10^{-11}
NME3	2.58×10^{-1}	-1.95×10^{0}	1.30×10^{-20}	1.35×10^{-19}
ZNF358	2.58×10^{-1}	-1.95×10^{0}	2.51×10^{-28}	5.08×10^{-27}
RPL10P9	2.59×10^{-1}	-1.95×10^{0}	6.54×10^{-6}	1.78×10^{-5}
HES6	2.59×10^{-1}	-1.95×10^{0}	2.12×10^{-16}	1.56×10^{-15}
HSPB1	2.59×10^{-1}	-1.95×10^{0}	9.23×10^{-15}	5.97×10^{-14}
DUOXA2	2.60×10^{-1}	-1.94×10^{0}	4.83×10^{-5}	1.18×10^{-4}
LGALS4	2.60×10^{-1}	-1.94×10^{0}	1.53×10^{-20}	1.57×10^{-19}
RPS28P4	2.61×10^{-1}	-1.94×10^{0}	4.56×10^{-7}	1.43×10^{-6}
RPLP1	2.61×10^{-1}	-1.94×10^{0}	5.88×10^{-28}	1.13×10^{-26}
ZNF524	2.62×10^{-1}	-1.93×10^{0}	2.43×10^{-30}	6.20×10^{-29}
MICOS13	2.63×10^{-1}	-1.93×10^{0}	1.75×10^{-28}	3.60×10^{-27}
FAM83E	2.64×10^{-1}	-1.92×10^{0}	4.96×10^{-20}	4.90×10^{-19}
ZG16	2.65×10^{-1}	-1.91×10^{0}	2.53×10^{-4}	5.62×10^{-4}
RPL8	2.65×10^{-1}	-1.91×10^{0}	1.76×10^{-20}	1.80×10^{-19}
PRSS8	2.66×10^{-1}	-1.91×10^{0}	5.16×10^{-20}	5.10×10^{-19}
CCDC124	2.67×10^{-1}	-1.91×10^{0}	1.95×10^{-26}	3.28×10^{-25}
C9orf16	2.67×10^{-1}	-1.90×10^{0}	5.53×10^{-27}	9.78×10^{-26}
AGPAT2	2.72×10^{-1}	-1.88×10^{0}	4.49×10^{-20}	4.46×10^{-19}
DPM3	2.72×10^{-1}	-1.88×10^{0}	6.39×10^{-19}	5.78×10^{-18}
JOSD2	2.72×10^{-1}	-1.88×10^{0}	1.93×10^{-23}	2.50×10^{-22}

Table A.50 (continued). The list of the top 100 downregulated DEGs identified in the CS2 subtype using limma as a result of four clustering analyzes.

SERINC2	2.73×10^{-1}	-1.87×10^{0}	1.00×10^{-20}	1.05×10^{-19}
B3GNT8	2.74×10^{-1}	-1.87×10^{0}	7.33×10^{-20}	7.14×10^{-19}
WNK4	2.74×10^{-1}	-1.87×10^{0}	7.22×10^{-15}	4.71×10^{-14}
ZDHHC12	2.76×10^{-1}	-1.85×10^{0}	4.22×10^{-27}	7.56×10^{-26}
SCRIB	2.76×10^{-1}	-1.85×10^{0}	3.88×10^{-23}	4.89×10^{-22}
EXOSC5	2.78×10^{-1}	-1.85×10^{0}	4.31×10^{-24}	5.86×10^{-23}
MFSD3	2.78×10^{-1}	-1.85×10^{0}	4.29×10^{-19}	3.94×10^{-18}
FAM174C	2.78×10^{-1}	-1.85×10^{0}	4.54×10^{-24}	6.15×10^{-23}
ELOB	2.79×10^{-1}	-1.84×10^{0}	4.04×10^{-23}	5.10×10^{-22}
HSPBP1	2.79×10^{-1}	-1.84×10^{0}	2.38×10^{-24}	3.31×10^{-23}
KCNQ1	2.79×10^{-1}	-1.84×10^{0}	4.79×10^{-14}	2.91×10^{-13}
CDHR5	2.80×10^{-1}	-1.83×10^{0}	1.39×10^{-22}	1.68×10^{-21}
RPS16	2.80×10^{-1}	-1.84×10^{0}	1.39×10^{-22}	1.68×10^{-21}
TSPO	2.81×10^{-1}	-1.83×10^{0}	1.37×10^{-20}	1.41×10^{-19}
RPL18AP3	2.83×10^{-1}	-1.82×10^{0}	5.64×10^{-15}	3.71×10^{-14}

IGSF8	2.83×10^{-1}	-1.82×10^{0}	2.75×10^{-28}	5.52×10^{-27}
ADH1C	2.84×10^{-1}	-1.81×10^{0}	1.03×10^{-4}	2.41×10^{-4}
KRT20	2.84×10^{-1}	-1.81×10^{0}	4.29×10^{-5}	1.05×10^{-4}
RPL21P16	2.85×10^{-1}	-1.81×10^{0}	1.21×10^{-9}	5.03×10^{-9}
AURKAIP1	2.86×10^{-1}	-1.81×10^{0}	6.70×10^{-23}	8.30×10^{-22}
AZGP1	2.86×10^{-1}	-1.81×10^{0}	9.27×10^{-9}	3.50×10^{-8}
ATP5F1D	2.86×10^{-1}	-1.81×10^{0}	6.88×10^{-20}	6.71×10^{-19}
THEM6	2.88×10^{-1}	-1.80×10^{0}	1.62×10^{-19}	1.53×10^{-18}
SSNA1	2.88×10^{-1}	-1.80×10^{0}	4.31×10^{-26}	7.01×10^{-25}
CDC42EP5	2.89×10^{-1}	-1.79×10^{0}	3.13×10^{-12}	1.64×10^{-11}
FKBP8	2.90×10^{-1}	-1.78×10^{0}	3.38×10^{-25}	5.08×10^{-24}
SHARPIN	2.90×10^{-1}	-1.78×10^{0}	1.73×10^{-27}	3.20×10^{-26}
DUOX2	2.92×10^{-1}	-1.77×10^{0}	2.27×10^{-4}	5.06×10^{-4}
RASSF7	2.92×10^{-1}	-1.77×10^{0}	5.18×10^{-23}	6.48×10^{-22}
SP5	2.93×10^{-1}	-1.77×10^{0}	6.30×10^{-8}	2.17×10^{-7}
TMUB1	2.94×10^{-1}	-1.76×10^{0}	9.71×10^{-29}	2.06×10^{-27}
NOP53	2.95×10^{-1}	-1.76×10^{0}	4.34×10^{-26}	7.06×10^{-25}
RPL10P6	2.96×10^{-1}	-1.76×10^{0}	1.81×10^{-4}	4.08×10^{-4}
CCL24	2.97×10^{-1}	-1.75×10^{0}	8.66×10^{-7}	2.63×10^{-6}
MYBL2	2.98×10^{-1}	-1.74×10^{0}	8.97×10^{-16}	6.29×10^{-15}
MRPL41	2.98×10^{-1}	-1.74×10^{0}	3.70×10^{-18}	3.14×10^{-17}
TMC4	3.00×10^{-1}	-1.74×10^{0}	1.42×10^{-25}	2.20×10^{-24}
PKP3	3.00×10^{-1}	-1.74×10^{0}	1.97×10^{-21}	2.17×10^{-20}

Table A.51. The list of the top 100 upregulated DEGs identified in the CS3 subtype using limma as a result of four clustering analyzes.

	fc	**log2fc**	**pvalue**	**padj**
TNNC2	6.22×10^{0}	2.64×10^{0}	1.07×10^{-29}	1.23×10^{-25}
AP003774.2	6.20×10^{0}	2.63×10^{0}	5.27×10^{-33}	1.51×10^{-28}
CEL	5.84×10^{0}	2.55×10^{0}	7.04×10^{-19}	1.93×10^{-16}
C10orf99	5.83×10^{0}	2.54×10^{0}	5.32×10^{-19}	1.51×10^{-16}
NOTUM	5.10×10^{0}	2.35×10^{0}	1.18×10^{-15}	1.26×10^{-13}
QPRT	4.80×10^{0}	2.26×10^{0}	9.49×10^{-29}	7.76×10^{-25}
ASCL2	4.54×10^{0}	2.18×10^{0}	2.02×10^{-28}	1.28×10^{-24}
GNG4	4.44×10^{0}	2.15×10^{0}	1.45×10^{-18}	3.51×10^{-16}
KRT23	4.32×10^{0}	2.11×10^{0}	3.67×10^{-14}	2.70×10^{-12}
CDHR1	4.11×10^{0}	2.04×10^{0}	5.32×10^{-19}	1.51×10^{-16}
DPEP1	3.99×10^{0}	2.00×10^{0}	1.17×10^{-13}	7.66×10^{-12}
TDGF1	3.64×10^{0}	1.86×10^{0}	3.99×10^{-24}	5.44×10^{-21}
CYP2B6	3.61×10^{0}	1.85×10^{0}	3.78×10^{-21}	2.10×10^{-18}
SLC39A5	3.59×10^{0}	1.84×10^{0}	6.10×10^{-21}	3.23×10^{-18}
CYP2W1	3.54×10^{0}	1.83×10^{0}	3.61×10^{-11}	1.33×10^{-9}
SLC26A3	3.45×10^{0}	1.79×10^{0}	1.26×10^{-7}	1.97×10^{-6}

ENPP3	3.44×10^{0}	1.78×10^{0}	1.42×10^{-16}	2.02×10^{-14}
RUBCNL	3.40×10^{0}	1.77×10^{0}	1.55×10^{-25}	3.45×10^{-22}
CELP	3.40×10^{0}	1.76×10^{0}	3.37×10^{-27}	1.55×10^{-23}
FABP1	3.24×10^{0}	1.70×10^{0}	1.32×10^{-7}	2.06×10^{-6}
Y_RNA.244	3.19×10^{0}	1.67×10^{0}	1.18×10^{-15}	1.26×10^{-13}
CXCL14	3.17×10^{0}	1.67×10^{0}	1.26×10^{-11}	5.18×10^{-10}
AL117382.1	3.17×10^{0}	1.66×10^{0}	4.99×10^{-26}	1.43×10^{-22}
LY6G6D	3.14×10^{0}	1.65×10^{0}	1.40×10^{-20}	6.69×10^{-18}
PLA2G12B	3.08×10^{0}	1.63×10^{0}	5.81×10^{-13}	3.20×10^{-11}
AXIN2	3.08×10^{0}	1.62×10^{0}	7.38×10^{-24}	8.62×10^{-21}
VAV3	3.08×10^{0}	1.62×10^{0}	2.45×10^{-19}	7.93×10^{-17}
EREG	3.03×10^{0}	1.60×10^{0}	1.50×10^{-10}	4.78×10^{-9}
APCDD1	3.02×10^{0}	1.59×10^{0}	2.61×10^{-15}	2.57×10^{-13}
FABP6	3.00×10^{0}	1.58×10^{0}	4.27×10^{-16}	5.19×10^{-14}
NKD1	2.97×10^{0}	1.57×10^{0}	2.03×10^{-15}	2.03×10^{-13}
LINC02418	2.96×10^{0}	1.57×10^{0}	1.12×10^{-13}	7.33×10^{-12}
GRM8	2.95×10^{0}	1.56×10^{0}	1.91×10^{-19}	6.47×10^{-17}
IHH	2.93×10^{0}	1.55×10^{0}	1.08×10^{-20}	5.23×10^{-18}
GPR143	2.90×10^{0}	1.54×10^{0}	7.08×10^{-19}	1.93×10^{-16}
SLC39A2	2.89×10^{0}	1.53×10^{0}	1.30×10^{-12}	6.67×10^{-11}
LINC02441	2.87×10^{0}	1.52×10^{0}	5.57×10^{-20}	2.20×10^{-17}
RBP2	2.84×10^{0}	1.51×10^{0}	1.03×10^{-10}	3.43×10^{-9}
SELENBP1	2.82×10^{0}	1.49×10^{0}	9.14×10^{-19}	2.37×10^{-16}
AIFM3	2.81×10^{0}	1.49×10^{0}	2.72×10^{-22}	1.95×10^{-19}

Table A.51 (continued). The list of the top 100 upregulated DEGs identified in the CS3 subtype using limma as a result of four clustering analyzes.

RPL39P40	2.77×10^{0}	1.47×10^{0}	3.71×10^{-16}	4.67×10^{-14}
RNF43	2.73×10^{0}	1.45×10^{0}	3.34×10^{-32}	6.37×10^{-28}
URAD	2.72×10^{0}	1.44×10^{0}	1.63×10^{-8}	3.16×10^{-7}
SATB2.AS1	2.70×10^{0}	1.43×10^{0}	2.41×10^{-22}	1.74×10^{-19}
HUNK	2.66×10^{0}	1.41×10^{0}	3.25×10^{-18}	7.15×10^{-16}
MEP1A	2.66×10^{0}	1.41×10^{0}	8.91×10^{-10}	2.35×10^{-8}
AC114291.1	2.64×10^{0}	1.40×10^{0}	1.45×10^{-16}	2.05×10^{-14}
CDX2	2.61×10^{0}	1.38×10^{0}	3.43×10^{-21}	1.97×10^{-18}
MAP7D2	2.60×10^{0}	1.38×10^{0}	7.47×10^{-11}	2.56×10^{-9}
ID1	2.59×10^{0}	1.37×10^{0}	2.61×10^{-14}	1.99×10^{-12}
BEX2	2.56×10^{0}	1.36×10^{0}	3.76×10^{-10}	1.08×10^{-8}
NOX1	2.56×10^{0}	1.36×10^{0}	5.73×10^{-12}	2.54×10^{-10}
ISX	2.55×10^{0}	1.35×10^{0}	1.10×10^{-12}	5.78×10^{-11}
HMGCS2	2.55×10^{0}	1.35×10^{0}	5.20×10^{-6}	5.37×10^{-5}
DDC	2.55×10^{0}	1.35×10^{0}	6.40×10^{-15}	5.58×10^{-13}
PPP1R14D	2.53×10^{0}	1.34×10^{0}	8.29×10^{-16}	9.21×10^{-14}
DIO3OS	2.52×10^{0}	1.33×10^{0}	1.72×10^{-17}	3.11×10^{-15}
SLC13A2	2.51×10^{0}	1.33×10^{0}	1.28×10^{-11}	5.24×10^{-10}

ANO9	2.51×10^{0}	1.33×10^{0}	1.50×10^{-25}	3.45×10^{-22}
AL354743.2	2.50×10^{0}	1.32×10^{0}	8.12×10^{-17}	1.21×10^{-14}
TINAG	2.50×10^{0}	1.32×10^{0}	2.81×10^{-17}	4.76×10^{-15}
R3HDML	2.49×10^{0}	1.32×10^{0}	7.67×10^{-22}	5.16×10^{-19}
MOGAT3	2.49×10^{0}	1.31×10^{0}	4.93×10^{-17}	7.77×10^{-15}
AL589669.1	2.48×10^{0}	1.31×10^{0}	2.63×10^{-16}	3.49×10^{-14}
CFTR	2.47×10^{0}	1.30×10^{0}	2.61×10^{-13}	1.57×10^{-11}
AL162413.1	2.45×10^{0}	1.29×10^{0}	4.09×10^{-7}	5.63×10^{-6}
LEFTY1	2.45×10^{0}	1.29×10^{0}	8.27×10^{-6}	8.04×10^{-5}
AC124067.4	2.43×10^{0}	1.28×10^{0}	5.91×10^{-18}	1.22×10^{-15}
GGT7	2.43×10^{0}	1.28×10^{0}	4.38×10^{-18}	9.28×10^{-16}
ENGASE	2.42×10^{0}	1.27×10^{0}	3.57×10^{-27}	1.55×10^{-23}
STYXL2	2.40×10^{0}	1.26×10^{0}	1.60×10^{-4}	1.04×10^{-3}
OXGR1	2.40×10^{0}	1.26×10^{0}	3.37×10^{-15}	3.21×10^{-13}
MAB21L4	2.40×10^{0}	1.26×10^{0}	1.32×10^{-14}	1.07×10^{-12}
MIR3131	2.37×10^{0}	1.24×10^{0}	2.53×10^{-11}	9.59×10^{-10}
AC108865.1	2.37×10^{0}	1.24×10^{0}	2.21×10^{-6}	2.51×10^{-5}
TUSC8	2.36×10^{0}	1.24×10^{0}	5.10×10^{-14}	3.66×10^{-12}
MUC12	2.35×10^{0}	1.23×10^{0}	2.55×10^{-8}	4.72×10^{-7}
PRDX5	2.34×10^{0}	1.23×10^{0}	1.26×10^{-22}	1.04×10^{-19}
PRAC1	2.34×10^{0}	1.23×10^{0}	2.48×10^{-3}	9.37×10^{-3}
SYT7	2.34×10^{0}	1.23×10^{0}	3.08×10^{-18}	6.84×10^{-16}
PLCB4	2.33×10^{0}	1.22×10^{0}	6.82×10^{-11}	2.35×10^{-9}

Table A.51 (continued). The list of the top 100 upregulated DEGs identified in the CS3 subtype using limma as a result of four clustering analyzes.

PRR15	2.33×10^{0}	1.22×10^{0}	1.01×10^{-25}	2.63×10^{-22}
HOXB9	2.33×10^{0}	1.22×10^{0}	2.68×10^{-9}	6.30×10^{-8}
CAB39L	2.32×10^{0}	1.22×10^{0}	6.97×10^{-17}	1.06×10^{-14}
SPINK1	2.32×10^{0}	1.21×10^{0}	7.63×10^{-8}	1.26×10^{-6}
AC005050.2	2.31×10^{0}	1.21×10^{0}	1.28×10^{-20}	6.16×10^{-18}
PTPRO	2.31×10^{0}	1.21×10^{0}	2.50×10^{-10}	7.52×10^{-9}
TMEM252	2.31×10^{0}	1.21×10^{0}	1.18×10^{-10}	3.86×10^{-9}
AC078993.1	2.30×10^{0}	1.20×10^{0}	2.88×10^{-11}	1.08×10^{-9}
PPP1R14C	2.30×10^{0}	1.20×10^{0}	5.40×10^{-12}	2.40×10^{-10}
NKD2	2.29×10^{0}	1.20×10^{0}	1.50×10^{-12}	7.60×10^{-11}
CKB	2.25×10^{0}	1.17×10^{0}	5.71×10^{-7}	7.55×10^{-6}
FAM3B	2.25×10^{0}	1.17×10^{0}	3.16×10^{-6}	3.46×10^{-5}
GSPT2	2.25×10^{0}	1.17×10^{0}	1.92×10^{-13}	1.19×10^{-11}
COL9A3	2.25×10^{0}	1.17×10^{0}	6.46×10^{-9}	1.38×10^{-7}
FGFR4	2.24×10^{0}	1.16×10^{0}	4.63×10^{-17}	7.33×10^{-15}
CKMT2	2.23×10^{0}	1.16×10^{0}	2.07×10^{-6}	2.36×10^{-5}
AC055717.2	2.23×10^{0}	1.16×10^{0}	2.74×10^{-13}	1.64×10^{-11}
AREG	2.23×10^{0}	1.15×10^{0}	3.12×10^{-10}	9.14×10^{-9}
NR1I2	2.22×10^{0}	1.15×10^{0}	2.04×10^{-16}	2.81×10^{-14}

Table A.52. The list of the top 100 downregulated DEGs identified in the CS3 subtype using limma as a result of four clustering analyzes.

	fc	log2fc	pvalue	padj
REG4	1.42×10^{-1}	-2.82×10^{0}	4.59×10^{-12}	2.07×10^{-10}
CTSE	1.71×10^{-1}	-2.55×10^{0}	3.82×10^{-17}	6.26×10^{-15}
PLA2G2A	2.03×10^{-1}	-2.30×10^{0}	8.31×10^{-13}	4.44×10^{-11}
CCL18	2.31×10^{-1}	-2.11×10^{0}	1.29×10^{-17}	2.44×10^{-15}
DUSP4	2.51×10^{-1}	-1.99×10^{0}	3.79×10^{-27}	1.55×10^{-23}
RAMP1	2.61×10^{-1}	-1.94×10^{0}	4.48×10^{-17}	7.18×10^{-15}
LYZ	2.63×10^{-1}	-1.93×10^{0}	3.23×10^{-15}	3.10×10^{-13}
CLDN18	2.64×10^{-1}	-1.92×10^{0}	6.62×10^{-14}	4.57×10^{-12}
CXCL13	2.69×10^{-1}	-1.89×10^{0}	1.02×10^{-21}	6.74×10^{-19}
SPP1	2.70×10^{-1}	-1.89×10^{0}	5.30×10^{-12}	2.37×10^{-10}
TCN1	2.86×10^{-1}	-1.81×10^{0}	3.69×10^{-10}	1.06×10^{-8}
REG1A	2.88×10^{-1}	-1.80×10^{0}	5.74×10^{-5}	4.41×10^{-4}
CXCL9	2.97×10^{-1}	-1.75×10^{0}	6.30×10^{-16}	7.32×10^{-14}
TFF2	3.02×10^{-1}	-1.73×10^{0}	2.80×10^{-10}	8.29×10^{-9}
VNN1	3.17×10^{-1}	-1.66×10^{0}	5.14×10^{-19}	1.47×10^{-16}
GJB5	3.21×10^{-1}	-1.64×10^{0}	1.53×10^{-13}	9.72×10^{-12}
SPON1	3.21×10^{-1}	-1.64×10^{0}	5.02×10^{-20}	1.99×10^{-17}
MUC5AC	3.21×10^{-1}	-1.64×10^{0}	4.28×10^{-13}	2.43×10^{-11}

Table A.52 (continued). The list of the top 100 downregulated DEGs identified in the CS3 subtype using limma as a result of four clustering analyzes.

CXCL10	3.21×10^{-1}	-1.64×10^{0}	3.08×10^{-15}	2.98×10^{-13}
FCGR3A	3.25×10^{-1}	-1.62×10^{0}	3.03×10^{-18}	6.78×10^{-16}
TRNP1	3.26×10^{-1}	-1.62×10^{0}	8.71×10^{-22}	5.80×10^{-19}
RARRES1	3.34×10^{-1}	-1.58×10^{0}	7.39×10^{-21}	3.81×10^{-18}
MUC2	3.37×10^{-1}	-1.57×10^{0}	7.69×10^{-6}	7.54×10^{-5}
GBP4	3.37×10^{-1}	-1.57×10^{0}	1.48×10^{-22}	1.18×10^{-19}
IL1RN	3.40×10^{-1}	-1.55×10^{0}	3.19×10^{-20}	1.37×10^{-17}
IGLV3.1	3.45×10^{-1}	-1.54×10^{0}	1.45×10^{-6}	1.73×10^{-5}
RAB27B	3.47×10^{-1}	-1.53×10^{0}	7.96×10^{-30}	1.14×10^{-25}
CD109	3.47×10^{-1}	-1.53×10^{0}	6.66×10^{-24}	8.01×10^{-21}
IGHG1	3.48×10^{-1}	-1.52×10^{0}	9.50×10^{-7}	1.19×10^{-5}
SERPINB5	3.51×10^{-1}	-1.51×10^{0}	3.18×10^{-11}	1.19×10^{-9}
IGLV3.25	3.59×10^{-1}	-1.48×10^{0}	2.36×10^{-6}	2.66×10^{-5}
TNNT1	3.60×10^{-1}	-1.48×10^{0}	3.72×10^{-14}	2.74×10^{-12}
CXCR4	3.62×10^{-1}	-1.47×10^{0}	4.85×10^{-26}	1.43×10^{-22}
IGLV3.21	3.64×10^{-1}	-1.46×10^{0}	3.28×10^{-6}	3.57×10^{-5}
MMP12	3.65×10^{-1}	-1.45×10^{0}	4.04×10^{-12}	1.84×10^{-10}
IGHV1.24	3.66×10^{-1}	-1.45×10^{0}	1.13×10^{-6}	1.38×10^{-5}
CCL5	3.67×10^{-1}	-1.45×10^{0}	2.00×10^{-19}	6.66×10^{-17}
IGHG4	3.68×10^{-1}	-1.44×10^{0}	2.73×10^{-6}	3.02×10^{-5}
HLA.DQA1	3.70×10^{-1}	-1.43×10^{0}	1.92×10^{-17}	3.42×10^{-15}

CD163	3.73×10^{-1}	-1.42×10^{0}	1.85×10^{-15}	1.88×10^{-13}
IGHV4.39	3.74×10^{-1}	-1.42×10^{0}	9.36×10^{-6}	8.96×10^{-5}
SDR16C5	3.75×10^{-1}	-1.41×10^{0}	9.61×10^{-12}	4.08×10^{-10}
HLA.DRA	3.78×10^{-1}	-1.40×10^{0}	5.27×10^{-16}	6.28×10^{-14}
MMP1	3.78×10^{-1}	-1.40×10^{0}	2.32×10^{-8}	4.34×10^{-7}
IGHV3.21	3.78×10^{-1}	-1.40×10^{0}	6.89×10^{-6}	6.84×10^{-5}
TRIB2	3.79×10^{-1}	-1.40×10^{0}	3.11×10^{-33}	1.51×10^{-28}
MARCO	3.79×10^{-1}	-1.40×10^{0}	3.65×10^{-11}	1.34×10^{-9}
IGLV3.19	3.81×10^{-1}	-1.39×10^{0}	4.75×10^{-6}	4.95×10^{-5}
DAPK1	3.82×10^{-1}	-1.39×10^{0}	4.11×10^{-24}	5.47×10^{-21}
OAS2	3.84×10^{-1}	-1.38×10^{0}	2.47×10^{-18}	5.65×10^{-16}
SRGN	3.86×10^{-1}	-1.38×10^{0}	1.44×10^{-19}	5.23×10^{-17}
IGHV4.34	3.86×10^{-1}	-1.37×10^{0}	1.35×10^{-6}	1.62×10^{-5}
IGLV2.14	3.86×10^{-1}	-1.37×10^{0}	1.33×10^{-5}	1.22×10^{-4}
HLA.DPA1	3.86×10^{-1}	-1.37×10^{0}	4.51×10^{-15}	4.12×10^{-13}
PLA2G4A	3.87×10^{-1}	-1.37×10^{0}	1.01×10^{-14}	8.38×10^{-13}
IGHV2.70	3.88×10^{-1}	-1.37×10^{0}	2.37×10^{-7}	3.47×10^{-6}
KCTD12	3.88×10^{-1}	-1.37×10^{0}	7.26×10^{-19}	1.96×10^{-16}
PTAFR	3.89×10^{-1}	-1.36×10^{0}	4.70×10^{-25}	8.67×10^{-22}
ANXA10	3.90×10^{-1}	-1.36×10^{0}	7.12×10^{-16}	8.04×10^{-14}

Table A.52 (continued). The list of the top 100 downregulated DEGs identified in the CS3 subtype using limma as a result of four clustering analyzes.

PTGS2	3.90×10^{-1}	-1.36×10^{0}	6.81×10^{-15}	5.89×10^{-13}
GZMA	3.93×10^{-1}	-1.35×10^{0}	5.37×10^{-18}	1.12×10^{-15}
EVI2B	3.94×10^{-1}	-1.34×10^{0}	1.38×10^{-23}	1.46×10^{-20}
ANO1	3.95×10^{-1}	-1.34×10^{0}	1.17×10^{-18}	2.91×10^{-16}
CCL13	3.95×10^{-1}	-1.34×10^{0}	1.42×10^{-13}	9.08×10^{-12}
IGHV1.69	3.96×10^{-1}	-1.34×10^{0}	1.19×10^{-6}	1.45×10^{-5}
PLEK	3.96×10^{-1}	-1.34×10^{0}	1.14×10^{-16}	1.65×10^{-14}
MT1E	3.97×10^{-1}	-1.33×10^{0}	2.17×10^{-10}	6.61×10^{-9}
SECTM1	3.97×10^{-1}	-1.33×10^{0}	1.31×10^{-17}	2.47×10^{-15}
TM4SF4	3.98×10^{-1}	-1.33×10^{0}	2.82×10^{-9}	6.60×10^{-8}
PLAAT4	3.98×10^{-1}	-1.33×10^{0}	7.89×10^{-15}	6.73×10^{-13}
IGHV5.51	3.98×10^{-1}	-1.33×10^{0}	3.76×10^{-5}	3.05×10^{-4}
IGHV1.69D	3.98×10^{-1}	-1.33×10^{0}	7.16×10^{-6}	7.08×10^{-5}
PTPRC	4.01×10^{-1}	-1.32×10^{0}	3.08×10^{-18}	6.84×10^{-16}
RGS2	4.01×10^{-1}	-1.32×10^{0}	2.04×10^{-22}	1.60×10^{-19}
GBP5	4.02×10^{-1}	-1.32×10^{0}	8.41×10^{-19}	2.22×10^{-16}
CD53	4.04×10^{-1}	-1.31×10^{0}	3.71×10^{-18}	7.94×10^{-16}
CXCL8	4.04×10^{-1}	-1.31×10^{0}	2.91×10^{-9}	6.81×10^{-8}
FPR3	4.04×10^{-1}	-1.31×10^{0}	5.09×10^{-16}	6.08×10^{-14}
IGHG3	4.05×10^{-1}	-1.30×10^{0}	6.37×10^{-6}	6.39×10^{-5}
IGLV6.57	4.06×10^{-1}	-1.30×10^{0}	2.16×10^{-5}	1.89×10^{-4}
SAMD9L	4.06×10^{-1}	-1.30×10^{0}	5.32×10^{-25}	9.22×10^{-22}

DPYD	4.06×10^{-1}	-1.30×10^{0}	5.04×10^{-28}	2.88×10^{-24}
IGHV3.30	4.07×10^{-1}	-1.30×10^{0}	1.17×10^{-5}	1.09×10^{-4}
MUC17	4.07×10^{-1}	-1.30×10^{0}	2.75×10^{-7}	3.96×10^{-6}
CXCL11	4.08×10^{-1}	-1.29×10^{0}	8.67×10^{-10}	2.29×10^{-8}
IDO1	4.08×10^{-1}	-1.29×10^{0}	9.61×10^{-12}	4.08×10^{-10}
HLA.DRB5	4.09×10^{-1}	-1.29×10^{0}	1.07×10^{-10}	3.54×10^{-9}
BCL2A1	4.09×10^{-1}	-1.29×10^{0}	2.41×10^{-17}	4.15×10^{-15}
IGHV1.18	4.09×10^{-1}	-1.29×10^{0}	4.07×10^{-5}	3.27×10^{-4}
TRIM7	4.10×10^{-1}	-1.29×10^{0}	5.26×10^{-24}	6.84×10^{-21}
CREB3L1	4.11×10^{-1}	-1.28×10^{0}	4.35×10^{-12}	1.97×10^{-10}
IGHV2.26	4.11×10^{-1}	-1.28×10^{0}	1.12×10^{-6}	1.37×10^{-5}
FDCSP	4.13×10^{-1}	-1.28×10^{0}	1.63×10^{-8}	3.15×10^{-7}
IGHGP	4.13×10^{-1}	-1.28×10^{0}	2.51×10^{-5}	2.15×10^{-4}
NKG7	4.14×10^{-1}	-1.27×10^{0}	6.45×10^{-16}	7.42×10^{-14}
MSR1	4.14×10^{-1}	-1.27×10^{0}	5.08×10^{-17}	7.96×10^{-15}
PRRX1	4.15×10^{-1}	-1.27×10^{0}	9.78×10^{-18}	1.92×10^{-15}
GNLY	4.15×10^{-1}	-1.27×10^{0}	1.74×10^{-17}	3.13×10^{-15}
AQP3	4.17×10^{-1}	-1.26×10^{0}	6.03×10^{-11}	2.11×10^{-9}
FSCN1	4.18×10^{-1}	-1.26×10^{0}	5.07×10^{-15}	4.58×10^{-13}

Table A.53. The list of the top 100 upregulated DEGs identified in the CS4 subtype using limma as a result of four clustering analyzes.

	fc	**log2fc**	**pvalue**	**padj**
REG4	3.33×10^{1}	5.06×10^{0}	1.14×10^{-23}	1.31×10^{-19}
CTSE	1.86×10^{1}	4.22×10^{0}	1.52×10^{-29}	8.70×10^{-25}
SPINK4	9.99×10^{0}	3.32×10^{0}	1.29×10^{-11}	1.93×10^{-9}
REG1A	8.86×10^{0}	3.15×10^{0}	3.48×10^{-8}	1.56×10^{-6}
TFF1	7.73×10^{0}	2.95×10^{0}	8.67×10^{-17}	6.88×10^{-14}
MUC2	7.56×10^{0}	2.92×10^{0}	5.23×10^{-11}	6.38×10^{-9}
TFF2	7.11×10^{0}	2.83×10^{0}	2.84×10^{-16}	1.91×10^{-13}
TCN1	6.69×10^{0}	2.74×10^{0}	9.17×10^{-14}	2.78×10^{-11}
SPDEF	6.01×10^{0}	2.59×10^{0}	1.79×10^{-18}	2.85×10^{-15}
MUC5AC	5.87×10^{0}	2.55×10^{0}	3.78×10^{-19}	7.47×10^{-16}
FCGBP	5.74×10^{0}	2.52×10^{0}	3.04×10^{-10}	2.87×10^{-8}
REG3A	5.11×10^{0}	2.35×10^{0}	6.43×10^{-7}	1.78×10^{-5}
AGR3	4.81×10^{0}	2.27×10^{0}	1.33×10^{-14}	5.28×10^{-12}
GJB5	4.54×10^{0}	2.18×10^{0}	2.42×10^{-14}	8.86×10^{-12}
AGR2	4.41×10^{0}	2.14×10^{0}	2.47×10^{-27}	7.06×10^{-23}
CREB3L1	4.34×10^{0}	2.12×10^{0}	9.67×10^{-20}	2.64×10^{-16}
REG1B	4.23×10^{0}	2.08×10^{0}	1.56×10^{-6}	3.71×10^{-5}
CA9	4.22×10^{0}	2.08×10^{0}	4.54×10^{-9}	2.80×10^{-7}
MUC5B	4.16×10^{0}	2.06×10^{0}	1.65×10^{-8}	8.29×10^{-7}
SDR16C5	4.16×10^{0}	2.06×10^{0}	9.52×10^{-15}	3.95×10^{-12}
CLCA1	4.04×10^{0}	2.02×10^{0}	1.11×10^{-4}	1.31×10^{-3}
TM4SF4	4.00×10^{0}	2.00×10^{0}	2.72×10^{-12}	5.13×10^{-10}

FFAR4	3.98×10^{0}	1.99×10^{0}	2.63×10^{-16}	1.79×10^{-13}
MLPH	3.85×10^{0}	1.94×10^{0}	1.94×10^{-18}	3.00×10^{-15}
KLK11	3.69×10^{0}	1.88×10^{0}	5.15×10^{-13}	1.26×10^{-10}
PIGR	3.67×10^{0}	1.87×10^{0}	6.75×10^{-5}	8.77×10^{-4}
GCNT3	3.56×10^{0}	1.83×10^{0}	1.05×10^{-11}	1.62×10^{-9}
GP2	3.55×10^{0}	1.83×10^{0}	3.34×10^{-17}	3.03×10^{-14}
DMBT1	3.52×10^{0}	1.81×10^{0}	9.19×10^{-6}	1.65×10^{-4}
LINC00261	3.49×10^{0}	1.80×10^{0}	9.62×10^{-12}	1.51×10^{-9}
ATOH1	3.40×10^{0}	1.77×10^{0}	6.88×10^{-9}	3.95×10^{-7}
HEPACAM2	3.33×10^{0}	1.73×10^{0}	1.41×10^{-8}	7.27×10^{-7}
PRSS2	3.31×10^{0}	1.73×10^{0}	5.71×10^{-5}	7.64×10^{-4}
BARX2	3.30×10^{0}	1.72×10^{0}	1.77×10^{-17}	1.81×10^{-14}
ZBTB7C	3.30×10^{0}	1.72×10^{0}	4.20×10^{-18}	5.46×10^{-15}
IL1R2	3.25×10^{0}	1.70×10^{0}	2.14×10^{-18}	3.15×10^{-15}
PLAC8	3.22×10^{0}	1.69×10^{0}	2.14×10^{-11}	3.01×10^{-9}
AQP3	3.18×10^{0}	1.67×10^{0}	2.03×10^{-11}	2.87×10^{-9}
AL121761.1	3.14×10^{0}	1.65×10^{0}	6.24×10^{-16}	3.84×10^{-13}
B3GNT6	3.14×10^{0}	1.65×10^{0}	5.47×10^{-7}	1.57×10^{-5}

Table A.53 (continued). The list of the top 100 upregulated DEGs identified in the CS4 subtype using limma as a result of four clustering analyzes.

SERPINA1	3.14×10^{0}	1.65×10^{0}	9.48×10^{-10}	7.35×10^{-8}
ITLN1	3.13×10^{0}	1.65×10^{0}	6.06×10^{-4}	5.33×10^{-3}
HYAL1	3.12×10^{0}	1.64×10^{0}	8.63×10^{-13}	1.96×10^{-10}
LCN2	3.12×10^{0}	1.64×10^{0}	3.19×10^{-7}	1.00×10^{-5}
RAB26	3.08×10^{0}	1.62×10^{0}	3.34×10^{-19}	6.83×10^{-16}
KLK12	3.05×10^{0}	1.61×10^{0}	3.73×10^{-11}	4.79×10^{-9}
AP002498.1	3.04×10^{0}	1.61×10^{0}	3.69×10^{-13}	9.27×10^{-11}
SPRR1A	2.93×10^{0}	1.55×10^{0}	6.08×10^{-7}	1.71×10^{-5}
VSIG2	2.93×10^{0}	1.55×10^{0}	1.72×10^{-5}	2.79×10^{-4}
MYRF	2.93×10^{0}	1.55×10^{0}	1.96×10^{-14}	7.42×10^{-12}
SERPINB5	2.90×10^{0}	1.54×10^{0}	2.61×10^{-7}	8.45×10^{-6}
LRRC26	2.89×10^{0}	1.53×10^{0}	1.16×10^{-10}	1.27×10^{-8}
MT1E	2.88×10^{0}	1.53×10^{0}	2.27×10^{-8}	1.09×10^{-6}
MUC1	2.87×10^{0}	1.52×10^{0}	9.58×10^{-10}	7.41×10^{-8}
RAP1GAP	2.86×10^{0}	1.51×10^{0}	2.88×10^{-14}	1.04×10^{-11}
LINC02489	2.86×10^{0}	1.51×10^{0}	2.54×10^{-20}	8.55×10^{-17}
CA8	2.83×10^{0}	1.50×10^{0}	6.39×10^{-13}	1.51×10^{-10}
ST6GALNAC1	2.80×10^{0}	1.49×10^{0}	2.14×10^{-9}	1.46×10^{-7}
CAPN9	2.78×10^{0}	1.47×10^{0}	1.15×10^{-9}	8.66×10^{-8}
ALDH1L1	2.74×10^{0}	1.45×10^{0}	2.11×10^{-11}	2.97×10^{-9}
TFF3	2.73×10^{0}	1.45×10^{0}	7.88×10^{-9}	4.42×10^{-7}
RHOV	2.71×10^{0}	1.44×10^{0}	8.76×10^{-14}	2.68×10^{-11}
B3GALT5	2.70×10^{0}	1.43×10^{0}	1.94×10^{-11}	2.77×10^{-9}

GABRP	2.68×10^{0}	1.42×10^{0}	1.31×10^{-8}	6.80×10^{-7}
L1TD1	2.66×10^{0}	1.41×10^{0}	8.66×10^{-5}	1.07×10^{-3}
NEURL1	2.65×10^{0}	1.41×10^{0}	8.48×10^{-11}	9.68×10^{-9}
KLK1	2.64×10^{0}	1.40×10^{0}	6.68×10^{-10}	5.48×10^{-8}
SLITRK6	2.62×10^{0}	1.39×10^{0}	6.43×10^{-7}	1.78×10^{-5}
C2CD4A	2.61×10^{0}	1.38×10^{0}	1.13×10^{-10}	1.24×10^{-8}
TSPAN1	2.58×10^{0}	1.37×10^{0}	1.19×10^{-12}	2.56×10^{-10}
NOS2	2.57×10^{0}	1.36×10^{0}	7.21×10^{-7}	1.95×10^{-5}
TFAP2A	2.57×10^{0}	1.36×10^{0}	7.83×10^{-19}	1.40×10^{-15}
CHST4	2.56×10^{0}	1.36×10^{0}	1.69×10^{-8}	8.47×10^{-7}
ANG	2.56×10^{0}	1.36×10^{0}	1.82×10^{-22}	1.16×10^{-18}
CHST5	2.54×10^{0}	1.35×10^{0}	8.20×10^{-16}	4.79×10^{-13}
VSTM5	2.52×10^{0}	1.33×10^{0}	5.68×10^{-23}	4.13×10^{-19}
PLLP	2.51×10^{0}	1.33×10^{0}	3.97×10^{-21}	1.62×10^{-17}
NXPH4	2.51×10^{0}	1.33×10^{0}	9.76×10^{-8}	3.70×10^{-6}
FAM177B	2.50×10^{0}	1.32×10^{0}	9.71×10^{-16}	5.50×10^{-13}
S100P	2.49×10^{0}	1.32×10^{0}	1.11×10^{-9}	8.36×10^{-8}

Table A.53 (continued). The list of the top 100 upregulated DEGs identified in the CS4 subtype using limma as a result of four clustering analyzes.

FER1L6	2.49×10^{0}	1.31×10^{0}	2.86×10^{-12}	5.37×10^{-10}
AC005256.1	2.47×10^{0}	1.30×10^{0}	9.34×10^{-16}	5.35×10^{-13}
ENTPD8	2.47×10^{0}	1.30×10^{0}	1.93×10^{-7}	6.50×10^{-6}
ZNF488	2.46×10^{0}	1.30×10^{0}	2.63×10^{-19}	5.79×10^{-16}
C4BPB	2.44×10^{0}	1.28×10^{0}	2.55×10^{-13}	6.78×10^{-11}
MRAP2	2.44×10^{0}	1.28×10^{0}	6.80×10^{-12}	1.12×10^{-9}
SLC4A4	2.43×10^{0}	1.28×10^{0}	1.67×10^{-9}	1.19×10^{-7}
MSLN	2.37×10^{0}	1.25×10^{0}	2.62×10^{-4}	2.69×10^{-3}
PI3	2.37×10^{0}	1.24×10^{0}	7.71×10^{-4}	6.49×10^{-3}
TMEM61	2.37×10^{0}	1.24×10^{0}	5.64×10^{-20}	1.62×10^{-16}
FABP2	2.37×10^{0}	1.24×10^{0}	1.41×10^{-6}	3.40×10^{-5}
PDZK1IP1	2.36×10^{0}	1.24×10^{0}	8.33×10^{-10}	6.58×10^{-8}
SYTL1	2.36×10^{0}	1.24×10^{0}	5.13×10^{-15}	2.31×10^{-12}
KCNK1	2.35×10^{0}	1.23×10^{0}	2.33×10^{-14}	8.62×10^{-12}
HSD17B2	2.35×10^{0}	1.23×10^{0}	6.40×10^{-13}	1.51×10^{-10}
ULBP2	2.34×10^{0}	1.22×10^{0}	1.23×10^{-11}	1.86×10^{-9}
SMIM31	2.33×10^{0}	1.22×10^{0}	3.87×10^{-11}	4.93×10^{-9}
TMEM231P1	2.31×10^{0}	1.21×10^{0}	7.66×10^{-16}	4.57×10^{-13}
HID1	2.31×10^{0}	1.21×10^{0}	2.77×10^{-15}	1.39×10^{-12}
CPS1	2.28×10^{0}	1.19×10^{0}	3.09×10^{-8}	1.41×10^{-6}

Table A.54. The list of the top 100 downregulated DEGs identified in the CS4 subtype using limma as a result of four clustering analyzes.

	fc	**log2fc**	**pvalue**	**padj**
EREG	1.69×10^{-1}	-2.57×10^{0}	4.48×10^{-16}	2.79×10^{-13}

Y_RNA.244	2.27×10^{-1}	-2.14×10^{0}	2.26×10^{-15}	1.16×10^{-12}
PTPRO	2.82×10^{-1}	-1.83×10^{0}	5.67×10^{-14}	1.80×10^{-11}
SRPX2	3.14×10^{-1}	-1.67×10^{0}	1.06×10^{-15}	5.84×10^{-13}
AOAH	3.15×10^{-1}	-1.67×10^{0}	2.73×10^{-17}	2.61×10^{-14}
MPP1	3.15×10^{-1}	-1.67×10^{0}	1.01×10^{-21}	5.25×10^{-18}
NPTX2	3.32×10^{-1}	-1.59×10^{0}	2.18×10^{-7}	7.21×10^{-6}
ST6GAL1	3.41×10^{-1}	-1.55×10^{0}	1.37×10^{-17}	1.51×10^{-14}
R3HDML	3.46×10^{-1}	-1.53×10^{0}	1.62×10^{-17}	1.71×10^{-14}
CKMT2	3.47×10^{-1}	-1.53×10^{0}	1.27×10^{-6}	3.13×10^{-5}
REEP1	3.53×10^{-1}	-1.50×10^{0}	2.90×10^{-15}	1.43×10^{-12}
APOLD1	3.67×10^{-1}	-1.45×10^{0}	4.61×10^{-12}	7.96×10^{-10}
AC108134.3	3.68×10^{-1}	-1.44×10^{0}	2.45×10^{-15}	1.24×10^{-12}
ZCCHC24	3.73×10^{-1}	-1.42×10^{0}	5.71×10^{-17}	4.81×10^{-14}
SLC6A6	3.75×10^{-1}	-1.41×10^{0}	3.20×10^{-21}	1.41×10^{-17}
AC078993.1	3.79×10^{-1}	-1.40×10^{0}	2.61×10^{-9}	1.72×10^{-7}
SHROOM4	3.81×10^{-1}	-1.39×10^{0}	3.05×10^{-21}	1.41×10^{-17}

Table A.54 (continued). The list of the top 100 downregulated DEGs identified in the CS4 subtype using limma as a result of four clustering analyzes.

FARP1	3.83×10^{-1}	-1.38×10^{0}	3.16×10^{-25}	6.03×10^{-21}
HSPB6	3.84×10^{-1}	-1.38×10^{0}	2.49×10^{-10}	2.41×10^{-8}
SLC26A2	3.91×10^{-1}	-1.35×10^{0}	2.21×10^{-7}	7.30×10^{-6}
SLC13A3	3.95×10^{-1}	-1.34×10^{0}	2.73×10^{-10}	2.62×10^{-8}
APOD	3.96×10^{-1}	-1.34×10^{0}	7.10×10^{-7}	1.93×10^{-5}
TSPOAP1.AS1	4.00×10^{-1}	-1.32×10^{0}	3.91×10^{-18}	5.33×10^{-15}
MAGEB17	4.00×10^{-1}	-1.32×10^{0}	4.65×10^{-9}	2.85×10^{-7}
AC108865.1	4.02×10^{-1}	-1.31×10^{0}	1.20×10^{-4}	1.41×10^{-3}
SEMA3A	4.12×10^{-1}	-1.28×10^{0}	4.44×10^{-15}	2.02×10^{-12}
SORBS1	4.12×10^{-1}	-1.28×10^{0}	6.21×10^{-13}	1.48×10^{-10}
OXGR1	4.13×10^{-1}	-1.28×10^{0}	1.50×10^{-9}	1.08×10^{-7}
AC123023.1	4.13×10^{-1}	-1.28×10^{0}	3.49×10^{-10}	3.20×10^{-8}
ACTG2	4.14×10^{-1}	-1.27×10^{0}	1.84×10^{-5}	2.95×10^{-4}
FREM1	4.18×10^{-1}	-1.26×10^{0}	1.22×10^{-7}	4.45×10^{-6}
PDE3A	4.18×10^{-1}	-1.26×10^{0}	6.61×10^{-12}	1.09×10^{-9}
FRG1CP	4.20×10^{-1}	-1.25×10^{0}	5.47×10^{-10}	4.60×10^{-8}
ARL11	4.24×10^{-1}	-1.24×10^{0}	1.95×10^{-13}	5.44×10^{-11}
AC019330.1	4.26×10^{-1}	-1.23×10^{0}	6.80×10^{-14}	2.13×10^{-11}
ERP27	4.29×10^{-1}	-1.22×10^{0}	4.23×10^{-7}	1.27×10^{-5}
PIPOX	4.30×10^{-1}	-1.22×10^{0}	1.26×10^{-8}	6.59×10^{-7}
NINL	4.33×10^{-1}	-1.21×10^{0}	1.34×10^{-11}	1.99×10^{-9}
SALL4	4.38×10^{-1}	-1.19×10^{0}	3.11×10^{-15}	1.51×10^{-12}
GABRE	4.40×10^{-1}	-1.19×10^{0}	2.46×10^{-11}	3.40×10^{-9}
EMB	4.40×10^{-1}	-1.18×10^{0}	2.41×10^{-7}	7.89×10^{-6}
TEX43	4.41×10^{-1}	-1.18×10^{0}	1.20×10^{-11}	1.82×10^{-9}

KLF7	4.44×10^{-1}	-1.17×10^{0}	1.43×10^{-17}	1.54×10^{-14}
DMD	4.44×10^{-1}	-1.17×10^{0}	1.51×10^{-19}	3.61×10^{-16}
RNU2.6P	4.47×10^{-1}	-1.16×10^{0}	1.94×10^{-8}	9.53×10^{-7}
CAMK1D	4.48×10^{-1}	-1.16×10^{0}	2.24×10^{-12}	4.37×10^{-10}
MPV17L	4.49×10^{-1}	-1.15×10^{0}	9.03×10^{-7}	2.36×10^{-5}
AK4	4.50×10^{-1}	-1.15×10^{0}	3.64×10^{-9}	2.31×10^{-7}
ZNF606	4.51×10^{-1}	-1.15×10^{0}	1.04×10^{-19}	2.70×10^{-16}
SATB2	4.52×10^{-1}	-1.15×10^{0}	3.07×10^{-10}	2.88×10^{-8}
HCG11	4.52×10^{-1}	-1.15×10^{0}	3.08×10^{-13}	7.93×10^{-11}
NFATC2	4.53×10^{-1}	-1.14×10^{0}	3.33×10^{-17}	3.03×10^{-14}
FAM217B	4.53×10^{-1}	-1.14×10^{0}	6.51×10^{-21}	2.48×10^{-17}
ZNF43	4.53×10^{-1}	-1.14×10^{0}	1.83×10^{-12}	3.68×10^{-10}
L1CAM	4.54×10^{-1}	-1.14×10^{0}	3.72×10^{-7}	1.14×10^{-5}
MIR196A1	4.56×10^{-1}	-1.13×10^{0}	1.02×10^{-5}	1.81×10^{-4}
RPS6KA6	4.57×10^{-1}	-1.13×10^{0}	4.71×10^{-13}	1.17×10^{-10}

Table A.54 (continued). The list of the top 100 downregulated DEGs identified in the CS4 subtype using limma as a result of four clustering analyzes.

CHN2.AS1	4.60×10^{-1}	-1.12×10^{0}	2.59×10^{-12}	4.91×10^{-10}
ZBTB10	4.60×10^{-1}	-1.12×10^{0}	1.73×10^{-13}	4.97×10^{-11}
PIP4P2	4.61×10^{-1}	-1.12×10^{0}	1.74×10^{-20}	6.22×10^{-17}
FNBP1	4.61×10^{-1}	-1.12×10^{0}	3.38×10^{-16}	2.22×10^{-13}
DAB2	4.64×10^{-1}	-1.11×10^{0}	8.90×10^{-17}	6.88×10^{-14}
ACE2	4.65×10^{-1}	-1.11×10^{0}	6.35×10^{-9}	3.68×10^{-7}
EPM2AIP1	4.65×10^{-1}	-1.10×10^{0}	1.23×10^{-14}	4.95×10^{-12}
LDLRAD3	4.65×10^{-1}	-1.10×10^{0}	1.93×10^{-14}	7.38×10^{-12}
PPP1R3D	4.66×10^{-1}	-1.10×10^{0}	5.77×10^{-23}	4.13×10^{-19}
RGS5	4.67×10^{-1}	-1.10×10^{0}	3.82×10^{-10}	3.45×10^{-8}
SPIN3	4.67×10^{-1}	-1.10×10^{0}	2.14×10^{-18}	3.15×10^{-15}
LINC00654	4.68×10^{-1}	-1.09×10^{0}	2.66×10^{-11}	3.64×10^{-9}
PCDHGC3	4.70×10^{-1}	-1.09×10^{0}	3.59×10^{-11}	4.67×10^{-9}
AC092070.2	4.71×10^{-1}	-1.09×10^{0}	3.91×10^{-14}	1.32×10^{-11}
ACSL6	4.72×10^{-1}	-1.08×10^{0}	9.01×10^{-9}	4.97×10^{-7}
EDNRA	4.72×10^{-1}	-1.08×10^{0}	3.46×10^{-10}	3.18×10^{-8}
PLA1A	4.73×10^{-1}	-1.08×10^{0}	5.49×10^{-10}	4.60×10^{-8}
SEMA3C	4.75×10^{-1}	-1.07×10^{0}	2.57×10^{-12}	4.89×10^{-10}
MALAT1	4.76×10^{-1}	-1.07×10^{0}	5.09×10^{-5}	6.93×10^{-4}
PLAGL1	4.76×10^{-1}	-1.07×10^{0}	1.28×10^{-12}	2.74×10^{-10}
ITGA9	4.77×10^{-1}	-1.07×10^{0}	4.47×10^{-12}	7.78×10^{-10}
Z83843.1	4.77×10^{-1}	-1.07×10^{0}	5.70×10^{-9}	3.36×10^{-7}
PM20D2	4.78×10^{-1}	-1.07×10^{0}	2.46×10^{-12}	4.72×10^{-10}
CARD11	4.79×10^{-1}	-1.06×10^{0}	6.91×10^{-6}	1.30×10^{-4}
TBC1D9	4.80×10^{-1}	-1.06×10^{0}	7.34×10^{-14}	2.28×10^{-11}
RDX	4.80×10^{-1}	-1.06×10^{0}	5.15×10^{-11}	6.34×10^{-9}
RNF217	4.81×10^{-1}	-1.05×10^{0}	5.20×10^{-14}	1.68×10^{-11}

ELAPOR2	4.81×10^{-1}	-1.05×10^{0}	1.57×10^{-8}	7.95×10^{-7}
ANKRD10.IT1	4.82×10^{-1}	-1.05×10^{0}	2.59×10^{-8}	1.22×10^{-6}
NAALADL2	4.83×10^{-1}	-1.05×10^{0}	1.69×10^{-14}	6.50×10^{-12}
AL139396.1	4.83×10^{-1}	-1.05×10^{0}	1.26×10^{-6}	3.10×10^{-5}
IGF2	4.85×10^{-1}	-1.04×10^{0}	4.64×10^{-4}	4.30×10^{-3}
CYCSP34	4.88×10^{-1}	-1.04×10^{0}	5.14×10^{-11}	6.34×10^{-9}
ZNF880	4.88×10^{-1}	-1.04×10^{0}	1.22×10^{-12}	2.62×10^{-10}
HDGFL3	4.90×10^{-1}	-1.03×10^{0}	1.08×10^{-11}	1.65×10^{-9}
PCMTD2	4.91×10^{-1}	-1.03×10^{0}	5.30×10^{-18}	6.60×10^{-15}
NNAT	4.92×10^{-1}	-1.02×10^{0}	8.41×10^{-9}	4.68×10^{-7}
SLC6A4	4.94×10^{-1}	-1.02×10^{0}	1.78×10^{-9}	1.25×10^{-7}
ZNF141	4.94×10^{-1}	-1.02×10^{0}	1.51×10^{-16}	1.08×10^{-13}
EDAR	4.94×10^{-1}	-1.02×10^{0}	8.03×10^{-5}	1.01×10^{-3}

Table A.54 (continued). The list of the top 100 downregulated DEGs identified in the CS4 subtype using limma as a result of four clustering analyzes.

HOXD10	4.94×10^{-1}	-1.02×10^{0}	1.75×10^{-6}	4.09×10^{-5}
ZNF736	4.95×10^{-1}	-1.01×10^{0}	6.10×10^{-14}	1.92×10^{-11}
PROX1	4.96×10^{-1}	-1.01×10^{0}	1.91×10^{-8}	9.38×10^{-7}

APPENDIX B Drug Sensitivity Results of All Subtypes

Table B.1. Response of all clustering results to chemotherapeutic drugs in p-value.

Subtypes **Drugs**	**2 Clustering**	**3 Clustering**	**4 Clustering**
BMS-536924	2.20×10^{-16}	2.20×10^{-16}	2.20×10^{-16}
BI-2536	9.10×10^{-11}	6.10×10^{-9}	3.60×10^{-9}
WZ-1-84	1.60×10^{-2}	1.60×10^{-2}	1.20×10^{-5}
WH-4-023	4.60×10^{-1}	2.40×10^{-4}	2.30×10^{-9}
A-770041	5.00×10^{-2}	4.40×10^{-5}	4.80×10^{-9}
CGP-082996	2.80×10^{-2}	1.10×10^{-3}	3.80×10^{-6}
CGP-60474	2.30×10^{-7}	1.70×10^{-9}	8.20×10^{-13}
GNF-2	4.80×10^{-1}	3.10×10^{-1}	2.20×10^{-2}
DASATINIB	5.30×10^{-1}	1.30×10^{-3}	3.20×10^{-6}
Z-LLNle-CHO	2.00×10^{-13}	5.00×10^{-12}	1.50×10^{-12}
S-Trithl-L-cysteine	5.80×10^{-6}	9.60×10^{-9}	3.10×10^{-15}
SARACATINIB	2.50×10^{-1}	2.30×10^{-2}	3.20×10^{-1}
CRIZOTINIB	3.80×10^{-6}	4.80×10^{-10}	3.90×10^{-12}
TAE684	2.20×10^{-16}	2.20×10^{-16}	2.20×10^{-16}
IMATINIB	2.00×10^{-5}	1.90×10^{-5}	1.20×10^{-9}
VX-680	1.80×10^{-4}	6.40×10^{-5}	3.70×10^{-6}
SORAFENIB	7.00×10^{-5}	2.30×10^{-3}	3.30×10^{-2}

AZ628	1.90×10^{-3}	4.00×10^{-3}	1.10×10^{-1}
CYCLOPAMINE	3.30×10^{-3}	1.40×10^{-10}	2.20×10^{-16}
PACLITAXEL	1.70×10^{-6}	4.10×10^{-7}	8.90×10^{-11}
MG-132	7.30×10^{-2}	1.30×10^{-1}	4.30×10^{-8}
PHA-665752	2.90×10^{-7}	6.20×10^{-5}	6.50×10^{-5}
SUNITINIB	2.00×10^{-8}	6.90×10^{-9}	7.50×10^{-11}
RAPAMYCIN	6.60×10^{-11}	1.40×10^{-11}	7.60×10^{-15}
ERLOTINIB	4.90×10^{-6}	4.80×10^{-11}	6.30×10^{-12}
BRYOSTATIN 1	1.40×10^{-5}	2.80×10^{-12}	2.20×10^{-16}
PHENFORMIN	2.20×10^{-16}	2.20×10^{-16}	2.20×10^{-16}
AUY922	1.00×10^{-8}	2.20×10^{-16}	2.20×10^{-16}
GW-2580	2.20×10^{-16}	2.20×10^{-16}	2.20×10^{-16}
LFM-A13	2.80×10^{-12}	9.60×10^{-15}	2.20×10^{-16}

Table B.1 (continued). Response of all clustering results to chemotherapeutic drugs in p-value.

BLEOMYCIN	2.20×10^{-16}	2.20×10^{-16}	2.20×10^{-16}
BEXAROTENE	2.20×10^{-16}	2.20×10^{-16}	9.00×10^{-16}
LISITINIB	2.20×10^{-16}	2.20×10^{-16}	2.20×10^{-16}
BMS-754807	2.20×10^{-15}	2.20×10^{-16}	2.20×10^{-16}
OBATOCLAX MESYLATE	8.50×10^{-2}	7.20×10^{-7}	7.70×10^{-10}
THAPSIGARGIN	6.10×10^{-7}	1.30×10^{-5}	2.40×10^{-6}
5-FLUOROURACIL	1.70×10^{-10}	9.80×10^{-10}	6.70×10^{-11}
BAY 61-3606	2.20×10^{-16}	2.20×10^{-16}	2.20×10^{-16}
GSK-650394	7.50×10^{-4}	1.30×10^{-2}	1.70×10^{-3}
IPA-3	5.20×10^{-5}	2.20×10^{-16}	2.20×10^{-16}
PAC-1	1.10×10^{-4}	2.90×10^{-4}	7.00×10^{-4}
FH535	7.50×10^{-4}	2.90×10^{-3}	2.30×10^{-5}
EMBELIN	8.90×10^{-8}	4.40×10^{-11}	8.50×10^{-16}
AKT INHIBITOR VIII	2.10×10^{-5}	8.70×10^{-4}	9.20×10^{-8}
SHIKONIN	6.00×10^{-1}	3.50×10^{-5}	2.10×10^{-7}
OSU-03012	1.90×10^{-5}	8.00×10^{-8}	3.40×10^{-10}
FTI-277	2.20×10^{-16}	2.20×10^{-16}	2.20×10^{-16}
DMOG	2.40×10^{-1}	1.60×10^{-1}	1.10×10^{-4}
JQ12	3.00×10^{-4}	5.00×10^{-4}	1.70×10^{-5}
JQ1	1.40×10^{-3}	9.80×10^{-5}	1.20×10^{-6}
HG-6-64-1	1.50×10^{-6}	2.60×10^{-9}	1.70×10^{-12}
PF-562271	4.20×10^{-4}	3.20×10^{-3}	1.00×10^{-1}
JNK-9L	1.00×10^{-2}	1.70×10^{-1}	6.90×10^{-2}
AZD6482	8.30×10^{-8}	5.40×10^{-9}	8.90×10^{-15}
AP-24534	2.90×10^{-9}	2.80×10^{-11}	2.00×10^{-11}
CHIR-99021	9.30×10^{-2}	8.30×10^{-14}	2.20×10^{-16}
MIDOSTAURIN	2.80×10^{-14}	2.20×10^{-16}	2.20×10^{-16}

CP466722	1.10×10^{-12}	1.60×10^{-15}	2.20×10^{-16}
QS11	4.30×10^{-2}	1.40×10^{-5}	3.80×10^{-11}
BICALUTAMIDE	6.70×10^{-1}	7.80×10^{-3}	1.30×10^{-4}
NSC-87877	4.30×10^{-1}	1.40×10^{-2}	1.40×10^{-2}
VINORELBINE	8.90×10^{-15}	3.70×10^{-13}	2.30×10^{-12}
MITOMYCIN C	2.40×10^{-1}	4.60×10^{-1}	1.30×10^{-1}
GEMCITABINE	6.90×10^{-13}	4.20×10^{-13}	7.10×10^{-14}
ETOPOSIDE	2.10×10^{-12}	1.20×10^{-12}	5.20×10^{-11}
DOXORUBICIN	3.80×10^{-6}	5.00×10^{-11}	3.90×10^{-16}
GSK269962A	4.10×10^{-12}	1.40×10^{-13}	6.30×10^{-14}
LAPATINIB	2.00×10^{-2}	5.10×10^{-14}	2.20×10^{-16}
SALUBRINAL	2.30×10^{-4}	9.80×10^{-3}	4.50×10^{-3}

Table B.1 (continued). Response of all clustering results to chemotherapeutic drugs in p-value.

ROSCOVITINE	8.10×10^{-1}	1.10×10^{-9}	2.20×10^{-16}
XMD8-85	3.20×10^{-1}	2.80×10^{-8}	2.60×10^{-16}
BORTEZOMIB	9.10×10^{-1}	1.30×10^{-1}	4.40×10^{-1}
TGX221	3.70×10^{-2}	8.70×10^{-5}	3.60×10^{-9}
KIN001-135	2.10×10^{-2}	5.10×10^{-8}	2.20×10^{-16}
PARTHENOLIDE	1.30×10^{-10}	6.00×10^{-12}	2.90×10^{-9}
MS-275	1.70×10^{-1}	5.40×10^{-8}	4.40×10^{-14}
GW843682X	1.50×10^{-3}	8.60×10^{-6}	5.50×10^{-10}
A-443654	3.30×10^{-5}	4.40×10^{-4}	1.50×10^{-4}
JW-7-52-1	3.50×10^{-1}	4.70×10^{-3}	4.40×10^{-5}
PYRIMETHAMINE	8.30×10^{-1}	6.30×10^{-1}	7.60×10^{-3}
CMK	5.70×10^{-7}	2.70×10^{-15}	4.90×10^{-15}
BMS-509744	4.90×10^{-1}	1.50×10^{-2}	3.00×10^{-5}
GW 441756	3.10×10^{-13}	1.40×10^{-12}	4.70×10^{-15}
AZD7762	2.20×10^{-16}	2.20×10^{-16}	2.20×10^{-16}
AXITINIB	8.40×10^{-12}	2.90×10^{-16}	5.90×10^{-16}
LENALIDOMIDE	5.40×10^{-14}	3.10×10^{-15}	1.40×10^{-8}
BOSUTINIB	2.20×10^{-16}	2.20×10^{-16}	2.20×10^{-16}
VELIPARIB	9.10×10^{-12}	1.70×10^{-9}	5.50×10^{-7}
OLAPARIB	2.20×10^{-16}	2.20×10^{-16}	2.20×10^{-16}
TEMSIROLIMUS	1.40×10^{-9}	1.80×10^{-13}	2.20×10^{-16}
CI-1040	3.90×10^{-2}	1.20×10^{-10}	1.10×10^{-10}
RDEA119	3.30×10^{-3}	2.10×10^{-10}	4.20×10^{-9}
NILOTINIB	9.10×10^{-10}	3.90×10^{-10}	3.90×10^{-6}
VORINOSTAT	4.60×10^{-1}	9.50×10^{-13}	2.70×10^{-16}
NAVITOCLAX	1.80×10^{-1}	1.30×10^{-9}	2.20×10^{-16}
GEFITINIB	1.10×10^{-2}	4.20×10^{-8}	1.50×10^{-7}
ATRA	7.40×10^{-3}	4.10×10^{-9}	2.20×10^{-16}
METHOTREXATE	3.10×10^{-1}	9.20×10^{-1}	3.40×10^{-1}
DOCETAXEL	2.10×10^{-8}	3.10×10^{-9}	1.90×10^{-11}

CYTARABINE	1.80×10^{-10}	3.20×10^{-15}	1.50×10^{-14}
CISPLATIN	2.00×10^{-15}	2.20×10^{-16}	2.20×10^{-16}
VINBLASTINE	2.20×10^{-16}	2.20×10^{-16}	2.20×10^{-16}
CAMPTOTHECIN	8.70×10^{-10}	1.20×10^{-12}	4.50×10^{-10}
AICAR	2.40×10^{-2}	2.10×10^{-12}	2.40×10^{-15}
THZ-2-102-1	2.30×10^{-5}	1.90×10^{-10}	2.40×10^{-11}
KIN001-270	9.00×10^{-15}	2.20×10^{-16}	2.20×10^{-16}
THZ-2-49	2.20×10^{-6}	1.90×10^{-5}	1.20×10^{-9}
EX-527	1.10×10^{-12}	4.80×10^{-15}	8.10×10^{-10}
T0901317	1.10×10^{-11}	2.20×10^{-16}	2.20×10^{-16}
XMD15-27	5.30×10^{-10}	2.20×10^{-16}	2.20×10^{-16}

Table B.1 (continued). Response of all clustering results to chemotherapeutic drugs in p-value.

QL-X-138	3.20×10^{-9}	1.30×10^{-14}	2.20×10^{-16}
XMD13-2	3.10×10^{-15}	2.50×10^{-14}	1.80×10^{-15}
QL-XI-92	1.00×10^{-10}	2.20×10^{-16}	2.20×10^{-16}
SNX-2112	3.30×10^{-9}	1.30×10^{-9}	6.70×10^{-10}
GSK690693	5.00×10^{-14}	7.40×10^{-12}	1.50×10^{-11}
TIVOZANIB	2.20×10^{-16}	2.20×10^{-16}	2.20×10^{-16}
YM201636	6.40×10^{-6}	2.90×10^{-4}	5.90×10^{-4}
Y-39983	6.30×10^{-13}	2.20×10^{-16}	2.20×10^{-16}
FORETINIB	2.20×10^{-16}	2.20×10^{-16}	2.20×10^{-16}
TG101348	5.10×10^{-9}	1.20×10^{-9}	1.20×10^{-7}
TPCA-1	1.20×10^{-13}	9.50×10^{-16}	7.10×10^{-16}
SB52334	1.10×10^{-3}	4.90×10^{-3}	8.50×10^{-3}
PIK-93	2.20×10^{-16}	2.20×10^{-16}	2.20×10^{-16}
PI-103	1.20×10^{-7}	2.20×10^{-16}	2.20×10^{-16}
PHA-793887	2.20×10^{-16}	2.20×10^{-16}	2.20×10^{-16}
CX-5461	1.80×10^{-9}	1.40×10^{-7}	1.10×10^{-6}
OSI-027	5.40×10^{-5}	3.20×10^{-9}	1.80×10^{-15}
OSI-930	5.10×10^{-1}	2.80×10^{-5}	5.20×10^{-6}
BHG712	4.50×10^{-5}	6.30×10^{-4}	2.40×10^{-3}
MPS-1-IN-1	1.70×10^{-1}	2.90×10^{-1}	7.30×10^{-1}
MP470	9.80×10^{-1}	2.40×10^{-4}	1.10×10^{-13}
MASITINIB	5.70×10^{-2}	1.50×10^{-1}	3.50×10^{-1}
KIN001-266	8.20×10^{-10}	3.00×10^{-14}	3.50×10^{-10}
KIN001-260	2.20×10^{-16}	2.20×10^{-16}	2.20×10^{-16}
KIN001-055	6.50×10^{-8}	6.70×10^{-11}	5.60×10^{-11}
KIN001-244	2.20×10^{-16}	2.20×10^{-16}	2.20×10^{-16}
KIN001-236	2.20×10^{-16}	2.20×10^{-16}	2.20×10^{-16}
GSK2126458	1.10×10^{-3}	3.40×10^{-3}	3.60×10^{-7}
EKB-569	9.00×10^{-1}	2.50×10^{-2}	5.80×10^{-6}
CH5424802	4.80×10^{-2}	2.90×10^{-3}	4.20×10^{-5}
BIX02189	2.20×10^{-16}	2.20×10^{-16}	3.50×10^{-13}

CAY10603	1.70×10^{-7}	2.40×10^{-15}	2.20×10^{-16}
I-BET-762	1.30×10^{-9}	7.60×10^{-8}	5.70×10^{-9}
BELINOSTAT	5.40×10^{-4}	8.30×10^{-6}	1.80×10^{-5}
CUDC-101	2.70×10^{-8}	8.60×10^{-13}	2.10×10^{-15}
AR-42	3.00×10^{-7}	2.20×10^{-16}	2.20×10^{-16}
NSC-207895	2.20×10^{-16}	2.20×10^{-16}	2.20×10^{-16}
YM155	1.80×10^{-15}	2.20×10^{-16}	2.20×10^{-16}
ZIBOTENTAN	2.20×10^{-12}	4.30×10^{-16}	9.00×10^{-14}
TUBASTATIN A	3.30×10^{-15}	7.80×10^{-16}	3.00×10^{-12}
FR-180204	3.50×10^{-11}	5.10×10^{-10}	4.60×10^{-10}

Table B.1 (continued). Response of all clustering results to chemotherapeutic drugs in p-value.

VX-11E	1.80×10^{-1}	3.70×10^{-3}	2.20×10^{-7}
TL-1-85	1.30×10^{-13}	2.20×10^{-16}	2.20×10^{-16}
NG-25	6.30×10^{-16}	2.20×10^{-16}	2.20×10^{-16}
STF-62247	2.20×10^{-16}	2.20×10^{-16}	2.20×10^{-16}
NPK76-II-72-1	2.20×10^{-16}	2.20×10^{-16}	1.10×10^{-15}
JW-7-24-1	1.90×10^{-1}	7.50×10^{-8}	1.60×10^{-13}
CP724714	3.50×10^{-7}	2.20×10^{-6}	3.50×10^{-4}
AC220	1.00×10^{-5}	4.50×10^{-7}	4.80×10^{-8}
XMD14-99	2.00×10^{-13}	7.70×10^{-16}	7.60×10^{-11}
WZ3105	1.80×10^{-12}	2.50×10^{-12}	2.20×10^{-16}
XL-184	2.20×10^{-16}	2.20×10^{-16}	2.20×10^{-16}
UNC0638	2.40×10^{-5}	1.30×10^{-11}	6.10×10^{-13}
CAL-101	8.60×10^{-6}	1.20×10^{-6}	5.00×10^{-9}
QL-XII-47	7.00×10^{-3}	2.20×10^{-14}	2.20×10^{-16}
FMK	1.10×10^{-10}	4.50×10^{-13}	2.40×10^{-8}
GSK429286A	1.10×10^{-9}	2.20×10^{-16}	2.20×10^{-16}
LY317615	4.40×10^{-2}	9.50×10^{-7}	1.70×10^{-12}
KIN001-102	1.20×10^{-5}	1.70×10^{-5}	1.20×10^{-6}
GSK1070916	4.60×10^{-3}	7.60×10^{-5}	7.30×10^{-3}
GENENTECH CPD 10	1.10×10^{-3}	3.90×10^{-7}	1.10×10^{-7}
AS605240	9.20×10^{-1}	1.50×10^{-1}	9.90×10^{-5}
ZSTK474	6.40×10^{-5}	7.80×10^{-7}	1.50×10^{-11}
BX-912	4.00×10^{-9}	2.20×10^{-16}	2.20×10^{-16}
TAK-715	1.40×10^{-8}	4.70×10^{-10}	4.80×10^{-6}
AT-7519	2.20×10^{-16}	4.70×10^{-16}	2.20×10^{-16}
TL-2-105	3.00×10^{-11}	3.50×10^{-11}	4.20×10^{-8}
ISPINESIB MESYLATE	2.70×10^{-8}	2.70×10^{-6}	4.30×10^{-6}
AS601245	2.20×10^{-16}	2.20×10^{-16}	2.20×10^{-16}
RUXOLITINIB	1.30×10^{-15}	2.20×10^{-16}	2.20×10^{-16}
BMS-708163	1.50×10^{-1}	4.00×10^{-7}	5.70×10^{-13}

TIPIFARNIB	1.60×10^{-10}	1.30×10^{-10}	1.80×10^{-12}
BMS345541	7.50×10^{-7}	2.70×10^{-10}	9.10×10^{-9}
GSK1904529A	2.20×10^{-16}	2.20×10^{-16}	2.20×10^{-16}
EPOTHILONE B	2.60×10^{-1}	1.40×10^{-6}	3.40×10^{-7}
LAQ824	3.60×10^{-2}	2.30×10^{-7}	1.10×10^{-11}
PAZOPANIB	2.50×10^{-16}	2.20×10^{-16}	2.20×10^{-16}
MLN4924	2.20×10^{-16}	2.20×10^{-16}	4.60×10^{-16}
SN-38	5.70×10^{-15}	1.50×10^{-14}	5.10×10^{-13}
BLEOMYCIN	2.20×10^{-16}	2.20×10^{-16}	2.20×10^{-16}
TEMOZOLOMIDE	2.60×10^{-7}	1.80×10^{-10}	1.70×10^{-10}

Table B.1 (continued). Response of all clustering results to chemotherapeutic drugs in p-value.

DABRAFENIB	5.20×10^{-16}	2.20×10^{-16}	2.20×10^{-16}
TRAMETINIB	7.40×10^{-1}	7.00×10^{-2}	5.30×10^{-2}
XAV939	4.70×10^{-14}	2.20×10^{-16}	2.20×10^{-16}
SGC0946	2.20×10^{-16}	2.20×10^{-16}	2.20×10^{-16}
UNC1215	6.60×10^{-9}	4.90×10^{-8}	7.90×10^{-10}
rTRAIL	1.30×10^{-3}	1.60×10^{-10}	6.50×10^{-16}
TALAZOPARIB	2.20×10^{-16}	2.20×10^{-16}	2.20×10^{-16}
FK866	2.20×10^{-16}	2.20×10^{-16}	1.20×10^{-15}
PIPERLONGUMINE	6.30×10^{-13}	2.20×10^{-16}	2.20×10^{-16}
(5Z)-7-OXOZEAENOL	1.30×10^{-1}	2.20×10^{-5}	9.70×10^{-9}
YK 4-279	1.10×10^{-4}	1.70×10^{-3}	1.90×10^{-1}
IOX2	1.40×10^{-9}	2.60×10^{-16}	2.80×10^{-16}
PFI-1	6.70×10^{-3}	3.90×10^{-7}	2.20×10^{-16}
QL-XII-61	4.50×10^{-10}	3.90×10^{-7}	3.20×10^{-14}
TAMOXIFEN	4.00×10^{-4}	3.70×10^{-8}	1.30×10^{-15}
SB 505124	2.40×10^{-1}	1.80×10^{-12}	2.20×10^{-16}
AG-014699	2.70×10^{-2}	1.20×10^{-1}	7.80×10^{-1}
CCT018159	2.20×10^{-16}	2.20×10^{-16}	2.20×10^{-16}
QL-VII-58	5.20×10^{-5}	8.40×10^{-15}	2.20×10^{-16}
XMD8-92	1.10×10^{-5}	2.20×10^{-16}	2.20×10^{-16}
ZG-10	6.30×10^{-12}	2.20×10^{-16}	2.20×10^{-16}
XMD11-85h	3.60×10^{-7}	2.80×10^{-15}	2.20×10^{-16}
TW37	3.20×10^{-6}	1.50×10^{-11}	1.10×10^{-11}
HG-5-88-01	6.50×10^{-3}	1.00×10^{-4}	4.80×10^{-10}
HG-5-113-01	1.50×10^{-9}	2.20×10^{-16}	2.20×10^{-16}
JNJ-268554165	5.90×10^{-14}	1.20×10^{-13}	3.40×10^{-14}
PF-4708671	3.20×10^{-13}	3.20×10^{-11}	4.80×10^{-9}
CETUXIMAB	1.10×10^{-1}	5.50×10^{-13}	2.20×10^{-16}
EHT 1864	4.20×10^{-2}	5.90×10^{-4}	9.80×10^{-6}
CCT007093	4.40×10^{-1}	3.10×10^{-5}	9.60×10^{-5}
SELUMETINIB	2.20×10^{-16}	2.20×10^{-16}	2.20×10^{-16}

SB590885	1.70×10^{-1}	1.80×10^{-6}	3.90×10^{-11}
PD-0325901	1.40×10^{-2}	6.20×10^{-6}	1.30×10^{-4}
AZD8055	3.40×10^{-14}	2.20×10^{-16}	2.20×10^{-16}
GDC0941	4.20×10^{-8}	1.40×10^{-6}	5.20×10^{-15}
BEZ235	1.70×10^{-14}	2.20×10^{-16}	2.20×10^{-16}
PD-0332991	4.40×10^{-5}	2.80×10^{-5}	5.80×10^{-8}
MK-2206	3.50×10^{-7}	3.40×10^{-6}	2.20×10^{-16}
RO-3306	2.10×10^{-9}	2.20×10^{-16}	2.20×10^{-16}
ZM-447439	4.20×10^{-1}	7.40×10^{-1}	1.20×10^{-1}

Table B.1 (continued). Response of all clustering results to chemotherapeutic drugs in p-value.

PD-173074	9.50×10^{-6}	5.40×10^{-6}	9.30×10^{-9}
NUTLIN-3A(-)	2.10×10^{-7}	1.10×10^{-13}	1.30×10^{-11}
681640	1.20×10^{-10}	2.20×10^{-16}	2.20×10^{-16}
JNK INHIBITOR VIII	2.60×10^{-10}	2.20×10^{-16}	2.20×10^{-16}
BIRB 0796	7.70×10^{-2}	2.60×10^{-9}	2.60×10^{-15}
SL 0101-1	1.10×10^{-1}	8.70×10^{-7}	3.10×10^{-8}
NU-7441	1.30×10^{-11}	3.60×10^{-11}	2.20×10^{-16}
BX-795	2.20×10^{-16}	2.20×10^{-16}	2.20×10^{-16}
PLX4720	2.10×10^{-15}	2.50×10^{-15}	2.20×10^{-16}
GDC0449	8.10×10^{-1}	6.20×10^{-2}	5.50×10^{-4}
AFATINIB	2.50×10^{-1}	2.30×10^{-2}	8.90×10^{-6}
ELESCLOMOL	1.50×10^{-8}	2.20×10^{-16}	2.20×10^{-16}
KU-55933	4.90×10^{-12}	5.60×10^{-14}	4.40×10^{-16}
AMG-706	1.60×10^{-4}	1.30×10^{-6}	1.90×10^{-15}
VX-702	6.30×10^{-5}	1.70×10^{-7}	1.90×10^{-4}
17-AAG	4.10×10^{-2}	3.00×10^{-11}	2.20×10^{-16}
SB 216763	5.70×10^{-12}	4.70×10^{-14}	1.60×10^{-8}
CEP-701	1.40×10^{-11}	1.40×10^{-14}	2.20×10^{-16}

AUTOBIOGRAPHY

Name Surname **:** Güllü Elif ÖZDEMİR

Foreign Language **:** English

Education

Degree	Department/Program	University	Graduation Year	GPA
Master of Science	Bioengineering	Marmara University	2024	3.79
Bachelor of Science	Biology	Hacettepe University	2020	3.06

Work Experience

Year	Company/Institution	Position
12/2023 - Continues	Ataşehir Genetik	Bioinformatics Specialist
09/2023 - 11/2023 (Seasonal)	Eres Biotechnology	Bioinformatics Instructor
09/2018 - 02/2020	Genz Biotechnology	Intern
09/2017 - 09/2018	Ankara University Biotechnology Institute	Intern

Publications:

1. Kori, M.; Ozdemir, G.E.; Arga, K.Y.; Sinha, R. A Pan-Cancer Atlas of Differentially Interacting Hallmarks of Cancer Proteins. J. Pers. Med. 2022, 12, 1919.

Presentations:

1. Kori, M, Özdemir, E., Arga, K.Y., Sinha, R. A Pan-Cancer Atlas of Differentially Interacting Hallmarks of Cancer Proteins. Cell Symposia, Hallmarks of Cancer, San Diego, October 30 November 1, 2022.

Projects:

1. 2023-2024 Marmara University Research Fund Project No: 10719 and title: "Kişiselleştirilmiş glioblastoma tedavisi için 3 boyutlu tümör mikroçevrenin oluşturulması ve transkriptom analizi ile belirlenen proteazomal sisteme etkili moleküllerin bu modelde denenmesi".

Fellowship & Awards:

1. Marmara University Research Universities Support Program (2023-2024).

Computer Skills:

- Linux/Bash
- R
- Python
- Microsoft Office

Areas of Expertise:

- Bioinformatics
- Systems biology
- Multi-omic data analysis
- Personalized treatment